Validation of an *ex vivo*, loaded, circumfusion culture system for living cancellous bone explants.

Thesis submitted in candidature for the degree of Doctor of Philosophy at Cardiff University.

AO Research Institute
Clavadelerstrasse, Davos Platz, CH7270
Switzerland
www.aofoundation.org

Connective Tissue Biology Laboratories
School of Biosciences, Cardiff University
Wales, CF10 3US,United Kingdom
www. cf.ac.uk/biosi/research/connective/index.html

By
Catrin Meleri Davies
2005

UMI Number: U584780

All rights reserved

INFORMATION TO ALL USERS
The quality of this reproduction is dependent upon the quality of the copy submitted.

In the unlikely event that the author did not send a complete manuscript
and there are missing pages, these will be noted. Also, if material had to be removed,
a note will indicate the deletion.

UMI U584780
Published by ProQuest LLC 2013. Copyright in the Dissertation held by the Author.
Microform Edition © ProQuest LLC.
All rights reserved. This work is protected against
unauthorized copying under Title 17, United States Code.

ProQuest LLC
789 East Eisenhower Parkway
P.O. Box 1346
Ann Arbor, MI 48106-1346

To John, Rose and Dafydd

"It is very clearly apparent from the admonitions of Galen how great is the usefulness of a knowledge of the bones, since the bones are the foundation of the rest of the parts of the body and all the members rest upon them and are supported, as proceeding from a primary base. Thus if any one is ignorant of the structure of the bones it follows necessarily that he will be ignorant of very many other things along with them."-- Niccolo Massa, 1559

Abstract

The goal of this project was to validate a novel, mechanically loaded culture system, for the maintenance of cancellous bone explants *ex vivo*. The Zetos system utilised cancellous biopsies (5 mm high, 10 mm diameter) from ovine distal femora, bovine distal metacarpals and human femoral heads loaded daily for 300 cycles, at 1 Hz, giving 4,000 microstrain.

Prior to culture, qualitative evaluation of bone density and overall morphology was conducted. These tissues were highly variable with bovine tissue being the most homogenous with regards to density and that each species contained different ratios of red and yellow marrow.

The viability of bone cells and matrix synthesis were analysed using a variety of techniques. The outcome of this study was that diffusion constraints were the major limitation of this system. Chamber design was not optimal for bathing the explants, which was inferior to submerged static culture in centrifuge tubes. Harvesting the tissue created damage to the bone core that resulted in a maximal volume loss of 36%, which also encouraged unwanted growth of a fibrous-like tissue over the explant periphery in a wound-like response, possibly enhanced by foetal calf serum in the media.

Nevertheless, ^{3}H-glycine incorporation detected proteins synthesised during day 7 and 14 of culture. Collagen was the predominant protein synthesised. Fluorochrome labelling demonstrated human bone apposition during culture, but was unsuccessful with bovine and ovine tissue. Mechanically loaded explants were qualitatively more viable than unloaded disuse explants and submerged static controls. These results demonstrate cell viability at least 15 days post-harvest.

If the limitations can be improved, then there is potential for this system to become routinely used in bone research. This system would provide a future means to allow bone-biomaterial interactions and interfaces to be studied, reducing, refining and replacing the need for animal experimentation.

Acknowledgements

I would like to express my deepest gratitude to my family and friends for all their guidance throughout the last 4 years, without their constant moral support and encouraging advice this thesis may not have come to be. I would like to especially thank my mother, Louise and Shamit for always being there to listen to my problems (which occurred quite often, if not on a daily basis!!)You are all fantastic :o) **Thank You All!**

I would like to thank my main supervisor Geoff Richards for being a kind and generous boss to work for and for being someone I could depend on whenever a problem arose. Without all your help and encouragement this work would not have been possible – you've been great. Special thanks to Mauro Alini for helpful discussion and advice regarding biochemistry. Pamela you have been an amazing help. Only wish you arrived sooner. Thanks a million, you truly are "the best". I am also grateful to Prof. Schneider for allowing me to be a part of the AO Research Institute.

To Charlie Archer, my supervisor at Cardiff University, I would like to say "you are a star" for always reading through my work and sending back the corrections. I understand how busy you were and I would like you to know how much I appreciated this. I would also like to thank his group for always making me welcome when I was there; especially to Garry Dowthwaite for helping me with lab work, Joanna Bishop for photocopies and Sam Redman for teaching me autoradiography.

I would like to thank David Jones, and Everett Smith, for technical input; and to the whole of Dept. Experimental Orthopeadics and Biomechanics at Marburg University for making me feel welcome while I stayed there for 7 months, special thanks to Marita Kratz, Eckhard Bröeckmann, Torsten Pohl, Kai Koller, Florian Martens and Miguel Miron.

Several parts of this thesis would not have been available had it not been for the help of several people at the AO Research Institute, Davos. First of all, I would like to thank all the members who have passed through the Interface Biology group; for helping to keep me sane, and for passing on some of their valuable knowledge; particularly to Louise Baxter and Llinos Harris for SEM images. I would like to thank the members of the Biochemistry group especially Cyndi Lee, Robert Peter and Sibylle Grad for always being approachable and helping to answer all of my questions. I would like to thank Berton Rahn, Christoph Sprecher, Iris Keller, and Nora Goudsouzian for histological advice. To Christina Eckhardt, I am

indebted for making all the μCT images of the bone cores. I would also like to thank Ralph Müller (ETH, Zurich) for his μCT images presented in the general discussion.

Thanks also to Sonia Wahl, Margrit Wipf, Elsbeth Wenzinger, Helga Klebel, Peter Stutz, Ladina Kaufmann, and Robi Moor for administrative help over the last 4 years.

I would like to thank Juerg Gasser for all of his time and helpful advice, Beat Gasser RMS for the chambers used during this study, and to all of the other Zetos users for helping me to develop as an independent researcher.

Finally, thank you to

- **3R Foundation grants # 78/01 & # 86/03 for funding this whole project.**

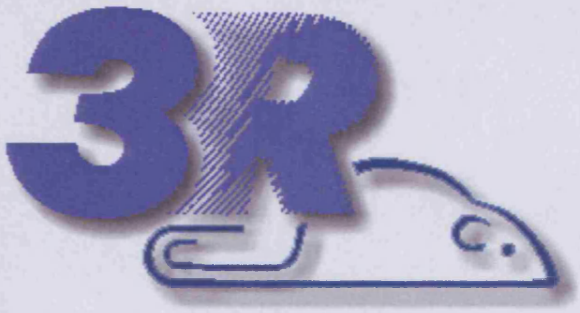

- **The author acknowledges the Swiss Society for Biomaterials for their financial support for the thesis printing and binding.**

SSB

Swiss Society for Biomaterials
Société Suisse des Biomatériaux
Schweizerische Gesellschaft für Biomaterialien
Società Svizzera Biomateriali

Contents

Abbreviations

AlP	alkaline phosphatase
B	bovine
BMPs	bone morphogenic proteins
βGP	beta-glycerophosphate
BMU	bone multicellular unit
BS	bone surface
BSE	backscattered electrons
BSPII	bone sialoprotein
BS/BV	bone surface to volume ratio
BV	bone volume
BV/TV	bone volume to tissue volume
CbFa1	core binding factor
cm	centimetre
CMFDA	CellTraker Green & 5-chloromethylfluorescein diacetate
D-MEM	Dulbecco's Modified Eagle Media
EBSS	Earle's balanced salt solutions
ECM	extracellular matrix
ECMV	extracellular matrix vesicles
ER	endoplasmic reticulum
EthD-1	ethidium homodimer 1
FCS	foetal calf serum
FDA	fluorescein diacetate
FGF	fibroblastic growth factor
Fig.	Figure
GAG	glycosaminoglycan
GLA	gama carboyglutamic acid
G6PD	glucose 6-phosphate dehydrogenase
Gly	glycine
GM-CFU	granulocyte/macrophage colony-forming unit
GST	glutathione S-transferase
H	human
HBSS	Hanks' balanced salt solutions
H and E	haematoxylin and eosin

IGF	insulin-like growth factor
kV	kilovolt
LDH	lactate dehydrogenase
μCT or microCT	micro computer tomography
MAR	mineral apposition rate
MESm	minimum effective strain
mm	millimetre
MMA	methylmethacrylate
MPa	Mega Pascal
MSC	mesenchymal stem cell
MTT	(3-4,5-dimethylthiazol-2-yl)-2,5-diphenyl tetrazolium bromide
NBT	nitro blue tetrazolium chloride
NO	nitric oxide
NR	neutral red
O	ovine
OC	osteocalcin
ON	osteonectin
OP	osteopontin
PBS	phosphate buffered saline
PDGF	platelet-derived growth factor
Pen/Strep	penicillin/streptomycin
PG	prostaglandin
PI	phosphatidyl inositol
PINP	procollagen type I aminopropeptide
PM	pericellular matrix
PTH	parathyroid hormone
PTHrP	parathyroid hormone-related protein
SE	secondary electrons
SEM	scanning Electron Microscopy
SMI	structure model index
Tb.N	trabecular number
Tb.Sp	trabecular separation
Tb.Th	trabecular thickness
TEM	transmission Electron Microscopy

TGFβ	transforming growth factor beta
TRAP	tartrate resistant acid phosphatase
TV	tissue volume
3D	three dimensional
2D	two dimensional
VitC	vitamin C – 2 phosphate
VOI	volume of interest
XTT	3'-[1-[(phenylamino)-carbonyl]-3,4-tetrazolium]-bis(4-methoxy-6-nitro)benzene-sulfonic acid hydrate.

Chapter 1.
Introduction

1.a. Bone

Bone is a highly specialised form of connective tissue and one of the hardest structures of the body. It is a dynamic tissue constantly being turned over. Hence, it is not an inert stone-like material as some people may believe but is a living matrix composed of organic materials, salts, water and cells. It has been estimated that within a period of 10 years, the tissue of the skeleton has been completely replaced from the pre-existing form. The role of the skeleton is varied. It functions as an ion reservoir, sequesters growth factors e.g. bone morphogenic proteins (BMPs), as well as a pool for haemopoietic cells; it supports the body allowing muscles to attach and move for locomotion; and finally some bones, such as the ribs and skull, protect internal organs.

Since the evolution of the human race man is assumed to have been aware of the vertebrate skeleton. Bone's ability to resist rapid degradation made it an ideal object for weapons and tools. It also shaped human ideas on life and death during prehistoric times. Many references to bone and the skeleton occur in the bible as well as Greek mythology.

Physicians from antiquity through the Renaissance discussed the form and function of the skeleton. Galen (A.D. 129) was one of the earliest physician/philosophers to investigate the skeleton. It was through his work that Greek medicine was transmitted to the Renaissance scholars. It was not until 1543 that our basic scientific knowledge began to take shape through the work of the anatomist Andreas Vesalius who recorded human bone anatomy. Over a century later Galileo (1638) began a division of bone based on engineering skills with his observation of a relationship between bone shape, cross-sectional width and mechanical demands. This work was at its greatest during late 19th early 20th century with the work of von Mayer (1867), Culman (1866), and Wolff (1870; 1892), which lead to the development of the hypothesis of functional adaptation by Roux (1885).

Ricqlès *et al.*, (1991) reviewed the development of our understanding of bone today from as far back as the invention of the compound microscope in 1590 by Zaccharias Janssen. This was a major advance in scientific research in all aspects of biology including

bone. It allowed scientists such as Leeuwenhoeck (1685, 1696), Gagliardi (1723), Malpighi (1743), and Havers (1661) to think of bone in terms of a tissue rather than a physical construction. Each contributed to our understanding of bone's microstructure with regard to the presence of canals, lacunae and bone lamellae.

In 1757, Albinius discovered bone had its own specific blood supply. Then with the development of the cell theory (Scheiden & Schwann, 1838/9) and the demonstration of cells within bone (Goodsir, 1845), the foundation for experiments conducted by the likes of Humphery (1858), Gegenbaur (1864), and Ranvier (1873) had been laid down, thus, developing the background to our current understanding of bone as a living tissue with constituent cells. Apart from cells, the chemical nature of the matrix was also studied, one of the first to accomplish this was Verduc in 1643, but it was not until 1758 before Herissant discovered its dual mineral and organic components and a further decade before Gann (1769) revealed calcium phosphate as a constituent of the organic phase (as cited by Ricqlès *et al.*, 1991).

Advances in the understanding of skeletal development also began during the 18th century. Belchier (1736) and Duhamel (1739, 1742) helped decipher the role of the periosteum in radial growth, and the role of the epiphyses in longitudinal growth was established by Hales (1731) later refined by Hunter (1797).

To this date, there are a number of unanswered questions regarding bone as a tissue and as an organ. Our quest for knowledge stems from a need to understand the mechanisms underlying the pathogenesis of bone disease. Today the life expectancy of the general population has increased and associated with this is an increase in the number of diseases linked with the aging process, for example, osteoporosis, osteoarthritis, rheumatoid arthritis, and bone malignancies to name but a few.

Unfortunately, the methods used to study bone have not changed much over the last century. *In vivo* work, involving the use of animals and humans, has the potential to allow us to gain insight into the development, growth and fracture repair of bone. It has the advantages of demonstrating experimental effects on the body as a whole.
However, by today animal experimentation has become a political issue making it increasingly difficult to conduct such research and in order to be granted a licence rigorous assessment has to be conducted. There is a need to pursue alternative technologies in order to further our understanding.

Another means to study bone is through tissue culture. Tissue culture is concerned with the study of cells, tissues and organs maintained or grown *in vitro* for more than 24 hours. It was initiated as early as 1902 by Leob in Germany. By today the term "tissue culture" has become the predominant generic term used for all types of culture. There are three main branches summarised below: -

i) Cell culture – the growth of cells no longer organised into tissues *in vitro*, where cells are harvested from tissue either mechanically or through enzyme digestion and propagated in a cell suspension or attached to a surface as a monolayer.

ii) Tissue culture – the maintenance of tissue fragments *in vitro*, not necessarily preserving tissue architecture.

iii) Organ culture – the maintenance or growth of tissue, or organs (in whole or in part) *in vitro*, which may allow differentiation and preservation of architecture and function.

The introduction of cell culture in 1907 by Harrison and 1912 by Alexis Carrel allowed cell culture to develop into the common practice of today. Carrel first introduced the flask culture technique in 1923 and was able to culture cells *in vitro* for long periods only through the strict use of aseptic techniques. Unfortunately, the problem of microbial contamination slowed its development in the scientific world. In the 1940's, after the discovery of antibiotics, cell culture became a more feasible technique. Cell culture work was further aided by the fact the enzyme trypsin had been discovered in 1916, though not commonly used until the 1950's, which allowed cells to be removed from the flasks and subcultured once they became confluent. One of the first people to culture bone cells in this manner was Peck *et al.*, in 1964.

Advantages of using cell culture include the great number of molecular and biochemical tools currently available and the fact that experimental replicates can be virtually identical, reducing the need for statistical analysis of variance thus, making quantification easier. There are, however, limitations to cell culture. Cells often suffer from loss of phenotypic characteristics, a process known as phenotypic modulation or drift (Freshney, 2000), which may be due to dissociation of cells from their 3D geometry and their propagation on a 2D substrate. There are several factors that affect cell differentiation and cell proliferation such as serum, Ca^{2+} ions, and cell-matrix interactions and these require regulation. It is also necessary to control the nutritional and hormonal environment as well as cell density. The dynamic properties of cell culture are, therefore, difficult to control *in vitro* and it is also difficult to recreate the appropriate cell interaction found *in*

vivo, thus many people prefer to abandon serial propagation in favour of structural integrity of the original tissue.

Organ culture of bone tissue was pioneered by Dame Honour Fell in the 1920's (Strangeways and Fell, 1926; Fell and Robinson, 1929). The aim of organ culture was to retain and preserve the original structure and function of the tissue in question with regard to structural relationships of one cell type to others of the same or different lineage. Organ culture is advantageous in the fact that it is possible to observe changes in living tissue directly by watching and photographing the explants under the microscope. The greatest advantage of using organ culture to analyse skeletal tissue is that the technique allows the direct effects of experimental agents on cartilage and bone to be studied in the absence of the many complicating factors, which usually obscure this *in vivo*. However, the mere fact that those systemic factors are absent makes results difficult to extrapolate to the *in vivo* situation. Other limitations include costly, complicated, labour intensive experiments, the analysis of which mainly relies on histological observations. They cannot be used so well with biochemical and molecular techniques as it is difficult to attribute biochemical pathways to the specific cell type and sample variation makes comparisons between samples problematic. Cultures usually have a short life span, as they undergo central necrosis due to vascular occlusion and rate-limiting mass transfer. Unfortunately, once the organ has been explanted it loses the function of the vascular system. This loss has implications in limiting the size of organ that can be harvested, since cells now depend on diffusion of nutrients and metabolites as well as for the removal of waste. Most organ cultures do not grow, or if they do, proliferation is often limited to the outer cell layer, mitosis occurs around the periphery while necrosis occurs in the centre of explants (Freshney 2000). On the other hand, many researchers used unphysiological oxygen partial pressure, which may have affected the maintenance of the tissue.

One fundamental limitation to organ and cell culture, with regard to skeletal tissue is the lack of mechanical stimulation in the form of physiological loading. Without load, bone is believed to have a net increase in resorption, as is seen in patients after prolonged bed rest (Vico *et al.*, 1987) or astronauts in zero gravity (Spengler *et al.*, 1983).

The aim of this thesis is to validate a novel culture system to enable cancellous bone explants to be cultured *ex vivo*, in a mechanically relevant environment, allowing researchers to use this tool to give us insight in our quest to fully understand the skeleton which has eluded us for so many decades thus, overcoming the limitations experienced

during organ and cell culture and without the cost and ethical issues associated with *in vivo* experimentation.

The introduction to this thesis covers the form and function of the skeleton, its architecture and cell types as well as the role of mechanical stimulation. This introduction is followed by a detailed description of the Zetos culture system, its potential and previous works.

The second chapter, "Model Systems", takes a closer look at the cancellous bone models used during these studies (ovine, bovine and human) with specific regard to bone density and cell types, analysed by radiography, maceration, scanning electron microscopy (SEM), microcomputer tomography (microCT) and histology.

Cell viability is the topic covered in the third chapter. A number of potential stains and labels were analysed with the regard for detecting dead and living cells simultaneously.

The fourth chapter deals with constituents synthesised by bone cells. Bone matrix synthesis was followed by the use of fluorochrome labelling within the culture system as well as immunohistochemical staining of specific bone marker proteins of embedded culture samples (osteocalcin, osteonectin, osteopontin, bone sialoprotein alkaline phosphatase and procollagen type I). The use of tritiated glycine was used to demonstrate protein synthesis within the 3D structure of the bone cores allowing active cells to be localised and the area of dead tissue to be quantified.

Finally, a general discussion combines the results obtained throughout this project allowing the *pros* and cons of this culture system to be considered.

1.a.i. Form and Function

The human body contains 206 bones (Figure 1.a1.).

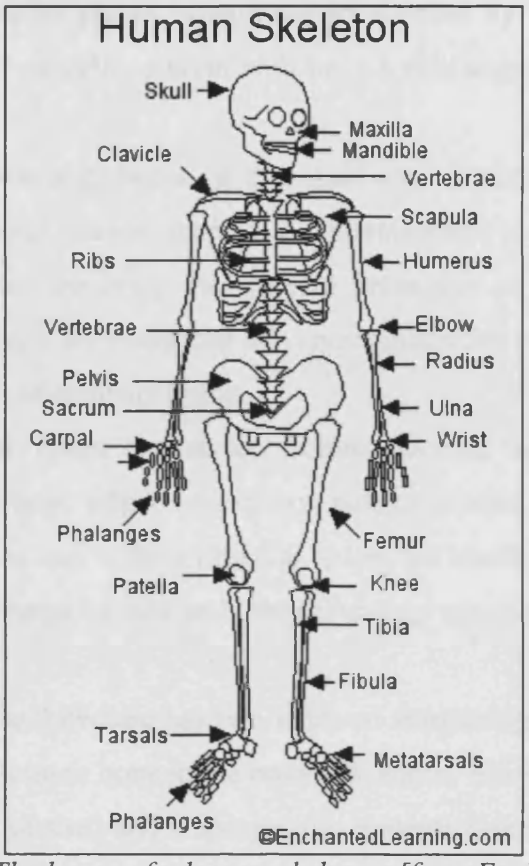

Figure 1.a.1. *The bones of a human skeleton. [from Enchanted Learning.com]*

These bones can be divided into four classes: Long, Short, Flat and Irregular (Warwick and Williams, 1973).

The **long bones** (e.g. clavicle, humerus, radius, ulna, femur, tibia, fibula, metacarpal and metatarsal bones, and the phalanges) are found in the limbs where they form a system of levers with the function of sustaining the weight of the body and to aid in locomotion. The structure of the long bone is usually depicted as a shaft and two extremities. The shaft is a hollow cylinder that forms the medullary canal. The wall of the shaft is composed of dense compact bone, thick in the middle but thinner at the extremities. The extremities are expanded and are articulated. Internally, the extremities are composed of spongy tissue with only a thin covering of compact tissue. The long bones themselves are not straight, but curved, providing greater strength to the bone as does their tubular structure.

The **short bones** (e.g. carpus and tarsus) are found in regions where strength and compactness are required, with slight and limited motion. Usually, these bones are divided into a number of smaller pieces often attached together by ligaments. These bones are composed entirely of cancellous bone with only a thin segment of compact bone at the periphery.

The **flat bones** (e.g. bones of the skull and shoulder blade, occipital, parietal, frontal, nasal, lachrymal, vomer, scapula, os innominatum, sternum, ribs and patella) are found around areas of the body that require protection or broad surfaces for muscle attachment. These bones are composed of various quantities of cancellous tissue enclosed within two thin layers of compact tissue.

The irregular bones (vertebrae, sacrum, coccyx, temporal, sphenoid, ethmoid, malar, superior maxillary, inferior maxillary, palate, inferior turbinated, and hyoid) also known as mixed bones due to their irregular shape, are similar in composition to the long bones with external compact tissue and internal spongy cancellous tissue.

Bone's basic architecture has two kinds of morphology. It is possible to see from figure 1.a.2. that the longest bone in the body, the femur, when cut open, has a dense outer layer forming a kind of shell and a sponge-like contents forming the interior. These types of bone are called cortical and cancellous bone respectively.

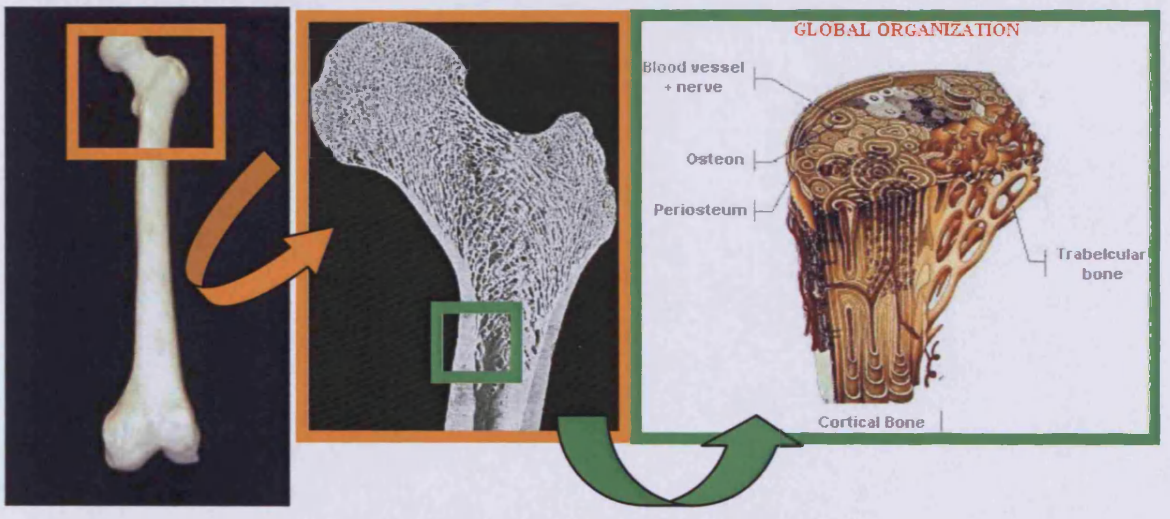

Figure 1.a.2. *The human femur, a cross-section through the frontal plane of a dried proximal end plus microstructure of compact and cancellous bone tissue within is depicted in both transverse and longitudinal section. [Adapted from Warwick and Williams, 1973]*

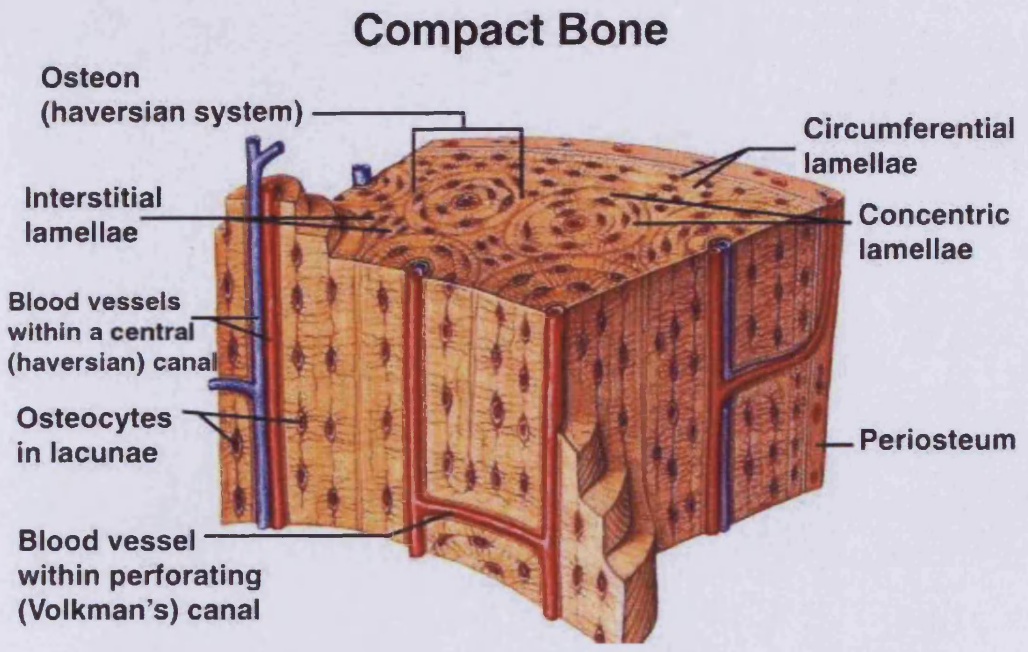

Figure 1.a.3. *The microarchitecture of cortical bone tissue [http://academic.wsc.edu/faculty/jatodd1/351/ch4outline.html]*

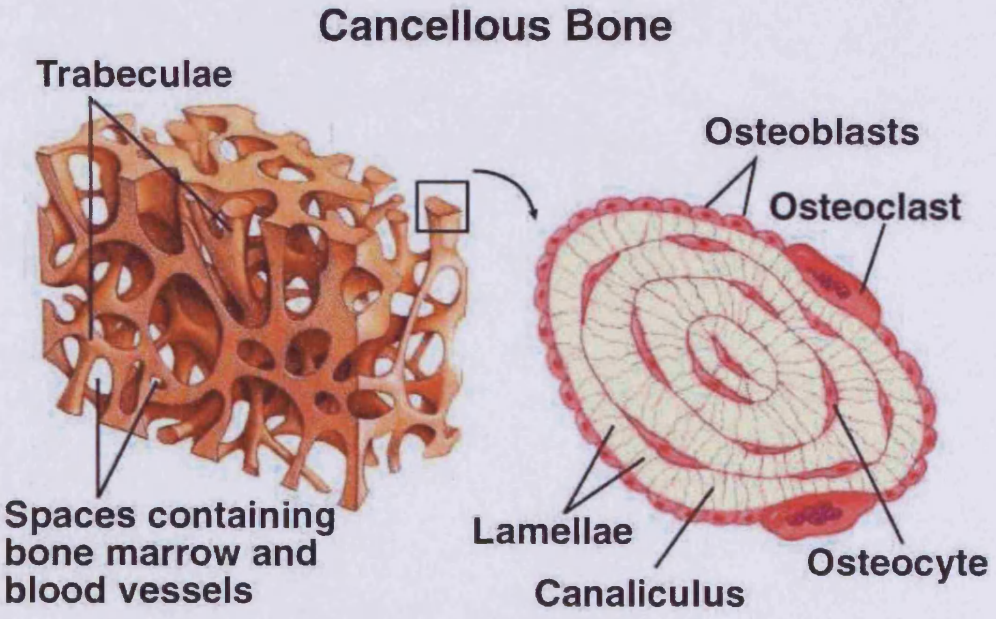

Figure 1.a.4. *The microarchitecture of cancellous bone tissue* [http://academic.wsc.edu/faculty/jatodd1/351/ch4outline.html]

Cortical bone (also known as compact bone) usually forms the outer wall of all bones. Its function is mainly supportive and protective (Fig.1.a.2). Cortical bone is dense and solid making 80% of the skeletal mass in the adult human skeleton (Fig.1.a.3). **Cancellous bone** (also known as spongy bone or trabecular bone) is found on the inner parts of bones and makes up the remaining 20% of mass (see Figure 1.a.2.). The main function of cancellous tissue is to serve as a reservoir for ions, especially calcium, regulating uptake and release of these ions to meet the body's requirements. In bones of weight bearing function, trabecular pattern is arranged to provide maximum resistance to physical stresses to which the bone is normally subjected. Differences between cortical and cancellous bone are both structural and functional. Individual bones vary in the distribution of cortical and cancellous bone, for example, the ulna is composed of 92% cortical bone and 8% cancellous bone, while a typical vertebra consists of 62% cortical and 38% cancellous bone (Jee, 2001). In addition to function, these bone types differ in their development, architecture, proximity to the bone marrow, blood supply, rapidity of turnover time, and magnitude of age-dependent changes and fractures (Fig.1.a.5)

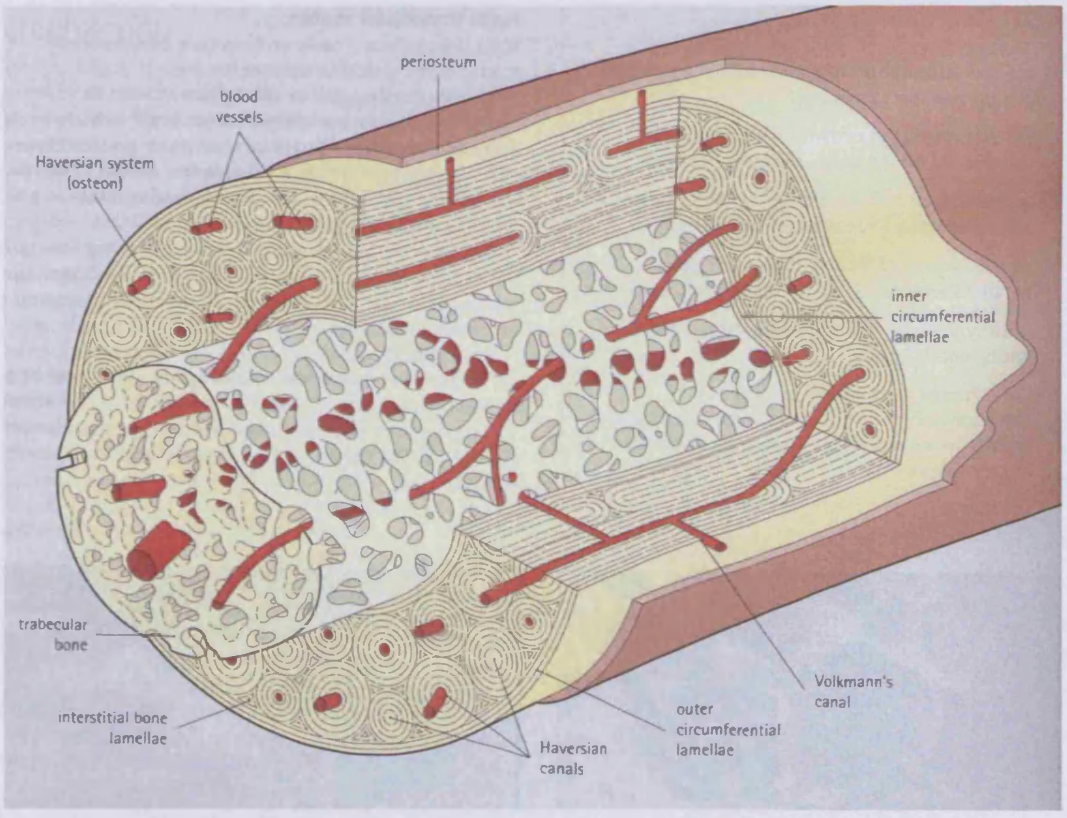

Figure 1.a.5. *A bone is composed of two different tissues, compact bone and cancellous bone. [Adapted from Stevens & Lowe 1997]*

Two thirds of cortical bone consists of concentric rings of lamella surrounding a longitudinally orientated vascular channel that forms a structural unit known as an osteon or a Haversian system (Fig.1.a.3). A typical osteon is 200-250 μm in diameter (Stevens & Lowe 1997). The outer border of the osteon is composed of a mineralised matrix known as a cement line which is 1-2 μm thick and devoid of collagen fibers. Cement lines are either irregular and scalloped (reversal lines) or smooth (arrest lines). Between osteons are small angular fragments of what were formely Harversian systems, now regarded as interstitial lamellae. Circumferential lamellae extend uninterrupted around part, or all, of the circumference of the bone, internally and externally. Both the interstitial lamellae and circumferential lamellae make up the remaining third of cortical bone. Cancellous bone consists of spicules or trabeculae, with a plate-like or rod-like configurations, that are also composed of hemi-osteon shaped crescents and interstitial lamellae (Fig.1.a.4). Trabecular packets usually have a radius of 600 μm, 50 μm thick and 1mm long, which are held together by cement lines (Jee, 2001).

Both cortical and cancellous bone contain small cavities, known as lacunae, which house a special type of cell, an osteocyte. The lacunae also contain cavities or channels, known as canaliculi. Long processes from the osteocytes fill these channels which enables the cells to communicate with other cells through gap junctions.

Cortical bone and cancellous bone are arranged in one of two types, woven or lamellar. **Woven bone** is usually present during embryogenesis or during fracture healing. Woven bone consists of a matrix of interwoven coarse collagen fibers with randomly distributed osteocytes within. Osteoblasts secret the bone matrix from one side, it is laid down directly with no need for free bone surfaces. Mineralisation is rapid and diffuse without clear seams and without relation to collagen fibers. The matrix is unorganised due to the speed of its deposition and mechanically weak. It is usually resorbed and replaced by a more organised lamellar bone. In human long bones, woven bone is replaced by lamellar bone between 2-3 years. **Lamellar bone** is formed during apposition to existing surfaces. It is secreted from one side of the osteoblast giving rise to a matrix that resembles plywood in the fact it is made up of a number of layers, approximately 3-7 μm thick, that contain collagen that run in the same direction. Adjacent layers differ in fiber axis, as much as 90°, thus giving a distinct banded pattern when viewed under polarised light. Virtually all bone in adult tissue is lamellar bone, which is regarded as being mechanically strong (Jee, 2001).

The bone matrix is a composite material which consists of collagen, noncollagenous proteins, mineral, lipids and water. Typically 65% is mineral and 35% is made up of organic matrix, cells and water. Of the organic matrix 90% is composed of collagen and the remaining 5-8 % of various noncollagenous proteins. The most abundant noncollagenous proteins are osteocalcin, osteonectin, osteopontin, and bone sialoprotein. It is the organic phase that is responsible for bone's compliancy, while it is the mineral that gives bone its strength and rigidity. The mineral, calcium and phosphate in the form of hydroxyapatite [$Ca_{10}(PO_4)_6(OH)_2$], is in the form of small crystals in the shape of needles, plates and rods located within the collagen molecules. The hydroxyapatite itself is not pure and contains other constituents incorporated into the crystal lattice or onto the crystal surface, such as carbonate, citrate, magnesium, fluoride, silica, and strontium (Jee, 2001).

The bone surface, apart from articulated surfaces, and at the junctions of tendons and ligaments, is usually coated with a fibrous membrane called the periosteum. It is through this skin that the bone is permeated by nerves, lymph, and blood vessels. The periosteum itself is composed of two layers. The outer layer is formed mainly of connective tissue, while the inner layer (cambium layer) consists of osteoblasts and their precursors of undifferentiated cells. The periosteum has the potential to form bone and cartilage during growth and fracture healing (Stevens & Lowe 1997).

Bone growth, modelling and remodelling is dependent on the vascular system, not only for oxygen and nutrients, but also for waste removal and a source of precursor cells. Preosteoclasts in the bone marrow leave through capillaries and travel with the blood circulation to required locations. Due to the importance of blood vessels in facilitating the transport of cells and metabolites it is believed that no bone cell is further than 200 μm away from functioning vessels.

Not much is known regarding the nerve supply of bone. Harversian canals, periosteum and medullary vessels are innervated, with poor myelinated nerve fibers present within the Haversian canals (Jee, 2001). A better understanding of this field will further improve bone regeneration.

1.a.ii. Embryogenesis

During the development of the human embryo it is possible to observe the advancement of the bony skeleton as early as the eighth week of gestation. Prior to this time, the outlines of bone tissue are present in the form of hyaline cartilage or condensed mesenchyme. It is, therefore, possible to say that a soft tissue model appears first and is gradually converted into hard osseous tissue by the development of osteogenesis (*Warwick and Williams, 1973*), thus, primary bone formation requires condensation of mesenchyme. Figure 1.a.6. shows the distribution of ossification within a nine-week old human foetus. The cartilaginous model is unstained (white) whereas the bone produced at the primary ossification centres has taken up the stain alizarin and is shown in red.

Figure 1.a.6. *A nine-week old foetus stained with alizarin and cleared to show the distribution and character of the primary ossification centres. [Adapted from Warwick and Williams, 1973]*

Much of the osteogenesis occurs during embryonic life, but some bones do not appear until prenatal life, or even until well after birth (Warwick and Williams, 1973) continuing development until the tenth year of childhood. Two different kinds of ossification occur depending on bone type and location. Intramembranous ossification is associated with the development of flat bones, bones of the sense organs and facial skeleton and contributes to the cortical shafts in long bones. Endrochondral ossification forms most of the cancellous bone, base of the skull, vertebral column, pelvis, and extremities.

Intramembranous Ossification

Intramembranous bone formation is achieved by the direct transformation of mesenchymal cells into osteoblasts (Karaplis, 2002). This process is preceded by fibro-cellular membrane formation rather than a cartilaginous one. Spindle shaped mesenchyme cells proliferate and condense around a profuse capillary network, a point regarded as the centre of ossification. These cells enlarge, develop abundant rough endoplasmic reticulum and produce a fine meshwork of collagen fibers and an associated amorphous ground substance giving the earliest sign of bone production. Stimulated by this activity the mesenchymal cells become either polygonal, roughly cuboidal, or low columnar over the surface of the secreted matrix. These cells are now termed osteoblasts. They begin to extrude bone matrix (osteoid) into small islands or spicules within the extracellular space which in turn becomes calcified (Warwick and Williams, 1973). The osteoid is arranged in a haphazard way and is so called the primary spongiosa. As more and more osteoid is produced, the matrix becomes condensed with some osteoblasts becoming trapped in their own secretions to form osteocytes, cells embedded within the calcified bone matrix. Further generations of osteoblasts form on the trabecular surfaces by transformation of adjacent vascular mesenchymal cells. As this procedure continues, the trabeculae thicken and the vascular spaces narrow. Remodelling begins instantly by combined osteoblast and osteoclast activity to form a network of trabecular bone. Bone marrow of the haemopoietic kind develops from the mesenchymal cells and fills the empty spaces (Stevens and Lowe, 1997). Further development is associated with increased bone formation on the outer and inner surfaces to form complete flattened plates of bone. During compact bone formation, the thickening of trabeculae and thinning of vessels continue. Collagen is secreted in a more organised fashion forming parallel and longitudinal bundles forming concentric sequential rows around a central vascular canal. This type of bone is termed primary osteons or a typical Haversian system (Jee, 2001). Over time, this type of bone is eroded and replaced by generations of lamellar bone known as secondary osteons. Concurrently, mesenchyme surrounding the compact bone condenses as a fibro-vascular tissue around the edges and surfaces giving rise to the periosteum. The molecular mechanism behind this type of bone formation is yet to be fully defined, though it is known to involve complex signalling molecules regulated by growth factors and transcription factors (Karaplis, 2002).

Endochondral Ossification

Bones that grow through endochondral ossification replace a cartilaginous model with newly formed bone (Karaplis, 2002). Hyaline cartilage rods are formed from a mass of immature mesenchymal tissue giving rise to a structure the approximate shape of the future bone surrounded by condensed mesenchyme or perichondrium (spindle-shaped mesenchymal cells, chondroblasts and some osteoprogenitor cells). For example, a typical long bone would include a shaft (diaphysis) with club-shaped expansions (epiphyses). A primary ossification centre begins when cartilage cells within the shaft of the bone enlarge and accumulate glycogen, and the matrix thins. These cells continue to enlarge until they die leaving their empty enlarged lacunae behind. The underlying matrix becomes calcified and the cells transform to osteoblasts laying down bone matrix (Warwick and Williams, 1973). Following the same mechanism as with intramembranous ossification a "periosteal collar" is formed (Fig. 1.a.7.). This development of bone tissue expands from the shaft to the extremities. Concomitantly, the chondrocytes within the cartilage model multiply increasing its length and breadth. Vascular channels from the periosteum invade the periosteal collar. Accompanying cells divide and form osteoblasts and osteoclasts. Chondroclasts erode into the calcified cartilage forming the medullary cavity and the spaces become filled with bone marrow and the calcified cartilage becomes covered with osteoblasts which lay down osteoid, as woven bone in the primary spongiosa (Jee, 2001). The spicules in the primary spongiosa are composed of mosaic pieces of calcified cores surrounded by woven bone tissue. These processes cause the diaphysis of the bone to increase in diameter. Remodelling of these surfaces produces a network of trabecular bone which occupies the core of the diaphysis and merges with the denser compact bone of the peripheral bone collar. Woven bone is replaced by lamellar bone forming the secondary spongiosa. Some bones develop from a single ossification centre, such as the carpus and tarsus, though most bones develop from several separate foci (Warwick and Williams, 1973). A second ossification centre usually forms towards the bone extremities near the time of birth. However, these centres do not replace all of the cartilage. Long bones continue to grow throughout childhood and into adolescence.

Endochondral ossification permits bone elongation and thickening during foetal development and throughout childhood until the bone ceases to grow. Bone grows appositionally due to the non-expendable nature of the mineralised tissue. Thus, most of bone's activities occur on the surfaces. There are two main surfaces in bone, the periosteal

and endosteal. The endosteal surfaces can be subdivided into intracortical, endocortical, and trabecular surfaces. At any given time the bone surfaces can be in one of three states; forming, resorbing or quiescent. Typically 6% of trabecular surfaces and 3% of cortical surfaces are in a formative state, while 1.2% of trabecular surfaces and 0.6% of cortical surfaces are being resorbed, leaving 92.8% of trabecular surfaces and 96.6% of cortical surfaces in a quiescent phase (Jee, 2001).

To enable bones to increase in length a junction of cartilage cells, known as the epiphyseal plate, remains separating the diaphysis and epiphysis. New cartilage is apposed to the ends of the diaphysis, which is then converted to cancellous tissue continuing until after puberty where the space once filled by the cartilaginous plate is filled with cancellous bone forming the metaphysis. Figure 1.a.8. depicts the process in greater detail. Cartilage on the epiphyseal side proliferates to form columns of chondrocytes embedded in a cartilaginous matrix. The most distal cells become enlarged and start to produce alkaline phosphatase (AlP). This enzyme aids the cells in calcifying the cartilaginous matrix. Osteoblasts lay down their organic matrix onto this calcified scaffold, which in turn becomes remodelled and incorporated into the diaphysis.

The circumference of the diaphysis increases through apposition of new bone on the outer surfaces of the cortical bone, while the inner surface undergoes resorption. This process also thickens the cortical bone allowing it to withstand the physical demands associated with body weight and physical activity. However, this is a complex process and does not only involve periosteal formation and endosteal resorption.

It is quite astonishing to note that, bone that formed from cartilage had been distinguished from bone that formed directly as far back as the seventeenth century by Spigelius (1631) and Bartholinius (1676). It was in 1770 when Portal suggested that the embryonic skeleton was first formed in cartilage and later formed in bone, and it was not untill a century and a half later that Müller demonstrated that the cartilage was actually replaced by bone and that the cartilage was destroyed in the process (cited by Hall, 1992).

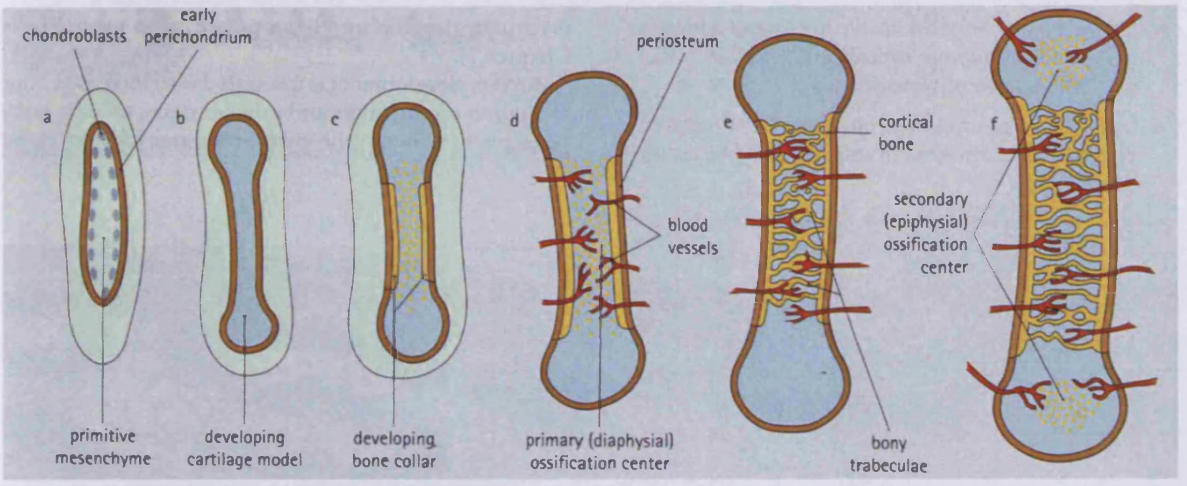

Figure 1.a.7. *Endochondral ossification. a) chondroblasts develop in primitive mesenchyme to form early perichondrium and cartilage scaffold. b) Cartilage rod assumes the shape of the bone. c) At the mid shaft of the diaphysis a bone collar forms through intamembranous ossification. d) Blood vessels grow through the periosteum and bone collar to establish primary ossification centre. e) Bony trabeculae develop to fill diaphysis and joins cortical bone of the collar. Epiphysis is still cartilaginous. f) Secondary ossification centres appear in the epiphysis close to birth.*
[Adapted from Stevens and Lowe, 1997]

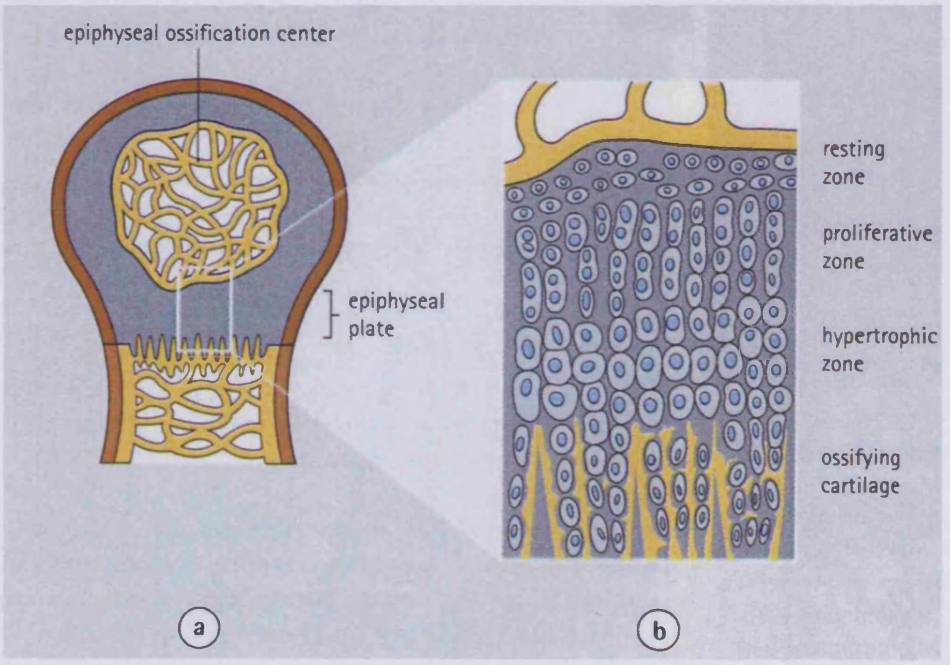

Figure 1.a.8. *a) Enlargement of the secondary ossification centre within the epiphyseal cartilage. b) Fine detail of the epiphyseal plate between secondary ossification centre and developing diaphyseal trabecular bone. Chondrocytes within the plate proliferate in column and, become hypertrophied as they deposit cartilage matrix. Matrix is mineralised before osteoblasts lay down osteoid on calcified model.*
[Adapted from Stevens and Lowe, 1997]

1.a.iii. Bone Cells

Bone is composed of four main cell types (see Figure 1.a.9.). Osteoblasts, osteoclasts and bone lining cells are present on the bone surface, while osteocytes are located within the mineralised bone matrix. Other cells are also present in the bone microenvironment, but a detailed description of these cells can be found in the introduction to chapter 2.

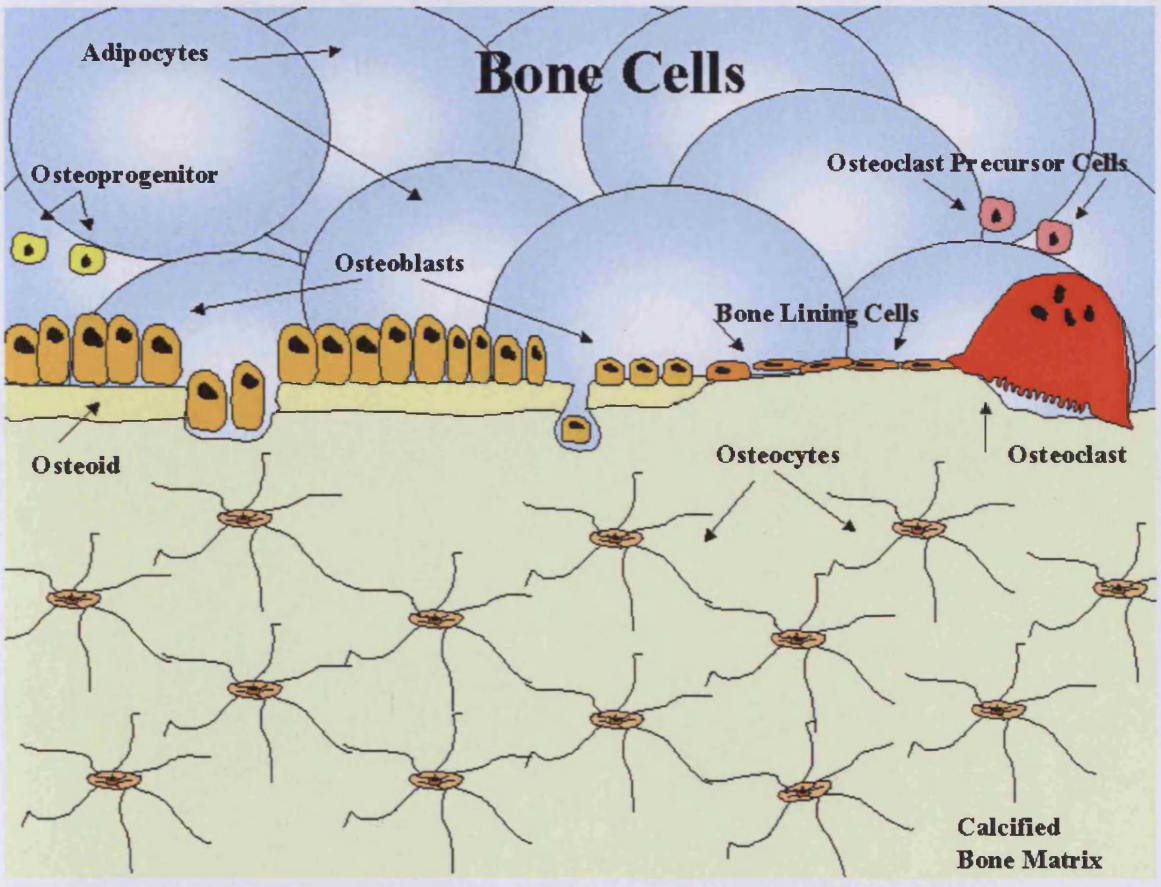

Figure 1.a.9 *The local microenvironment of bone cells, their origins and locations. [Adapted from Marks and Popoff, 1988]*

Osteoblasts, osteocytes and lining cells are closely related, and represent different stages in the maturation of a single cell type. The osteoblast linage is a subset in the developmental linage of other connective tissues such as muscle, fat and cartilage cells. The osteoblasts are derived from pre-osteoblasts which are unable to form bone yet, but are capable of dividing. The osteoclasts, on the other hand, are an extension of the monocyte cell lineage, part of the haematopoietic family that also includes all of the circulating blood cells (*Marks and Popoff, 1988*).

Bone Lining Cells

The bone lining cells are also known as resting osteoblasts as they are no longer actively forming bone. They are believed to be derived from osteoblasts that have become inactive or are precursor cells that have ceased activity. Little is known of their history. It is believed that they can become active again, though they may return to the stem cell/preosteoblast pool or may apoptose. They have a distinct morphological phenotype; flattened, elongated cells (1 μm thick and up to 12 μm long), within close proximity to the bone surface. They form a connective tissue barrier that separates mineralised bone and the soft tissue of the marrow. The cells lie on an osteoid layer 1 μm thick above the mineralised tissue known as endosteum. They have few cytoplasmic organelles, a flat nuclear profile and an attenuated cytoplasm. Adjacent lining cells as well as osteocytes communicate with each other via gap junctions. Their role in bone has not been fully defined. They are known to locate to areas that require resorption, they digest surface osteoid with neutral proteases before contracting and allowing osteoclasts access to the bone surface, and secrete factors which activate osteoclasts (see chapter 4). Their location and morphology allows them to serve as a ion barrier between fluids of the osteocyte/lacunar/canalicular system and the interstitial fluids. This may have a role in regulating fluxes of calcium and phosphate in bone fluid as well as controlling the microenvironment. The three-dimensional network of lining cells and osteocytes have been postulated to be able to sense stresses and strain placed upon the tissue and then influence bone's adaptive changes at the surface where new bone formation/resorption is possible. Hence, lining cells may be involved in homeostatic and restructuring processes that regulate bone mass and architecture.

Osteoblasts

It was Carl Gegenbauar who named the bone forming cells osteoblasts (Gegenbaur, 1864). Osteoblasts are the main cells responsible for synthesising the main constituents of the bone matrix and regulating its mineralisation. They also participate in bone resorption and in maintaining calcium and phosphate homeostasis. Active osteoblasts are polar and cuboidal in shape usually 15 – 30 μm thick, they rarely undergo mitosis (Owen, 1967). They have a distinct phenotype that is typical for a protein producing cell. They have a large nucleus, prominent Golgi apparatus and an abundance of rough endoplasmic reticulum. They secrete mainly collagen type I in a glycosaminoglycan gel containing

specific glycoproteins, and a number of noncollagenous proteins such as osteonectin, osteopontin, osteocalcin, and bone sialoprotein into a structure which is termed the osteoid seam. The osteoid seam is around 10 μm in width and adult human apposition rate is approximately 0.55 μm/day (Jee, 2001). The mechanism of calcification and the role of all the secreted components are not clearly defined nor well understood, but the enzyme AlP found in the cell membrane is believed to play a key role. Once bone formation is complete the osteoblasts are believed to either become inactive bone lining cells, osteocytes embedded within the bone matrix or apoptose.

Osteoblasts are derived from mesenchymal progenitors (stem cells), which are located near bone surfaces. These cells are believed to arise from local undifferentiated intraskeletal mesenchymal cells that are capable of mitosis, but the exact cell type that becomes osteoblast progenitor cells is unknown. Once a cell is committed to the osteoblast lineage, osteoblast precursor cells proliferate and then differentiate into preosteoblasts before becoming mature osteoblasts. Osteoblast differentiation is believed to be under the control of the transcription factor known as core-binding factor (CbFa1) and Runx-2. It performs a dominant and nonredundant role in osteoblast differentiation and controls bone formation after osteoblast differentiation is achieved.

Osteoblasts possess receptors on their surface for a number of bone agents, such as parathyroid hormone (PTH), parathyroid hormone-related protein (PTHrP), prostaglandins, vitamin D metabolites, gonadal and adrenal steroids, and certain cytokines and lymphokines.

Osteocytes

During bone formation some osteoblasts become surrounded in their own secretions and become what is known as osteocytes, embedded in the bone matrix within a cavity called a lacuna. This is thought to be arranged haphazardly, though they do have their long axis parallel to the collagen fibers around them (Holtrop, 1991). Osteocytes are the most abundant cell type in mature bone. There are approximately ten times more osteocytes than osteoblasts in mature human bone (Parfitt, 1991). Osteocytes are described as having a stellate shape and have lost much of the organelles associated with protein production, have decreased in size by approximately 30% (Holtrop, 1991), and have acquired long slender processes which permeate the matrix in channels called canaliculi. These processes enable the osteocytes to communicate with other osteocytes, osteoblasts

and bone lining cells through gap junctions (Doty 1981). Gap junctions are transmembrane channels composed of the protein connexin (types 26, 32, and 43), which connect the cytoplasm of two adjacent cells usually 2-4 nm in space. They permit small molecules and ions to pass through from one cell to another contributing to intracellular signalling. No microtubules are found in the cell processes, but bundles of microfilaments fill them (aid transport of small molecules).

Though osteocytes have little synthetic activity they may still remodel their local environment to prevent mineral precipitation onto the lacunar surfaces. Hypermineralisation of a lacunae is associated with the loss of osteocytes during aging. It is hypothesised that osteocytes secrete mineral binding proteins such as osteocalcin as they contain abundant mRNA. It is estimated that osteocytes have a life-span of 20-25 years (Parfitt, 1991) though many are removed prior to this.

Osteocytes are ideally situated to be able to sense changes in strain distribution and magnitudes and transducing this information to other bone cells at the surface. Thus, osteocytes are believed to influence modeling and remodeling. They are also believed to have a homeostatic role in regulating an appropriate local ionic milieu in conjunction with the bone lining cells as well as sensing microdamage in the surrounding matrix and triggering appropriate adaptive responses.

Osteoclasts

It was Albrecht Kölliker who named the bone resorbing cells osteoclasts (Kölliker, 1873). Osteoclasts are usually located in scalloped concavities known as Howship's lacunae (Howship, 1817). Their role is to resorb bone. Osteoclasts are derived form the mononuclear/phagocytic lineage of haematopoietic marrow, specifically the granulocyte/macrophage colony-forming unit (GM-CFU) (see intro chapter 2). Osteoclasts are multinucleated giant cells with 1-50 nuclei and are 20-100 μm in diameter. A unique characteristic of the osteoclasts is a striated appearance on its surface adjacent to the bone's surface. This structure is known as a ruffled border and is an area of extensive membrane enfolding. Around the ruffled border is an area devoid of organelles known as the clear zone. It does, however, contain many actin filaments that allow the osteoclast to adhere to the bone surface forming a permeable seal keeping the microenvironment under the cell optimal for bone resorption. From the ruffled border numerous products are secreted in order to break down the bone matrix. Osteoclasts are capable of solubilising both the

mineral and organic component of the bone matrix. Once the cell is attached to the bone surface it secretes H^+ ions which maintain the pH at around 3.5 causing the bone mineral to dissolve. The H^+ ions are generated by the action of carbonic anhydrase on H_2CO_3 and are released from the cell through an electrogenic ATPase proton pump. The H+ ions neutralise the negatively charged OH^- ions and PO_4^{3-} ions which are present in the bone mineral hydroxyapatite. To remove the organic phase from the matrix the cell secretes proteolytic enzymes such as metalloproteinases, cystiene-proteinases, phosphatase, and cathepsin K (Fig.1.a.10).

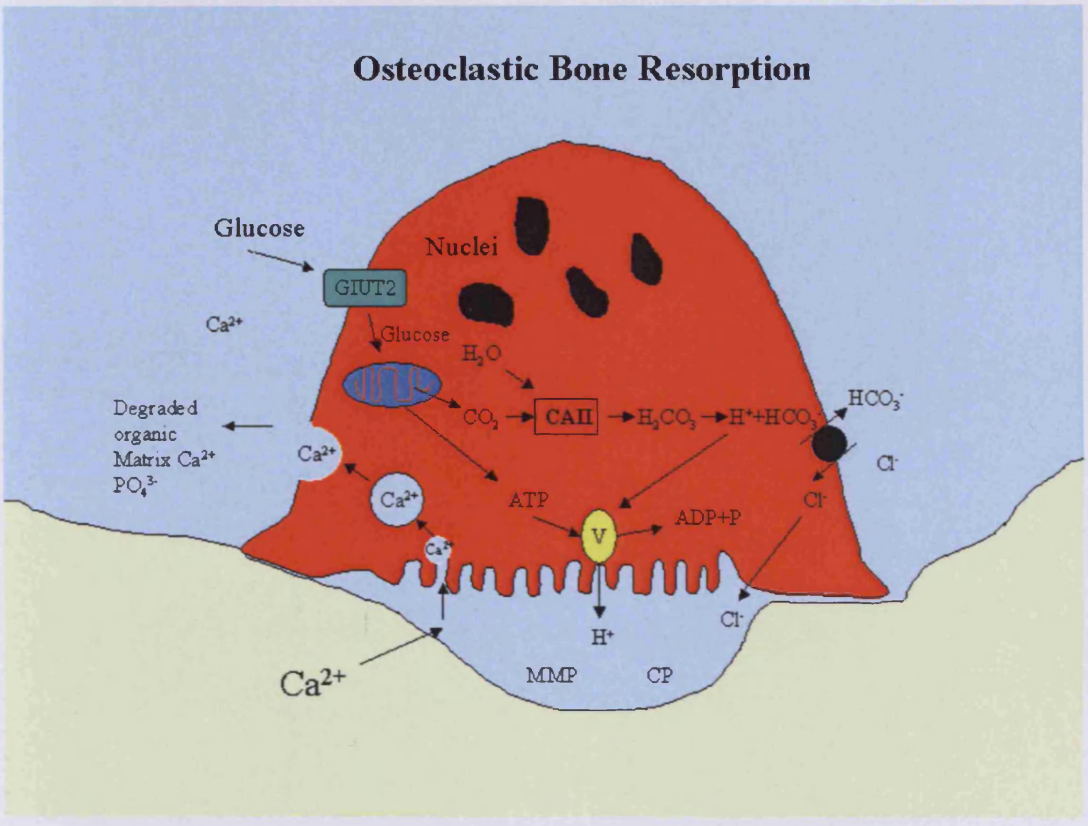

Figure 1.a.10. *The action of osteoclasts during bone resorption. Mature osteoclasts form a tight seal over the bone surface and resorb bone by secreting hydrochloric acid and proteolytic enzymes through the "ruffled border" into a space beneath the osteoclast (Howship's lacuna). The hydrochloric acid secreted by osteoclasts dissolves hydroxyapatite and allows proteolytic enzymes (mainly Cathepsin K and matrix metalloproteinases MMP) to degrade collagen and other matrix proteins. Carbonic anhydrase II (CAII) catalyses formation of hydrogen ions within osteoclasts. Glucose binds to glucose transporter 2 (GLUT2) to provide energy to the cell. [Adapted from Marks and Popoff, 1988]*

1.a.iv. The Effect of Mechanical Stimulation

Researchers believe that strain (change in bone length relative to original length) is the controlling agent in bone growth and growth related adaptation. By adjusting bone architecture in relation to strain, cells are believed to participate in a feedback loop - a method known as mechanotransduction. Mechanotransduction is a process that recognises and responds to mechanical stimuli. For strain to influence remodelling it must elicit some kind of chemical response within a strain sensitive population. Once this response has been achieved the mechanically-engineered chemical message must compete for a response with all other biochemical messages that cells are exposed to. Duncan and Turner (1995) proposed four different mechanisms for the transduction of a mechanical stimulus to an intracellular biochemical signal. One, the extracellular matrix (ECM) interacts with the cytoskeletal and nuclear matrix through intergrins. Two, via stretched activated cation channels. Three, through G-protein dependent pathways, and finally, by linkage between the cytoskeleton and phospholipase C pathways and cAMP. Osteocytes are thought to be the key cell that is influenced by the amount and distribution of strain, and in turn they influence modelling and remodelling of surrounding tissue through chemical methods or cell-cell interactions. Osteocytes are well placed for this role and are known to communicate with each other and cells on bone surfaces.

The general form of each bone, its attachments, and its anatomical arrangements are genetically determined, and will develop in the absence of functional influences. However, the particular structural architecture (mass, girth, cortical thickness, curvature, density and arrangement of trabeculae) depends on the presence of continual functional load-bearing. Therefore, normal skeletal architecture, peak bone mass, or mass at any time are not genetically determined, but rather a reflection of modelling and remodelling history which was influenced by mechanical load-bearing. In the absence of normal loading, those normal architectural features do not develop. Thus, girth, curvature cortical thickness, trabecular number thickness and connectivity are all deficient in bones that develop in the absence of functional loading. Lack of functional loading has different consequences depending on stage of bone development. If loading is reduced during growth, bone formation is stimulated less, and the bone does not develop to its normal size. If loading is reduced in adulthood, resorption is increased, and bone tissue is lost usually by thinning of the cortex from the endosteum and porosis within the cortex. This phenomenon can be

observed in example, patients after prolonged bed rest / immobilisation (Vico *et al.*, 1987) or astronauts in zero gravity (Spenger *et al.*, 1983).

Loading of bone is believed to be the cause of cell deformation, which in turn is believed to be the stimulus for functional adaptation (Roux, 1885). Wolf's Law can explain functional adaptation, which is a relationship between form and function (Wolff 1870, 1892). It is believed that what governs the shape and mass of each bone is the requirement to resist the effects of mechanical forces (Currey, 1984; Lanyon, 1992; Rubin & Lanyon, 1985). It is unknown how deformation stimulates bone cells, nor the mechanisms that take place.

A number of responses have been observed to occur after mechanical loading. One of the first responses to take place in a bone cell that has been cyclically loaded *in vitro* is a rise in intracellular calcium. Jones *et al.*, (1991) deformed osteoblast-like cells with a single stretch cycle and saw a rise in intracellular calcium within 90-100 msec. Following this Ca rise, a number of different secondary messenger pathways are believed to be activated. Binderman *et al.*, (1988) and Jones *et al.*, (1991) observed phospholipase A2 activation between 5 sec to 15 min post-loading, while Jones *et al.*, (1991) also saw protein kinase C activation approximately 90 sec post-loading. One of the earliest responses observed *in vivo* and with explant culture was a change in matrix orientation, which occurred at approximately 6 min post-loading (Skerry *et al.*, 1988; 1990) as well as an increase in the activity of glucose 6-phosphate dehydrogenase (G6PD) (Skerry *et al.*, 1989). Between 5-15 min post-loading, a rise in prostaglandin (PG) E2 expression was observed in cell culture and explant culture (Somjen *et al.*, 1980; Rawlinson *et al.*, 1991) and after 15 min an increase in nitric oxide (NO) production (Pitsillides *et al.*, 1995). A number of studies have observed early response gene activation (c-fos, TGFβ, IGF-1, type I collagen) between 1-18 hours post stimulation in all three types of culture (cell, explant, and *in vivo*) (Zaman *et al.*, 1992; Raab Cullen *et al.*, 1994; Inaoka *et al.*, 1995;). Many other responses have been observed in the *in vivo* situation including cell proliferation (8-24 h post loading Lanyon, 1987; Dallas *et al.*, 1993), matrix synthesis (48 h post loading Pead *et al.*, 1988), increase in protein mRNA expression (72 h post loading) (Lean *et al.*, 1995), and finally the formation of mineralised matrix (96 h post loading Pead *et al.*, 1988; Lanyon 1992; Torrance et al., 1994; Hillam and Skerry 1995).

Frost introduced the mechanostat hypothesis in 1987. It was developed to explain the biological mechanism that affects skeletal mass and architecture to an individual's

normal physical activity. Thus, explaining how mechanical usage regulates bone mass and architecture. It was hypothesised that the biological mechanism would act similar to a thermostat, turning on in response to an error and off in its absence.

The concept of the mechanostat relies on there being a set point of effective strain present within bone tissue. Overloading of this set point would cause an increase in bone mass and strength, where as an underload would cause bone mass to diminish. Thus, the set point elicits a range of strain that causes no response. This hypothesis can be explained in figure 1.a. 11.

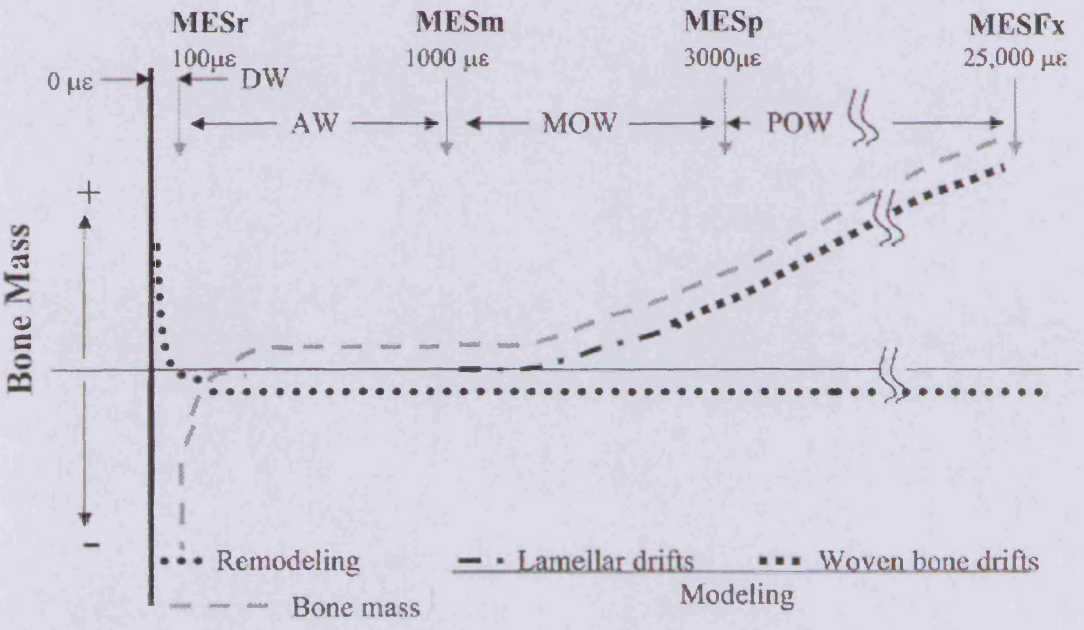

Figure 1.a.11. *The mechanostat hypothesis summarised in terms of different thresholds. MES =minimum effective strain, r = remodeling, m = modeling, p = pathology, Fx = fracture, με = microstrain,* DW = disuse window, AW = adapted window, *MOW =mild overload window, POW = pathologicoverload window [Adapted from Jee, 2001]*

This mechanism also works in a feed-back loop system limiting the amount of response exerted to a given stimulus. Carter (1981, 1982) and Cowin (1984) also suggested a number of effective strains that might elicit responses in bone tissue.

Frost (1999) also developed the Utah Paradigm of skeletal physiology to explain how nonmechanical agents (hormones, calcium, vitamin D, cytokines, genes etc.) affect changes in bone mass and strength. These nonmechanical agents are known to influence

mechanical regulation and have a direct effect on bone cells independent of mechanical stimuli. Both are equally important to skeletal development.

A number of hypothesises have been postulated on the mechanisms of mechanotransduction. It has been suggested that deformation of bone affects cells by means of fluid flow through the interstices of the cortex though the exact mechanism is unclear (Piekarski and Munro, 1977; Knothe-Tate, 1998). Deformation of bone induces electrical potentials. The "piezoelectric effect in bone" (Fukada and Yasuda 1975) hypothesised that these electric potentials had a role in bone remodelling and repair.

Streaming potentials (SP's) arise when electrolytes within the interstitial fluid are forced through small channels, causing some charges to bind to the channel wall, thus leaving the fluid in a charge of opposite sign. These SP's are important because of their potential role in transducing mechanical stimulus into a biological response during the adaptive remodelling and maintenance of bone (Weinbaum, 1994). However, it is now believed that streaming potentials and interstitial fluid flow may be one and the same phenomenon (Knothe-Tate, 2001).

To this date, it is unclear which of these mechanisms are responsible for mechanotransduction, nor if they all contribute in their unique way to skeletal adaptation. The effect of mechanical stimulation has been studied for several decades through a vast number of techniques both *in vivo* and *in vitro*.

Several animal and human models have been developed to evaluate the effect of altering mechanical loading of bone tissue. Osteotomy models (Lanyon *et al.*, 1979; Goodship *et al.*, 1979; Burr *et al.*, 1989; Rubin *et al.*, 1984); casting and bandaging models (Jaworski *et al.*, 1980; and Li *et al.*, 1990); neurectomy (Goshi *et al.*, 1989; and Weinreb *et al.*, 1989); models for generalised bone loss (Spengler *et al.*, 1983); models of increased bone loading (Smith *et al.*, 1984; Barlet *et al.*, 1995; Thorsten *et al.*, 1996; Ayalon *et al.*, 1987; Woo *et al.*, 1991; Raab *et al.*, 1991); models affecting physiological activity (Jones *et al.*, 1977); and finally models that apply load through implants (Hert *et al.*, 1971; Churches *et al.*, 1982; Pead *et al.*, 1988) or non-invasive applied loads (Turner *et al.*, 1991; and Torrance *et al.*, 1994).

There are several limitations regarding this kind of work, namely that the surgery initiated can have an affect on bone formation rather than the article in question. In order to reduce false results, sham surgeries are performed simultaneously to control for the effects of the preparation method. It is also crucial to control the animal or human use of the tissue

in question i.e. exercise history prior, during and post experiment; hormonal status and nutrition; and be aware of the effect of season, diet, and illness.

In vitro loading experiments are usually performed on tissue explants or extracted cells. One of the commonest failings with such experiments is the lack of controlled loading. Most applied loads are neither measured nor calibrated. Loading conditions often used do not mimic that of the *in vivo* situation. For example, applying loads of 3000 microstrain to rat calvarial cells, which usually receive less than 50 microstrain in the *in vivo* situation. Also explanted tissue cultured in this manner seems to suffer from disuse effects.

The effects of loading of single cells or cell monolayers are difficult to extrapolate to the *in vivo* situation due to the lack of 3D matrix. Deformation of cells through bending of culture substrate can cause a series of undesirable effects such as stimulation through fluid flow or shear stresses. It is also essential to measure all parameters as frequency rate, and magnitude of load will all affect cellular responses.

No method is free from flaws. To study the processes whereby skeletal tissue reacts to mechanical stresses, experimental systems are needed that allow direct measurement of cell proliferation, differentiation, and matrix metabolism under controlled loading conditions. A novel *ex vivo* mechanically loaded culture system for cancellous bone tissue was developed by David. B. Jones (since September 1996) to overcome the limitations discussed above for both cell culture and organ culture. Compression and force can be applied and measured with high precision (+/- 3%) (Jones *et al.*, 2003) thus allowing reproducible results to be obtained regarding amplitude, direction of load, loading frequency mimicking that of the *in vivo* situation. However, it should be born in mind that physiological loading of bone tissue is a highly complex factor.

The described system offers other advantages. The physiochemical environment (pH, temperature, osmotic pressure, and O_2/CO_2 tension) can be strictly controlled as with *in vitro*. This *ex vivo* bone chamber device allows observation of bone formation and resorption with online readings. On the whole this culture method is cheap, and avoids the legal, moral, and ethical issues regarding animal experimentation in the *in vivo* situation.

1.b. Zetos Culture System

The Zetos culture system was designed for long term, *ex vivo* culture of cancellous bone explants, though, it may also be adapted for possible future use with cartilage tissue (United States Patent 6th July, 1998, No.: US 6,171,812: Everett L. Smith, David Jones: Combined perfusion and mechanical loading system for explanted bone. United States Patent 19th March, 2002, No.: US 6,357,303 B2: Everett L. Smith, David Jones: Mechanical testing device.). The system consists of two main parts: a set of circumfusion chambers and a computer controlled loading device (Fig.1.b.1). Hence, the name Zetos stems from **Zeta** ζ the Greek symbol sometimes used for strain and **os** Greek for bone. The Zetos system is based on a similar system devised by El Haj *et al.*, (1990) for short term tissue culture of cancellous bone biopsies subjected to mechanical load. The aim in developing this "Zetos" system was to overcome limitations seen with a number of *in vivo* and *in vitro* loading experiments where accurate measurements of real-time force and deformation under dynamic loading were not achieved. The development of the engineering side of this system is reviewed by Jones *et al.*, (2003).

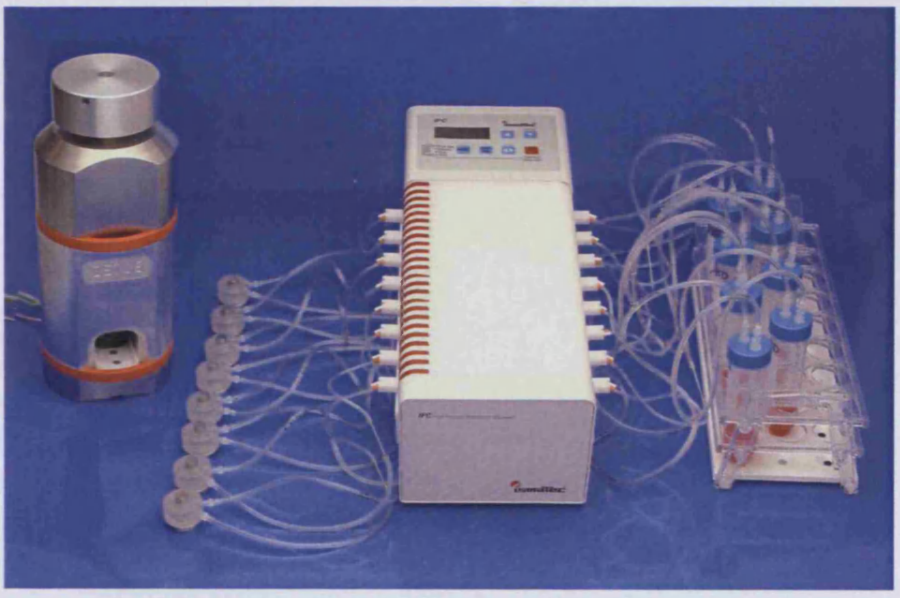

Figure 1.b.1. *The Zetos culture system which comprises of a loading device, and a set of culture chambers, each with their own media supply fed from a reservoir through Tygon tubing with the aid of an Ismatech pump.*

1.b.i. Components of the System

The Set up

The system is set up within a small room especially equipped to carry out such experiments. The room is small and unused for any other purpose, which limits the amount of people entering thus, reducing the possibility of microbial contamination. The walls of the room are covered with insulating tiles and there is a heater set to a thermostat to keep the room at 37°C. A fan in the roof keeps the temperature at the ceiling no greater than 38°C. Without this fan the temperature would exceed 60°C. There is a UV light attached to the wall to kill any micro-organisms in the air prior to making a media change. There is a table to set the system upon and adequate power supply to run the pumps. The door to the room has a glass pane running down the middle to allow the user to visualise the computer screen from inside the room. The computer unit and monitor along with the voltage amplifier are kept in an outside room free from the temperature and are linked to the loading device via an insulated connector (Fig.1.b.2). For accurate measurements of mechanical properties, bone specimens should be tested at 37°C (Turner and Burr, 1993).

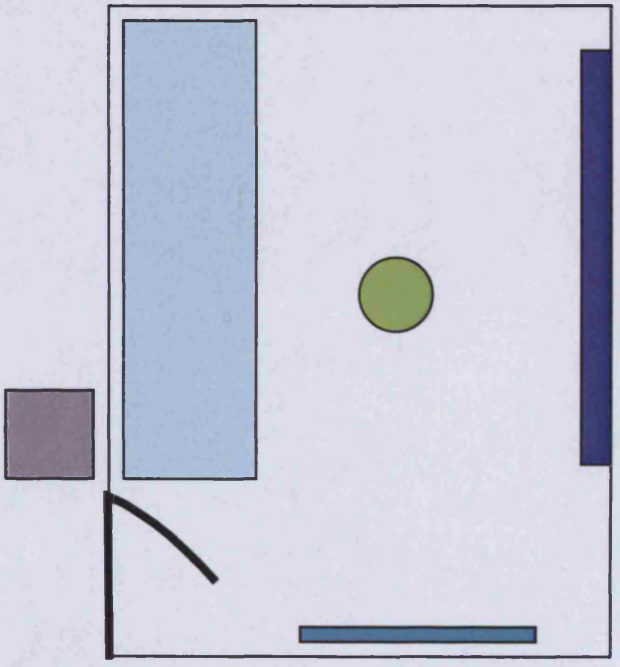

Figure 1.b.2. *Plan of the culture room. The light blue oblong represents the table, the green circle represents the fan, the dark blue oblong represents the UV light, the turquoise oblong represents the heater. The door open inwards and is represented by a thick black line. The grey square represents the computer and voltage amplifier.*

The Culture Chambers

In order to keep bone explants (5 mm high and 10 mm in diameter) viable over a number of days, housing is required which allows the bone cells to receive adequate nutrient and removal of waste products without disturbing its natural milieu. This housing must also allow adequate oxygen supply and keep the cells free from potential contamination. An innovative culture chamber was designed and constructed that allowed the bone explant to be bathed in nutrient media and physiologically loaded at the same time.

The chamber itself is constructed from polycarbonate with a stainless steel or titanium base plate and piston (Fig.1.b.3). At the bottom there is a black neoprene O-ring that helps seal the chamber to the base plate. On top the piston is inserted. The piston is used to transmit the force of loading onto the bone core within. Surrounding the piston is an X-ring. This X-ring also stops leakage of media but also allows for non parallelity of the bone core due to its X- like structure. There are also internal black neoprene gaskets which are responsible for keeping the media from flowing around the bone, but allowing it to bathe and cover the core thus, allowing diffusion to occur.

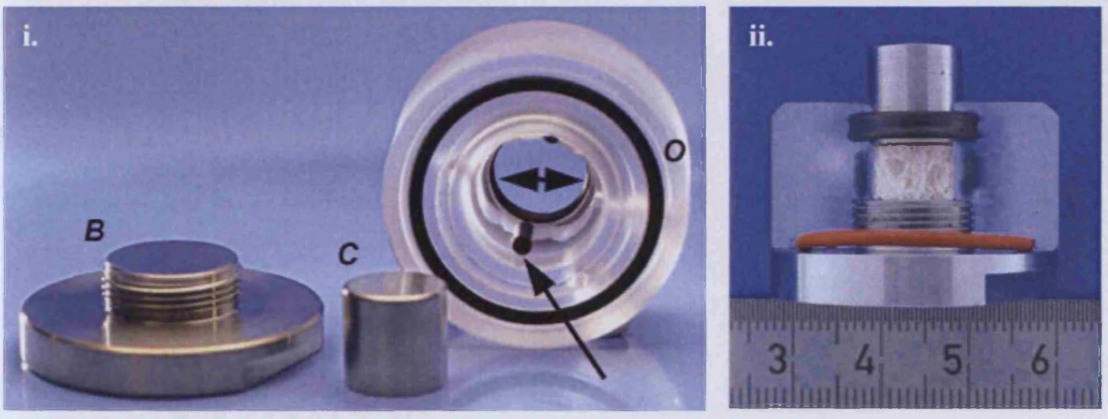

Figure 1.b.3. i) *Components of the chamber are displayed. The bone core (10 mm in diameter and 5 mm high) is situated within the polycarbonate chamber (O) though not present here, the base plate (B) is attached to the bottom of the chamber, while the piston (C) is inserted at the top. The X-ring is indicated by a double headed arrow, while the gaskets are indicated by a single headed arrow.* **ii)** A cross-section through *the assembled chamber can be seen complete with bone core [provided by David Jones]*

With a single Ismatech pump (IPC-ISM934) it is possible to have a maximum of 24 chambers in use at any given time. Though, it is possible to use 2 pumps simultaneously doubling the capacity of the system.

The Loading Device

One of the unique features of the Zetos culture system is the ability to apply a defined load to the culturing explant. This is achieved by inserting the culture chamber into the opening of the loading device (Fig.1.b.4.). The loading stack is composed of a stainless steel shell which surrounds a piezoelectric stack. The piezo stack is linked to a voltage amplifier which causes it to expand and contract. When a chamber is inserted into the loading device, the piezo stack is lowered onto the piston of the chamber, with approximately 5N of load given to ensure that all surfaces are in contact. Then, when the voltage is applied the force is displaced from the piston on to the bone core. In conjunction with a computer program, it is possible to apply a quantifiable force or displacement upon the bone core housed within the culture-loading chamber. A detailed review of the working, calibration and mechanics of the system can be seen by Jones *et al.*, 2003.

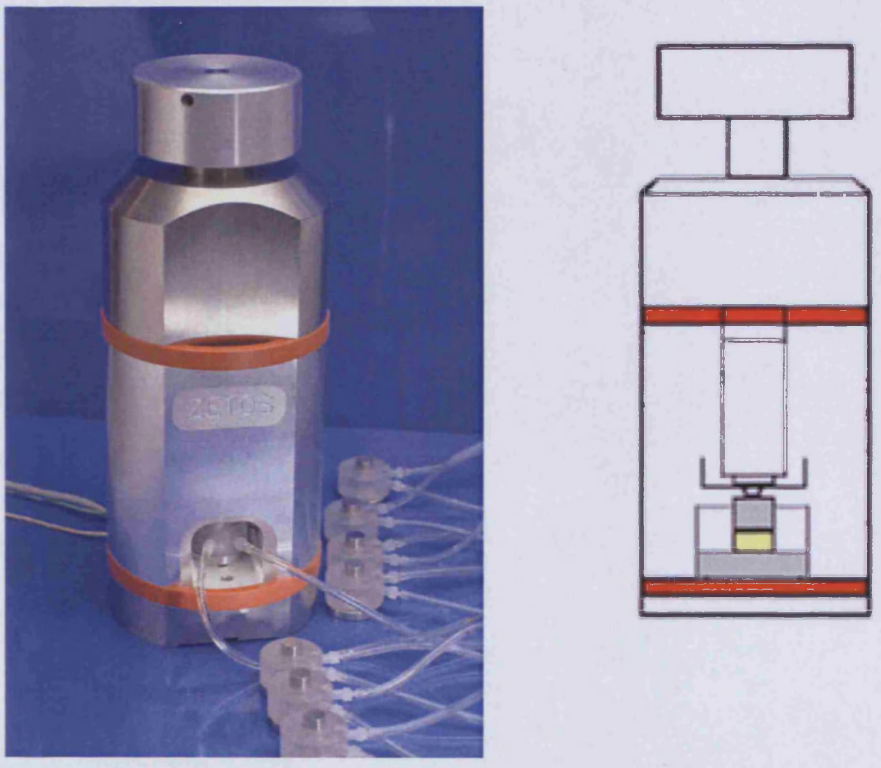

Figure 1.b.4. *The Zetos loading device applies physiological mechanical stimulation to cancellous bone explants housed within culture chambers. The schematic diagram depicts the chamber within the loading device where a piezo stack expands and contracts to dynamically load the bone tissue (yellow).*

The Computer Interface

The unique design of this system allows the bone explants to be stressed by unique user defined oscillation patterns. These can mimic walking, running jumping etc (Fig 1.b.5). It is also possible to set the desired amplitude of loading; this can be either in the form of min/max μm compression, mix/max volts or min/max Newtons. Repetition of loading frequencies can be set between 0.1 Hz to 50 Hz for a duration of any given period.

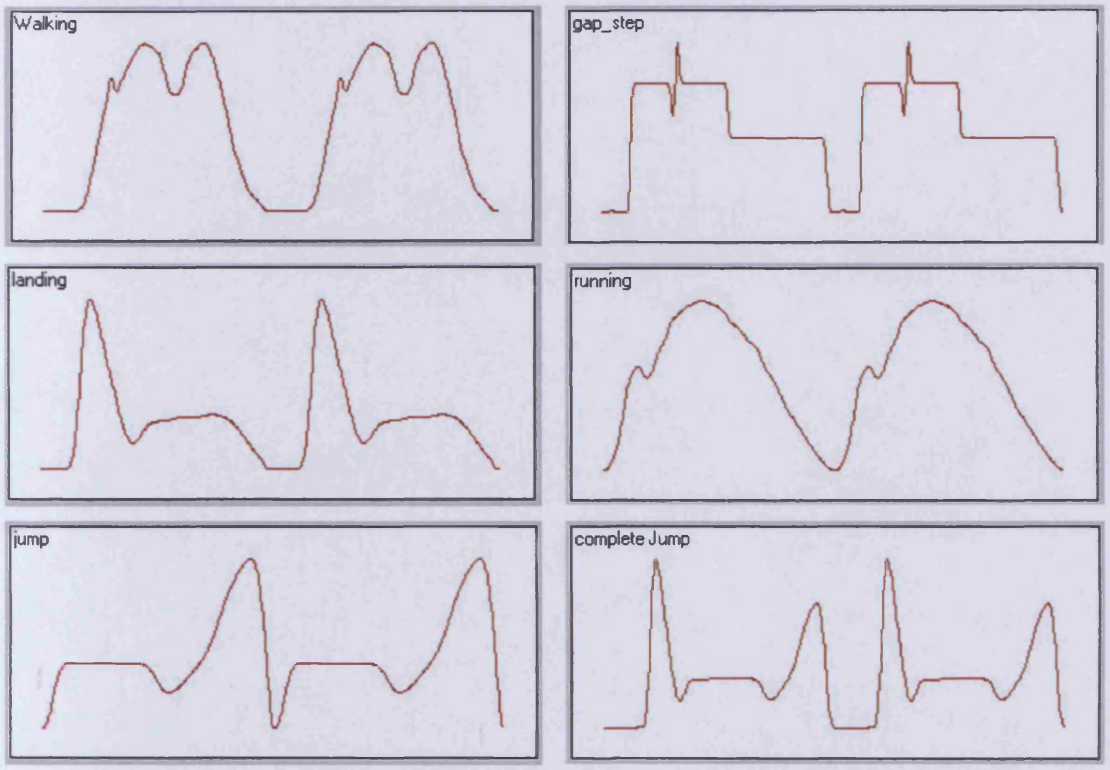

Figure 1.b.5. *Examples of different physiological waveforms that can be applied to cancellous bone cores cultured in the Zetos system.* [*Bröckmann, 2002*]

In our system cancellous bone cores were loaded daily under dynamic compression (Hert *et al.*, 1969; Rubin and Lanyon, 1985) for 300 cycles, at 1 Hz, with a complete jump (dual peak) waveform, giving a maximum and minimum compression of 20 μm and 5 μm respectively (Pead et al., 1988; and Boppart et al., 1998) to produce 4000 microstrain (Rubin and Lanyon, 1984 and 1985). Some of the samples remain unloaded as disuse controls. Though these samples did not receive stimulus through dynamic loading, they did however receive a 30s static load every four days. Prior to all loading, a preload $1/10^{th}$ of the ultimate force used was placed on each sample in order to get a more linear curve and enable a more accurate modulus to be calculated.

Once mechanical stimulation was complete, a quasi-static measurement was taken to plot the specimen's apparent stiffness - its Young's modulus over time (MPa). Measurement started at zero and increases to a preset maximum compression (usually 20 μm) in small incremental steps over a period of 30 s. Force and displacement were measured simultaneously. There was a slow release to avoid activating cells. The programme calculated the apparent Young's modulus (E) by linear regression with best linear fit within the selected interval (k) (Fig.1.b.6). The calculation uses cylindrical parameters radius (r) and height (h) for normalisation so that the extracted value is no longer dependent on the geometric dimensions of the body:

$$E = k \cdot \frac{h}{\pi r^2} \qquad (1)$$

Using a quasi-static measurement has the advantage of eliminating the nonlinearities of the system. This allows a value to be obtained which can be practically associated with the mechanical properties of other materials (Jones *et al.*, 2003).

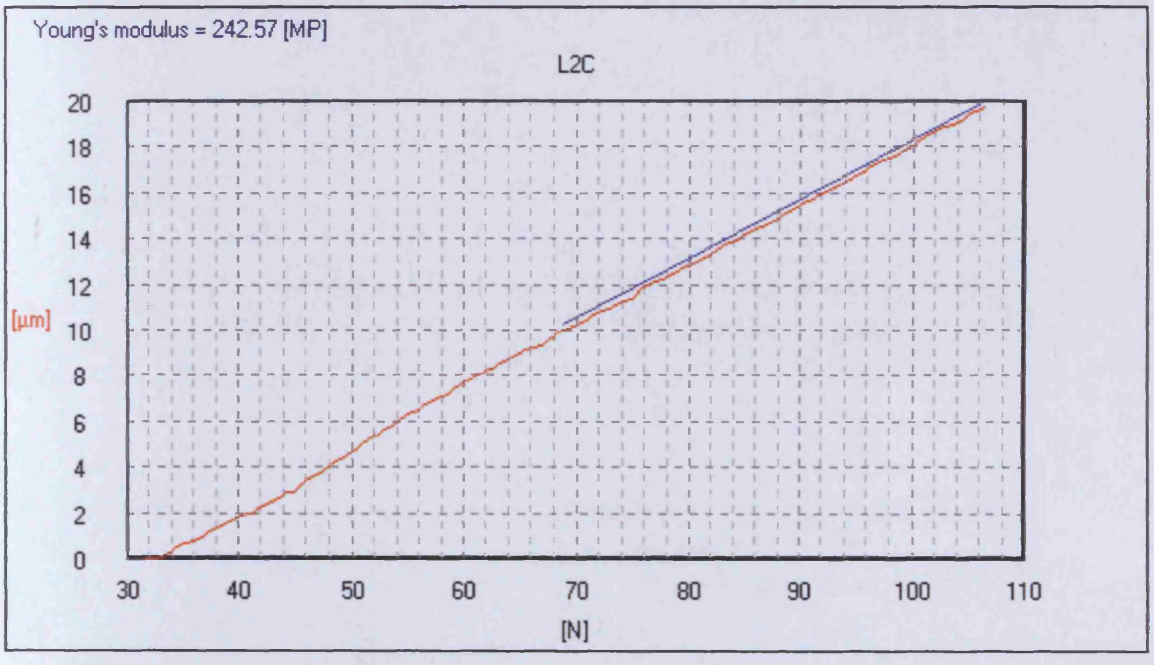

Figure 1.b.6. *Determining apparent Young's modulus from quasi static loading.*

The system allows the stiffness of the sample to be followed from the beginning of the experiment until the end. It is hypothesised that healthy tissue is in net bone formation and that this can be detected by a rise in sample stiffness due to the fact that compressive strength of bone is approximately proportional to the square of the apparent density, and

the compressive modulus is approximately proportional to the cube of the apparent density (Carter and Hayes, 1977). Unloaded samples mimic disuse and should decrease in stiffness due to net bone resorption. The static compression that these unloaded cores received every four days should not stimulate the cells (Lanyon and Rubin, 1984). Thus, online measurements can be compiled for each individual bone explant.

To accurately measure sample stiffness, the surface of the sample to be measured needs to be parallel, as only a perfect plan parallel body will follow Hook's law (though such a surface does not really exist) (Fig 1.b.7 image a). If the surfaces are not parallel then the effective area under load increases as the force increases, thus, a function of force over compression will be non-linear (Fig 1.b.7 image b). If the surfaces are parallel but rough, then the curve will be linear after a short initial non-linear phase (Fig 1.b.7 image c). However, there does remain an inaccuracy about the effective area, which may lead to an incorrect Young's modulus. In order to obtain precise results great care is needed in preparing the samples to be tested (Bröckmann, 2002).

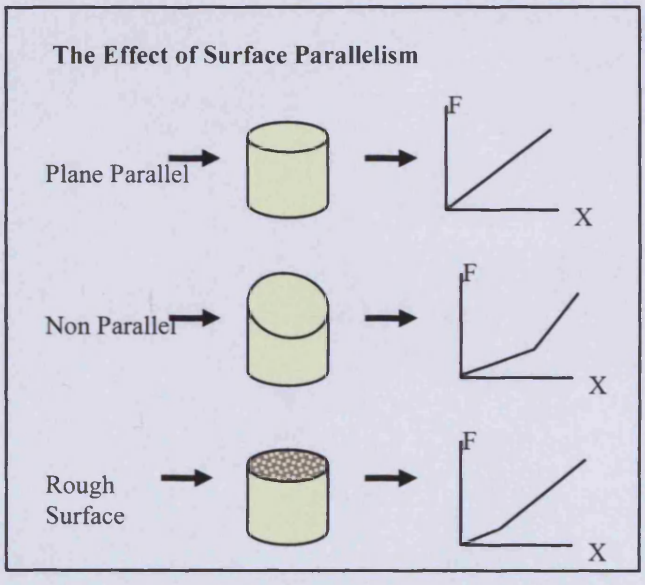

Figure 1.b.7. *Effect of samples surface and parallelism on the measure of Young's modulus.* [*Bröckmann, 2002*]

In order to help eliminate the problem of surface parallelism, it is important to bring all surfaces in contact with one another. To achieve this, a small preload is placed upon the chamber ~2.5 N prior to loading, thus the surface of the piezo actuator is in contact with the piston, which is in turn in contact with the bone core, the under side of the bone core is in contact with the base plate and this in turn in contact with the bottom of the loading device. Data is usually recorded daily for the duration of the experiment, though

the readings for the first day are excluded due to artefacts caused by nonparalelity and surface roughness.

It is not possible to determine absolute stiffness of the samples due to the machining of the sample core biopsies. Trabecular struts that were once supported are now cut and this leads to a platen effect, where bone faces are misaligned with the loading platen (piston and base plate). Thus, data obtained from this system cannot be extrapolated to the whole bone tissue.

Cutting of the cores causes an "end effect" due to the machining of the specimen (Fig.1.b.8.). Trabeculae at the boundary of the core are unsupported, thus strain is greater at the edge of the specimen than in the middle. Due to an elevated strain at the end of the specimen in contact with the loading platen an overestimation of strain can cause an underestimation of Young's modulus (Odgaard *et al.*, 1989).

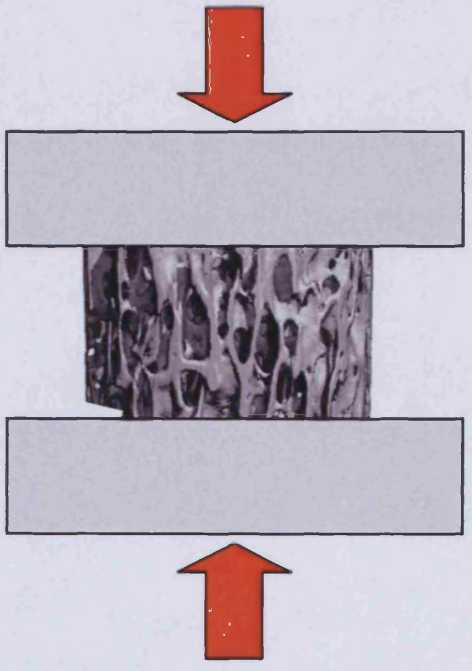

Figure 1.b.8. *Effect of loading non parallel cancellous bone cylinders. Higher stresses at the right edge of the specimen leading to inaccurate results. [Adapted from Turner and Burr, 1993]*

The use of bone cements would greatly reduce this effect, by stabilising the cut ends, but due to the culture constraints of this system it would greatly affect the diffusion of medium from reaching bone cells within the explant and equally removal of waste from the explant.

1.b.ii. Harvesting and maintaining the explants

Cancellous bone explants were obtained either from ovine distal femora (3-6 years of age), bovine distal metacarpals (4 months of age) or human femoral heads (70-81 years of age) as these contained the largest volume of cancellous tissue. No animal was directly sacrificed for these studies. One of the main aims of this system is to reduce the amount of animal experimentation conducted for bone research. This entire study was funded by 3R Research Foundation Switzerland, who promote: -

Reducing the number of experimental animals per experiment.

Refining experiments on animals by minimising animal discomfort.

Replacing animal experiments by methods not requiring experimental animals.

Once excised, the skin, muscle, and tissue were removed from the ovine and bovine bone under sterile conditions, in a laminar flow hood (Fig.1.b.8.i). The human femoral head, provided by the hospital, contained no soft tissue. The bone tissue was cut into 9 mm thick sections with an Exakt 300 band saw (Fig1.b.8.ii). Cores, 10 mm in diameter, were drilled from the sections with a specially designed diamond tipped, hollow, flutted, drill (Fig1.b.8.iii). The cores were cut parallel with a Leica annular saw, to the height of 5 mm (Fig.1.b.8.iv). This was necessary to reduce the platen effect during compressive loading. Bone cores (5 mm high and 10 mm in diameter) were chosen for the amount of cells present, approximately 2 million, for biochemical analysis (Burger, 2001). Also, the minimum size core required for biomechanical testing would be 7.5 mm diameter and 6.5 mm high (Linde, Hvid and Madsen, 1992). Any smaller and the mechanics are effected due to the disintegration of the cut surface in contact with the loading platen. Throughout all cutting procedures, the bone was irrigated with sterile 0.9% NaCl at 4°C to remove bone debris, and to limit the amount of damage caused to the cells by heat, as well as stopping the bone from drying out. The environment where cutting was performed was sterilised as completely as possible. All surfaces and machines were cleaned with 70% ethanol and antibacterial fluids 24 h and 12 h before the cutting process. Sterile hats, gloves masks and gowns were worn at all times. After harvesting the bone, cores required washing in order to remove as much bone dust and debris as possible, which may be clogging soft tissue or pores. In order to achieve this end, the bone cores were placed in separate labelled 15 ml centrifuge tubes and covered with 12ml of Hank's Balanced Salt Solution (HBSS). The centrifuge tubes were then placed onto an overhead shaker (Heidolph REAX 2), in a 37°C room, set at the slowest speed and left to rotate for 10

minutes. The samples were removed by means of sterile forceps and placed into a fresh set of centrifuge tubes and repeated in total for 3 x 10 minutes. It was not possible to aspirate the media from the tubes as the bone debris blocks the glass pipette, or remains at the bottom of the tube. Once completed, the bone cores were washed for a final time with HBSS containing a powerful combination of antibiotics and antimycotics (100,000 IU Penicillin/Streptomycin, 500 μg fungizone and 150 mg gentamicin per litre). This step was crucial for removing any possible contaminants that encountered the tissue during the harvest procedure. Again, the bone cores were placed into a fresh set of centrifuge tubes and covered with 12 ml of the medium, they were set in the overhead shaker and left to wash for 30 min before being inserted into the chambers (Fig. 1.b.9.i-iv). The assembled system was placed into a 37°C room and left to settle for 24 hours (Fig.1.b.9.v). Throughout the experiment, all bone cores were perfused with Dulbecco's Modified Eagle Medium (DMEM) media containing 10% Foetal Calf Serum (FCS) (Smith *et al.*, 2000) (same batch used throughout), 10 mM HEPES, 2 mM L-glutamine, 10 mg L-ascorbic acid-2-phosphate, 5 mM β-glycerophosphate disodiumhydrate, 4 mM $NaHCO_3$ and 50,000 IU Penicillin/Streptomycin per litre, at pH 7.25 at a flow rate of 100 μl/min. Media was changed every day, pH readings were taken and samples (2 ml each) were collected for biological analysis. The flow rate was chosen to supply adequate oxygen without disrupting or mechanically activating bone and marrow cells with shear forces (Koller, 2004; personal communication with David Jones).

Controls

At least two bone cores were fixed in 70% ethanol as soon as harvest procedure was complete in order to act as positive controls. Bone explants cultured in static culture, submerged in media, are known to suffer from necrosis therefore, some bone cores were cultured submerged in 10 ml media in 50 ml centrifuge tubes to act as positive controls for necrosis as well as a negative control for explant culture. Explants placed in the Zetos culture chambers, but not dynamically loaded, were used as a negative control for loading stimulation (these cores received a static load for 30 s every 4 days). In each of these culture environments, dead tissue (purposely killed explants) was used to permit negative controls for all viability and synthesis experiments. Explants were "killed" by placing the cores after washing into an incubator (56°C) for 6 to 8 hours. This was enough to kill the cells, but did not alter the mechanical properties of the tissue.

Sharkey *et al.*, (1991) found that cancellous bone cores 8 mm in diameter and 7 mm high incubated at 60°C for 20h displayed an increase of 47% in yield strain and a decrease of 25% in elastic modulus, while bone cores incubated at 56°C for 20 h showed no alterations in mechanical behaviour. Temperatures above 80°C caused significant reductions in mechanical strength (Von Garrel and Knaepler, 1993). Chemical fixation and freezing were considered as a means to kill the cells, however, they are also known to cause changes in the tissue's mechanical properties (Martin and Sharkey, 2001).

During freezing ice crystals form in the extracellular water and then within the cells, due to an osmotic gradient that is produce across the membrane, thus causing the cells to become hypertonic and dehydrated. During thawing damaged cells may lyse and release enzymes capable of degrading the tissues. However, the freeze-thawing itself does not seem to cause change in the tissues mechanical properties (Linde and Sorensen, 1993).

Linde and Sorensen, (1993) also looked at the effects storing cancellous bone explants in 70% ethanol at 10°C would have on the mechanical properties. Though they saw a decrease in elastic modulus this was not regarded as significant.

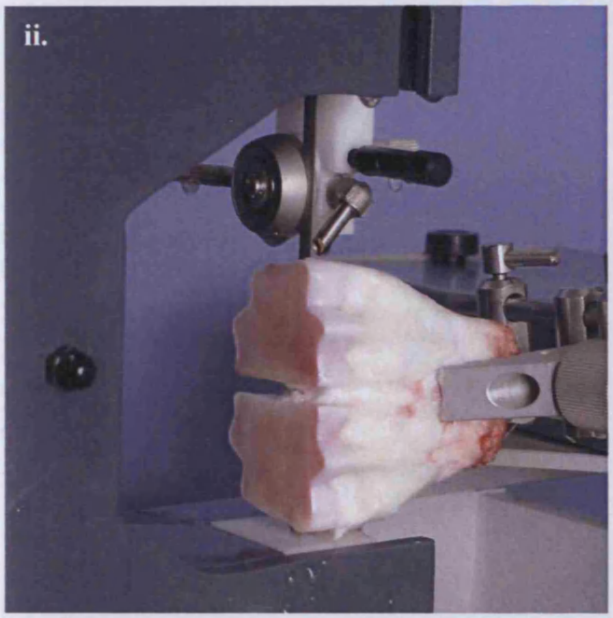

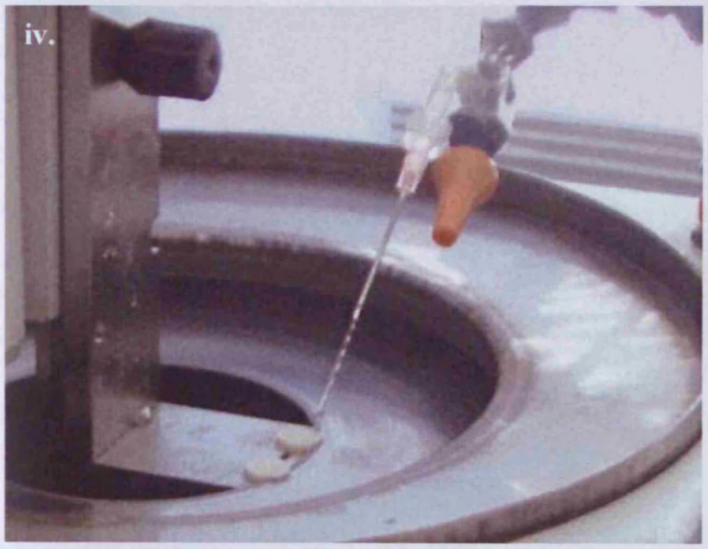

Figure 1.b.8. i.) *Soft tissue removal from ovine femur under sterile conditions in a laminar flow hood.* **ii.)** *Bone slabs cut from bovine metacarpal with the Exakt band saw.* **iii)** *Cores bored from bovine metacarpal with a hollow diamond rimmed drill bit.* **iv)***Bone cores cut parallel with an annular saw to provide surface parallelism to the cylinders. During all cutting procedures 0.9% NaCl was used for irrigation.*

Figure 1.b.9. i) *Insertion of bone cores into the housing chambers under sterile conditions of laminar flow hood.* **ii)** *The cancellous bone core fits into the centre of the polycarbonate midpiece within the two black neoprene gaskets.* **iii)** *The stainless steel or titanium base pate is screwed on tight and sealed by the O-ring to prevent leakage.* **iv)** *The corresponding piston is inserted into the top of the chamber to sit on top of the bone core cushioned by the X-ring.* **v)** *The chambers are connected to a media reservoir and linked to a pump and left to settle for 24 h at 37℃ before loading begins.*

1.b.iii. Previous Studies

The Zetos culture system has been under development since September 1996. To date a number of studies have been conducted, mostly at Phillips University, Marburg, under the guidance of Professor David B. Jones and Professor Everett Smith.

One of the most significant findings was recently published in the Journal of Cell Biology by Clarke *et al.*, (2003). They detected viable bone marrow within the cancellous explants that constitutively produced platelets after four days of *ex vivo* culture. However, no functional assessment of the cells were possible due to the small number of particles, nonetheless transmission electron microscope (TEM) of cell morphology were consistent with healthy blood platelets.

Jones *et al.*, (2001) have cultured bone explants for 72 days and observed a rise in prostaglandin E2 and insulin-like growth factor 1 after a few hours of loading at 0.4% compression. Bone formations rates of 0.6 μm a day were estimated, comparable to that of the *in vivo* situation. Osteocyte viability was estimated to be around 95% after 21 days of loaded culture, less than 60% in unloaded explants and 100% inactive in heat treated negative controls, evaluated in a double blind study with the viability stain MTT ((3-4,5-dimethylthiazol-2-yl)-2,5-diphenyl tetrazolium bromide).

Martens *et al.*, (2000) observed no significant change in the bone or bone marrow histology after 60 days of culture. Nerve cells had disappeared but cells were still present even within blood vessels. Whereas, David *et al.*, (2003), observed that bone formation parameters (osteoid parameters, mineral apposition rate and bone formation rate) were increased in loaded versus unloaded explants by 48%, 30% and 48%, respectively.

Human tissue cultured in the Zetos system for 49 days, analysed with fluorescent triple label (calcein day 19 & 32, and alizarin day 44), demonstrated 79% of surfaces labelled with alizarin and 15% of surfaces stained with the double label (calcein and alizarin). The mineral apposition rate (MAR) was determined to average 0.48 μm a day (Smith *et al.*, 2003). This study suggested that osteoclasts and osteoblasts were still viable nearly 50 days post-harvest.

To our understanding there is no other similar long-term loaded culture system for cancellous bone tissue. Though, a similar method to the Zetos culture system was currently being developed at the AO Research Institute for cortical bone tissue without loading (Ahrens *et al.*, 2003). This system was not fully validated.

The advantage of this system is its ability to allow dynamic events such as, bone formation, bone resorption and tissue morphogenesis to be studied. Tissue fluids flowing through the lacunar-canalicular system of the calcified matrix are believed to help supply nutrients (and remove waste) to the cells *in vivo*. This flow is driven by blood pressure and mechanical loading in the *in vivo* situation (Bronk *et al.*, 1993; Knothe *et al.*, 1998). This is the possible key for maintaining cancellous bone explants viable *ex vivo*. Postneonatal bone organ cultures usually suffer from necrosis due to lack of oxygen and the difficulty associated with supplying nutrient through diffusion alone. The mineralized ECM poses a substantial barrier to diffusion, thus embryonic, foetal, or neonatal tissues are usually more successful. It is hypothesised that mechanical stimulation provided by the Zetos culture system may continue to allow the fluid (tissue culture media) to flow through the lacunar-canalicular system maintaining cell viability. In recent years it has been discovered that it is imperative to sustain the osteocytes within the ECM viable as these cells are believed to be the mechanosensors within the tissue controlling both bone resorption and formation in its turn. Osteocytes are believed to apoptose in response to microdamage within the tissue (Verborgt *et al.*, 2000) or due to hormonal deprivation (Tomkinson *et al.*, 1997). This is a trigger for osteoclast recruitment and subsequent resorption. Later, the resorption pit is filled with fresh organic matrix by the osteoblasts, which then mineralises it to reform the existing tissue. This complex cellular microenvironment and the effect of nonosseous tissues on bone cells can not be duplicated *in vitro*. Thus, a thorough validation of this system is required in order to enable future work with cancellous explants to be conducted.

1.b.iv. Potential of the System

The Zetos culture system could be used to study numerous parameters, some examples are as follows:-

The interaction of bone cells with biomaterials could be analysed, allowing the initial reactions of bone biomaterial interfaces to be studied without the need of animals. This could include metal implants, polymers or ceramics. The effect of different topographies and surface chemistries of the biomaterials could also be investigated.

Different aspects of bone modelling and remodelling could be examined, such as, proliferation, regulation, and differentiation as well as metabolic activity of bone cells, allowing biochemical pathways to be delineated.

Action of hormones, cytokines, growth factors and other signalling molecules on human tissue could be investigated prior to pre-clinical trials saving time and money. This would also be beneficial in the field of osteoporosis and osteoarthritis.

Finally, the biomechanical aspect of cancellous bone deformation could be analysed. The effect of altering the loading parameters (such as load duration, frequency, magnitude and strain rate) could be elucidated and applied in future studies.

The list could become endless. Further advances in the pipeline include possible adaptation of the system to culture cartilage *ex vivo*, as well as possible movements into the field of tissue engineering. Engineered scaffolds could be seeded with numerous cell lineages and propagated within the Zetos culture system.

Aims

The main goal of the work conducted within this thesis was to ascertain whether maintenance of cancellous bone explants in the loaded environment of the Zetos culture system, providing 4,000 microstrain at 1Hz for 300 cycles daily, maintained the tissue in a more "viable" condition than disuse control explants also maintained in the Zetos culture chambers and disuse control explants maintained bathed in static media within 50 ml centrifuge tubes. The parameters used were as follows:-

- Cell viability of the explants were analysed through undecalcified histology; detection of tartrate resistant acid phosphatase, the use of different viability dyes allowing both live and dead cells to be observed simultaneously; measuring the explant's apparent Young's modulus and pH; and detecting lactate dehydrogenase.
- Cell matrix synthesis was analysed through location of bone marker proteins, namely procollagen type I, osteocalcin, osteonectin, osteopontin, and bone sialoprotein, immunohistochemically; identification of *de novo* bone apposition through the use of two different fluorophores; analysing the media for the presence of alkaline phosphatase (AlP); and finally locating the presence of *de novo* protein synthesis through the incorporation of tritiated glycine into protein molecules.

Simultaneous assessment of ovine (distal femora), bovine (distal metacarpal) and human bone structure (human femoral head) was conducted in order to have a better understanding of the tissue maintained *ex vivo*. Analysis of matrix density and structure was conducted by radiography, bone maceration, Micro Computer Tomography (μCT), Scanning Electron Microscopy (SEM) while routine undecalcifed bone histology was used

to analyse cellular morphology. The ultimate aim of this work was to find a routine method to analyse tissue before harvest and maintenance in the Zetos culture system to provide a reference point allowing only events taking place *ex vivo* to be analysed rather than pre-existing events.

Chapter 2.
Model Systems

2.a. Introduction

The Zetos culture system utilises cancellous bone due to its porous nature and the potential to keep cells alive with nutrient perfusion, which would be far more difficult with dense cortical bone.

Figure 2.a.1. demonstrates the anatomical location of where cancellous bone cores were harvested from ovine distal femora, for culture is the Zetos system. These bone cores were fixed in 70% ethanol and processed for embedding. Sections 6 μm thick were cut from each block and stained with toluidine blue, a metachromatic histological stain. It was possible to see from this image that the cancellous bone from sample 1C was denser than that of sample 4B. Sample 1C was from the most distal plane closest in proximity to the articular surface. Sample 4B was from the most proximal plane within close proximity of the medulary cavity.

These differences in samples make comparing samples cultured in the Zetos system very difficult. There is variability in bone remodelling and structure throughout the skeleton. There are also variations in bone remodelling and cancellous bone structure within the same location, thus changes in one site may not necessarily reflect those occurring elsewhere. This demonstrated the need to fully understand the models of bone used for culture in the Zetos system.

This chapter deals with the analysis of cancellous bone harvested from ovine distal femora, bovine metacarpals and human femoral heads, and their comparison with regard to bone density and histological morphology. This introduction to chapter 2 covers the structure of cancellous bone, which is cultured within the *ex vivo* system, followed by the three animal models used (human, ovine and bovine). A description of the concept and theory behind each mode of analysis, radiography, bone maceration, Micro Computer Tomography (μCT), Scanning Electron Microscopy (SEM) and routine undecalcifed bone histology is given.

The aim of the work conducted within this chapter was to use a number of different techniques (radiography, bone maceration, Micro Computer Tomography (μCT), Scanning

Electron Microscopy (SEM) and routine undecalcifed bone histology) in order to gain a better understanding of cancellous tissue with regards to trabecular type, density and orientation, as well as cell types, numbers and locations. The ultimate aim was to find a way to analyse the above mentioned characteristics, pre- and post- culture, in order to establish what changes occurred to the tissue explants during *ex vivo* culture within the Zetos culture system. This would thus, avoid inaccurately associating pre-existing *in vivo* characteristics (i.e. low core density and absence of specific cell types), observed within individual cores, to the *ex vivo* culture condition.

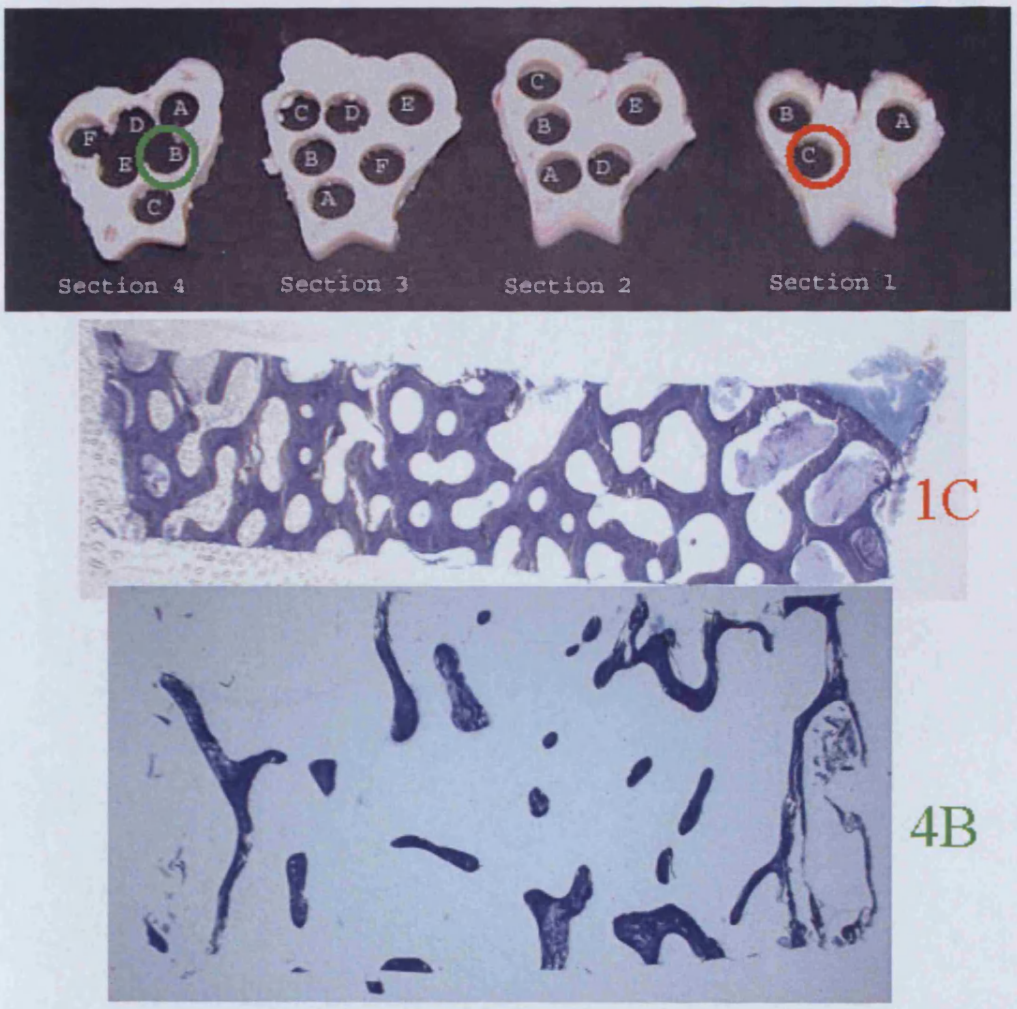

Figure 2.a.1. *Four transverse sections, 7mm thick, through an ovine distal femur (Sheep number 5, 4 years and 10 months old at day of sacrifice.) Section 1 is the most distal region and section 4 is the most proximal being in close proximity to the medulary cavity. Bone cores were harvested from each section, fixed in 70% ethanol and embedded in MMA resin. Below the femoral sections are two 6 μm sections from two different bone cores harvested from different locations. Sample 1C is from the distal plane and sample 4B in from the most proximal plane. Both sections were stained with toluidine blue.*

2.a.i. Cancellous Bone

Only 20% of bone mass is made up of cancellous bone, the rest is composed of cortical bone, but cancellous bone contributes to more than 61% of the total bone surface area due to its surface to volume ration (20 mm^2 /mm^3), eight times that of cortical bone (2.5 mm^2 /mm^3).

Cancellous bone is composed of large plates and rods known as trabeculae. It is a highly porous, lattice-like structure, found mainly at the end of long bones and in the vertebral bodies. The role of cancellous bone is to distribute mechanical loads from the articular cartilage to the cortical shaft.

In 1978, Inderbir Singh reported that human cancellous bone could be classified into seven different groups, Type I, II a, II b, II c, III a, III b, III c.

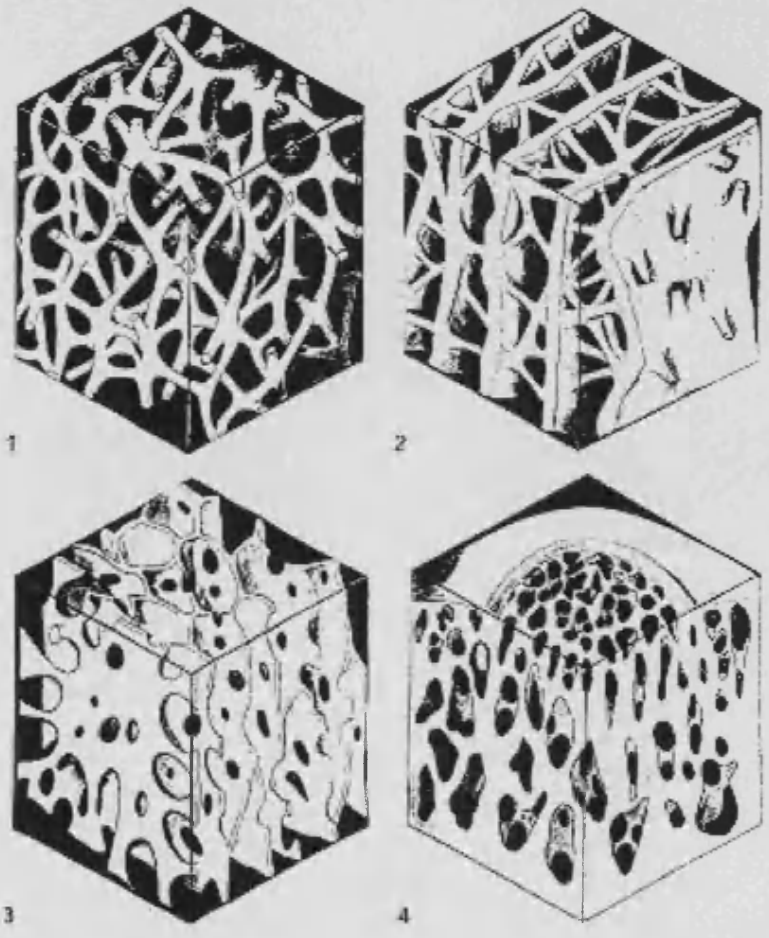

Figure 2.a.2 *These four images represent some of the different kinds of cancellous bone found in the human body. Image 1. is a representation of Type I cancellous bone. Image 2 represents Type II c bone. Image 3and 4 represents bone Type III b and Type III c respectively. [Adapted from* Singh 1978.]

Type I cancellous bone is composed of very fine straight or curved rods 0.08-0.14 mm in diameter and approximately 1 mm in length, see image 1 in figure 2.a.2 It is the most delicate type found mainly in deeper parts of the long bones. **Type II** cancellous bone is composed of both plates and rods, and can be subdivided into three subgroups. The subgroup **II a**, is similar to type I but some of the meshwork has been replaced by delicate plates of bone 0.1-0.2 mm thick and 1 mm long. **Type II b** differs from **a** in the fact that some of the plates are much more extensive with a specific orientation, and that some of the rods can be much thicker and longer (0.5 mm thick and several mm in length). This type of bone can be seen mainly in the calcaneum. Cancellous bone **Type II c** is usually seen close to articular cartilage. It consists of plates, 0.16-0.3 mm thick, arranged in a parallel layer 0.4-0.8 mm apart which is traversed by numerous rod structures, which when viewed at certain angles seem to look like they hold the plates apart, see image 2 in figure 2.a.2 **Type III** bone is usually composed of only plates of varying sizes, which contain a number of fenestrations. **Type III a,** is made up entirely of plates 0.1-0.2 mm thick and approximately 1mm in length. **Type III b,** is composed of what seems as parallel plates without the presence of rods. The rods have been placed with plates that form a tubular meshwork, see image 3 in Figure 2.a.2. These tubes have a distinct orientation, which usually run along the direction of stress, having a diameter of 0.7-2.00 mm. This type of cancellous bone is usually seen at the ends of the tibia adjacent to the articular cartilage. Cancellous bone **Type III c** is normally seen where dense cancellous bone underlies articular cartilage such as in the head of the femur. The bone is made up of plates that connect to enclose spaces, forming a honeycomb structure. These differences observed in structure imply a different requirement in function, though this is only a qualitative assessment.

Whitehouse, Dyson and Jackson (1971) used the scanning electron microscope (SEM) to study trabecular bone in the human vertebral body, followed by the proximal end of the human femur (Whitehouse and Dyson, 1974). The low magnification images obtained demonstrated wide variations in trabecular architecture within millimetres of neighbouring regions, suggesting that comparison from one area to another requires caution.

Hence, it was established in the 1970's that cancellous bone structure varies with anatomical location. However, in the 1980's it was noted that differences in architecture

also had an effect on the mechanical properties of cancellous bone. Steven Goldstein (1983) looked at the mechanical properties of human tibial trabecular bone as a function of metaphyseal location. His results indicated that the medial side of the bone was stronger and stiffer than the lateral, with individual tibias showing as much as two orders of magnitude differential. This correlates with the belief that bone is stronger and stiffer directly beneath load bearing areas. Goldstein (1987) provides us with a review of work carried out on the mechanical properties of trabecular bone with regard to anatomic location and function which supports the hypothesis that cancellous bone tissue is highly variable.

A more detailed analysis regarding mechanical properties of cancellous explants was conducted by Hobatho *et al.* 1997. Specimens of human cancellous bone from the tibia, femur, patella, lumbar spine, and humerus of eight different subjects were analysed. The elastic properties of these bone explants differed significantly ($p<0.05$) between subjects and the mechanical properties varied along the length and periphery of the tissue.

Collectively, these observed variations in the mechanical properties of cancellous bones explants have been shown to be a function of anatomic position, loading direction, methods of storage and testing conditions.

It has been hypothesised that trabeculae of cancellous bone are organised along the lines of principal stresses (Meyer, 1867). Bones function to distribute large contact stresses applied at the articular surfaces to the compact bone of the cortical shaft (Hayes *et al.*, 1978). This function directly influences the structure and strength of metaphyseal bone, a relationship known as Wolff's Law (Wolff 1870, 1892).

The strength and stiffness of cancellous bone is known to be proportional to its mineral density and orientation of the trabeculae (Behrens *et al.*, 1974). Compressive strength is related to the square of the apparent density and the compressive modulus is proportional to the cube of the density (Carter & Hayes 1977). The strength of bone was found to be proportional to the strain rate raised to the 0.06 power, and viscous stiffening due to *in situ* marrow was only significant at very high strain rates (Carter & Hayes 1977). These factors should be born in mind when comparing numerous cancellous bone explants from various locations, individual bones and species especially when exploiting them to mechanical testing as would be done with the Zetos culture system.

2.a.ii. Ovine Model

The ovine model is used primarily for orthopaedic implant studies as aged animals are in ready supply, they are docile, easy to work with and require simple husbandry. At the AO Research Institute, there is a possibility to obtain femora from deceased Swiss Alpine ewes or ewes sacrificed for other research studies where the femora were not needed Fig 2a.3. The age of these ewes ranged from 3-6 years and 40-70 kg in weight. Potential life span for a sheep is 15-20 years (Hecker, 1983), the growth plate closes at 15 months of age, and therefore these animals were considered as young adults that were skeletally mature. As the aim of the "Zetos" system was to reduce the amount of animals used in orthopaedic research, no animal was ever sacrificed directly for *ex vivo* tissue culture. The advantage of using this system was that each animal has a full medical record which was kept at the animal house. Therefore it was known which drugs the animals had received or the illnesses suffered. Sometimes, if the animal was used in another study it already has the fluorochrome labels calcein green and xylenol orange incorporated into mineralised bone. This allowed bone growth in the *ex vivo* culture to be directly compared to that *in vivo* and will also disclose areas of active resorption of the tissue formed *in vivo*.

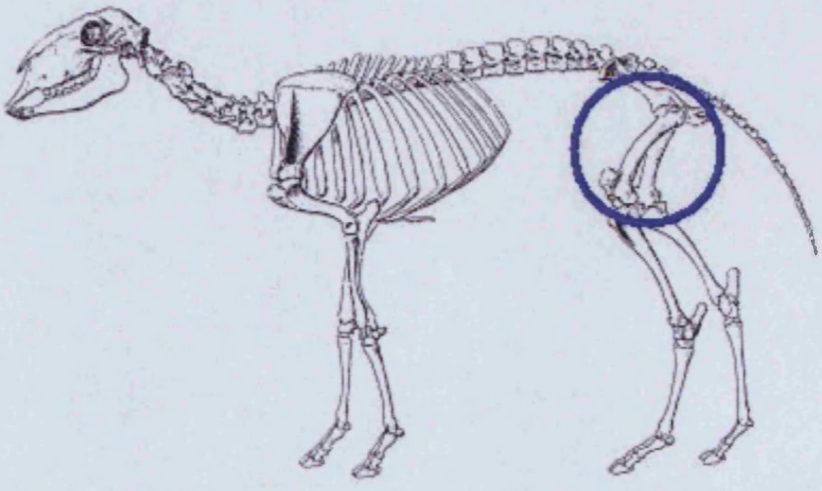

Figure 2.a.3. *The ovine skeleton. The femora are encircled with a blue ring. Usually only the distal end was harvested for culture as this is where the greatest amount of cancellous bone was found.*

One disadvantage associated with using ovine tissue is that the skeleton undergoes seasonal variation in bone loss and bone mass. For example, bone formation rates are severely depressed in the winter months (Rosen *et al.*, 1999). Also, there are not a lot of antibodies available that are specifically directed towards this species. However, it would

have been possible to have antibodies specifically made, or the possibility that the epitopes of some proteins were conserved within a number of species and, therefore, would demonstrate reactivity.

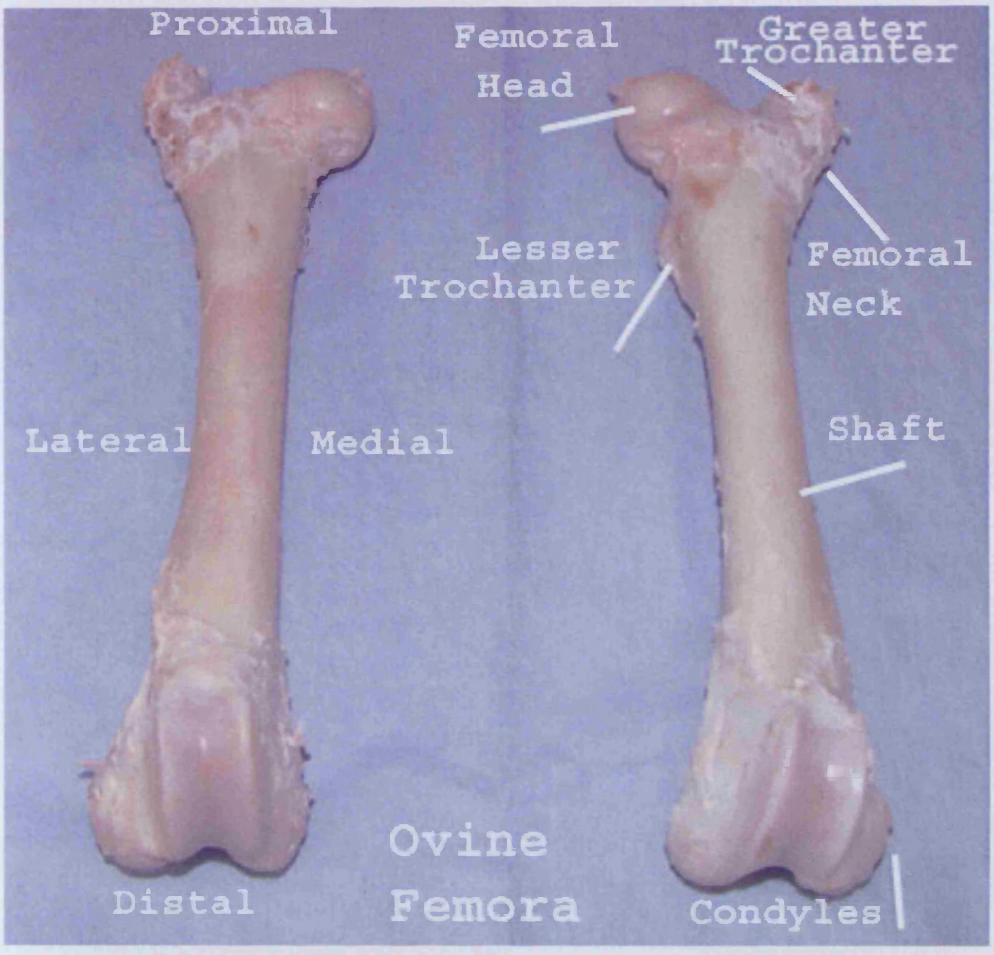

Figure 2.a.4. *The ovine femora from sheep number 181, age 3 years, weight 49 kg.*

The femur is the longest, largest and strongest bone in the body(Fig.2.a.4). Its main role is to form part of a system of levers which have to sustain the weight of the body and, to confer the power of locomotion. The femur of the sheep has a fairly regular diameter throughout its length and is very rounded apart from the caudal surface where it becomes narrow and rough, this area is known as the linea aspera. The distal end of the shaft, at the cranial side, is a convex curve that extends from one extremity to the other, thus affording greater strength to the bone (Gray, 1974). The main nutrient vessels, nutrient foramen, enters through cortex at the junction of the middle and distal thirds of the medial side of

the caudal surface where it enables sufficient blood supply to the medullary cavity of the long bone.

For culture in the "Zetos" system bone was harvested from the distal end of the femora at the condyles (see Figure 2.a.5).

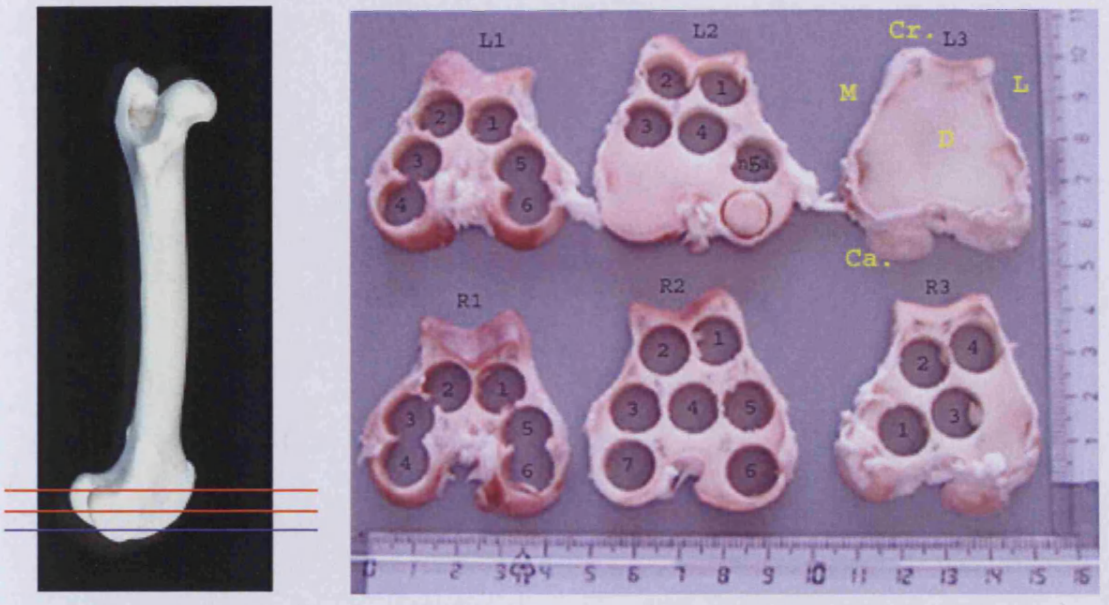

Figure 2.a.5. *The image on the left demonstrates how the cancellous bone within the condyle region was obtained. The first cut was discarded as it contained articular cartilage (blue line), then up to 4 sections 7 mm in thickness were obtained from the rest of the distal region before reaching the marrow cavity in the shaft (red lines). The image on the right demonstrates the transverse plane of the sections obtained and where bone cores were usually harvested. Sections were labelled corresponding to whether they were from the right or left leg (L/R) and the sequential number of each section was denoted with a number (1 being the most distal section). Section number L3 was labelled with yellow letters depicting its anatomical orientation; M = medial; L =lateral; Cr. = cranial, Ca. = caudal, D = distal.*

2.a.iii. Bovine Model

The bovine model is used primarily for work with antibodies, as many antibodies are directed only towards the rodent, human and bovine models. Very few antibodies can be found for ovine models. The local slaughterhouse sacrifices cows approximately 4-months-old on a weekly basis, thus provides a regular supply of tissue.

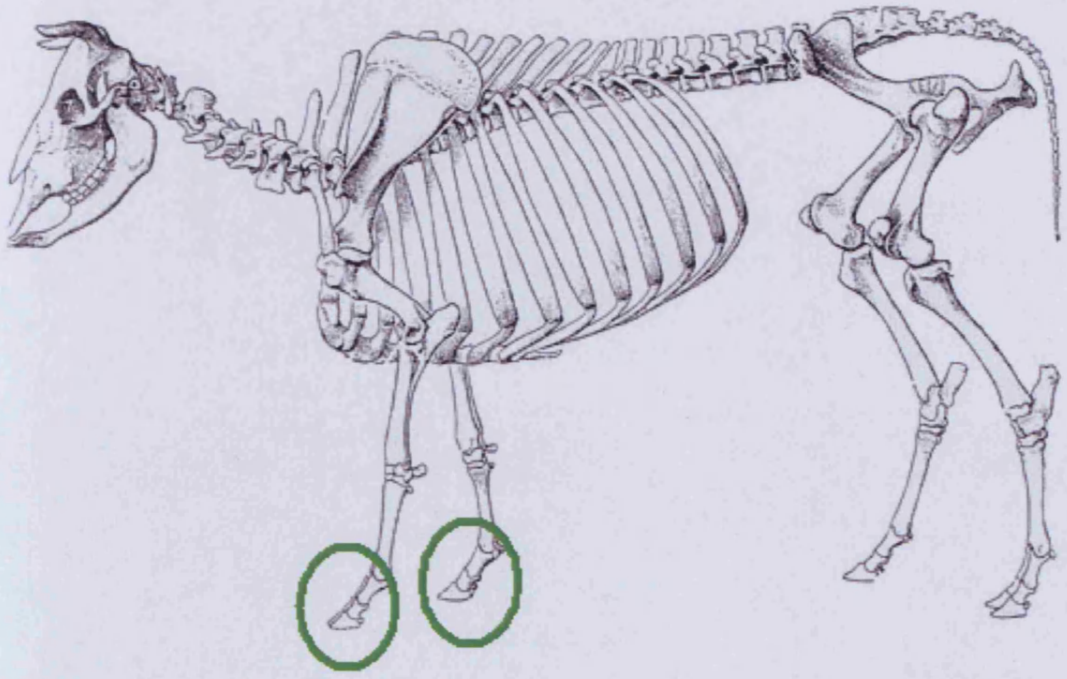

Figure 2.a.6. *The bovine skeleton. The fetlock joints are encircled with a green ring. Usually only the cancellous bone from the metacarpal is used.*

It was possible to obtain the fetlock joints (also known as the metacarpophalangeal joint) (Figure 2.a.6), which comprises the distal part of the thoracic limb that includes the carpus, metacarpus and phalanges (Figure 2.a.7). One of the disadvantages of using the metacarpal bone is that they are prone to damage in the growing cow. The metacarpal and metatarsal fractures comprise 50% of all bovine fractures (Web ref.1). On the whole, it is not known what illnesses or treatment these animals have had which may affect the cultured tissue. Usually as an experimental animal the cow suffers from being expensive to purchase and maintain, and require more space than other large animals and, has generally, been replaced by other animals such as sheep and pigs that are slaughtered for food. The advantage of using bovine tissue is that it is cheap and frequent to obtain.

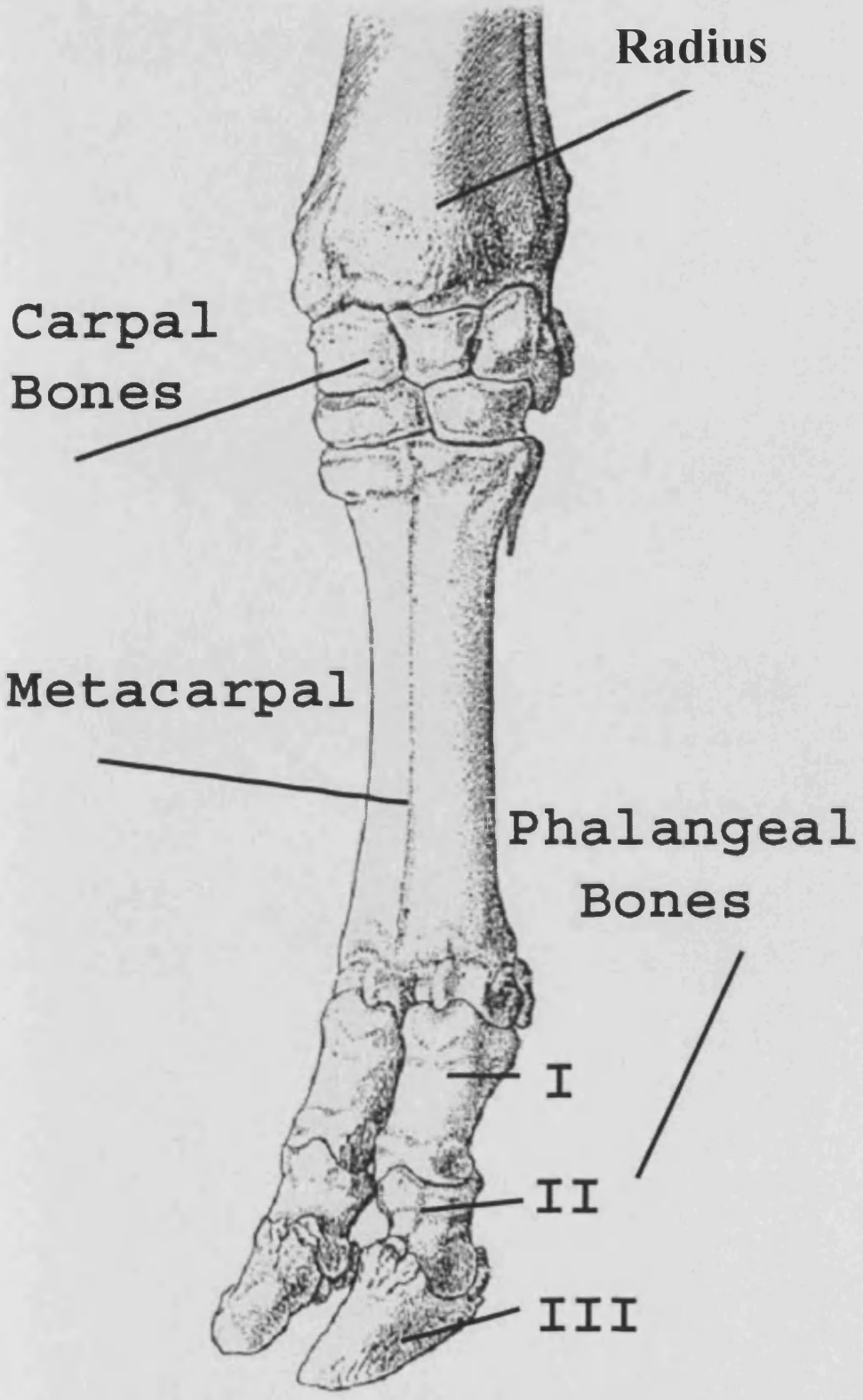

Figure 2.a.7. *Bovine distal forelimb. In ruminants the metacarpal bone is composed of two bones fused to form one. These digits support the weight of the whole body and hence tend to be larger than the metatarsal in the legs. [Adapted from Nickel et al., 1992]*

The palmar side of the fetlock joint can bee seen on the left in figure 2.a.8. The metacarpal has to be dissected out under sterile conditions.

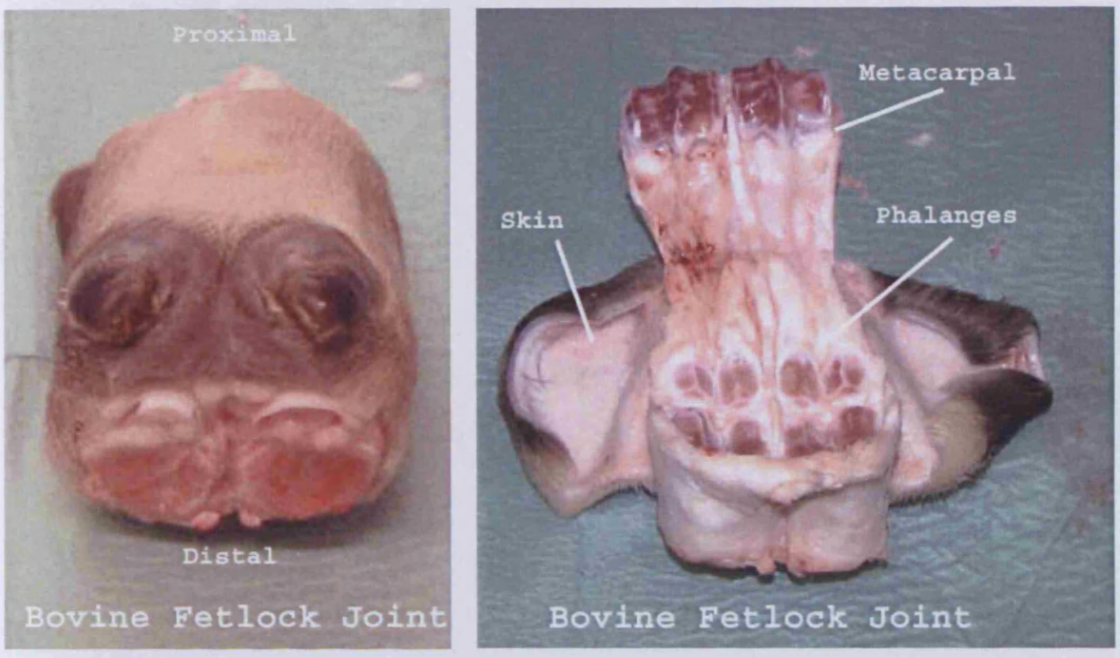

Figure 2.a.8. *The image on the left demonstrates how the fetlock joint is received from the abattoir. The view is from the palmar side showing the dewclaws. The image on the right shows how the bones are located within the joint. The metacarpal has been lifted out of its position to show the phalanges that lie beneath it.*

The bovine metacarpal is responsible for bearing most of the animal weight as can be seen from figure 2.a.6., and that most of the weight is at the cranial end. Therefore, this bone is usually larger than the corresponding bone in the pelvic limb, the metatarsal. Cattle and sheep have cursorial limbs, long limbs adapted for running. In both ruminants and pigs two digits normally support the weight of the body these are digits 3 and 4 which are enlarged and fused to form a long cannon bone, unlike humans who have five, and cats and dogs that have four and horses which have only one. In ruminants, the two non-weight supporting digits (2 and 5) are vestigial and are called dewclaws (see Figure 2.a.7).

For culture in the "Zetos" system, bone is harvested from the distal end of the metacarpal (see Figure 2.a.9).

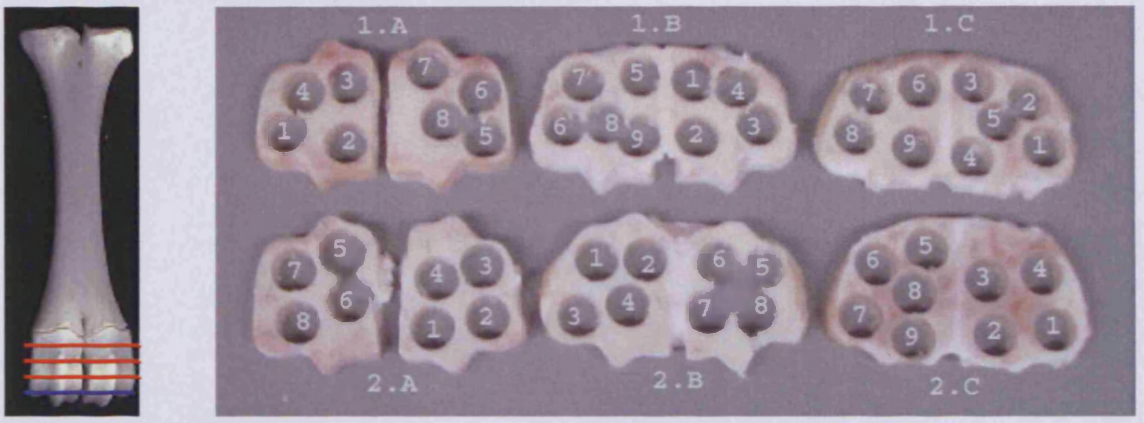

Figure 2.a.9. *The image on the left demonstrates how the cancellous bone within the metacarpal is obtained. The first cut is discarded as it contains articular cartilage (blue line), then up to 4 sections 7 mm in thickness can be obtained from the rest of the distal region before reaching the marrow cavity in the shaft (red lines). The image on the right demonstrates the transverse plane of the sections obtained and where bone cores are usually harvested. Sections are labelled corresponding to the joint they were obtained from (1/2) and the sequential number of each section is denoted with a letter (A being the most distal section).*

As mentioned previously, we have access to bone from Swiss calves usually 4-months-old. Generally calves reach maturity at approximately 24-months of age and can have a natural life span of 20-25 years (Web ref.2). These calves are regarded as immature animals as the growth plate is still open. Thus, bovine tissue would be structurally weaker than ovine tissue comprising of more woven bone than lamellar bone. It would also be less calcified.

The growth plate is also known as the epiphyseal plate (greek word physis = growth). Most bones have two epiphyses but the metacarpal, metatarsal, and phalangeal bones only have one epiphysis and, thus, only one metaphyseal growth plate (Sumner-Smith, 1982). The metaphyseal growth plates are unipolar, which means that growth takes place in one direction only. The growth plate is the only cartilage structure present in bone, once ossification is complete, apart from joint cartilage.

The cartilage of the metaphyseal growth plate is highly specialised. It consists of distinct zones. A zone of resting cells is seen closest to the epiphysis. This zone is also known as the zone of germinal cells, since it is these cells that initiate mitotic division (responsible for post-foetal growth). The zone below the resting cells contains proliferating

cells, which is characterised by small flattened dividing chondrocytes. This configuration allows the columns of chondrocytes to elongate and is the site of cartilaginous ECM accumulation. Following the zone of proliferating cells, is a zone of maturating cells hypertrophing chondrocytes. These cells are much larger in size and have ceased dividing. The final zone, the cells that are in closest proximity to the metaphysis, is a zone containing hypertrophying cells. The chondrocytes in this region degenerate and die, the surrounding matrix calcifies and cells of mesenchymal origin invade the cartilage. Chondroclasts erode and resorb the calcified cartilage matrix allowing osteogenic cells from the marrow to invade and differentiate into osteoblasts. The osteoblasts line the surface of the cartilage and secrete a thin layer of bone matrix, the osteoid that becomes mineralised as apposition of new unmineralized matrix occurs (Marks and Odgren, 2002).

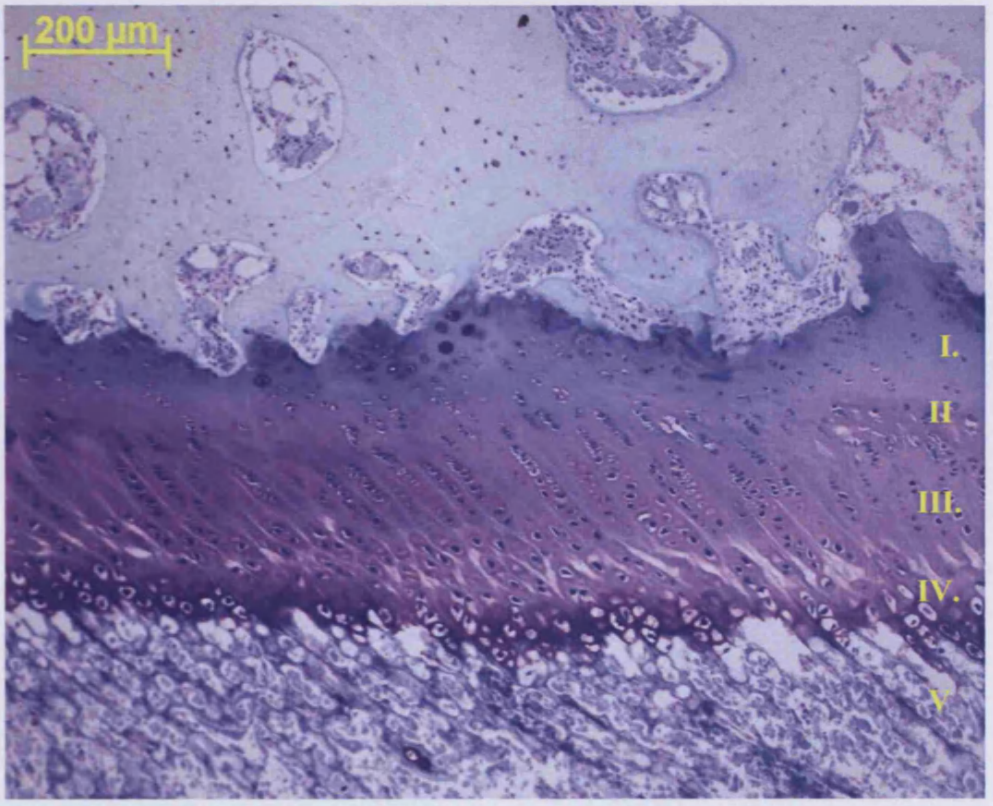

Figure 2.a.10. *The mammalian growth plate consists of four zones. Chondrocytes in the reserve zone are randomly arranged within a large amount of collagen type II and proteoglycans* (I)*.Cells arrange themselves into long columns in the proliferative zone* (II)*.Chondrocytes mature* (III) *and enlarge in size producing collagen type X in the hypertrophic zone* (IV)*. These cells undergo programmed cell death leaving lacunae that eventually become calcified and invaded by blood vessels. Osteoblasts from bone marrow stromal cells lay down osteoid on to the calcified cartilage which forms woven bone. In turn, the woven bone is remodelled to give lamellar bone* (V)*. Toluidine blue stained ovine tissue fixed in 70% ethanol, embedded in Technovit 9100.*

2.a.iv. Human Model

The human model is used primarily to study the effect of drugs on human tissue and to study osteoporotic and osteoarthritic bone. The Zetos system is currently the only systems in the world that allows *ex vivo* studies to be conducted with living human bones. There is a possibility to obtain femoral heads from the local hospital (Davos) from individuals who will receive hip prostheses [Ethical Commission Graubünden (18/02)]. The age of the tissue expected to be obtained can vary from late 50's to early 90's from either male or female patients receiving total hip arothplasty. This is considered old bone and can be very osteoporotic in nature.

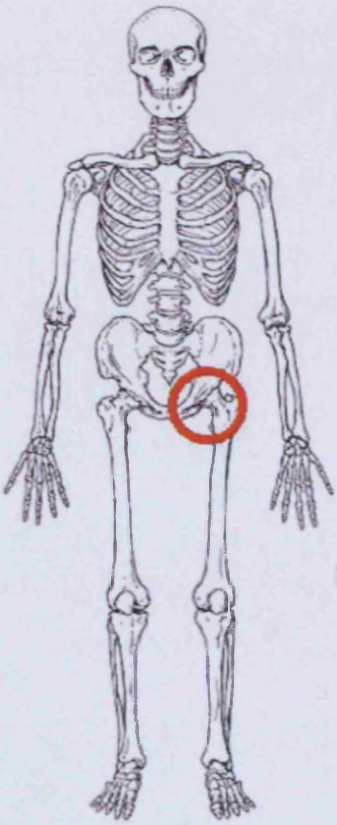

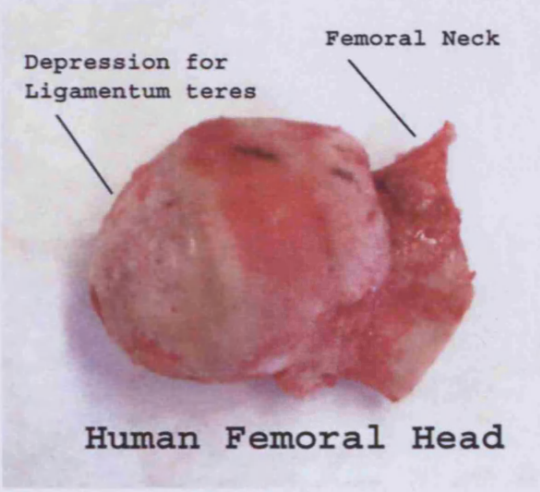

Figure 2.a.11. *The human skeleton comprises 206 bones. The femoral head is encircled with a red ring. Usually the femoral head obtained from the hospital has diseased cartilage, bone, or both.*

The femoral head is globular in shape, smooth and covered with articular cartilage. Just a little below centre there is usually a depression for the attachment of ligament. The femoral head is connected to the shaft via the femoral neck, a flattened pyramidal process.

For culture in the "Zetos" system, bone was harvested from the femoral head (see Figure 2.a.12).

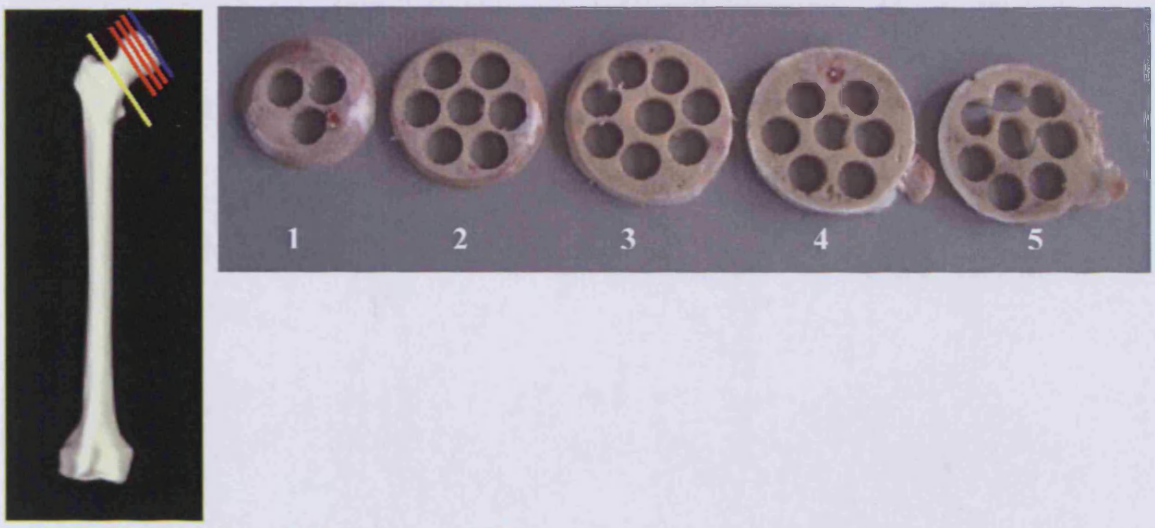

Figure 2.a.12. *This image on the left demonstrates how the cancellous bone within the femoral head was obtained. The first cut was discarded as it contained articular cartilage (blue line), then up to 5 sections 7 mm thick were obtained from the rest of the region before reaching the femoral neck (red lines). The image on the right demonstrates the transverse plane of the sections obtained and where bone cores were usually harvested. Sections were labelled sequentially (1 being the most medial).*

Osteoporosis is a heterogeneous disorder with several kinds of bone remodelling abnormalities, which is explained in greater details in chapter 4. Its main characteristic is fractures caused by cancellous bone alterations such as fenestration of bone plates, and thinning and reduction of bone trabeculae. It is estimated that annually, in Britain, 70,000 hip, 120,000 spine, 50,000 wrist fractures occur due to osteoporosis with one in three women being affected and 1 in 12 men (Web ref.3). There are two types of osteoporosis, primary and secondary. Primary osteoporosis occurs in association to the normal aging process, while secondary osteoporosis is caused by certain medical conditions or medications that affect bone formation.

Other diseases in the skeleton, such as osteoarthritis, might be related to the mechanical properties of the subchondral bone under the affected cartilage and that of the cancellous bone supporting it. It is possible to obtain femoral heads where the primary reason for removal may have been due to a defect in the cartilage as well as bone tissue. All of the subchondral bone utilised during these studies were healthy.

2.a.v. Radiography

Conventional radiography is a non-invasive method used to visualise bone structure providing qualitative information on bone density. A decrease in bone density is depicted as radiolucency on the radiographs. This lucency is caused by a decrease in the volume of mineralised bone and a decrease in the amount of calcium (Jiang, Zaho & Genant, 2002). This method is still widely used to detect osteoporotic related fractures and to differentiate various bone disorders such as osteoporosis and osteomalacia. Changes in bone density are more prominent in cancellous bone tissue than cortical tissue due to the greater surface area of cancellous bone allowing it to adapt faster. Usually, as bone mineral is lost, the non-weight bearing trabeculae are resorbed first. The remaining weight bearing trabeculae become more widely separated and may undergo compensatory thickening in the direction of mechanical stress (Jiang *et al.*, 2002). Clinicians and radiologists are able to grade bones in such a way as to determine the risk of fracture in certain individuals, for examples the Genant scoring method for vertebral fracture (Genant *et al.*, 1993) and the Singh index for the proximal femur (Singh *et al.*, 1972).

Microradiography utilises high resolution contact radiographs to display trabecular structure of bone slabs in order to asses bone morphometry. This method is useful to aid detection of lesions or faults present in bone tissue. Bone slabs give a more detailed image than whole specimens used during clinical radiology. A Faxitron cabinet X-ray system is a tabletop unit used for this purpose. The unit is approximately 56cm wide x 51cm deep x 89 cm high, has an energy output between 10-110 kV, adjustable shelves for flim to source distances (31 mm – 61 mm), and is fully lead lined to protect the operator (Callis, 2002). It is possible to quantify the degree of mineralisation and secondary mineralisation by using aluminium calibration step wedges. Grayscale images with a range of values are converted into binary images with only two values black (no bone) and white (bone) (Jiang *et al.*, 2002). However, this technique is influenced by factors such as tissue thickness, radiographic exposure, the film used and film processing (Callis, 2002). The aim of using this method was to analyse the density of the cancellous tissue from the different species as well as observing any post-harvest fractures that may be present.

2.a.vi. Bone Maceration

Maceration is a process whereby soft tissue is removed from bones leaving behind the calcified tissue. This removal allows the 3D structure of the bones to be visualised including the cortical and cancellous bone tissue in relation to the whole bone.

2.a.vii. Micro Computer Tomography (μCT)

MicroCT measurements can provide 2D and 3D structure parameters such as bone volume to total volume, bone surface area to bone volume, trabecular number, thickness and separation in a non destructive way (Rüegsegger, Koller, and Müller, 1996). This imaging system is based on standard X-ray CT principles but utilises specialised hardware to obtain bone images at extremely high resolutions (up to ~ 10 μm) (Feldkamp *et al.*, 1989; Kinney *et al.*, 1995; Lang *et al.*, 1998). The μCT enables the 3D microarchitecture distribution of cancellous bone to be measured enabling correlations between bone architecture (i.e. trabecular connectivity) and bone strength to be determined. Structure model index (SMI) is a morphometric parameter used to determine the amount of plates and rods that characterise that structure. It is calculated by 3D image analysis based on a differential analysis of the triangulated bone surface (Jiang *et al.*, 2002). An ideal plate structure would have an SMI value of 0 and an ideal rod structure would have an ideal value of 3. Values between 0-3 depict a structure with both plates and rods of equal thickness but with differing ratios. The aim of using microCT was to obtain a 3D image of bone explants that would be potentially maintained within the Zetos culture system.

2.a.viii. Scanning Electron Microscopy (SEM)

The electron microscope was invented back in the early 1930's by Ernst Ruska and Max Knoll, and the first scanning electron microscope (SEM) was constructed in 1938 by von Ardenne (Bozzola and Russell, 1992). One of the main advantages of using the SEM is its high resolution (up to 1.5 nm) and the ability to create a 3D image of the specimen due to the large depth of field and the shadow-relief effect of the secondary (SE) and backscattered (BSE) electrons (Goldstein *et al.*, 1992). The SEM produces an electron beam which scans the surface of the specimen to generate SE and BSE from the specimen that is detected by sensors. The apparent three-dimensional (3D) image is produced due to differences in contrast between various structural features of the specimen. Contrast arises

when different parts of the specimen generate different amounts of SE or BSE when the electron beam strikes them. Brighter areas produce more SE (Bozzola and Russell, 1992). This method was utilised by Whitehouse, Dyson and Jackson (1971) followed by Whitehouse and Dyson (1974) to assess the differences in cancellous bone density.

2.a.ix. Histology

It was over 300 years ago, in the early 1690's that the first observations of bone histology were made by Leeuwenhoek (1693) and Havers (1691-2). They were the first to visualise the tissue in a 3D structure and noted small holes within the microarchitecture of bone which they called Haversian canals after Havers.

Before a sample can be analysed histologically, the tissue in question must undergo relevant processing. The aim of tissue processing is to embed the tissue in a solid medium firm enough to support the tissue and give it sufficient rigidity to enable thin sections to be cut, and yet soft enough not to damage the knife or tissue (Callis, 2002). Before this can be achieved, a number of steps must be carried out; **fixing, dehydrating, clearing, impregnating and embedding**. The embedded sample is then sectioned and stained. Only once these procedures are complete can the samples be analysed microscopically – a process which can take several weeks depending on sample size. Each and every step mentioned above can affect the quality of the sample to be analysed and several factors must be taken into consideration at each stage. It is essential that tissue should resemble the living state as close as possible and not change shape or volume once it has been fixed.

The stains chosen for these experiments were giemsa, Toluidine blue, Movat pentachrome, and the Masson Goldner trichrome method - to distinguish bone from freshly synthesised osteoid. With the Masson and Movat stains the calcified tissue takes up the fibre stain and to some extent the haemotoxylin, and the osteoid reacts with the cytoplasmic stain. Toluidine blue has the advantage of demonstrating the mineralised front in the bone trabeculae, while giemsa allows haemopietic cells to be distinguished.

The aim of using histology was to compare the various morphologies of the differing tissues including soft tissue as well as the calcified matrix, which is not possible with the other techniques.

2.b. Materials and Methods

Herein is a detailed description of all methods and materials used during this study. Additional information on techniques, machinery and chemicals can be found in the relevant Appendices.

2.b.i. Radiology

Comparison of bone slabs from ovine (distal femora), bovine (distal metacarpal) and human tissue (human femoral head) qualitatively analysed by eye for any fractures or cysts within the calcified matrix. The numbers of ovine, bovine and human limbs assessed in this manner were 22, 7, and 3 respectively

Ovine distal femora, bovine distal metacarpals and human femoral heads were cut into 7 mm thick sections with the Exakt 300 band saw (Exakt 300 CL/CP) [Appendix A]. These sections were placed in individual Petri dishes (Falcon, 351029) filled with 0.9% NaCl (Fresenius Kabi NI2516) for transportation to radiology. The faxitron (Faxitron 804, Faxitron Company, Illinois, USA) and developer (Structurix NDT M) were switched on and allowed to warm up for 10 minutes before use. The bones were dried with tissue paper and placed on the photographic film (AGFA Structurix D4 film). Each radiograph was labelled with the sample number, date and sample name and contained calibration bars to determine bone density. These samples were placed into the bottom shelf inside the faxiton, with a number 1 steel filter placed on the top shelf. The machine was set to 35 kV for 2½ minutes. Once exposed, the samples and photographic film were removed. The samples were placed back into the Petri dishes. Following this procedure, the photographic film was developed in the dark room. A light box was used to view the radiograph and scanner was used to digitise the radiographs.

2.b.ii. Bone Maceration

Comparison of ovine (femora), bovine (metacarpals) and human tissue (human femoral heads) qualitatively analysed by eye for any fractures or cysts within the calcified matrix or decrease in calcified matrix. The two limbs from each species (ovine femora, bovine metacarpals and human femoral heads) were assessed in this manner.

Ovine femora, bovine metacarpals and human femoral heads were obtained and cleaned to remove as much soft tissue as possible. A hole was drilled in through the bone in order to allow all the marrow to be washed out with water, or blown out with an air gun. The bones were boiled for 5-15 minutes in order to denature the proteins, and then they were placed for several days in a 1% solution of papain (Fluka 76222) at 65 °C to remove all the cellular material. The papain solution was changed daily until the papain was clear. The tissue was then washed for 24 hours under running water and a brush was used to remove any remaining tissue. A 3.5% solution of hydrogen peroxide (Fluka 95299) was used to deactivate the papain by boiling the bones for 1-2 hours, followed by a brief wash under running water and air dried. The fat was removed from the tissue by placing the bones in choloroform (Fluka, 25669) for 24 hours and then leaving the samples to air dry. Once dry, it was possible to image the bones with a scanner allowing calcified tissue and bone trabeculae to be detected.

2.b.iii Micro computed Tomography (μCT)

Comparison of bone cores from ovine (distal femora), bovine (distal metacarpal) and human tissue (human femoral head) quantitatively analysed by microCT for bone volume to tissue volume, trabecular number and trabecular thickness and qualitatively analysed by eye for trabecular microstructure (plate or rods) and trabecular orientation. The numbers of ovine, bovine and human limbs assessed in this manner were 2, 1, and 1 respectively.

Ovine distal femora, bovine distal metacarpals and human femoral heads were cut into 7 mm thick sections with the Exakt 300 band saw. These sections were placed in individual Petri dishes (Falcon, 351029) and filled with 0.9% NaCl (Fresenius Kabi NI2516) to stop the tissue from drying. The sections were transferred to a Teflon plate that was secured to an x-y table under a bench drill (Eco MAC 212). A diamond tipped drill bit (D256) was used to bore bone cores with a diameter of 10 mm from the cancellous tissue. The bone cores were placed in individually labelled 15ml centrifuge tubes (Miliam TTK120) filled with 5ml of 0.9% NaCl and stored at –20°C. Samples were defrosted before being measured with the MicroCT 20. Voxel size of 26 x 26 x 26 μm^3 was chosen. For the evaluation procedure, a VOI (Volume of Interest), which was smaller than the

explant was chosen to eliminate particles from drilling and sawing. The VOI was a cylinder with a diameter of app. 8.944 mm and a height of 4.888 mm. The chosen segmentation parameters were sigma 1.0, support 2, and threshold 250. Sigma and support are the parameters of the Gauss filter. The threshold was necessary to distinguish between bone and no-bone because a binary structure is required for microCT evaluations. These parameters were machine specific. Samples were imaged by Christina Eckhardt at Research Services, AO Research Institute, Davos.

2.b.iv. Scanning Electron Microscopy (SEM)

Comparison of bone cores from ovine (distal femora), bovine (distal metacarpal) and human tissue (human femoral head) qualitatively analysed by eye for trabecular microstructure (plate or rods). The number of ovine, bovine and human cores assessed in this manner was 2.

Ovine distal femora, bovine distal metacarpals and human femoral heads were cut into 7 mm thick sections with the Exakt 300 band saw. These sections were placed in individual Petri dishes (Falcon, 351029) filled with 0.9% NaCl (Fresenius Kabi NI2516) to stop the tissue from drying. The sections were transferred to a Teflon plate, which was secured to an x-y table under a bench drill (Eco MAC 212). A diamond tipped drill bit (D256) was used to bore bone cores with a diameter of 10 mm from the cancellous tissue. The bone cores were placed in individually labelled 50ml centrifuge tubes (OmniLab AG, 91050) filled with 30ml of 2% papain (Fluka 76222) and incubated at 60°C. The papain solution was changed every second day for 2 weeks to make sure all soft tissue was removed from the canaliculi. The bone cores were placed in a beaker containing 50 ml 3.5% hydrogen peroxide (H_2O_2) (Fluka 95299). These beakers were placed onto a hot plate, under the fume hood and boiled at 200 °C in order to deactivate the papain. Boiling was carried out until the bone cores became white and stopped bubbling. The bone cores were then left for 20 min to dry before being placed in clean beakers containing 100 ml chloroform (Fluka, 25669), covered and left to defat overnight in the fume hood. Once defatted the bone cores were placed in small Perti dishes to dry.

Once dried, the bone cores were freeze-fractured in liquid nitrogen. This technique involved placing the bone cores onto a bespoke jig, placing the jig into a plastic

Tupperware box and filling it with liquid nitrogen. A blade was connected to the jig and was tapped gently with a hammer so that the bone was fractured rather than being cut. Once fractured, the lid of the box, which had a hose connected to it, was replaced to allow the nitrogen to boil off while stopping condensation to accumulate on the bone specimens.

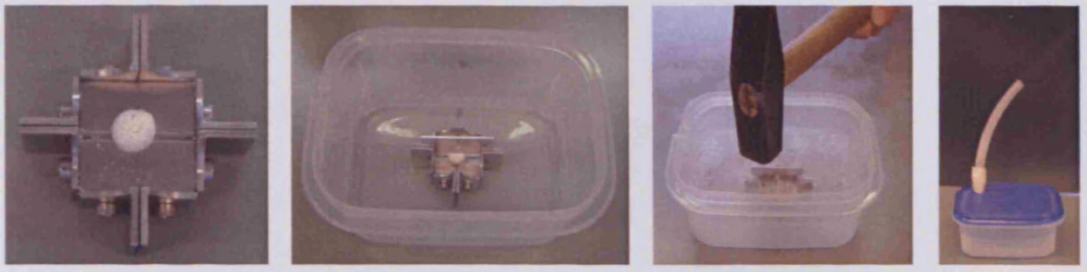

Figure 2.b.1. *The novel technique to freeze-fracture bone cores. Adapted from [ap Gwyn et al., 2002]*

The bone fragments were mounted onto a stub. This procedure involved sticking black carbon discs (Provac AG, PRHL140085) onto the stubs (Provac AG, PRHP14001T) then placing the bone fragments onto these followed by covering the surface with silverdag (Provac AG, PRHC14020). The stubs were placed into a sputter coater and coated with gold-palladium (Baltec Med 020). Once coated, the specimens were stored in a plastic container to avoid dust contamination until they were ready for image analysis. Images of the bones were taken with Hitachi S-4700 FESEM by Dr Llinos Harris and Louise Baxter, Interface Biology Group, AO Research Institute, Davos.

2.b.v. Histology

Comparison of bone sections from ovine (distal femora), bovine (distal metacarpal) and human tissue (human femoral head) qualitatively analysed by eye for calcified matrix density, cell location and cell types. Qualitative analysis of different morphological stains and resins regarding tissue staining patterns. Twenty sections obtained from the centre of the core and twenty sections obtained from the surface of the core, was assessed in this manner from a group where n=6 for each species (ovine, bovine and human).

Bone cores from ovine distal femora, bovine distal metacarpals and human femoral heads were obtained by sectioning the tissue into 7 mm thick sections with the Exakt 300 band saw and boring 10 mm diameter cores from the cancellous region with a diamond tipped fluted drill bit (D256) and bench drill (Eco MAC 212). These cores were cut parallel to the height of 5 mm with a Leica annular saw (Leica AG, Glattbrugg, CH). The cores

were fixed with 20 ml 70% ethanol in 50 ml centrifuge tubes, for five days, at 4°C, with two changes a day. The cores were then dehydrated in an ethanol series (80%, 90%, 96%, 100%, 100%) with 20 ml in 50 ml centrifuge tubes, for one day, at 4°C, with two changes a day. The ethanol was cleared from the samples by immersing the samples in xylene (Siegfried, 235120-04) for 6-8 hours at room temperature (20-22°C) under the fume hood. Samples were ready for immersion in resin once the cores were completely defatted and had become transparent in appearance. Samples were either embedded in methylmethacrylate (MMA) resin or Technovit 9100 New (a derivative of MMA).

For MMA embedding cores were placed in glass jars containing enough MMA solution 1 (Fluka, 64200) to cover the sample for 3 days at 4°C, then transferred to solution 2 for 3 days at 4°C and then finally in solution 3 for 5 days at 4°C before being placed in a water bath at 20°C for polymerisation. When the resin was fully polymerised the samples were obtained by smashing the glass.

For Technovit 9100 New (Heraeus Kulzer GmbH, Germany) embedding, a series of solutions were prepared. The samples were infiltrated in solution 1 for half a day (~12 hours) at 4°C , solution 2 for 24 hours at 4°C, solution 3 for 24 hours at 4°C and finally solution 4 for 4 days at 4°C. The polymerisation mixture was stored as two separate solutions which were mixed immediately before use in the ratio of 9 parts solution A to 1 part solution B. One bone sample per mould was inserted and covered with the polymerisation mixture until the mould was full to eliminate the oxygen. Labelled samples were placed in 24 well plates for stability and then placed at –20°C. The samples usually polymerised within 5-10 days.

Polymerised cores were cut with the Polycut E microtome (Reichert-Jung Leica, Glattbrugg, CH) or HM355S rotary microtome (Microm International) with a D blade to give 6 μm thick sections. Sections were adhered to SuperFrost® Plus (Roth, Karlsruhe, D, no. H867) glass slides with 80% ethanol and covered with polyethylene foil and paper before being clamped for 24 hours at 50 °C.

Prior to staining, the residual resin was removed from the tissue sections by placing the glass slide in MEA (1-acetoxy-2-methoxy-ethane) (Fluka, 00860) for 2 x 30 min, then through a graded ethanol series (100%, 96%) before being placed in water ready for morphological staining.

Masson-Goldner Trichrome:- Samples were placed in Weigert's haematoxylin (Merck, 1.15973./1 and 1.15973./2) stain for 1 hour, rinsed under lukewarm water for 5 minutes, immersed in Masson solution (Fluka, 84600, and 81465) for 15 minutes, differentiated in 1% acetic acid (fresh) (Fluka, 45731) before being placed in phosphomolybdic acid - orange G (Fluka, 79560, and Fluka, 75380) for 8 minutes. Samples were rinsed in 1% acetic acid, immersed in 0.1% Light green SF yellowish (Merck, 15941) for 12 minutes, rinsed in 1% acetic acid then de-ionised water, 96% ethanol, absolute ethanol (2x 2 minutes), rinsed in xylene and then immersed in xylene for 5 minutes and mounted with Eukitt (O. Kindler GmbH & Co., Freiburg, Germany).

Toluidine blue: - Samples were stained with 1% Toluidine blue for 30 minutes, rinsed in water followed by immersion in 96% ethanol for 5–10 seconds, rinsed in absolute ethanol (2 x 3 minutes), rinsed in xylene for 5 minutes and mounted with Eukitt.

Giemsa:- Samples were immersed in 15% Giemsa (Fluka, 48900) for 40 min., rinsed for a few seconds in water to check staining intensity, differentiated in 96% ethanol for 1 min before being placed in 100% ethanol for 5 min. Sections were finally rinsed in xylene for 5 min and mounted with Eukitt.

Movat Pentachrome:- Samples were stained with alcian blue (Fluka, 05500) for 10 min, then rinsed in running water for 6 min. Sections were then immersed in alkaline alcohol (Siegfried, 106440-01) for 60 min, then rinsed in running water for 10 min. Next, sections were stained with Weigert's haematoxylin (Merck, 1.15973./1 and 1.15973./2) stain for 20 min, rinsed under lukewarm water for 15 minutes, and then differentiated in 96% ethanol. Sections were rinsed in dH_2O before being immersed in brilliantcrocein/fuchsine acid for 20 min. Sectioned were rinsed in 0.5% acetic acid before being stained with 5% phosphotungstic acid (Fluka, 79690) for 20 min. Sections were then rinsed in 0.5% acetic acid before being stained with Saffron alcohol for 40 min. Finally, sections were washed three times in 100% ethanol, 5 min in each change of ethanol before rinsed in xylene for 5 min and mounted with Eukitt.

Imaging of the samples was conducted with a Zeiss 2 epifluorescence light microscope. The light path was switched to 3200K for reproducibility, and the grey filters were set at 6%. The light path was to the camera only. Black and white references were made for every image as well as adjusting the condenser. A fixed exposure time was selected to increase image reproducibility. Focus was determined by the computer.

2c. Results

Herein is a detailed description of all the results obtained during this study. Additional information on techniques, machinery and chemicals can be found in the relevant Appendices.

2c.i. Radiology

Ovine Distal Femora

The right and left distal femoral from a total of 11 ewes were observed by radiographs. The age range of these sheep was between 3 and 5 years. Their weight ranged between 40-63 kg. It was possible to obtain at least three sections 7 mm thick from each leg and if the sheep weighed over 60 kg then it was possible to obtain four sections per leg. Two examples are shown and can be seen in Figures 2c.1, 2, 3 and 4.

The first sections (the most distal region) contained the densest amount of trabeculae (see Figure 2c.1 & 2c.2) there after, further towards the medulary cavity the sections became less dense. Usually, the centre of sections two and three contained very little bone as can be seen in Figure 2c.3 and 4.

Sheep are known to suffer from cysts, as are humans. These cysts are most apparent in ewe number 206, where it is possible to see bone-like tissue in the digital image 2c.1., but only an empty void in the radiograph (Figure 2c.2)

Bovine Distal Metacarpals

The distal metacarpals from a total of 7 calves were observed by radiographs. The age range of these animals was approximately 4 months. It was not possible to find out the weight of the animals as this was not a standard practice at the abattoir. It was possible to obtain at least three sections 7 mm thick from each bone before reaching the growth plate and a further three if including the growth plate. Two examples are shown and can be seen in Figures 2c.5, 6, 7 and 8.

The first sections (the most distal region) contained the densest amount of trabeculae (see Figure 2c.6 & 2c.8), thereafter, the following sections contained the growth plate, and a final section before reaching the cavity of the bone. No loss of tissue due to cyst was observed in any samples.

Human Femoral Heads

The femoral heads from a total of 3 patients were observed by radiographs. The age of these ranged from 69-81 years. It was possible to obtain at least three sections 4 mm thick from each head. Two examples are shown and can be seen in Figures 2c.9, 10,11 and 12.

The first sections (the most medial region) contained the densest amount of trabeculae (see Figure 2c.9 & 2c.10), there after, the further towards the femoral neck the sections became less dense. Usually the last section contained very little bone as can be seen in Figure 2c.11 and Figure 2c.12.

Humans are also known to suffer from cysts. These cysts are most apparent in the 80-year-old human, where it was possible to observe voids within the digital image 2c.9., as well as in the radiograph (Figure 2c.10).

This technique would be beneficial to use prior to tissue harvest for the Zetos system in order to locate areas within the sections to avoid. However, the effect that making radiographs has on bone cells viability would have to be conducted. If the technique is not found to be too detrimental to the viability of the cells, then it should be possible to conduct under relatively sterile conditions as not to infect the tissue with microorganisms.

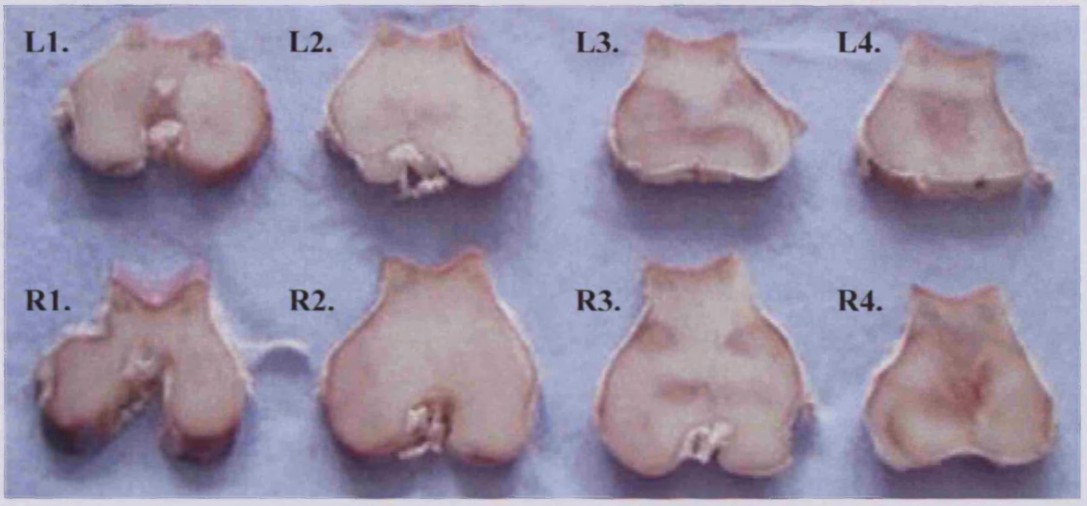

Figure 2c.1. *Digital image of the distal femora from ewe number 206, 3 years of age and 60.5 kg in weight. Labelled sections correspond to whether they were from the right or left leg (L/R) and the sequential number denotes location of section within the femora (1 being the most distal section). [A representation of 22 limbs analysed in this manner]*

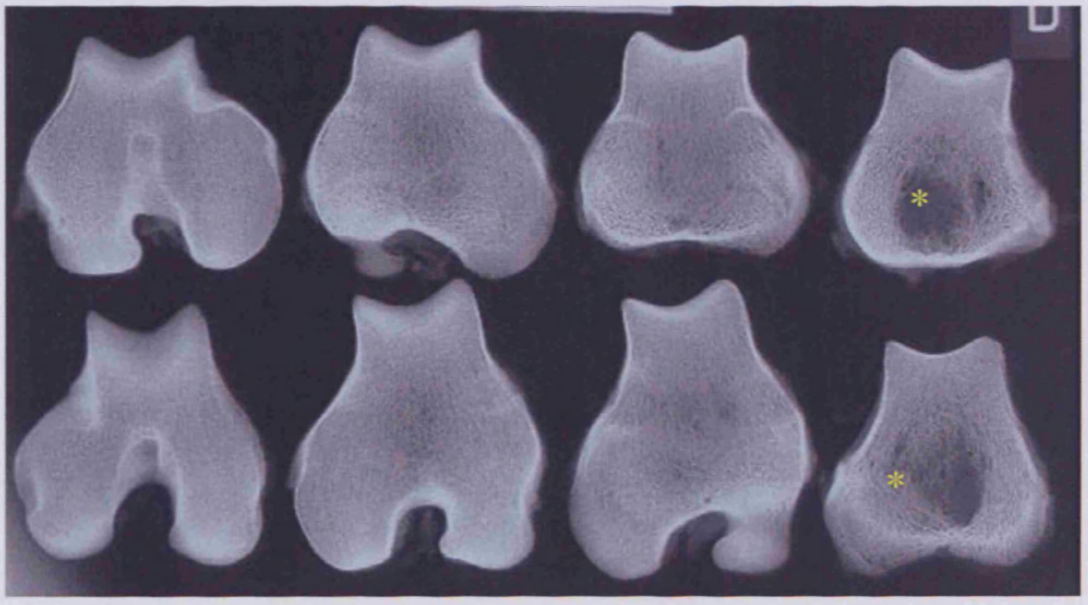

Figure 2c.2. *Radiograph of the distal femora from ewe number 206, 3 years of age and 60.5 kg in weight. Image was taken with 35 kV for 2 min 30 s. Yellow star represents areas where cysts are present. [A representation of 22 limbs analysed in this manner]*

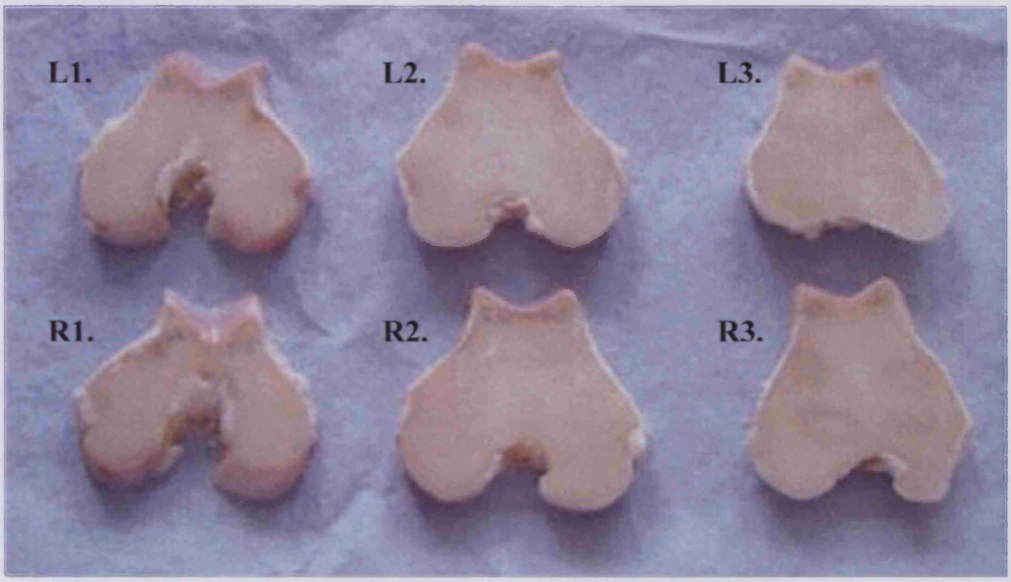

Figure 2c.3. *Digital image of the distal femora from ewe number 181, 3 years of age and 49 kg in weight. Labelled sections correspond to whether they were from the right or left leg (L/R) and the sequential number denotes location of section within the femora (1 being the most distal section). [A representation of 22 limbs analysed in this manner]*

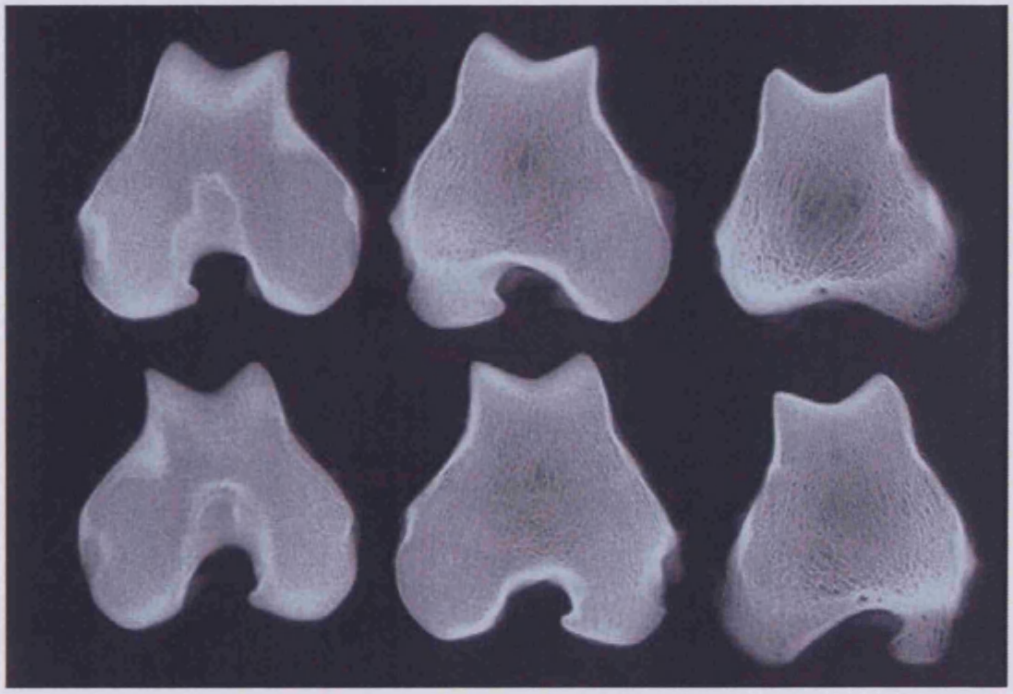

Figure 2c.4. *Radiograph of the distal femora from ewe number 181, 3 years of age and 49 kg in weight. Image was taken with 35 kV for 2 min 30 s. [A representation of 22 limbs analysed in this manner]*

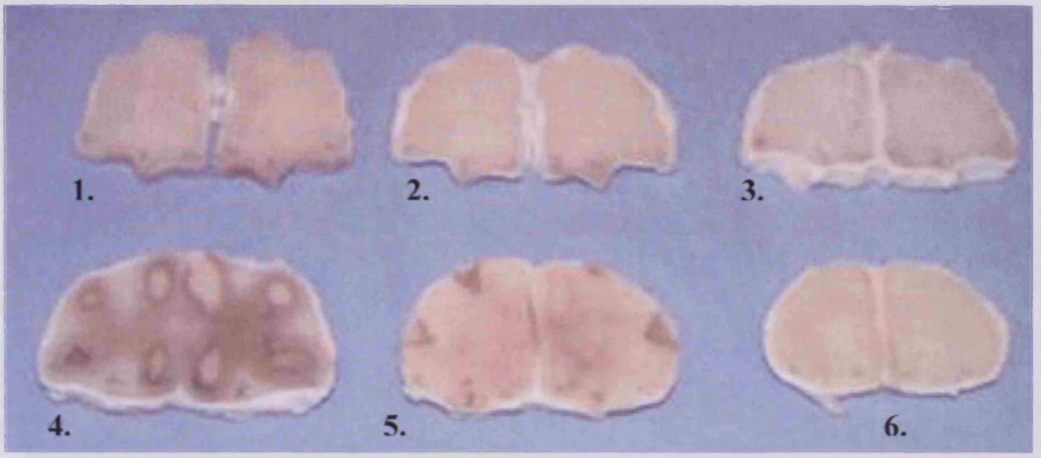

Figure 2c.5. *Digital image of the distal metacarpal from calf number 1, 4 months of age. Labelled sections correspond to the location of the section within the metacarpal (1 being the most distal section). [A representation of 7 limbs analysed in this manner]*

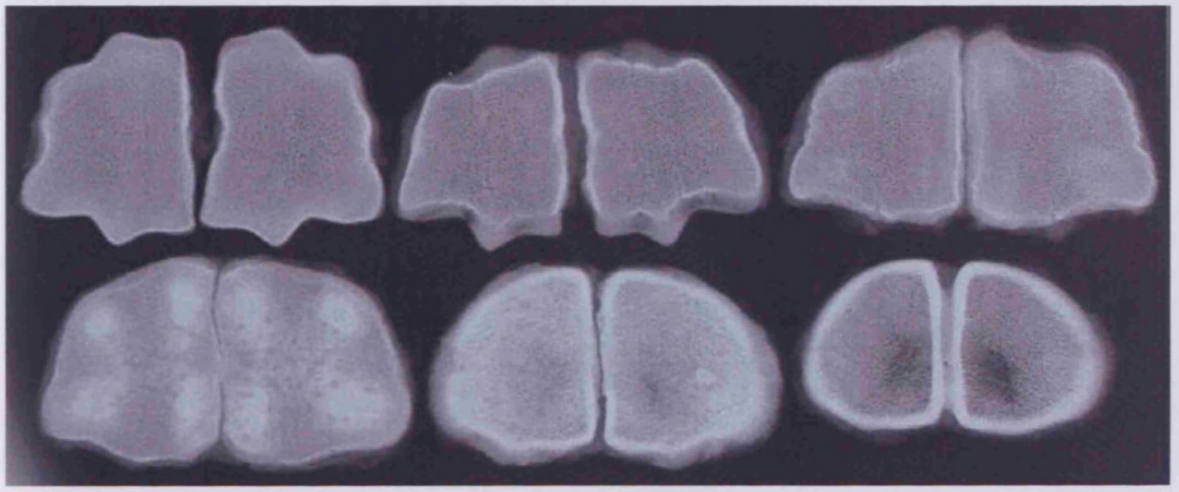

***Figure* 2c.6.** *Radiograph of the distal metacarpal from calf number 1, 4 months of age. Image was taken with 35 kV for 2 min 30 s. [A representation of 7 limbs analysed in this manner]*

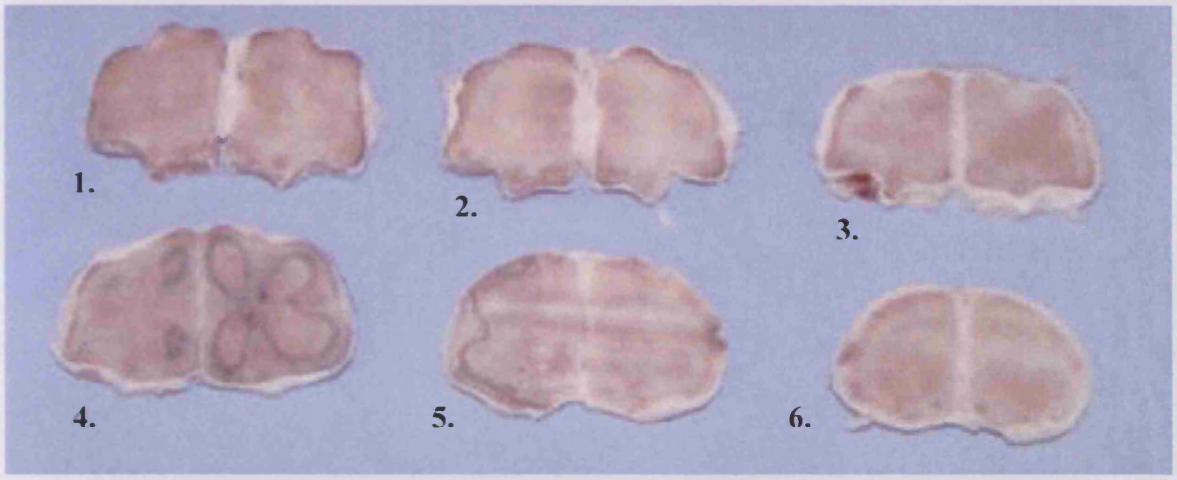

***Figure* 2c.7.** *Digital image of the distal metacarpal from calf number 2, 4 months of age. Labelled sections correspond to the location of the section within the metacarpal (1 being the most distal section). [A representation of 7 limbs analysed in this manner]*

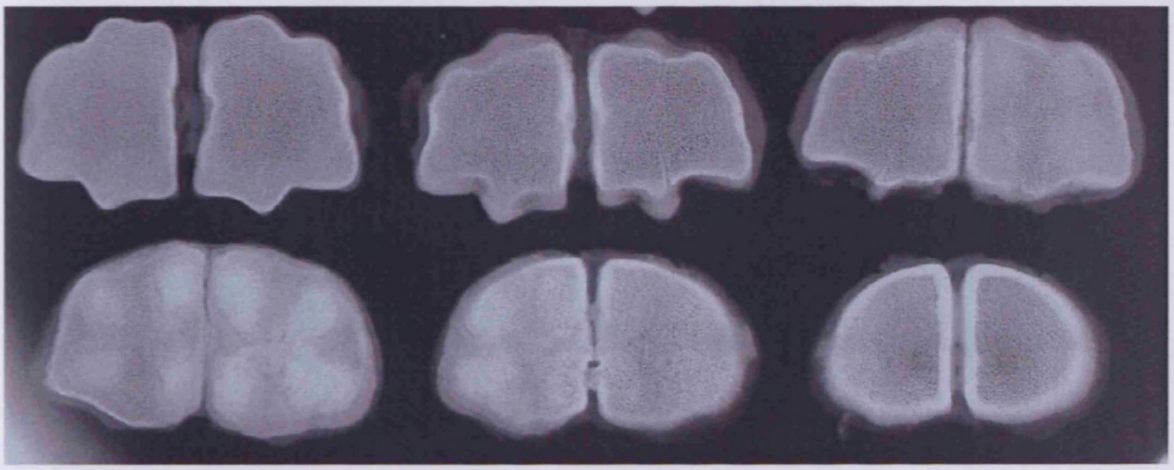

***Figure* 2c.8.** *Radiograph of the distal metacarpal from calf number 2, 4 months of age. Image was taken with 35 kV for 2 min 30 s. [A representation of 7 limbs analysed in this manner]*

***Figure* 2c.9.** *Digital image of human femoral head from a female patient, 80 years of age. Labelled sections correspond to location of section within the femora (1 being the most medial section). [A representation of 3 limbs analysed in this manner]*

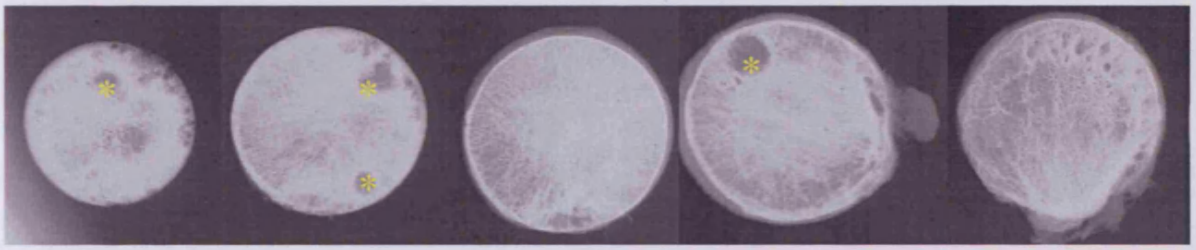

Figure 2c.10. *Radiograph of human femoral head from a female patient, 80 years of age. Image was taken with 35 kV for 2 min 30 s. Yellow star represents areas where cysts are present. [A representation of 3 limbs analysed in this manner]*

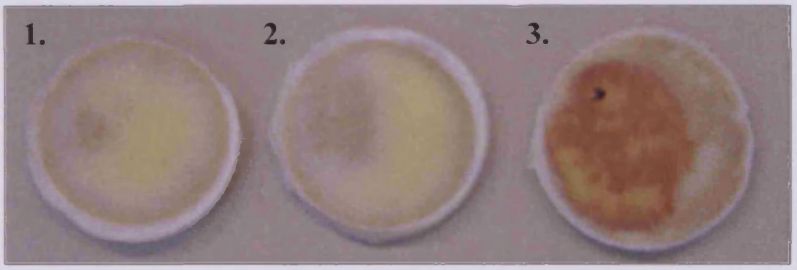

Figure 2c.11. *Digital image of human femoral head from a female patient, 69 years of age. Labelled sections correspond to location of section within the femora (1 being the most medial section). [A representation of 3 limbs analysed in this manner]*

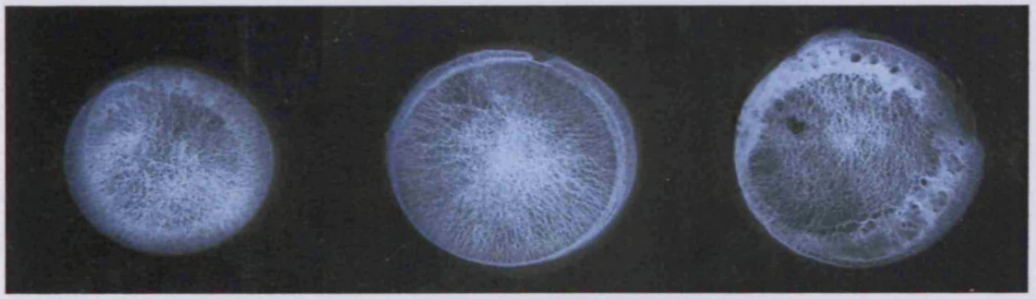

Figure 2c.12. *Radiograph of human femoral head from a female patient, 69 years of age. Image was taken with 35 kV for 2 min 30 s. [A representation of 3 limbs analysed in this manner]*

2c.ii. Bone Maceration

The maceration of the tissue allowed the samples to be preserved and also allowed the structure of the bone as a whole to be viewed without the presence of soft tissue.

Ovine tissue

The internal structure of the ovine femora can be seen in figure 2c.13. It is possible to see that it is not very big, and that it would not be possible to harvest many bone cores from the femoral head, unlike that of human tissue. The trabecular structure and orientation can also be observed. The trabeculae become much sparser as they get closer to the medullary cavity.

Bovine tissue

The internal structure of the bovine metacarpals can be seen in figure 2c.14. It is possible to see the growth plate present at the distal region (The growth plate is no longer present in the ovine and human tissue). Just above the growth plate a fracture can be seen (blue arrow). It is common for calves to fracture their metacarpals as this bone supports much of the animals' weight. The trabecular structure and orientation can also be observed. They become much sparser as they get closer to the medullary cavity.

Human tissue

The internal structure of the human proximal femora can be seen in figure 2c.15. It is possible to see that it is larger than the ovine bone. The trabecular structure and orientation can be observed and compared to that of an osteoporotic individual figure 2c.16. The trabeculae within the cancellous tissue are fewer in number and much thinner than in the previous example. This causes the tissue to become more fragile, leading to possible fractures.

Generally this technique has no advantages to be further utilised in Zetos experiments, though it does enhance the understanding of the system models.

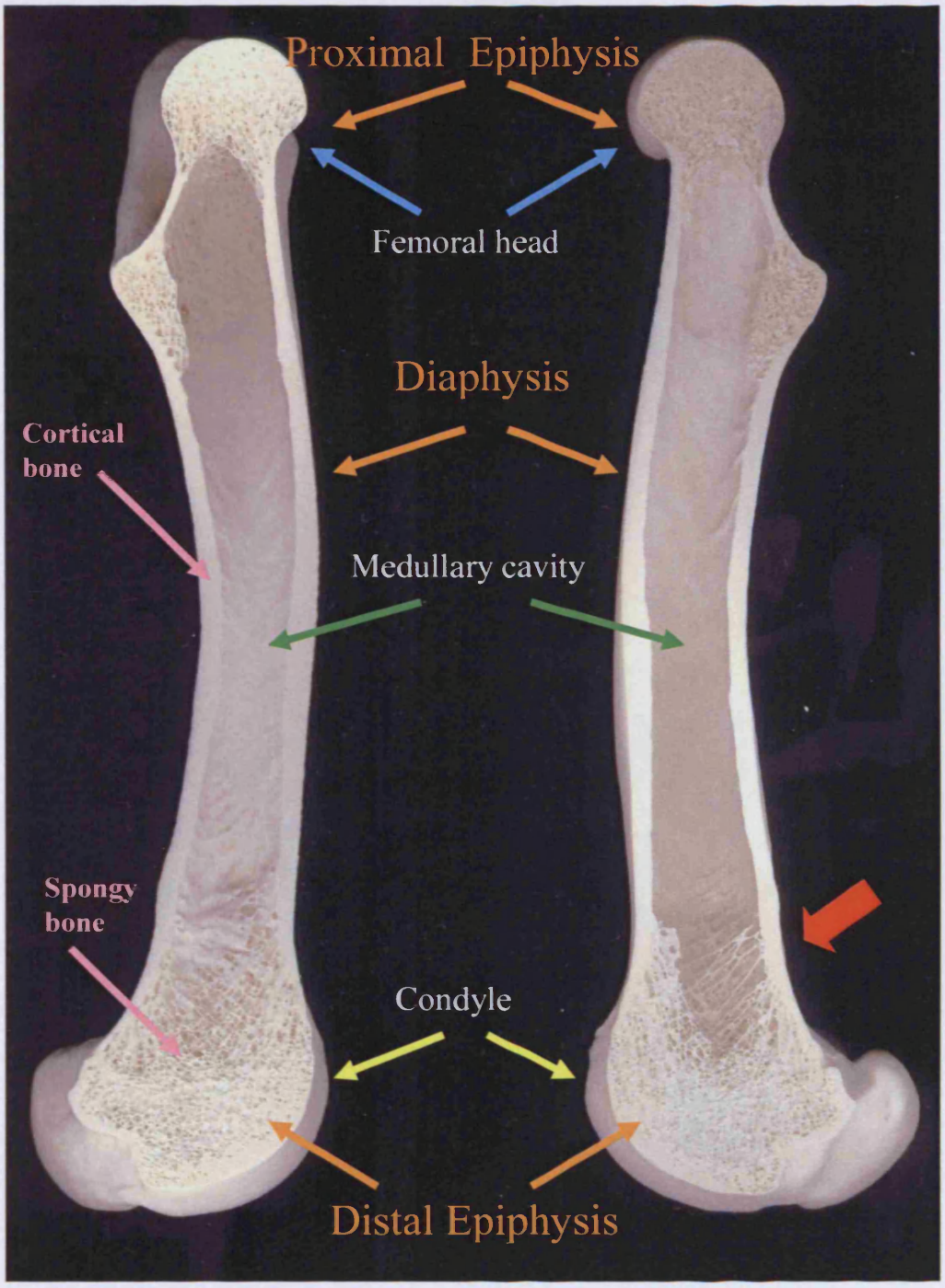

Figure 2c.13. *A transverse plane of the left femora of a 4-year-old ewe. It is possible to see that the femoral head is too small to harvest tissue from and that there is more area in the distal region. It is possible to see cortical tissue surrounding the outer surface of the bone and the cancellous tissue within. It is also possible to see the thinning of the cancellous tissue as it approaches the marrow cavity of the diaphysis (red arrow).*
[A representation of 2 limbs analysed in this manner]

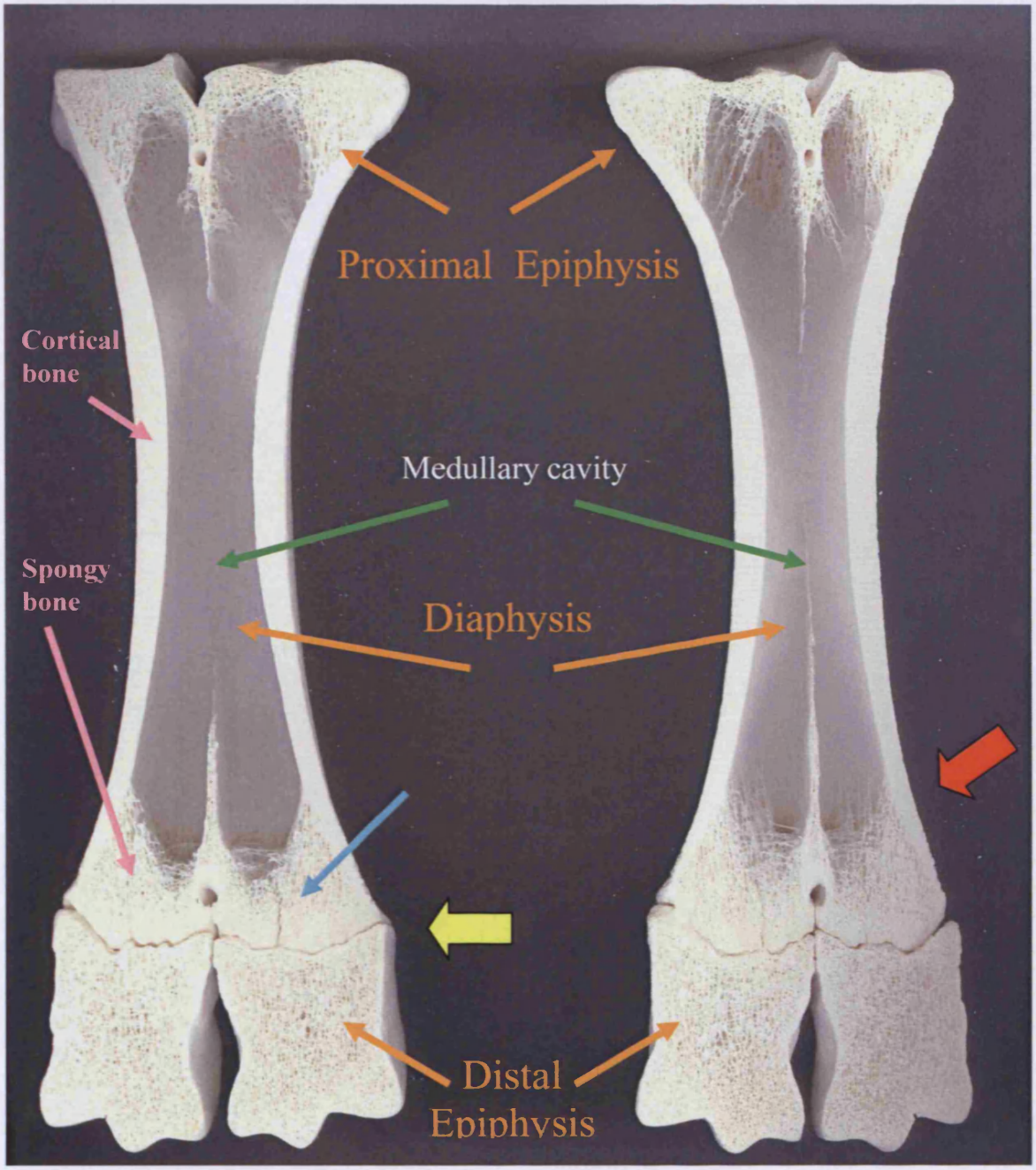

Figure 2c.14. *A transverse plane of the metacarpal of a 4-month -old calf. It is possible to see the growth plate above the distal condyle(yellow arrow). Cortical tissue surrounding the outer surface of the bone and the cancellous tissue within can be seen. It is also possible to see the thinning of the cancellous tissue as it approaches the marrow cavity (red arrow). A fracture can be seen above the growth plate (blue arrow). [A representation of 2 limbs analysed in this manner]*

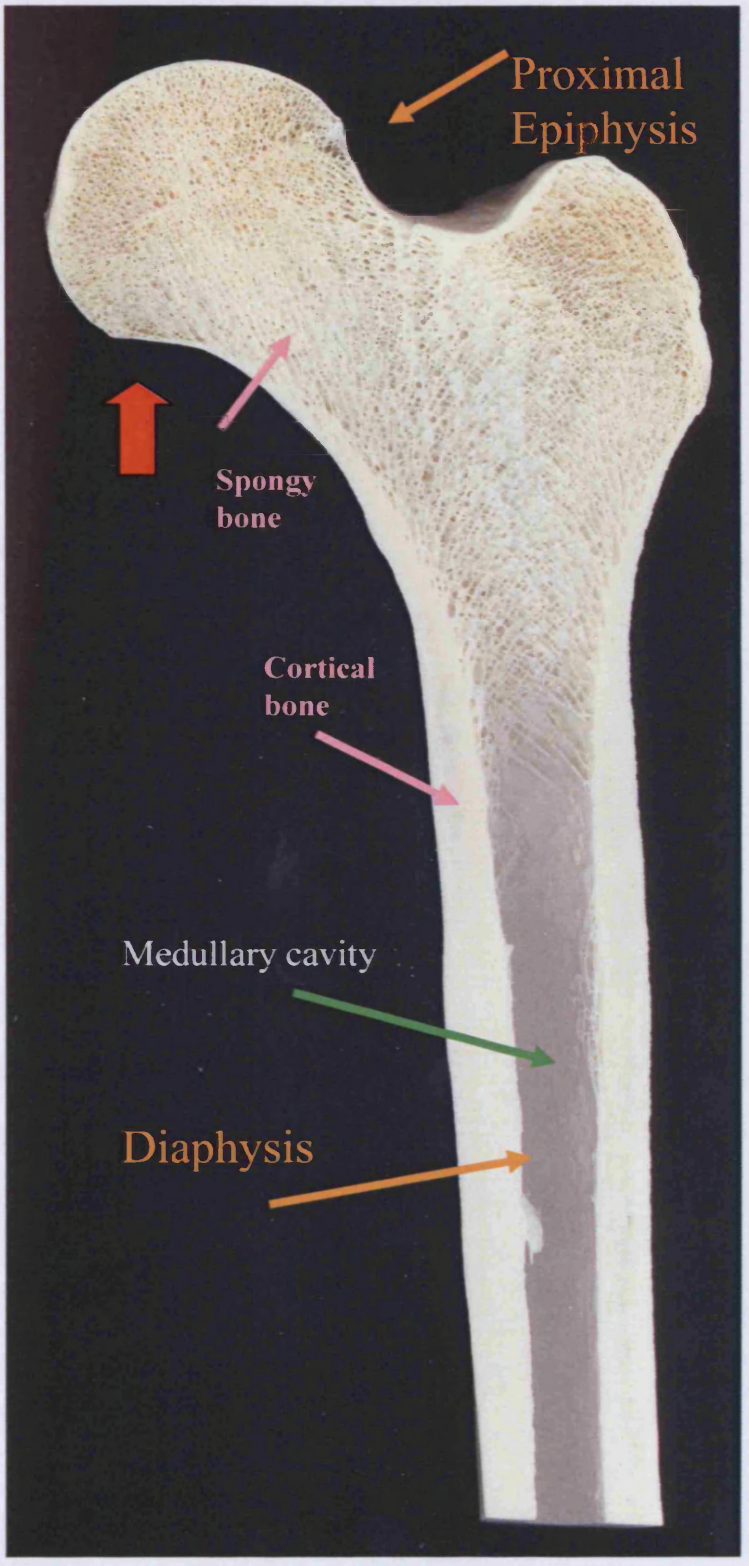

Figure 2c.15. *A frontal/coronal plane of the femur of average human. Cortical tissue surrounding the outer surface of the bone and the cancellous tissue within can be seen. It is also possible to see the orientation of the trabeculae (red arrow). [A representation of 2 limbs analysed in this manner]*

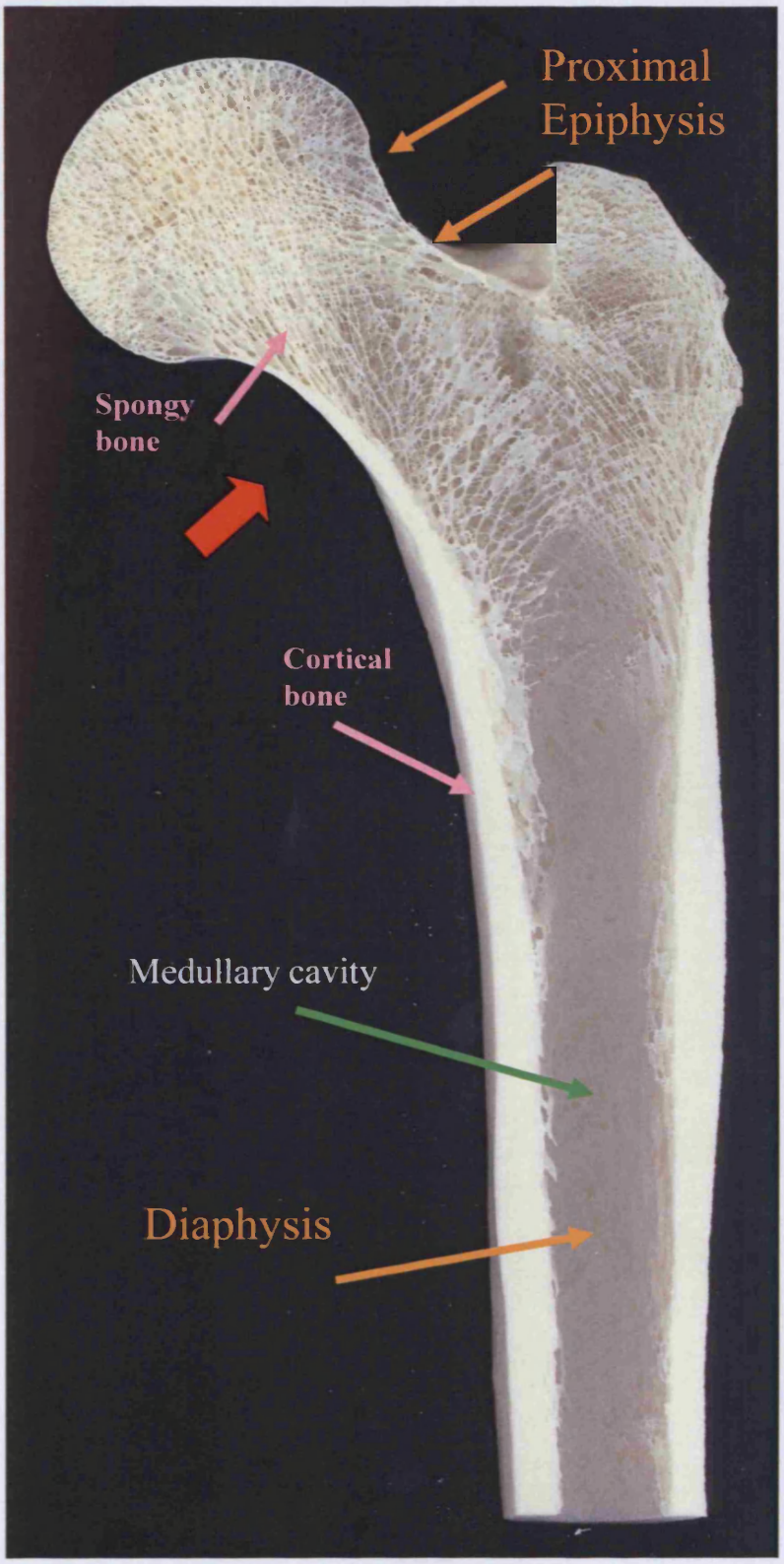

Figure 2c.16. *A frontal/coronal plane of the femur from an osteoporotic human. Cortical tissue surrounding the outer surface of the bone and the cancellous tissue within can be seen. There is a loss in trabeculae thickness and number (red arrow). [A representation of 2 limbs analysed in this manner]*

2c.iii Micro-computed Tomography (μCT)

This technique provided a 3D image of the cancellous bone explants. The aim of making μCT analysis on individual bone cores was to show an appreciation that each sample (whether located adjacent to each other or far apart) differed in their microarchitecture. Thus, implying that comparison of one sample to another is not as simple as it is with more homogenous tissue such as cartilage." For example, core 2G in figure 2c18 is composed or rod-like trabeculae while an adjacent core 2E is composed mainly of plate-like trabeculae. It was also possible to obtain detailed histomorphometrical data regarding bone volume, bone surface area, trabecular thickness and number. If this technique could be shown to maintain cells viable it would be ideal to use with cores cultured with the Zetos system before initiating of culture and after termination, though the resolution may be a little low to see differences.

Ovine Distal Femora

A total of 17 bone cores were obtained from the right distal femur of a 5-year-old ewe, number 166, 63 kg in weight. Histomorphometry conducted on each bone core (summarised in Table 2c.1). It was deduced that sample 1c had the highest bone volume (BV) at 91.7206 mm^2 and sample 2g the lowest with 25.7847 mm^2. The sample with the greatest bone surface as well as trabeculae number per mm^2 was explant 2f with 458.91 mm^2 and 2.0897 mm^2 respectively. The sample with least bone surface as well as least number of trabeculae per mm^2 was sample 2g with 477.64 mm^2 and 0.7723 mm^2 respectively. The thickest bone trabeculae were seen in sample 3e (0.1247 mm) and the thinnest were seen in sample 2d (0.0884 mm). Figure 2c.17 to 2c.19. depicts the anatomical location of each bone specimen as well as the μCT image generated for each explant.

Bovine Distal Metacarpal

A total of 18 bone cores were obtained from the distal metacarpal of a 4-month-old calf. Histomorphometry conducted on each bone core (summarised in Table 2c.2). It was deduced that sample 1.2 had the highest bone volume (BV) at 95.2985 mm^2 and sample 3.5 the lowest with 45.6236 mm^2. The sample with the greatest bone surface as well as trabeculae number per mm^2 was explant 1.3 with 1353.96 mm^2 and 2.2785mm^2 respectively. The sample with least bone surface as well as least number of trabeculae per

mm^2 was sample 3.5 with 810.21 mm^2 and 1.3635 mm^2 respectively. The thickest bone trabeculae were seen in sample 1.2 (0.1413 mm) and the thinnest were seen in sample 1.3 (0.1096 mm). Figure 2c.20 to 2c.22 depicts the anatomical location of each bone specimen as well as the μCT image generated for each explant.

Human Femoral Head

A total of 33 bone cores were obtained from the femoral head of an 80-year-old female patient. Histomorphometry conducted on each bone core (summarised in Table 2c.3). It was deduced that sample 2b had the highest bone volume (BV) at 130.562 mm^2 and sample 4e the lowest with 40.758 mm^2. The sample with the greatest bone surface as well as trabeculae number per mm^2 was explant 2g with 1041.37 mm^2 and 1.7312 mm^2 respectively. The sample with least bone surface as well as least number of trabeculae per mm^2 was sample 5c with 477.64 mm^2 and 0.7940 mm^2 respectively. The thickest bone trabeculae were seen in sample 5b (0.3266 mm) and the thinnest were seen in sample 3f (0.1377 mm). Figure 2c.23 to 2c.27 depicts the anatomical location of each bone specimen as well as the μCT image generated for each explant.

For each species, a normal distribution was assumed. The mean and standard deviation were taken for bone volume to tissue volume, trabecular number and trabecular thickness, which were then used to calculate a p-value for each number. Numbers in red were statistically high (in the upper tail), and the numbers in blue were too low (in the lower tail). For statistical analysis these samples were outliers and should be omitted from any studies.

Table 2c.1. Histomophometry of ovine explants

Sample	TV [mm³]	BV [mm³]	BV/TV [1]	BS [mm²]	BS/BV [1/mm]	SMI [1]	Tb.N [1/mm]	Tb.Th [mm]	Tb.Sp [mm]
1a	297.11	69.9598	0.2355	1169.58	16.7180	0.3002	1.9682	0.1196	0.3884
1b	297.11	55.7706	0.1877	909.95	16.3160	0.8785	1.5313	0.1226	0.5305
1c	297.11	91.7206	**0.3087**	1229.17	13.4013	-0.412	2.0685	0.1492	0.3342
1d	297.11	52.0346	0.1751	940.48	18.0741	0.8195	1.5827	0.1107	0.5212
2a	297.11	56.9606	0.1917	988.51	17.3543	0.5616	1.6635	0.1152	0.4859
2b	297.11	49.5441	0.1668	911.48	18.3973	0.7020	1.5339	0.1087	0.5432
2c	297.11	31.4849	0.1060	711.04	22.5837	1.3211	1.1966	0.0886	0.7471
2d	297.11	34.0250	0.1145	770.14	22.6344	1.1871	1.2960	0.0884	0.6832
2e	297.11	62.2548	0.2095	998.40	16.0374	0.3720	1.6802	0.1247	0.4705
2f	297.11	91.0736	**0.3065**	1241.74	13.6345	-0.340	2.0897	0.1467	0.3319
2g	297.11	25.7847	0.0868	458.91	17.7978	1.6821	**0.7723**	0.1124	1.1825
3a	297.11	55.8613	0.1880	806.65	14.4402	0.4159	1.3575	0.1385	0.5982
3b	297.11	36.4828	0.1228	645.16	17.6838	0.9933	1.0857	0.1131	0.8080
3c	297.11	59.1740	0.1992	1022.09	17.2726	0.5545	1.7200	0.1158	0.4656
3d	297.11	46.7725	0.1574	686.70	14.6816	0.5375	1.1556	0.1362	0.7291
3e	297.11	81.0111	0.2727	867.93	10.7137	-0.351	1.4606	**0.1867**	0.4980
3f	297.11	33.2928	0.1121	549.61	16.5083	1.0772	0.9249	0.1212	0.9600

Table 2c.2 Histomophometry of bovine explants.

Sample	TV [mm³]	BV [mm³]	BV/TV [1]	BS [mm²]	BS/BV [1/mm]	SMI [1]	Tb.N [1/mm]	Tb.Th [mm]	Tb.Sp [mm]
1.1	297.11	68.3927	0.2322	1139.80	16.5230	0.4257	1.9181	0.1210	0.4003
1.2	297.11	95.2985	**0.3207**	1349.07	14.1563	-0.415	**2.2703**	**0.1413**	0.2992
1.3	297.11	74.2075	0.2498	1353.96	18.2455	0.1932	**2.2785**	0.1096	0.3293
1.4	297.11	68.9743	0.2321	1244.25	18.0393	0.3071	2.0939	0.1109	0.3667
1.5	297.11	77.1911	0.2598	1265.77	16.3981	0.0465	2.1301	0.1220	0.3475
1.6	297.11	61.8266	0.2081	1075.32	17.3926	0.5275	1.8096	0.1150	0.4376
2.1	297.11	58.2555	0.1961	1017.85	17.4721	0.4493	1.7129	0.1145	0.4693
2.2	297.11	55.7814	0.1877	961.06	17.2290	0.7771	1.6173	0.1161	0.5022
2.3	297.11	64.0811	0.2157	1032.82	16.1173	0.3571	1.7381	0.1241	0.4513
2.4	297.11	46.1620	0.1554	901.85	19.5366	0.8372	1.5177	**0.1024**	0.5565
2.5	297.11	57.6059	0.1939	976.75	16.9557	0.4919	1.6437	0.1180	0.4904
2.6	297.11	50.1814	0.1689	881.90	17.5742	0.8589	1.4841	0.1138	0.5600
3.1	297.11	52.2430	0.1758	879.03	16.8258	0.7371	1.4793	0.1189	0.5571
3.2	297.11	49.7156	0.1673	877.38	17.6480	0.8102	1.4765	0.1133	0.5639
3.3	297.11	49.6624	0.1671	881.21	17.7440	0.7151	1.4830	0.1127	0.5616
3.4	297.11	53.2064	0.1791	915.04	17.1979	0.6461	1.5399	0.1163	0.5331
3.5	297.11	45.6236	0.1536	810.21	17.7585	0.8873	1.3635	0.1126	0.6208
3.6	297.11	49.5774	0.1669	843.30	17.0097	0.6702	1.4192	0.1176	0.5871

TV = *tissue volume;* **BV** = *bone volume;* **BV/TV** = *bone volume to tissue volume;* **BS** = *bone surface;* **BS/BV** = *bone surface to volume ratio;* **SMI** = *structure model index ;* **Tb.N** = *trabecular number,* **Tb.Th** = *trabecular thickness;* **Tb.Sp** = *trabecular separation.*

Table 2c.3. Histomophometry of human explants.

Sample	TV [mm^3]	BV [mm^3]	BV/TV [1]	BS [mm^2]	BS/BV [1/mm]	SMI [1]	Tb.N [1/mm]	Tb.Th [mm]	Tb.Sp [mm]
1a	300.77	46.3059	0.1540	671.58	14.5032	1.7680	1.1164	0.1379	0.7578
1b	300.77	75.8536	0.2522	931.43	12.2793	0.4890	1.5484	0.1629	0.4829
1c	300.77	91.672	0.3048	675.10	7.3643	-0.753	1.1223	0.2716	0.6195
2a	300.77	85.002	0.2826	949.01	11.1645	0.3721	1.5776	0.1791	0.4547
2b	300.77	130.562	**0.4341**	987.73	7.5652	-1.311	1.6420	0.2644	0.3446
2c	300.77	88.9799	0.2958	935.39	10.5123	0.2882	1.5550	0.1903	0.4528
2d	300.77	60.4021	0.2008	839.99	13.9066	1.0500	1.3964	0.1438	0.5723
2e	300.77	102.05	0.3393	940.74	9.2181	0.3081	1.5639	0.2170	0.4225
2f	300.77	93.8252	0.3120	867.16	9.2423	0.1993	1.4416	0.2164	0.4773
2g	300.77	98.4857	0.3274	1041.37	10.5738	0.1651	1.7312	0.1891	0.3885
3a	300.77	103.875	0.3454	1016.70	9.7877	-0.058	1.6902	0.2043	0.3873
3b	300.77	96.4367	0.3206	995.67	10.3246	0.1776	1.6552	0.1937	0.4104
3c	300.77	93.9409	0.3123	912.23	9.7107	0.1738	1.5165	0.2060	0.4535
3d	300.77	94.1863	0.3132	740.20	7.8589	0.4710	1.2305	0.2545	0.5582
3e	300.77	48.6506	0.1618	688.55	14.1529	1.4158	1.1446	0.1413	0.7323
3f	300.77	59.2863	0.1971	860.83	14.5199	0.9227	1.4310	0.1377	0.5610
3g	300.77	74.5037	0.2477	848.33	11.3864	0.7088	1.4103	0.1756	0.5334
3h	300.77	94.3409	0.3137	928.90	9.8462	0.2174	1.5442	0.2031	0.4445
4a	300.77	95.7813	0.3185	889.12	9.2828	0.2038	1.4781	0.2155	0.4611
4b	300.77	80.1123	0.2664	799.63	9.9813	0.8944	1.3293	0.2004	0.5519
4c	300.77	104.744	0.3483	870.58	8.3115	0.1061	1.4473	0.2406	0.4503
4d	300.77	45.4915	0.1513	558.43	12.2755	1.7011	**0.9283**	0.1629	0.9143
4e	300.77	40.7582	**0.1355**	585.24	14.3588	1.5891	0.9729	0.1393	0.8886
4f	300.77	55.2601	0.1837	790.42	14.3036	1.3518	1.3140	0.1398	0.6212
4g	300.77	96.8529	0.3220	851.73	8.7940	-0.043	1.4159	0.2274	0.4788
5a	300.77	62.1771	0.2067	749.90	12.0606	1.3570	1.2466	0.1658	0.6363
5b	300.77	100.229	0.3332	613.84	6.1244	-0.552	1.0204	**0.3266**	0.6534
5c	300.77	45.4433	0.1511	477.64	10.5108	2.1765	**0.7940**	0.1903	1.0691
5d	300.77	47.1688	0.1568	618.39	13.1101	1.4033	1.0280	0.1526	0.8202
5e	300.77	88.5557	0.2944	799.20	9.0249	0.5418	1.3286	0.2216	0.5311
5f	300.77	81.8441	0.2721	829.32	10.1330	0.6704	1.3787	0.1974	0.5280
5g	300.77	81.2103	0.2700	738.85	9.0980	0.5307	1.2283	0.2198	0.5943
5h	300.77	92.7385	0.3083	670.44	7.2294	0.7187	1.1145	**0.2766**	0.6206

TV = *tissue volume;* **BV** = *bone volume;* **BV/TV** = *bone volume to tissue volume;* **BS** = *bone surface;* **BS/BV** = *bone surface to volume ratio;* **SMI** = *structure model index ;* **Tb.N** = *trabecular number;* **Tb.Th** = *trabecular thickness;* **Tb.Sp** = *trabecular separation.*

Different colours represent the different plane the cores were harvested from. Numbers highlighted in red were regarded as statistically high, while numbers in blue were regarded as significantly low.

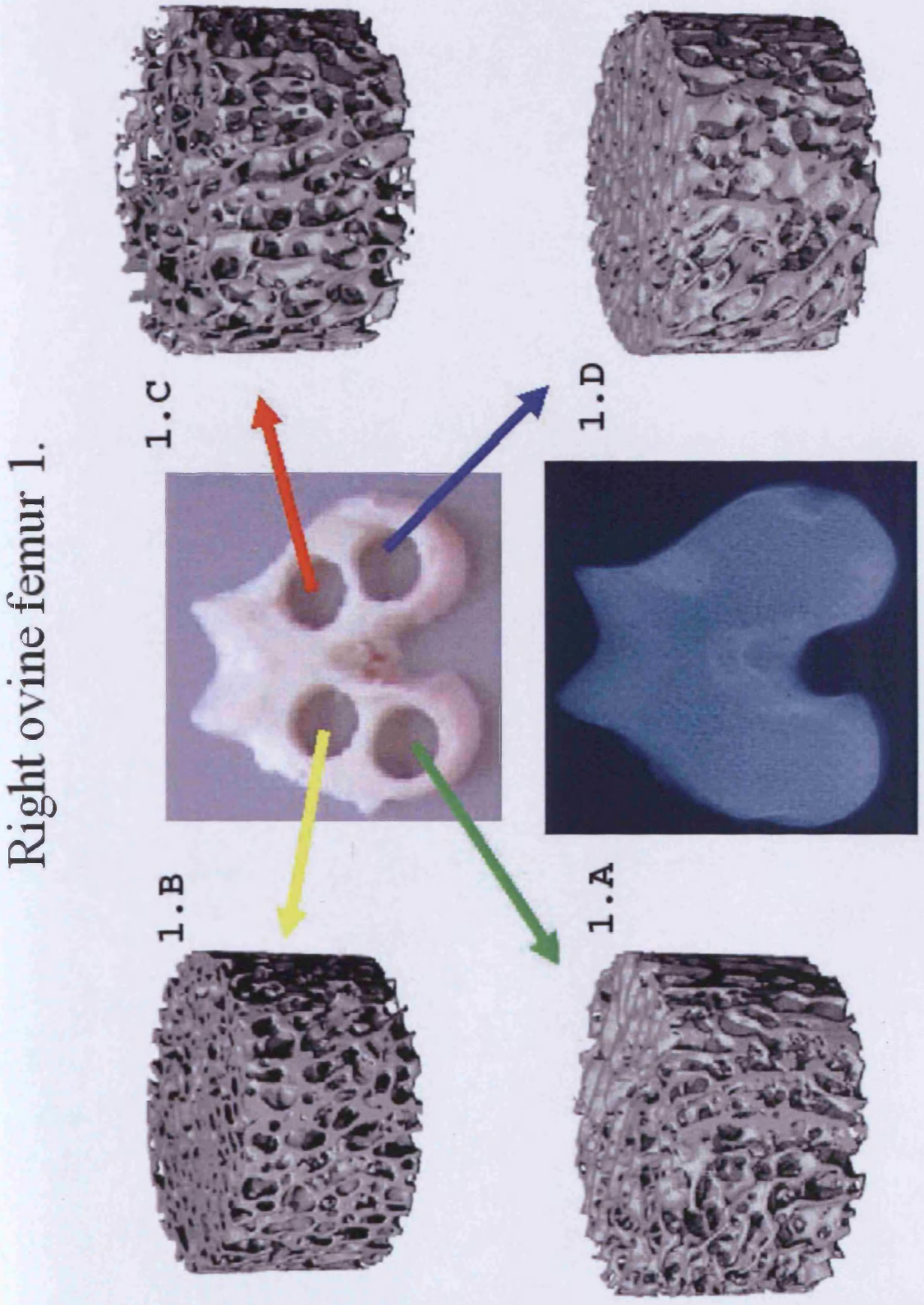

Figure 2c.17. *Architecture of bone cores harvested from the right distal femur of a 5 -year -old ewe, number 166, 63 kg in weight.*
[A representation of 35 cores from 2 limbs analysed in this manner]

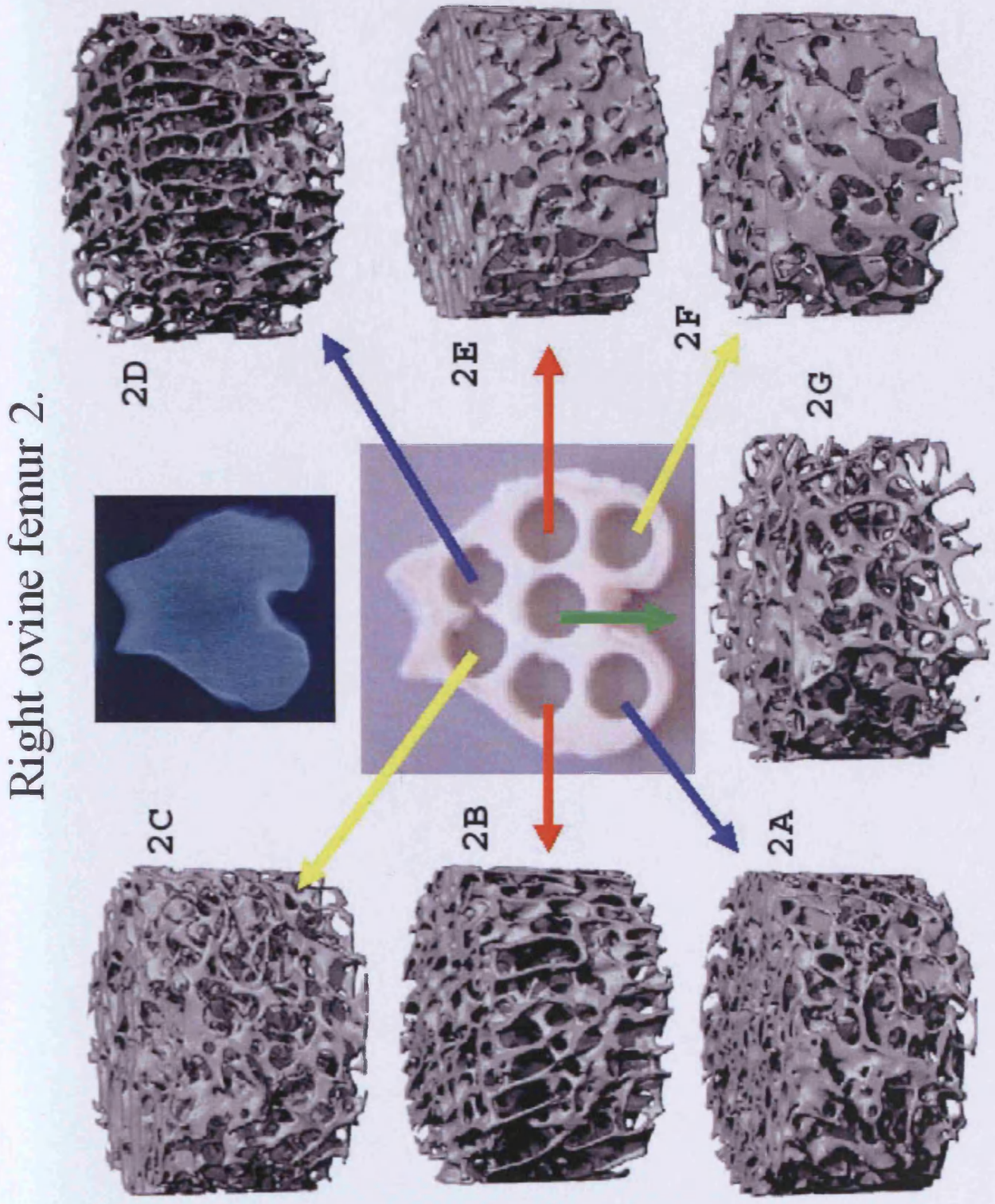

Figure 2c.18. *Architecture of bone cores harvested from the right distal femur of a 5-year -old ewe, number 166, 63 kg in weight.*
[A representation of 35 cores from 2 limbs analysed in this manner]

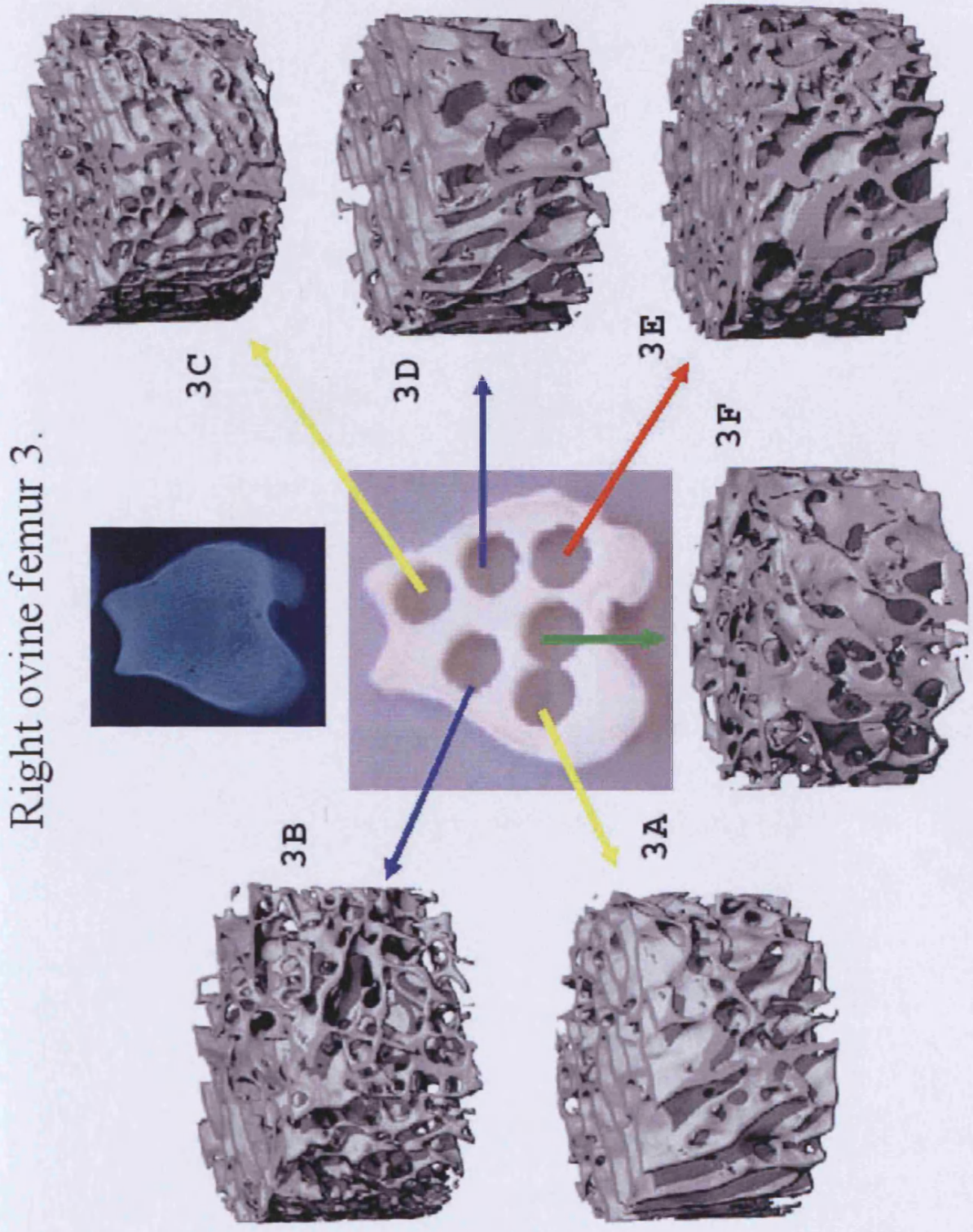

Figure 2c.19. *Architecture of bone cores harvested from the right distal femur of a 5-year -old ewe, number 166, 63 kg in weight.*
[A representation of 35 cores from 2 limbs analysed in this manner]

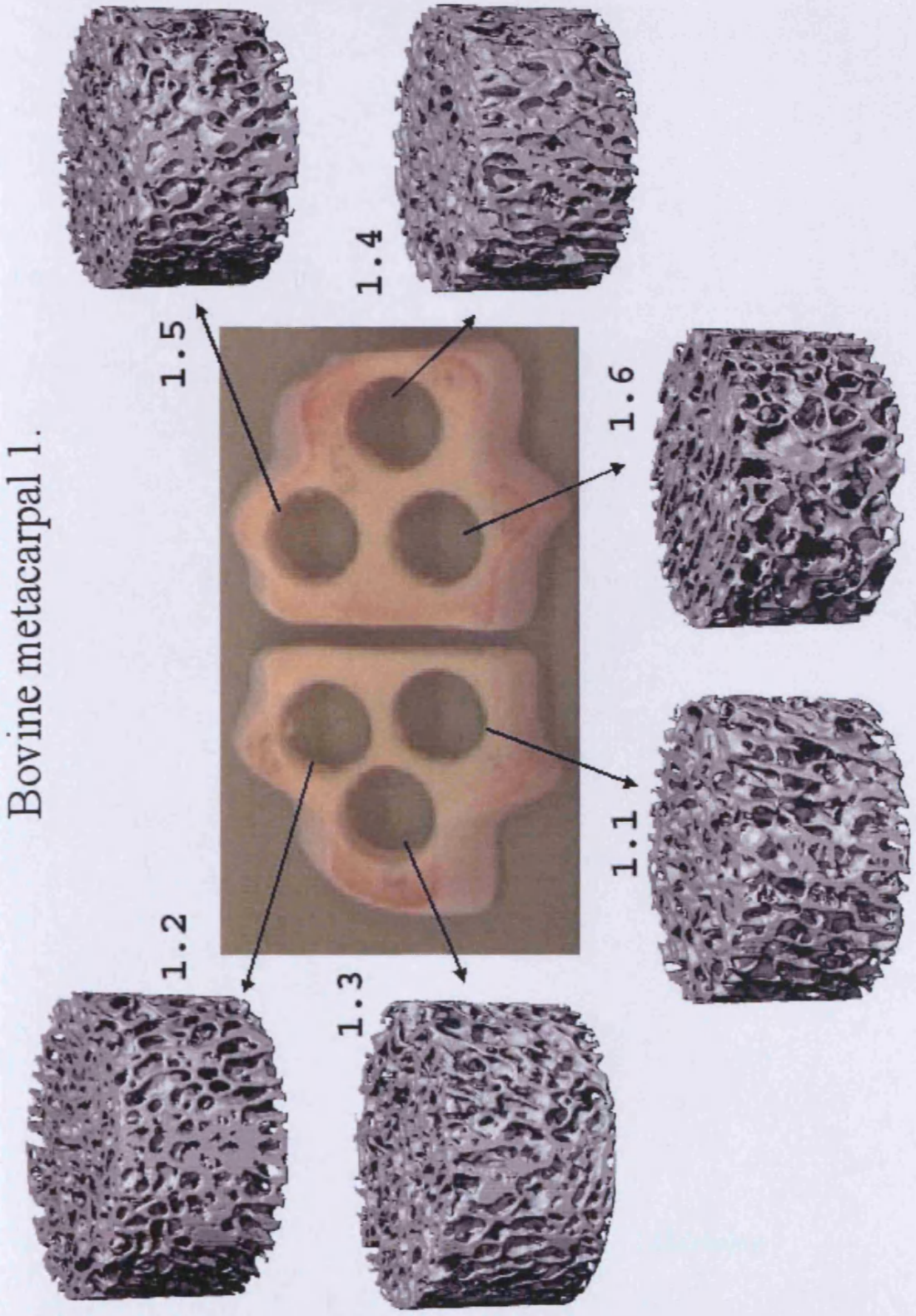

Figure 2c.20. *Architecture of bone cores harvested from the distal metacarpal of a 4-month-old calf. [A representation of 18 cores from 1 limbs analysed in this manner]*

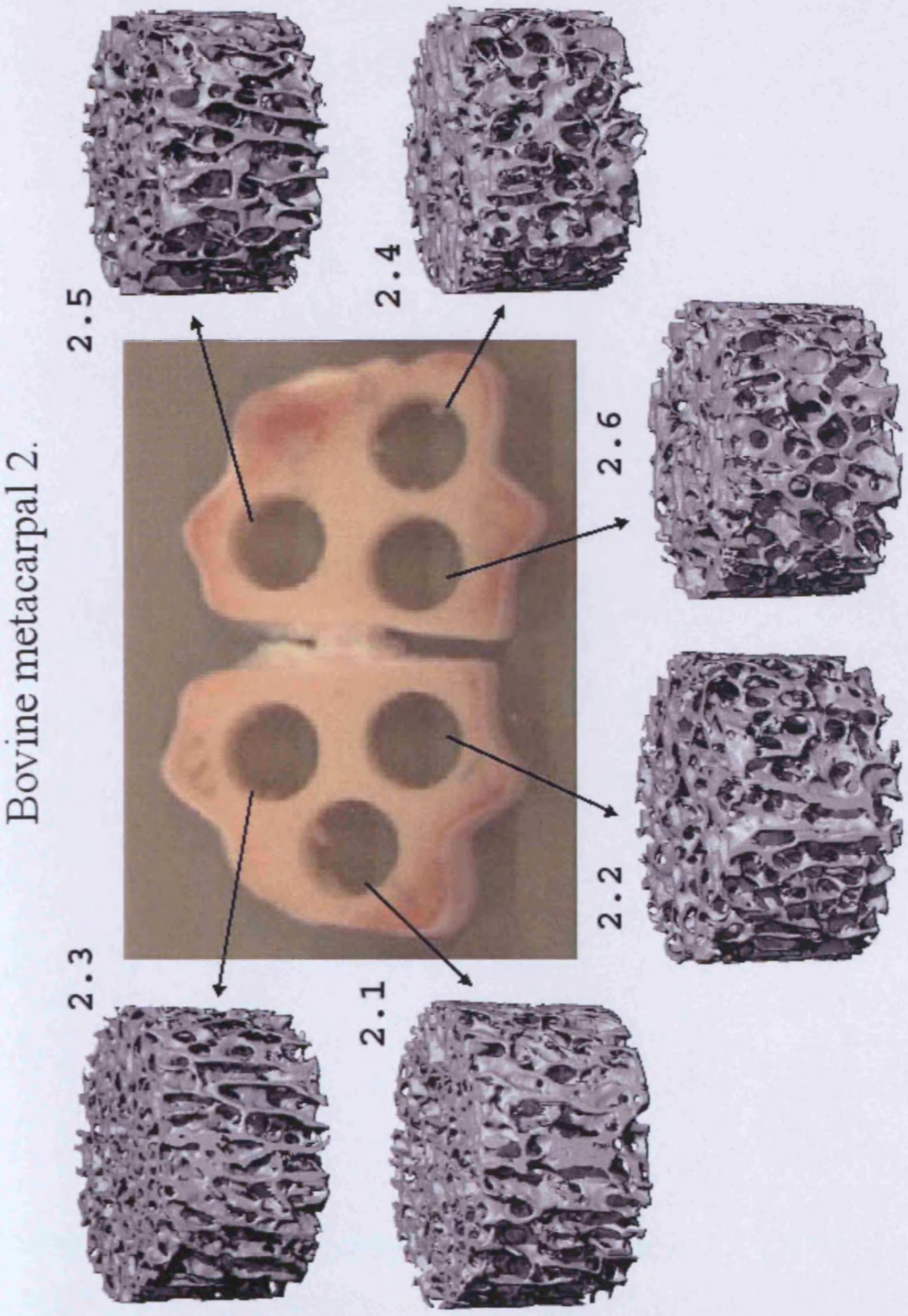

Figure 2c.21. *Architecture of bone cores harvested from the distal metacarpal of a 4-month-old calf. [A representation of 18 cores from 1 limbs analysed in this manner]*

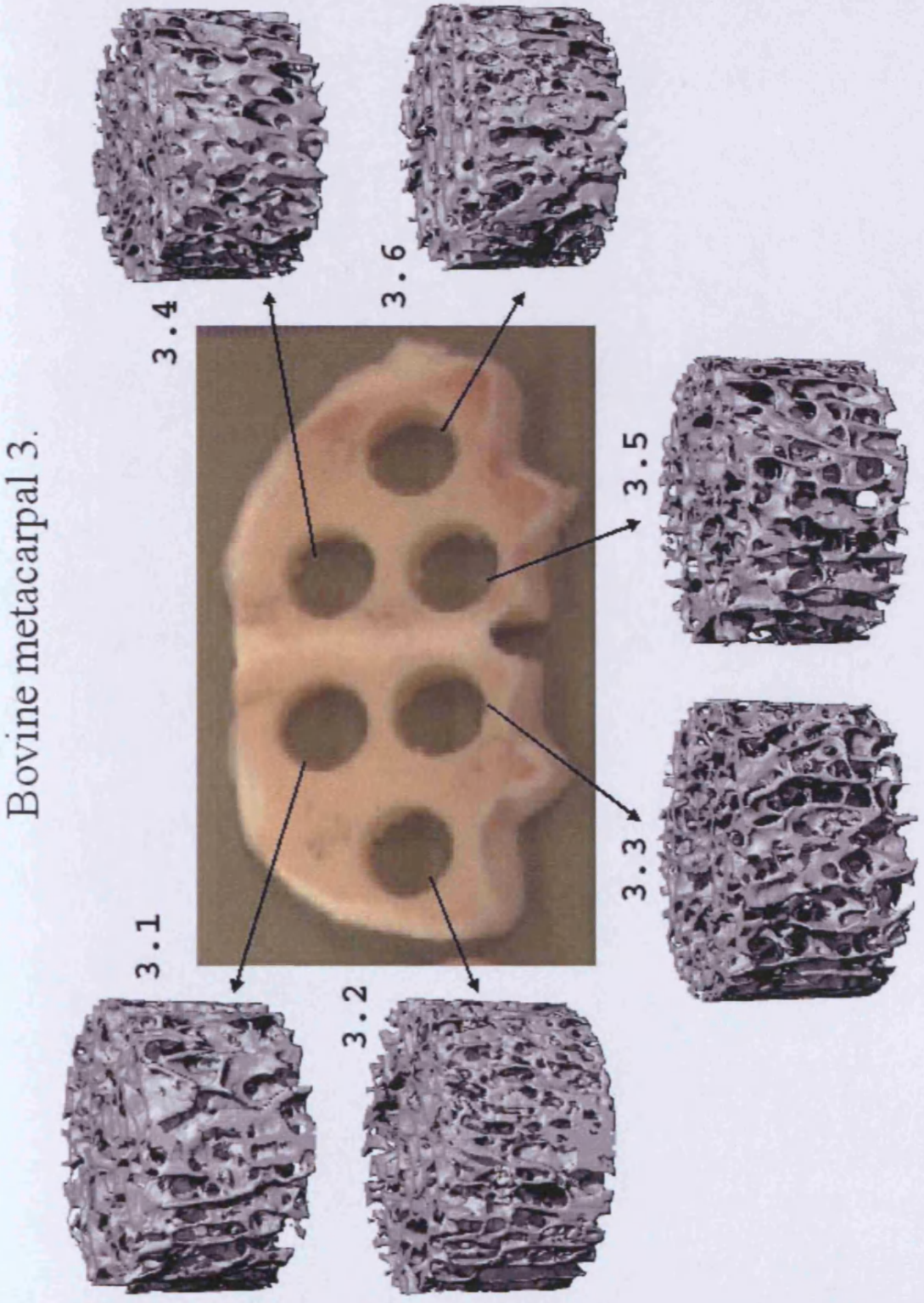

Figure 2c.22. *Architecture of bone cores harvested from the distal metacarpal of a 4-month-old calf. [A representation of 18 cores from 1 limbs analysed in this manner]*

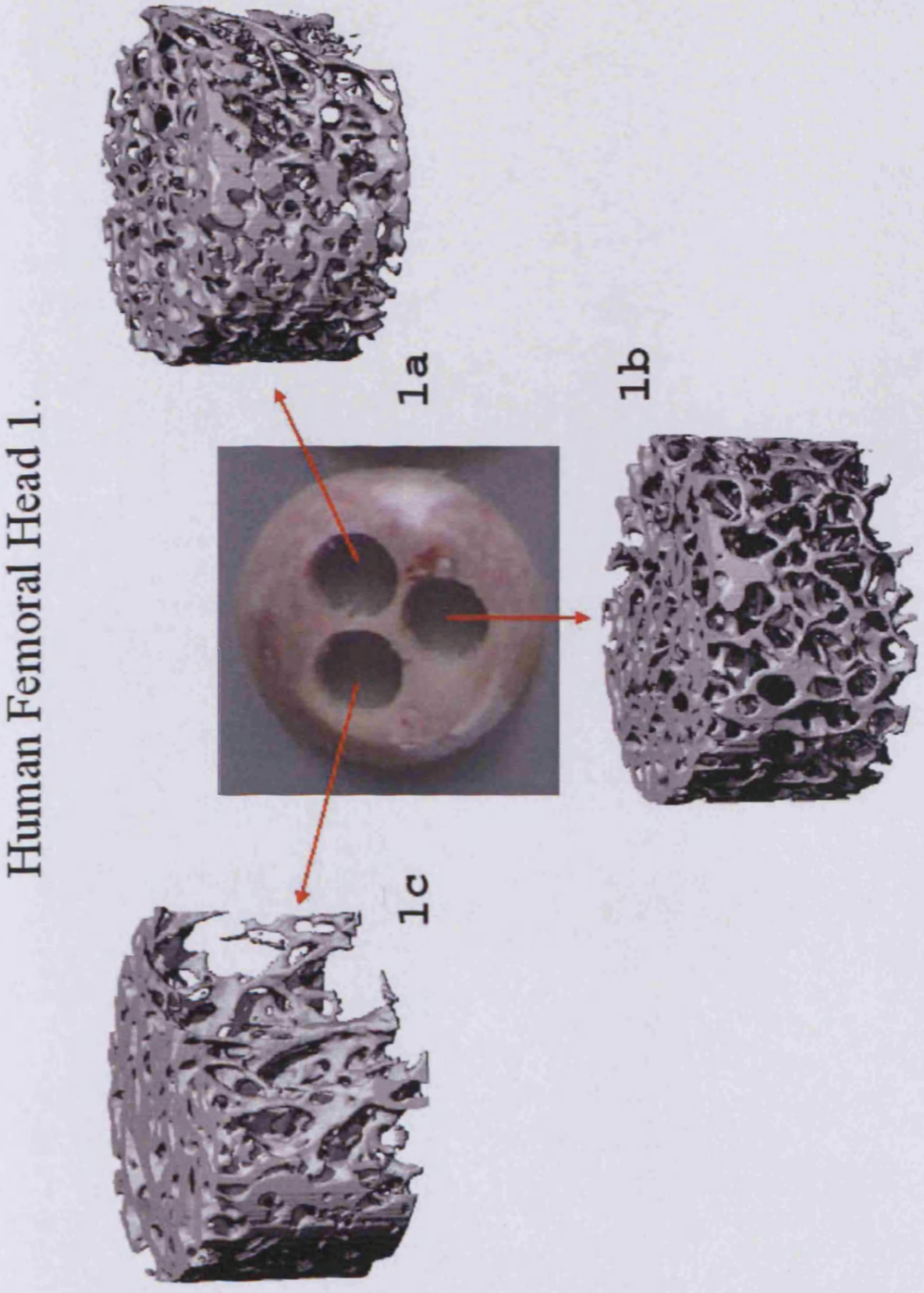

Figure 2c.23. *Architecture of bone cores harvested from the femoral head of an 80-year-old female patient. [A representation of 33 cores from 1 limbs analysed in this manner]*

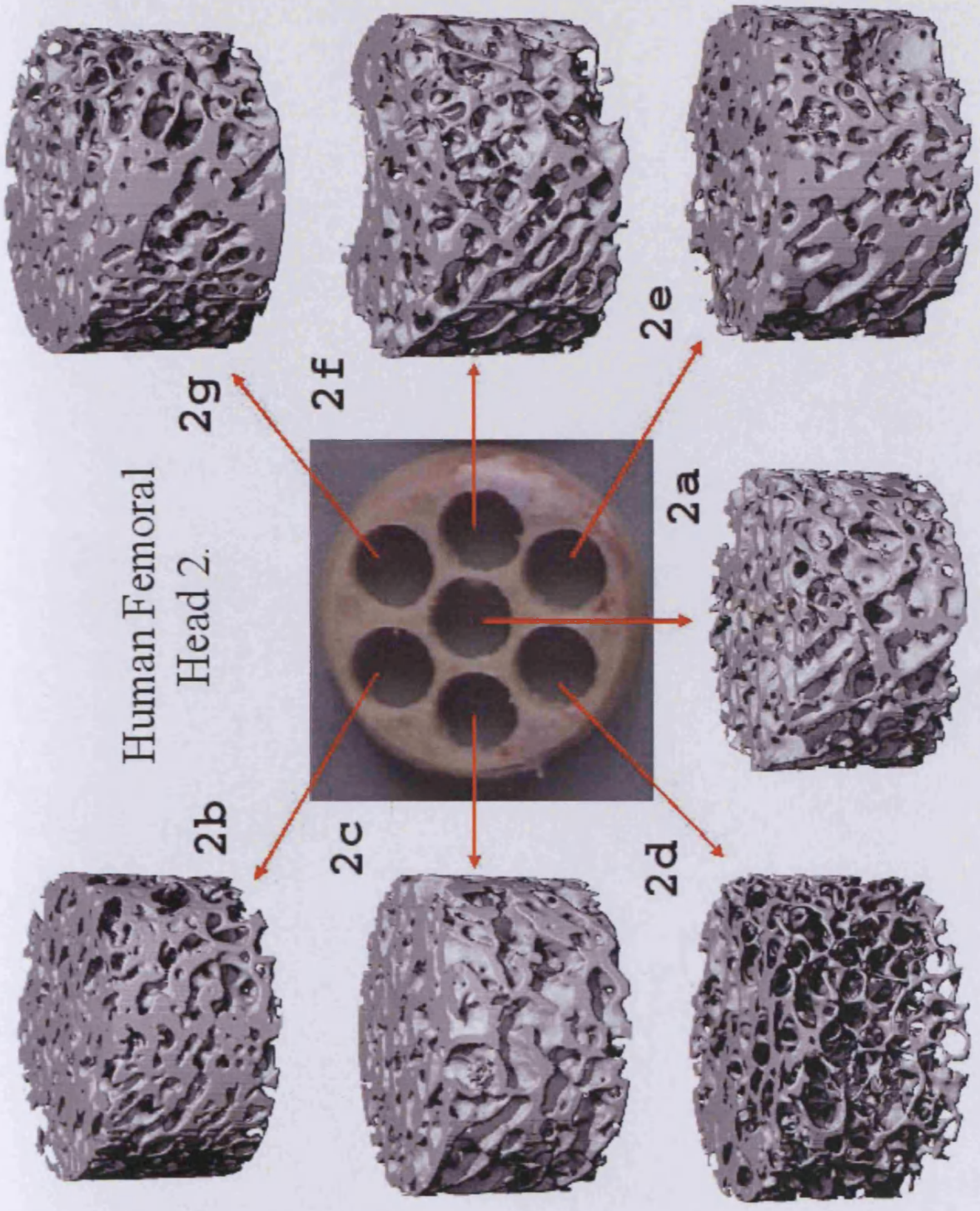

Figure 2c.24. *Architecture of bone cores harvested from the femoral head of an 80-year-old female patient. [A representation of 33 cores from 1 limbs analysed in this manner]*

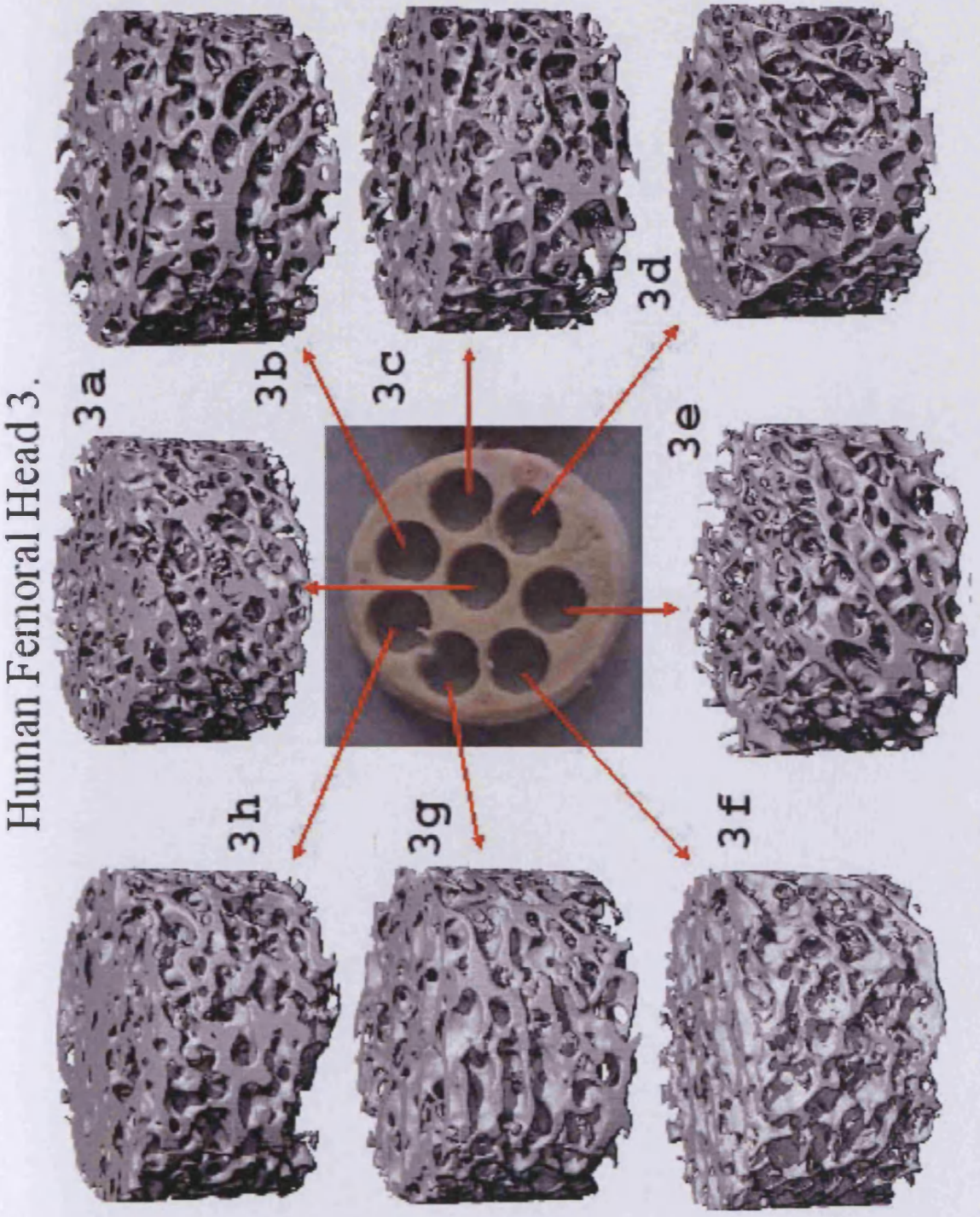

Figure 2c.25. *Architecture of bone cores harvested from the femoral head of an 80-year-old female patient. [A representation of 33 cores from 1 limbs analysed in this manner]*

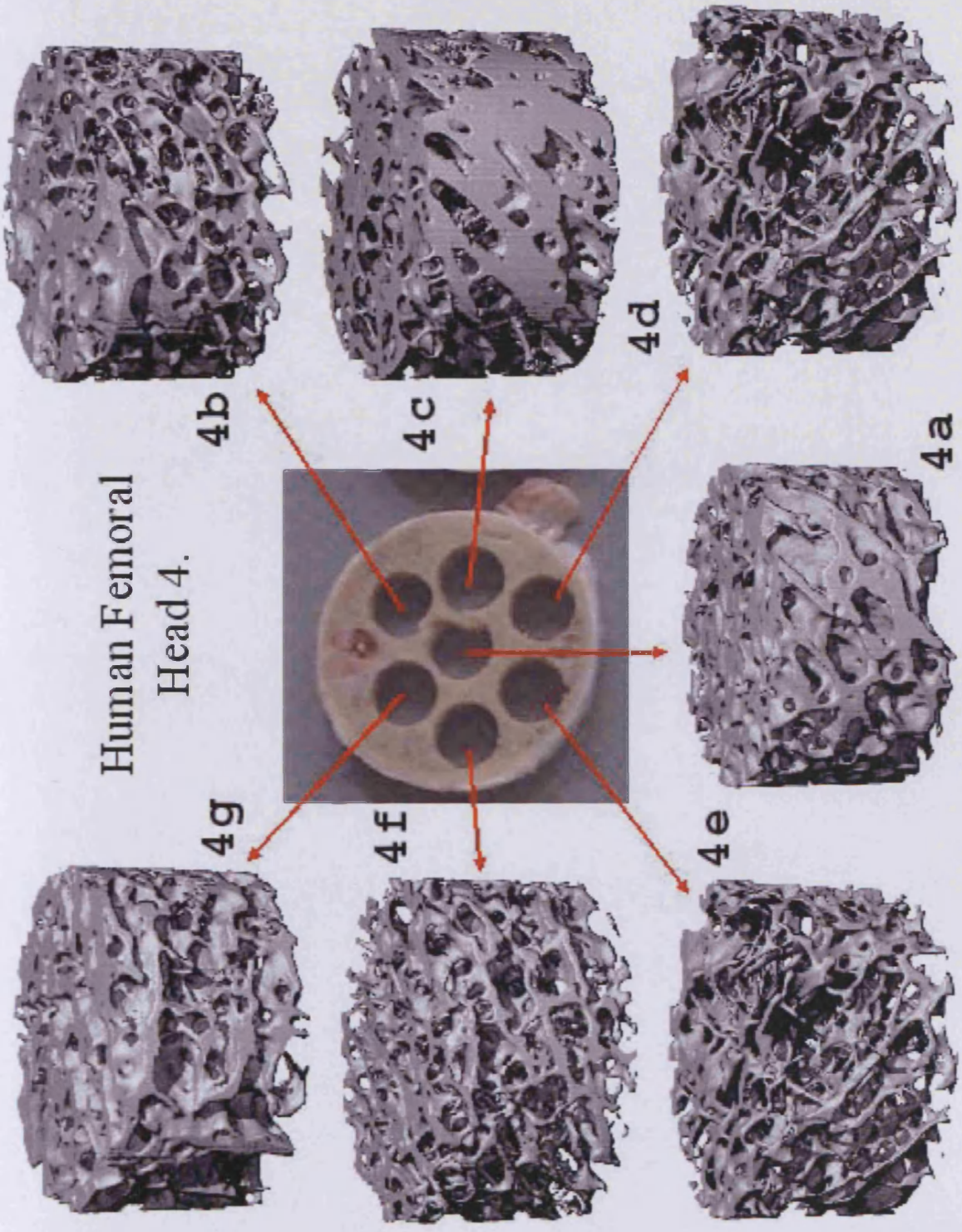

Figure 2c.26. *Architecture of bone cores harvested from the femoral head of an 80-year-old female patient. [A representation of 33 cores from 1 limbs analysed in this manner]*

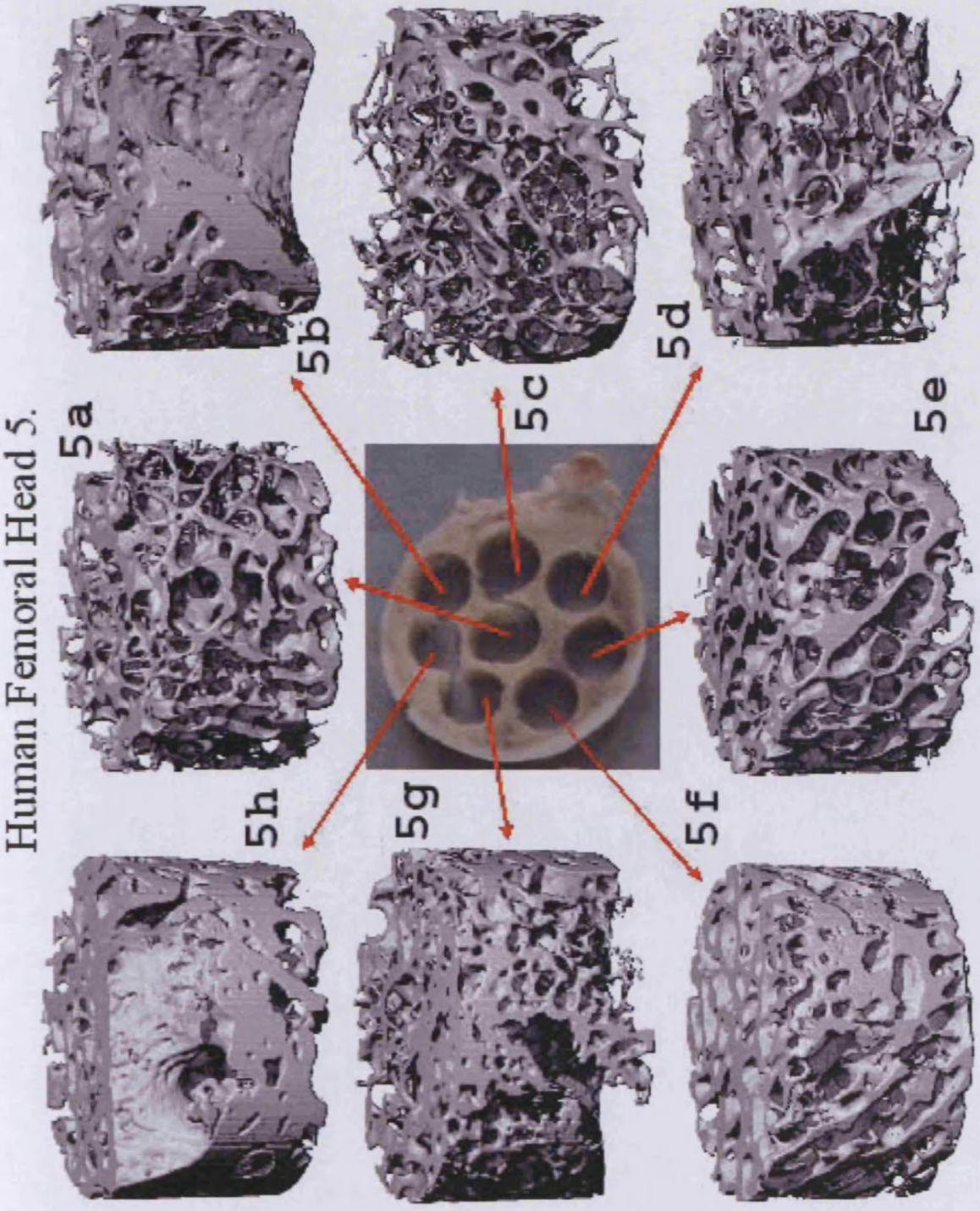

Figure 2c.27. *Architecture of bone cores harvested from the femoral head of an 80-year-old female patient. [A representation of 33 cores from 1 limbs analysed in this manner]*

2c.iv. Scanning Electron Microscopy (SEM)

The SEM allowed the trabecular architecture to be viewed. However, this technique did not provide any additional information than that gained from the other techniques employed. It was inferior to the data gained from μCT, regarding non visual information. One advantage was the ability to zoom into interesting areas, for example osteocyte lacunae. It was also possible to see the canaliculi and convert the image to obtain a 3D view of depth into the lacunae (Fig.2c.31).

Ovine Distal Femora

From the images produced by the SEM it was possible to see that the ovine tissue was composed of a plate-like arrangement of trabeculae, with very few rod shaped structures (Fig.2c.28). Numerous osteocyte lacunae could be observed within the calcified matrix. This observation was limited to a small area of tissue, due to the nature of the technique.

Bovine Distal Metacarpal

From the images produced by the SEM it was possible to see that the bovine tissue was also composed of a plate-like arrangement of trabeculae, with very few rod shaped structures (Fig.2c.29). Numerous osteocyte lacunae could be observed within the calcified matrix. This observation was limited to a small area of tissue, due to the nature of the technique.

Human Femoral Head

From the images produced by the SEM it was possible to see that the human tissue was composed of a rod-like arrangement of trabeculae, with very few plate-like structures (Fig.2c.30). Numerous osteocyte lacunae could be observed within the calcified matrix. This observation was limited to a small area of tissue, due to the nature of the technique.

CARDIFF UNIVERSITY

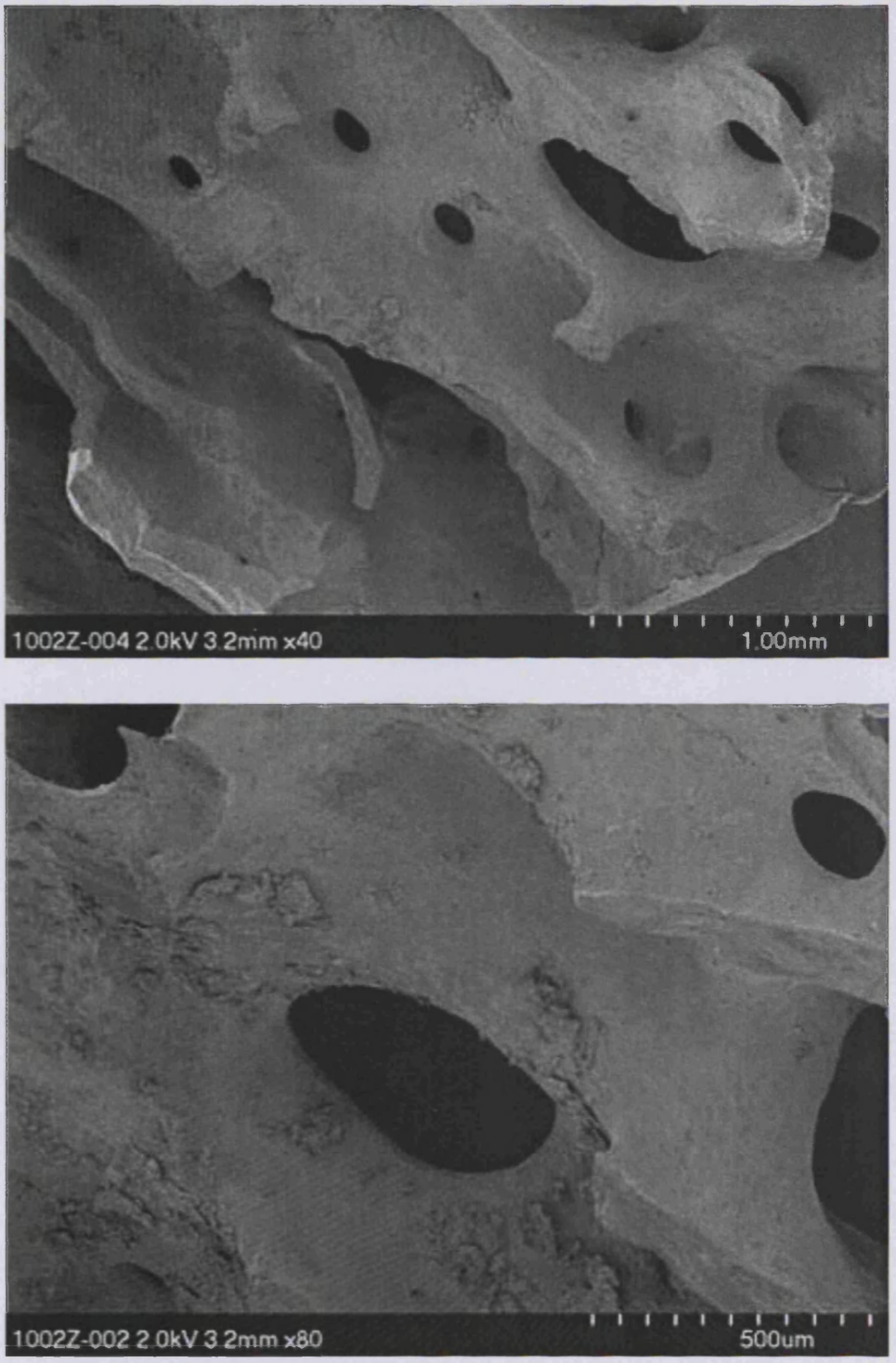

Figure 2c.28. *Images of ovine tissue (5-year-old, 61kg). It is possible to see that the calcified cancellous tissue is composed mainly of plate-like trabeculae. [A representation of 2 cores from 1 limbs analysed in this manner]*

Figure 2c.29. *Images of bovine tissue (4-month-old). It is possible to see that the calcified cancellous tissue is composed mainly of plate-like trabeculae. [A representation of 2 cores from 1 limbs analysed in this manner]*

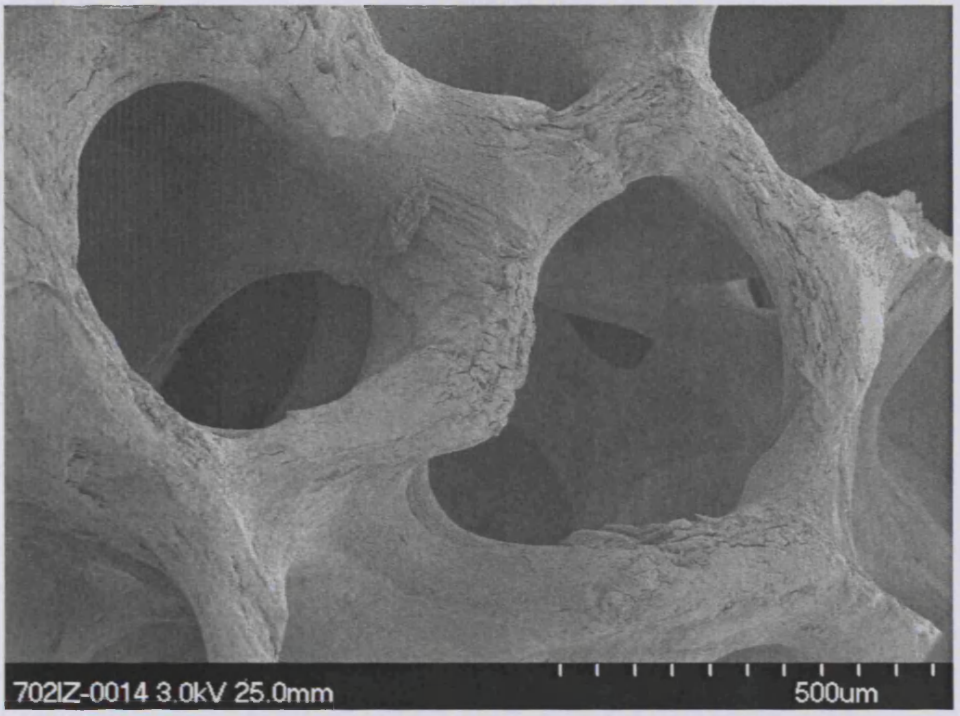

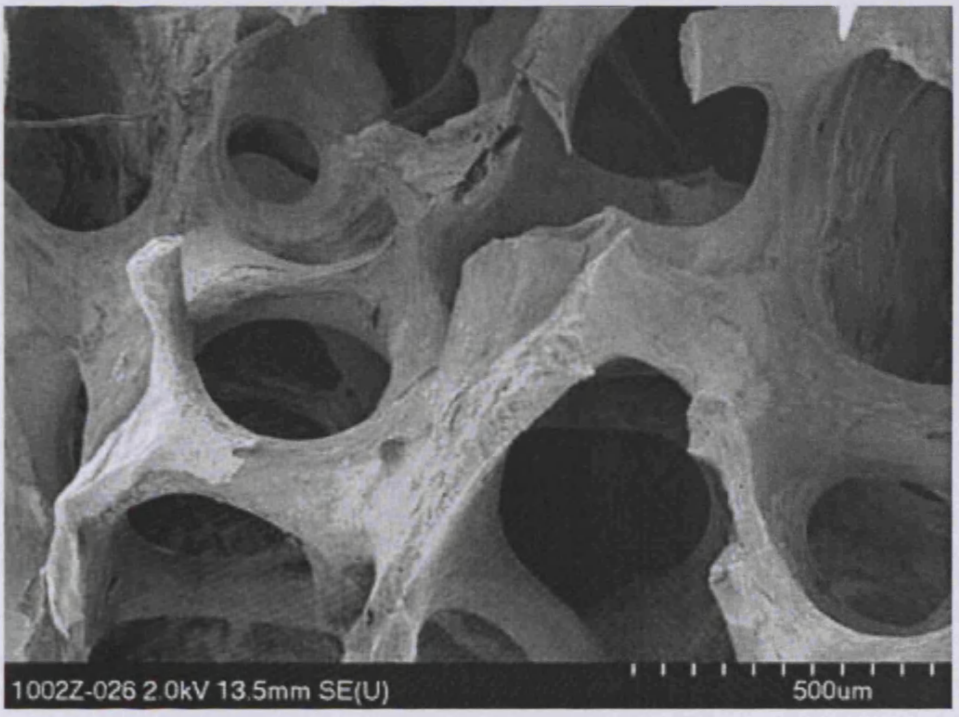

Figure 2c.30. *Images of human tissue (71-year-old female). It is possible to see that the calcified cancellous tissue is composed mainly of rod-like trabeculae. [A representation of 2 cores from 1 limbs analysed in this manner]*

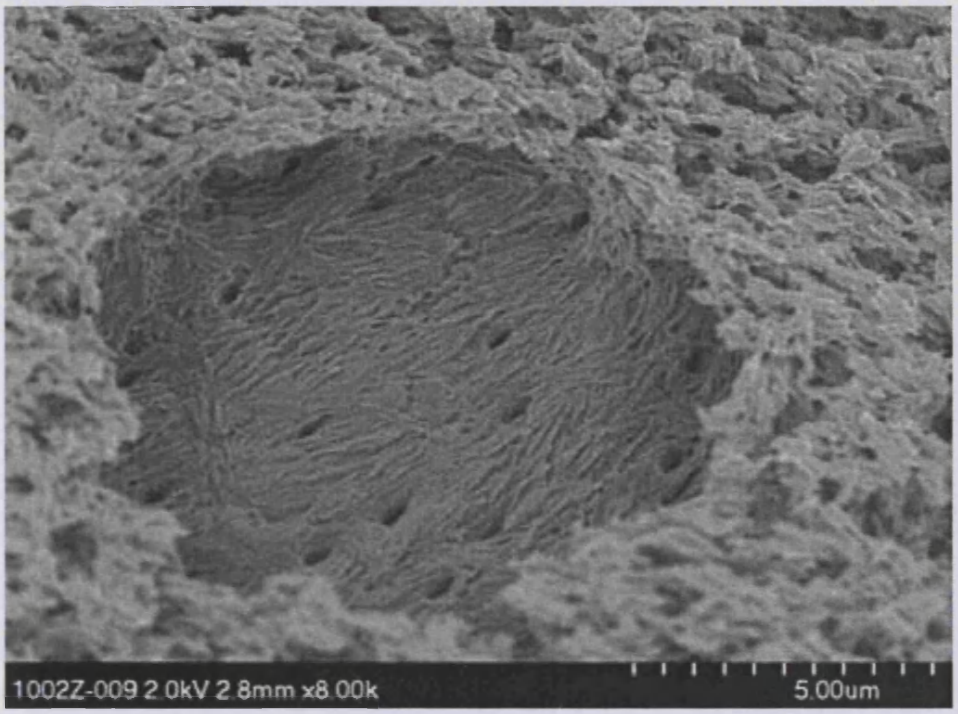

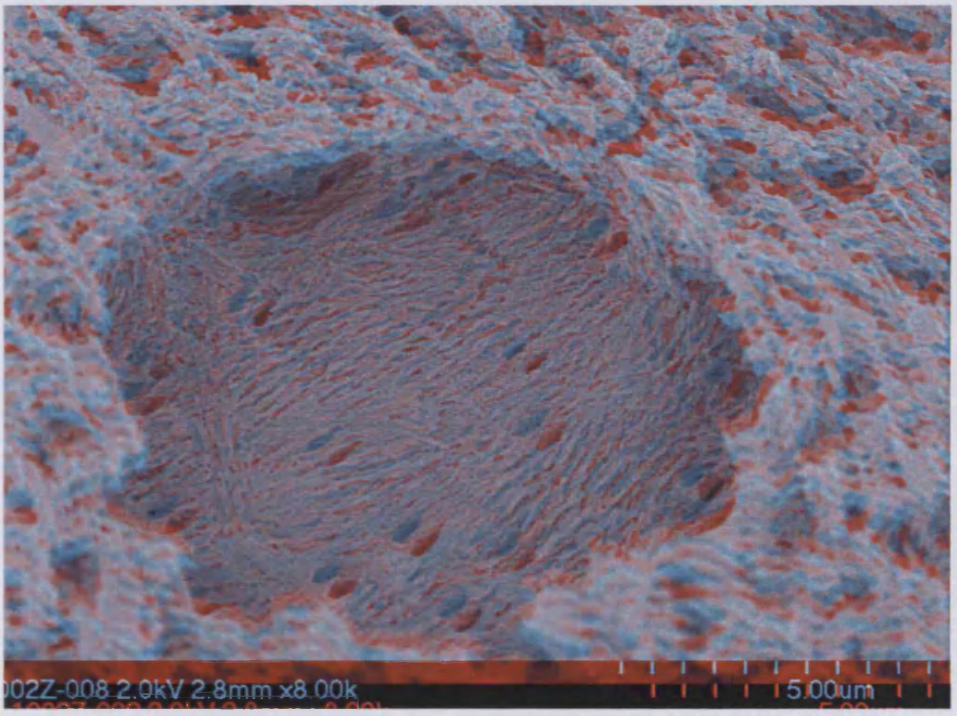

Figure 2c.31. *Images of bovine tissue (4-month-old). It is possible to see the canaliculi within the osteocyte lacunae. The lower image is in stereo (red/cyan). When viewed with stereo glasses, it gives a feeing of depth to the image. [A representation of 2 cores from 1 limbs analysed in this manner]*

2c.v. Histology

Histology is the only technique that allows the visualisation of the calcified matrix and the cells simultaneously. For the purpose of this Zetos validation work a novel embedding medium (Technovit 9100 New) was standardised, for the histology of undecalcified cancellous bone tissue as well as immunolabelling (Yang *et al.*, 2003).

Characteristic morphology of cancellous bone tissue can be seen in figure 2c.32i. The calcified ECM can be seen in the form of trabeculae (yellow) surrounded by adipocytes (fat cells). The adipocytes are large cells that contain a droplet of fat (that was removed during the clearing stage). The cells have a peripheral eccentric nucleus and are supported by a fine network of collagen fibres. The adipocytes are also known as yellow marrow. Occasionally, blood vessels can be seen within the marrow (soft tissue). Osteocytes are clearly seen entombed within the ECM, and two areas of freshly laid unmineralised matrix (osteoid seams). Active osteoblasts are cuboidal in shape (Fig.2c.32ii). In time the osteoblasts will calcify the osteoid seam, making it indistinguishable from the rest of the calcified tissue. Quiescent bone lining cells cover the entire surface of the trabeculae, but these are difficult to see at low magnifications. Other significant active areas in bone tissue are the scalloped shaped, Howships lacunae, filled with osteoclasts resorbing the surface of the ECM (Fig.2c32iii). These images depicted in Fig.2c32 are representations of cancellous bone tissue that was fixed in 70% ethanol and embedded in Technovit 9100 New. Different fixation, resin, dyes, and staining technique can give an altered view of the bone morphology. It is common for osteoid seams, from tissue embedded in Technovit 9100 New resin, to have a distinct staining between the unmineralised matrix and the cells (Fig.2c.32ii). This is not seen with tissue embedded in standard MMA (Fig.2c36v and vi) This could imply that mineralisation was altered, proceeding from the cells outward towards the ECM, rather than from the ECM towards the cells. This would be misleading as this staining is also seen in freshly fixed tissue. It has been hypothesised that this extra layer may be collagen fibers (Gasser and Jones personal communications). The use of MMA for this study was inadequate due to its inability to preserve tissue antigenicity for immunolabelling. Therefore, it is imperative to understand the method in question.

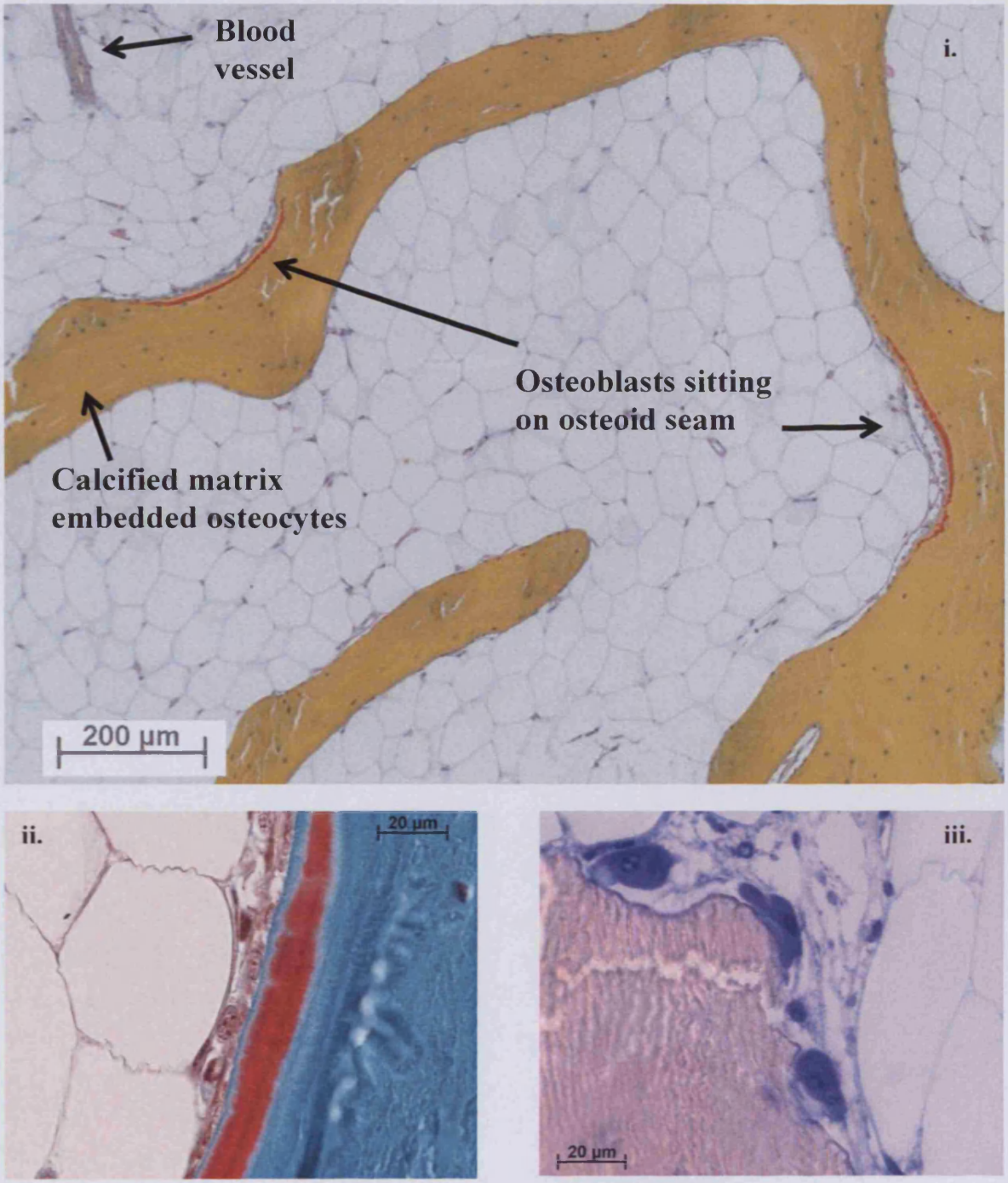

Figure 2c.32. i) *Ovine tissue (3-years-old, 61kg). Calcified matrix (yellow) can be seen surrounded by adipocytes. Two freshly deposited osteoid seams (red) can be observed as well as the active osteoblasts and entombed osteocytes (Movat stained, Technovit embedded).* **ii)** *High power image of an osteoid seam and active osteoblasts (Masson stained, Technovit embedded (Human tissue, 70-year-old male).* **iii)** *Giemsa stained Technovit embedded section, depicting 3 osteoclasts resorbing calcified matrix (Ovine tissue, 4-year-old, 56kg). [Characteristic image from one of twenty sections obtained from the centre of the core, providing a representation from a group n=6]*

The staining of tissue with dyes is a common practice, but very little is known about its mechanism. Throughout this study four different histological stains were employed, each with their own characteristic staining pattern, advantages and disadvantages.

Serial sections of the same tissue were used to compare the stains giemsa, Masson Goldner, Movat pentachrome and toluidine blue.

An overview of a cross-section from freshly fixed human cancellous tissue (70-year-old, male) can be seen in figure 2c.33. The blue square represents the location of the magnified images, depicting calcified ECM and haemopoietic cells, seen below the overview. Tissue in figure 2c.33i was stained with giemsa. It has stained the ECM purple-pink, and the cells a various shade of blue, purple and pink. It also stains calcified cartilage dark blue, osteoid seams pale blue, nuclei dark blue and erythrocytes pink. This neutral stain is a mixture of two dyes, methylene blue and its derivative as well as eosin and its derivatives. Methylene blue and its derivatives are basic dyes. In solution they exist as cations (positively charged). These dyes bind to basophilic tissue components. An example of a basophilic component is the cell nucleus. The nuclei contain acid groups, which bind to the basic dye through salt linkages. Eosin derivatives are acidic dyes. In solution they exist as anions (negatively charged). These dyes bind to acidophilic tissue components. An example of an acidophilic component is the cell's protoplasm. The protoplasm contains basic groups, which bind to the acidic dye through salt linkages. The acid and the basic dyes are stored in solution by excess amount of either component. A giemsa precipitate is formed that is soluble in ethanol. The methylene blue is responsible for staining the tissue components blue; eosin is responsible for staining the tissue components pink; the oxidation products of methylene blue, called azures, are responsible for staining the tissue components redish-purple; and a complex of dyes from the mixture is responsible for staining the tissue components a pale lilac. It is possible to see how this dye stains the haemopoietic cells in figure 2c.34i, and osteoid seams in figure 2c.35i. This stain is one of the best for staining haemopoietic cells. It is used routinely in hospitals to stain cells in blood smears. Unfortunately it is not so good at low magnifications, and also not the best at staining osteoclasts. Osteoclasts are often seen as dark blue blobs, where the nuclei are difficult to observe (Fig.2c.32iii).

Figure 2c.33ii, 34ii and 35ii, are all stained with the Masson Goldner stain (1938) a variant of the Masson stain (1929). This method is more complex than that of the giemsa,

with several stages to achieve the trichrome staining. It characteristically stained the ECM green, the osteoid and cells red (sometimes brown-grey), and the nuclei black (calcified cartilage was red). This staining method is based on the competition of different dyes for the same tissue component. Firstly the tissue is stained with haematoxylin, a basic dye, which colours the nuclei red. By placing the tissue in a weak alkali (tap water) and differentiating in ethanol, the nuclei become blue. Next the tissue is immersed in Masson solution (acid fuchsin) (Mr 586). The anions bind strongly to collagen, as collagen contains cationic groups of proteins. Following this, the tissue is stained with the mordant phosphomolybdic acid – orange G (Mr 452). It is a strong acidic dye, which acts as a colourless acid dye. It competes with the Masson solution. It gains access to the collagen easily expelling the Masson dye. The collagen is now free to be stained with a larger molecular weight dye – Light green SF yellowish (Mr 793). This dye is a strong acid, too big to penetrate small pores. It electrostatically binds to the free terminal amino groups and basic side chains of proteins. Therefore, when a tissue is treated with a range of acidic dyes (anionic) in aqueous solution, red blood cells will be coloured by dyes of the smallest molecular size, the cytoplasm by intermediary molecules and collagen by dyes of a larger molecular weight. The staining mechanisms are not entirely understood, but may be related to the penetration and diffusion phenomena. This stain is the best for highlighting osteoclasts. It is also good for differentiating calcified tissue and osteoid, though at times the red colour can be lost from the tissue. This is clarified by comparing to MMA embedded tissue (Fig.2c.36v). It is possible that the Technovit 9100 New resin may affect the chemical properties of the tissue. Due to the complex binding of dye to tissue components any changes may alter the staining pattern. It was also noted that tissue stained with Masson Goldner lacked osteocytes present within their lacunae. This could be detrimental to tissue analysis of explants cultured in the Zetos system, as empty lacunae is usually associated with dead tissue (see Chapter 3). It is therefore important not to rely on a single staining technique in order to avoid misinterpreting results.

Movat pentachrome is a staining technique that can stain tissue components one of five colours. Its characteristic staining pattern dyes nuclei blue-black, cytoplasm red, osteoid red, connective tissue bright yellow and mineralised cartilage blue-green. This can be seen in figures 2c.33iii, 34iii, and 35iii. It works in a similar manner to the Masson stain. Firstly, the tissue is stained with Alcian blue, a basic dye, which has a high affinity for anionic sites of polysaccharides, forming a reversible electrostatic bond. Placing the

tissue in alkaline alcohol converts the alcian blue into an insoluble fast blue. A basic haematoxylin is used to stain the nuclei blue-black (Weigert's haematoxylin). Brilliant crocein used in conjunction with acid fuchsin to stain the collagen red. Some of the dye is removed by the mordant phosphotungstic acid, allowing the rest of the connective tissue to be stained yellow in colour by saffron alcohol. This stain is the best for differentiating calcified matrix from the osteoid. It also stains haemopoietic cells and osteoclasts much better than giemsa and toluidine blue. However, due to its complex staining procedure the tissue becomes damaged easily and often soft tissue is lost or the calcified matrix is broken.

The final dye used to stain the tissue serial section, was toluidine blue. This is a basic dye used in an alkaline solution. It stains all bone tissue components various shades of blue when the dye is in its orthochromatic phase. This stain has a unique property known as metachromasia – the ability to stain constituents of tissue a different colour from the dye itself. In the metachromatic phase they will stain tissue a purple-red. For example, closely packed sulphate groups found in polysaccharides stain red-purple. This colour shift is caused by an intercalation of water when the dye is bound close enough (0.5 nm) thus, causing a change in the way the dye absorbs light. This stain provides minimal specific chemical information about the tissue. On the positive side it is possible to observed the mineralisation fronts between the osteoid and the calcified matrix. It is also the best stain for tissue preservation.

Preservation of the section is of great importance. It was observed during this study that the majority of tissue loss occurred at the staining stage, rather than during sectioning. Figure 2c36i-iv demonstrates how it is possible for some sections to have the tissue preserved, while other serial sections lost a vast amount of soft tissue. The worst staining technique for tissue loss was the Masson and Movat stains, due to the long immersion times in solutions causing tissue loosening. Though at times it was possible to lose tissue from giemsa and toluidine blue stained sections.

Each of these staining procedures has advantages and disadvantages. Some properties were unique to the tissue embedded in Technovit 9100 New. Therefore, it would be ideal to incorporate all four staining methods for analysis of Zetos cultured bone explants.

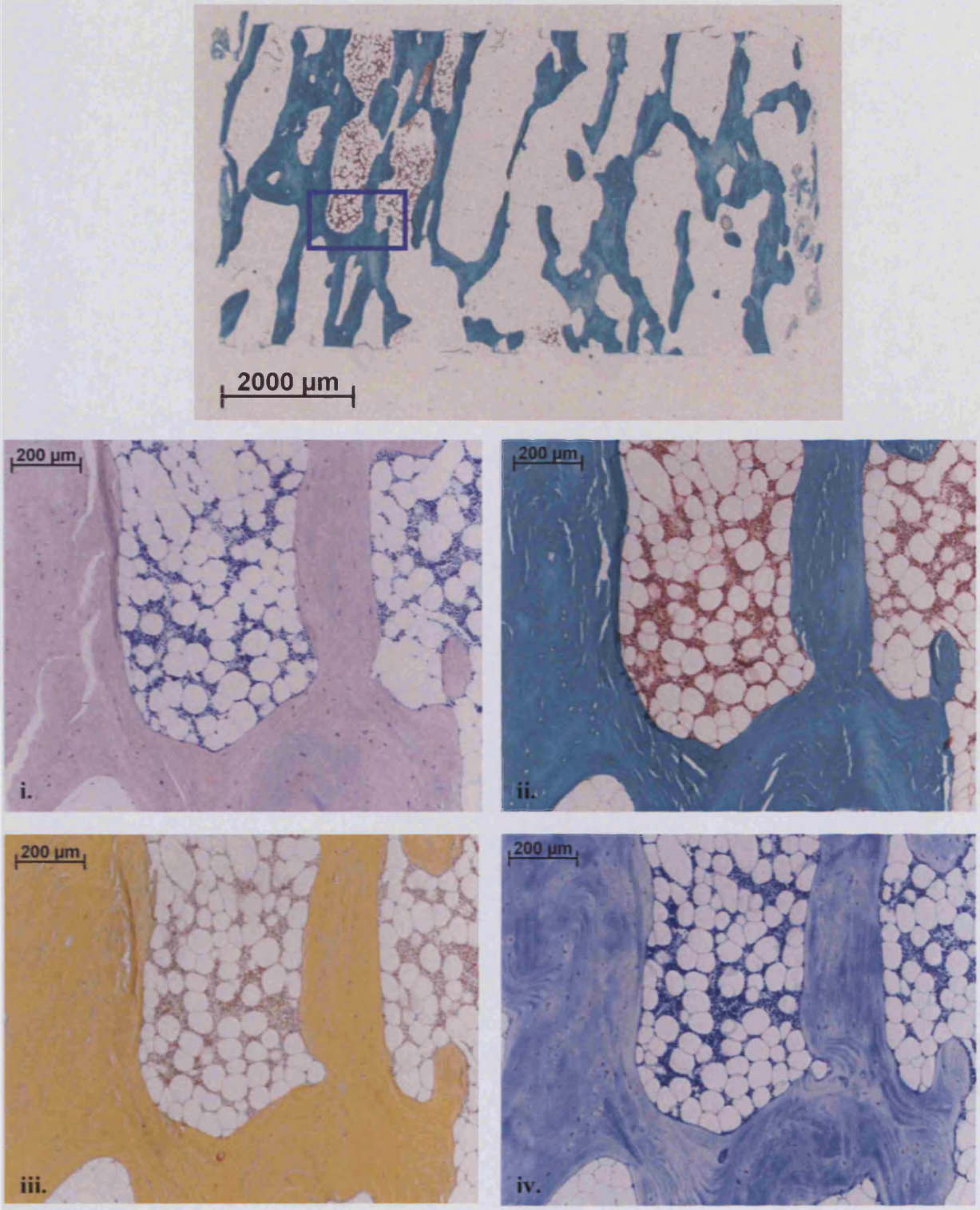

Figure 2c.33. *Cross-sectional overview of a section from freshly fixed human tissue (70-year-old male). Blue square represents location of magnified images.* **i)** *Giemsa stained serial section.* **ii)** *Masson stained serial section.* **iii)** *Movat stained serial section.* **iv)** *Toluidine blue stained serial section. All depict calcified trabecular matrix, adipocytes and haemopoietic cells. [Characteristic image from one of twenty sections obtained from the centre of the core, providing a representation from a group n=6]*

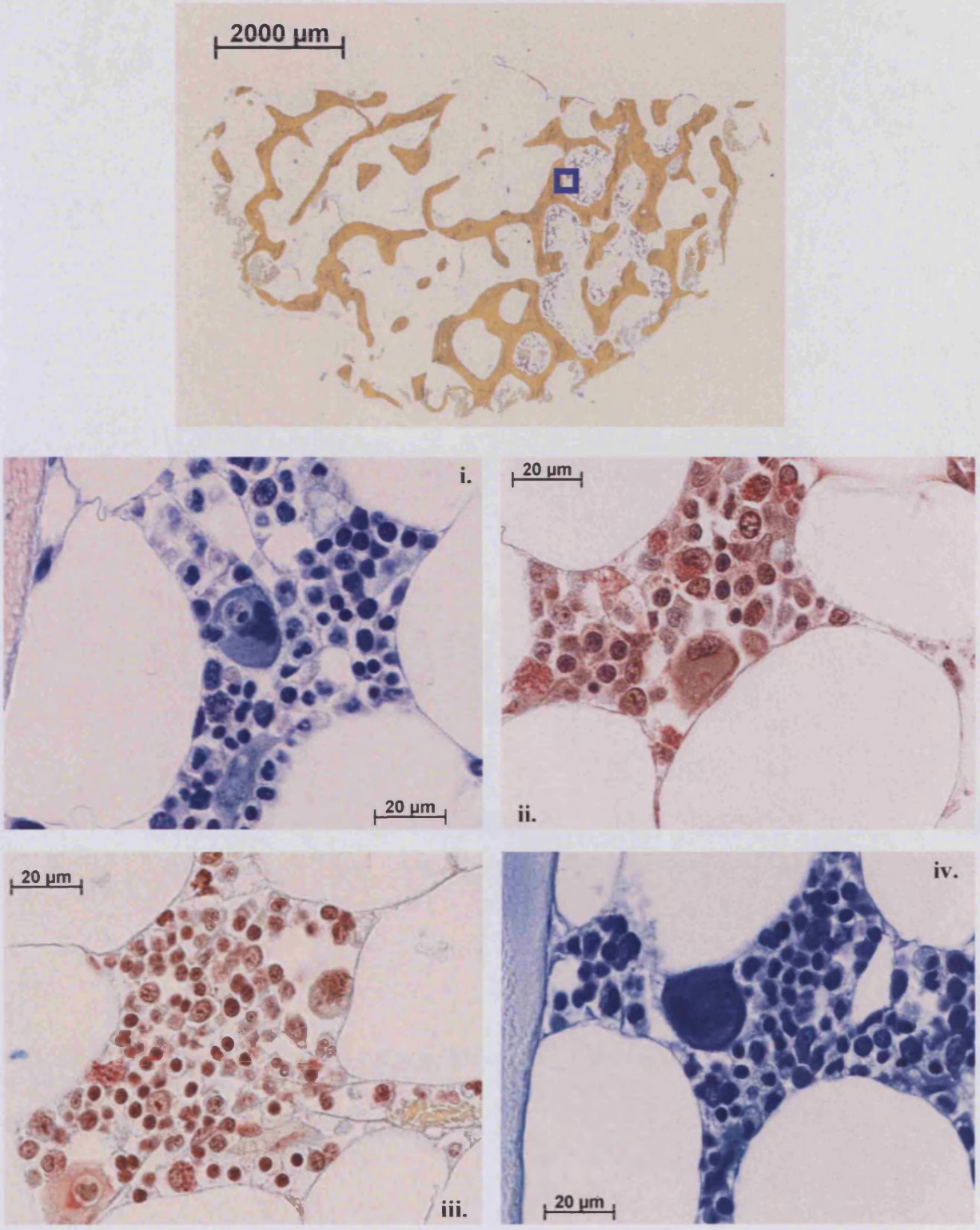

Figure 2c.34. *Transverse-sectional overview of a section from freshly fixed human tissue (70-year-old male). Blue square represents location of magnified images.* **i)** *Giemsa stained serial section.* **ii)** *Masson stained serial section.* **iii)** *Movat stained serial section.* **iv)** *Toluidine blue stained serial section. All depict haemopoietic cells. [Characteristic image from one of twenty sections obtained from the surface of the core, providing a representation from a group n=6]*

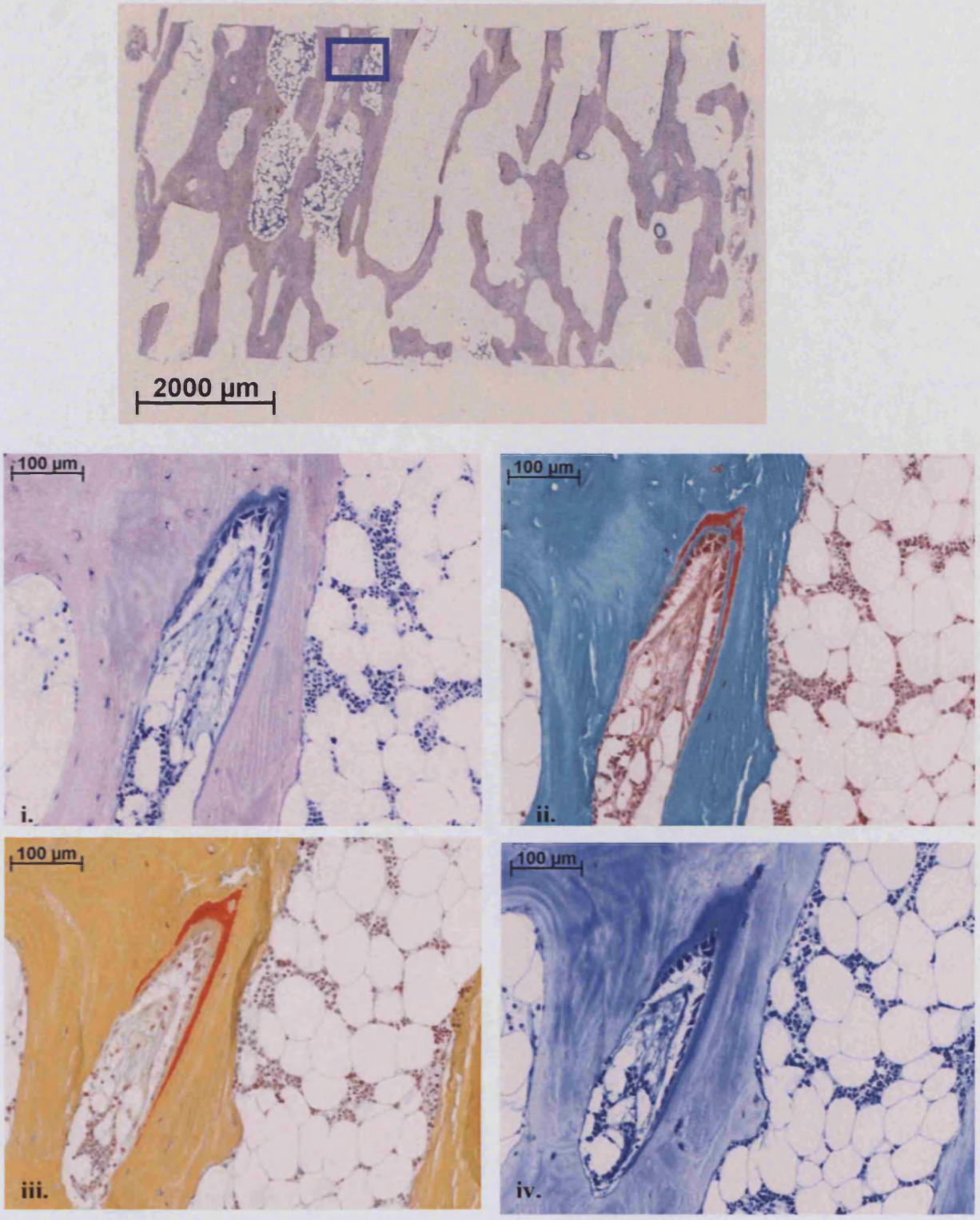

Figure 2c.35. *Cross-sectional overview of a section from freshly fixed human tissue (70-year-old male). Blue square represents location of magnified images.* **i)** *Giemsa stained serial section.* **ii)** *Masson stained serial section.* **iii)** *Movat stained serial section.* **iv)** *Toluidine blue stained serial section. All depict calcified trabecular matrix, adipocytes and haemopoietic cells and freshly laid uncalcified matrix (osteoid seam). [Characteristic image from one of twenty sections obtained from the centre of the core, providing a representation from a group n=6]*

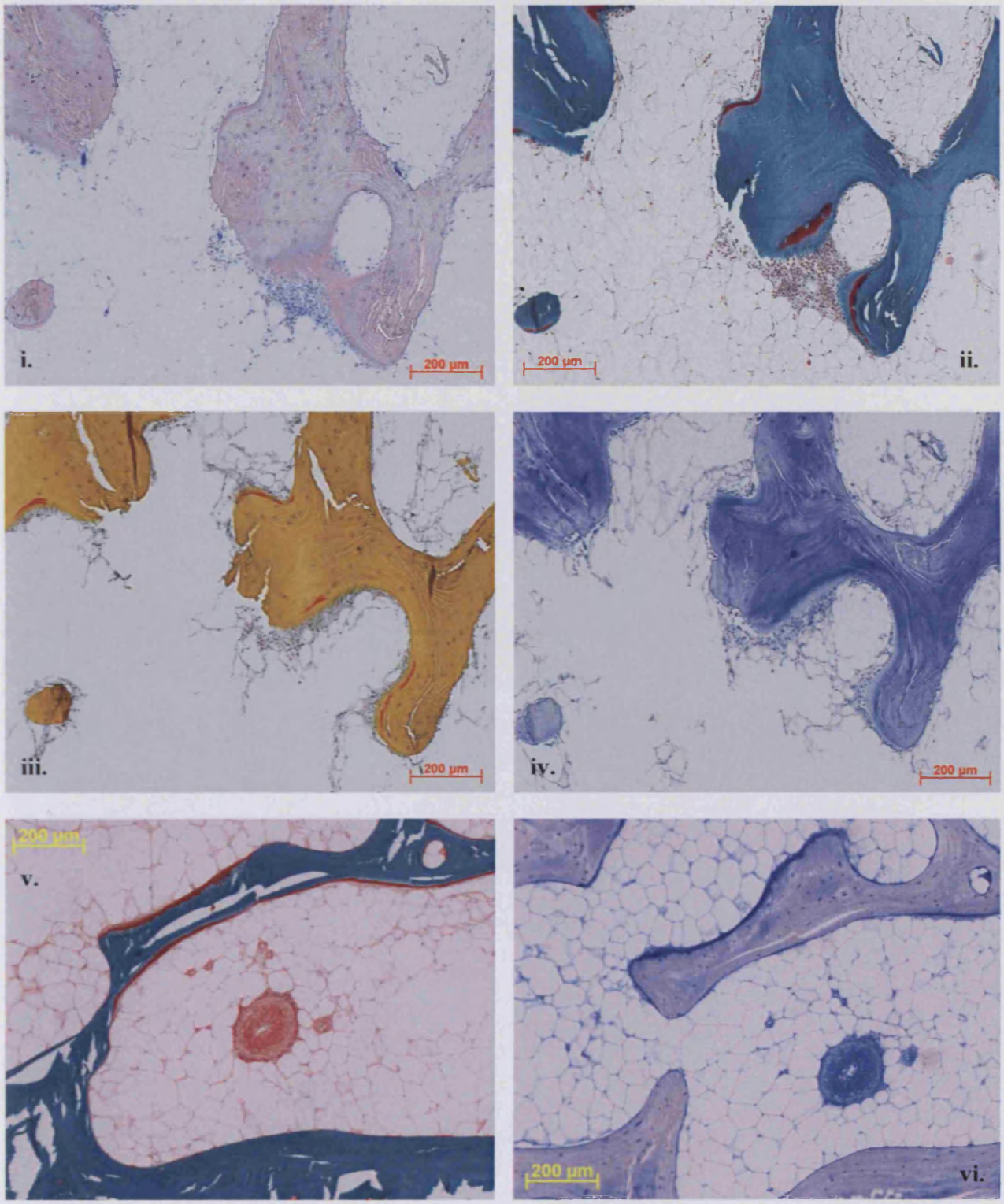

Figure 2c.36. i) *Giemsa stained serial section.* **ii)** *Masson stained serial section.* **iii)** *Movat stained serial section.* **iv)** *Toluidine blue stained serial section. All depict calcified trabecular matrix, adipocytes and osteoid seams (bovine tissue, 4-months-old).* **v)** *Masson stained MMA embedded section* **vi)** *Toliuidine blue stained MMA embedded section. Differences in staining pattern was observed. [Characteristic image from one of twenty sections obtained from the centre of the core, providing a representation from a group n=6]*

Ovine Distal Femora

Tissue used from ewes between 3 and 6 years of age is regarded as mature tissue. It is possible to observe from figure 2c.37 that the spaces between the trabeculae were mostly occupied by adipocytes. However, occasionally haemopoietic cells can be seen in discrete locations (Fig.2c.37i). Osteoblasts can be seen secreting unmineralised bone matrix (blue) as well as a non-functioning blood vessel in figure 2c.37ii. Osteoclasts can be observed resorbing calcified bone surfaces (Fig.2c.37iii). Unfortunately, giemsa and toluidine blue tend to stain these cells very dark due to their basophilic nature. Masson is a much better dye for differentiating the cells numerous nuclei. A resorption lacunae and osteoid seam can be observed in figure 2c.37iv. Much of the ovine tissue had most of its surfaces in a quiescent state this is outlined in figure 2c.37v. Some more bone apposition sites were observed in figure 2c.37vi. Nothing out of the ordinary was observed.

Bovine Distal Metacarpals

Tissue used from calves 4 months of age is regarded as immature tissue. The growth plate of the tissue is still open and some of the tissue is composed of woven bone (pink) apposed onto a calcified cartilaginous scaffold (dark blue) (Fig.2c.38iii). Most of the tissue is composed of lamellar bone as can be seen in figures 2c.38i,ii,iv. A bone modelling unit can be seen in figure 2c.38i. This is where the osteoclast resorbs the surface and is followed by osteoblasts filling in new bone (more details in chapter 4). A resorption lacunae filled with osteoblasts can be seen in figure 2c.38ii. The mineralisation front of the osteoid is coloured bright blue. Five different osteoid seams can be seen in figure 2c.38iv, indicating that the young tissue is very active and not in a quiescent state as the adult ovine tissue. Areas of haemopoietic cells were observed (Fig.2c.38v), as well as osteoclasts modelling the secondary ossification centre (Fig.2c.38vi). Differences observed between the ovine and bovine tissue was the amount of cell activity as well as the differences in cell and tissue types.

Human Femoral Heads

Tissue used from humans between 70 and 81 years of age is regarded as mature tissue. Like the ovine tissue, the bone surfaces were in a quiescent state (Fig.2c.39i,v,vi). Some osteoid seams were observed (Fig.2c.39ii-iii), but few and far between. Osteoclasts were observed in Howship's lacunae (Fig.2c.39iv) as seen with all three species. One difference

between the human tissue compared with that of the ovine and bovine tissue was the vast amount of haemopoietic cells. However, the cancellous bone morphology of all three species was quite similar.

One significant factor that became apparent by analysing several sections from the numerous explants, harvested from the model systems, was the differences in trabecular, number, density and orientation. Fifteen random sections from each species were used to highlight this phenomenon. Low power images of core cross-sections and transverse-sections can be seen in figure 2c.40, 41 and 42. The ovine and human samples were most heterogeneous in trabecular density as previously confirmed by radiographs and μCT images. If enough samples per bone could be obtained, it may be worth while to exclude some cores that differ greatly from the mean form participating in the Zetos culture studies. Unfortunately, very few samples can be harvested from a single bone, making this impractical. Possibly in other laboratories where numerous bones can be obtained this would be more feasible.

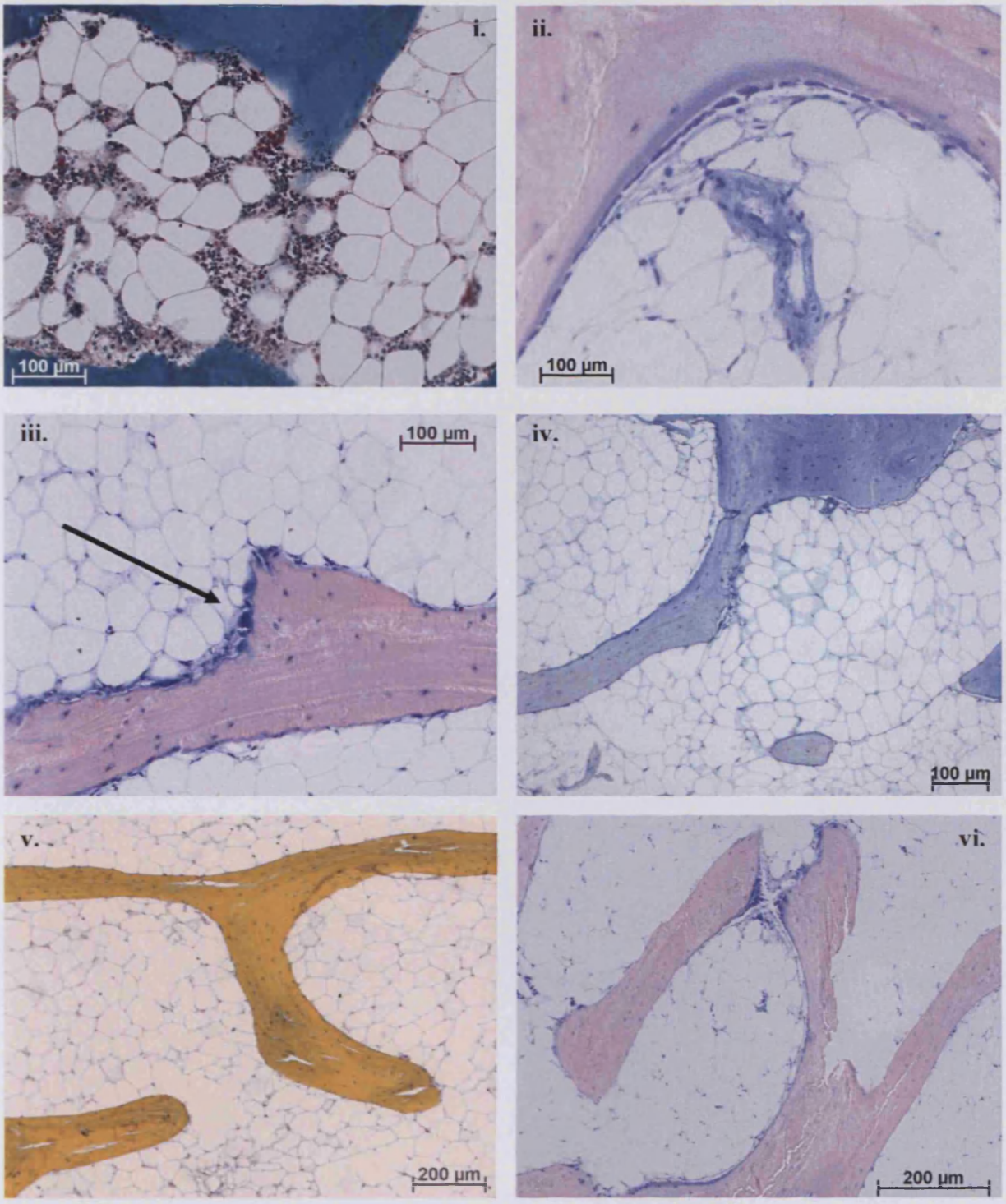

Figure 2c.37 *Ethanol fixed, Technovit embedded, 6 µm thick section from ovine tissue (4-years-old, 56 kg in weight).* **i)** *Masson stained image depicting haemopoietic tissue between the adipocytes.* **ii)** *Giemsa stained image of osteoblast over osteoid seam.* **iii)** *Giemsa stained image of osteoclasts on the surface of a trabeculae (black arrow).* **iv)** *Toluidine blue stained image of bone and soft tissue.* **v)** *Movat stained image of tissue lacking osteoid seams.* **vi)** *Giemsa stained image demonstrating two active areas of bone apposition. [Characteristic image from one of twenty sections obtained from the centre of the core, providing a representation from a group n=6]*

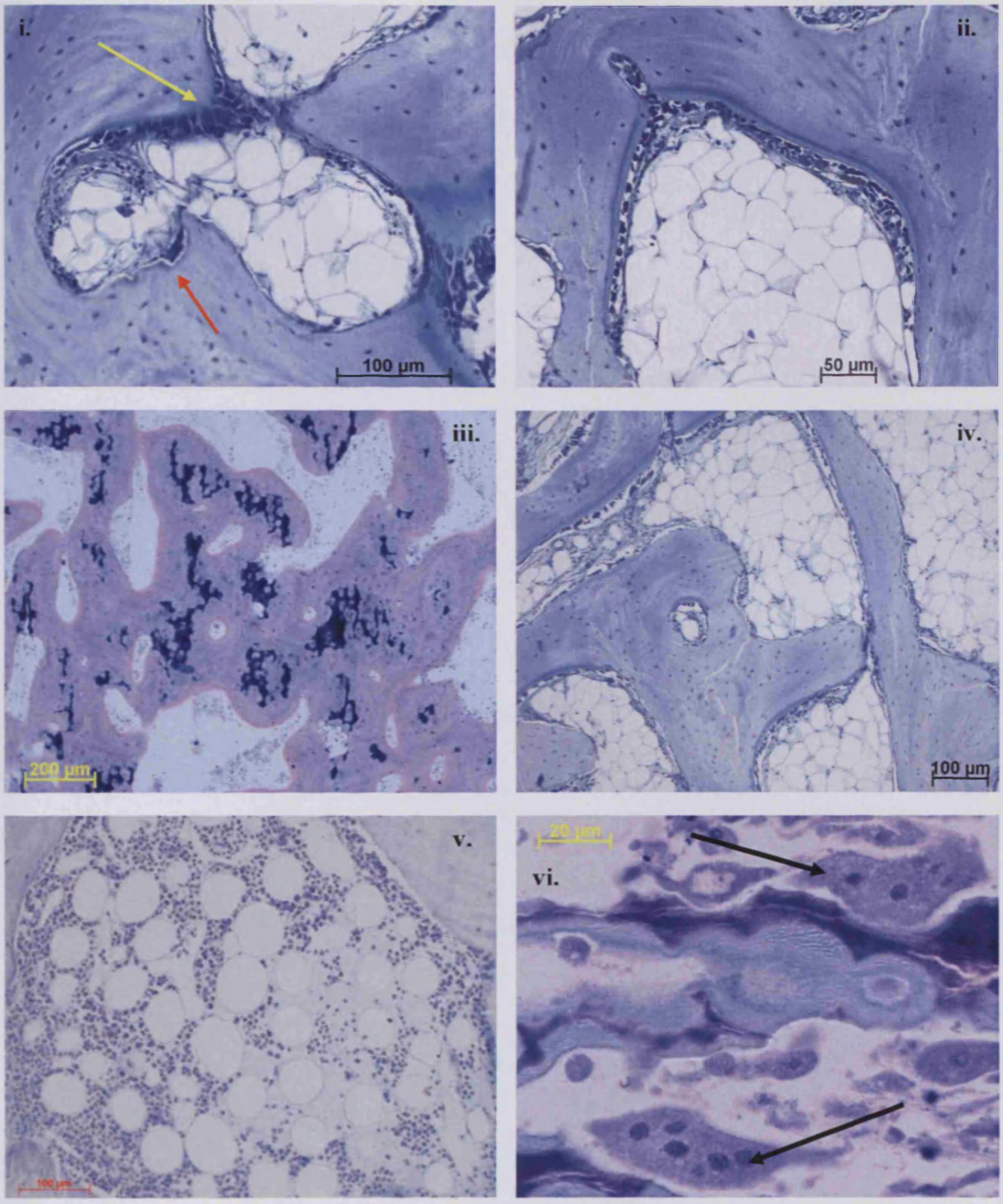

Figure 2c.38. *Ethanol fixed, Technovit embedded, 6 µm thick section from bovine tissue (female, 4-months-old).* **i)** *Toluidine blue stained section depicting osteoblasts (yellow arrow) and osteoclasts (red arrow).* **ii)** *Toluidine blue stained section depicting osteoid and mineralisation front (bright blue).* **iii)** *Giemsa stained section localising calcified cartilage (dark blue) within woven bone tissue.* **iv)** *Toluidine blue stained section of trabeculae and osteoid.* **v)** *Toluidine blue stained section of haemopoietic cells within the marrow.* **vi)** *Toluidine blue stained section of osteoclasts resorbing calcified matrix (black arrows). [Characteristic image from one of twenty sections obtained from the centre of the core, providing a representation from a group n=6]*

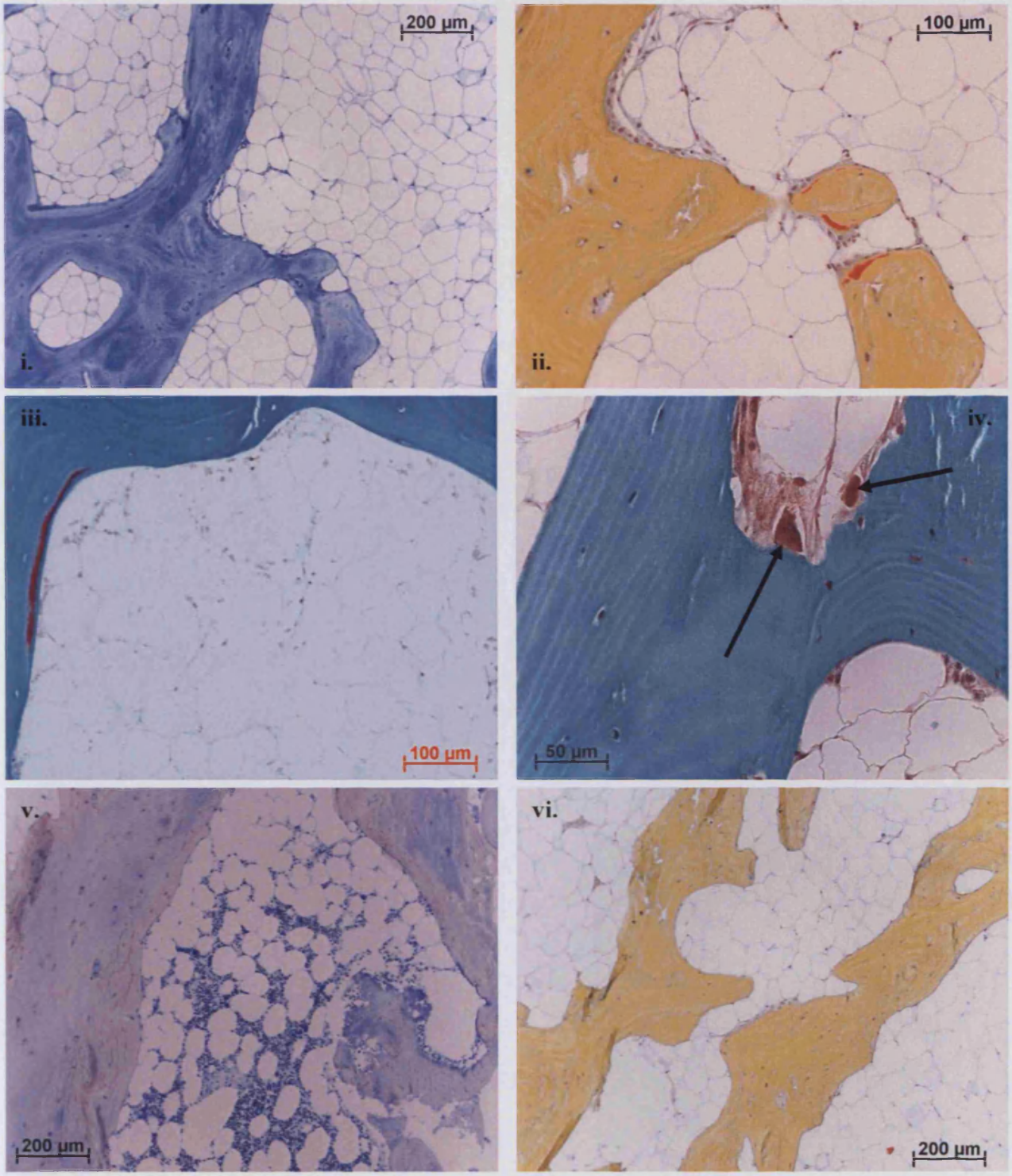

Figure 2c.39. *Ethanol fixed, Technovit embedded, 6 µm thick section from human tissue (male, 70-year-old).* **i)** *Toluidine blue stained section depicting cancellous tissue and adipocytes.* **ii)** *Movat stained section depicting some osteoid (red).* **iii)** *Masson stained section localising more osteoid.* **iv)** *Movat stained section of osteoclasts resorbing calcified matrix (black arrows).* **v)** *Giemsa stained section of hemopoietic cells within the marrow.* **vi)** *Movat stained section highlighting the lack of bone apposition. [Characteristic image from one of twenty sections obtained from the centre of the core, providing a representation from a group n=6]*

Figure 2c.40. *Overview of ovine bone cores (3 ½ -year-old, 88.5kg) in both cross-section and transverse-section. There is a difference in trabecular orientation and shape.*

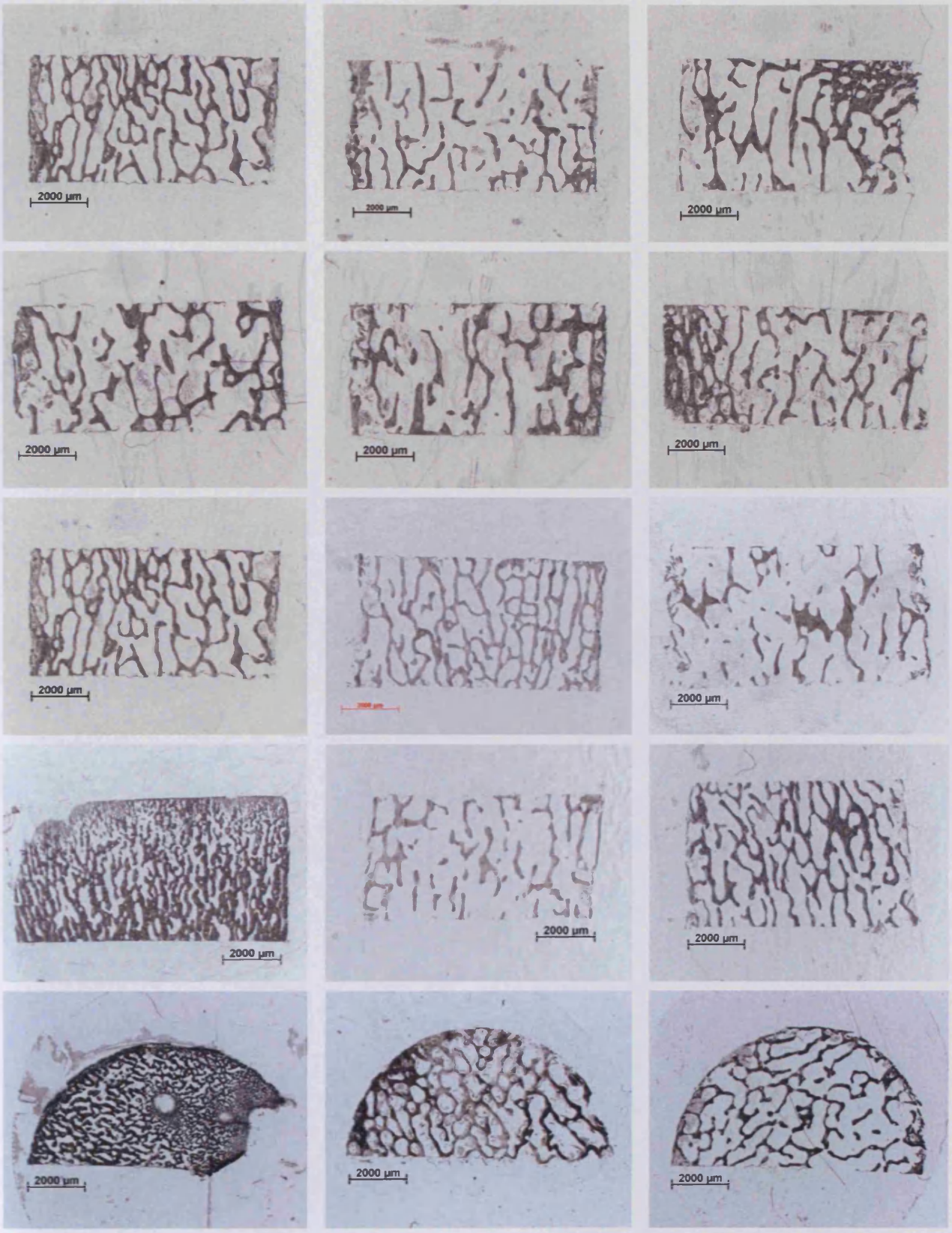

Figure 2c.41. *Overview of bovine bone cores (4 -months-old) in both cross-section and transverse-section. There is a difference in trabecular orientation and shape.*

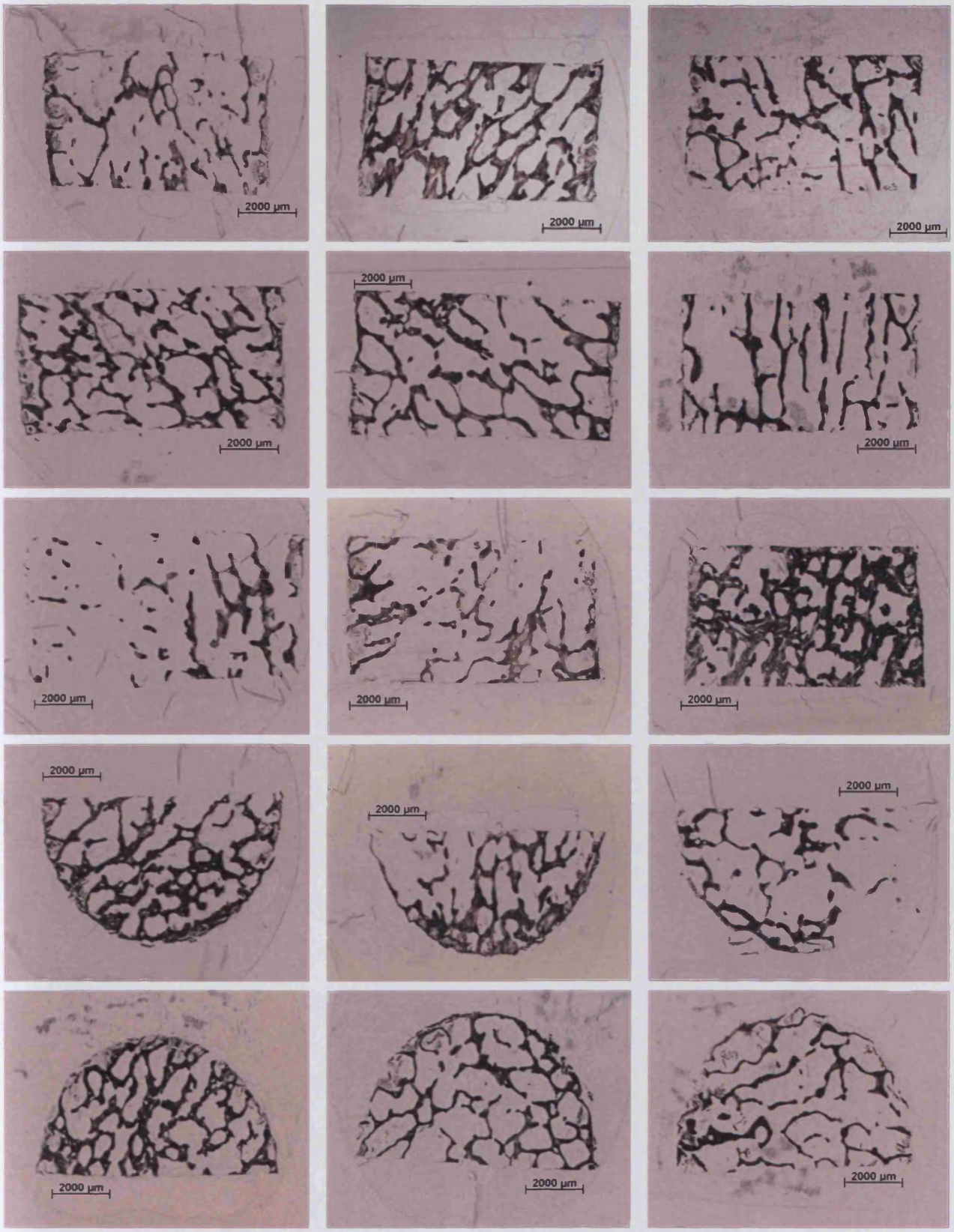

Figure 2c.42. *Overview of human bone cores (70-year-old, male) in both cross-section and transverse-section. There is a difference in trabecular orientation and shape.*

2.d. Discussion

Cancellous bone is a highly porous material with a complex internal structure. It is composed of struts and rods of trabeculae, which are the actual load bearing constituents of bone. The trabecular architecture of cancellous bone varies from location to location resembling very different shapes such as strut-like, plate-like, or honeycomb-like mesh-works. It is the presence of certain preferred trabecular orientation that causes the bone to be anisotropic meaning the tissue displays different properties in different directions.

A thorough understanding of the model system employed is required in order to gain the maximum information from Zetos based experiments. By randomly inserting bone cores with low bone density into control groups where net bone resorption would be expected, and high density bone cores into a loaded situation where net bone growth would be expected, one could draw the wrong conclusion if it were assumed that each bone core had a relatively average density to begin with.

It is also useful to be able to analyse skeletal integrity, in order to observe any damage to the tissue or locate any undesirable artifices such as cysts. Also, as animals and humans age, their skeletal architecture may change whether due to trauma or disease. In humans especially, as the bone ages the skeleton loses its ability to adapt to mechanical forces. For example, cortical and cancellous bone becomes thinner increasing bone porosity, thus, increasing bone fragility and increase risk in fractures.

The aim of this chapter was to use a number of different techniques in order to gain a better understanding of cancellous tissue and to possibly find a routine method to analyse tissue before harvest and maintenance in the Zetos culture system.

Maceration of the three different bones (two femora and a metacarpal) preserved the calcified trabeculae structures within the cancellous region. This technique demonstrated that the cancellous tissue differed in amount and orientation. Though this can not be fully explained, it has been believed for over a century that trabeculae orientate themselves along lines of primary stresses (Meyer, 1867), though no mathematical law has ever been found. It would be best to align the explants for the Zetos system, to these orientations, in order to reproduce the stresses and strains experienced *in vivo*. Though, it would also be interesting to see if bones adapted to altered patterns of loading, by orientating them differently to that of the *in vivo* situation as it is believed that bone should adapt its structure to resist certain levels of stress, a process known as functional adaptation.

Radiography demonstrated that bovine distal metacarpal tissue was by far the most homogenous with regards to trabecular density, with ovine distal femora and human femoral heads prone heterogeneity due to the possible occurrence of cysts. This would suggest that the bovine metacarpal tissue would be best for culture in the Zetos system, as samples would be more comparable to each other. However, it is known from literature that trabecular bone from skeletally immature animals (such as that seen in our bovine models), is weaker, less stiff, more deformable before failure; and has higher shock-absorptive qualities than skeletally mature animals (Nafei, Danielsen, Linde & Hvid; 2000). Therefore, these properties may not be desirable for cancellous explants that would be cultured in a loaded environment. Thus, it is not only bones' apparent density that causes variations in the compressive elastic properties of cancellous tissue. The collagen content and the mineral content are also major predictors too. This is something to bear in mind when selecting tissue for culture in the Zetos system.

Limitations to this technique is that plain film radiography does not record the real architecture of bone, but an apparent one which is created by superposition of the X-ray shadows produced by calcified tissues. Thus, in order to get non-artifactual results each bone section requires the same thickness throughout its entirety. The quality of the radiographs may also be affected by the presence of soft tissue on the bone's outer surface, which can cause blurred images. Finally, radiography only gives a 2D view of the tissue and says nothing of the quality or connectivity through the volume of the section. Though this technique is not perfect, it does have potential to be used prior to explant harvest, in order to assess the quality of the tissue qualitatively and to show areas to avoid harvesting from, if the technique can be shown not to harm the cells.

An advantage over radiography would be a technique that showed the 3D structure of cancellous bone tissue. This is possible with the microCT. The availability of 3D measuring techniques and 3D image processing methods allow direct quantification of unbiased morphometric parameters, such as volume and surface area. MicroCT allow the capture of true trabecular architecture without assumptions of the structure type. The results from this analysis confirmed that seen with radiography, indicating that that ovine distal femur and human femoral heads were more heterogeneous than the bovine distal metacarpal.

This method is advantageous in the fact that, unlike radiography, it can measure connectivity. The 3D connectivity of a sample is defined as the degree to which a structure

is multiply connected. Changes in connectivity are associated with changes in elastic stiffness, though, the absolute measure of connectivity is not directly related to mechanical strength, (Kinney and Ladd, 1998). There is no functional relationship between connectivity and elastic modulus *per se* because connectivity does not discriminate between rod-like connections and fenestrated plates, which brings us to the limitations of this technique.

Another disadvantage of using this technique is that the results obtained for the architecture of individual bone cores harvested from ovine, bovine, and human tissues were generated using the "Plate Model". This method assumes all trabecular bone was organised in infinite parallel plates. These results are, therefore, only valid under the assumption of a plate model. The results would be biased if all trabecular bone was not organised in parallel plates. Therefore, some parameters may be biased to some unknown extend. This is a limitation to using model-based approaches (Kinney *et al.*, 1995).

Currently microCT is not suitable in clinical settings as it has a high radiation dose and only possible to generate a 3D image with small biopsies. It may not be possible to use this on explants to be cultured within the Zetos system as the bone and marrow cells may be permanently damaged. If, however, a technique was found to enable the bone samples to retain their viability, microCT images taken pre and post culture would be invaluable to calculate where and how much bone was resorbed and deposited *ex vivo*. This is one of the Zetos development team's goals.

SEM analysis of the cancellous tissue again supported the results observed from tissue maceration, radiology, and microCT, that the bovine cancellous tissue appeared to be denser than that of the ovine and human samples. This method of analysis was inferior, with regards to tissue density, compared to radiography and microCT and thus, would not become a routine method of analysis for explants cultured within the Zetos system.

Histology was the only technique used that allowed cellular morphology as well as calcified tissue to be analysed. It was observed that explants from bovine metacarpals and human femoral heads contained a mass of haemopoietic cells throughout its entirety, while ovine explants from the distal femora was composed mainly of adipocytes, with the sparse isolated areas containing haemopoietic cells (Fig.2c.37, 38, and 39). These differences in cell populations would have a marked effect of the reactions that may occur during *ex vivo* culture. Samples may act very differently. Harvesting tissue from different anatomical sites may give rise to cells at different stages of differentiation, which may also show true

phenotypic variations and a distinct set of subpopulations. It is believed that younger animals have more undifferentiated progenitor cells which would give them a greater capacity for growth and differentiation. For example, in the bovine tissue, the vast number of potential cell precursors and stem cells would suggest a better capacity for growth, when compared to ovine and human explants. On the other hand, the vast number of cells present in the bovine explants, compared with the ovine tissue, may utilise more nutrients and create more waste products, thus affecting the microenvironment. Human and ovine tissue were in a quiescent state, while bovine tissue was highly active in tissue remodeling. In areas in close proximity to the growth plate, the bovine tissue was composed of woven bone apposed to a calcified cartilage scaffold (Fig.2c.38). This was not observed in the mature ovine and human tissues. It was hypothesised that the lack of activity in ovine tissue may be due to the fact that ovine bone aged one month corresponds approximately to that of one year in man (Nafei *et al.*; 2000). Therefore a 6-year-old would have tissue corresponding to a 72-year-old human.

The differing density of trabecular tissue was also reiterated with this technique, further corroborating the premise that bovine tissue was the most homogeneous of the three species in question (Fig.2c.40, 41, 42).

The results of the staining technique established that the binding of dyes to tissue is dependent on many physiochemical factors such as pH, temperature, method of fixation and embedding medium employed. Staining with four common histological stains (Giemsa, Masson Goldner, Movat pentachrome and Toluidine blue) yielded an altered staining that that observed with standard MMA embedded tissue (specifically the osteoid seems). This was most pronounced with the Masson stain. For example, soft tissue of tissue embedded in Technovit resin did not stain as strongly as tissue embedded in MMA (Fig.2c.36ii and v). It was also observed that osteoid seams present in tissue embedded in Technovit 9100 New resin displayed an extra layer between the unmineralised osteoid and the cells. It has been hypothesised that this may be collagen fibers (personal communications with D.B. Jones and J. Gasser). It was deduced that each stain had its advantages and disadvantages. Giemsa was the best stain to detect individual cells of the haemopoietic lineage, but did not stain osteoclasts as well as some of the other stains. Masson Goldner was one of the best stains for staining osteoclasts, but also caused the loss of osteocytes from their lacunae, which could lead to misinterpretation. Movat was the best stain to emphasise osteoid seams from calcified matrix. Though Masson was also good, at

times the red dye could be lost from the tissue sections, which caused a lack of osteoid staining. Unfortunately, both the Masson staining and the Movat staining was prone to the loss of soft tissue, and tears of the calcified tissue, due to the prolonged immersion of sections in solutions. Toluidine blue was the best stain to preserve the morphology of the sections. Sadly, this dye was limited in its differentiation of tissue components when compared to the Masson staining and Movat. However, unlike the other stains, the toluidine blue stain did highlight the mineralisation fronts observed within the osteoid. It was therefore concluded that each stain should be used with serial sections in order to overcome the limitation of each stain individually.

The disadvantage of this technique is that the images obtained were 2D representations of a 3D structure. Not all cells and structures are present. To be able to extrapolate the data into 3D quantities a stereological formulae must be used. This assumes that sampling is unbiased and random, and that the structure is isotropic (evenly dispersed and randomly orientated in space.). This is not the case with cancellous bone tissue thus, this method is prone to errors. However, this technique can be used to compare groupings provided that the same consistent approach is adopted (Compston, 1998). Limitations also include intra- and inter-observer variations, sampling variation, and methodological factors such as staining method, magnification etc. It is also difficult to assess what was present within bone explants prior to excision and what was new since culture. A further limitation to this technique is that it does not tell us the active state of the cells present. For example, the presence of resorption cavities does not necessarily indicate active resorption, but may reflect a failure of osteoblasts to synthesise and mineralise matrix in these cavities. Histology is not a useful technique for analysing formation and resorption on its own, but should be used in conjunction with a number of other methods.

In conclusion, cancellous bone is dramatically heterogeneous and great care should be taken to get representative and reproducible results. There is intersite and interindividual variability. Caution is required when extrapolating data obtained from one model to other models and to the situation *in vivo*.

Apart from differences in bone density, there may be difficulties with interspecies differences, and the possibility of phenotypic heterogeneity of cells from animals of different ages, or bone from different anatomical location. For example, though many genes are conserved throughout several species, there may be differences in certain gene sequences and protein sequences, as well as the amount of expression. Cells may be at

different developmental stages, show different cross-reactivity to different hormones, cytokines and growth factors with a range of differentiated phenotypes.

The trabecular arrangement in cancellous bone is obviously not random. Some regions are very dense, whereas others are very sparse. In some regions the trabeculae are coarse, whereas in other regions they are fine. It was observed that the mean orientation, and therefore the degree of anisotropy, varies between anatomical sites and individuals. This variation in cancellous bone architecture was the basis for the formulation of Wolff's Law (Wolff, 1870). This law links trabecular architecture to mechanical usage by adaptation. Data obtained for histomorphometrical parameters regarding bone volume, bone surface area, trabecular thickness and number (Tables 2c.1-3) suggests a number of cores are higher or lower than the mean for that group. This makes comparing one individual bone core to another difficult. In studies with a more homogenous tissue, for example articular cartilage, matched pairs are used with adjacent samples placed in different groups (load vs. no load). This would not be possible with cancellous bone cores. It would also be impossible to determine which cores were statistical outliers without making μCT analysis. However, the results obtained in Tables 2c.1-3 were only conducted once and is thus not enough for a reliable conclusion form the analysis. Thus, more limbs are required from each species and cores harvested from each section to be analysed several times. It would then be possible to statistically analyse the variance associated with the cancellous bone explants.

The need for understanding the model in question before beginning experimentation has been demonstrated. Thus, a better understanding of the results obtained can be made.

Summary

- Cancellous bone is heterogeneous with regard to trabecular thickness and orientation and no explants harvested from adjacent sites are identical. This statement was concluded from analysing ovine (distal femora), bovine (distal metacarpal) and human tissue (human femoral head) by radiography, bone maceration, Micro Computer Tomography (μCT), Scanning Electron Microscopy (SEM) and routine undecalcifed bone histology. Thus, care should be taken when extrapolating data obtained from one core to another, one model to other models and to the situation *in vivo*.

- It would not be possible to use adjacent cores as match pair controls for comparisons between different experimental treatments. This statement was concluded from the above mentioned analysis.
- Most analysis was only conducted on one limb, thus more samples would make the conclusions more significant.

Chapter 3.

Cell Viability

3.A. Introduction

There is a considerable need for a reliable viability assay for the bone explants cultured in the Zetos System. There are several techniques available to test for cell viability. Unfortunately, they are mainly suited for cell monolayers cultured *in vitro*. A technique is required, that tests for the viability of bone cells present in a 3D explant of bone, where matrix, bone cells, and bone marrow, are all present.

The use of the Zetos, culture system, to maintain cancellous bone explants, is becoming more widespread. Systems are now present in Marburg, Germany; Davos, Switzerland; St Etienne, France; Edinburgh, Scotland; Madison, USA; and Leuven, Belgium. A technique is sought, which is reproducible, and easy to use. This test would allow the percentage of cells killed during the harvest procedure, and during the culture period, to be determined. It would also enable the optimum *in vitro* culture period to be calculated. This would then provide an overview of whether tissue at the periphery, or in the centre of the core, was best maintained.

To date, Jones and Smith have demonstrated that 95% of osteocytes were still viable after 21 days of culture in the Zetos system (Jones D.B., *et al.*, 2001)(Fig.3a.1).

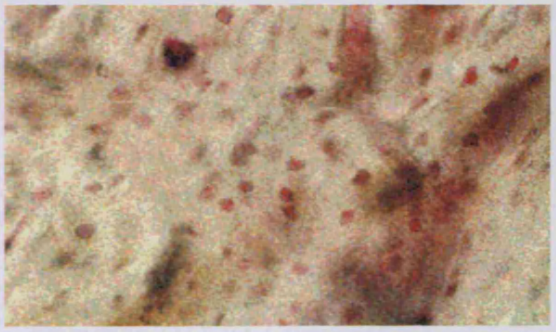

Figure 3a.1. *Living osteocytes within mineralised bone matrix were stained red in colour due to the cleavage of MTT to form formazan – [David Jones et al., 2001.]*

This percentage of viable cells was confirmed in a double blind study analysed by 3 independent scientists, where the bone cores were stained with MTT (3-4,5-dimethylthiazol-2-yl)-2,5-diphenyl tetrazolium bromide). MTT is a tetrazolium salt incorporated into cells with intact membranes and reduced by succinate dehydrogenase in

the mitochondria and/or NADH and NADPH. When reduced, it becomes a water-insoluble, brightly coloured (reddish-purple-blue) precipitate, which is easily visualized, and allows percentage of viable cells to be calculated. They examined 6 sections from each bone core, and found that MTT labelling did not differ between levels, nor within the diameter of the cores, regardless of time in culture. However, they did find two regions in which viable cells were absent or diminished. The first was at the top and bottom, where the cores interfaced with the piston and base plate. There, 2-4 cell layers were not viable, and the second, in some of the peripheral trabeculae. Unfortunately, this method has severe limitations, which are mentioned in detail later. Its main drawback is the fact that these sections of tissue have to be visualised immediately. Tissue fixation and embedding is not possible. Due to lack of sectioning or cutting, the samples are difficult to visualise, image and interpret as the samples are too thick (5 mm in height). It is also difficult to assess accurately the number of dead cells due to lack of labelling. The results obtained correlate to 80% cell viability observed by Val Mann (personal communication).

Work conducted by Clarke *et al.,* (2003) also suggested that the cells within the cancellous explants were viable. They analysed platelets over a four day culture period. As platelets are believed to have a life-span of around 10 days (Parfitt, 1995), this data was not 100% conclusive and would have been advantageous to extend this study after to a fortnight of culture, possibly even one month. No functional assessment was conducted, but transmission electron microscope analysis demonstrated morphology comparable to blood derived platelets.

The aim of the work conducted within this chapter was to analyse cell viability within ovine, bovine and human cancellous bone explants (5mm high and 10mm in diameter) maintained *ex vivo* for over 14 days in the Zetos loaded culture system in comparison to unloaded explants. This was conducted as follows:-

1. Analysis of the morphology of the explants maintained *ex vivo* through undecalcified histology to ascertain if any changes occurred to the tissue compared to that of fresh tissue fixed on the day of harvest. The detection of tartrate resistant acid phosphatase was also conducted in order to identify active osteoclasts within the cancellous explants.

2. Comparison of the labelling properties of different viability dyes in order to find a combination of dyes that will remain within the tissue through the histological processing technique, thus, allowing both live and dead cells to be observed

simultaneously. Following this, the best viability dyes were used to determine the amount of live and dead cells present within cancellous explants maintained *ex vivo*.

3. Observation of daily changes in the explant's apparent Young's modulus, as it is hypothesised that loaded explants should become stiffer as an adaptation to the load applied, while unloaded explants should become less stiff due to an increase in bone resorption as is seen with bones in disuse. Comparison of explant stiffness and anatomical location was made in order to determine if location of the harvested cores bore any relevance to explant stiffness.

4. Assessment of explant viability using LDH and pH would indicate if the cells within the explants were dying as the enzymes presence in the media would only have come from cells with compromised membranes. Concomitantly, measurement of the pH was made in order to observe the status of the tissue being cultured. For example dead tissue was not expected to alter their pH, while living tissue would constantly utilise the nutrients in the media and release lactic acid (a by-product of metabolism) and should cause the pH of the media to fall. It also provided an early indication if the tissue was contaminated with bacterial or fungal organisms as the pH of the media would rapidly drop, as well as become cloudy and opaque.

This introduction gives an overview of the different kinds of cell death, different ways of detecting cell death and the advantages/disadvantages of these techniques. Finally a detailed description of each of the dyes used during this study is given.

3.a.i Apoptosis & Necrosis

Cell death can be classified into two different types – necrosis (death of living tissue due to infection or injury) or apoptosis (programmed cell death) (Wylie et al., 1980; Kerr et al., 1972).

Necrosis is characterised by loss of membrane function giving rise to abnormal permeability and disruption of organells such as lysosomes and mitochondria. Cellular activities rapidly decline. Usually, a large number of connective cells are affected, typically caused by injury (Clark, 1996). A key feature associated with necrosis is the activation and attraction of inflammatory cells to the near proximity. A second characteristic feature is the influx of fluid into the dying cells, consequently causing them to swell, burst and disintegrate. Cells retain their nuclear membrane and diffuse dispersal of genomic DNA until bursting.

Apoptosis, on the other hand, is a predictable physiological death. It is regarded as being a precisely regulated, energy dependent, form of death, unlike that of necrosis. It usually occurs in the removal of unwanted cells during embryogenesis. Apoptosis is an ancient Greek term that means "the falling off, as of leaves from a tree". Apoptosis in bone is normal. It ends the life of an unwanted cell. For example, apoptosis allows osteoclasts at the end of their resorption phase to be eliminated (Fuller *et al.,* 1993); it also reduces the number of osteoblasts, ones that do not become osteocytes, or bone lining cells (McCabe *et al.,* 1995). Recent hypotheses believe that osteocytes in close proximity to microcracks may apoptose, causing a signal for osteoclasts to resorb that area (Elmardi *et al.,* 1990). Also, in endochondral bone development, the apoptosis of hypertrophic chondrocytes allow bone formation (Roach et al., 1995). These are but a few known examples. It would, therefore, be expected that some cells within the explants cultured in the Zetos system, would be undergoing apoptosis. It is generally considered that apoptosis and necrosis lie at a continuum where intermediary forms of cell death also exist. It is known that when cartilage is injured some cells die from necrosis and some by apoptosis, but it is not programmed and the same may apply for bone cells.

During apoptosis, single cells shrink and the cell surface changes its characteristic shape by containing invaginations. However, the membrane remains intact as well as organelles such as lysosomes and mitochondria (until very late phase). Changes in the nucleus are the most characteristic. Chromatin clumps into aggregates around the nuclear membrane. Even distribution is seen in viable cells. The chromatin then becomes condensed with crescent-shaped aggregates appearing and the prominence of the nucleolus, resembling dense balls. Following this condensation, the disintegration of the nuclear membrane releases chromatin aggregates into the cytoplasm. Fluid moves out of the cell, allowing transglutaminase-mediated, cytoplasmic, protein cross-linking to take place. This loss of fluid results in cytoplasmic condensation and cell shrinkage. Cells then lose their ability to adhere to surfaces. Eventually, they form multiple membrane-bound condensed apoptotic bodies that become engulfed and phagocytosed by neighbouring cells (Boyce, Hughes, and Wright, 1998). Unlike necrosis, no phagocytes or immune cells appear. During early stages of apoptosis internucleosomal cleavage of the chromatin occurs in a pattern indicative of endogenous endonuclease activation (Wyllie, 1981). This damages the DNA through Ca^{2+}/Mg^{2+} dependent pathways. Other characteristic features

include the release of caspase enzymes and externalisation of phosphatidylserine at the plasma membrane (Noble and Stevens, 2003).

Methods of detection include analysis of cell morphology with the SEM and TEM; observing cell loss, DNA fragmentation, internucleosomal sized increments of DNA produced during DNA destruction. It may be difficult to assess the reasons why cells undergo apoptosis. Is it due to normal end of lifespan, or due to insufficient culture conditions within the Zetos system? Not all of these methods of detection would be applicable to organ culture without destroying the tissue as a whole, and would, therefore, not be advantageous to Zetos users.

3.a.ii. The requirements of the Zetos system

Viability is not easily defined in terms of physiological or morphological parameters (as discussed above), therefore it is desirable to combine several different measures.

Morphological signs of poor viability in bone tissue include pyknotic nuclei and empty lacunae. Cancellous tissue, from the femoral heads of old patients were found to contain significantly more empty osteocyte lacunae, compared to young patients (Dunstan, *et al.*, 1990). This increase in empty lacunae was also confirmed by the work of Noble *et al.*, (1997). Good visualisation of condensation, blebbing or fragmentation of the nucleus prior to packaging of nuclear and cytoplasmic contents into apoptotic bodies can be obtained with the histological stain, toluidine blue (Noble and Stevens, 2003), allowing cells undergoing apoptosis to be visualised. Cells undergoing apoptosis can also be visualised with haematoxylin and eosin staining (H&E, histological stain), as these cells stain more intensely than surrounding viable cells. Apoptotic cells also lose their attachment to neighbouring cells, thus, they usually have a clear space around them. These parameters are compatible for use with the cores cultured in the Zetos system.

Both the cells, and the extracellular matrix, should be maintained in a homeostatic condition, relative to the *in vivo* state. If the cells of the specimen die, its mechanical properties are believed to change over time. Even when the tissue is stored in a wet state at body temperature, lytic enzymes are likely to be produced through autolysis of the cells within the specimen (Martin and Sharkey, 2001). These enzymes would affect the organic matrix, and if there was not an adequate buffering system, then the mineral component of the tissue would also deteriorate, severely affecting the specimen's mechanical properties.

When bone suffers from nutrient deprivation, cells tend to die from necrosis. Necrosis produces enzymes capable of compromising the physical structure and mechanical properties of extracellular matrix (Martin and Sharkey, 2001). Daily readings of the bone's apparent Young's modulus, over a 15 day period, should be able to detect any change in sample stiffness over time, indicating that the tissue may be suffering from necrosis.

It is also possible that the mineral content of bone is altered by storage of samples in supersaturated solutions as it may cause mineral deposits on the bone surface. It is believed that bone cells are responsible for maintaining the degree of mineralisation within the tissue as well as participating in it. Body fluids are supersaturated compared with the hydroxyapatite present in bone and hence, osteocytes must, therefore, continuously transport mineral ions out of the bone matrix. Frost (1960) hypothesesd this to be the case as, after osteocyte death, the matrix surrounding the lacunae becomes hypercalcified. This hypercalcification may also be detected through morphological investigation of the explants histology and stiffness measurements.

A number of studies have been conducted that suggest that the elastic modulus and hardness of bone diminishes postexplantation. For example, Linde and Sorensen (1993) studied the effect of 24 h storage of 74 cancellous bone explants (6.5mm in diameter by 6.5mm high) in saline at room temperature. They found that during axial compression, there was a significant decrease of 10% in modulus after storage as opposed to prior storage in saline. It is known that minerals leach from bone when kept in saline (Martin and Sharkey, 2001). Again, this could be observed over time by measuring the sample's apparent stiffness with the computer controlled loading apparatus of the Zetos system.

Lactate dehydrogenase (LDH) is a stable enzyme, predominantly present, in the cytoplasm of all cells of the body. It is important for the metabolism of carbohydrates. Its role is to transfer hydrogen using NAD+ as a hydrogen acceptor, thus, catalyzing the oxidation of L-lactate to pyruvate. LDH is released upon cell lysis, making it a good marker for determining cell membrane integrity and cell viability. Biochemical assays for this enzyme in the media would be better suited to these experiments, rather than staining for its activity within living explants.

The presence of the cytoplasmic enzyme, tartrate resistant acid phosphatase (TRAP) within osteoclasts identifies viable cells. This staining method may also identify osteoclasts undergoing apoptosis, as these cells stain more intensely, due to either continued production of TRAP or difficulty in secretion (van de Wijngaert and Burger,

1986). This test could be conducted on histological sections of explants cultured within the Zetos system. Active osteoclasts or TRAP + cells hydrolyse naphthol AS-BI phosphoric acid substrate to Naphthol AS-BI enzymatically. Free Naphthol AS-BI couples immediately to fast garnet GBC forming insoluble maroon dye deposits at the site of activity. Cells that are tartaric acid-sensitive acid phosphatase are not active. Mononuclear cells containing tartaric acid-resistant phosphatases are not affected.

3.a.iii. History of cell viability

The use of *in vitro* assays to enumerate the proportion of live and dead cells in a population has been around since the mid 1940's when the screening of potential anti-cancer agents became common. It is now used routinely to evaluate the safety of compounds such as drugs, cosmetics, food additives, pesticides, and industrial chemicals (Freshney R.I. 1986). Such cytotoxic and viability assays are based on *in vitro* testing as it has considerable economic advantages over *in vivo* testing. For example, animal models have the limitations to human models due to the metabolic differences between species, and moralistic concerns in terms of reducing animal experimentations.

Some of the most common assays involve measuring enzymatic activity, membrane permeability, or redox potential (see table 3.1). Each has its advantages and disadvantages.

Table 3.1. Different methods to assess cell viability

Membrane Integrity - stains dead cells	**Enzymatic Activity** - stains living cells	**Redox Potential** - stains living cells
Trypan Blue, Eosin Y, Naphthalene Black, Nigrosin (green), Erythrosine B, Nile blue Sulphate and Fast green	Fluorescein diacetate, Calcein AM, SYTO, CellTracker Green	MTT, XTT, NBT, Methylene blue

One of the earliest techniques to test cell viability was the incorporation of radioactive labelled essential amino acids into cellular proteins. However, these procedures have the limitations of being mutagenic, extremely time consuming and costly.

Over the years, people have sought after simplified methods that are less hazardous. For example, trypan blue dye exclusion by viable cells is one of many viability dyes, which have been used to determine membrane integrity. Membrane integrity is the most frequently used measure of cell viability. It gives an instantaneous interpretation of damage, or progressive damage, caused to cells since only the dead cells take up the stain. However, these stains are best suited to suspension cultures as dead cells in monolayer culture tend to round up and float away, thus being lost from the assay (Freshney, 1986).

Trypan blue is limited in its use due to the fact that the colorimetric assay must be completed within 3-5 min of dye incorporation because the stain is relatively toxic to cells causing the number of blue-staining cells to increase with time after the addition of the dye, thus giving a false estimation of dead cells present in a given population (Jones & Senft, 1985). It is also extremely laborious and time consuming. Due to these flaws, this stain would not be applicable to test bone explants cultured in the Zetos system.

In 1983, Mossman developed a colorimetric assay to estimate the number of viable cells growing inside wells of a microtitre tray. The assay was based on the ability of living cells to cleave a tetrazolium salt MTT (3-4,5-dimethylthiazol-2-yl)-2,5-diphenyl tetrazolium bromide) (Fig.3a.2) into an insoluble blue/purple coloured product known as formazan, through the use of a mitochondrial enzyme succinate-dehydrogenase. This reaction was first hypothesesd by Slater *et al.*, (1963). These coloured products could be easily quantified by colorimetric measurements in an automatic microplate scanning spectrophotometer. This technique had the advantage of saving time compared to traditional techniques of counting cells with a haemocytometer (trypan blue dye exclusion)

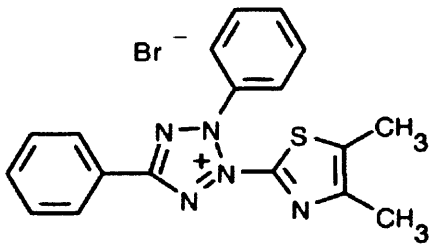

Figure 3a.2. *MTT, which has a molecular formula of $C_{18}H_{16}BrN_5S$ and a molecular weight of 414.32 g/mol. [Adapted from Molecular Probes]*

Denizot and Lang (1986) found that there were several limitations to the original technique, including less than optimal sensitivity, background staining due to protein

precipitation in the media and low solubility of the product. They managed to overcome these problems by choosing a better wavelength spectrophotometer, a higher concentration of MTT, and half area microtitre trays thus avoiding serum and phenol red in the media while staining and finally using pure propanol or ethanol to solublise the formazan. With these modifications implemented, the reliability and sensitivity of the assay was shown to be equal to that of tritiated-thymidine uptake assay to measure cell proliferation. Though the MTT assay offers major advantages in speed, simplicity, cost and safety over the conventional assays using the uptake of radiolabelled compounds, one aspect to keep in mind is that the MTT assay is dependent on the number of cells present and the mitochondrial activity per cell (as the reaction would be more pronounced in active cells than resting cells). Plus, the density of formazan is dependent on concentration of MTT used, as well as incubation time (Twentymn, 1987). Recently it has been determined that in addition to dehydrogenases, MTT is reduced by glutathione S-transferase (GST). Therefore, MTT may not always be a reliable cell viability probe in cells treated with compounds that affect GST activity (Web ref.4).

Paull *et al.*, (1988) synthesised a new tetrazolium salt called XTT 3'-[1-[(phenylamino)-carbonyl]-3,4-tetrazolium]-bis(4-methoxy-6-nitro)benzene-sulfonic acid hydrate that produced an orange coloured formazan product on reduction. It had the advantage of being water soluble, allowing direct spectrophotometric absorbance measurements without having to first dissolve the crystals (Roehm N.W., *et al.*, 1991). However, it also shares the same pitfalls as MTT (Scudiero, 1988)

Nitro blue tetrazolium chloride (NBT) is another tetrazolium salt with a deep blue coloured formazan product, which like MTT is not water soluble. Another viability assay based on dehydrogenase activity is that of methylene blue. Cell death is indicated by non-reduction of the dye. The disadvantage of this method is that it is not quantitative.

However, there is one common draw back with all the above mentioned viability/cytotoxic assays, and that is the fact that you can only detect "live" or "dead" cells, mainly for single cells/monolayer and not tissues. In reality, in order to estimate precisely how many cells are dead and how many are alive a combination of stains should be used simultaneously.

Such kits can be purchased from Molecular Probes called LIVE/DEAD, which allows viability and cytotoxicity assays to be conducted in a wide variety of cells, including those of animal origin as well as bacteria and yeast, each with its own advantages

and disadvantages. The main drawback of using the above kits on bone tissue would come in imaging the stained cells within the mineralised matrix without prior embedding, as the relatively thick sections of the bone core (~ 150 μm) would be out of focus in several areas with respect to others. The only way around this problem would be to attempt to embed the bone cores in a suitable resin and determine if the stain remained unaffected during the processing and then imaging thin (6 μm) sections.

3.a.iv. Potential stains and their mode of action

This work involved analysing the potential of 5 different fluorescent stains to be used as viability markers for 3D bone cores that contain bone matrix, bone cells, fat cells and marrow cells. Four of these stains show living cells depicted as green fluorescent cells (Fluorescein diacetate, Calcein AM, CellTracker Green and SYTO24) while one depicts dead cells as red fluorescent cells (Ethidium Homodimer -1). Of these five stains, two are DNA binding molecules (Ethidium Homodimer -1 and SYTO24) and the other three are derivatives of fluorescein, which become fluorescent in the cell cytoplasm upon cleavage by esterases. The fluorescein derivatives are viability probes that measure both enzymatic activity, which is required to activate their fluorescence, and cell-membrane integrity, which is required for intracellular retention of their fluorescent products.

Fluorescein diacetate (FDA) was one of the first probes to be used as a fluorescent indicator of cell viability (Rotman and Papermaster, 1966). Fluorescein dye hydrolysis is a common marker of cell viability. On its own, fluorescein diacetate is non-fluorescent (Fig.3a.3). When placed in culture, it penetrates living cells without disrupting the membrane, a process known as flurochromasia. Esterases present in the cytoplasm split the dye to fluorescein, which remains inside cells with intact membranes. The dye can only leave cells with broken membranes, thus giving us an estimation of viable cells within a population (Persidsky and Baillie, 1977). A disadvantage to this mechanism, with regard to viability of bone cells, is that the fluorescein molecule is difficult to distinguish from the natural green autofluorescence of bone and, that it leaks from the cells quite quickly (Hulett *et al.*, 1970).

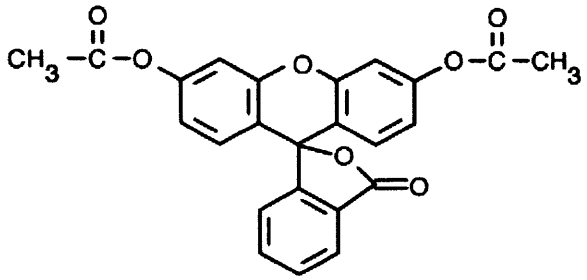

Figure 3a.3. *Fluorescein diacetate, which has a molecular formula of $C_{24}H_{16}O_7$ and has a molecular weight of 416.39 g/mol. [Adapted from Molecular Probes]*

Calcein AM is hydrolysed within a cell to calcein. Calcein is a polyanionic derivative of fluorescein (Fig.3a.4), with the advantage of being retained in cells better than most stains and is not sensitive to the surrounding pH. Calcein AM is an uncharged molecule that can permeate cell membranes. It is cleaved by esterases in the cell cytoplasm. Esterases remove the lipophilic component of the calcein molecule, thus, giving the molecule a charge that makes it harder for it to be released from the cell. However, this dye can have some potential artefacts such as incomplete hydrolysis of the molecule, compartmentalisation of the dye within membranous organelles, or may produce toxic by-products such as formaldehyde or acetic acid, which is also true of all fluorescein derived compounds.

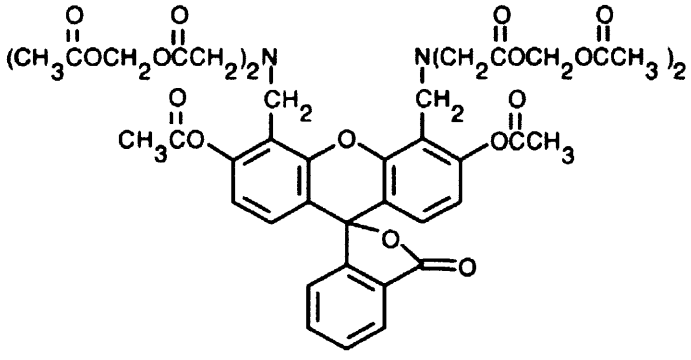

Figure 3a.4. *Calcein AM, which has a molecular formula of $C_{46}H_{46}N_2O_{23}$ and has a molecular weight of 994.87 g/mol. [Adapted from Molecular Probes]*

CellTracker Green (CMFDA), 5-chloromethylfluorescein diacetate (Fig.3a.5), is patented to Molecular Probes. It is a molecule which can freely diffuse into cells, where once in the cytoplasm, its thiol reactive moieties react with intracellular thiols allowing acetate groups to be cleaved by cytoplamic esterases. However, CMFDA may react with

both glutathione and proteins, thus, cells with membranes that become compromised after staining may retain some residual fluorescent conjugates. This problem can be overcome by combining this stain with a membrane-impermeant probe such as ethidium homodimer 1.

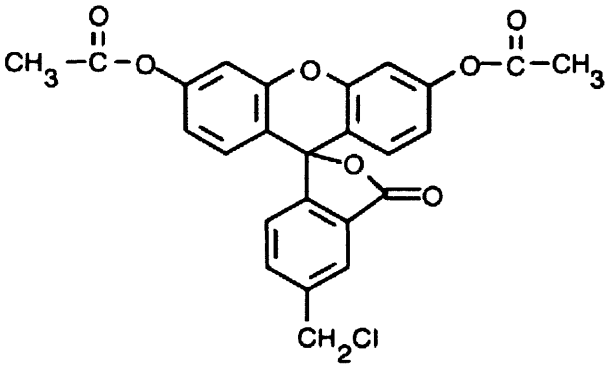

Figure 3a.5. *CellTracker Green, which has a molecular formula of $C_{25}H_{17}ClO_7$ and has a molecular weight of 464.86 g/mol. [Adapted from Molecular Probes]*

Ethidium Homodimer 1 (EthD-1) is a cationic, cell-impermeant, red fluorescent dye that is commonly used to detect dead or dying cells (Fig.3a.6). It binds to DNA causing a 40 times enhancement of the fluorescence. It has a greater advantage than ethidium bromide as it is highly charged and binds to DNA 1,000 times more tightly. This dye has a large Stokes shift allowing it to be used in conjunction with fluorescein based probes to give a two colour application.

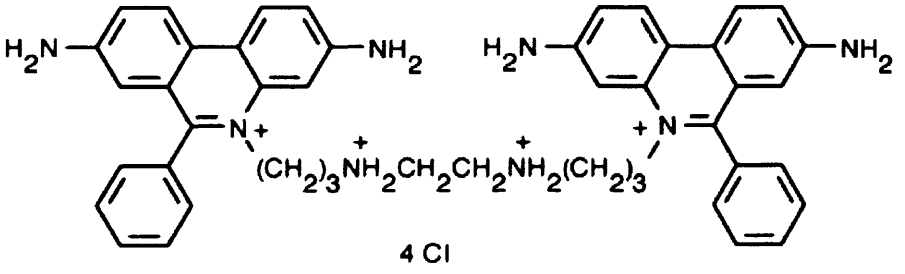

Figure 3a.6. *Ethidium Homodimer -1, which has a molecular formula of $C_{46}H_{50}Cl_4N_8$ and has a molecular weight of 856.77 g/mol. [Adapted from Molecular Probes]*

SYTO24 is a DNA binding fluorescent molecule, which can be used to determine living cells when used in conjunction with EthD-1. This dye differs from the other

mentioned dyes as they react and stain within the whole cytoplasm, while this dye binds to nucleic acids. This dye is freely permeable to most cells, and is essentially nonfluorescent until it binds to nucleic acids. Once bound, their fluorescence quantum increases 1000 fold or more, though they can be displaced by higher affinity nucleic acid stains such as EthD-1. Thus, when used together, they can be taken as a measure of live and dead cells when the green fluorescent SYTO dye is displaced by the red fluorescent ethidium dye producing a yellow-orange and red fluorescent population of dead cells. There are 32 different SYTO dyes with emission maxima in the range of 441 nm and 678 nm. SYTO24 was chosen for its compatibility with Ethidium Homodimer 1.

3.B. Materials & Methods

Herein is a detailed description of all materials and methods used during this study. Additional information on techniques, machinery and chemicals can be found in the relevant Appendices.

3.b.i. Culture in the Zetos System

Harvesting the tissue.

Bone cores from ovine distal femora, bovine distal metacarpals and human femoral heads were obtained by sectioning the tissue into 7 mm thick sections with the Exakt 300 band saw and boring 10 mm diameter cores from the cancellous region with a diamond tipped fluted drill bit (D256) and bench drill (Eco MAC 212). These cores were cut parallel to the height of 5 mm with a Leica annular saw (Leica AG, Glattbrugg, CH) (see Chapter 1b. for a more detailed description). The cores were randomly assigned into groups (Freshly harvested live and dead explants (heat killed at 55°C 4-8h); live and dead explants cultured in the Zetos chambers with load; live and dead explants cultured in the Zetos chambers without load; and live and dead explants cultured in the centrifuge tubes). The number of each sample per group depended upon the total number of cores harvested (Fig.3b.1).

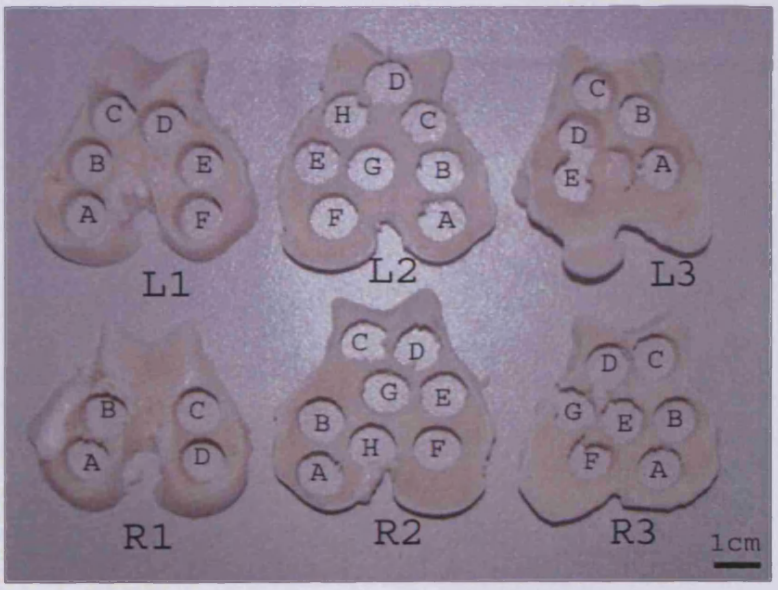

Figure 3b.1. Image demonstrating the location of each individual bone core. Ovine bone, L= left leg, R= right leg, 3 ½ years of age, 88.5 kg in weight.

Maintenance of the tissue.

Powdered DMEM with high glucose was used in this study (Gibco, Cat. No. 12800-058, Lot No. 1143722). Single packages, enough to make 1L at a time, were used. The powder was produced without sodium bicarbonate to increase its stability and shelf life. However, bicarbonate is a necessary component of the medium and is required by most mammalian cells due to its nutritional benefits (Swim & Parker, 1958) as well as buffering the medium. It was one of several components supplemented to the culture media. L-Glutamine was also included at a concentration of 584.00 mg/L. L-Glutamine is an essential component of cell culture media, which is very unstable, spontaneously decomposing in aqueous, neutral solutions, therefore, 2 mM was added.

To prepare 1L of DMEM the following procedure was used: - A plastic 1L measuring cylinder and a magnet was rinsed with distilled water. The measuring cylinder was placed onto a stir plate. One packet containing 13.5g of DMEM powder was added to the cylinder. The remaining powder in the packet was washed with distilled water over the cylinder. Once the packet was clean, it was discarded. MilliQ water water was added ~ 400 ml. The magnet was inserted and the solution stirred. Foetal Calf Serum (FCS), Vitamin C Pen/Strep and L-Glutamine were taken from the -20°C freezer and placed in a hot bath at 20°C to thaw. To the stirring solution 2.38g HEPES (Sigma, Cat.No. H-3375), 0.12g Sodium hydrogen carbonate (Merck, Cat.No. 6329), and 1.08g -glycerophosphate disodiumhydrate (Sigma, Cat.No. G9891) were added, giving a final concentration of 10 mM, 4 mM β-, 5 mM respectively. Distilled water was filled to 750 ml by running the water around the wall of the cylinder to make sure all the powder was in the solution and not still stuck to the wall. Finally, 10 mg L-ascorbic acid-2-phosphate and 50 000 IU Pen/Strep were also added. A piece of aluminium foil was placed on top of the cylinder to reduce possible contamination and was left to stir for 30 min to ensure thorough mixing of the solution. Once mixed the pH of the medium was adjusted to 7.25 and the cylinder filled with MilliQ water to a volume of 1000ml. With 100 ml discarded (the pH will normally rise 0.1-0.3 upon filtration). The solution was filtered into a 1L glass bottle with 0.22 μm Bottle top filter (Falcon, No. 7105). To this, 100 ml of FCS (Biochrome-S 0113/5 Lot 615B) was sterile filtered with a 0.22μm Syringe Filter (Milipore, No. SLGS 025 0S). The media was labelled and stored at 4°C until use. The shelf life of the media was one week. If it was not used by then it was discarded. On the 3rd day extra L-ascorbic acid-2-phosphate was added 1

mg/100ml. After the first week of culture, Pen/Strep was no longer included in the medium.

The media was aliquoted under sterile conditions into 50 ml centrifuge tubes to a volume of 10ml. Daily media changes were made after the loading stimulation. Media change involved warming the media to 37°C by leaving the tubes in the warm room for 30 min. The negative control (centrifuge tube cultured explants) were taken to the fume hood and under sterile conditions, transferred with a tweezers into a fresh tube of warmed media. The samples were placed back in the 37°C room. To change the media of the Zetos cultured samples the utmost care was needed. The room was sprayed with 70% ethanol and left to air dry. A face mask, hat and gloves were worn at all times. Gloves were sterilised with 70% ethanol between each sample change. The pump was turned off to ensure that no air and possible microbial contamination was taken inside the system. The centrifuge tubes were released from the tubing and exchanged with fresh media as quickly as possible; limiting the amount of time the tubing was in contact with the air. Once all samples were changed, the pump was switched back on. The media was measured for pH, and 2 ml aliquots were stored at -20°C for future biochemical analysis. The rest of the media was discarded.

At least two bone cores were fixed in 70% ethanol as soon as harvest procedure was complete in order to act as positive controls. Bone explants cultured in static culture, submerged in media, are known to suffer from necrosis therefore, some bone cores were cultured submerged in 10 ml media in 50 ml centrifuge tubes to act as positive controls for necrosis as well as a negative control for explant culture. Explants placed in the Zetos culture chambers, but not dynamically loaded, were used as a negative control for loading stimulation (these cores received a static load for 30 s every 4 days). In each of these culture environments, dead tissue (purposely killed explants) was used to permit negative controls for all viability and synthesis experiments. Explants were "killed" by placing the cores after washing into an incubator (56°C) for 6 to 8 hours. This was enough to kill the cells, but did not alter the mechanical properties of the tissue.

Quantitative analysis of media pH for tissue explants maintained *ex vivo* in the Zetos loaded culture system, in comparison to positive and negative control tissue explants. A fall in pH would be interpreted as a sign that the tissue was utilising nutrients and forming lactic acid. A similar change in pH as disuse or necrotic tissue would be a sign that the tissue was not being maintained *ex vivo*. A similar change in pH to dead tissue or blank

media would suggest the technique was artefactual and not sensitive to use to detect changes occurring post-harvest or that the tissue was dead. The number of ovine, bovine and human cores assessed in this manner was 46.

Loading of the Zetos cultured explants.

Before any loading took place, the loading device was calibrated. Calibration involved placing a steel 1200 calibration probe into the loading device and measuring its stiffness. This would adjust the settings according to changes obtained with the steel probe, for example, the effect that temperature would have on the readings.

Daily, each chamber containing the cancellous explant was placed within the loading device. A preload of 10N was placed onto the chamber piston, to make sure all surfaces were in contact. The samples were then mechanically stimulated for 5 min each, at 1Hz, with a double peak waveform (resembling a complete jump), giving each sample approximately 4,000 microstrain. The maximum displacement of the tissue was 20 μm, and minimum 5 μm. Once complete the computer readouts were saved and the piezo released from the samples.

The samples were then measured with a quasi-static static load, slowly increasing displacement to 20 μm, over 1 min, in the form of a ramp. The load was slowly released as not to stimulate the samples. The Young's modulus of the samples was calculated and saved. Unloaded controls were measured in this manner every 4 days. At least two bone cores were fixed in 70% ethanol as soon as harvest procedure was complete in order to act as positive controls. Bone explants cultured in static culture, submerged in media, are known to suffer from necrosis therefore, some bone cores were cultured submerged in 10 ml media in 50 ml centrifuge tubes to act as positive controls for necrosis as well as a negative control for explant culture. Explants placed in the Zetos culture chambers, but not dynamically loaded, were used as a negative control for loading stimulation (these cores received a static load for 30 s every 4 days). In each of these culture environments, dead tissue (purposely killed explants) was used to permit negative controls for all viability and synthesis experiments. Explants were "killed" by placing the cores after washing into an incubator (56°C) for 6 to 8 hours. This was enough to kill the cells, but did not alter the mechanical properties of the tissue.

Quantitative analysis of core stiffness, for explants maintained *ex vivo* in the Zetos loaded culture system, in comparison to negative control tissue. An increase in stiffness

would be interpreted as a sign that the tissue was metabolically active forming new bone to resist the force being placed upon it. A similar change in stiffness to disuse or necrotic tissue would be a sign that the tissue was not being maintained *ex vivo* and possibly in a state of resorption. A similar change in stiffness to dead tissue would suggest the technique was artefactual and not sensitive to use to detect changes occurring post-harvest. The number of ovine, bovine and human cores assessed in this manner was 46.

3.b.ii. Explant Analysis

Sample processing

The samples were fixed in 70% ethanol at 4°C and dehydrated in an ethanol series before being embedded in technovit resin (see Chapter 2b. for a more detailed description). Once embedded, the bone cores were sectioned, stained and imaged with the Zeiss microscope and camera (Axioplan Imaging), and processed with Axiocam and Axiovision package.

Qualitative analysis of tissue morphology regarding cell types and location of tissue sections from explants maintained *ex vivo* in the Zetos loaded culture system, in comparison to positive and negative control tissue explants. Similar morphology to fresh samples would be interpreted as a good sign that the tissue was healthy. Similar morphology to disuse or necrotic tissue would be a sign that the tissue was not being maintained *ex vivo*. Similar staining to dead tissue would suggest the technique was not sensitive to use to detect changes occurring post-harvest. Twenty sections obtained from the centre of the core and twenty sections obtained from the surface of the core, were assessed in this manner from a group where n=26, 40, 18, for each species ovine, bovine and human respectively. Summarised in table 3b.2

TRAP staining of embedded tissue [Sigma 387]

Sections were deacrylated to allow the stain to penetrate. This was accomplished through the following procedure:-

The glass slides were placed in MEA (1-acetoxy-2-methoxy-ethane) (Fluka, 00860) for 2 x 30 min, then through a graded ethanol series (100%, 96%) before being placed in water ready for staining.

The slides were incubated in 0.2M Tris buffer pH9 for 1 hour at 37°C. Tris buffer is the preferred phosphate buffer system for diagnostic reagents due to low metal content

providing better control of pH above 7.5. Slides were rinsed in dH_2O for 5 min before being placed in one of 2 Coplin jars: -

Table. 3b.1. Solution for controlled TRAP staining

Reagents	- control	+ control
37°C dH_2O	45 ml	45 ml
Fast Garnet & sodium nitrate solution*	1 ml	1 ml
Napthol AS-BI	0.5 ml	0.5 ml
Acetate	2 ml	2 ml
Tartrate	-	1 ml

* Solution made by placing 0.5 ml Fast Garnet and 0.5 ml sodium nitrate into Eppendorf tubes, mixing, and leaving to stand for 30 s.

The solutions were placed over the slides, and incubated in the dark at 37°C (water bath) for 1 hour. Slides were then rinsed in dH_2O for 5 min before being counterstained in hematoxylin. In order to turn the nuclei blue, the slides were rinsed in alkaline tap water. The slides were dehydrated, rinsed in xylene, and then immersed in xylene for 30 minutes and mounted with Eukitt (O. Kindler GmbH & Co., Freiburg, Germany).

3.b.iii. Media Analysis

Lactate dehydrogenase (LDH) assay [bioMérieux® sa REF63400]

Media was sent to a local company (MEDITEST) for quantification of LDH secreted from compromised cells. In principle the following reaction should occur:

$$\text{Pyruvate} + \text{NADH} + H^+ \xrightleftharpoons{\text{LDH}} \text{L-lactate} + NAD^+$$

The reagents were prepared as follows: -

2.8 ml Phosphate buffer was mixed with 2.8 ml NADH. From this reagent 840 µl was added to 30 µl of sample media, and 30 µl pyruvate in a thermostatically controlled cuvette (37°C). After 45 seconds the mean decrease of absorbance was measured per min for a maximum of 1 min. The results were recorded as U/L the equivalent of 1 mmol of substrate catalysed per min. A control consisting of normal media was provided.

Quantitative analysis of cell death within tissue sections from explants maintained *ex vivo* in the Zetos loaded culture system, in comparison to positive and negative control tissue explants. The presence of the enzyme would be interpreted as a bad sign that the tissue was dying. A similar quantity to disuse or necrotic tissue would be a sign that the tissue was not being maintained *ex vivo*. A similar quantity to dead tissue or blank media would suggest the technique was artefactual and not sensitive to use to detect changes occurring post-harvest or that the tissue was dead. Nine human cores, from one limb were analysed in this manner

3.b.iv. Viability Stains

Several viability stains were used to assess the viability of bone cores cultured in the Zetos system. The preparation of these dyes is outlined below:

Calcein AM [Fluka, Cat. No. 17783]

A stock solution of Calcein AM was made, which consisted of 1 mg/ml in DMSO and was stored in small aliquots at -80°C. Working solution 1 µl/ml of stock solution in sterile PBS was used.

Ethidium Homodimer 1. [Fluka, Cat. No. 46043]

A stock solution of Ethidium homodimer-1 was also made, which consisted of 1 mg/ml in 20% DMSO in H_2O and stored in small aliquots at -80°C. Working solution of 1 µl/ml of stock solution in sterile PBS was used.

Fluorescein diacetate [Sigma F 7378]

A stock solution of fluorescein diacetate was freshly made by placing 1mg/ml of acetone to give a concentration of 2.13 mM. It was diluted 1:100 with PBS to give a working concentration of 21.3 µM.

Cell Tracker™ Green [Molecular Probes, C-2925]

A stock solution of CFMDA was made, which consisted of 1 mg in 0.215 ml DMSO and stored in small aliquots at -20°C. A working solution of 25 µM in a 5 ml volume of PBS was required.

SYTO24 [Molecular Probes S-7559]

The stock solution of SYTO24 (5 mM) was stored in small aliquots at -20°C. A working solution of 5 μM in a 5 ml volume of PBS was required. This dye should be protected from light whenever possible and, during, use a double layer of gloves should be worn as this dye is extremely mutagenic.

3.b.v. Staining Procedure

Several viability stains were used simultaneously to assess the viability of bone cores cultured in the Zetos system. The staining procedures for each of these dyes are outlined below.

Qualitative analysis of live vs. dead cells within tissue sections from explants maintained *ex vivo* in the Zetos loaded culture system, in comparison to positive and negative control tissue explants. Similar labelling to fresh samples would be interpreted as a good sign that the tissue was healthy. Similar morphology to disuse or necrotic tissue would be a sign that the tissue was not being maintained *ex vivo*. Dead tissue, irrespective of culture condition should only stain cells as dead and not living. Table 3b.2 summarises the number of cores analysed during these studies.

Fluorescein diacetate

Approximately 5 ml of the working solution was placed over each bone core in a multi-well plate and left to incubate at 37°C for 35 min. After incubation, the cores were washed and rinsed in separate centrifuge tubes filled with 10 ml PBS. The cores were imaged on the Zeiss microscope and camera (Axioplan Imaging), and processed with Axiocam and Axiovision package.

Calcein AM & Ethidium Homodimer 1.

When required, a working solution of 1 μl/ml of each stock solution was prepared in sterile PBS. Usually, 4 ml of sterile PBS was placed into a 50 ml (Omnilab AG, Cat no. 91050) centrifuge tube, and added to it was 4 μl of Calcein AM and 4 μl EthD-1. The centrifuge tube was vortexed in order to mix the stains. If bone cores had previously been in contact with calf serum they were washed 3 x 30 min in 10 ml sterile PBS. Bone cores were then placed in the staining solution, the tube covered with aluminium foil to block out light, and incubated at 37°C for initially 2 hours (before lack of diffusion was observed). After

incubation, the cores were washed and rinsed in separate centrifuge tubes filled with 10 ml PBS. The cores were imaged on the Zeiss photomicroscope (Axioplan Imaging) and processed with Axiocam and Axiovision.

For future experiments, incubation increased to 8 hours once it was observed that diffusion to the centre of the core took approximately 6 hours (Koller, 2004). Once stained, bone cores were rinsed 3 x 30 min in 10 ml sterile PBS to remove residual stain and then fixed in 70% ethanol at 4°C for 1 week. Samples were dehydrated in an ethanol series and embedded in Technovit resin (see Chapter 2b. for a more detailed description). Once embedded, the bone cores were sectioned and imaged with the Zeiss photomicroscope and (Axioplan Imaging) and processed with Axiocam and Axiovision package.

Cell Tracker™ Green & Ethidium Homodimer 1.

If bone cores had previously been in contact with calf serum they were washed 3 x 30 min in 10 ml sterile PBS. Bone cores were then placed in a centrifuge tube containing the vortexed staining solution (5 ml PBS, 12.5 µl CMFDA and 5 µl EthD-1), the tube covered with aluminium foil to block out light, and incubated at 37°C for 8 hours. Once stained, bone cores were rinsed 3 x 30 min in 10 ml sterile PBS to remove residual stain and then fixed in 70% ethanol at 4°C, before being dehydrated in an ethanol series and embedded in Technovit resin (see Chapter 2b. for a more detailed description). Undeacrylated 6 µm thick sections were imaged with the Zeiss photomicroscope (Axioplan Imaging) and processed with Axiocam and Axiovision package.

SYTO24 & Ethidium Homodimer 1.

If bone cores had previously been in contact with calf serum, they were washed 3 x 30 min in 10 ml sterile PBS. Bone cores were then placed in a centrifuge tube containing the vortexed staining solution (5 ml PBS, 5 µl SYTO24 and 5 µl EthD-1), the tube covered with aluminium foil to block out light, and incubated at 37°C for 8 hours. Once stained bone cores were rinsed 3 x 30 min in 10 ml sterile PBS to remove residual stain and then fixed in 70% ethanol at 4°C, before being dehydrated in an ethanol series and embedded in technovit resin (see Chapter 2b. for a more detailed description). Undeacrylated 6 µm thick sections were imaged with the Zeiss photomicroscope (Axioplan Imaging) and processed with Axiocam and Axiovision package.

Summary of tissue used and the length of culture *ex vivo.*

Table. 3b.2. Summary of experiments conducted

Experiment	Animal Species	Number of limbs	Number of cores	Number of cores in each group*	Number of Days Maintained *ex vivo.*
General Morphology	Ovine	2	26	LFr=1, DFr=1, LL=4, DL=4, LU=4, DU=4, LC=4, DC=4,	15 days
General Morphology	Bovine	2	40	LFr=4, LL=12, LU=12, LC=12,	Four from each group at day 19, 24 and 29. Including gaskets in chambers
General Morphology	Bovine	1	14	LFr=1, DFr=1, LL=2, DL=2, LU=2, DU=2, LC=2, DC=2,	23 days
General Morphology	Human	1	18	LFr=2, DFr=2, LL=3, DL=3, LU=2, DU=2, LC=2, DC=2,	15 days
Fluorescein diacetate	Bovine	1	4	LFr=4,	Stained fresh to determine properties
Calcein AM & EthD-1	Bovine	1	4	LFr=4,	Stained fresh to determine properties
CMFDA & EthD-1	Bovine	1	2	LFr=2,	Stained fresh to determine properties
SYTO 24 & EthD-1	Bovine	1	2	LFr=2,	Stained fresh to determine properties
Viability of cells (CMFDA & EthD-1)	Bovine	1	8	LFr=2, LL=2, LU=2, LC=2,	30 days Including gaskets in chambers.
Viability of cells (CMFDA & EthD-1)	Bovine	2	30	LFr=3, DFr=1, LL=5, DL=5, LU=4, DU=4, LC=4, DC=4,	One from each group at day 1,3,5,7 and loaded only at day 15.
Viability of cells (CMFDA & EthD-1)	Ovine	2	7	LFr=1, LL=2, LU=2, LC=2,	One from each group at day 7 the other day 14.

* Key to grouping. LFr= Live cores fixed Freshly after harvest procedure, DFr= Live cores fixed Freshly after harvest procedure, LL = Live cores Loaded in the Zetos culture system, DL = Live cores Loaded in the Zetos culture system, LU = Live cores Unloaded in the Zetos culture system, DU = Dead cores Unloaded in the Zetos culture system, LC = Live cores cultured in centrifuge tubes, DC = Dead cores cultured in centrifuge tubes

3.C. Results

3.c.i. General Morphology

One characteristic way of identifying dead cells is by observing a number of empty lacunae or cells with pyknotic nuclei within the tissue. General morphology of the tissue from all three species (ovine, bovine and human) was comparable to fresh tissue fixed on the day of harvest (Fig.2c.37-39). No masses of dead cells were observed. However, before detailed analysis of cell viability could take place, a number of characteristics not associated with *in vivo* tissue were observed.

In nearly every sample a lot of bone debris was blown into the surrounding marrow (Fig.3c.1). A cross-section through an ovine core, cultured within the Zetos system for 15 days, demonstrated that this occurred primarily at the periphery of the sample, in close proximity to the surfaces cut by the drill (black arrows, Fig.3c.1i), rather than the surfaces cut with the annular saw (red arrow, Fig.3c.1i). A transverse section from the same sample confirmed this, showing that most of the debris was pushed within the soft tissue at the surfaces where the drill would have been in contact to the tissue (black arrows, Fig.3c.1ii). However, it was also possible to see that a small amount of debris was left within the soft tissue at surfaces cut with the annular saw, but not to such an extent as the drill (red arrows, Fig.3c.1ii). The presence of bone debris suggests there may be an irrigation problem during sample harvest, even though the drill bit has a unique fluted surface (Fig.1b.8), designed primarily to allow saline to reach the bone, thus, allowing the sample and blade to be cooled and the debris to be released. It is obvious that not enough dust is being removed and is, thus, being compacted within the soft tissue. This is generally avoided with the surface cuts (annular and Exakt saws) as there is more free space around the sample allowing the saline to push the dust away. Cross-sectional images (human tissue, cultured within the system for 15 days) from figures 3c.1iii. and 1iv., show that the distance the debris can penetrate into the samples can be up to 1mm. Thus, up to 36% of tissue volume could be lost due to debris damage. Figure 3c.1v illustrates how the debris can affect areas of active bone apposition and mineralisation by removing all of the bone and marrow cells (human tissue cultured for 15 days). Though the damage is not as severe on the upper and lower surfaces, cut by the annular saw, small deposits of debris was occasionally seen (red arrow), often surrounded by fibrous-like cells (white arrow) (Fig.3c.1vi. Ovine tissue cultured within the system for 15 days).

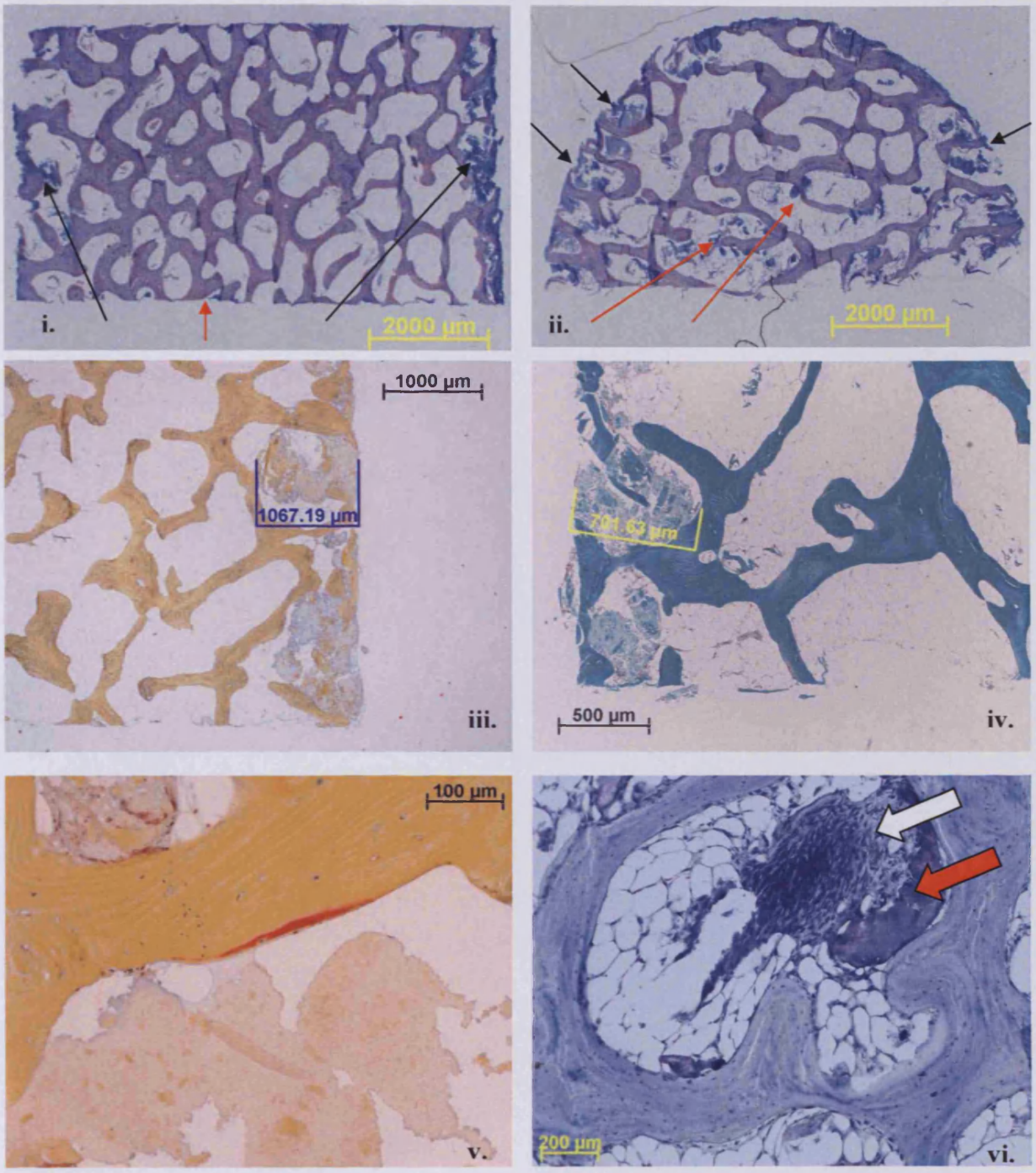

Figure 3c.1 i) *Giemsa stained cross-section, showing debris all along periphery (black arrows) little on surfaces (red arrow).* **ii)** *Transverse-section from sample i. Bone debris can be seen in areas that came into contact with the drill (black arrows) some debris on surface (red arrows).* **iii)** *Movat stained cross-section, demonstrating bone debris having been pushed at least 1mm into the soft tissue.* ***iv)*** *Masson stained cross-section, demonstrating debris at least 0.7mm into the soft tissue. Sparse debris can be seen on the bottom and top surfaces, suggesting that the drill bit causes most damage.* **v)** *Movat stained cross-section, demonstrating damage to active surface.* **vi)** *Toluidine blue stained transverse-section, demonstrating fibrous-like tissue (white arrow) in close proximity to surface bone debris (red arrow). [Characteristic image from one of twenty sections obtained from the centre of the core, providing a representation from a group n=128] [Characteristic image from one of twenty sections obtained from the surface of the core, providing a representation from a group n=66]*

Another noticeable difference that was observed with cultured tissue when compared to the *in vivo* situation. A mass of fibrous-like tissue developed over the outer surfaces of the cores (Fig.3c.2). With bovine tissue, this fibrous-like tissue had formed a dense skin-like covering over the outer regions of the core that was visible by eye (Fig.3c.2i). This fibrous-like encapsulation was more pronounced with control samples cultured in centrifuge tubes, but was also observed with Zetos cultured, loaded, and unloaded cores. No fibrous tissue was observed around dead control bone samples. Fibrous tissue was also observed with human tissue and, to a slightly lesser extent, with ovine tissue. This difference in the amount of fibrous-like tissue may be due to a more varied cell population within the human and bovine explants. Bovine and human marrow has a lot of hemopoietic cells (red marrow) within the marrow. Microscopically, the fibrous-like layer of cells was observed on all surfaces (drill cut or annular cut). Figures 3c 2ii-iv demonstrates how the fibrous-like tissue covered the outer surfaces of human bone (81 year old male) cultured within the Zetos system for 23 days. The higher power images show that the fibrous-like skin was several cell layers thick, in places reaching 300μm. In other areas, the fibrous layer was much thinner, around 50μm, as seen in the bovine tissue in figure 3c 2v (yellow arrow). Also visible was a vast amount of bone debris within the trabecular bone (red arrow). A similar scene is evident in figure 3c 2vi, with the fibrous-like cells filling the space between trabeculae and surrounding adipocytes.

After removing some of the cores from the culture chamber, it became clear that the black neoprene gaskets used to hold the bone cores in position, and to aid the transport of the media through the core, were in fact, damaging the cancellous bone cores, and possibly affecting the loading of the explants. Low power images demonstrated broken trabeculae (Fig.3c.3i) and an obstruction to media flow (Fig.3c.3i).

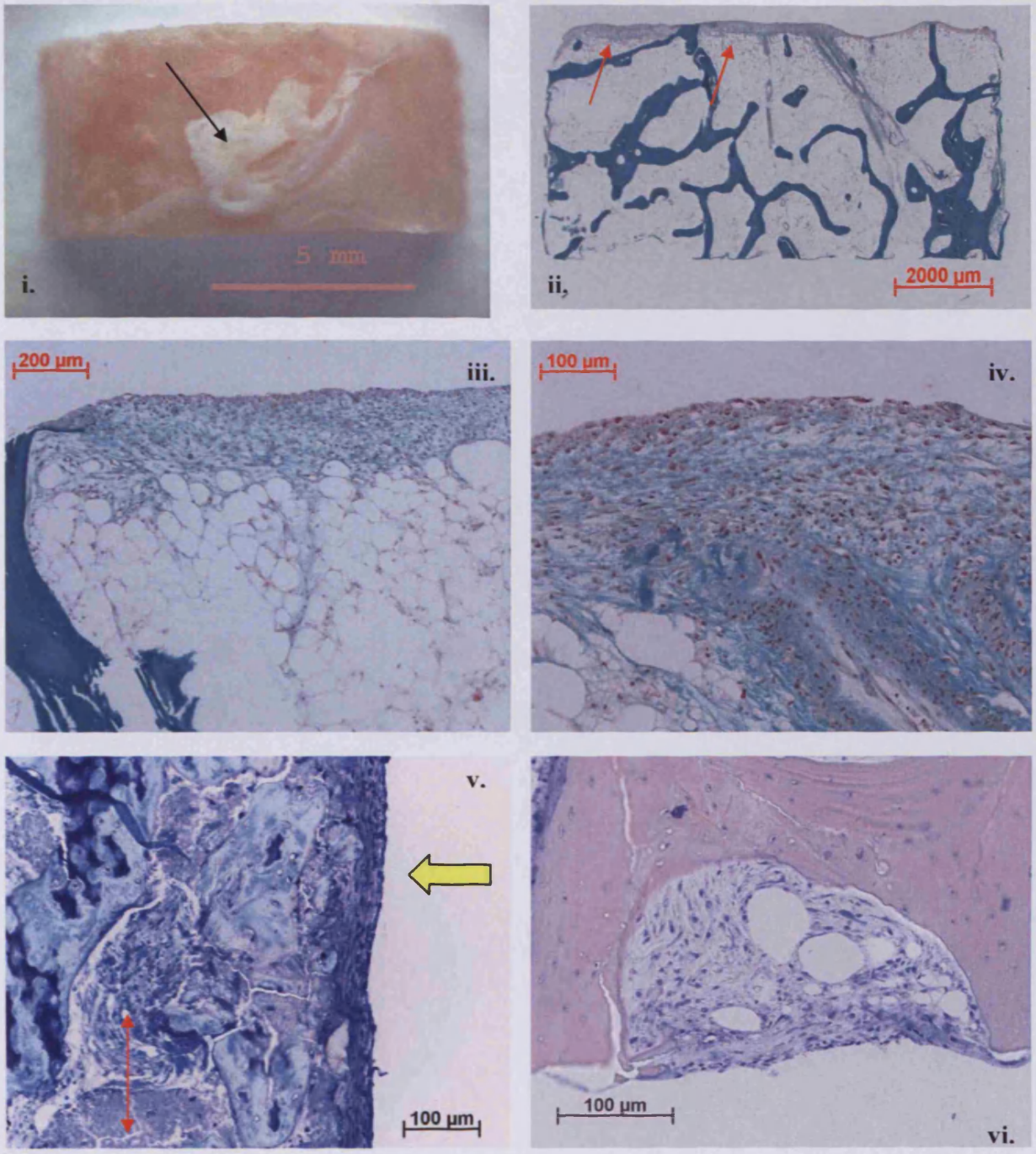

Figure 3c.2 i) *Bovine bone core cultured within the Zetos system for 30 days. A fibrous-like skin can be seen surrounding the outer periphery (black arrow).* **ii)** *Low power image of a cross-section through a human core (81 yr, 26 day culture), Masson stained. Red arrows depict fibrous-like layer of cells.* **iii)** *High magnification of previous image to highlight extent of fibrous-like tissue.* **iv)** *High magnification of fibrous-like cells from previous image.* **v)** *Toluidine blue stained, cross-section of bovine tissue cultured within the chamber for 23 days. Fibrous layer can be seen surrounding bone debris at the periphery of the sample (red arrow).* **vi)** *Giemsa stained cross-section, bovine tissue cultured for 23 days. Fibrous-like tissue contained within calcified matrix. [Characteristic image from one of twenty sections obtained from the centre of living cores, providing a representation from a group n=53][Characteristic image from one of twenty sections obtained from the surface of living cores, providing a representation from a group n=53]*

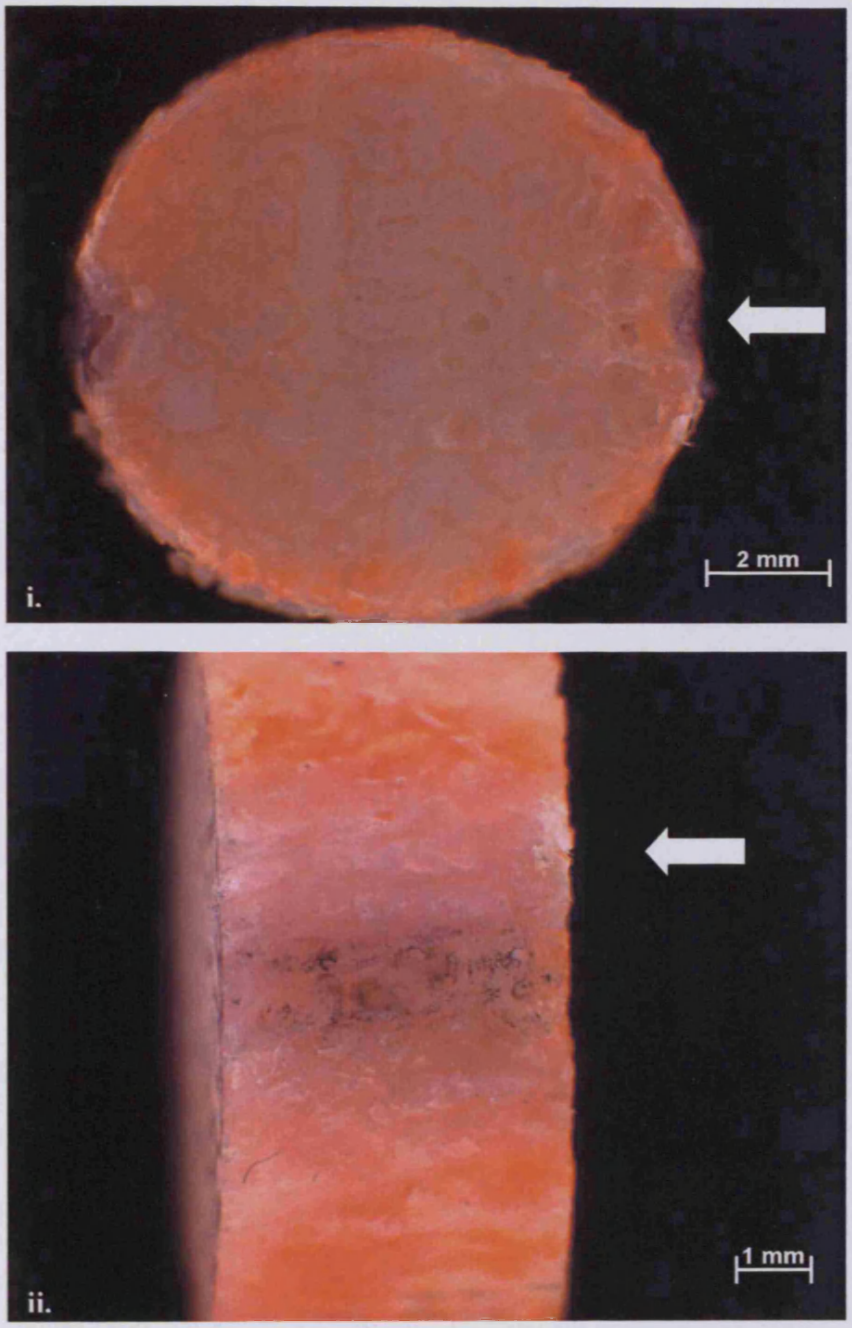

Figure. 3c.3. i) *Images of a whole bone core, demonstrating damage to outer surface caused by black neoprene gaskets located within the chamber (white arrow).* **ii)** *Apart from black residue, a lack of staining can be seen in close proximity to the gasket (white arrow). These were initial observations. No histological evaluations of cores cultured within Zetos chambers containing gaskets were included within the rest of the thesis. [A representation of 24 cores from 2 limbs analysed in this manner] [Image taken by Christoph Sprecher with a digital camera].*

However, despite some of these flaws, overall good morphology was observed in cancellous explants cultured in a loaded environment of the Zetos system. Connectivity of trabeculae was observed with no broken struts due to overloading. Osteocytes were observed throughout the calcified matrix. Red and white blood cells as well as adipocytes were observed between trabeculae. In places, non-functioning blood vessels were seen, as well as osteoblasts laying down osteoid and osteoclasts within their Howship's lacunae. This morphology was similar for all three species as can be see from Figures 3c.4, 3c.5 and 3c.6.

Ovine Tissue

Osteoclasts were visible at the surface of a trabecule in ovine tissue cultured within the Zetos system for 15 days (Fig.3c.4i). A low power image of soft tissue and calcified tissue highlights good tissue preservation (Figure 3c.4ii). There was no osteoid present. In fact, nearly no osteoid was present in any ovine samples (including cores fixed freshly on day of harvest). This may be due to the fact that most of the ovine tissue was harvested for culture over winter months, and it is believed that sheep reduce their bone turnover (Rosen *et al.*, 1999). This lack of osteoid is again emphasised in Figure 3c.4iii of ovine tissue cultured in the Zetos system for 15 days. Cells on the surface of the tissue were differentiating to a more fibrous-like appearance (Figure 3c.4iv). The lack of osteoid present within the tissue is further highlighted (Figure 3c.4v and 4vi of ovine tissue cultured in the Zetos system for 15 days)

Bovine Tissue

Bovine tissue suggested a much higher activity, presumably due to the young age of the animal. Good tissue preservation was observed (low power image 3c.5i, from bovine tissue 4 month old, cultured in the Zetos system for 23 days). Osteoid seams were present in bovine tissue cultured in the system for 23 days (Figure 3c.5ii). The mineralisation front can be seen as a dark blue band (black arrow) the uncalcified region is in a lighter shade of blue. Movat staining in shows the osteoid as a red layer and within the marrow a non-functioning blood vessel can be seen (Fig. 3c.5iii). Three osteoclasts in their scalloped edge Howship's lacunae were observed (Fig. 3c.5iv). Areas of endochondral ossification were observed in some cores (Figures 3c.5v and 5vi, bovine tissue, 4 month old, cultured 23 days). Woven bone (pink) can be seen surrounding a cartilage scaffold (dark blue) with two osteoclasts/chondroclasts within the soft tissue (Figure 3c.5v). Spicules covered with osteoblasts and osteoclasts were common (Figure 3c.5vi).

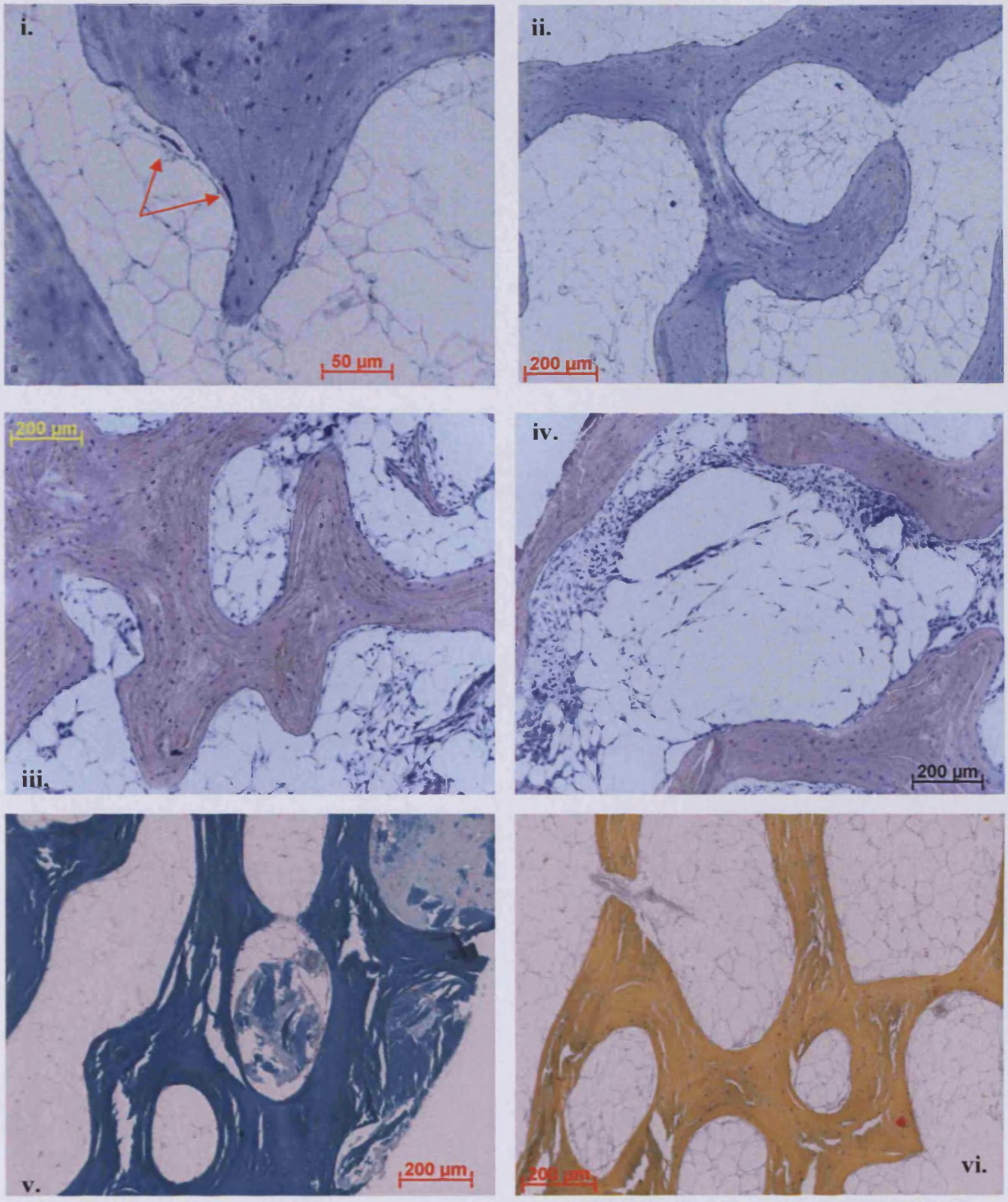

Figure 3c.4. i) *Toluidine blue stained cross-section of ovine tissue depicting osteoclasts on trabecule surface (red arrows).* **ii)** *Toluidine blue stained cross-section depicting morphology of sparse osteoid seams.* **iii)** *Giemsa stained transverse-section showing no empty lacunae and no osteoid.* **iv)** *Giemsa stained transverse-section showing fibrous-like cells aligning the trabeculae, again no osteoid.* **v)** *Masson stained transverse-section depicting general morphology, no osteoid seams. Bone debris can be seen filling soft tissue.* **vi)** *Movat stained cross-section depicting general morphology of sparse osteoid seams. [Characteristic image from one of twenty sections obtained from the centre of the core, providing a representation from a group n=26]*

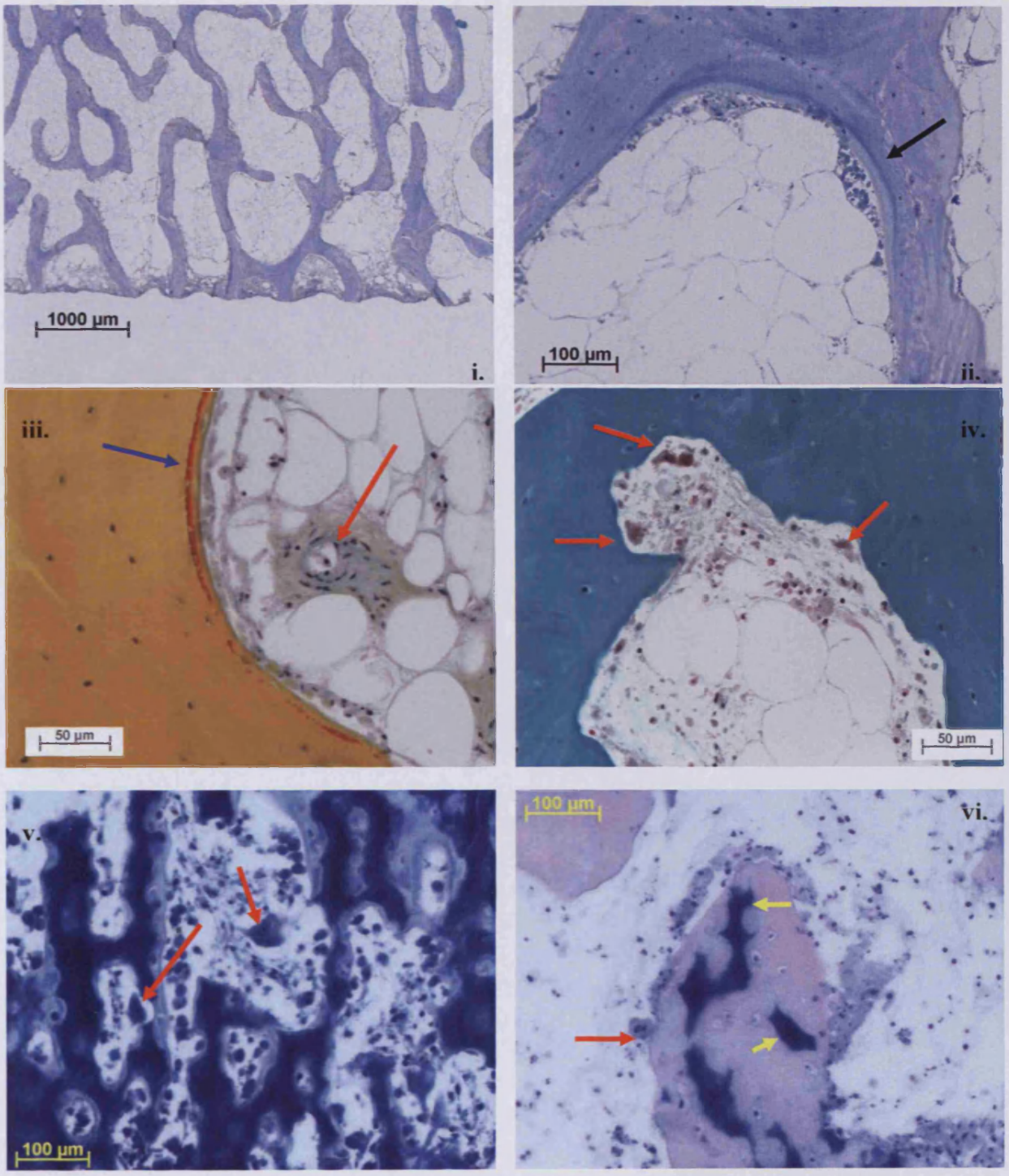

Figure 3c.5. i) *Toluidine blue stained cross-section of bovine tissue showing good tissue preservation.* **ii)** *Toluidine blue stained tissue (23 day culture) depicting freshly laid osteoid seam (pale blue), mineralisation front (black arrow).* **iii)** *Movat stained tissue (23 day culture) depicting freshly laid osteoid seam (blue arrow) with a blood vessel within the marrow (red arrow).* **iv)** *Three osteoclasts seen within a Howship's lacunae (red arrows). Masson stained section from bovine tissue cultured 23 days.* **v)** *Toluidine blue stained bovine section cultured for 23 days. A cartilaginous scaffold can be seen as well as fresh bone; osteoclast within soft tissue (red arrows).* **vi)** *Osteoclasts (red arrow) and osteoblasts on a bone spicule still containing cartilage (yellow arrows). Giemsa stained section from bovine tissue cultured 23 days. [Characteristic image from one of twenty sections obtained from the centre of the core, providing a representation from a group n=14]*

Human tissue

The general cross-sectional morphology of loaded human bone tissue (71 yr old male) cultured within the Zetos culture system for 15 days is shown in Figure 3c.6i and 6ii. Like the ovine tissue, there was little osteoid present. This lack of osteoid was also true for the freshly fixed samples. Large non-functional blood vessel could also be observed (red arrow) (Figure 3c.6ii). Fibrous-like tissue could be seen forming a ring at the surface of the explant (black arrow) (transverse-section, 71 yr old male, cultured for 15days) (Figure 3c.6iii). Several thin osteoid seams could be observed as red bands with the Movat stained human tissue (green arrows) (Figure 3c.6iv). Osteoclasts within scalloped shaped lacunae were observed in figure 3c.6v (red arrows) (male 81 yr old tissue cultured for 21 days). Vast amount of haemopoietic cells (blue arrows) were present in the human tissue, red and white blood cells surround the adipocytes (male 81 yr old tissue cultured for 21 days) (Figure 3c.6vi).. All of these images suggested morphology similar to that seen in the *in vivo* situation.

Control tissue

Negative control tissue from dead samples (heat killed, 60°C, 4-8h), centrifuge cultured samples and unloaded Zetos cultured samples, are shown in Fig 3c.7. These could also be compared with fresh tissue (positive control) seen in Fig.2c37-39. No clear differences in morphology can be seen.

Unloaded samples (Figure 3c.7i and 7ii), from human tissue 71 yr old male, shows the same morphology, with lack of osteoid seems. No extra osteoclasts were observed, as was hypothesised, that tissue in disuse has an increased bone resorption. The tissue was living, as seen by the formation of fibrous-like cells at the samples surface (black arrow) (Figure 3c.7ii). Dead tissue, imaged in figure 3c.7iii and 7iv, show a lack of cells within areas (blue arrows), but the vast majority remaind, osteoid seams also remain (green arrow). No fibrous-like cells were observed in any dead explant regardless of species (71 yr old male, 15 day culture). Living explants cultured for 15 days in centrifuge tubes also showed morphology comparable to that of loaded tissue (Figure 3c.7v and 7vi). Small amounts of osteoid could be seen (red) (Figure 3c.7vi) (71 yr old male, 15 day culture), which does not imply tissue is growing as they are still present in dead tissue (Figure 3c.7iii).

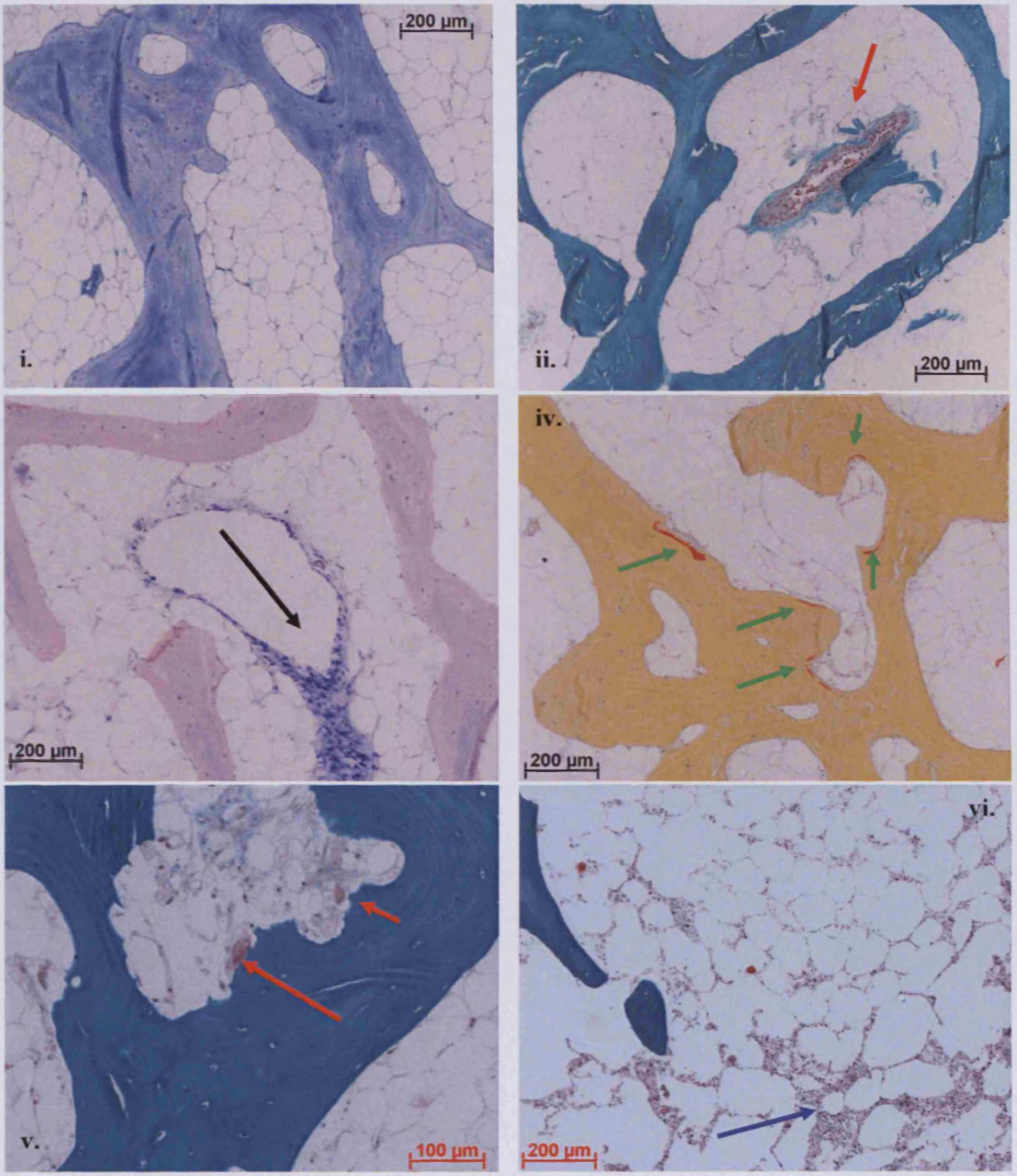

Figure 3c.6. i) *Toluidine blue stained human tissue (71 yr), cultured loaded within the Zetos system for 15 days. Not much new bone formation visible, most surfaces were quiescent.* **ii)** *Masson stained human tissue (71 yr), cultured for 15 days. A blood vessel can be seen within the soft tissue (red arrow).* **iii)** *Fibrous cells can be seen on the surface within the marrow (black arrow). Again most trabeculae are quiescent. Giemsa stained human tissue (71 yr), 15 day culture.* **iv)** *Osteoid seams can be seen (red)(green arrows) on the bone surface (yellow). Movat stained human tissue (71 yr), 15 day culture.* **v)** *Masson stained, human tissue (81 yr), cultured in the loaded system for 21 days. Osteoclasts present in Howship's lacunae (red arrows).* **vi)** *Red marrow seen within the adipocytes (yellow marrow) (blue arrow). Masson stained human tissue (81 yr), 21 day culture. [Characteristic image from one of twenty sections obtained from the centre of the core, providing a representation from a group n=18]*

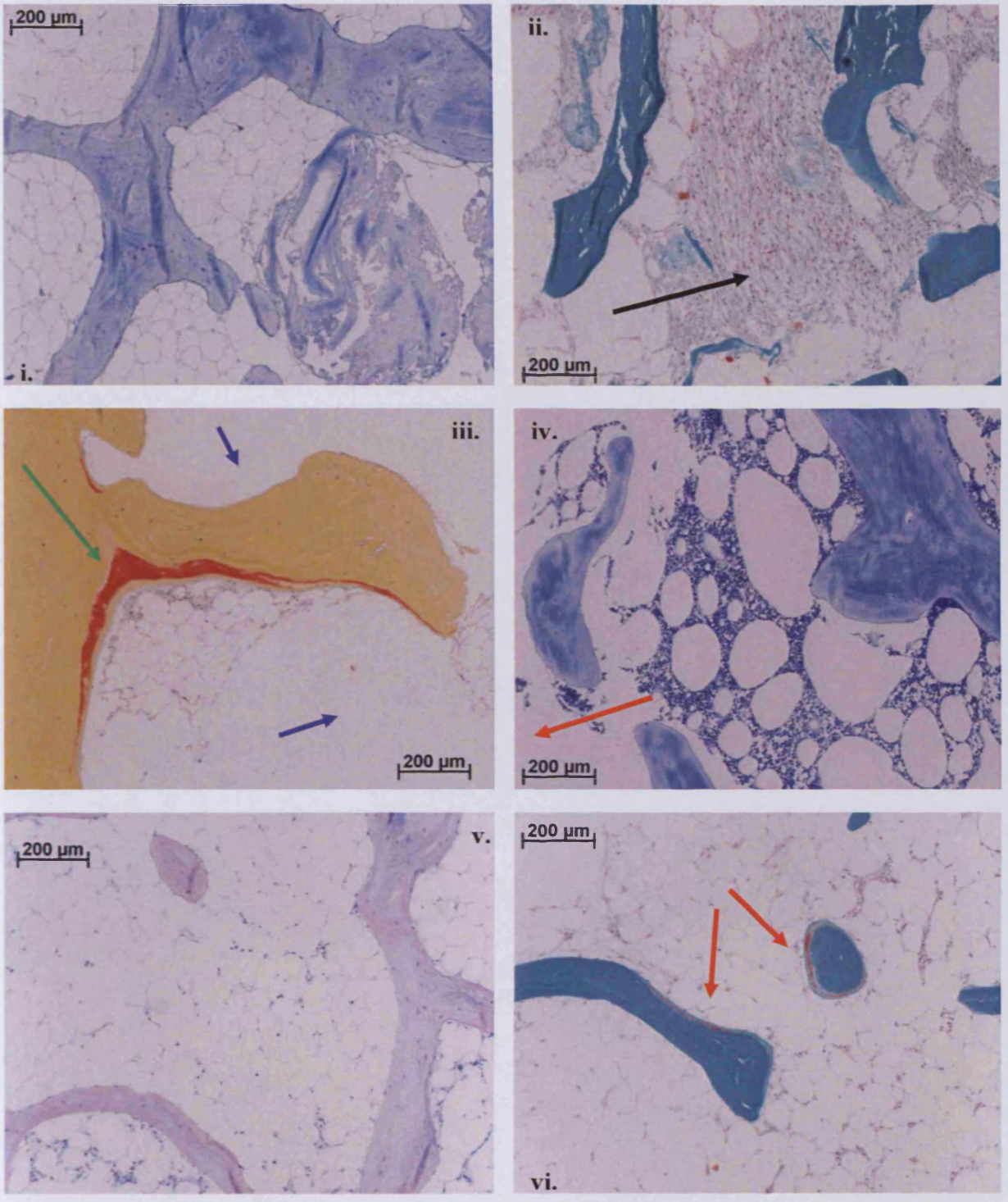

Figure 3c.7 i) *Toluidine blue stained cross-section from human tissue cultured within the Zetos system, unloaded for 15 days.* **ii)** *Masson stained transverse-section from human tissue cultured within the Zetos system unloaded. Fibrous-like cells were present on the surfaces (black arrow)* **iii)** *Movat stained cross-section from dead human tissue cultured within the Zetos system. Loos of cells were observed (blue arrows) as well as retention of osteoid seams (green arrow).* **iv)** *Toluidine blue stained cross-section from dead human tissue cultured within the Zetos system for 15 days. Loss of cells is also visible (red arrow).* **v)** *Giemas stained cross-section from human tissue cultured within centrifuge tubes. Lack of osteoid was observed.* **vi)** *Masson stained transverse-section from human tissue cultured within centrifuge tubes for 15 days. Osteoid seams (red arrows)*

3.c.ii. Viability Labels

Several viability labels were used to assess their ability to be used as viability markers for bone cells within 3D bone tissue cultured in the Zetos system.

Fluorescein diacetate

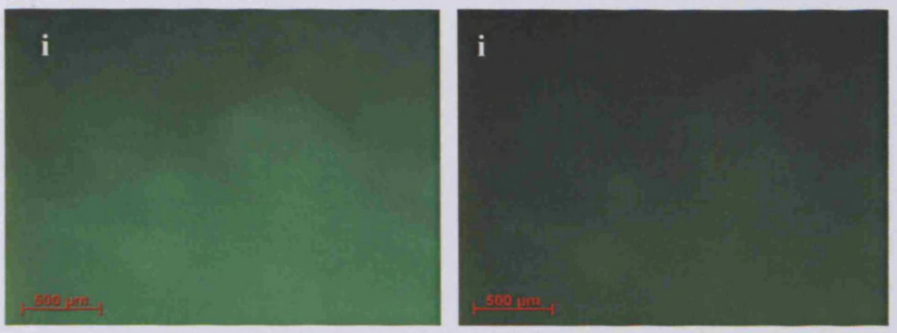

Figure 3c 8 i) *Unfocussed image immediately taken.* **ii)** *The same image 10 s later. The bovine bone and bone cells are not distinguishable. [A representation of 4 bovine cores analysed in this manner]*

Fluorescein diacetate was used alone to assess the number of viable cells present in a freshly harvested and stained core (5 mm high, 10 mm in diameter) without prior sectioning or cutting. Unfortunately, the bone cores that were stained with fluorescein diacetate made it difficult to distinguish cells from background fluorescence (Fig.3c.8). When the light was focused onto the sections for imaging, the fluorescence would fade within 10 seconds, before an image could be taken (Fig.3c.8ii). In order to demonstrate this phenomenon the section had to be imaged immediately before focussing could take place or the fluorescence would be lost.

Calcein AM & EthD-1

Calcein AM used in conjunction with EthD-1 demonstrated a layer of dead cells ~ 1 mm in depth around the periphery of the bone cores (Fig.3c.10). The cores stained with calcein AM and ethidium homodimer-1 simultaneously were far easier to image than the fluorescein diacetate stained cores. An overview of the core was taken at the edge of the sample (Fig.3.c.9). Here it was possible to see the trabecular bone stained grey, the live marrow cells in between were stained green, and the dead cells, which were mainly seen on the periphery were stained red. The blue fibre-like structures were artefacts caused by dust particles.

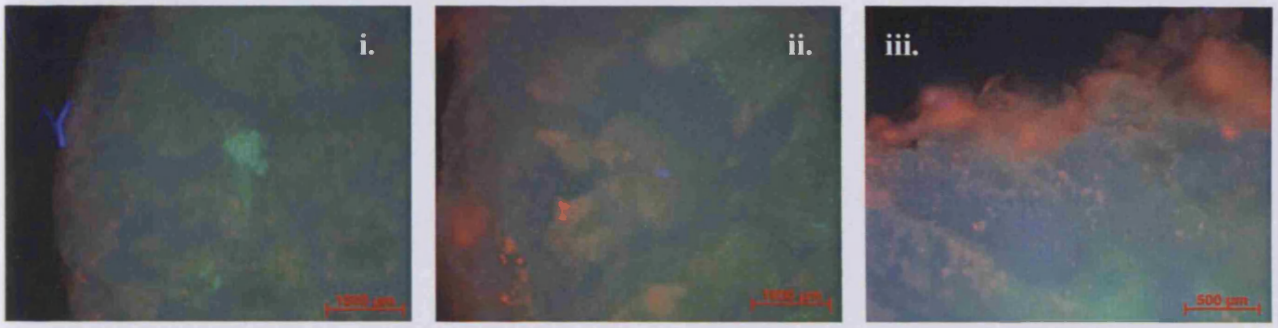

Figure 3c.9 i) *Overview of a bovine bone core.* **ii)** *Closer view of the same area.* **iii)** *High power image of the bone core periphery. Trabeculae are grey, while living cells were labelled green and dead cells labelled red. Due to core thickness single cells were not visible. [A representation of 4 bovine cores analysed in this manner]*

A higher powered close up of the same view allowed the surface cells to be seen in more detail, dead cells were labelled red while living cells were labelled green (Fig.3c.9.ii). Each red dot represents a cell; the background staining is due to the depth of the bone marrow, which is not in focus compared with the surface.

High power examination clearly demonstrated that drilling of the cores killed the cells on the periphery of the bone core (Fig.3c.9.iii). It was surprising to note that the surface area did not show as much cell death as there was at the periphery. This effect may be due to less irrigation of the bone core whilst drilling compared to sawing, thus producing more heat to kill cells. This problem could be overcome with increased irrigation during drilling.

Fixing the above imaged bone cores in 70% ethanol at 4°C preserved the labelling of the cells (Fig.3c.10.). However, the calcein stain did not remain within the cells through the embedding procedure, though EthD-1 did survive the process.

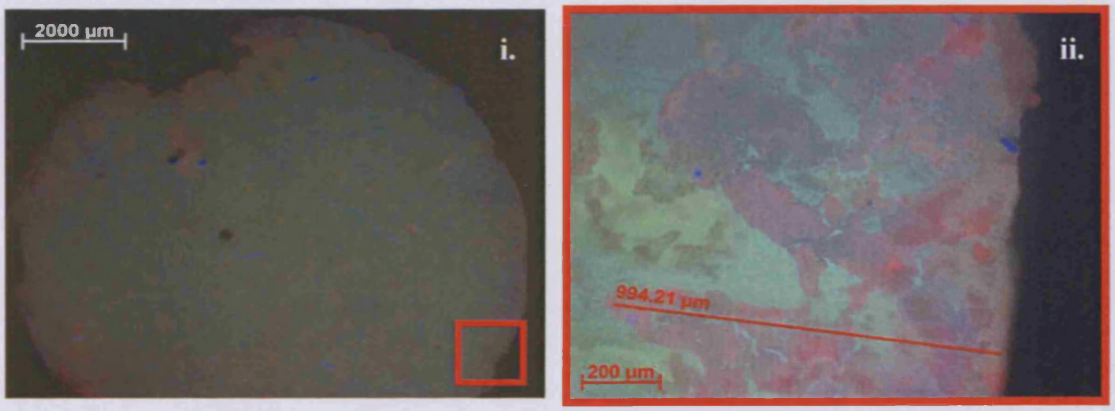

Figure 3c.10 i) *Bovine bone core stained for viability after fixation in 70% ethanol before embedding* **ii)** *Distance of dead cells from the periphery of the core to the centre.*

Figure 3c.10 shows that cell death was apparent approximately 1 mm in to the core. This distance would mean that, in theory up to 36% of the bone volume would be lost before culture began.

Calcein AM and EthD-1 was also used to evaluate the viability of bone cores cultured with the Zetos system. This labelling required increasing the culture period in order to make sure the stain diffused to the centre of the bone cores. Incubation time was increased from 2 hours to 8 hours at 37°C. Bone cores were then fixed before being cut in half and viewed. However, this technique was not optimal, and a better staining technique was sought.

SYTO24 & EthD-1

These stains worked well in conjunction with each other. They both allowed single cells to be visualised (Fig.3c.11i). The stain also survived the tissue processing and embedding (Fig.3c.11ii). However, with this staining technique it was not easy to define dead from living cells. All cells were initially stained green by the SYTO24, then the EthD-1 would displace the SYTO24 from the DNA of dead cells, thus turning the cells an orange colour. In places some cells were still stained green, suggesting that the EthD-1 was not always displaceing the SYTO24. If this was the case then using this stain would underestimate dead cells. For this reason this stain was not used for Zetos cultured cores.

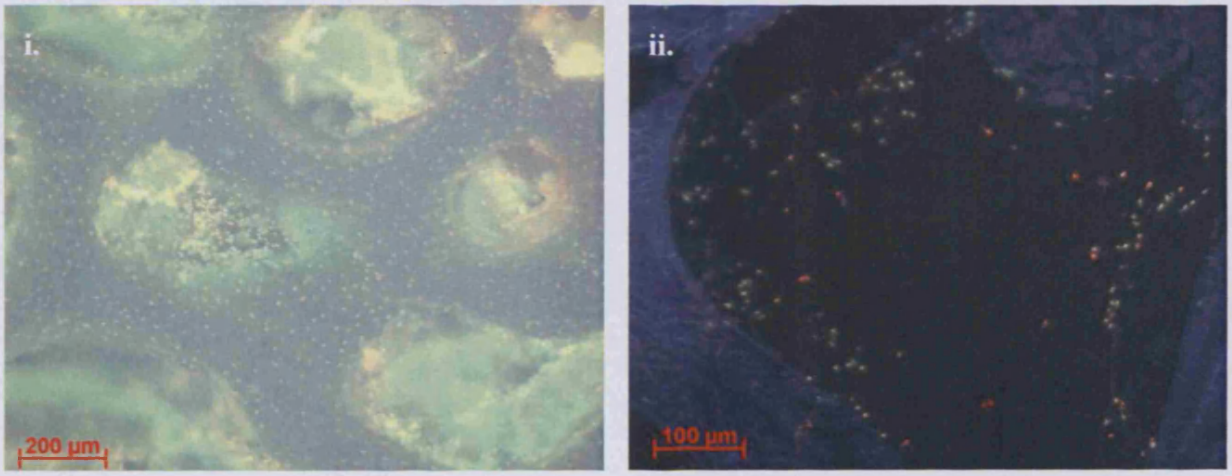

Figure 3c.11 i) *This image was taken from a heat killed sample, left for 6 hours at 60°C in saline (bovine tissue). The osteocytes can be seen very well. The marrow seems to be disrupted. Unfortunately it is not clear which cells are alive and which are dead.* **ii)** *The stain remained within the cells through fixation (70% ethanol) and embedding in Technovit 9100 New resin. However, again it was not clear which cells were dead and which were alive. [A representation of 2 bovine cores analysed in this manner]*

Cell Tracker™ Green & EthD-1

It was observed that these labels remained within the cells throughout the tissue processing to produce an embedded sample. Sections 6 μm thick were cut and imaged. It was possible to see a range of living green fluorescent cells, bone lining cells and active osteoblasts resting on calcified trabeculae (grey-blue fluorescence), which was distinguishable from red fluorescent dead cells.

Images from a cross-section of an explant cultured in a loaded condition within the Zetos system, for 30 days, is shown in Figure 3c.12. However, it was observed that most of the label only penetrated as far as the thick fibrous-like tissue that surrounded the outer periphery.

Images from a sample cultured in the Zetos system (without load) are shown Figure 3c.13. Again it is possible to see living cells within the fibrous membrane, but also a number of dead cells were observed in the soft tissue and lining the trabeculae. It was also noted that the stain did not penetrate much further than 200 μm into the tissue.

A similar outcome was seen for cells within the explants cultured statically in centrifuge tubes (Fig.3c.14). By comparing these results with that seen for fresh tissue, stained and fixed at the day of harvest (Fig.3c.15), it is possible to conclude that the label did not penetrate deep into the tissue, but more bone cells within the core were labelled due to the lack of fibrous tissue covering the outer surfaces to hinder diffusion. A negative control of dead tissue was used to show the CMFDA did not stain the cells (Fig.3c15v and vi).

The fibrous layer obviously adds a barrier to the diffusion of solutes. This barrier would probably stop the labels from being removed during the washing phase, causing EthD-1 to label cells during the fixation process, thus, possibly overestimating dead cells. In theory, this labelling technique seems appropriate, but in reality was not suited to the explants cultured within the Zetos system.

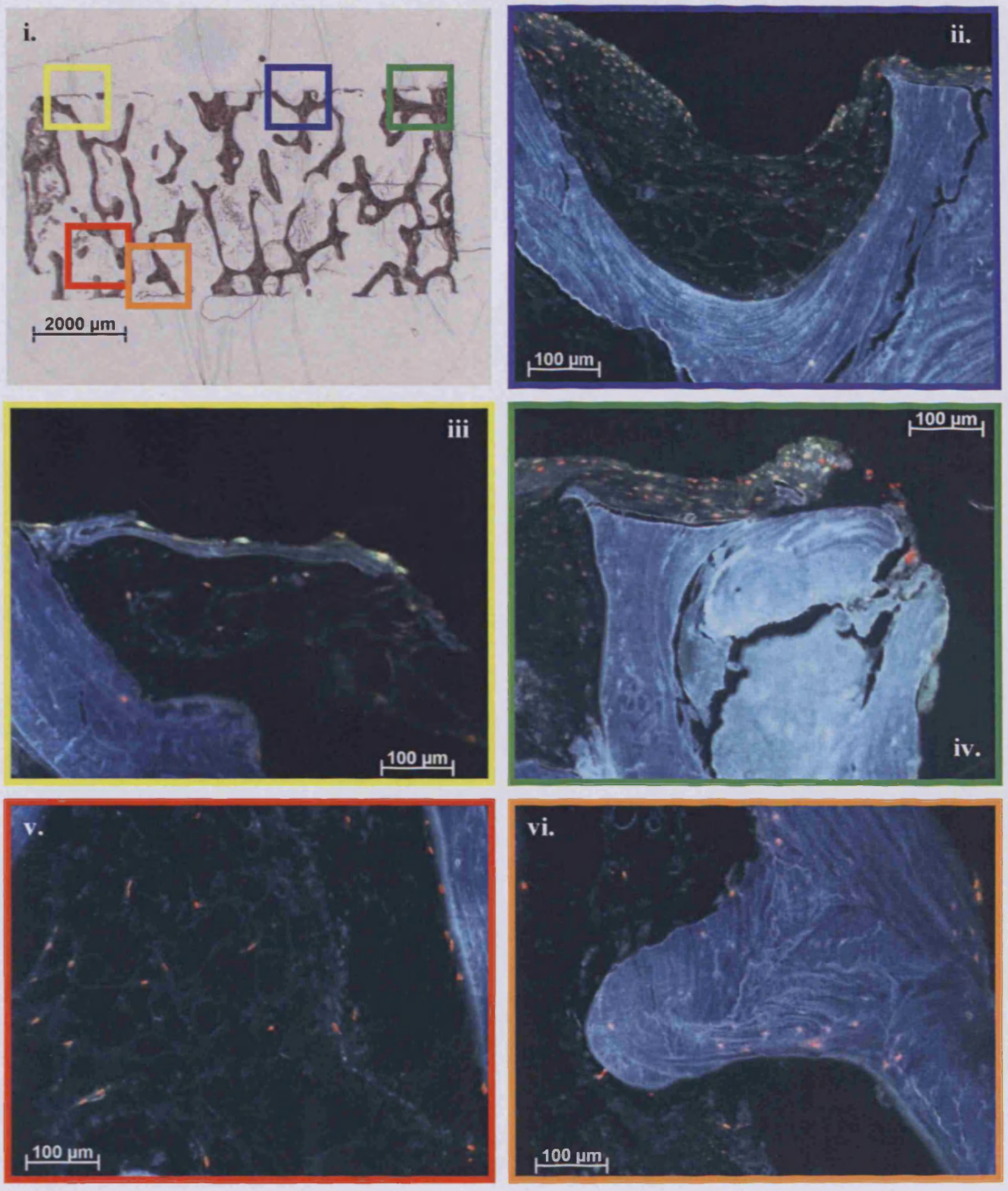

Figure 3c.12 *A cross-section from bovine tissue (4 months old) cultured in a loaded environment with the Zetos culture system for 30 days. Tissue labelled with CMFDA and EthD-1. Magnified images from certain regions of the tissue can be seen. The label did not penetrate well into the tissue, mainly reaching the fibrous tissue.The calcified bone is unlabeled and fluoresces blue, while living cells were labeled green due to the cleavage of CMFDA by esterases. Membrane compromised dead cells were labelled with EthD-1causing the cells to be labelled in red. [A representation of 2 bovine cores analysed in this manner]*

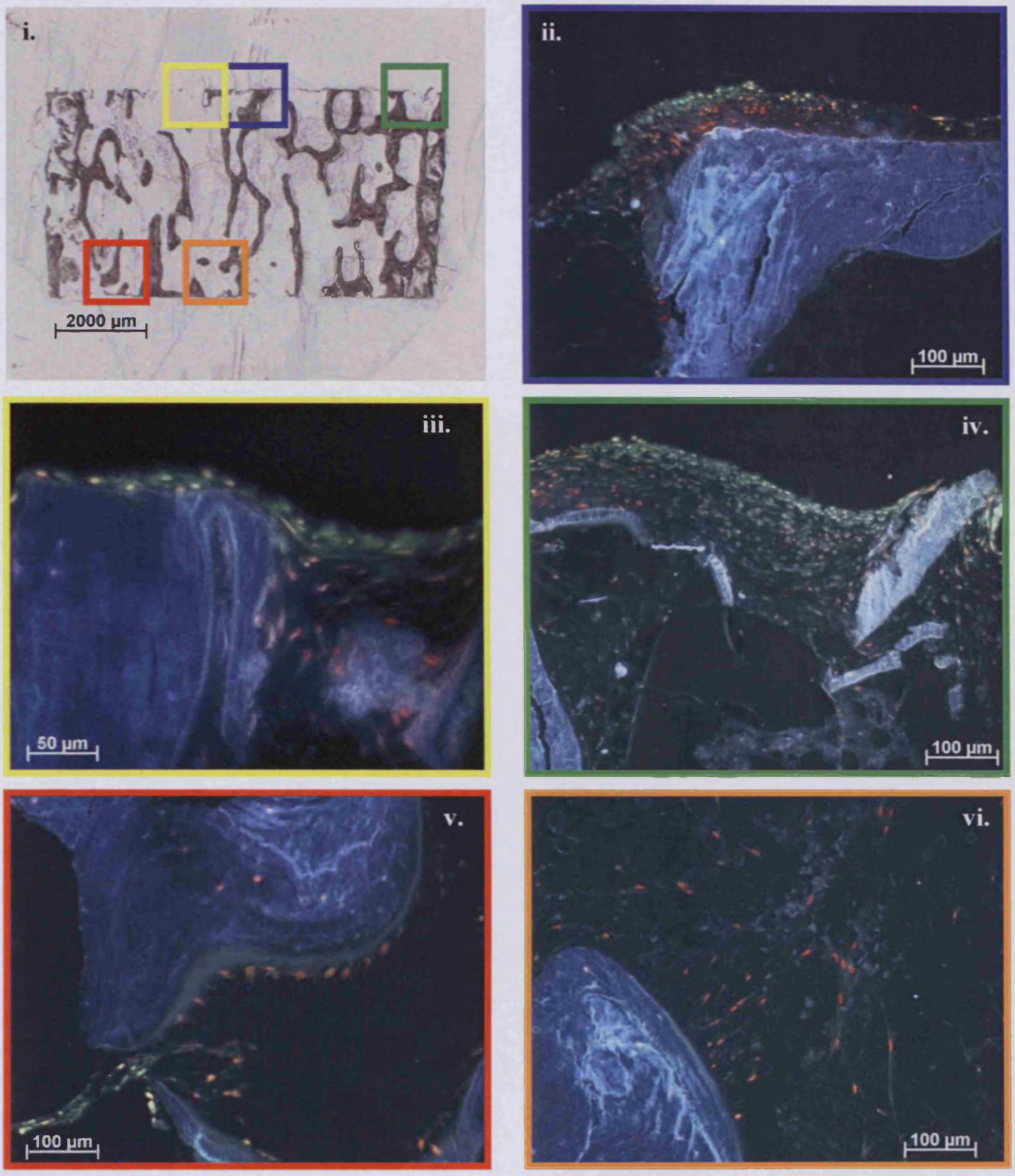

Figure 3c.13. *A cross-section from bovine tissue (4 months old) cultured in an unloaded environment with the Zetos culture system for 30 days. Tissue labelled with CMFDA and EthD-1. Magnified images from certain regions of the tissue can be seen. The label did not penetrate well into the tissue, mainly reaching the fibrous tissue. Dead cells are apparent, with live tissue towards the outer region of the fibrous tissue. The calcified bone is unlabeled and fluoresces blue, while living cells were labeled green due to the cleavage of CMFDA by esterases. Membrane compromised dead cells were labelled with EthD-1causing the cells to be labelled in red. [A representation of 2 bovine cores analysed in this manner]*

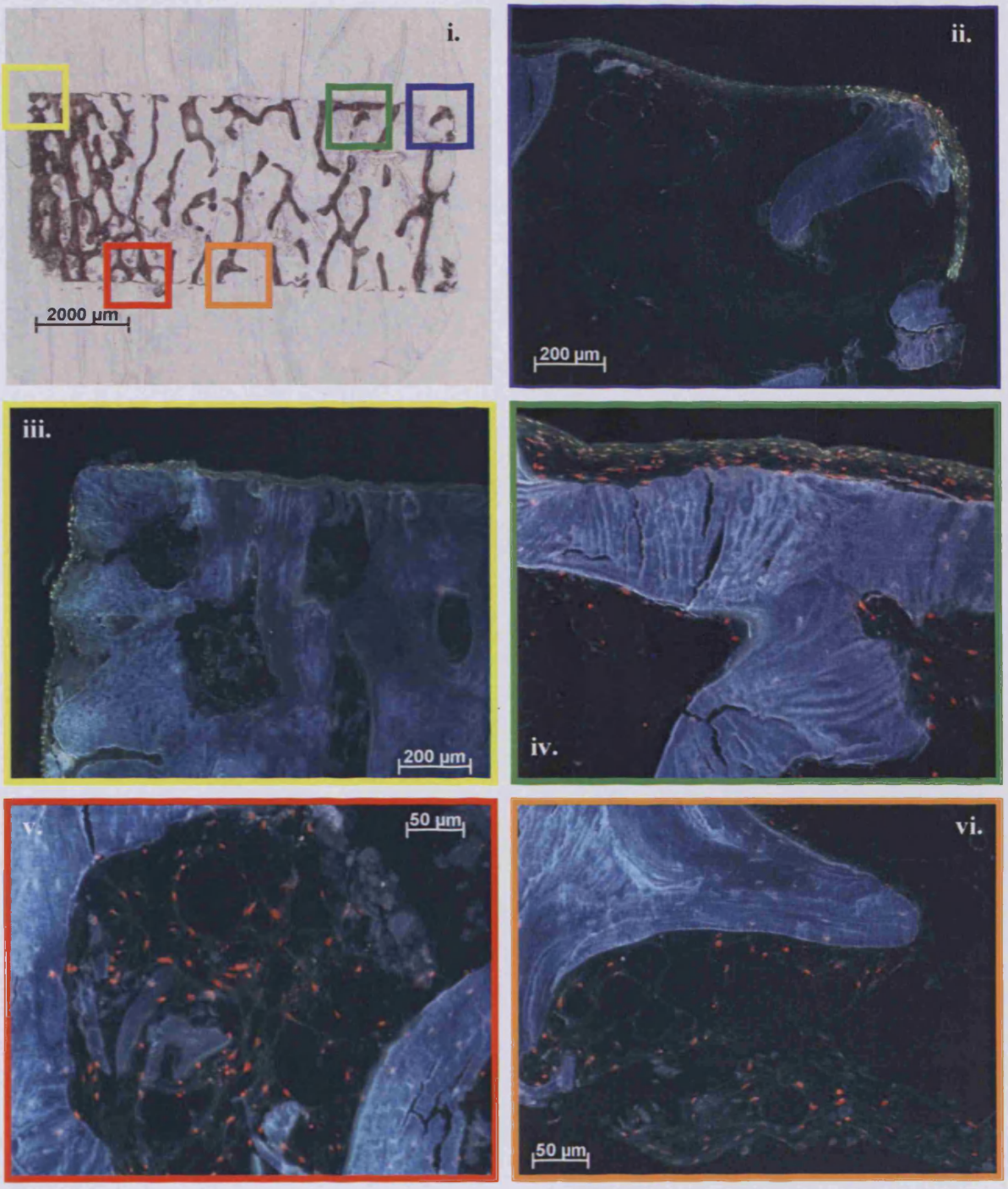

Figure 3c.14. *A cross-section from bovine tissue (4 months old) cultured in a centrifuge tube of media for 30 days. Tissue labelled with CMFDA and EthD-1. Magnified images from certain regions of the tissue can be seen. The label did not penetrate well into the tissue, mainly reaching the fibrous tissue. Dead cells are apparent, with live tissue towards the outer region of the fibrous tissue. The calcified bone is unlabeled and fluoresces blue, while living cells were labeled green due to the cleavage of CMFDA by esterases. Membrane compromised dead cells were labelled with EthD-1 causing the cells to be labelled in red. [A representation of 2 bovine cores analysed in this manner]*

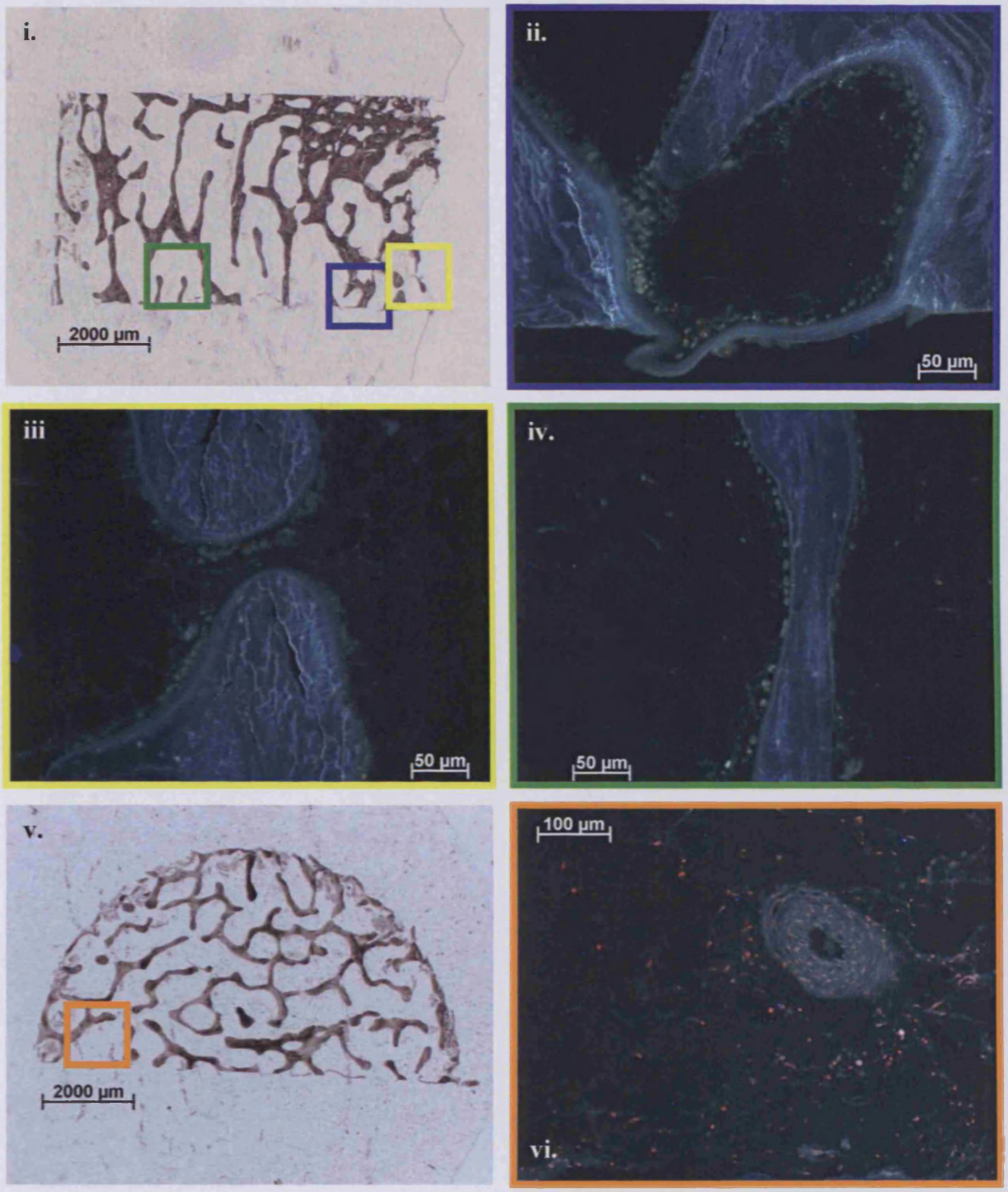

Figure 3c.15. i) *A cross-section from freshly labelled (with CMFDA and EthD-1) and fixed bovine tissue (4 months old). Magnified images from certain regions of the tissue can be seen.Most osteoblasts can be seen as living. Label only penetrated the outersurfaces of the tissue. No fibrous tissue was present.* **v)** *A transvers-section from freshly labelled (with CMFDA and EthD-1) and fixed dead control bovine tissue (4 months old). Magnified image shows dead cells and blood vessel. Label only penetrated the outersurfaces of the tissue. The calcified bone is unlabeled and fluoresces blue, while living cells were labeled green due to the cleavage of CMFDA by esterases. Membrane compromised dead cells were labelled with EthD-1causing the cells to be labelled in red. [A representation of 2 bovine cores analysed in this manner]*

A clear diffusion barrier was observed with the cancellous bone tissue. This may have been more problematic due to the presence of a thick layer of fibrous tissue surrounding the outer periphery of the explants. To eliminate this problem, thinner sections (~500 – 1000 μm) thick, leftover from sectioning the bone cores with the annular saw, were used. Figure 3c.16 demonstrates that this was more successful than thick (5 mm high and 10 mm in diameter) Zetos cultured explants.

It was possible to see living osteoblasts resting upon the surface of the calcified matrix. Some dead osteocytes were also observed, possibly damaged from the sawing procedure. Viable chondrocytes within the growth plate were also observed.

Figure 3c.17. demonstrates a number of serial sections of the above sample. It is possible to observe good morphology with the giemsa (17iii) and Masson stained sections (17v). Living bone cells can be seen in figure 17iv. The same serial sections were used for immunohistochemical evaluation of bone marker proteins (procollagen type I and osteocalcin). In figure 3c.17i, it is posible to see strong labelling for procollagen within the cells. The same image can be seen under fluorescent light to distinguish the cells from the calcified tissue. This result suggests that the live-dead stain CMFDA and EthD-1 does not interfere with immunohistochemistry and can be used in conjunction with general morphology and immunohistochemistry. Thinner tissue samples also appeared to improve diffusion of label into the explants. Figure 3c.17vi, depicting osteocalcin was not as intensly labelled as procollagen type I. This was probably due to lack of specificity to bovine tissue. Other bone marker proteins (osteonectin, osteopontin, and bone sialoprotein) were also compatible for use in conjunction with CMFDA and EthD-1 (results not shown), providing a useful method for analysing bone tissue.

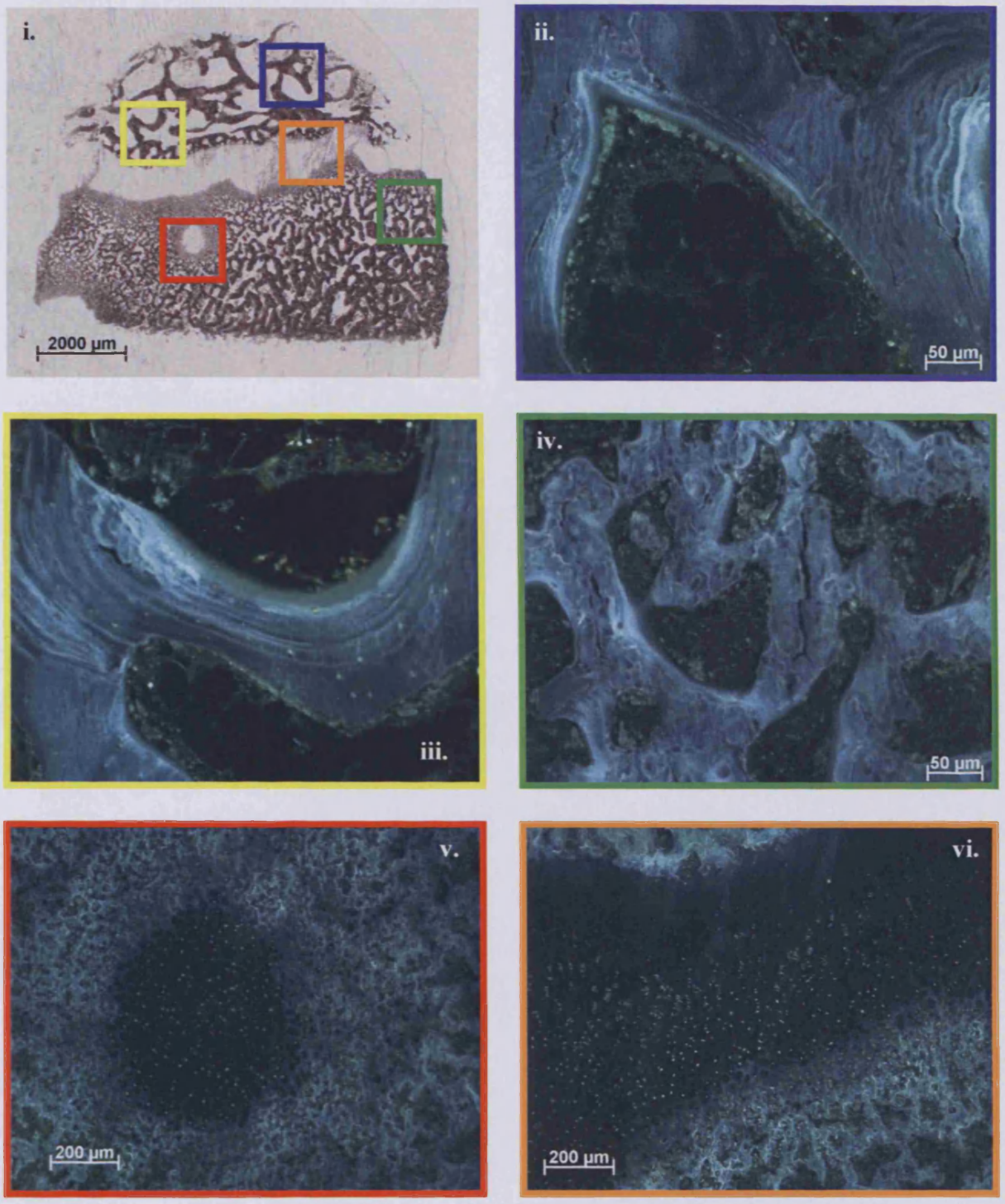

Figure 3c.16. *A transverse-section from thin (~500 µm) freshly labelled (with CMFDA and EthD-1) and fixed bovine tissue (4 months old). Magnified images from certain regions of the tissue can be seen. Most osteoblasts and chondrocytes can be seen as living. Stained penetrated the whole tissue. No fibrous tissue was present. The calcified bone is unlabeled and fluoresces blue, while living cells were labeled green due to the cleavege of CMFDA by esterases. Membrane comprimised dead cells were labelled with EthD-1causing the cells to be labelled in red. [A representation of 2 bovine cores analysed in this manner]*

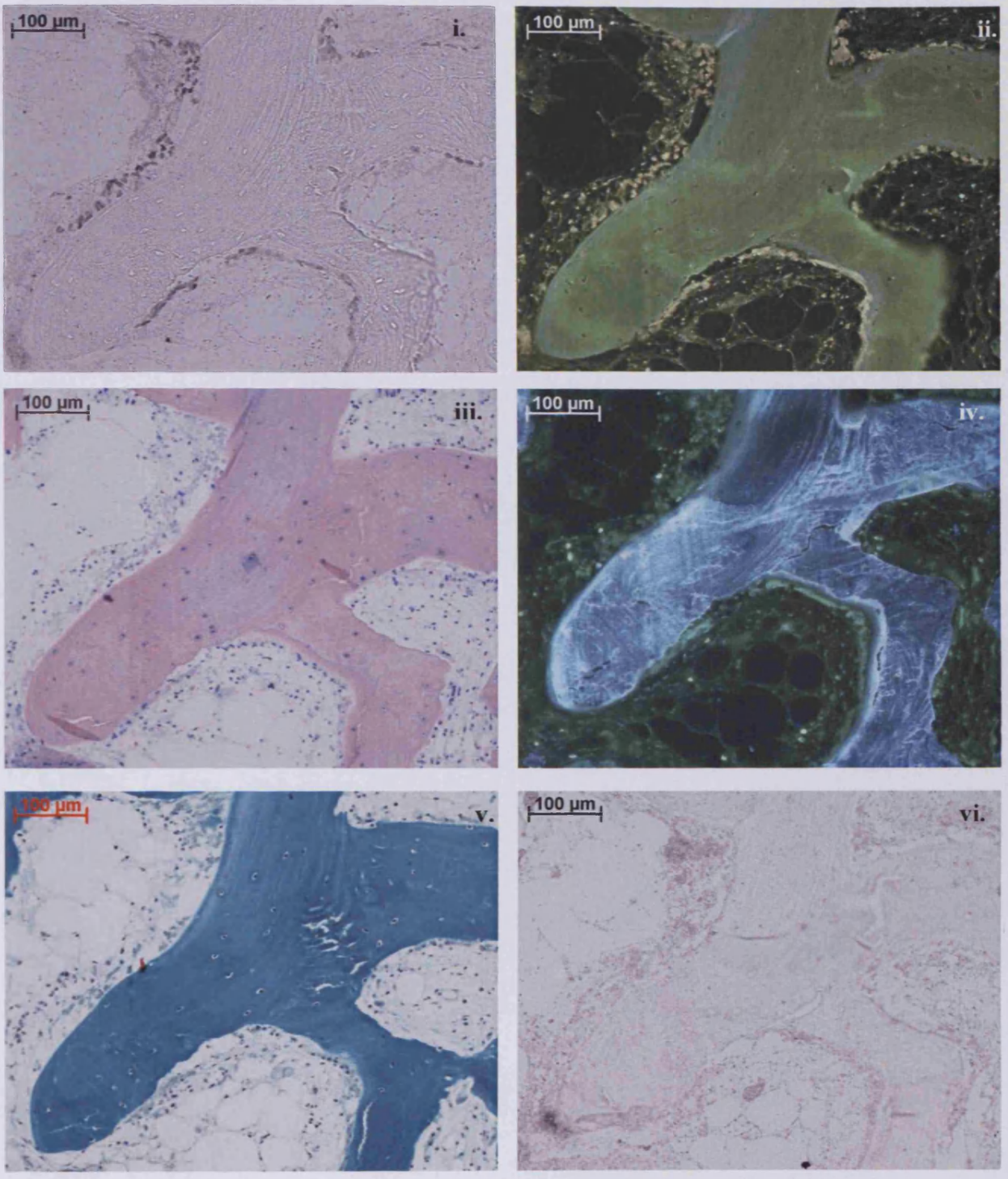

Figure 3c.17 *A transverse-section from thin (~500 µm) freshly stained (with CMFDA and EthD-1) and fixed bovine tissue (4 months old)* **i)** *Image stained for procollagen type I (PINP)(7µg/ml monoclonal goat anti-rabbit).* **ii)** *Fluorescent image of i. showing the cells.* **iii)** *Giemsa stained serial section.* **iv)** *Fluorescent image showing live CMFDA stained cells.* **v)** *Masson stained serial section.* **vi)** *Immunolabelled serial section for osteocalcin (10µg/ml polyclonal goat anti-rabbit). [A representation of 2 bovine cores analysed in this manner]*

3.c.iii. Sample stiffness

Daily loading of the explants within the Zetos culture system allowed the sample stiffness to be analysed over the entire culture period. It was noted that the explants from the different species had a different range. Bovine tissue was the least stiff, ranging from 100-500 MPa. This low stiffness was probably due to the presence of a cartilage scaffold in some areas, as well as woven bone. It was also possible that the tissue was not fully calcified. The calves were not regarded as having mature bone. The next lowest was seen with the human tissue, ranging from 200-600 MPa. It is probably that human tissue, because of its age (70-80 yrs), has lost most of its strength due to damage in the collagen as well as containing less mineral. The stiffest tissue was that from the ewes. It ranges from 500-1400 MPa. Ovine tissue and human tissue were both regarded as being mature. Examples of readings from three explants from each species can be seen in Fig.3c.18. Jumps in measured stiffness were believed to be caused by human error during positioning of chamber in the loading device (blue circle). No correlation from sample location and sample stiffness was observed (Fig. 3c.19 and 20 - ovine tissue). Unlabeled cores were not cultured within the system, and thus, their stiffness could not be calculated. However, readings obtained for sample stiffness (Fig. 3c.19 and 20 - ovine tissue) clearly shows that distinct segments exhibit heterogeneity in stiffness. In the *in vivo* situation it would not be expected that each trabeculae within each core would receive the same strain. By placing 4,000 microstrain on each sample this may not be representative of the physiological situation for individual trabeculae. On the other hand, it ensures that each core, irrespective of its stiffness, receives the same deformation, which is regarded as more physiological than giving each core the same force.

It was also observed that, over time, the stiffness of the tissue slightly increased or remained constant. This increase in stiffness suggested that there was no, or very little, leaching of minerals from the explants during culture thus, no damage to the matrix was caused from necrosis. It also suggests that no net resorption was taking place. An experiment with ovine tissue can be seen in figure 3c.21. Green coloured explants were alive and red coloured explants were dead (heat killed). Unfortunately, dead tissue was also observed to increase in stiffness. This increase in stiffness suggests that possible calcium phosphate precipitation was taking place, causing the tissue to become stiffer. Sometimes, operator error caused small leaps in the stiffness readings such as inaccurately placed chambers within the loading device (blue circle, Fig.3c.21).

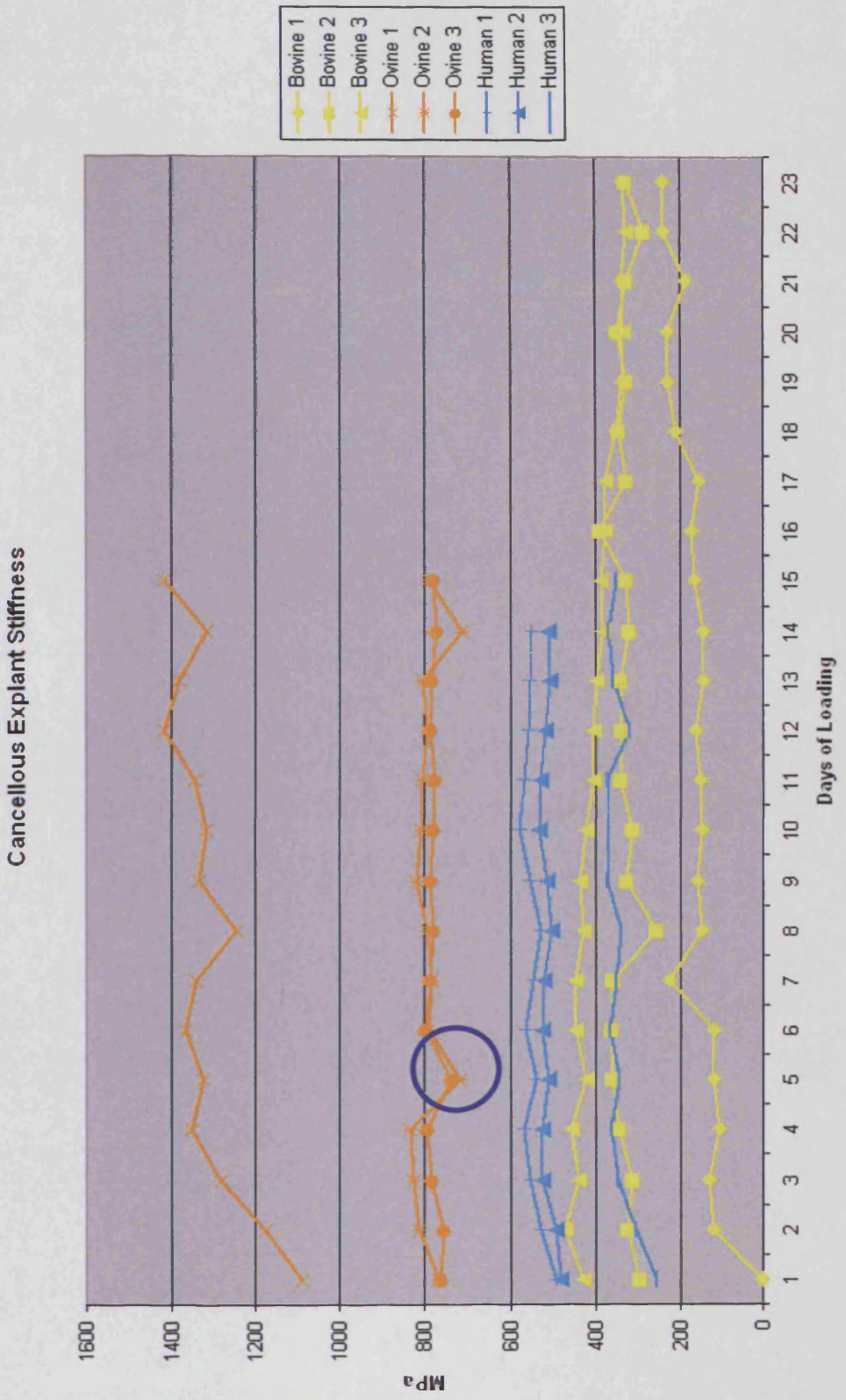

Figure 3c.18. *Ovine tissue is represented by orange, human is represented by blue, and bovine is represented by yellow coloured lines. Ovine was the most stiff, followed by human, then bovine. Jumps in stiffness were caused by human error during positioning of chamber in the loading device (blue circle). [A representation of 46 cores, from the three species, analysed in this manner]*

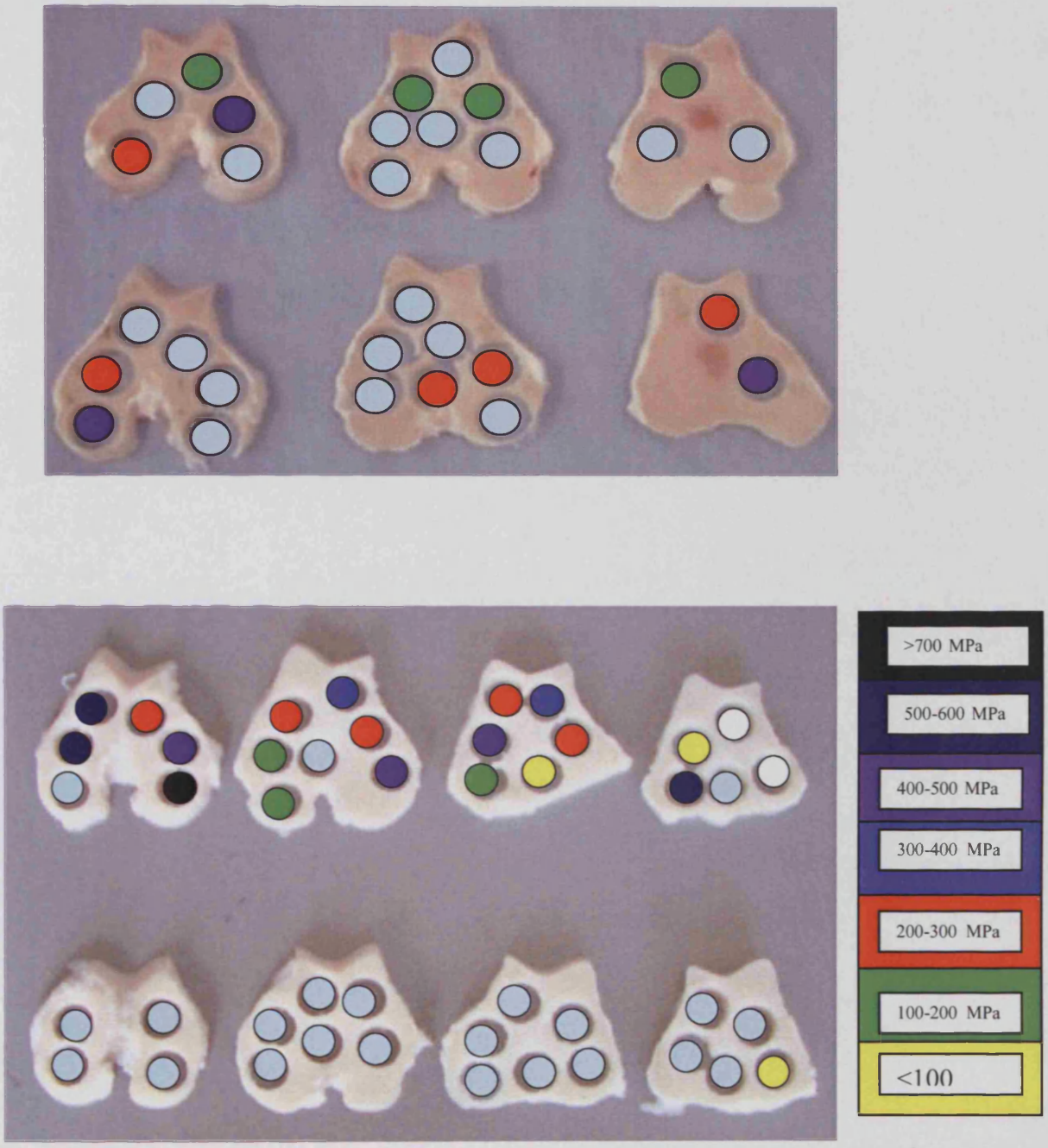

Figure 3c.19. *Ovine tissue depicting location of explants and their measured apparent stiffness. There is no correlation with explant location and explant stiffness. Only half of the samples were cultured within the Zetos system (the rest in centrifuge tubes) therefore explant stiffness was not measured (pale blue cores).*

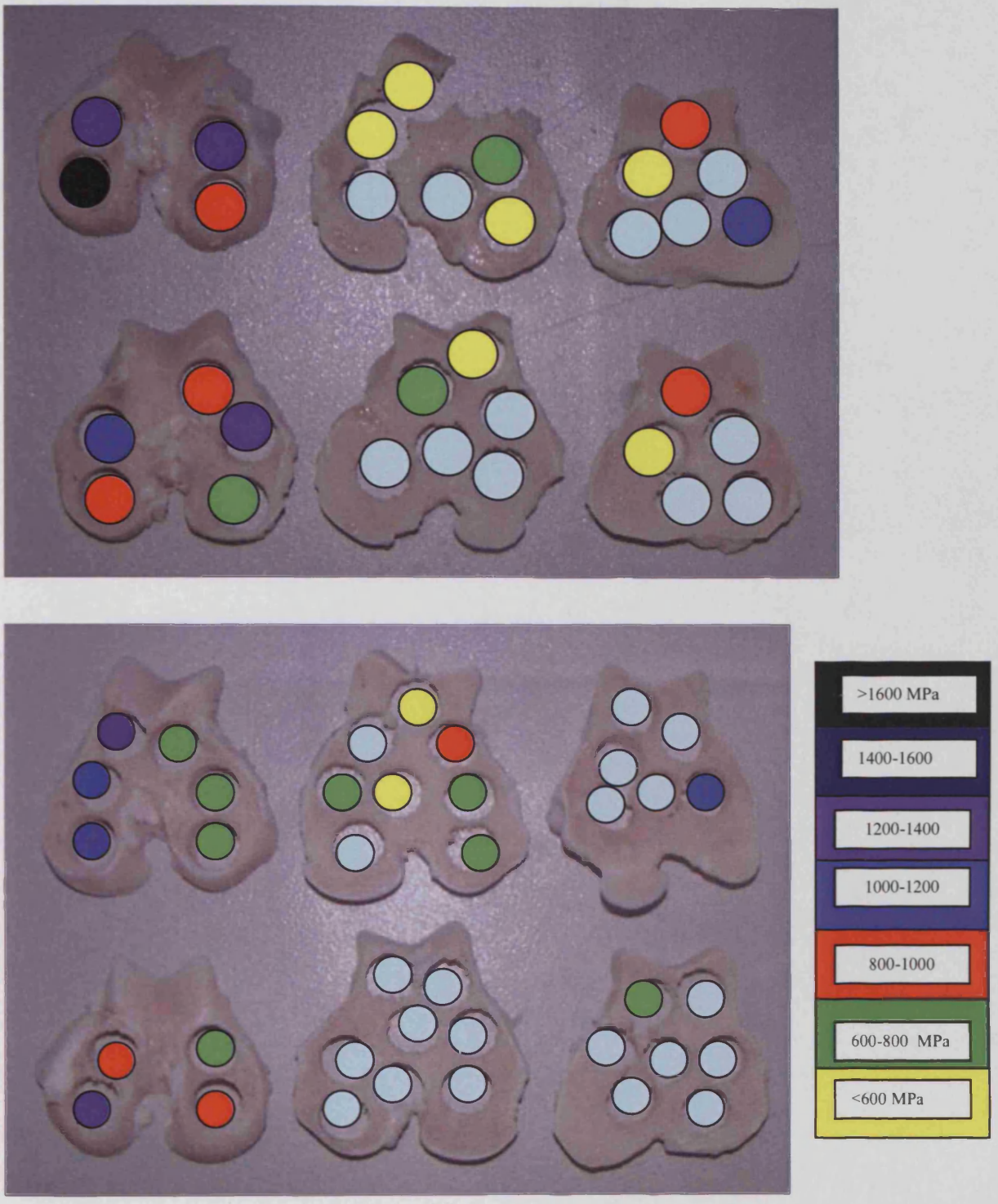

Figure 3c.20. *Ovine tissue depicting location of explants and their measured apparent stiffness. There is no correlation with explant location and explant stiffness. Only half of the samples were cultured within the Zetos system (the rest in centrifuge tubes) therefore explant stiffness was not measured (pale blue cores).*

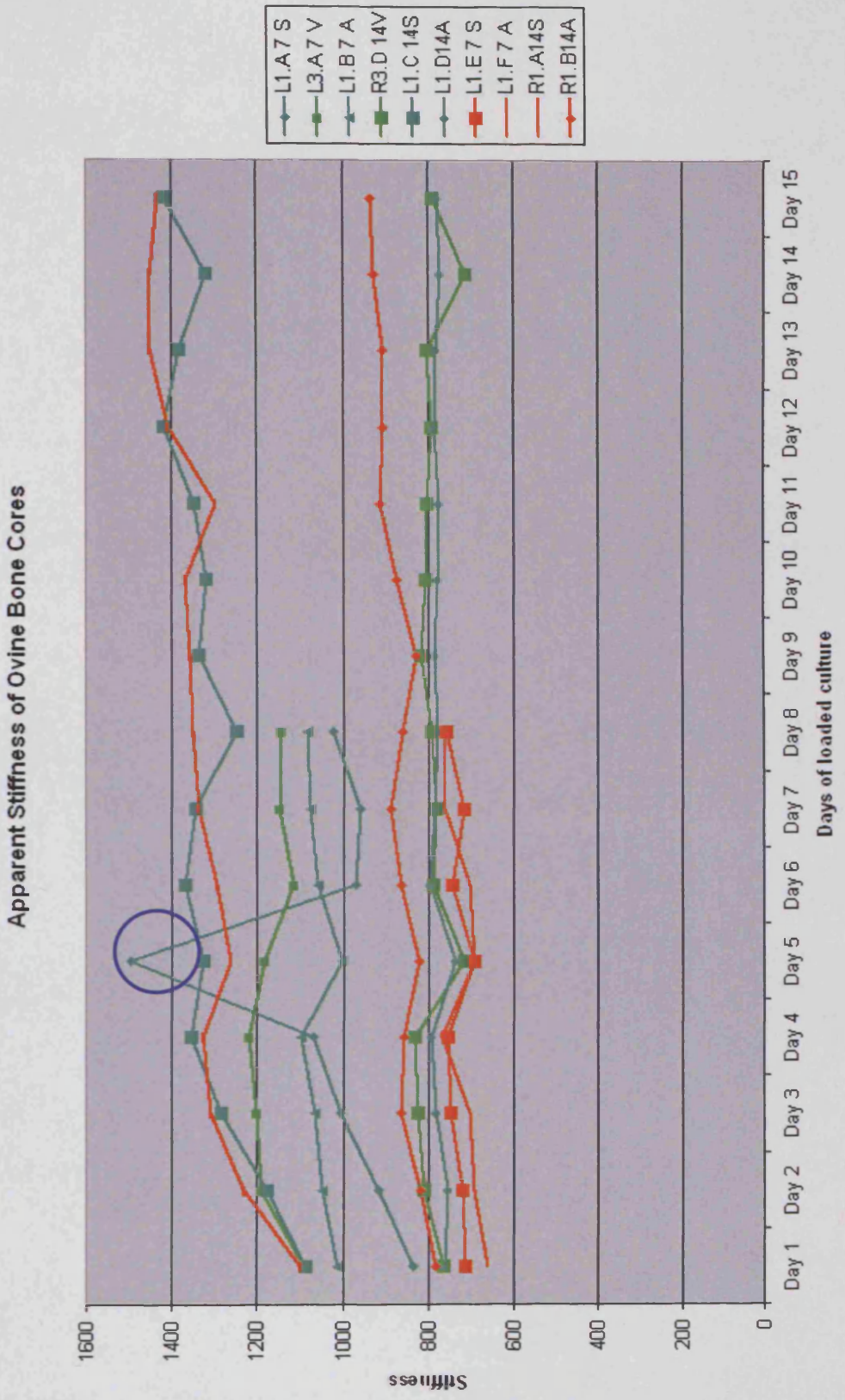

Figure 3c.21. Ovine tissue cultured within the Zetos system for 15 days. Some samples were harvested early after 1 week. Living tissue is represented by the green line; dead tissue is represented by red. The blue circle indicates an error, probably due to misplacement of the chamber within the loading device.

3.c.iv. Biochemical analysis

Daily media changes provided daily readings of sample pH. This enabled constant supervision of the status of the tissue being cultured, for example dead tissue would not be expected to alter their pH, while living tissue would constantly utilise the nutrients in the media and release lactic acid (a by-product of metabolism) causing the pH of the media to fall. It also provided an early indication if the tissue was contaminated with bacterial or fungal organisms as the pH of the media would rapidly drop, as well as become cloudy and opaque.

Generally, dead tissue had a higher media pH than living tissue (Figure 3c.22) (Dead explants red or orange; living explants shades of green), which was expected as no nutrients were being depleted and no accumulation of lactate was occurring. It was also observed that samples cultured in the centrifuge tubes had a lower pH than samples cultured within the Zetos chambers. This observed difference was probably due to the fact that the media was static, while in the Zetos chambers the media was constantly being pumped through the tubing and chambers. Submerged, static, centrifuge cultured samples can be seen as orange and light green in fig 3c.22.

The analysis of the media for lactate dehydrogenase (LDH) was conducted by MEDITEST. The results indicated that there was no more LDH present than there was in control media (black) (Figure 3c.23). There is a suggestion that levels of LDH in living tissue may have been higher during the first few days (blue circle). This hypothesis can not be proved as media from day 0 and 1 were not collected. A high level of LDH should have been secreted into the media from compromised cells damaged from the sawing procedures. Fortunately, these results suggest that the tissue was being maintained in a optimal environment over the 15 day culture period, as well as samples cultured in an unloaded environment (Zetos cultured and submerged, static, centrifuge culture).

Analysis of the explant sections for the enzyme tartrate resistant acid phosphatase (TRAP) was not successful. It is hypothesised that the tissue processing and embedding may have damaged the enzyme activity. No results shown.

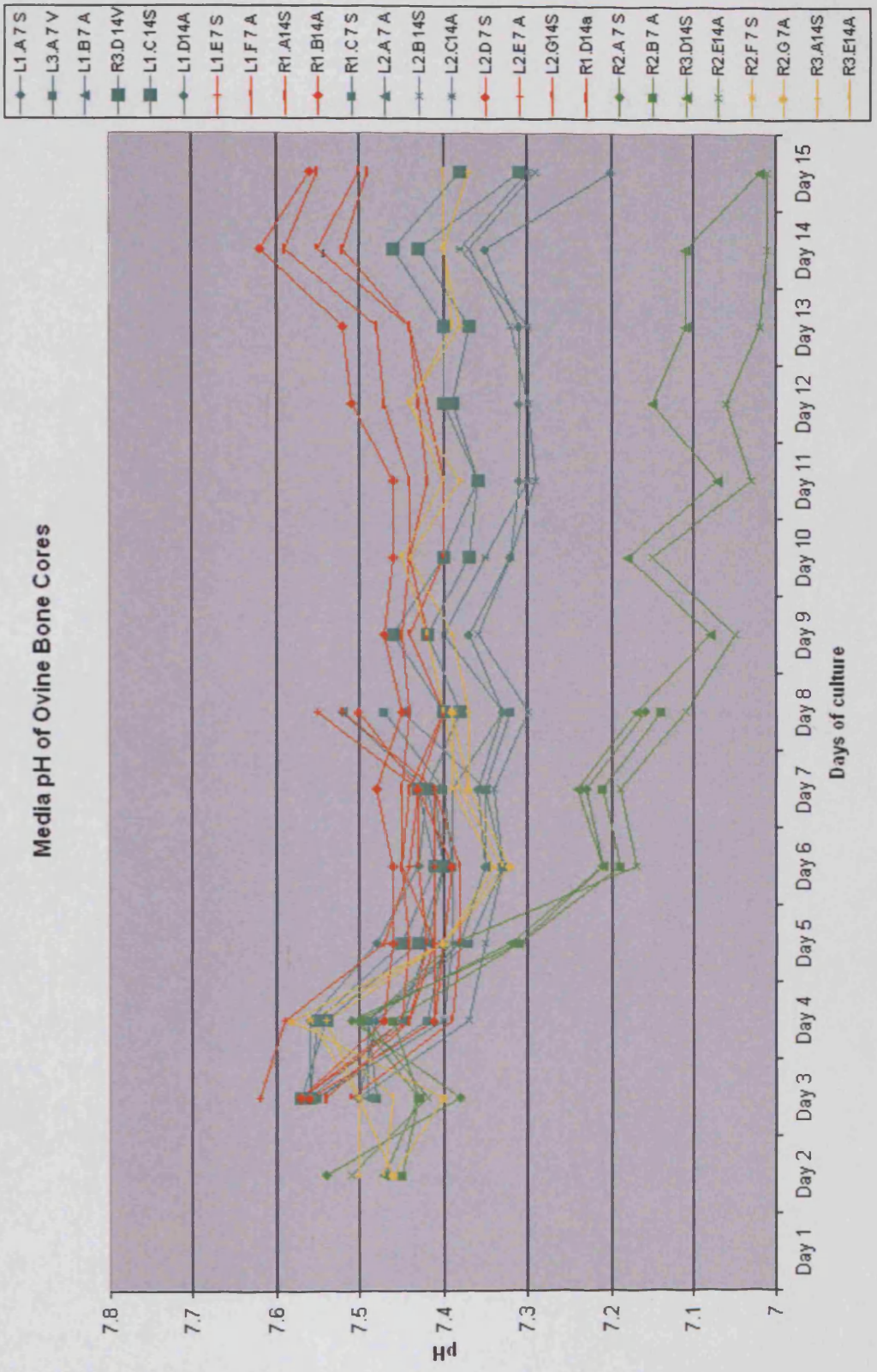

Figure 3c.22 *Media pH from ovine bone cores cultured (red=dead, green=live) in Zetos chambers, and centrifuge tubes (orange=dead, light green=live) for 15 days. Day one was omitted. Dead tissue seems not to utilise nutrients, while live centrifuge cultured explants seems to use the most. Optimal pH is around 7.4 as is the blood. [A representation of 46 cores, from the three species, analysed in this manner].*

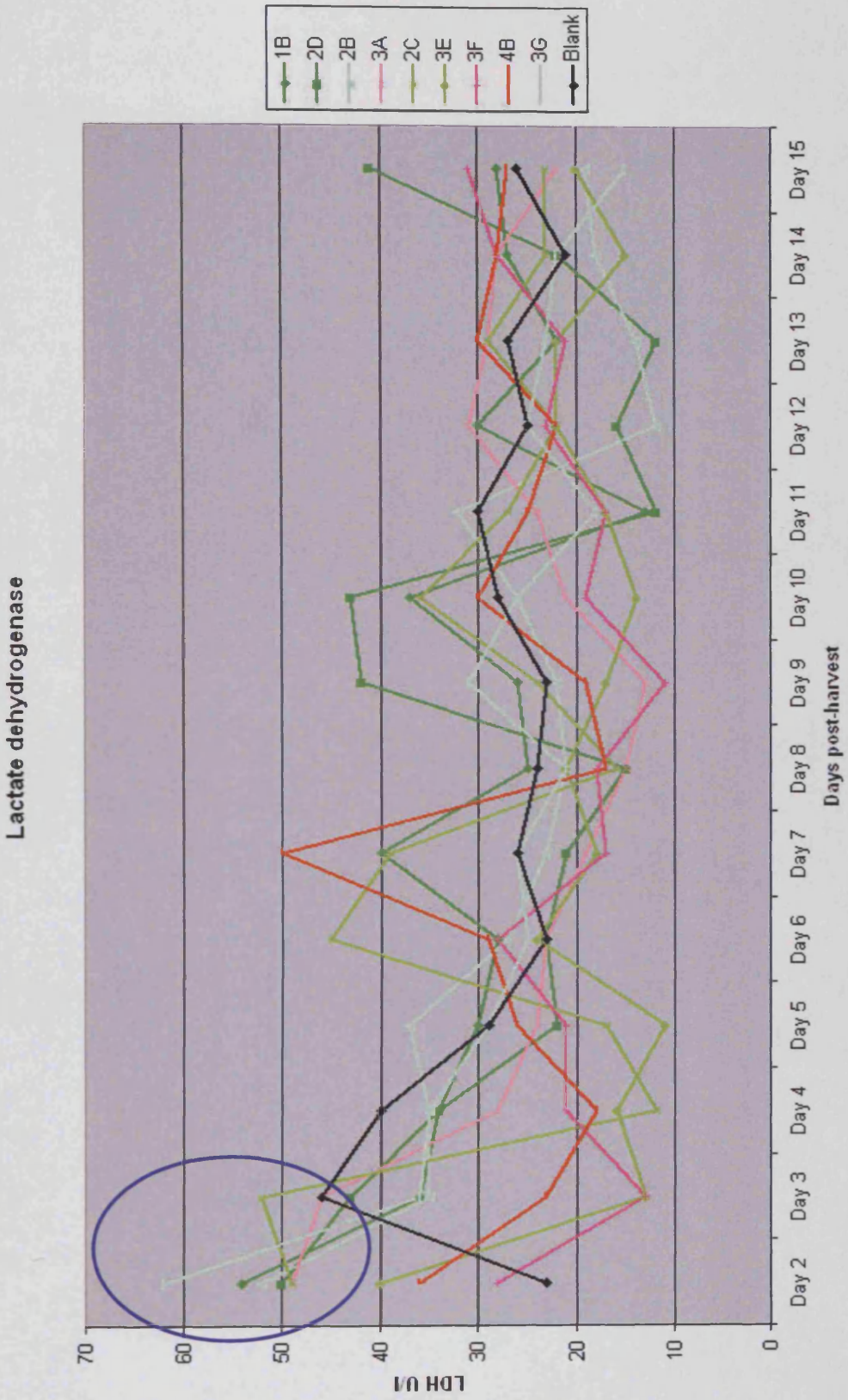

Figure 3c.23. *Media from human bone explants measured for LDH. The measure was random, including the blank/plain media (black). Possibly the levels were higher on day 1 after harvest. Damaged cells would have secreted LDH into the media (blue circle). [A representation of 9 human cores, from one limb, analysed in this manner]*

3.D. Discussion

The aim of this chapter was to find a technique that allowed the percentage of live and dead cells, present within a cancellous bone explant (10 mm in diameter and 5 mm high), to be determined. A number of fluorescent labels were used (fluorescein diacetate, calcein AM, STO24, CMFDA and ethidium homodimer-1), unfortunately, none of these were deemed compatible for future studies with the Zetos system. These labels did not penetrate the tissue, irrespective of any modifications made to try and improve them (higher concentration and prolonged labelling times).

In theory these labels had a lot of positive aspects. Fluorescent-based cell viability and proliferation assays are generally less hazardous and less expensive than radioisotopic techniques, more sensitive than colorimetric methods and more convenient than traditional testing methods. They are reliable and easy to perform and consist of a simple protocol allowing for simultaneous two-colour assessment of numbers of live and dead cells within a population.

It was noted during these studies that fluorescein diacetate bleached from the tissue before analysis could be undertaken, and that this label, along with calcein AM, could only be used with unfixed and embedded tissue. These stains did not survive the embedding process to allow single cells to be visualised within 6 μm thick sections. Nevertheless, it was suggested by staining whole bone cores with calcein AM and ethidium homodimer-1, that damage caused to the tissue during harvest penetrated up to 1 mm into the tissue (Fig.3c.4ii). This result correlates to the distance debris penetrated into the tissue by the drilling procedure.

The nuclear binding stain, SYTO, was advantageous in the fact that it survived the embedding process, and that it could detect single cells within tissue sections. However, it was very difficult to distinguish which cells were alive and which cells were dead. Instead of a clear red (dead) green (live) comparison, a more yellow (live) orange (dead) colour ensued. It was observed that SYTO24 bound to the DNA with a stronger affinity than ethidium homodimer-1 and hence, ethidium homodimer-1 could not displace SYTO24. This lack of specificity caused an overestimation of living cells within a "dead" sample. Other SYTO dyes may prove to be more compatible, and thus have a role for the Zetos system, if they can penetrate far enough into the tissue.

One ideally suited combination of stains was found – CMFDA and ethidium homodimer-1. They provided clear visualisation of live and dead cells (green and red respectively), and were retained within the cells after the polymerisation procedure with Technovit 9100 New. The only drawback was the fact that these stains did not penetrate more than 300 μm into the cancellous bone cores (10mm in diameter and 5 mm high). Zetos cultured samples (as well as centrifuge cultured samples) analysed by this method were stained, mainly at the fibrous-like region (Fig.3c.12, 13 and 14). Most of the fibrous-like cells were stained as living (green). However, some inner layers of cells stained red, suggesting these cells were dead. These cells may have been dead, but it is more probable (in the light of new evidence discussed in Chapter 4) that these cells were indeed alive during culture, and were labelled as dead due to an artefact of labelling. It is possible that residual stain trapped within the tissue could not be washed out (due to diffusion limitations) and stained the cells during the fixation procedure, when the cells would have lost their membrane integrity. Even doubling the concentration of the label, and increasing the incubation period to 24 h did not improve labelling and label penetration. On the other hand, this method was found to be successful with thinner pieces of tissue, approximately 500 μm to 1000 μm thick (Fig.3c.16). Thus, this labelling technique may have potential to be used as an indicator of cell viability on thin slivers of tissue, where the majority of the tissue is used for histopathology, for example. This labelling method did not seem to interfere with immunohistochemical evaluation of bone marker proteins (osteocalcin, osteonectin, osteopontin, bone sialoprotein, and pro-collagen type I) (Fig.3c.17), as was observed by (Poole *et al.*, 1996) for other connective tissues.

With this aside, it was possible to assess the viability of the cells within the cancellous bone explants cultured, *ex vivo*, with the Zetos system. This assessment was achieved through two different methods. Firstly, through histological evaluation of tissue morphology. No masses of empty lacunae or a vast number of cells with pyknotic nuclei were observed. These signs are characteristic of dead cells and tissue. Tissue from all three species demonstrated characteristic morphology (i.e. soft tissue, osteoblasts, osteoclasts, and osteocytes) comparable to that of freshly harvested tissue (Fig.2c.37-39). Unfortunately, this in itself does not tell us directly if the tissue was alive, active, or functioning as it would *in vivo*. It only provides a visual guide to structure, cell types, and location. There is no indication whether the cell's activities have been up-regulated, down-regulated or remained the same. Osteoclast nuclei and osteoblasts have life-spans within

the range of 10-120 days (Parfitt, 1995). Though some osteoclasts may have been created during culture within this system, this is not, on its own, conclusive. Signs of active metabolite synthesis and secretions are required and are evaluated in the following chapter. Disappointingly not much osteoid was observed in ovine or human tissue (including fresh controls) suggesting most of the tissue was in a quiescent state. Bovine tissue, being very young, was far more active. It would have been interesting to change the orientation of the tissue or the mechanical stimulation pattern used, as these are known to affect bone adaptation, and then to see how much resorption and apposition took place, and if this differed from control samples. These kinds of studies will be implemented in the future. Analysis of submerged static centrifuge tube cultured, and unloaded controls, showed the same typical morphology of loaded and fresh samples, as can be seen in figure 3c.7. This undistinguishable morphology was not expected, as they were supposed to stimulate tissue undergoing necrosis.

Secondly, viability of the tissue was concurred by analysis of the media (from human tissue) for lactate dehydrogenase (LDH). LDH is a stable, cytosolic enzyme, released upon cell lysis, and is a good marker for determining cell membrane integrity and cell viability. It is regarded as being more sensitive than trypan blue staining. Lactate dehydrogenase transfers hydrogen using NAD+ as a hydrogen acceptor, thus, catalyzing the oxidation of L-lactate to pyruvate. LDH activity is present in all the cells of the body, predominantly in the cytoplasm of the cell. Tissue levels are 500 times greater than those in serum, thus, even a small mass of damaged tissue causes leakage of enzyme and increasing its level in serum significantly. No amount of this enzyme was being secreted into the media, thus, suggesting that the cells were viable (or were at least still intact). It would have been ideal to been able to analyse media from day 0 and 1, to see if there was LDH released from cells at the surface of the explant, as they would have been damaged from the cutting procedure. This is currently being carried out at the AO Research Institute, Davos, Switzerland. Surprisingly, but again concurring with the morphology results, the control unloaded and centrifuge cultured samples also seemed to have retained viability. This was unexpected, as organ culture without load, should only last a few days before necrosis sets in, these types of culture were chosen specifically as a negative control for the Zetos system. It was important that the histology of the samples appeared correct in order to be sure that the biochemical tests were looking at physiological responses rather than pathological ones, which seems to be the case. A drawback to biochemical assays is the

fact that you cannot say which cells are responsible for producing the chemical due to the heterogeneity of the samples.

Sections were incubated for acid phosphatase in the presence or absence of tartrate, to investigate the feasibility of tartrate-resistant acid phosphatase as a histochemical marker for osteoclast identification. Acid phosphatase activity sensitive to tartrate inhibition (TS-AP) was demonstrated in macrophages from spleen, bone marrow, and loose connective tissue surrounding bone rudiments (van de Wijngaert and Burger, 1986). Acid phosphatase activity resistant to tartrate inhibition (TR-AP), was detected in multi-nuclear osteoclasts and in some mononuclear cells from bone marrow and periosteum (van de Wijngaert and Burger, 1986). Unfortunately, no positive labelling of osteoclasts was observed. This lack in labelling was due to the rarity of osteoclasts in the sections, and the loss of soft tissue from the sections during staining. It was also possible that the processing of the tissue and embedding damaged the enzyme. Though this protocol was specific for methacrylate embedded sections (Web ref.5), most TRAP staining is conducted with cryo-fixed tissue (Noble and Stevens, 2003).

Other features observed during these studies included a fibroblast-like tissue encapsulation of the bone cores, being most pronounced in cores cultured in centrifuge tubes, followed by Zetos cultured loaded, and Zetos cultured unloaded samples (Fig.3c.2). This encapsulation was greater in bovine and human tissue, with less surrounding ovine tissue. This observed difference in fibrous-like tissue encapsulation may be due to the fact that both bovine and human tissue contained red marrow, and that ovine tissue does not. It is also known that fibroblasts, osteoblasts, adipocytes and chondrocytes all stem from the same lineage – mesenchymal stem cells (MSC). Certain conditions under culture may have caused these cells to transdifferentiate from one cell type to another.

This accumulation of fibrous-like cells mimics the *in vivo* wound response. Generally in wound healing, platelets facilitate formation of a haemostatic plug, secret multiple growth factors, and chemotactic factors that recruit inflammatory leukocytes to the wound site. Neutrophils cleanse the wounded area of foreign particles, releasing enzymes and toxic oxygen products. When complete, they are phagocytosed by macrophages or fibroblasts. Peripheral blood monocytes infiltrate the wound. Once activated, monocytes become macrophages. Macrophages demolish the necrotic tissue at the wound surface. Fibroblasts migrate to the surface and form a small zone. These cells are believed to secrete a reticular matrix to provide mechanical support for an emerging

vascular system that occurs *in vivo* (Davies and Hosseini, 2000). Work by Clarke et al., (2003) demonstrated platelet viability, after four days, in cancellous explants cultured in the Zetos system. Therefore, it was possible that these cells caused the migration of fibroblasts to the core periphery. Platelet-derived growth factor (PDGF) has been shown to be a mitogen to fibroblasts (Stiles, 1979). No *de novo* capillaries were observed in close proximity to the fibrous tissue as would be observed *in vivo*.

These fibroblast-like cells were probably enhanced by the use of serum within the media. It is believed that serum potentiates an already existing capacity within the tissue, rather than inducing it, and probably the reason why it was more pronounced in bovine and human tissue (the presence of haemopoietic cells). Serum is undefined chemically, and differs from batch to batch. It contains a number of growth factors, which make it ideal for stimulating cells to grow and differentiate. Serum was found to be essential for ossification to take place *in vitro* (Roach, 1987); it is also required for proliferation (Holley, 1975); and increases cell viability (Bingham and Raisz, 1974) When serum was not used, it was difficult to demonstrate unambiguous mineralisation. Unpublished data from David Jones, Marburg, showed that 5% serum was insufficient to sustain growth, and 15% caused even greater fibrous-like cells to encapsulate the explants. Thus, 10% serum was deemed best. It is common to exclude it from the media of organ culture to avoid unwanted growth of fibrous-like cells (Majeska and Gronowicz; 2002).Conversely, factors present in serum, may inactivate inhibitors and proteolytic enzymes released during tissue harvest (Bingham and Raisz; 1974) and as a consequence decreases the amount of necrotic cells observed in serum free cultures. It is an experimental dilemma on whether to use it or not. Due to the necessity to maintain the same standards as used with Zetos systems elsewhere in the world, it was included with all of these experiments. Fortunately, the same batch of serum was used throughout these studies, making all experiments comparable to each other and to ones conducted at other laboratories. In future, it may be possible to compose serum free media, or incorporate the use of plasma. As long as every group adopts the same method then the work can always be comparable.

Bone debris was observed on the surface of cut tissue, but to a greater extent at the sample periphery, causing as much as 36% loss of tissue volume (Fig.3c.1). This loss of tissue is not at all desirable. It suggests that the drill bit does not work optimally, and is causing the bone debris to be compacted into the soft tissue. Ideally, in the future, a new designed drill bit should be implemented. This debris may be blocking molecules such as

CMFDA and ethidium homodimer-1 from penetrating into the sample. It may be worse, and that the debris may actually be blocking the exchange of nutrients and waste from the centre of the bone core, limiting the life-span of the tissue in the culture.

The gaskets from within the chamber were initially designed to aid the flow of media through cancellous biopsy and stopping the media from escaping around the periphery of the bone (as fluid is known to flow through the path of least resistance). However, it was noticed that these gaskets caused damage to the cores (see Fig.3c.3) as well as affecting media from reaching the tissue within close proximity to it. It was believed that these neoprene gaskets also affected the loading of the samples. It was possible that the neoprene gaskets were blocking the piston from reaching the bone surface, and in effect, shielding the tissue from its mechanical stimulation (Fig.3d.1). Since this was first noted, all gaskets were removed from the chambers, leaving the bone cores to be cultured without them. This did not seem to affect sample loading and positioning within the chamber. The work of Jones (personal communication) and Koller (2004), in Davos, showed that it was not possible to force the media through the tissue, and therefore removing the gaskets should have no effect on the diffusion of solutes into and out of the sample.

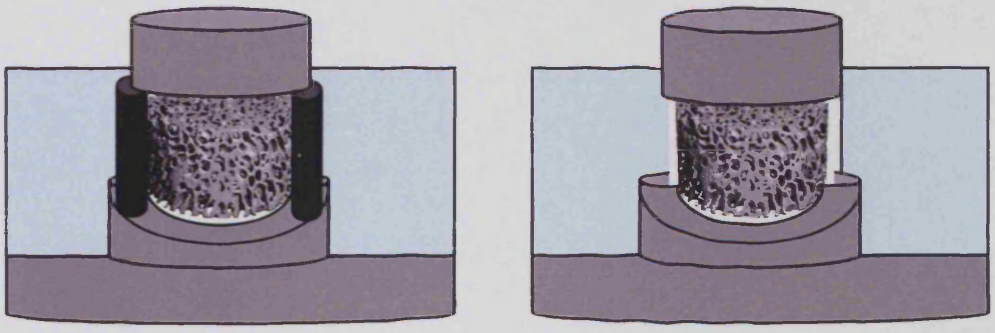

Fig.3d.1 i) Image depicts how the black neoprene gaskets could interfere with the piston from loading the cancellous explant. **ii)** How the piston would load the explant without the presence of the gaskets. This also slightly increases the area for media to bathe the tissue.

The effect that loading had on the viability of the explants is more apparent in the following chapter, though it was demonstrated to be imperative to the maintenance of the tissue. Daily loading of the cores yielded a series of readings, providing an apparent Young's modulus for each individual sample. It was hypothesised that loaded cores would become stiffer over time, due to bone apposition, in order to withstand any altered stresses

and strains within the samples, thus changing the samples' architecture, in a process known as functional adaptation. As bone density is believed to have a cubic relationship to elastic modulus (Carter and Hayes; 1977).

It was also hypothesised that unloaded samples would mimic a disuse state. Although bone formation would occur in the unloaded explants, a net resorption would ensue, causing the sample to become progressively weaker. This net resorption is also true of the *in vivo* state, for example with astronauts, and prolonged bed rest (Spenger *et al.*, 1983; Vico *et al.*, 1987). Though these samples were loaded every four days it was not stimulatory (Lanyon and Rubin, 1984). Unfortunately, these hypotheses were difficult to prove or disprove. It was observed within several experiments (using bone cores from all three species) that sample stiffness of the loaded samples tended to increase over time, though this was also seen with "dead" control samples cultured simultaneously (Fig.3c.21). This increase in stiffness suggested that the tissue was being compacted over time, or that small surface ridges were being flattened (Koller, 2004) or that the supersaturated media caused calcium phosphate precipitation onto the surfaces, thus, increasing samples stiffness.

Unloaded controls, that were statically loaded every four days for 1 min, were difficult to evaluate in terms of change in stiffness as, usually, not enough readings were made during the course of an experiment. It was also noted that there was a large difference between sample stiffness from the first to second day of loading, suggesting that the tissue adjusted to its surroundings. This jump in stiffness also influenced readings for the unloaded controls, as their second loading period was several days after the loaded tissue (loaded tissue received 300 cycles of load at 1Hz daily). Thus, by the end of the experiments unloaded samples had not finished their "settling" period. While assessing sample stiffness, the first day's readings were generally omitted and compared to the second day's results. It was hypothesised that this short static loading of the "unloaded" control samples may have been enough of a stimulation to keep the tissue from being in a disused state. In future work, these explants will be completely unloaded (as with the submerged static centrifuge cultured control explants).

It is known the Young's Modulus of cancellous bone can vary from 0.1-4.5 GPa depending on bone density and trabecular orientation. (Turner *et al.*, 1990). This is because bone is anisotropic. It was noted during these experiments that bovine tissue was the least stiff, ranging in stiffness from 100-500 MPa. In contrast, ovine tissue ranged from 500-

1400 MPa, and human 200-600 MPa (Fig.3c.18). This can be explained by the fact that the bovine tissue was immature and that the ovine and human bone was mature. Thus, lamellar bone was not as calcified as mature lamellar bone. In areas, bovine bone consisted mainly of woven bone on a calcified cartilage scaffold. These differences were observed in the tissue morphology (Fig.3c.5) and may be responsible for differences seen with solute diffusion (see Chapter 4). No correlation between sample location and stiffness was observed (Fig.3c.19&20). It is interesting to note that bone mass is the primary factor contributing to bone strength. Quantitative relationships between bone mass and biomechanical stiffness and strength have been demonstrated (Rice *et al.*, 1988; Lang *et al.*, 1988; Weaver and Chalmers 1966).

The pH of the media, that was changed daily, indicated that the samples were metabolically active, with a lower pH observed with living tissue than dead control tissue (Fig.3c.22). The media from the cores cultured within the centrifuge tubes tended to be lower than Zetos cultured samples. Fortunately, throughout the course of these studies, no bacterial or fungal contamination occurred. If such an event had occurred, it would have been observed by lowering the pH of the media and causing it to become orange and opaque.

In conclusion, tissue viability was partially confirmed through histological morphology and lack of LDH secreted into the media. To substantiate these findings, proof of cellular activity will be sought in the next chapter. Fluorescent dyes had difficulty penetrating into the cores, maybe due to a combination of bone debris and fibrous-like tissue encapsulation. To overcome possible diffusion issues of the tissue, the validation of cell viability could be analysed by assessing cryo-fixed cores for the presence of LDH. This is currently being investigated at Davos in conjunction with Brendon Noble in Edinburgh, Scotland. Short-term changes implemented, involved removing the gaskets from the chambers. Long-term changes would be to change the drill bit, and to possibly find a serum free media, both of which may aid diffusion into the explants. It was thus discovered, that this system was not a perfusion system, as was first believed, but more of a circumfusion/diffusion system, in agreement with the work of K. Koller (2004).

Summary

- Tissue morphology of cancellous bone explants cultured *ex vivo* for over 15 days, with and without daily load of 4,000 microstrain, demonstrated no masses of empty

lacunae or a vast number of cells with pyknotic nuclei. However, this histological method was limited as it did not indicate whether the cell's activities have been up-regulated, down-regulated or remained the same. Alone this technique was not effective as it did not differ between dead and live tissue.

- Neoprene gaskets present within the culture chambers were observed to damage the integrity of the cancellous bone cores and were removed from after the initial study and not incorporated in any further studies.
- Bone debris was observed at the periphery of the cores in close proximity of the surfaces cut with the drill. The debris was observed in all cores of all species, even freshly harvested explants. This suggested that boring of the cores from the limbs caused this problem and not a cellular reaction some time post-harvest.
- Fibroblast-like cells were present on the periphery of all living cores of each species maintained *ex vivo*. The presence of this fibrous-like layer was irrespective of culture condition suggestion it was caused by the harvest procedure and the serum within the medium.
- The live/dead labels utilised to ascertain cell viability within cancellous explants were not ideally suited for use with 5 mm high and 10 mm diameter cores. This was based on the inability of these labels to fully perfuse into the centre of the explants.
- Sample stiffness increased for both live and dead explants. This suggests this mode of analysis is not sensitive to use to detect changes occurring post-harvest and that possibly the cores were being compressed making them stiffer.
- Quantitative analysis of media pH for all living cores demonstrated a fall in pH suggesting that the tissue was utilising nutrients and forming lactic acid. No such fall in pH was observed for dead tissue or blank media suggesting the technique was not artefactual
- Quantitative analysis of LDH activity was not significant as it was only conducted once. However, a similar level of LDH was observed as was observed with dead tissue and blank media suggesting the technique was not sensitive enough to use to detect changes occurring post-harvest

Chapter 4.
Matrix Synthesis

4.a. Introduction

The bone matrix is a composite material which consists of collagen, noncollagenous proteins, mineral, lipids and water (as discussed in chapter 1).

Osteoblasts are the main cells responsible for synthesising the main constituents of the bone matrix and regulating its mineralisation. The morphology/physiology of the cell is that of a typical protein producing cell. It secretes mainly collagen type I, and a number of noncollagenous proteins into a structure which is termed the osteoid seam. Osteoblasts also secrete transforming growth factor-β (TGFβ), insulin-like growth factor (IGF), bone morphogenic proteins (BMPs) and fibroblastic growth factor (FGF), which gets deposited and embedded into the bone matrix.

The aim of the work conducted within this chapter was to observe de novo matrix synthesis within ovine, bovine and human cancellous bone explants (5mm high and 10mm in diameter) maintained ex vivo for over 14 days in the Zetos loaded culture system in comparison to unloaded explants in bone explant cultures. This was conducted as follows:-

1. Labelling to locate bone marker proteins, namely procollagen type I, osteocalcin, osteonectin, osteopontin, and bone sialoprotein, immunohistochemically within the bone cells of explants maintained ex vivo for at least 15 days.

2. Analysis of de novo bone matrix apposition on existing calcified surfaces through the use of two different fluorophores. Calcein green was used as the first marker and either xylenol orange or alizarin red as the second marker as xylenol orange is less toxic than alizarin red, though previous experiments by David Jones utilised alizarin red.

3. Analysis of the media for the presence of alkaline phosphatase (AlP), an enzyme present in osteoblasts. The detection of this enzyme would suggest osteoblast activity, possibly in mineralisation.

4. Analysis of the media and bone explant tissue for the presence de novo protein synthesis. The incorporation of tritiated glycine into protein molecules would indicate cells were viable after harvesting. Autoradiography would allow the location of the

metabolically active cells to be determined, while SDS-page gels and Western blots would allow the nature of the proteins synthesised de novo to be revealed.

5. Analysis of indirect bone resorption through the identification of hydroxyproline within the circulating medium. This would show that the bone explants maintained ex vivo were releasing collagen into the media thus, infer that the cancellous explants were under going active tissue resorption.

The aim of this introduction is to give a brief overview of the processes that occur in bone during growth, development, and maintenance of skeletal tissue, thus, modelling and remodelling, whilst comparing the differences expected to be observed with each of the different tissues used with the Zetos culture system (ovine, bovine and human). Details on individual marker proteins are given defining their structure and role in bone biology. This is followed by an explanation of the techniques used to observe these processes in bone explants cultured in the Zetos system. Namely double labelling of the bone with fluorescent markers in order to locate *de novo* bone apposition, using radioactively labelled amino acids to detect proteins synthesised during culture and immunolabelling of key bone markers (procollagen type I, osteocalcin, osteonectin, osteopontin, and bone sialoprotein).

4.a.i. Modelling

In terms of human development, the first two decades of life are devoted to a process known as modelling. Modelling controls the growth, shape, size, strength, and anatomy of bones and joints during growth and stops once skeletal maturity is reached. During this phase, bone formation precedes and exceeds bone resorption. Physiological remodelling does not change bone shape, and consists of bone resorption followed by bone deposition in approximately the same location. Since it continues throughout life it appears to be important for maintenance of the skeleton, but its exact function remains obscure. Adaptive remodelling is the response of the bone to altered loads and may alter the strength, density and shape of bone (Buckwalter, 1987).

To summarise the activities of bone cells during modelling, osteoclasts resorb bone on the endosteal (inner) surface (marrow cavity) while osteoblasts add matrix on the periosteal (outer) surface. However, this is a complex process and does not only involve periosteal formation and endosteal resorption As the bone grows the osteoblastic and osteoclastic activities will lead to increases in bone size and changes in longitudinal and cross-sectional geometry that are characteristic of individual skeletal components. This process is deemed uncoupled as the amount of resorption and formation are unequal, and are located on different surfaces. It is usually a continuous process, covering over 90% of the surfaces, to produce a net gain in bone mass. Modelling is the main form of growth taking place in young bovine tissue used during Zetos culture. New bone is laid down on a calcified cartilaginous scaffold in a process known as endochondral ossification (see Introduction).

Frost (1987), developed a theory (the mechanostat) that bone cells can sense mechanical strain, and that there is a range, or a window, in where this affects bone formation and resorption. It is believed that when strains within the bone exceeds a "modelling threshold" then bone formation is initiated, causing an increase in bone mass and bone strength. This threshold is known as the minimum effective strain (MES_m) and is believed to be around 1,000 μstrain in young adults. If this threshold is not reached then bone tends to be inactive.

Jowsey (1960) showed through microradiographic studies that newly formed bone is 25% less dense than older bone, making woven bone structurally inferior to mature bone. Older bone has more densely packed crystal and is, therefore, more brittle. It is believed that in woven bone mineralisation is initiated away from the cell surface in matrix

vesicles that bud from the plasma membrane of osteoblasts (Fig.4a.1). In certain situations such as calcifying cartilage in the growth plate, and in tendons and ligaments collagen, matrix vesicles are also required to initiate mineralisation. Within the epiphyseal growth plate, membrane bound bodies, known as extracellular matrix vesicles (ECMV's), provide a site for the accumulation of mineral ions. They have an average diameter of 70 nm. They are the sites of initial mineral deposition in calcifying cartilage. They appear less frequently in newly mineralizing osteoid. The vesicles are believed to protect mineral ions, contain enzymes capable of degrading mineral nucleation, growth and proliferation inhibitors, provide a local increase in local ion concentration. For example, metalloproteinases degrade cartilage proteoglycans and ATPases hydrolyse nucleoside triphosphates (NTPs) both of which are inhibitors of apatite growth and formation.

Lamellar bone replaces woven bone in humans when they are 2-3 years old. In lamellar bone mineralisation is believed to begin within the gap between overlapping collagen molecules (Fig.4a.2). The collagen molecule is assumed to act as a template, initiating and propagating mineralisation along with the noncollagenous proteins, though the exact mechanism is unknown. There are few if any matrix vesicles present in this region, if any at all, and the cells themselves are always sitting upon a layer of unmineralised bone matrix.

In order for mineralisation to take place, alkaline phosphatase (AlP) is required to increase the local phosphate concentration during osteoid mineralisation. Also, a higher pH is necessary, as osteoblasts work best at around 7.2-7.8. It is believed that anionic proteins facilitate this environment which indirectly aids apatite deposition.

During modelling, where bone formation and bone resorption are not coupled, bone formation can occur on quiescent bone surfaces without preceding bone resorption and create smooth cement lines. Therefore, the combination of fluorochrome labelling and a smooth cement line without interruption of surrounding collagen fibers is regarded as evidence of minimodelling (Kobayashi, 2003). However, these sites accounted for less than 2% of the entire bone surface on average. Therefore, when performing bone histomorphometry of adult cancellous bone, minimodelling should be taken into account when dealing with parameters related to osteoid volume and mineralisation.

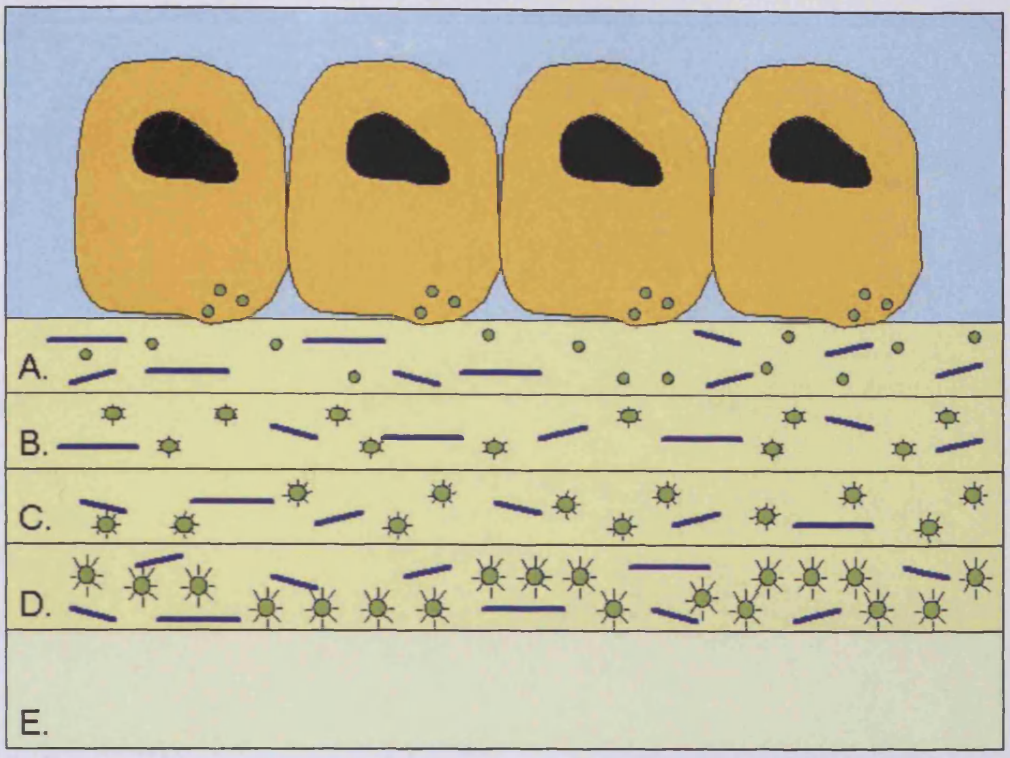

Figure 4.a.1. *Mineralisation of the osteoid seam through matrix vesicles.* ***A.*** *Osteoblasts secrete collagen (blue line) and glycosaminoglycans, as well as matrix vesicles (green circle).* ***B.*** *The matrix vesicles begin to accumulate crystals of hydroxyapatite.* ***C.*** *These crystals increase in size by accretion of mineral salts and are regarded as foci of mineralisation.* ***D.*** *Each foci is almost confluent.* ***E.*** *Fully mineralised bone. The junction between C and D is the calcification front. [Adapted from Stevens & Lowe, 1997]*

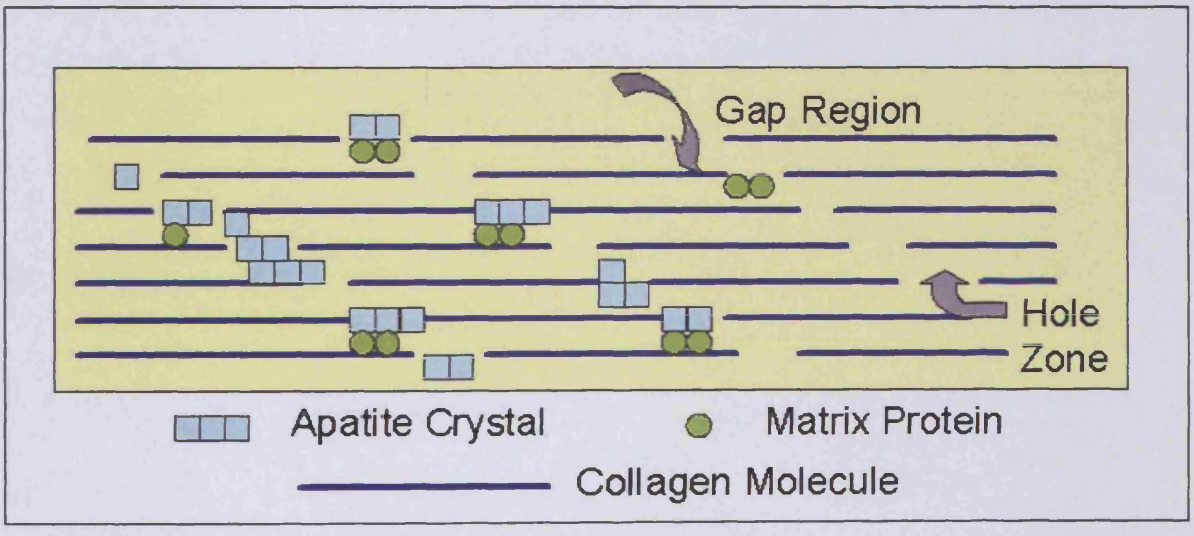

Figure 4.a.2. *Mineral deposition in bone is believed to occur within the hole and gap regions between the packed collagen fibrils. Noncollagenous proteins are thought to act as nucleators and are located within these spaces.*
[Adapted from Boskey and Paschalis, 2000]

4.a.ii. Remodelling

Remodelling is the term used for the continued maintenance of the adult skeleton, through continued removal and replacement of small fractions of bone each year. Usually this phase occurs for three decades or more after modelling ends (in terms of human development). Parfitt (1994) concluded that this process begins with localised resorption that is succeeded, at the same site, by precisely equal bone formation. Thus, bone formation equals bone resorption, therefore, these activities are said to be "coupled".

It is assumed that the aim of bone remodelling is to enable the bones to adapt to mechanical stresses. It allows the bone to maintain its strength by repairing microdamages caused through daily use, and allows mineral metabolism to be conducted. Continually renewing bone prevents accumulation of older, densely mineralised bone, which is more brittle.

Approximately 20% of the cancellous bone surface is being remodelled at any given time point, which will reoccur on average every 2 years, deemed "activation frequency" (Parfitt *et al.*, 1987).

In essence, bone remodelling in cancellous bone, begins once its "origination" has been decided and is carried out by a team of cells known as the basic multicellular unit (BMU). The life cycle of this unit consists of six phases; resting, activation, resorption, reversal (coupling), formation, mineralisation then returning back to resting. This first step requires the accumulation and proliferation of specific cells as well as hormones and cytokines at the desired resting surface of cancellous bone. What determines the exact location of the BMU is not known, though several hypotheses exist. The favourite hypothesis among bone biologists is that the osteocyte, and/or lining cells, sense changes in mechanical forces and reacts accordingly. Once the origination of the BMU has been determined and the secretion of hormones have taken place, lining cells on the surface of a trabecule change their shape from being flat epithelial-like cells to rounded cells, allowing some of the collagen matrix to be exposed. Usually lining cells rest upon a thin endosteal membrane (0.1 - 0.5 μm) which consists of unmineralised connective tissue that has fewer collagen fibers and less amorphous substances than bone. The lining cells also secrete collagenase to break down the collagen fibrils allowing the bone mineral to be exposed. Then the activated lining cells produce RANK Ligand on their cell membrane. Osteoclast progenitor cells in the near vicinity bind to this receptor via their membrane bound receptor

RANK, this causes precursor cells to fuse creating a mature, active, multinucleic osteoclast. This stage of the BMU can be seen in Figure 4.a.3. Image A.

The initial resorption phase is very rapid and lasts approximately 8 days, and forms what is referred to as a Howship's lacunae. This step is succeeded by a slower resorption phase conducted by mononuclear cells which lasts approximately 34 days (Ericksen *et al.*, 1984). Parfitt *et al.*, (1996) states that multinucleic osteoclasts are active for approximately 12 days before they undergo apoptosis (programmed cell death). Thus, a constant renewal of osteoclasts is required at the BMU "front". The BMUs in cancellous bone lie along the surface, rather than burrow through the bone as seen in cortical bone (Figure 4.a.3. Image B & C). The BMU forms a trench (half tunnel) or spreads out over a specific area. It can have a mean depth of approximately 60 μm.

After an optimal depth of resorption has been achieved a reversal phase occurs, which lasts approximately 9 days (Ericksen *et al.*, 1984) whereby plump active osteoblasts converge at the bottom of the pit ready to form osteoid (Figure 4.a.3. Image D.). Matrix deposition is usually polarised towards the bone surface. Initial apposition rate is 1.2μm/day, which gradually decreases to zero as the cavity is filled. According to Parfitt *et al.*, (1997) it takes approximately 17-20 days for osteoid to mature. Approximately fifteen days after osteoid formation mineralisation begins (Figure 4.a.3. Image E.). This increases to 27 days before gradually decreasing (Erikson *et al.*, 1984). In normal individuals it could take anything between 124-168 days to refill a resorption cavity (Ericksen *et al.*, 1984) (Figure 4.a.3. Image F-H.), after which the osteoblasts gradually begin to flatten until they become quiescent lining cells (Figure 4.a.3. Image I-L.). The evidence suggests that no new osteoblastic teams are recruited throughout the life span of the BMU (Parfitt *et al.*, 1997). During this formation phase some osteoblasts get surrounded in their own matrix. These cells remain embedded within the mineralised matrix as osteocytes. Unlike cortical bone remodelling, remodelling in cancellous bone occurs on surfaces that are lined with lining cells and are in close proximity to marrow cells, all of which could aid or participate in the remodelling process. It has been observed that bone remodelling is higher in areas with more red marrow and that the area occupied by fat cells increases as bone volume decreases (Meunier *et al.*, 1971).

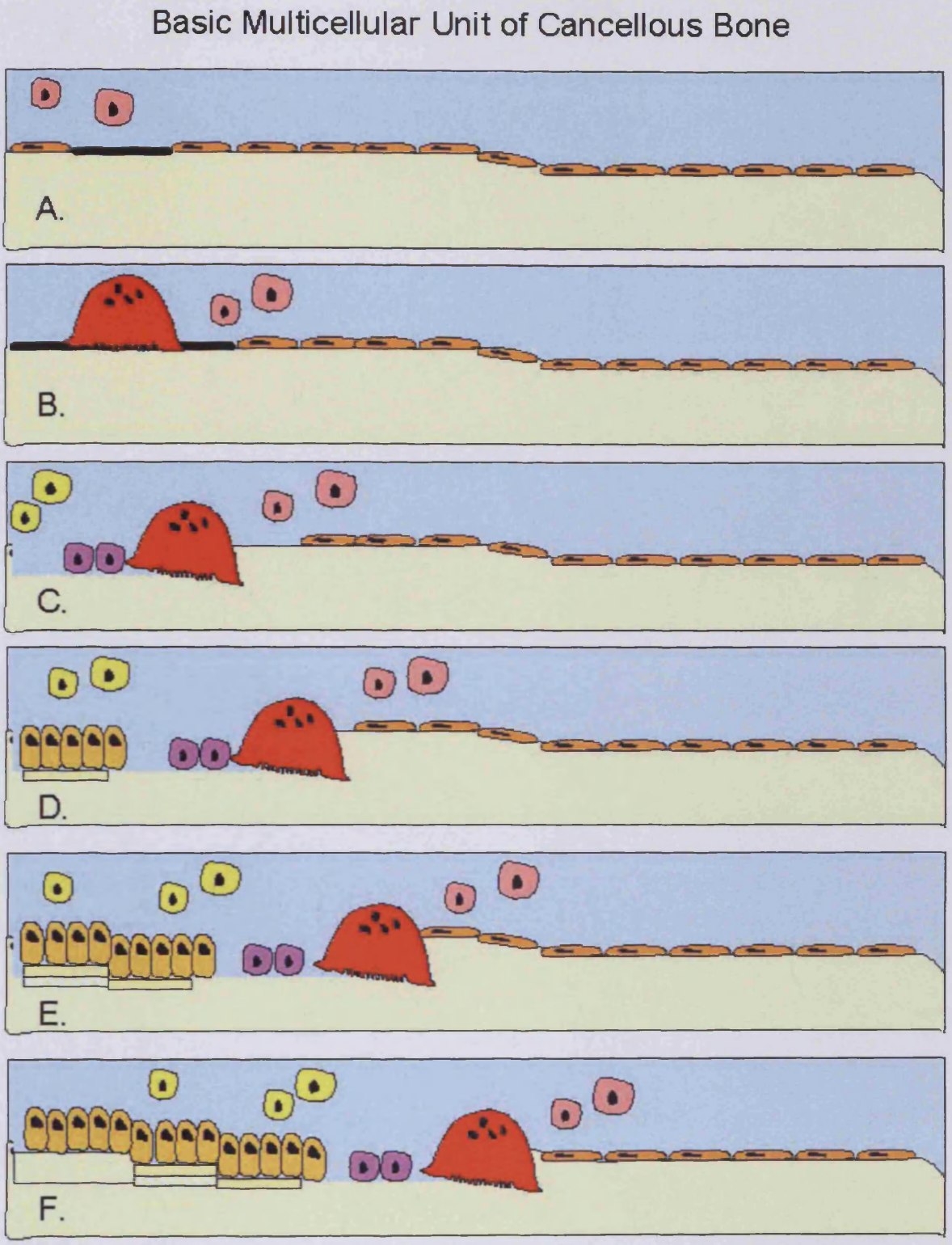

Figure 4.a.3. *The life-span of a BMU moving along the surface of cancellous bone is depicted above (Adapted from Ott, 2002). Each stage represents 10 days, moving at a rate of 10 μm each day.* ***A.*** *Origination of the BMU.* ***B.*** *Active osteoclasts are formed (red).* ***C.*** *Mononuclear cells (purple) continue resorption, while preosteoblasts (yellow) proliferate.* ***D.*** *Osteoblasts (orange) start to form osteoid (pale yellow).* ***E.*** *Osteoid secretion continues and begins to mineralise (cream).* ***F-H.*** *Continuation of formation and mineralisation.* ***I-J.*** *Osteoblasts begin to flatten.* ***K-L.*** *Osteoblasts become lining cells (dark orange).*

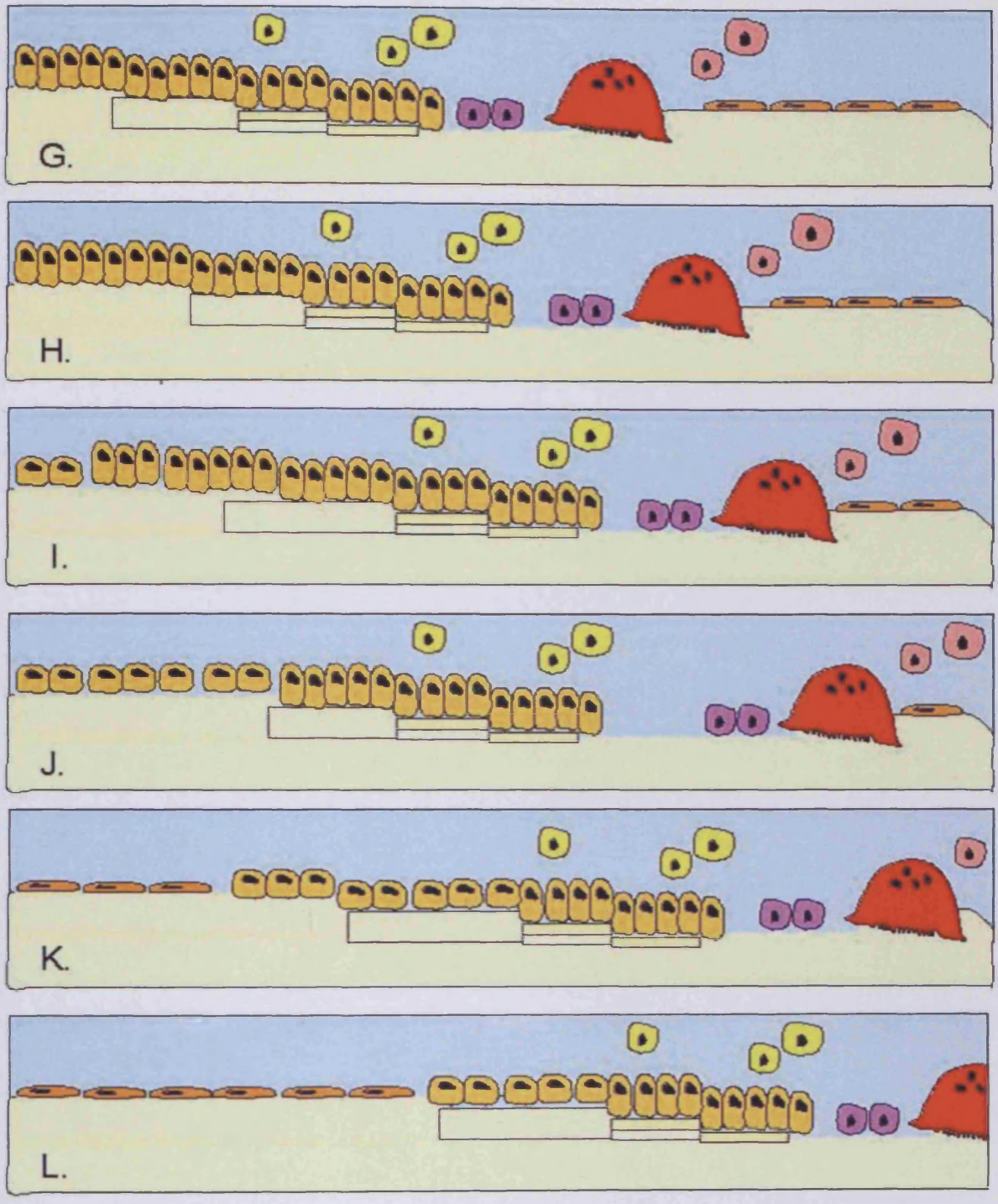

This figure however, does not account for osteoblasts becoming surrounded in their secretions to form osteocytes, nor does it account for the fact that there is a continuous renewal of osteoclastic cells throughout the lifespan of the BMU. New cells are continually recruited, though no new osteoblasts are believed to join.

4.a.iii. Osteoporotic bone

Sometime after the fifth decade of life, bone resorption and bone formation become once again uncoupled in the human skeleton. Bone formation fails to keep pace with bone resorption, causing a decrease in skeletal mass and the loss of trabecular connectivity. This in turn causes the skeleton to become weaker with a greater risk of fracture. Osteoporosis is a skeletal disease that is characterised by a decrease in bone strength.

Loss of connectivity causes isolated trabeculae to loose their ability to sense mechanical forces. Over time, these segments of bone will disappear due to further osteoclastic resorption causing a loss of bone mass. Once connectivity is lost it cannot be replaced.

Postmenopausal osteoporosis is associated with several kinds of irregularities at each stage of the remodelling process. It is believed that the menopause itself causes, i) an increase in the origination of BMU's. Manolags and Jilka (1995) believe that this increase in BMU's is because estrogen deficiency causes an increase of interleukin 6, as well as other cytokines, which in turn promotes the proliferation of osteoblasts and osteoclasts; and ii) an increased depth of resorption pits. Erikson *et al.*, (1999) believes postmenopausal osteoporosis is due to an increase in the life span of the osteoclast, while Kameda *et al.*, (1997) believes it is due to a decrease in osteoclast apoptosis. The main problem with osteoporosis is that aged osteoblasts do not fill the BMU with as much new bone as was there previously. This leads to a loss of bone mass causing greater bone loss the more BMU's there are, which in clinical terms is called senile osteoporosis. It has been shown by Arlot *et al.*, (1990) that women with postmenopausal osteoporosis have a lower mineral apposition rate compared with normal postmenopausal women. While Parfitt *et al.*, (1995) showed that there was a lower ratio of osteoblastic surface to osteoid surface in women with postmenopausal osteoporosis compared with normal postmenopausal women. There is also evidence suggesting that patients with osteoporosis show a high percentage of surface with unmineralised matrix (Jayasinghe *et al.*, 1993) indicating that bone formation at these sites are incomplete and that the BMU's are less active than in normal postmenopausal women. Ott (1993) noted that women with postmenopausal osteoporosis had a lower percentage of tetracycline labelled osteoid seams. This aspect should be kept in mind for analysing cancellous bone cores from elderly women cultured in the Zetos system.

4.a.iv. Collagen Type I

Bone consists mainly of type I collagen though trace amounts of collagen type III, V and X have been observed. These trace collagens may aid in organising matrix deposition and act as a template for type I collagen (type X), or may regulate the diameter of collagen fibrils (type III and V).

Each molecule of type I collagen is composed of two α1 chains and one α2 chain coiled around each other in a characteristic triple helix, though some molecules have been composed of 3 α1 chains. These chains are composed of Gly-X-Y repeats. This causes each chain to be coiled into a left-handed helix, with the triple helix being right-handed. The smallest molecule Gly is situated in the centre of the helix, while the other residues are at the surface. In one third of the cases X is proline and Y is hydroxyproline. Type I collagen is a fibrillar collagen, which characteristically consists of long continuous triple helix, which self-assembles into highly organised fibrils (Rossert and Crombrugghe, 2002).

The α chains of pre-procollagen are synthesised on ribosomes upon the endoplasmic reticulum. During this process hydroxylation of proline residues occur to obtain hydroxyproline (an imino acid unique to collagen). The reaction substitutes a hydroxyl group, OH, for a hydrogen atom, H, in the proline. The role of the hydroxylation reaction is to secure the chains in the triple helix of collagen. Hydroxylation is catalysed by the enzyme prolyl-4-hydroxylase with vitamin C being essential for the action of this enzyme. Also, hydroxylation of lysine residues occurs to obtain hydroxylysine. Hydroxylysine is needed to permit the cross-linking of the triple helices into the fibers. The enzyme peptidyl proline hydroxylase is essential for this. Glycosylation of some hydroxlysine residues takes place by adding glucose and galactose to the amino acid by the enzymes galactosyl transferase and glycosyl transferase (Rossert and Crombrugghe, 2002).

The assembly of the three alpha chains from procollagen polypeptide, involves the formation of disulphide bonds between parts of the polypeptide chains at the C-terminal. The three chains then associate and align allowing the triple helix to form in a zipper-fashion giving procollagen.

Procollagen molecules are secreted from the cells by exocytosis into the extra cellular space. In the extra cellular space, procollagen peptidases cleave the N telopeptide and the N telopeptide, resulting in the formation of collagen. Collagen molecules form collagen fibrils through self-assembly or polymerisation. Cross-linkage between adjacent collagen molecules stabilises the fibrils (Robins & Brady, 2002). The types of cross-links

made are based on the number of molecules involved. Bivalent (reducible): linking the N or C terminal (i.e. telopeptides) of one molecule to the helical region on another. Trivalent (stable or mature crosslink): linking the N or C terminals of two molecules to the helical region of the third.

In fibrils, molecules of collagen are aligned parallel to each other, overlapping by 67 nm. It is in this 40 nm gap region that mineralisation is assumed to initiate. This quarter-staggered assembly explains the banded aspect of type I collagen as seen with SEM.

4.a.v. Noncollagenous Matrix Proteins

The noncollagenous proteins in the bone matrix include glycoaminoglycan (GAG) containing proteins, glycoproteins, gamma carboxyglutamic acid (GLA) containing proteins as well as other proteins. The exact role of these proteins is not well understood though they are believed to play a key role in bone mineralisation and calcification. Observations involving knockout animals show that, if not lethal, the changes observed are not profound, implying that the process of mineralisation is redundantly controlled with more than one protein acting as a mineral nucleator or regulator of crystal growth. Most osteoid constituents are not bone specific, but its uniqueness relies upon the way it is organised (Robey, 2002).

Control of matrix composition is determined at the genetic level as all proteins are encoded in the genome. Messenger RNAs for each secretory protein are transcribed and processed in the nucleus, from there they are transported to the cytoplasm where they direct protein synthesis on ribosomes associated with the endoplasmic reticulum (ER). The proteins are packaged within the lumen of the ER and pass through a series of membrane-bound compartments of the Golgi apparatus. Most of these proteins undergo one or more post-translational modifications. For example, covalent cross-linking of amino acids (collagen); N- and O- glycosylations of amino acids to yield proteoglycans (e.g. biglycan and decorin) or other glycoproteins (osteopontin and bone sialoprotein); phosphorylation of amino acid residues (osteopontin); vitamin k dependent gamma-carboxylation of glutamate residues (osteocalcin). After modification the proteins fold into their mature 3D conformations and are packaged into secretory vesicles which fuse with the plasma membrane expelling their contents into the extracellular space.

Expression patterns of these proteins vary spatially and temporally. Osteonectin is expressed early on during mineralisation; AlP is also an early expressed enzyme that remains well into maturity; however, osteocalcin is expressed after the development of an established matrix; while osteopontin is also a late stage marker, produced just prior to mineralisation.

Proteoglycans

These molecules are characterised by the covalent attachment of long chain polysaccharides (GAGs) to core protein molecules. These GAG molecules are composed of repeating carbohydrate molecules are sulphated to varying degrees (Robey, 2002).

Decorin (PG-II), and biglycan (PG-I), are two small proteoglycans found within the bone matrix (Fischer *et al.,* 1989). They contain chondroitin sulfate chains and share a high degree of homology within their core proteins. However, they differ in pattern of expression (Bianco *et al.,* 1990). During endochondral bone formation, decorin is widely distributed matching that of type I collagen. Decorin is first expressed by preosteoblasts, and is continued in osteoblasts, before being down regulated when the osteoblasts become osteocytes embedded within the matrix. On the other hand, biglycan has a more distinct distribution. It is up regulated in osteoblasts and maintained through to osteocytes. Both appear in the osteoid and, therefore, potential candidates as nucleators of hydroxyapatite precipitation. Though neither is believed to be initiators of matrix mineralisation, due to decorin's inability to bind calcium or effect hydroxyapatite precipitation. Biglycan on the other hand, has a limited affinity for calcium at low concentrations where it facilitates hydroxyapatite precipitation, but inhibits precipitation at high concentrations. Both have been observed to bind transforming growth factor β (TGF β) and collagen (Robey, 2002).

Glycoproteins

The number of glycoproteins discovered in the bone matrix have increased since the development of cDNA libraries to screen sequence information. The most abundant with significant structural and metabolic roles are described below. Most of these proteins have been modified post-translationally to contain either N- or O- linked oligosaccharides, and further still with the addition of phosphate and/or sulphate. There are at least seven different glycoproteins that contain the RGD (Arg-Gly-Asp) amino acid sequence, which allows the protein to bind to integrin receptors usually found on cell surface

(thrombospondin, fibronectin, vitronectin, fibrillin, osteoadherin, osteopontin and bone sialoprotein). These proteins differ in abundance and pattern of expression during bone formation, *in vivo* and *in vitro* and in other tissues (Robey, 2002).

Alkaline phosphatase

Alkaline phosphatase (AlP) is a cell surface enzyme covalently bound to phosphatidyl inositol (PI) phospholipids complexes. It is released from cells by the PI-specific phospholipase C enzyme (Noda *et al.*, 1987). The tissue-non-specific form of the enzyme is expressed by osteoblasts. There are at least four isoforms, the other three have a tissue specific distribution. AlP is a phosphotransferase, potential Ca^{2+} carrier, and may hydrolyse inhibitors of mineral deposition such as pyrophosphates. The exact role of AlP has not been elucidated, but as AlP is present in a number of non-calcifying tissues (kidney and liver) it is believed to have an abundant physiological purpose.

Osteonectin (SPARC, Culture Shock Protein, and BM40)

Osteonectin (35-45 kDa) was one of the first intact proteins to be isolated from demineralised bone matrix (Yang *et al.*, 1999). It is also known as SPARC, which stands for secreted protein, acidic, rich in cysteine; Culture Shock Protein; and BM40. SPARC was identified at early stages of embryogenesis in teratocarcinoma cells; Culture Shock Protein was noticed within *in vitro* cultured cells that would not usually express this protein, such as decidual cells in the uterus and maturing cells of the testis; and BM40 is the name derived from basement membrane associated cells that constitutively express the protein, such as mammary epithelium, distal tube epithelium in the kidney, and salivary epithelium (Robey, 2002). As can be seen above, this protein is not specific to bone, but is highly expressed in cells associated with mineralisation, such as hypertrophic chondrocytes, osteoblasts, and odontoblasts. The molecule itself contains two EF hand high affinity calcium binding sites, allowing it to bind to Ca^{2+}, hydroxyapatite and collagen, thus may mediate deposition and nucleation of hydroxyapatite deposition (Termine *et al.*, 1981). It is regarded as a positive regulator of bone formation. Cell culture studies have also implicated the osteonectin protein in binding to growth factors and modulating enzymatic activities, as well as regulating and influencing the cell-cycle, cell shape, and cell matrix interactions, though these activities may not reflect its role *in vivo*

(Robey, 2002). Knockout mice have been seen to suffer from severe cataracts (Gilmour *et al.*, 1998) and develop osteopenia (Delany *et al.*, 1998).

Osteopontin (Spp, BSP-I)

Osteopontin (OP), which is also known as bone sialoprotein I (BSP-I), is a secreted, acidic glycoprotein normally found in mineralised matrices as well as in urine, kidney and most epithelia (Robey, 2002). It is a 264-301 amino acid protein characterised for its large quantity of sialic acid (Sodek *et al,* 2000). *In vitro*, OP binds to cells, inhibits mineralisation and NO synthesis, may regulate proliferation, tissue repair, and initiate mineralisation (Giachelli, 1999). It has the RGD adhesion domain similar to that of fibronectin and vitronectin (Butler, 1989). It has a fairly high affinity for Ca^{2+} but does not appear to nucleate hydroxyapatite formation, but appears to possess a collagen-binding domain (Butler, 1989). It is believed to be a regulator of bone resorption (Giachelli, 1999). Osteopontin is expressed at late stages of osteoblastic maturation during matrix formation and prior to mineralisation, and is synthesised by osteoclasts. It can be localised within the osteoid, as well as bone surfaces and cement lines (Roach, 1994). The osteopontin knockout mouse does not have any defect regarding mineralisation, though shows impaired osteoclast function (Rittling *et al.*, 1998). *In vitro* studies show that there is defective osteoclast development as it has been shown to mediate the attachment of many cell types, including osteoclasts (Noda and Denhardt, 2002).

Bone Sialoprotein (BSP-II)

Bone Sialoprotein (BSPII) is generally expressed during mineralisation, though a few exceptions have been noted. It has been observed in a number of skeletal bone cells, such as chondrocytes, hypertrophic cartilage, osteoblasts at the verge of mineralisation and in some cases osteoclasts (Bianco *et al.*, 1991). It is strongly localised in cement lines and collagen poor matrix.

BSP-II differs from osteopontin by the fact it is made up of polyglutamic acid instead of polyaspartic acid, as well as being composed of sialic acid 12% (50% carbohydrate) (Robey, 2002). Its expression in bone is more limited than osteopontin. BSP can bind to cells with its RGD sequence or its upstream tyrosine sulphated region, possibly through the vitronectin cells surface receptor (Fisher *et al.*, 1990). It binds Ca^{2+}, and may be a candidate for initiating mineralisation as it has been seen to nucleate hydroxyapatite deposition in a variety of assays, unlike OP (Robey, 2002). BSP knockout mice do not

show an altered phenotype and no differences in mechanical or crystallographic properties were noted (Boskey, 2001).

Other Proteins

Osteocalcin (bone gla protein, BGP)

One of the bone specific noncollagenous proteins is osteocalcin. Osteocalcin was first discovered in the mid 1970's (Hauschka 1975, Price 1976). It is a small vitamin K dependent, calcium binding peptide, who's main role is currently unknown, but is believed to be involved in regulating precursor and mature osteoclast activity; may mark a turning point between bone resorption and bone formation and may regulate mineral maturation. It is also know as Bone Gla protein (BGP) due to the presence of γ-carboxyglutamic acid. Osteocalcin is thought to interact directly with hydroxyapatite in bone through its Gla residue (Hauschka *et al.*, 1989)

The osteocalcin gene knockout mouse shows excessive bone formation that does not appear to be dependent on osteoclastic resorption, suggesting that it has an effect on bone formation (Boskey *et al.*, 1998; Ducy *et al.*, 1996). The crystal size of the hydroxyapatite mineral is roughly the same size as controls though does not show any maturation thus, implying that osteocalcin is important for mineral maturation. Osteocalcin synthesis is a relatively late event, it begins after AlP activity though, persists for longer.

4.a.vi Labelling *de novo* matrix synthesis

One of the first experiments regarding bone growth was conducted by Stephen Hales in 1727. He used holes that were bored into the shaft of chicken long bones as markers. Measurements from the holes to the ends of the bones clearly demonstrated that bones grew from their ends, rather than from the middle, as the distances between the holes remained constant, while the distance between the holes and the end of bones increased.

Today, a far simpler method is used to study bone growth. In the last 40 years, bone growth has been studied by using fluorescent markers. The advantage of fluorescent markers is that they give a high resolution and allow simultaneous microscopic evaluation to be made. These methods are based on observations made over 270 years ago by the surgeon John Belchier. Belchier (1736) noted that the pork being served at a dinner he was attending had red stained bones but the meat remained unstained. It was deduced that the pigs had been fed madder, a dye from the roots of the plant *Rubia tinctorum*. Belchier saw the potential to use this dye to study bone growth and began to perform experiments on

pigs and birds. However, it was Duhamel (1740) who made full use of the potential of this dye. He observed that the dye only stained bone that was deposited during feeding with madder. He discovered that by adding and subtracting the madder from the animals diet he could confirm that the bones grew from their ends and that growth in width occurred by the addition of new bone at the periphery. Duhamel also noted that bone was dynamic and not static as the madder stained bone was removed and replaced by unstained bone, and that the madder was taken up by bone which was laid down during fracture repair (Hall, 1992).

The active agent in madder is known as alizarin, and has subsequently been synthesised chemically. It has been widely used as a means of studying bone growth for several years. Many of these techniques were developed here at the AO Research Institute by Berton Rahn (1980). Other chemicals have been identified that fluoresce in different colours. These fluorochromes include tetracycline, which produces a yellow colour (Milch, Rall, and Tobie 1957) (Frost, 1960); calcein green (Suzuki and Mathews 1966); calcein blue (Rahn and Perren, 1970); xylenol orange (Rahn and Perren, 1971); and alizarin complexon, which produces a red colour (Rahn and Perren, 1972).

Ott (1993) noticed that 40-60% of osteoid surfaces do not contain tetracycline labeles, of this only 7% can be explained by the non start of mineralisation. Frost (1980) hypothesised that mineralisation is not a continuous process, that it stops and starts over a period of time. However, Patel *et al.*, (1999) administered quadruple tetracycline labels to postmenopausal women and they did not see any missing labels, which would indicate a pause in bone formation. The highest percentage of surface osteoid that was mineralising, as seen with tetracycline labelling, is approximately 15% and in actively growing children. Adults can range between 5-10%, which is also the case with premenopausal, postmenopausal and osteoporotic adults.

The proportion of double labels to single labels depends on the number of days between labelling as well as bone formation period. The shorter the interval or the longer the formation period, the higher the proportion of double labels compared to single labels. This technique allows calculation of dynamic bone formation and mineralisation. Fluorophores form a chelate complex with calcium, strontium, barium and thus, becomes permanently incorporated into the mineralisation fronts (Fig.4a.4).

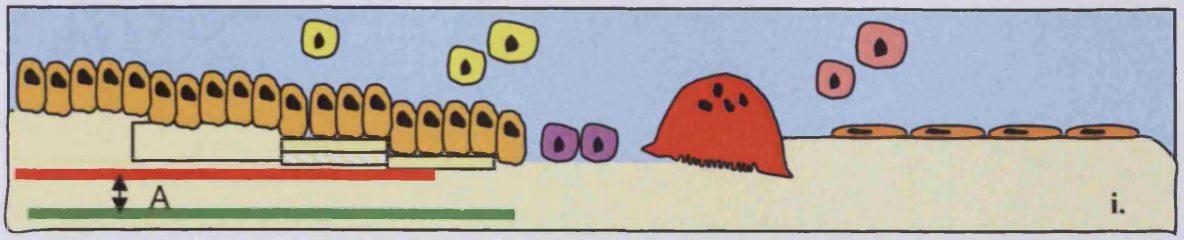

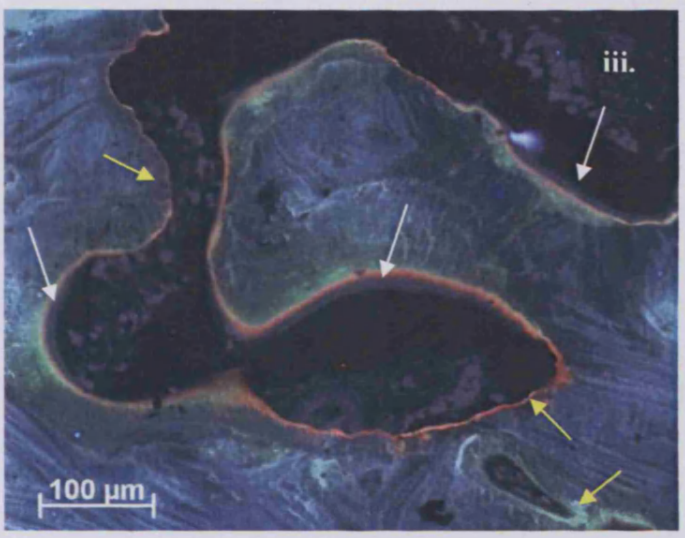

Figure 4.a.4. i) *A schematic diagram depicting how the fluorophores are incorporated into mineralised tissue. The distance between the centre of the first fluorophore (calcein green) to the second fluorophore (alizarin complexon) is the amount of bone apposition that took place during the administration period.* **ii)** *The different types of fluorophores that could be incorporated into a study.* **iii)** *An example of a double label incorporating calcein green and alizarin complexon into mineralising tissue. Regions of double labelling associated with light grey osteoid seams are indicated (white arrow) although the lack of resolution of the calcein green label prevents calculation of bone apposition rates.*

4.a.vii Labelling *de novo* protein synthesis

This method of radiolabelling has been used successfully for decades as an index of viability/cytotoxicity as protein synthesis is regarded as an essential metabolic process without which the cell would not survive. Most studies have used the incorporation of [^{3}H] leucine measured by liquid scintillation counting or [^{35}S] methionine incorporation (Freshney *et al.*, 1975) or measured using autofluorography (Freshney and Morgan, 1978). Radiolabelling specifically of cartilage or bone tissue has been conducted by a number of researchers (McKenzie *et al.*, 1977; Kaye and Henderson, 1988; Fedarko *et al.*, 1992). Culturing bone cores in the presence of radioactively labelled amino acids should, if the

tissue is living, create radioactive proteins which can be detected via autoradiography or with SDS-page (Fig.4a.5).

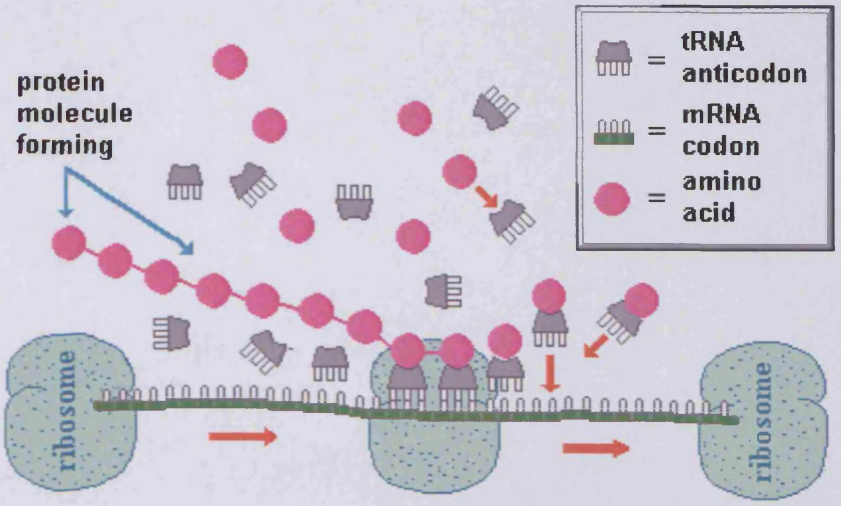

Figure 4a.5. *Cells synthesise proteins within protein structures known as ribosomes. tRNA molecules bring specific amino acids that correspond to the mRNA sequence together to form a polypeptide. This process is known as translation. If some of the free amino acids contained a radioactive tag, it would allow the detection for proteins synthesised during the administration period.*

Autoradiography is a means to directly visualise silver grain precipitate within cells, caused by radioactivity, providing localisation of metabolically active cells.

To extract collagen from the bone samples a solvent is used. In this case 0.5 M acetic acid containing 1 mg/ml of the enzyme pepsin. Pepsin degrades native collagen molecules from which the cross-links originate (Colowick and Kaplan, 1982). Ammonium sulphate precipitation is often used as the first purification and concentrating procedure. The proteins can be stored in ammonium sulphate solutions which reduces bacterial contamination, denaturation and proteolysis. Ammonium sulphate works by taking up the water molecules around the protein, thus, exposing the hydrophobic sites. Because hydrophobic groups tend to prefer to be together, the proteins will aggregate and thus, come out of solution. Ammonium sulphate is not the only salt that can be used, but it is the cheapest. The trick is to ensure that only the target protein precipitates, in this case collagen. This can be achieved by using an appropriate ammonium sulphate concentration. The concentration that should be used must be determined by experiment or from literature references. The precipitation reaction should be performed at low temperatures to prevent denaturation of the target protein. The ammonium sulphate must be added slowly and mixing is important to distribute the ammonium sulphate and to prevent inclusion of

unwanted proteins in the precipitate. Ammonium sulphate should be prepared as a stock solution at 4°C. The required final concentration is often reported as a v/v% ie. volume of saturated ammonium sulphate added/(volume of ammonium sulphate + starting volume of sample). After precipitation, the pellet is separated by centrifugation and washed in ammonium sulphate solution. The pellet is then dissolved in buffer for further purification or analysis. In this case the proteins will be separated on an SDS-page gel. Incubation of the gel with a photographic film should allow radioactivity within the protein bands to be detected.

4.a.viii Immunohistochemistry

Immunohistochemistry is a technique that uses labelled antibodies for localisation of specific tissue constituents *in situ*, making it a highly sensitive tool. Coons (1941) was the first to practice this method. There are two kinds of antibodies available for use, monoclonal antibodies and polyclonal antibodies. Monoclonal antibodies are all identical to each other, raised from lymphocytes fused to myeloma cells. By their nature, they react only to a single epitope making them highly specific. Polyclonal antibodies are harvested from animals that have been immunised with the antigen of interest. These antibodies recognise multiple epitopes, making them more tolerant of small changes in the nature of the antigen they recognise and offering a more robust reactivity profile but are less specific.

An antibody (monoclonal or polyclonal) recognises and binds to specific epitopes within tissue. These antibodies are known as primary antibodies (blue molecules) (Fig.4a.6). To amplify the localisation of the antigen in question, a secondary antibody is used (red molecules), which binds to the primary antibody. A marker, such as a gold probe, or fluorescent molecule, is attached to the secondary antibody to allow its detection either with light of fluorescent microscopy (yellow molecule).

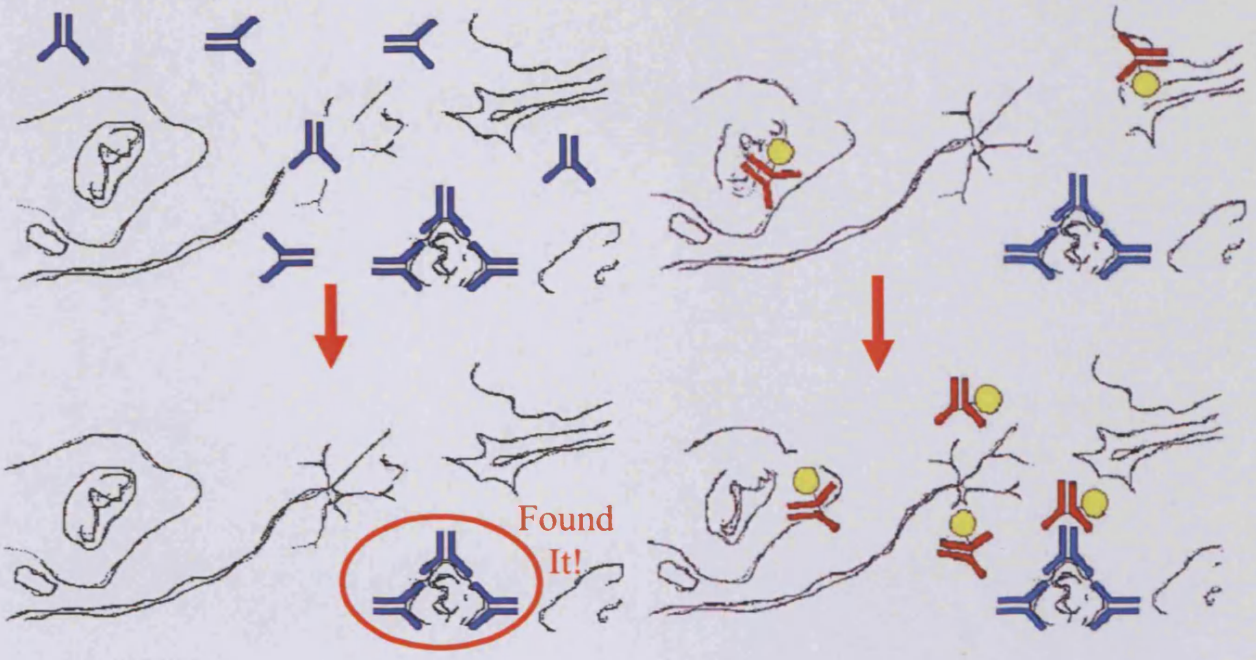

Figure 4a.6. Primary antibodies (blue molecules) are placed over a section of tissue. These molecules bind specifically to their antigen. Washing the tissue removes residual antibodies. Secondary antibodies (red molecules) with bound label (yellow molecules) are used to localise and visualise the primary antibodies and thus, the protein of interest. [permission from R.G. Richards]

4.B. Materials & Methods

Herein is a detailed description of all materials and methods used during this study. Additional information on techniques, machinery and chemicals can be found in the relevant Appendices.

4.b.i. Culture in the Zetos System

Ovine, bovine and human cancellous explants were harvested and maintained *ex vivo* as previously described in the Introduction and Materials and Methods 3B. Bovine bone cores were maintained *ex vivo* for 23 days, while both ovine and human bone cores were maintained *ex vivo* for 15 days.

4.b.ii. Immunohistochemistry of Bone Marker Proteins.

Antibodies: In total six different antibodies were used. Monoclonal mouse anti-bovine bone osteonectin (AON-1) (Bolander *et al.*, 1989); monoclonal mouse anti-ovine procollagen type I aminopropeptide (SP1.D8) (Foellmer *et al.*, 1983). Polyclonal rabbit anti-bovine bone osteocalcin (LF-32) (Ingram *et al.*, 1993); polyclonal rabbit anti-human osteopontin (LF-123) (Fisher *et al.*, 1995) (LF-166) and polyclonal rabbit anti-human bone sialoprotein (LF-120) (Fisher *et al.*, 1995). Mouse immunoglobulins (IgG) were purchased from Sigma (St. Louis, MO, USA) (I8765). Monoclonal mouse antibodies (IgG) against osteonectin (ON), and procollagen type 1 aminopropeptide (PINP), were obtained from the Developmental Studies Hybridoma Bank under the auspices of the NICHD and the University of Iowa, Department of Biological Sciences, Iowa City, IA 52242, USA: Polyclonal rabbit antibodies against osteocalcin (OC), osteopontin (OPN), and bone sialoprotein (BSP) were generous gifts from Dr. Larry W. Fisher of the National Institutes of Health, National Institute of Dental and Craniofacial Research, Craniofacial and Skeletal Diseases Branch, Bethesda, MD, USA:

Immunolabelling: The method was based on the immunolabelling method of Yang *et al.* (2003). The rinsing buffer was composed of 0.1M PIPES (Piperazine- NN'-bis-2-ethane sulphonic acid) (pH 7.4) and 1% Tween 20 + 1% BSA (bovine serum albumin) and 1% goat serum as blocking agents. This buffer was used for all washes, to dilute the primary and secondary antibodies, as well as to prepare the 6% goat serum used to block 'sticky' sites. Sections were first deacrylated with 1-acetoxy-2-methoxyethane, cleared through ethanol and rehydrated to distilled water through a decreasing ethanol series. Sections were

encircled with a water-repellent wax pen (Daido Sangyo Co., Tokyo, Japan) and slides were placed in a humidified chamber containing moist tissue. The procedure was carried out at room temperature (20-22°C). The volume of each wash and incubation was 200 μL.

Immunolabelling procedure: Sections were washed with rinsing buffer for 5 min each followed by 6% goat serum for 15 minutes to block non-specific binding by the primary antibody. Primary antibodies were incubated for 1 h (see Table 4b.1 for concentrations used). Sections were washed again 6 times with rinsing buffer followed by 6% goat serum for 15 minutes to block non-specific binding by the secodary antibody. Five nm gold-conjugated goat anti-mouse or anti-rabbit secondary antibody (1:200) (see table 1) was incubated for 2 h. Sections were then washed 6 times with rinsing and fixed with 1% glutaraldehyde in PIPES pH 7.4 for 5 minutes, followed by being washed 6 times with 0.1M PIPES and final rinsing with distilled water. Sections were silver enhanced (silver enhancement kit, British Biocell International, Cardiff, UK) for 20-30 min. The reaction was stopped by placing the slides in distilled water for 5 min. No counterstaining was used. Slides were dehydrated through a graded series of ethanol, cleared in xylene and Eukitt-mounted.

Table 4.b.1. Summary of primary and secondary antibody dilutions used on ovine (O), bovine (B) and human (H) sections.

Species of Bone	*1° Antibody*	*Dilution*	*2° Antibody*	*Dilution*
O, B, H	BSP rabbit anti-human (LF-120)	1:100	Goat anti-rabbit	1:200
O, B,H	Osteocalcin rabbit anti-bovine (LF-32)	1:300	Goat anti-rabbit	1:200
B	Osteopontin rabbit anti-human (LF-123)	1:200	Goat anti-rabbit	1:200
O & H	Osteopontin rabbit anti-human (LF-166)	1:200	Goat anti-rabbit	1:200
O, B, H	Osteonectin mouse anti-bovine (AON-1)	1:50	Goat anti-mouse	1:200
O, B, H	PINP mouse anti-ovine (SP1.D8)	1:100	Goat anti-mouse	1:200

Qualitative analysis of protein localisation in cells within tissue sections from explants maintained *ex vivo* in the Zetos loaded culture system, in comparison to positive and negative control tissue explants. Similar labelling to fresh samples would be interpreted as a good sign that the tissue was healthy. Similar labelling to disuse or necrotic tissue would be a sign that the tissue was not being maintained *ex vivo*. Similar staining to

dead tissue would suggest the technique was not sensitive to use to detect changes occurring post-harvest, or that the tissue was dead. Immunolabelling was conducted upon one of twenty sections (each stained for different proteins) obtained from the centre of the core, and one of twenty sections from the surface of the core, providing a representation from each experimental group n=2

4.b.iii. Fluorescent Double Labelling of Bone Apposition.

On day one of culture DMEM (without serum) plus calcein green (30 μg/ml) (Fluka 21030) was perfused around all of the explants for 8 hours. Explants were then perfused with three changes of DMEM (without serum) each for 30 min to washout any residual stain. Normal culture media was replaced. Ten days later, explants were perfused with DMEM (without serum) plus alizarin red (45 μg/ml) (Fluka 398817) for 8 hours, or DMEM (without serum) plus xylenol orange (12 μg/ml) (Fluka 95615) for 8 hours. Again, the explants were washed with three changes of DMEM (without serum) each for 30 min before being perfused with DMEM (10% FCS) for the remainder of the experiment (unless otherwise stated). Explants were harvested 5 days later to allow the fluorophores to fully bind to the matrix. Explants were fixed in 70% ethanol before being processed through Technovit 9100 New resin (as described in Chapter 2).

Qualitative analysis of bone apposition within tissue sections from explants maintained ex vivo in the Zetos loaded culture system, in comparison to positive and negative control tissue explants. The presence of double labelling would be interpreted as a good sign that the tissue was metabolically active. Similar labelling to disuse or necrotic tissue would be a sign that the tissue was not being maintained ex vivo. Similar labelling to dead tissue would suggest the technique was artefactual and not sensitive to use to detect changes occurring post-harvest or that the tissue was dead. Table 4b.2 summarises the number of cores analysed during these studies, the species used and length of culture.

4.b.iv. Biochemical Analysis of the Media

Hydroxyproline (Woessner J.F., 1961).

First Day: Samples of media, that was harvested daily and frozen, were removed from the –20°C freezer and left for 30 min to defrost. Once defrosted, each sample was vortexed for a few seconds to ensure sample was thoroughly mixed. Two hundred and fifty μl of sample media was placed in a labelled Wheaton 4 ml glass vial (Sterico AG no. 224742). Once

this had been achieved for all samples they were placed under the fume hood. A small volume of hydrochloric acid fuming 37% HCL conc. (12M) was placed into a glass beaker. A multiuse pipette was used to place the same volume of HCl to each sample (250µl). The caps were screwed tight onto the glass bottles to avoid sample evaporation during incubation (not too tight as the glass may expand and break). All tubes were placed into a metal rack in an incubator at 110°C for 15h.

Second Day: To the incubated samples 300 µl of 10M NaOH was added to neutralise the sample. Black precipitate in the sample corresponded to denatured proteins. Each sample was placed into clean labelled eppendorf tubes, where 50 mg of Charcoal-Resin mix (Fluka no. 05110 and Bio Rad no. 143-7425) was added. This mix was placed under agitation for a few hours at room temperature. This step adsorbed the proteins and removed the colour from the media. Once completed, the samples were spun at 19,720rcf for 15 min. The cleaned supernatant was removed from the Charcoal-Resin mix ready for use in the colorimetric assay.

Hydroxyproline (OHP) assay: 6 Standard test tubes were made as follows:

1) 40 µL OHP-stock (40 µg/mL) solution, filled with 1960 µL Milli-Q water, vortexed (-> 5 µg OHP)

2) 1000 µL from tube 1, 1000 µL Milli-Q water, vortexed (-> 2.5 µg OHP)

3) 1000 µL from tube 2, 1000 µL Milli-Q water, vortexed (-> 1.25 µg OHP)

4) 1000 µL from tube 3, 1000 µL Milli-Q water, vortexed (-> 0.625 µg OHP)

5) 1000 µL from tube 4, 1000 µL Milli-Q water, vortexed (-> 0.313 µg OHP)

6) 1000 µL from tube 5, 1000 µL Milli-Q water, vortexed (-> 0.156 µg OHP)

Duplicates of all samples were prepared. From each standard, 250 µL was removed and placed into thick walled glass tubes. To these, 250 µL NaCl (saturated) was added, followed by 500 µL Chloramin T. Tubes were vortexed and incubated for 4 min at room temperature. To each standard 500 µL (4-Dimethylamino-benzaldehyd, Fluka no. 39070) DABA was added, vortexed, and incubated for 12min at 65 °C then left cool down to room temperature. MilliQ water (plus NaCl, Chloramin T, DABA) was used for zero adjustment (neg. control). Next, 250 µL aliquots were transferred per well into 96 well assay plate. The same reagents were added to 250 µL of the media samples that were previously centrifuged. Then, once cooled, 250 µL of aliquot was transferred into the 96 well plate. The absorbance was measured with HTS 7000 Bio Assay Reader, 560 nm. The results

were calculated from a linear standard curve A(560) vs. OHP content and were documented in a file on the local computer.

Alkaline phosphatase [Enzyline® PAL optimise (REF 63 609)]

Media was sent to a local company (MEDITEST) for quantification of ALP secreted from compromised cells. In principle the following reaction occurred: -

$$\text{PNPP} \xrightarrow{\text{ALP}} \text{paranitrophenol} + \text{phosphate}$$

The rate in which paranitrophenol is freed from paranitrophenylphosphate (PNPP) is proportional to the ALP activity in the sample.

The reagents were prepared as follows: -
10 ml Diethanolamine buffer was mixed with 1 ml PNPP+NaN_3. From this reagent 1 ml was added to 20 µl of sample media in a thermostatically controlled cuvette (37°C). After 1 min the mean increase of absorbance was measured per min for a maximum of 3 min. The results were recorded as U/L the equivalent of 1 mmol of substrate catalysed per min. A control consisting of normal media was provided.

Quantitative analysis of cell activity within tissue sections from explants maintained *ex vivo* in the Zetos loaded culture system, in comparison to positive and negative control tissue explants. The presence of the enzyme would be interpreted as a good sign that the tissue was metabolically active. A similar quantity to disuse or necrotic tissue would be a sign that the tissue was not being maintained *ex vivo*. A similar quantity to dead tissue or blank media would suggest the technique was artefactual and not sensitive to use to detect changes occurring post-harvest or that the tissue was dead. Nine human cores, from one limb, analysed in this manner

4.b.v. Incorporation of ^{3}H-glycine into Synthesising Proteins

Radiolabelling of Bone Cores

At 0, 7 and 14 days, ovine, bovine, and human bone cores, from all culture conditions were placed within the wells of a 24 well plate (Falcon, 353504). Upon each sample 2ml of DMEM containing 10% serum and 25 µCi of ^{3}H-glycine (Amersham, TRK.71) was

placed, and left to incubate for 24 hours at 37°C. The media covering the cores was collected and stored in eppendorf tubes for analysis, and the cores were then washed 3x30 min in 2 ml phosphate buffered saline (PBS) (Sigma, P-4417) at 37°C.

Processing the bone cores for microautoradiography

Half of the samples were fixed in 4% paraformaldehyde (Fluka, 76240) at 4°C for 10 h, washed 3x30 min in 0.3M PIPES buffer (Fluka, 80636) and placed in 70% ethanol. The samples were then dehydrated and processed, as mentioned in Chapter 2 (2.b.v. Histology), for embedding in Technovit 9100 New resin. Polymerised samples were sectioned with a HM355S rotary microtome. The sections were deacrylated with 1-acetoxy-2-methoxyethane, brought to second 100% ethanol and left to air dry. In a dark room the slides were dipped into molten emulsion (Hypercoat EMI ^{3}-H from Amersham) 43-45 °C for 5 sec, removed slowly from the vessel with the count of 5 sec and held vertically over tissue paper for 5 sec. The back of the slides were wiped clean and the slides placed into a rack to dry. After 5-10 min when the slides were dry they were placed into a dark box and left at room temperature for 1 h. The box was then stored in a sealed dark bag at 4°C for 3 weeks. Once incubation was complete, the slides were developed in the dark room with D19 solution (Kodak) [1:1 with water] for 10 min. The reaction was stopped by placing the slides in 0.05% acetic acid for 1 min then the slides were fixed with Unifix (Kodak) [1:3 with water] for 10 min. Slides were then removed from the dark room and rinsed in gentle running tap water for 30 min. Sections were counterstained in haematoxylin and eosin . The slides were immersed in Mayer's haematoxylin for 30 sec and blued in lukewarm tap water 15s before being rinsed in dH_2O. Then, the samples were placed in 1% eosin for 30 sec and differentiated in tap H_2O for a few seconds. The sections were then dehydrated in 70% ethanol for 1 min, 96% ethanol for 2 min, rinsed in 100% ethanol then placed in fresh 100% ethanol for 5 min. Finally slides were rinsed in xylene for 30 minutes and mounted with Eukitt. The sections were imaged on the Zeiss microscope and camera (Axioplan Imaging), and processed with Axiocam and Axiovision package.

Qualitative analysis of protein synthesis within cells of tissue sections from explants maintained *ex vivo* in the Zetos loaded culture system, in comparison to positive and negative control tissue explants. The presence radiolabeled proteins would be interpreted as a good sign that the tissue was metabolically active. Similar labelling to

disuse or necrotic tissue would be a sign that the tissue was not being maintained *ex vivo*. Positive labelling of dead tissue would suggest the technique was artefactual and not sensitive to use to detect changes occurring post-harvest. Table 4b.2 summarises the number of cores analysed during these studies, the species used and length of culture.

Harvesting the radiolabelled protein from the media and bone cores

The other half of the radiolabelled samples were digested in 2 ml pepsin (SERVA, 31820) in a 24 well plate at 4°C for 24 h to degrade native collagen molecules from which the cross-links originate (minimized bacterial growth, enhances the solubility of native collagen, ensures the retention of native conformations of the solubilised collagens). The enzyme was added to the solvent in sufficient quantities to achieve a 1:10 ratio between the weight of enzymes and dry weight of the tissue extracted (Miller, 1972). The bone core was resuspended in 2ml of the solvent and again incubated at 4°C with continuous vigorous stirring. The yield of collagen from the second extraction should be markedly diminished. The media and the pepsin solution from the degraded bone cores were used to harvest protein. From either the media or pepsin solution, 1ml was placed into an Eppendorf tube with 1 ml 45% ammonium sulphate $(NH_4)_2SO_4$ and shaken vigorously at 4°C for 24 h. These solutions were then centrifuged at 19720 RCF for 10 min until a pellet formed at the back of the eppendorf tube thus, causing the solution to clarify and separating proteins from suspended tissue extracts. Pepsin is inactivated at neutral pH but persists at a significant contarninant (10%) in the solution. Salt/and or ethanol precipitation is sufficient to remove the pepsin. The supernatant was aspirated away and the pellet resuspended in 1 ml of ethanol. The samples were then centrifuged at 19720 RCF for 10 min until the pellet re-formed, the ethanol was aspirated away and this washing procedure was repeated 3 times. The remaining pellet was left in the opened eppendorf tube under a fume hood to air dry. Once dry the pellets were resuspended in 50 µl SDS-page sample buffer (1x). These were stored at -20°C until used on SDS-page gels.

Detecting the radiolabelled protein in SDS-page gels

To make the SDS-page gel to separate the proteins two different gels were made. The first was a 10% separating gel in 0.375M Tris pH 8.8 composed of the following components: 4.1 ml H_2O, 2.5 ml 1.5 M Tris-HCl pH8.8, 100 µl 10% (w/v) SDS, 3.3ml acrylamide 30%

bisacrylamide 37.5:1, 50 µl ammonium persulfate and 5 µl TEMED. The second was a 4% stacking gel in 0.125M Tris pH 6.8 composed of the following components: - 3.05 ml H_2O, 1.25 ml 0.5 M Tris-HCl pH6.8, 50 µl 10% (w/v) SDS, 0.65 ml Acrylamide 30% Bisacrylamide 37.5:1, 25 µl ammonium persulfate and 5 µl TEMED. The first gel (10% separating) was left to set between two glass slides in gel cassette ¾ from the top. Once set, the second gel (4% stacking gel) was placed above the first set gel where a 10 well comb was placed within to mould the gel. Once set the comb was removed. The gel cassette was removed from the casting frames and placed onto a clamping frame inside a gel tank. The tank and the gel were filled with 1x reservoir buffer. Inside the wells 10µl of the samples were placed and 5 µl of the protein standard (precision plus protein™ standard all blue BIORAD). The lid was placed on the tank and the samples left to run until the protein reached the bottom of the gel, this was conducted at room temperature and with 200V applied. When complete, the gel was removed and placed into a glass container containing enough Coomassie blue to stain the gel. The gel was set on an agitating table at 4°C for 5 min. The Coomassie was removed from the gel by rinsing in Coomassie blue destain (5% v/v methanol and 10% v/v glacial acetic acid) for 2 hours at 4°C with agitation. The gels were then soaked in Amplify™ solution (Amersham Biosciences – NAMP100) for 30 min at 4°C with agitation. The gel was rinsed in water and placed between two sheets of gel air cellophane support and left to dry. Once dried the gel was placed with a film (Hyperfilm™-MP from Amersham Biosciences –RPN6K) in a cassette which was stored at -80°C for 11 days. The film was developed as described in Chapter 2 (2.b.i. Radiology).

Qualitative analysis of protein synthesis within cells of tissue and media from explants maintained *ex vivo* in the Zetos loaded culture system, in comparison to positive and negative control tissue explants. The presence radiolabeled proteins would be interpreted as a good sign that the tissue was metabolically active. Similar labelling to disuse or necrotic tissue would be a sign that the tissue was not being maintained *ex vivo*. Positive labelling of dead tissue would suggest the technique was artefactual and not sensitive to use to detect changes occurring post-harvest. Table 4b.2 summarises the number of cores analysed during these studies, the species used and length of culture.

Western blot analysis

An SDS-page gel was made as described above but with a 7% gel. A PVDF (Polyvinylidene Difluoride) membrane was placed in methanol for a few seconds before being placed in 1x electroblotting buffer that contained 10% methanol, along with two sponges and four squares of filter paper (size of gel). The gel was also placed in some 1x electroblotting buffer that contained 10% methanol for 5 min. A sandwich was created, black arm of holder, sponge, 2 filter papers, gel, PVDF membrane, 2 filter papers, sponge, white edge of holder. The gel-membrane sandwich was placed onto a clamping frame inside a gel tank. The electroblotting buffer was placed over the sandwich and left to run for 30 min at 50V. The blot (PVDF membrane) was rinsed in H_2O, then placed in 100% methanol for a few seconds before being stained in Coomassie Blue R250 for one minute. The blot was destained in 50% methanol to remove the Coomassie. When destained, the blot was rinsed extensively in H_2O and then allowed to air dry. Care was taken not to touch the membrane with fingers to avoid contamination. The desired bands were cut from the membrane and placed in Eppendorf tubes.

Summary of tissue used and the length of culture *ex vivo*.

Table. 4b.2. Summary of experiments conducted

Experiment	Animal Species	Number of limbs	Number of cores	Number of cores in each group*	Number of Days Maintained *ex vivo*.
Immuno-histochemistry	Ovine	2	16	LFr=2, DFr=2, LL=2, DL=2, LU=2, DU=2, LC=2, DC=2,	15 days
Immuno-histochemistry	Bovine	2	14	LFr=1, DFr=1, LL=2, DL=2, LU=2, DU=2, LC=2, DC=2,	23 days
Immuno-histochemistry	Human	1	16	LFr=2, DFr=2, LL=2, DL=2, LU=2, DU=2, LC=2, DC=2,	15 days
Double labelling	Ovine	2	26	LFr=1, DFr=1, LLar=2, DLar=2, LUar=2, DUar=2, LCar=2, DCar=2, LLxo=2, DLxo=2, LUxo=2, DUxo=2,	15 days

				LCxo=2, DCxo=2,	
Double labelling	Bovine	2	14	LFr=1, DFr=1, LLar=2, DLar=2, LUar=2, DUar=2, LCar=2, DCar=2,	23 days
Double labelling	Human	1	18	LFr=2, DFr=2, LL=3, DL=3, LU=2, DU=2, LC=2, DC=2,	15 days
SDS-page	Bovine	1	12	LFr=1, DFr=1, LL7=1, DL7=1, LC7=1, DC7=1,	7 days
SDS-page	Ovine	2	17	LFr=2, DFr=2, LL7=2, DL7=1, LU7=1, DU7=1, LC7=1, DC7=1, LL14=1, DL14=1, LU14=1, DU14=1, LC14=1, DC14=1,	Half samples 7 days, rest 14 days
Autoradiography	Ovine	2	17	LFr=2, DFr=2, LL7=2, DL7=1, LU7=1, DU7=1, LC7=1, DC7=1, LL14=1, DL14=1, LU14=1, DU14=1, LC14=1, DC14=1,	Half samples 7 days, rest 14 days
Autoradiography	Bovine	1	12	LFr=2, DFr=2, LL7=2, DL7=2, LC7=2, DC7=2,	7 days
Autoradiography	Human	1	22	LFr=2, DFr=1, LL7=2, DL7=1, LU7=1, DU7=1, LC7=2, DC7=1, LL14=2, DL14=1, LU14=2, DU14=1, LC14=2, DC14=1,	15 days

* Key to grouping. LFr= Live cores fixed Freshly after harvest procedure, DFr= Dead cores fixed Freshly after harvest procedure, LL = Live cores Loaded in the Zetos culture system, DL = Dead cores Loaded in the Zetos culture system, LU = Live cores Unloaded in the Zetos culture system, DU = Dead cores Unloaded in the Zetos culture system, LC = Live cores cultured in centrifuge tubes, DC = Dead cores cultured in centrifuge tubes, 7 = 7 day culture, 14 = 14 day culture, ar = alizarin red, xo = xylenol orange.

4.C. Results

4.c.i. Immunohistochemical localisation of bone marker proteins.

Immunolabelling was used to detect what are regarded as bone marker proteins, osteocalcin, osteopontin, osteonectin, bone sialoprotein, and type I procollagen. Of these osteocalcin and BSPII are the most specific to bone cells, the others though present are common in many other tissues. Immunogold conjugated antibodies were used for labelling followed by silver enhancement. Each antibody was used on sequential sections including negative controls that omitted the use of the primary antibody. Positive labelling of tissue was easily distinguishable from the controls. Fluorescent images of the same sections were also made in order to give a more defined image of the tissue, which is not as clear in the immunolabelled section as the slides were not counterstained.

Serial sections from a bovine bone explant cultured and loaded in the Zetos system for 23 days were used for labelling (Fig.4c.1). Bone morphology can be seen in figure 4c.1ii and iii demonstrating the tissue was in a state of modelling rather than remodelling. The tissue was developing through endochondral ossification, apposing new bone onto a cartilaginous scaffold. The non-collagenous protein, osteocalcin, did not have a strong signal (4c.1v). The protein may not have been expressed in high enough concentrations to be detected. Osteonectin was present in a wide range of cells including bone cells and fibroblast-like cells, but not reversal lines or cement lines (Fig.4c.1vi). It is hypothesised that osteonectin, as well as osteocalcin, are involved in controlling the growth and size of hydroxyapatite crystals as they are present in fully calcified matrix, but sparsely seen in osteoid seems, and have high affinities for hydroxyapatite. Osteopontin is believed to be responsible for cell attachment as it contains the integrin binding motif RGD (Arg-Gly-Asp). Antibodies located this protein in soft tissue, specifically osteoblasts and osteoclasts, as well as in the ECM (Fig.4c.1vii). It had a similar expression as BSPII, which also contains an RGD motif and shares a lot of other features with osteopontin. It was also found present in soft tissue as well as in the ECM (Fig.4c.1viii). Unlike osteopontin, BSPII was not observed in osteoclasts. Osteopontin was clearly seen in reversal lines within the bone matrix along with BSPII, concurring with the results of Roach (1994). Type I procollagen the most abundant protein constituent of bone (90%) was present in active osteoblasts and in some fibrous-like cells at the core surface (Fig.4c.1ix) Similar results

were obtained for bovine tissue cultured in the Zetos system without dynamic loading (static load for 30 s every 4 days), and for explants cultured submerged in static media, all of which were comparable to fresh fixed tissue.

Ovine tissue was not as successful as bovine and human tissue (6-year-old ewe, 15 days culture). Due to the lack of active osteoblasts no positive labelling of osteocalcin, osteopontin, BSPII or procollagen type I was observed (Fig.4c.2i-v, vii-ix). This was also true of fresh fixed control tissue. However, positive labelling of osteocalcin and procollagen type I was observed in other ovine tissue, but the antibodies for osteopontin, and BSPII were shown to be non-reactive (Yang *et al.*, 2003). Osteonectin was observed throughout the tissue (Fig.4c.2vi), including explants cultured in the Zetos system without dynamic load, and for explants cultured submerged in static media.

Human tissue (70-year-old, cultured for 15 days) also had a limited amount of active osteoblasts (Fig.4c.3i-iii) and, therefore, did not show positive labelling for osteocalcin and procollagen type I (Fig.4c.3v and ix). Human tissue demonstrated a weaker labelling for osteonectin than ovine and bovine tissue (Fig.4c.3vi). Unlike the ovine tissue, the human tissue demonstrated high antigenicity to the osteopontin and BSPII antibodies (Fig.4c.3vii and viii). The strongest signal was localised at the periphery of the tissue that had been damaged from the harvest procedure thus, suggesting that these proteins were exposed from the mineralised matrix during fracturing. These proteins were also observed in reversal lines and cement lines, as well as active osteoblasts. It was interesting to note that osteopontin and BSPII were shown to be of a greater concentration within surfaces undergoing resorption (green arrow) than within osteoid seams (red arrows) (Fig.4c.4). Again, similar results were observed for unloaded explants and explants cultured in centrifuge tubes.

On their own these results do not confirm fully if these proteins were created in the culture system or not, but do show that, apart from the cells at the periphery, the bone cells have not changed their phenotype at least in qualitative terms. This technique will be of use to analyse future work with bone biomaterial interfaces.

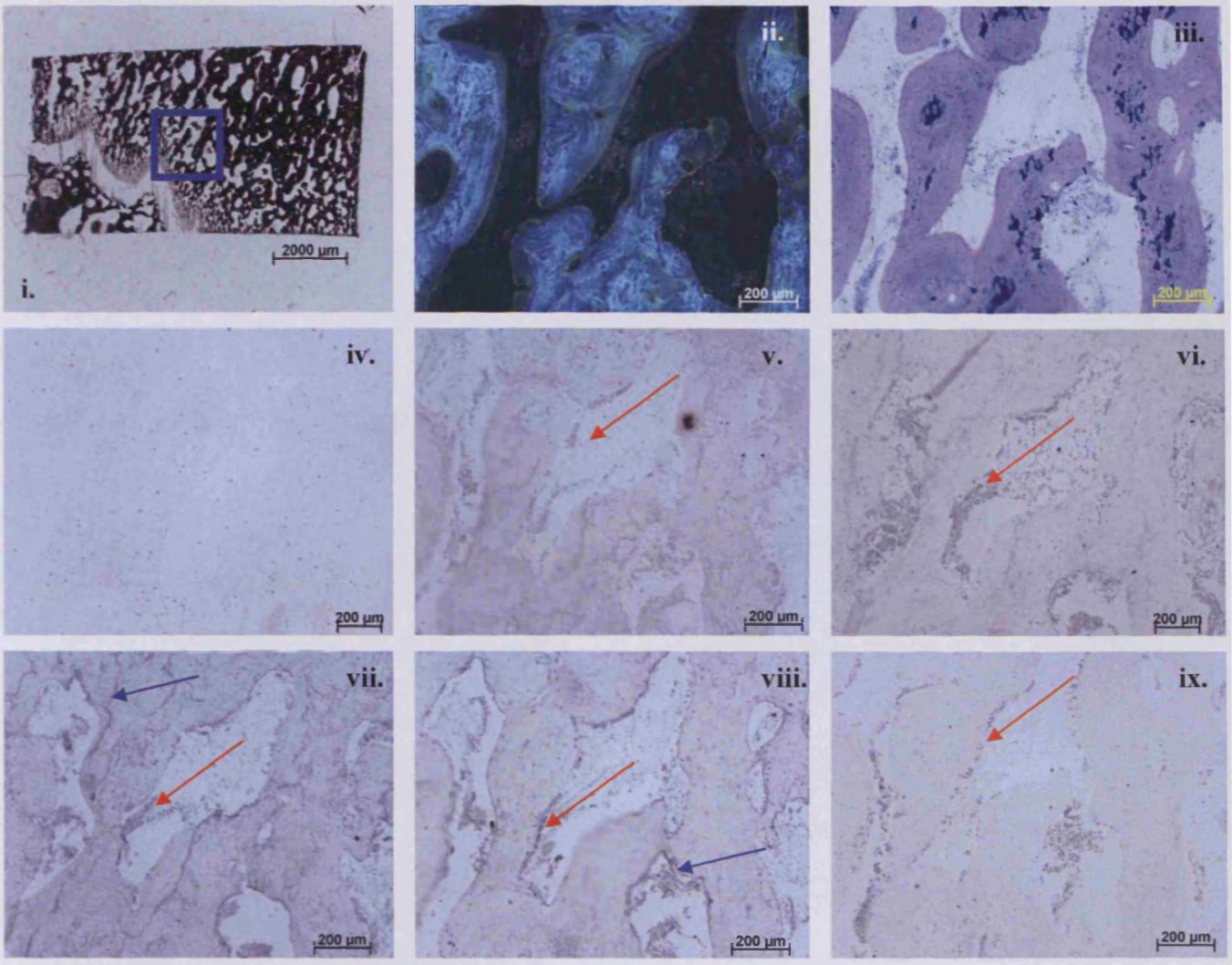

Figure 4c.1. *Bovine bone tissue from a 4 month old calf cultured in the Zetos system for 23 days.* **i)** *Overview of core cross-sections. Images were located from within the blue square. Serial sections were stained as follows:* **ii)** *Calcein green and alizarin red, that was incorporated into the tissue during culture ex vivo. Calcified tissue is in blue, labelling with calcein green is green, and bone marrow is a grey within a black background.* **iii)** *Giemsa, calcified tissue is pink, calcified cartilage is dark blue, and the cells are pale blue. Groups of serial sections were immunolabelled, with every second section used as an immunolabelling control without primary antibody. Only one control example is shown* **iv).** *The immunolabelling was as follows* **v)** *osteocalcin (10µg/ml polyclonal goat anti-rabbit),* **vi)** *osteonectin (8µg/ml monoclonal mouse anti-bovine),* **vii)** *osteopontin (10µg/ml polyclonal goat anti-rabbit),* **viii)** *bone sialoprotein (10µg/ml polyclonal rabbit anti-human),* **ix)** *procollagen type I (7µg/ml monoclonal goat anti-rabbit). Red arrows depict positive labelling within cells, while blue arrows depict positive labelling within the calcified matrix. [Characteristic image from one of twenty sections (each stained for different proteins) obtained from the centre of the core, providing a representation from a group n=2][Characteristic image from one of twenty sections (each stained for different proteins) obtained from the surface of the core, providing a representation from a group n=2]*

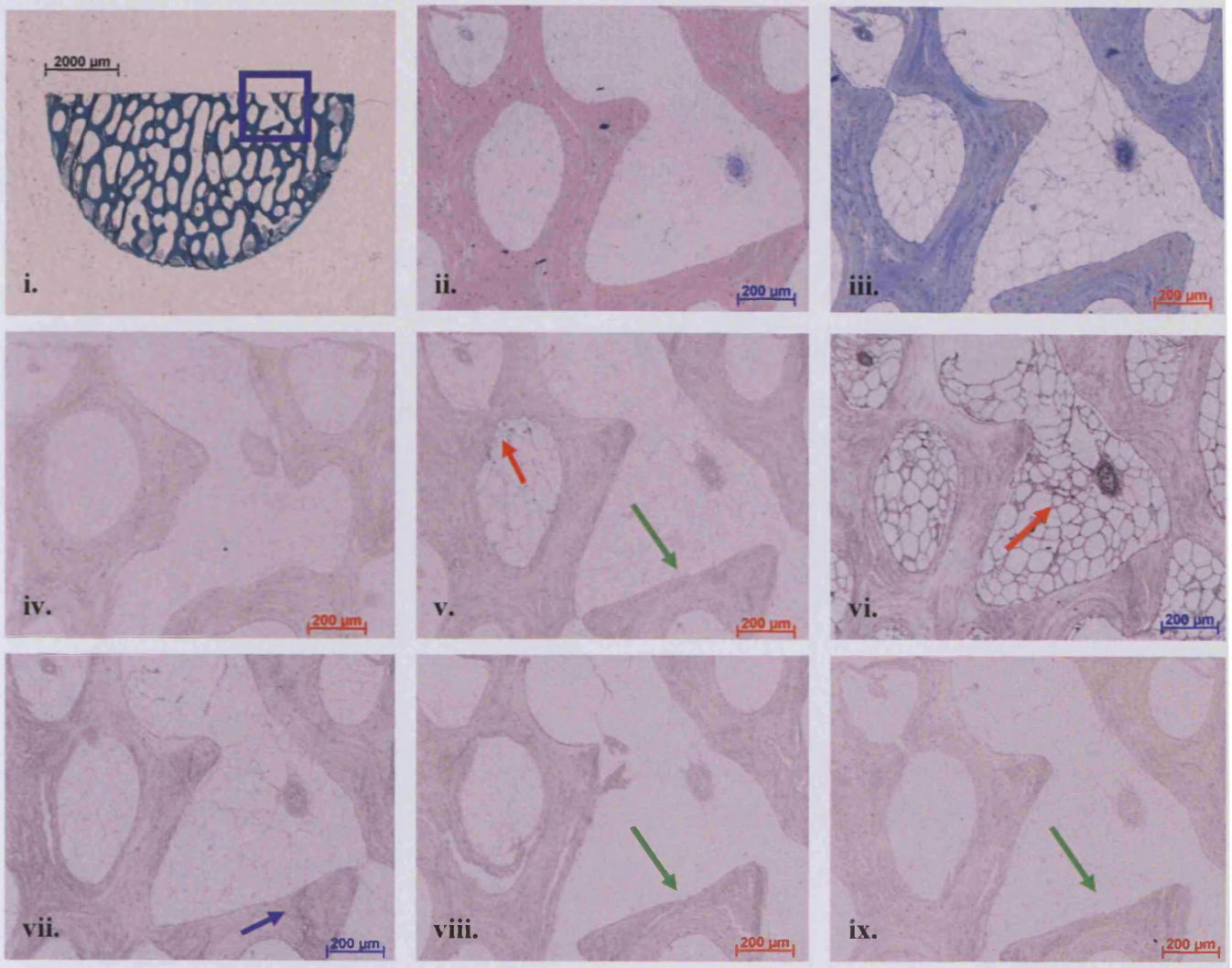

Figure 4c.2. *Ovine bone tissue from a 6 year old ewe cultured in the Zetos system for 15 days.* **i)** *Overview of core cross-sections. Images were located from within the blue square. Serial sections were stained as follows:* **ii)** *Giemsa, calcified tissue is pink and the cells are pale blue.* **iii)** *Toluidine blue, calcified tissue is dark blue and the cells are pale blue. Groups of serial sections were immunolabelled, with every second section used as an immunolabelling control without primary antibody. Only one control example is shown* **iv).** *The immunolabelling was as follows* **v)** *osteocalcin (10µg/ml polyclonal goat anti-rabbit),* **vi)** *osteonectin (8µg/ml monoclonal mouse anti-bovine),* **vii)** *osteopontin (10µg/ml polyclonal goat anti-rabbit),* **viii)** *bone sialoprotein (10µg/ml polyclonal rabbit anti-human),* **ix)** *procollagen type I (7µg/ml monoclonal goat anti-rabbit). Red arrows depict positive labelling within cells, while blue arrows depict positive labelling within the calcified matrix. Green arrows depict a lack of labelling. [Characteristic image from one of twenty sections (each stained for different proteins) obtained from the centre of the core, providing a representation from a group n=2]. [Characteristic image from one of twenty sections (each stained for different proteins) obtained from the surface of the core, providing a representation from a group n=2]*

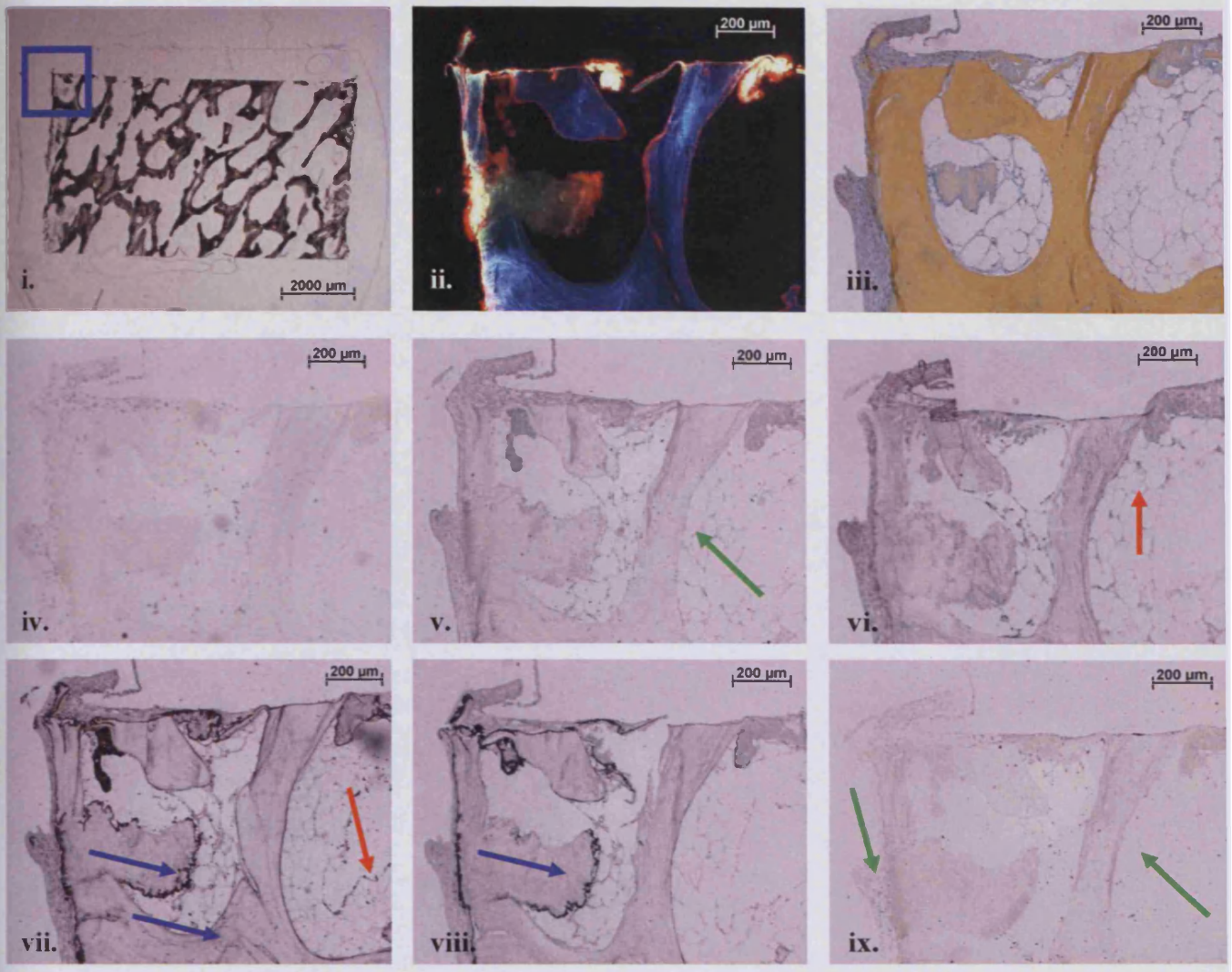

Figure 4c.3. *Human bone tissue from a 70 year old male, cultured in the Zetos system for 15 days.* **i)** *Overview of core cross-sections. Images were located from within the blue square. Serial sections were stained as follows:* **ii)** *Calcein green and alizarin red, that was incorporated into the tissue during culture ex vivo. Calcified tissue is in blue, labelling with calcein green and alizarin red is green and red respectively, and bone marrow is a grey within a black background.* ***iii)*** *Movat pentachrome, calcified tissue is yellow and the cells are pale blue . Groups of serial sections were immunolabelled, with every second section used as an immunolabelling control without primary antibody. Only one control example is shown* **iv)**. *The immunolabelling was as follows* **v)** *osteocalcin (10µg/ml polyclonal goat anti-rabbit),* **vi)** *osteonectin (8µg/ml monoclonal mouse anti-bovine),* **vii)** *osteopontin (10µg/ml polyclonal goat anti-rabbit),* **viii)** *bone sialoprotein (10µg/ml polyclonal rabbit anti-human),* **ix)** *procollagen type I (7µg/ml monoclonal goat anti-rabbit). Red arrows depict positive labelling within cells, while blue arrows depict positive labelling within the calcified matrix. Green arrows depict a lack of labelling.*
[Characteristic image from one of twenty sections (each stained for different proteins) obtained from the centre of the core, providing a representation from a group n=2]
[Characteristic image from one of twenty sections (each stained for different proteins) obtained from the surface of the core, providing a representation from a group n=2]

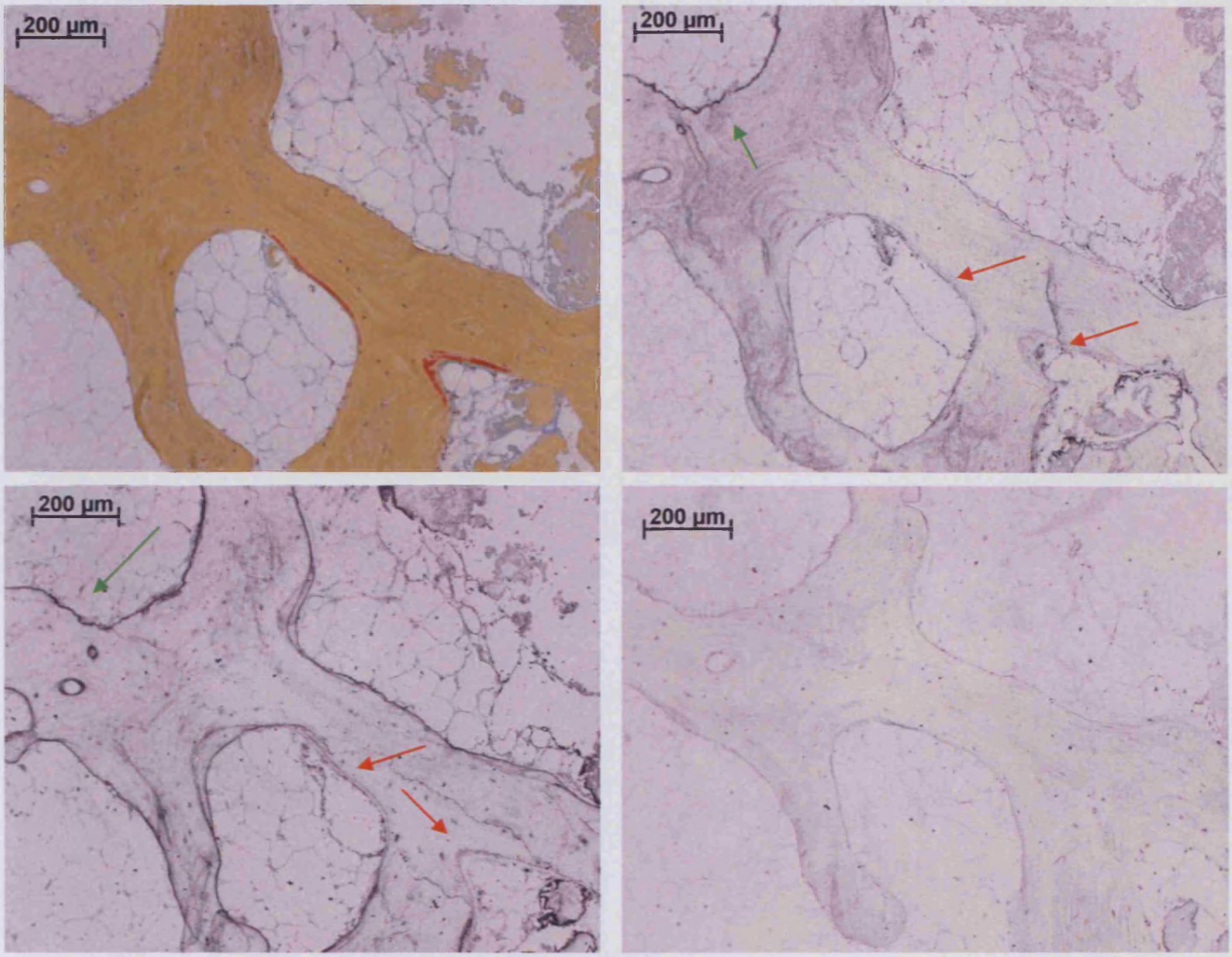

Figure 4c.4. *Human bone tissue from a 70 year old male, cultured in the Zetos system for 15 days.* **i)** *Movat stained section depicting osteoid seams in red and calcified tissue in yellow.* **ii)** *Bone sialoprotein labelled section (10µg/ml polyclonal rabbit anti-human). Surface undergoing resorption - green arrow, osteoid seam - red arrows.* ***iii)*** *Osteopontin stained section (10µg/ml polyclonal goat anti-rabbit). Surface undergoing resorption - green arrow, osteoid seam - red arrows.* **iv).** *Negative control – omission of primary antibody. [Characteristic image from one of twenty sections (each stained for different proteins) obtained from the centre of the core, providing a representation from a group n=2][Characteristic image from one of twenty sections (each stained for different proteins) obtained from the surface of the core, providing a representation from a group n=2]*

4.c.ii. Double fluorescent labelling of explants to measure bone apposition

One of the earliest observations made, during fluorescent labelling of the tissue, was the lack of staining of Zetos cultured explants. Figure 4c.5i compares the binding of the fluorescent stain alizarin, to an explant bathed in the solution for 8 hours (A) to a Zetos cultured explant circumfused with the solution for 8 hours (B). The black arrows depict the unstained areas which are at the under surface and at the sides. The yellow arrow represents the area of tissue that was directly adjacent to the area of the red arrow of Figure 4c.5ii. It is, therefore, clear that the base plate and the area adjacent to the inflow of media hamper the staining of the tissue, by possibly creating a barrier to the solution and stopping the tissue from being bathed. The unfortunate consequence of this may be the lack of nutrients being diffused from the surrounding media into the explant as well as waste products being removed.

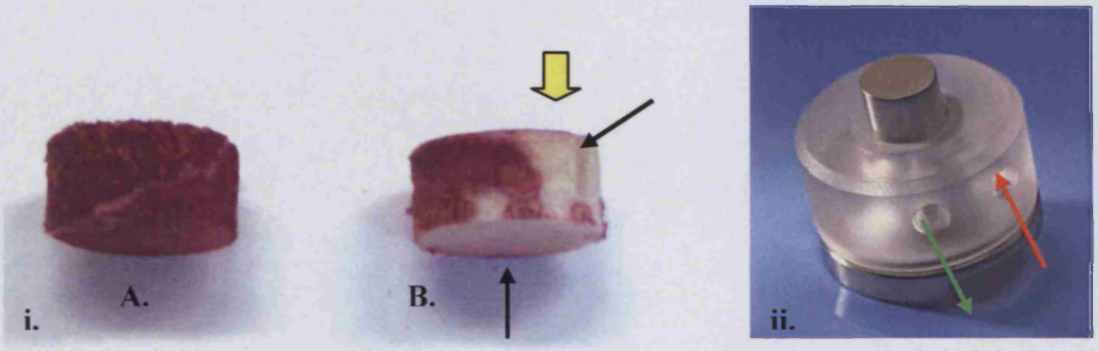

Figure 4c.5. i)*Bovine bone cores (4 month of age) stained with the fluorescent labels calcein and alizarin. Both were incubated within the stain solution for 8 hours. Explant cultured bathed in static culture of the centrifuge tube (A) was completely stained. Explant cultured within the Zetos culture chambers (B) had areas that were unstained (black arrows). The yellow arrow corresponds to the area adjacent to the red arrow in figure ii.* **ii)** *Assembled culture chamber, red arrow represents the in flow, while the green arrow represents the out flow of media.*

Analysis of embedded tissue presented unexpected results. One of the most prominent findings was that the staining pattern varied depending upon the orientation of the tissue being examined. Each core was cut and embedded to provide a cross-sectional image and a transverse-sectional image. Due to the observed difference in staining, each image's location was recorded from the area of tissue in question.

Ovine tissue

Figure 4c.6 depicts images from a cross-section through ovine tissue (6-years-old, 55 kg weight) stained with calcein green and xylenol orange for 8 hours on day 1 and 11 respectively. Several areas within the tissue appeared to have the presence of double labels (Fig.4c.6), indicating bone apposition took place during the culture period. However, the location of these labels indicated that they were in fact artefactual. Each label was at the outer perimeter of the explant where no cells would have been present. These areas were cut and drilled, which would have exposed free calcium for the fluorophores to bind. Another possibility may be that calcium phosphate in the supersaturated media may be depositing onto the outer surface of the explants causing the labels to be bound to the tissue and also give the impression of bone growth.

Another noticeable feature was the lack of penetration of these stains into the cancellous tissue. No visible fluorophore was present in Fig.4c.6v approximately 100 μm from the outer surface. The same was true for the centre of the core (Fig.4c.6iv). In fact, no fluorophores were observed apart from at the outer periphery.

A cross-section through ovine tissue (6-years-old, 55 kg weight) demonstrated that the alizarin fluorophore penetrated the tissue further than the xylenol orange did (Fig.4c.7ii-iii and v-vi) (stained with calcein and alizarin for 8 hours on day 1 and 11 respectively.). However, the penetration was not into the centre of the tissue, just the outer regions. Most of the centre was still unstained (Fig. 4c.7iv). It was also noted that all the bone debris, which surrounded the outer regions of the tissue, had absorbed a lot of the stains (Fig.4c.7ii-iii and v-vi). Both explants were of similar bone density. No positive double labels were observed for either staining conditions.

An identical pattern of staining was observed for Zetos cultured unloaded samples, and submerged static bathed explants cultured in centrifuge tubes. Surprisingly dead (heat treated) cores also stained in the same manner, results shown for human tissue (Fig.4c.14vi) and discussed later. Transverse-sectional sections were over stained with nearly all trabecular surfaces stained with alizarin (not with xylenol orange), results shown for human tissue (Fig.4c.11) and discussed later.

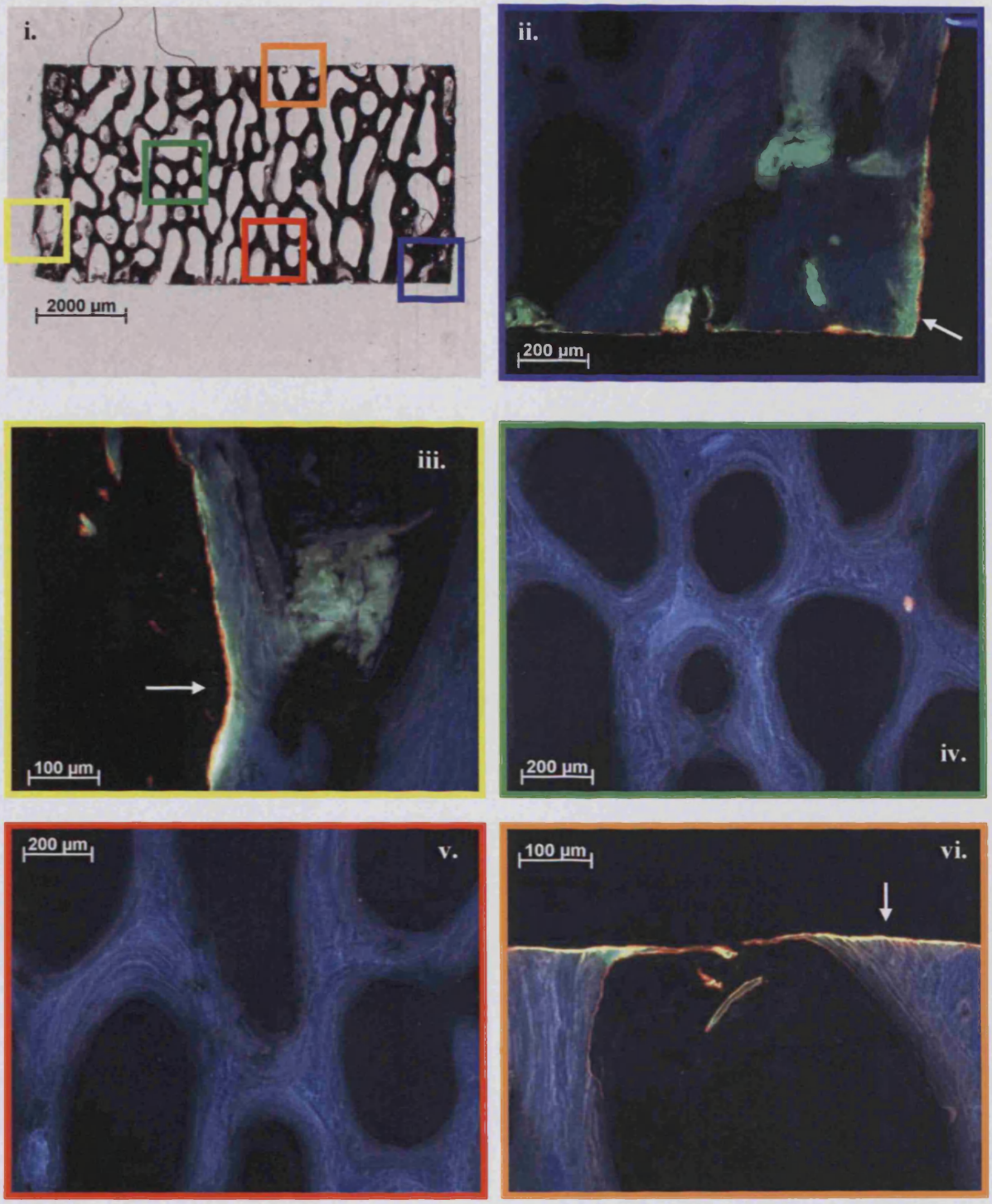

Figure 4c.6. *Cross-section through ovine tissue (6-years-old, 55 kg weight) stained with calcein (green) and xylenol orange for 8 hours on day 1 and 11 respectively. White arrows depict artefactual double label of tissue. Coloured boxes represent image location within the explant. [Characteristic image from one of twenty sections obtained from the centre of the core, providing a representation from a group n=2]*

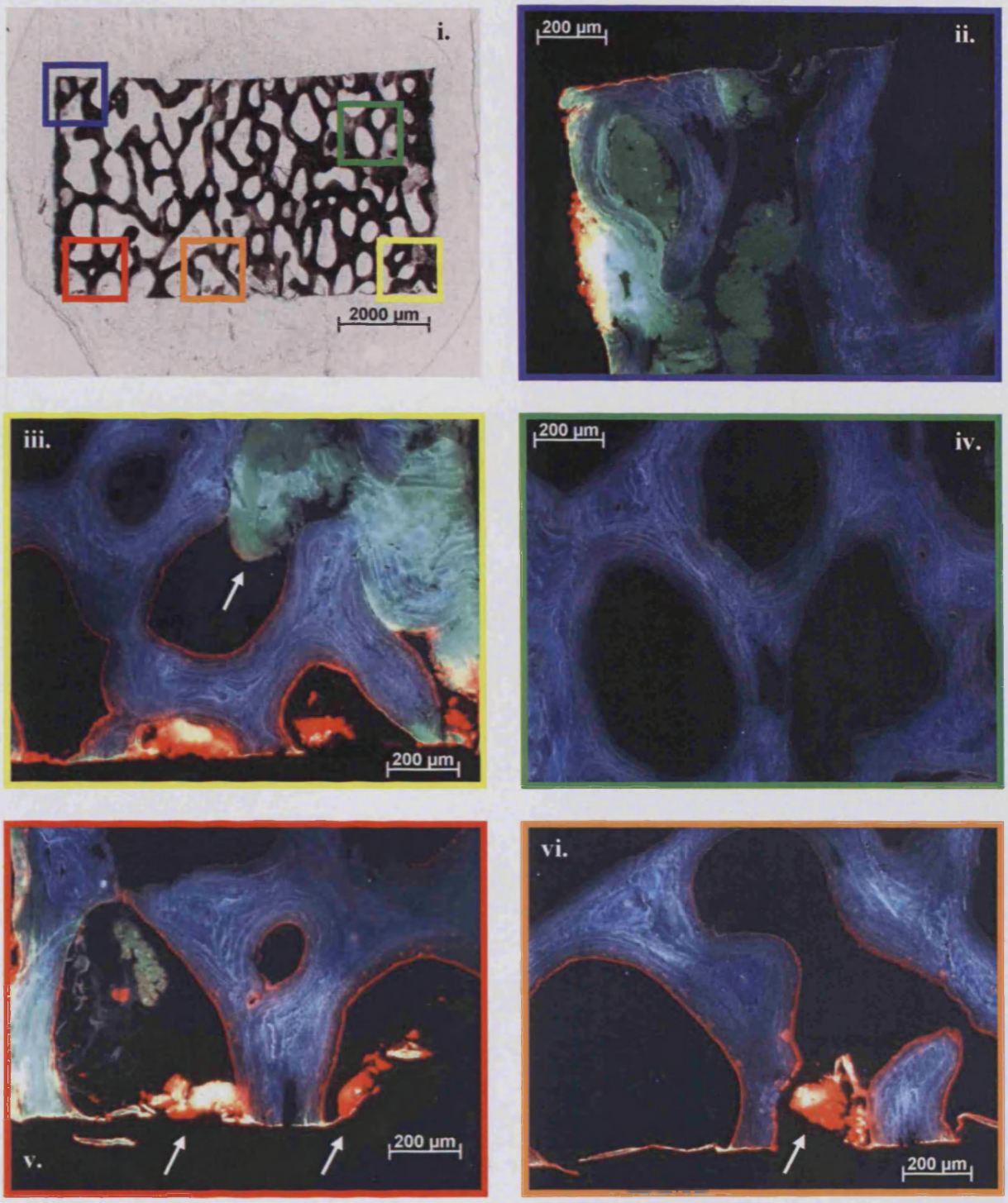

Figure 4c.7. *Cross-section through ovine tissue (6-years-old, 55 kg weight) stained with calcein (green) and alizarin (red) for 8 hours on day 1 and 11 respectively. White arrows depict stained bone debris. Coloured boxes represent image location within the explant. [Characteristic image from one of twenty sections obtained from the centre of the core, providing a representation from a group n=2]*

Bovine tissue

Unlike the ovine and human explant, the fluorophore staining of the immature bovine tissue (4-months-old, cultured for 20 days loaded in the Zetos culture system) resulted in stain uptake through the majority of the extracellular matrix (Fig.4c.8ii-iv) (stained with calcein green and xylenol orange for 8 hours on day 5 and 15 respectively). Though osteoid and cells can be seen in the images, it is difficult to ascertain whether these cells were functional and viable during harvest due to the lack of double staining. Double xylenol orange staining could be seen at certain points (white arrows) which could have lead to erroneous assumptions of bone apposition during culture, if xylenol orange had been used twice, instead of the calcein (Fig.4c.8ii-iv). For this reason, to avoid inaccuracies, it is always best to use two different fluorophores. Deeper penetration into the tissue, than that seen with ovine and human samples, probably resulted from the fact that the tissue was less calcified providing a less of a barrier for diffusion of solutes.

During a different study bovine explants (4-months-old, cultured for 23 days loaded in the Zetos culture system) demonstrated staining with only the calcein label with no alizarin present (Fig.4c.9ii-iii) (stained with calcein green and alizarin red for 8 hours on day 5 and 15 respectively). The density of this explant was much lower than previous and may explain why the calcein molecules penetrated further into the core, but does not explain the lack of alizarin labelling. Figure 4c.9iv depicts images from a cross-section through bovine tissue from the same study but from a different location within the metacarpal. This explant was close to the growth plate. The bone in this section was mainly woven in nature, thus, took up much of the dye into the matrix. The alizarin bound to the outer surfaces of the trabeculae, but this was unclear if it was due to bone apposition or to artefactual staining (Fig.4c.9v-vi).

A similar pattern of staining was also seen for Zetos cultured unloaded samples, and static bathed explants cultured in centrifuge tubes as well as dead tissue, correlating with the results obtained for both ovine and human tissue. No double labelling of bone apposition was observed in any culture condition situation.

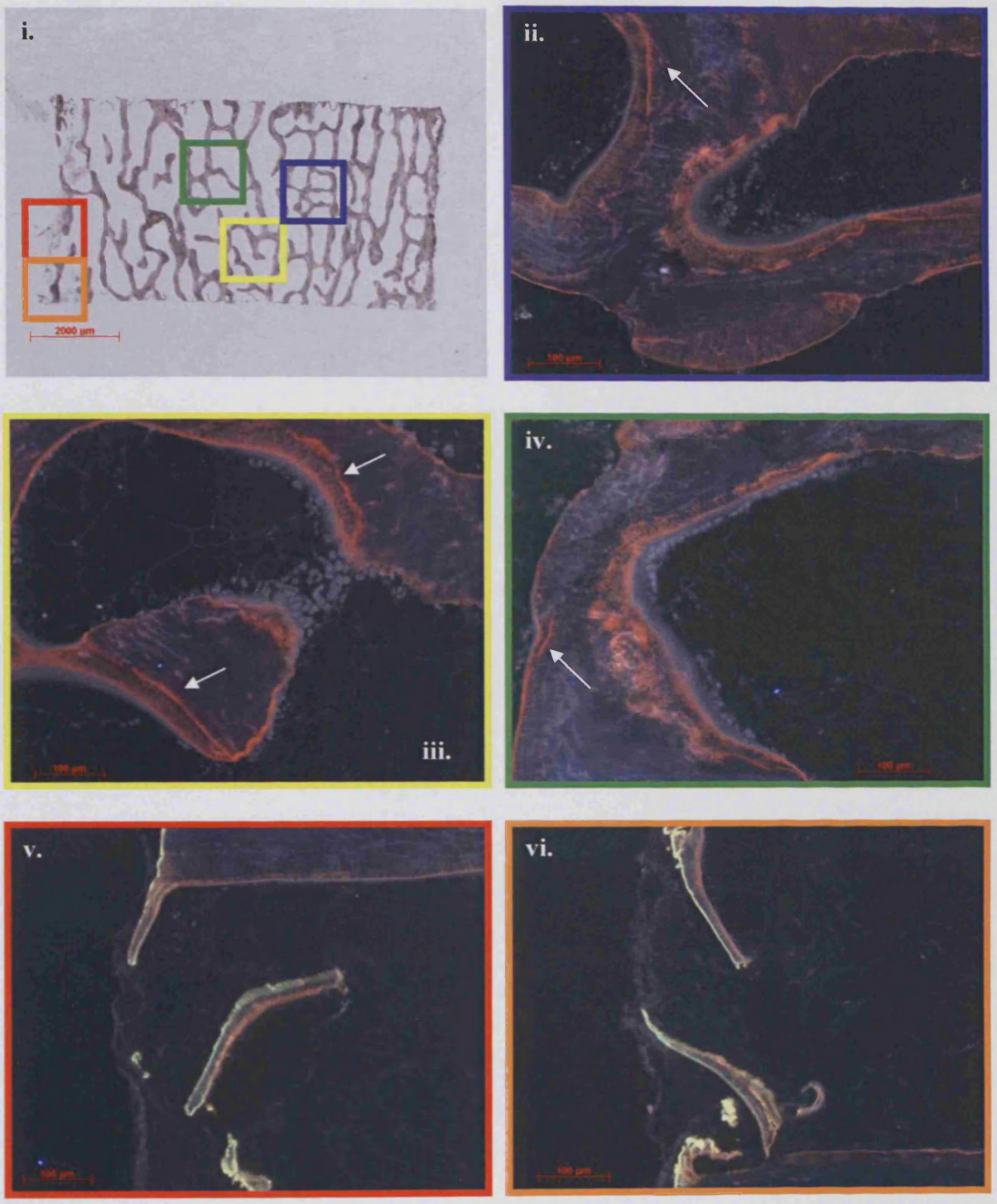

Figure 4c.8. *Cross-section through bovine tissue (4-months-old, cultured for 20 days loaded in the Zetos culture system) stained with calcein (green) and xylenol orange for 8 hours on day 5 and 15 respectively. White arrows depict artefactual double alizarin labelling. Coloured boxes represents image location within the explant. [Characteristic image from one of twenty sections obtained from the centre of the core, providing a representation from a group n=2]*

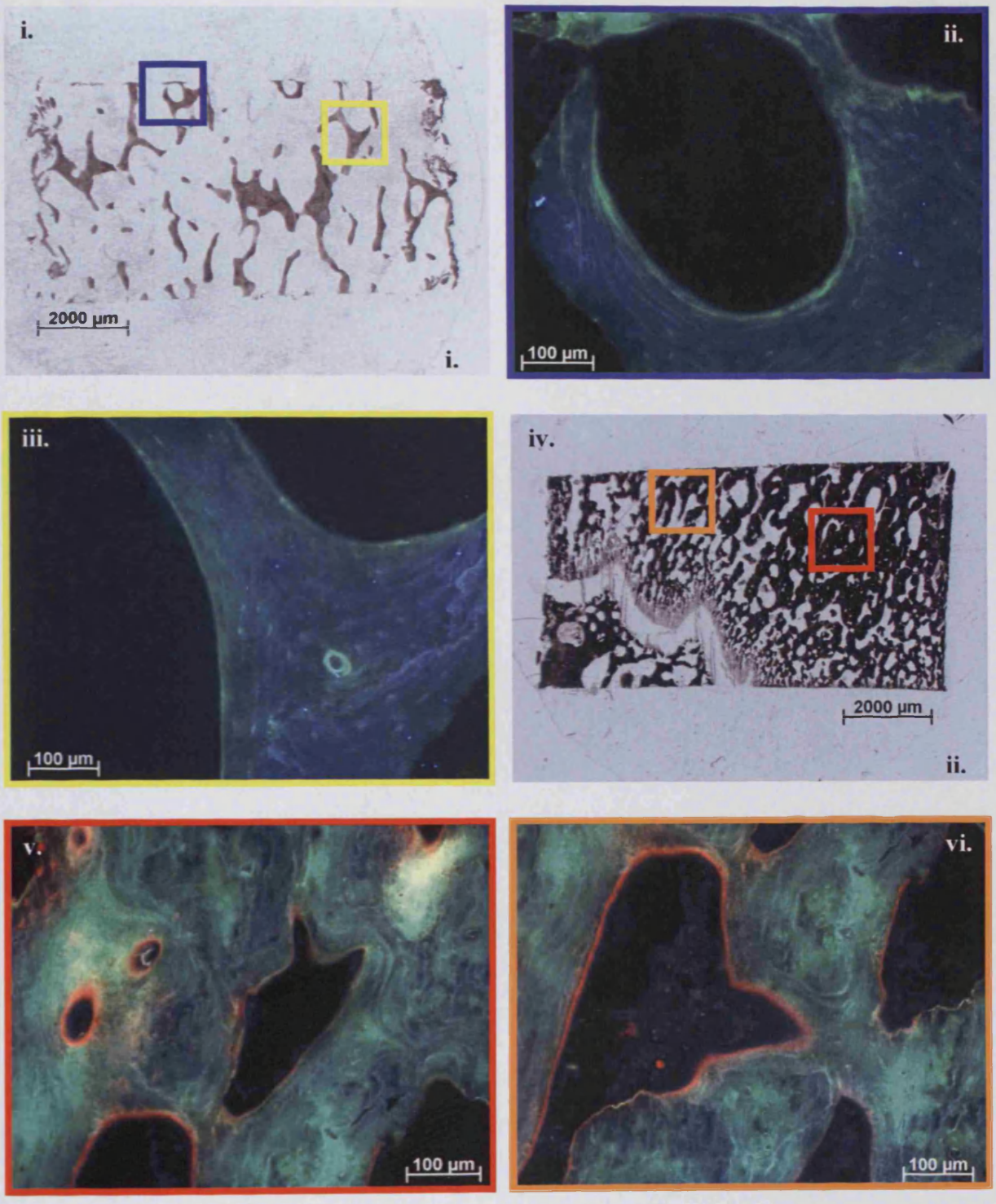

Figure 4c.9. i) *Cross-section through bovine tissue (4-months-old, cultured for 23 days loaded in the Zetos culture system) stained with calcein (green) and alizarin (red) for 8 hours on day 3 and 18 respectively. Coloured boxes represent image location within the explant.* **ii)** *Cross-section through bovine tissue (4-months-old, cultured for 23 days loaded in the Zetos culture system) stained with calcein (green) and alizarin (red) for 8 hours on day 3 and 18 respectively. Coloured boxes represent image location within the explant. [Characteristic image from one of twenty sections obtained from the centre of the core, providing a representation from a group n=2]*

Human tissue

Limited penetration of the fluorophores was observed with human tissue (70-years-old, cultured for 15 days loaded in the Zetos culture system) as was seen for ovine tissue (Fig.4c.10iii-v) (stained with calcein green and alizarin red for 8 hours on day 1 and 11 respectively) Though, labelling was seen at the outer periphery (Fig.4c.10ii and vi). One factor that was noted during the analysis of human tissue was the presence of tetracycline incorporated into the bone matrix (Fig.4c.10ii and vi). This is important to bear in mind during double labelling of bone growth to avoid any misinterpretations of the results.

Surface images taken from the transverse-sections of loaded tissue highlighted the over staining of the surface trabeculae with alizarin (Fig.4c.11). A number of double labels were also noted (Fig.4c.11ii-iv). These corresponded to areas of osteoid in morphological staining. A double label was also observed in other cores (Fig.4c.12ii). A single calcein label and a number of alizarin labels were also observed in that explant, as well as the staining of bone debris (Fig.4c.12iii-vi).

A couple of double labels were also observed in explants cultured bathed within static media, four surfaces double labelled with calcein and alizarin and their corresponding histological images depicting the calcified tissue and osteoid seams (Fig.4c.13).

A double label within a cross-section of a Zetos cultured loaded tissue was observed (Fig.4c.14ii). It is clear that tissue at the surfaces of the explants were still active and viable. It was difficult to ascertain the status of the tissue within the centre of the core, due to the lack of stain penetration.

Artefactual staining of dead tissue and bone debris was observed (Fig.4c.14vi). The precipitation of calcium phosphate onto the periphery of the cores may account for the fact that the dead tissue increases in stiffness over the culture period as does the loaded living samples (see Chapter 2).

This experiment highlights the need to depict image location within a sample when talking about double label results obtained with loaded bone explants cultured within the Zetos system.

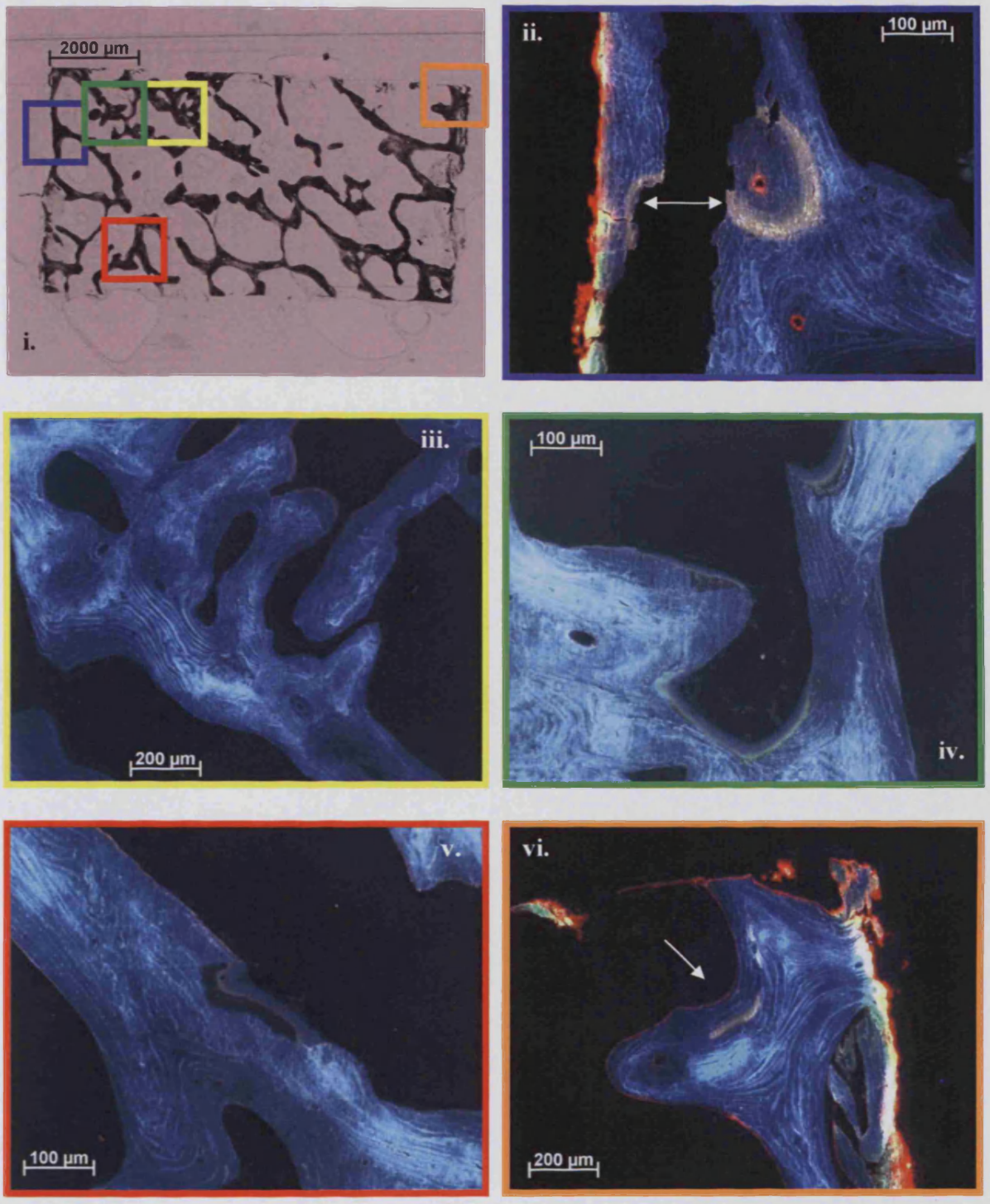

Figure 4c.10. *Cross-section through human tissue (70-years-old, cultured for 15 days loaded in the Zetos culture system) stained with calcein (green) and alizarin (red) for 8 hours on day 1 and 11 respectively. White arrows depict double tetracycline labelling of the tissue due to previous medication administered to the patient. Coloured boxes represent image location within the explant. [Characteristic image from one of twenty sections obtained from the centre of the core, providing a representation from a group n=2]*

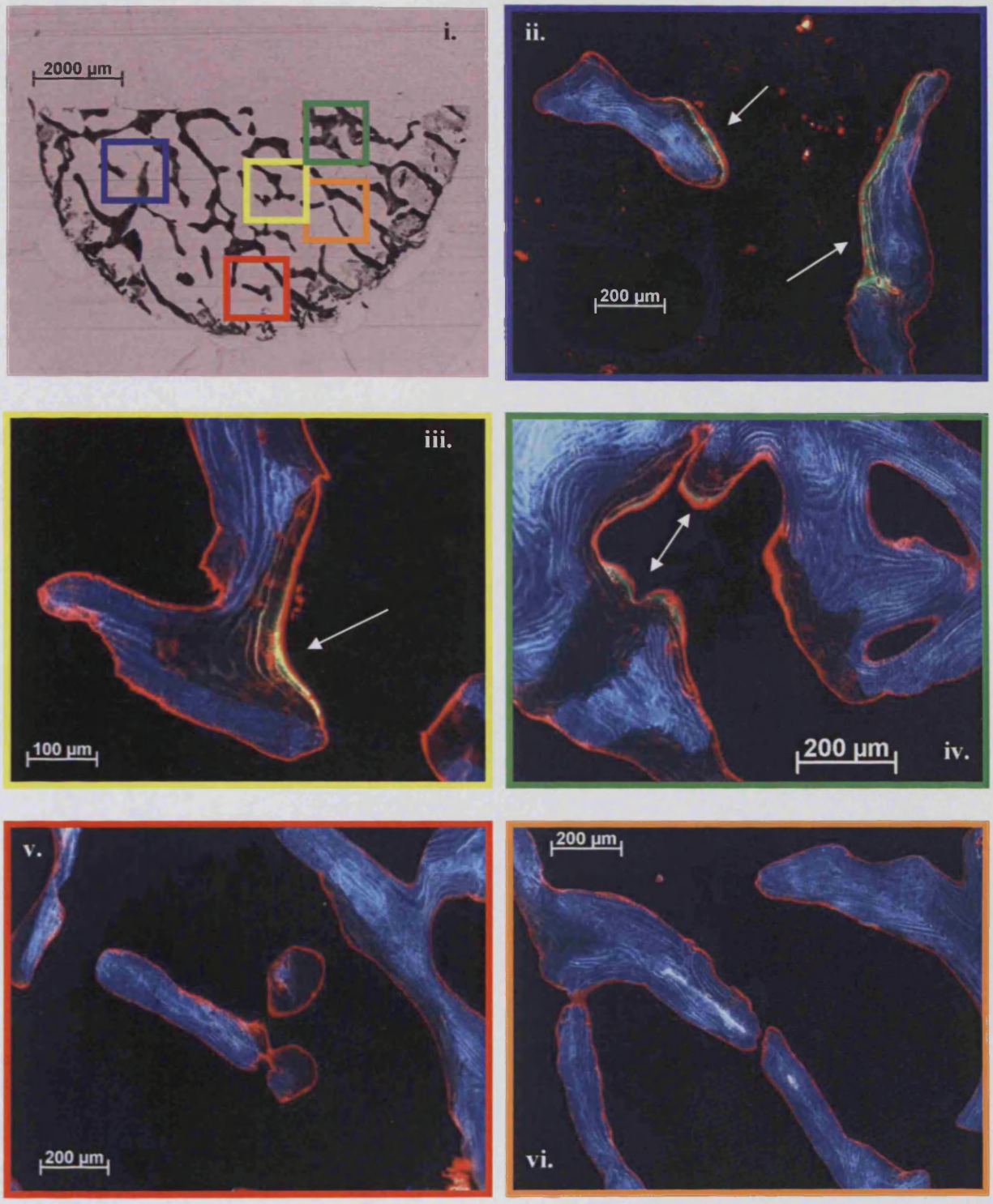

Figure 4c.11. *Transverse-section through human tissue (70-years-old, cultured for 15 days loaded in the Zetos culture system) stained with calcein (green) and alizarin (red) for 8 hours on day 1 and 11 respectively. White arrows depict double labelling. Coloured boxes represent image location within the explant. [Characteristic image from one of twenty sections obtained from the surface of the core, providing a representation from a group n=2]*

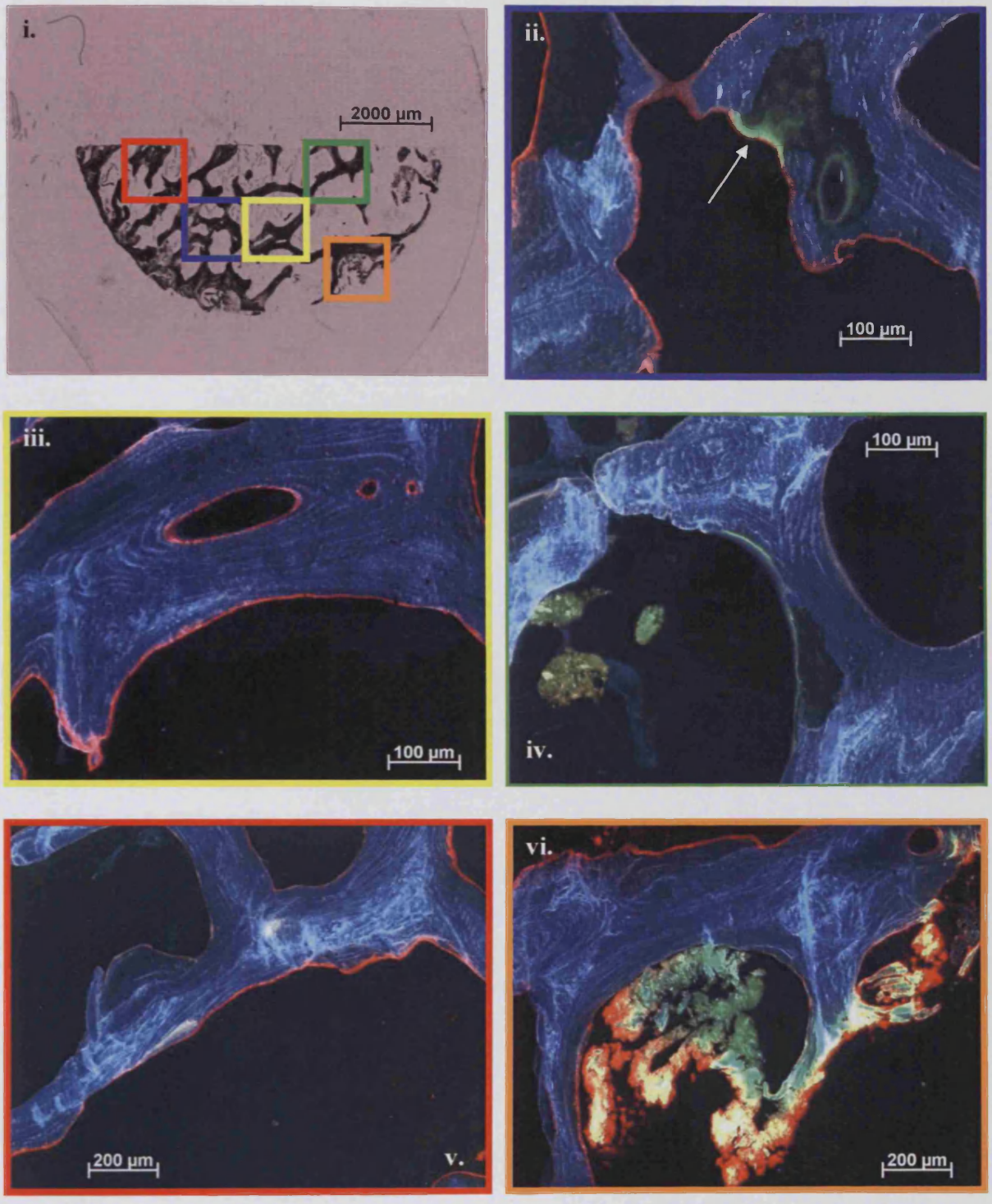

Figure 4c.12. *Transverse-section through human tissue (70-years-old, cultured for 15 days loaded in the Zetos culture system) stained with calcein (green) and alizarin (red) for 8 hours on day 1 and 11 respectively. White arrow depicts double labelling. Coloured boxes represent image location within the explant. [Characteristic image from one of twenty sections obtained from the surface of the core, providing a representation from a group n=2]*

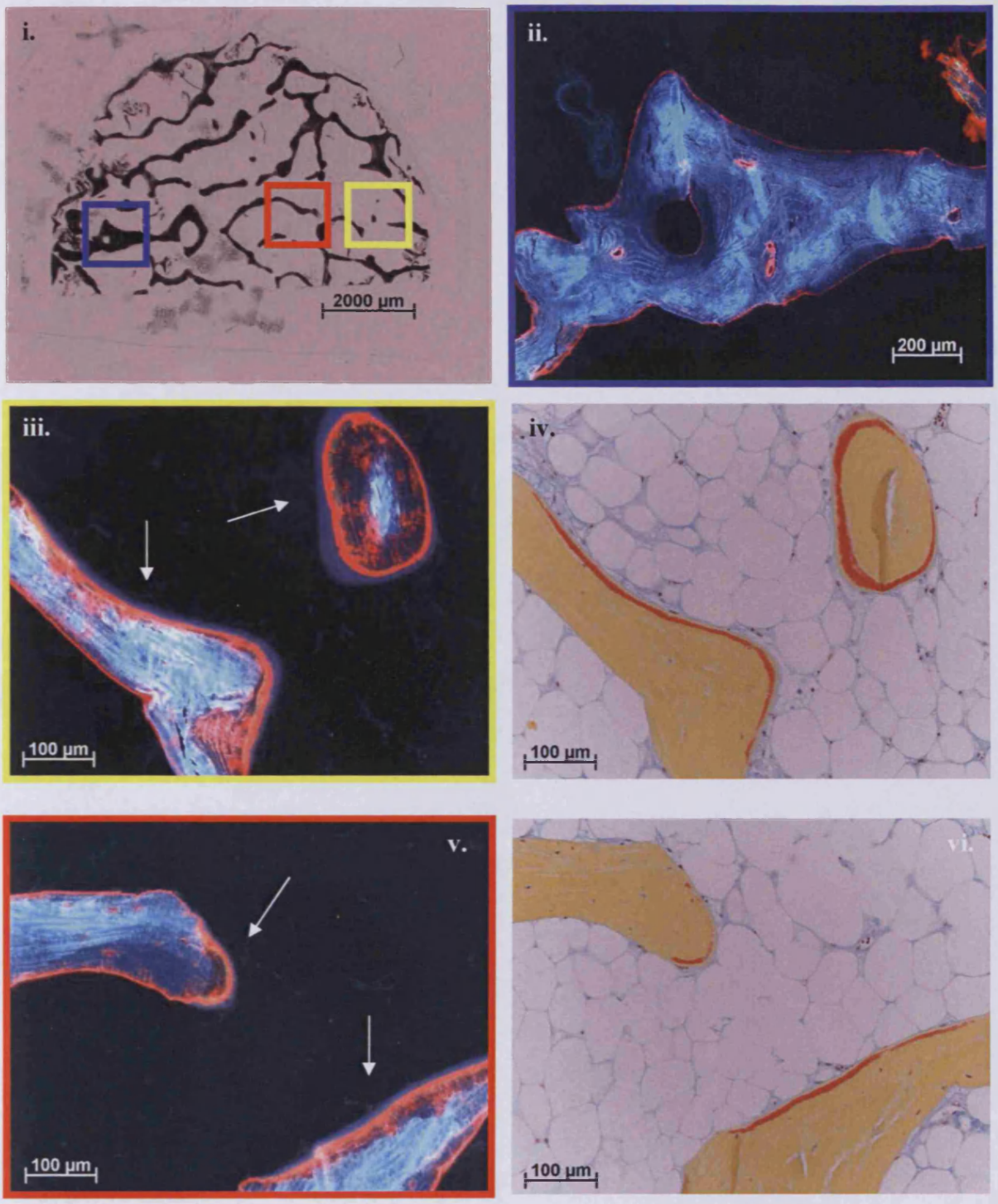

Figure 4c.13. *Transverse-section through human tissue (70-years-old, cultured for 15 days submerged static culture in centrifuge tubes) stained with calcein (green) and alizarin (red) for 8 hours on day 1 and 11 respectively. White arrows depict double labelling. Coloured boxes represent image location within the explant. [Characteristic image from one of twenty sections obtained from the surface of the core, providing a representation from a group n=2]*

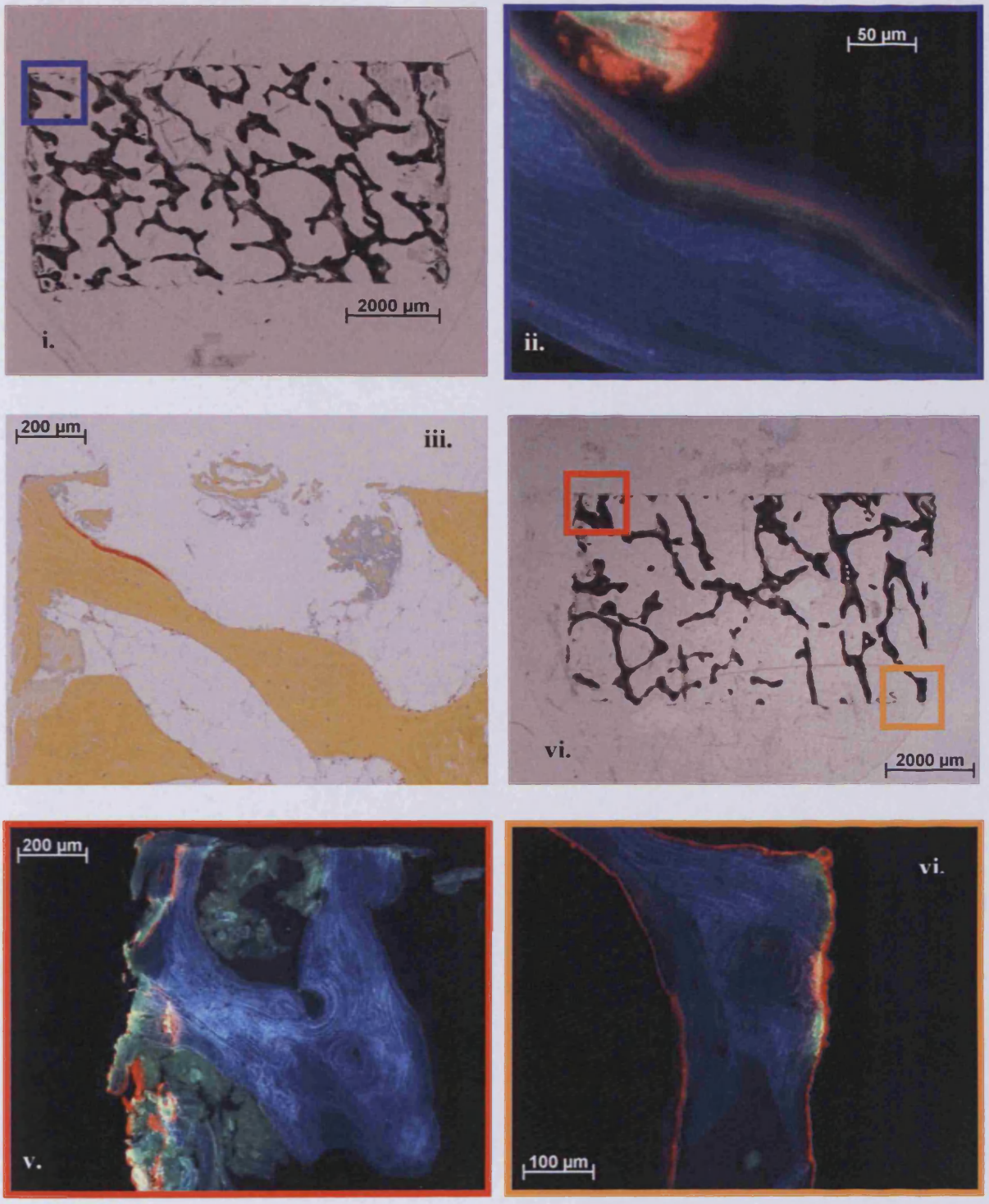

Figure 4c.14. i) *Cross-section through human tissue (70-years-old, cultured for 15 days loaded in the Zetos culture system) stained with calcein (green) and alizarin (red) for 8 hours on day 1 and 11 respectively. Coloured boxes represent image location within the explant.* **ii)** *Cross-section through "dead" (heat killed) human tissue (70-years-old, cultured for 15 days loaded in the Zetos culture system) stained with calcein (green) and alizarin (red) for 8 hours on day 1 and 11 respectively. Coloured boxes represent image location within the explant. [Characteristic image from one of twenty sections obtained from the centre of the core, providing a representation from a group n=2]*

4.c.iii. Biochemical evaluation of media

Hydroxyproline

The presence of hydroxyproline in the media was attempted for bovine bone samples (4-months-old) cultured in the Zetos loaded, unloaded and static bathed control explants. Unfortunately the levels were too low to be detected and thus, this technique was not continued.

Alkaline phosphatase

Alkaline phosphatase (AlP) is normally localised in the cell membrane, where it is covalently attached to phosphatidyl inosito (PI) phospholipid complexes where it can be released during mineralisation by PI-specific phospholipase C enzyme. The AlP enzyme associated with bone is one of four isoenzymes also found in liver and kidney tissue. Media harvested daily from the culture of human tissue (male, 71 years of age) was analysed for the presence of AlP. The results obtained were plotted on a graph, figure 4c.15. The results suggests show that active mineralisation was taking place up to 7 days post-harvest. The highest amount of AlP was observed within the living loaded explants (1B & 2D, bright green), followed by living unloaded explants (2C & 3E, brown-green) and finally explants cultured bathed in static media within centrifuge tubes (2B & 3G, pale green). This implies that mechanical loading may have had an influence in the amount of AlP produced. Dead samples (pink and red) showed as much reactivity as the blank media (black). This technique is currently being evaluated on a number of human samples cultured within the Zetos system.

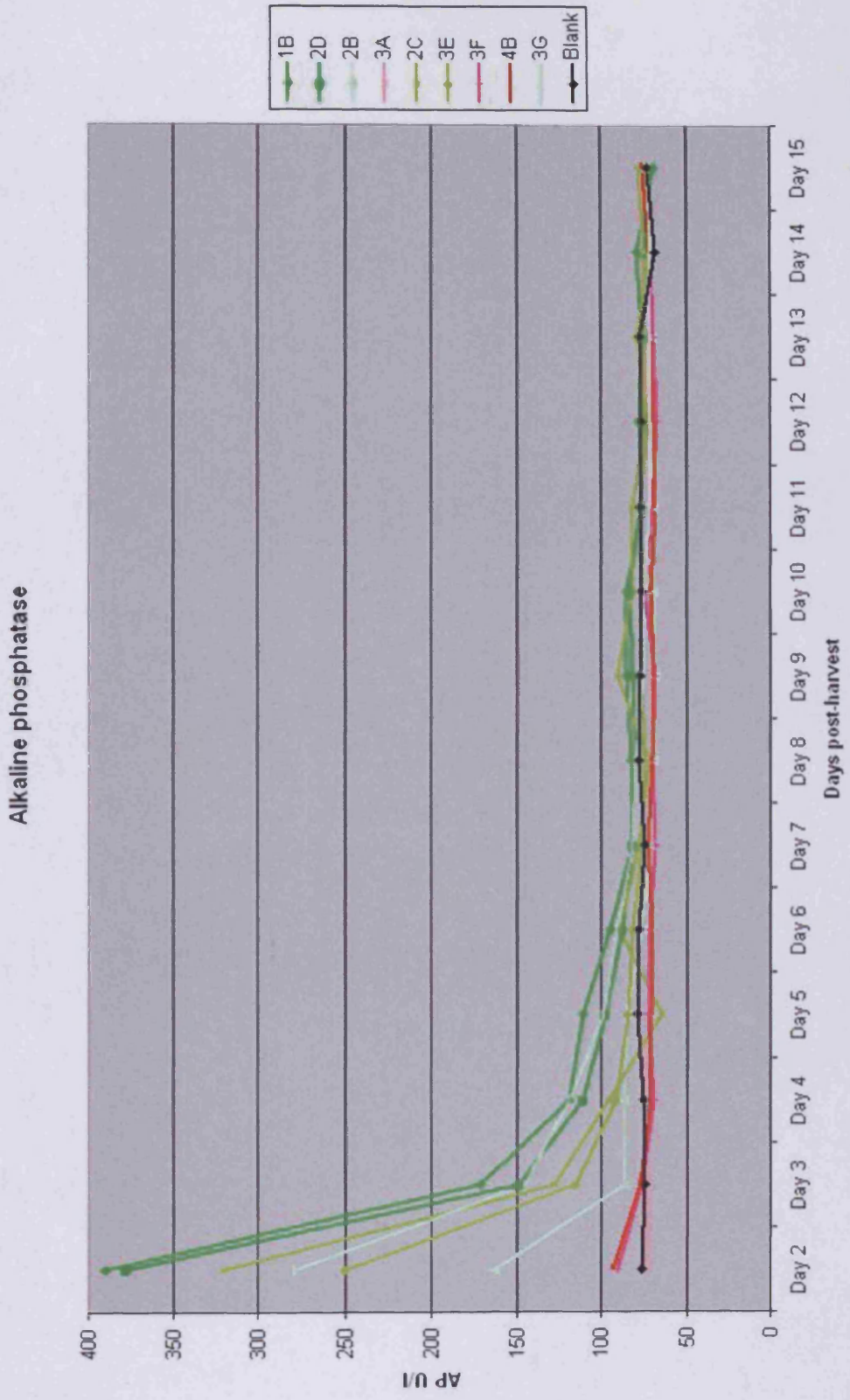

Figure 4c.15. *Media from human explants (male, 71 years of age) were analysed for AlP over 15 days culture ex vivo. Samples depicted as different shades of green were living, samples depicted as different shades of red were dead. Blank unused media was used as a control. Highest AlP was produced by loaded followed by unloaded and static samples. [A representation of 9 human cores, from one limb, analysed in this manner]*

4.c.iv. Active protein synthesis

Detection of radioactive protein within SDS gels.

The first indication that the cultured tissue was still living after 15 days of culture was by the change in media pH seen in Figure 4c.16 after 24 hour incubation with tritiated-glycine. The media of living tissue turned orange, while the media of the dead (heat killed) explants remained pink.

Figure 4c.16. *Incubation media containing ^{3}H-glycine that the ex vivo cultured bone cores were immersed in. Living tissue lowered the pH of the media turning the solution orange, while dead tissue did not affect the media so the solution remained pink.*

Proteins harvested from ovine and bovine tissue and media were separated on an SDS-page gel (Fig.4c.17.i). Protein bands were evident from all samples indicating that the harvest procedure had been successful. Extra protein bands were present in samples harvested from the media due to the presence of FCS. Similar banding can be seen with all samples.

Incubation of the gel with photographic film demonstrated the presence of radioactivity within protein harvested from media, and to a lesser extent tissue, of ovine explant cultured in the loaded Zetos system for 15 days (Fig.4c.17.ii). Similar positive results were obtained for explants cultured in the Zetos system but unloaded, and for explants cultured submerged in static media within centrifuge tubes. No positive results were seen for fresh tissue, thus suggesting the positive results for the *ex vivo* cultured tissue came from the fibrous-like tissue surrounding the explant periphery. Unfortunately, this technique does not indicate which cell or where within the tissue was active. The results from the autoradiography should clarify this.

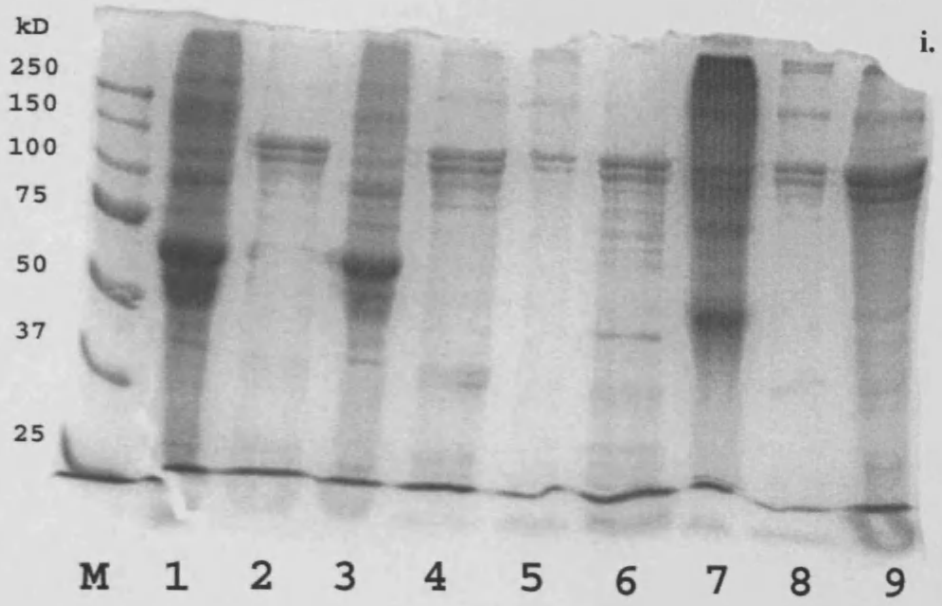

Figure 4c.17. i) Coomassie stained *SDS-page gel of proteins harvested from tissue and from media. M = Precision Plus Protein™ standards all blue (BIO-RAD)*
1 = L1C Zetos Cultured 14 days Living (ovine) protein harvested from media
2 = L1C Zetos Cultured 14 days Living (ovine) protein harvested from tissue
3 = R1A Zetos Cultured 14 days Dead (ovine) protein harvested from media
4 = R1A Zetos Cultured 14 days Dead (ovine) protein harvested from tissue
5 = L3D Fresh Live (ovine) protein harvested from media
6 = L3D Fresh Live (ovine) protein harvested from tissue
7 = L3B Fresh Dead (ovine) protein harvested from tissue
8 = L3B Fresh Dead (ovine) protein harvested from tissue
9 = No 5 Live (bovine) protein harvested from media

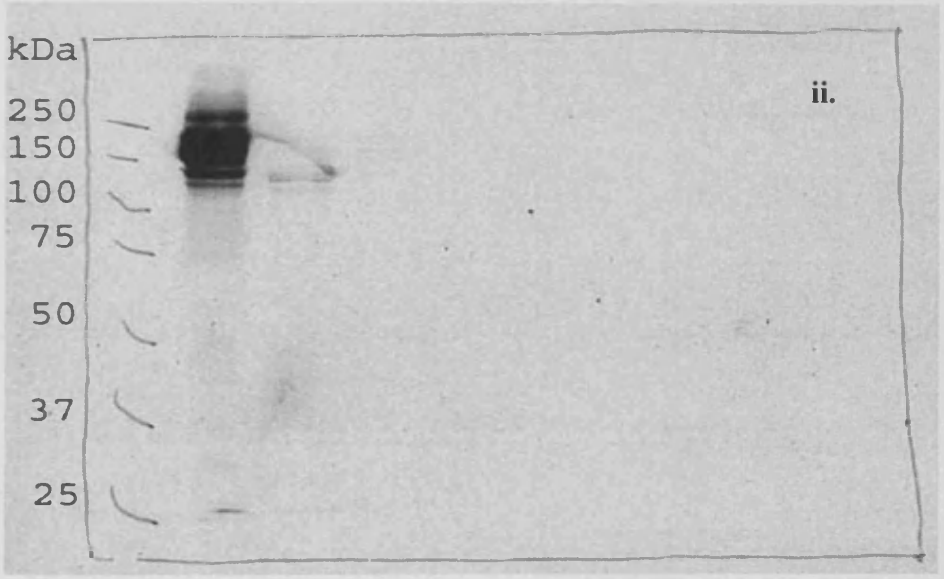

Figure 4c.17. ii) *Detection of radioactive protein bands from the SDS-page gel. Living tissue cultured in Zetos system for 14 days. [A representation of protein harvested from 18 ovine cores and 3 bovine cores (media and tissue) analysed in this manner]*

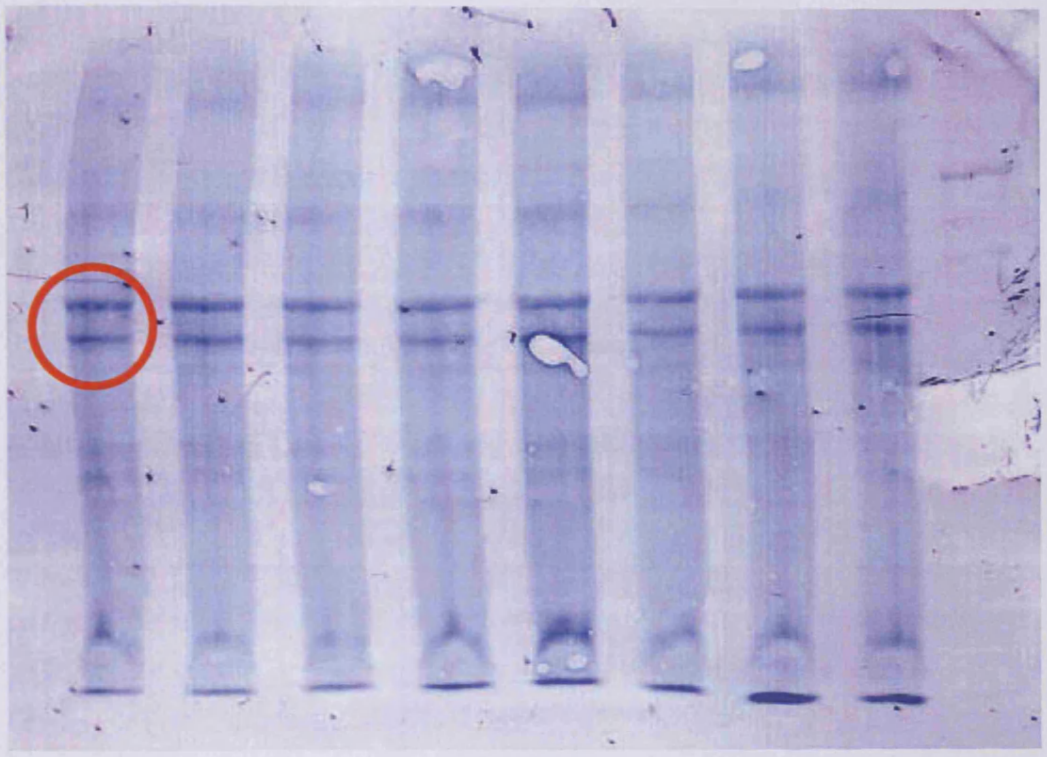

Figure 4c.18. *Two bands of interest (red circle) were removed from each lane of the Western blot (of the protein bands from sample L1C observed in figure 4c.17) to allow the proteins to be sequenced. Thus, allowing the protein being synthesised during day 15 of culture to be identified.*

The protein of interest was separated on a 7% SDS-page gel in order to get as little contamination as possible, when harvesting the radioactive bands from the western blot. These were then placed in Eppendorf tubes and sent to Dave McCourt, Midwest Analytical Inc. St Louis, MO. in the USA for sequencing. No one in the UK had the facilities to use radioactive incorporated proteins. N-terminal protein sequencing was conducted. The original chromatograms of the phenylthiohydantoin (PTH) amino acids were received, however, the results from this analysis were inconclusive. The proteins could not be fully identified but were strongly believed to be collagenous in nature due to the presence of hydroxyproline.

Ovine Tissue

The surface of the ovine explant (3½-year-old) cultured in a loaded environment of the Zetos culture system for 14 days, was still living 15 days post-harvest (Fig.4c.19). The majority of the radiolabel was seen within osteocyte lacunae (Fig.4c.19iv-v) and the fibroblast-like cells that resided within the soft tissue (Fig.4c.19ii-iii) as well as encircling bone debris (Fig.4c.19vi).

Consistent to this interpretation, the cross-sectional section (Fig.4c.20) demonstrated metabolically active osteocytes, in addition to fibrous like tissue at the explants periphery (Fig. 4c.19ii-iii). However, images from the centre of the core did not localise any radioactive precipitate, suggesting that either the cells were not active, or that the ^{3}H-glycine did not penetrate deep into the tissue (Fig.4c.19iv-vi). It is possible that both factors contributed to the results observed, as no active cells were observed within the centre of freshly stained cores at day zero. Nevertheless, there was a greater number of living cells within the centre of fresh tissue than observed with any *ex vivo* cultured explants.

Again, comparable results were obtained with Zetos cultured explants in the unloaded situation (Fig.4c.21), as well as the submerged, static cultured explants within centrifuge tubes (Fig.4c.22). Numerous protein synthesising cells were observed on the surface of the explants in transverse-sectional sections. Yet, the centre of the cores remained unlabeled. In unloaded explants, living cells could be observed in some areas (Fig.4c.21ii, v-vi), whereas no living cells were observed in others (Fig.4c.21iii-iv). Inactive cells were present in explant cultured for 14 days within a centrifuge tube (Fig.4c.22iii-iv, and vi). Active fibroblast-like cells could be seen surrounding bone debris (Fig.4c.22ii), while living osteocytes were only present as far as 500 μm into the tissue (Fig.4c.22v). More living cells were observed in the loaded tissue than explants maintained in other culture conditions. Additional protein synthesis was observed in explants only cultured for 7 days. No activity was observed in heat treated dead tissue explants.

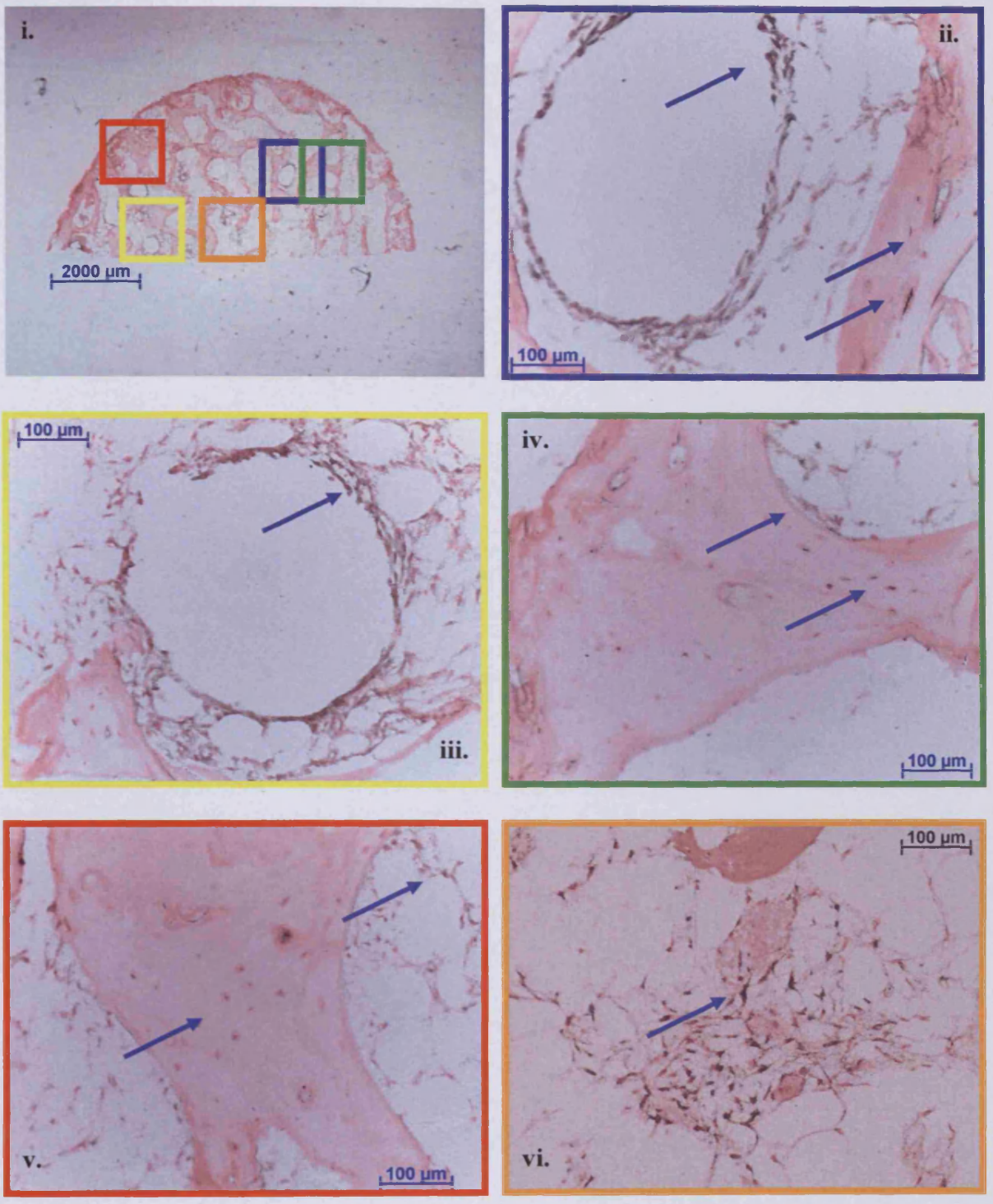

Figure 4c.19. *Transverse-section from ovine tissue (3½-years-old) cultured in a loaded environment of the Zetos culture system for 14 days. Radioactive protein can be seen as black precipitate. Most of the activity can be seen within the fibrous-like tissue surrounding the periphery of the explant. Coloured boxes represent image location within the explant. Blue arrows depict positive labelling, while green arrows depict lack of staining. [Characteristic image from one of ten sections obtained from the surface of the core, providing a representation from a group n=1]*

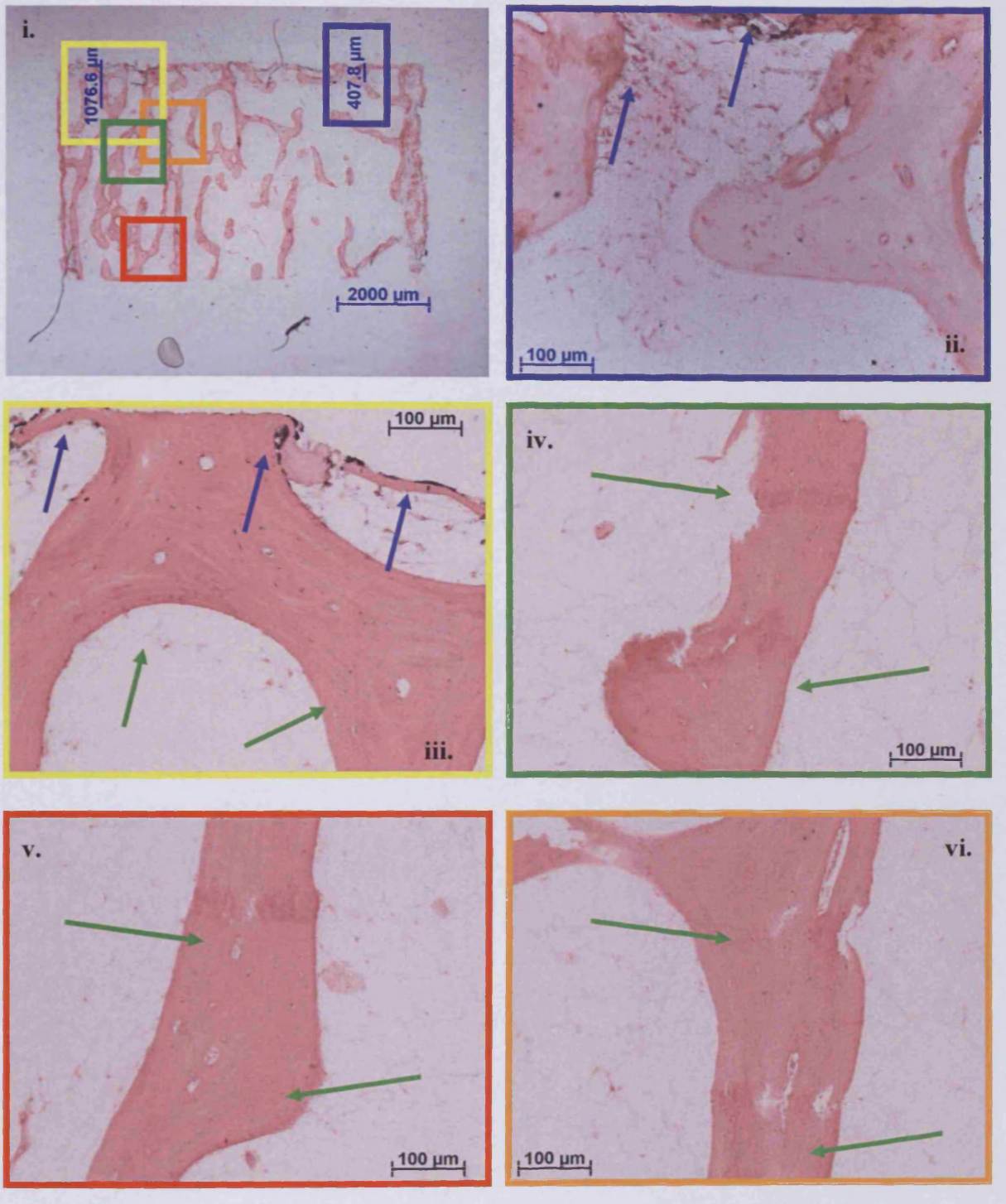

Figure 4c.20. *Cross-section from ovine tissue (3½-years-old) cultured in a loaded environment of the Zetos culture system for 14 days. Radioactive protein can be seen as black precipitate. Most of the activity can be seen within the fibrous-like tissue surrounding the periphery of the explant. Not much activity seen within the centre. Coloured boxes represent image location within the explant. Blue arrows depict positive labelling, while green arrows depict lack of staining. [Characteristic image from one of ten sections obtained from the centre of the core, providing a representation from a group n=1]*

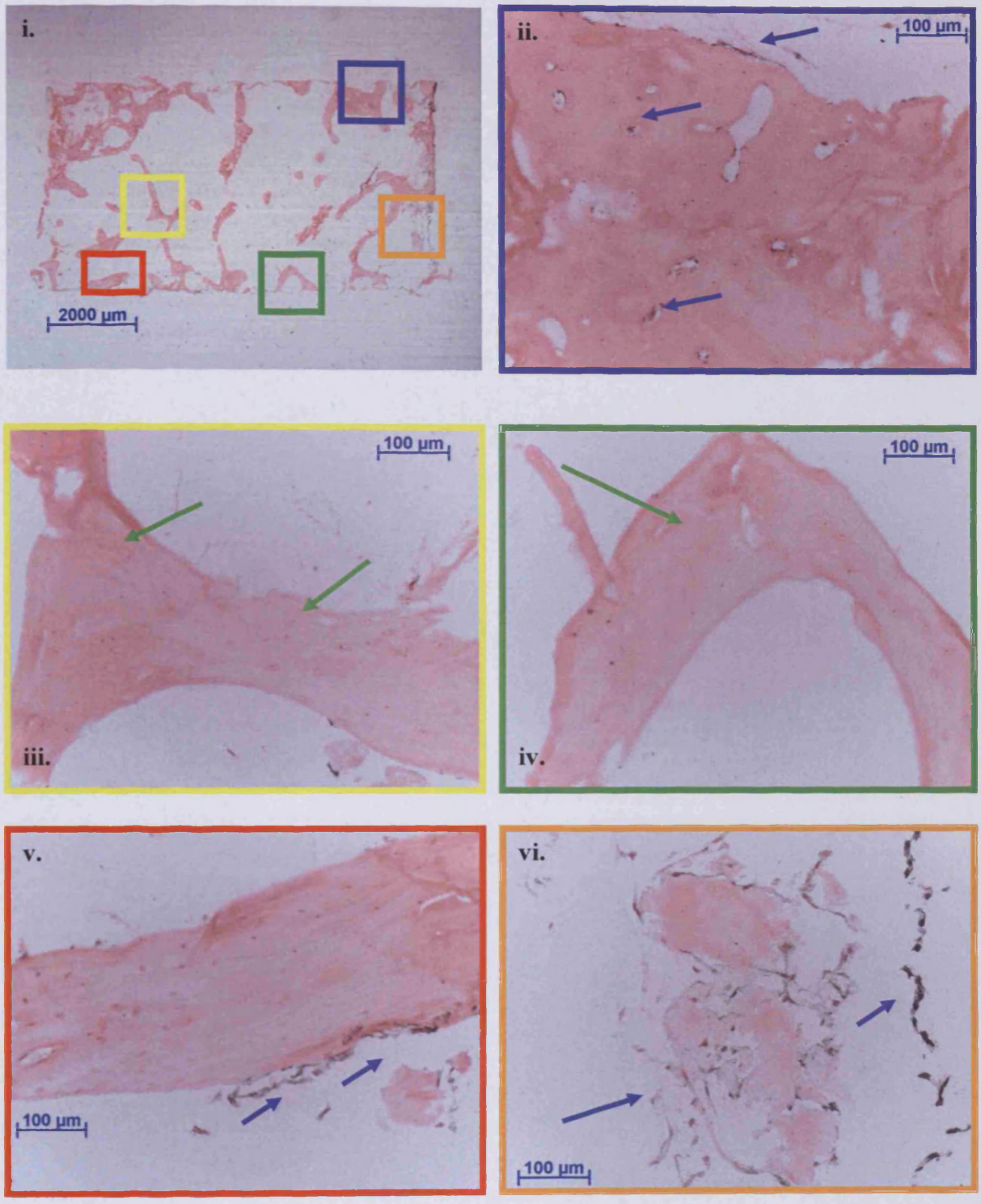

Figure 4c.21. *Cross-section from ovine tissue (3½-years-old) cultured in an unloaded environment of the Zetos culture system for 14 days. Radioactive protein can be seen as black precipitate. Most of the activity can be seen within the fibrous-like tissue surrounding the periphery of the explant. Not much activity seen within the centre.*
Coloured boxes represent image location within the explant. Blue arrows depict positive labelling, while green arrows depict lack of staining. [Characteristic image from one of ten sections obtained from the centre of the core, providing a representation from a group n=1]

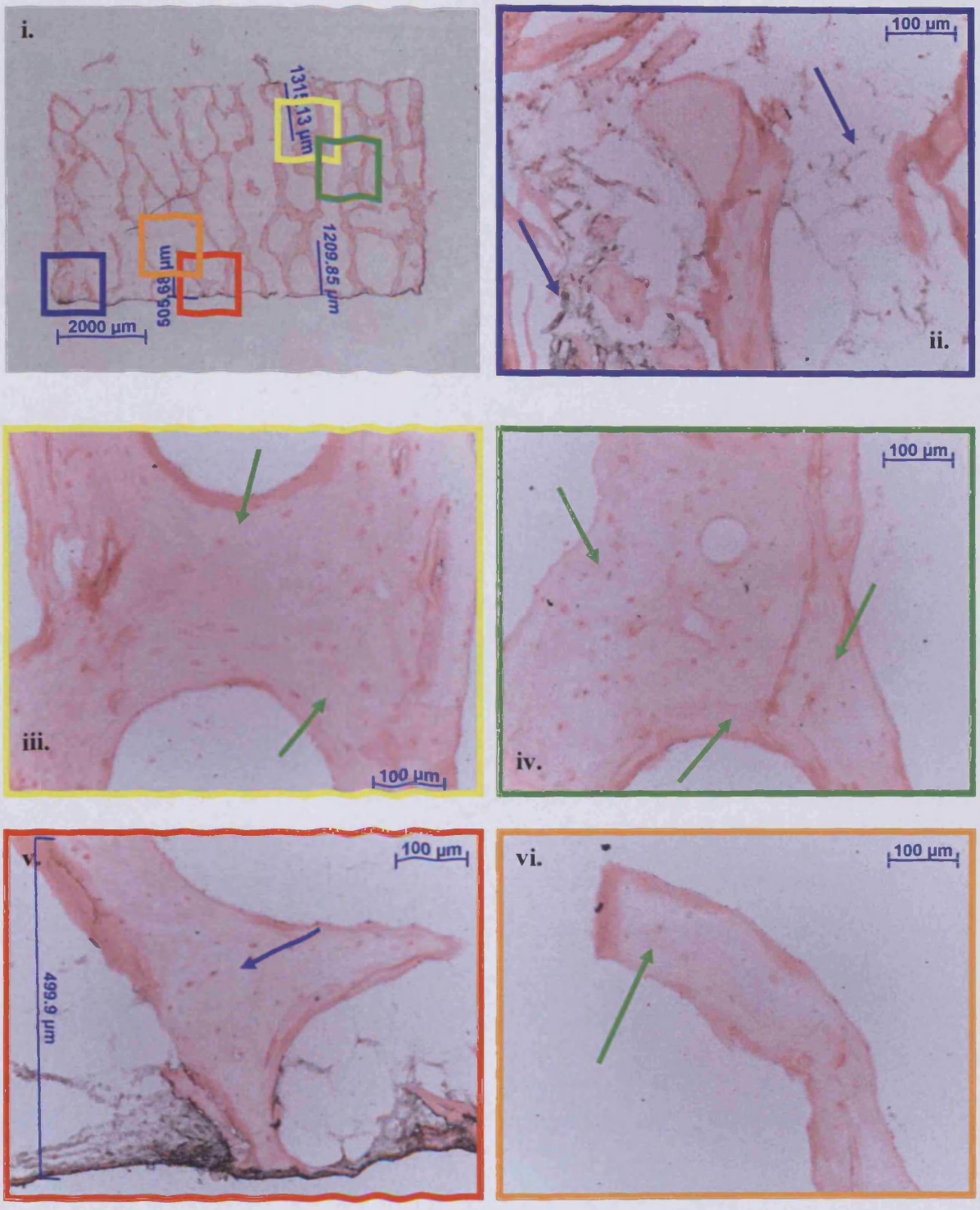

Figure 4c.22. *Cross-section from ovine tissue (3½-years-old) cultured in a submerged static environment of a centrifuge tube for 14 days. Radioactive protein can be seen as black precipitate. Most of the activity can be seen within the fibrous-like tissue surrounding the periphery of the explant. Not much activity seen within the centre. Coloured boxes represent image location within the explant. Blue arrows depict positive labelling, while green arrows depict lack of staining. [Characteristic image from one of ten sections obtained from the centre of the core, providing a representation from a group n=1]*

Bovine Tissue

Analysis of the fresh bovine tissue, fixed at time of harvested, demonstrated a ring of cell death around the outer periphery of the core (Fig.4c.23). Living cells were seen throughout the upper surface of the tissue (Fig.4c.23ii), suggesting the drill bit was the cause of the cell death and not the annular saw. The distance from the perimeter of the tissue to the first living cells was approximately 350 μm (Fig.4c.23v). This correlates with the results obtained in pervious chapters, to the damage that drilling exerts onto the tissue.

The bovine tissue was only examined after 7 days of culture as the heater in the culture room broke down during the experiment and all of the samples had been incubated with ^{3}H-glycine prematurely. Nevertheless, the results obtained were similar to those obtained for ovine and human tissue. It was possible to see living cells close to the periphery of the sample, especially within the fibrous-like cells (Fig.4c.24ii) of living, Zetos loaded explants. No metabolically active cells were seen within the centre of the tissue (Fig.4c.24iii).

A transverse-section of the surface of an explant culture for 7 days submerged within static media inside a centrifuge tube demonstrated a mass of living cells comparable to fresh tissue (Fig.4c.24v-vi).

The lack of staining within the centre of the explant may not necessarily be due to the fact that the tissue was dead, but may be unstained due to diffusion limitations of the radioactive amino acid from penetrating the centre during the incubation period (24 hours). On the other hand, the concentration of the radioactive amino acid may not have been sufficient with most of it being used at the outer regions and therefore not enough left over to stain the middle of the core. Further investigations would enable this question to be answered.

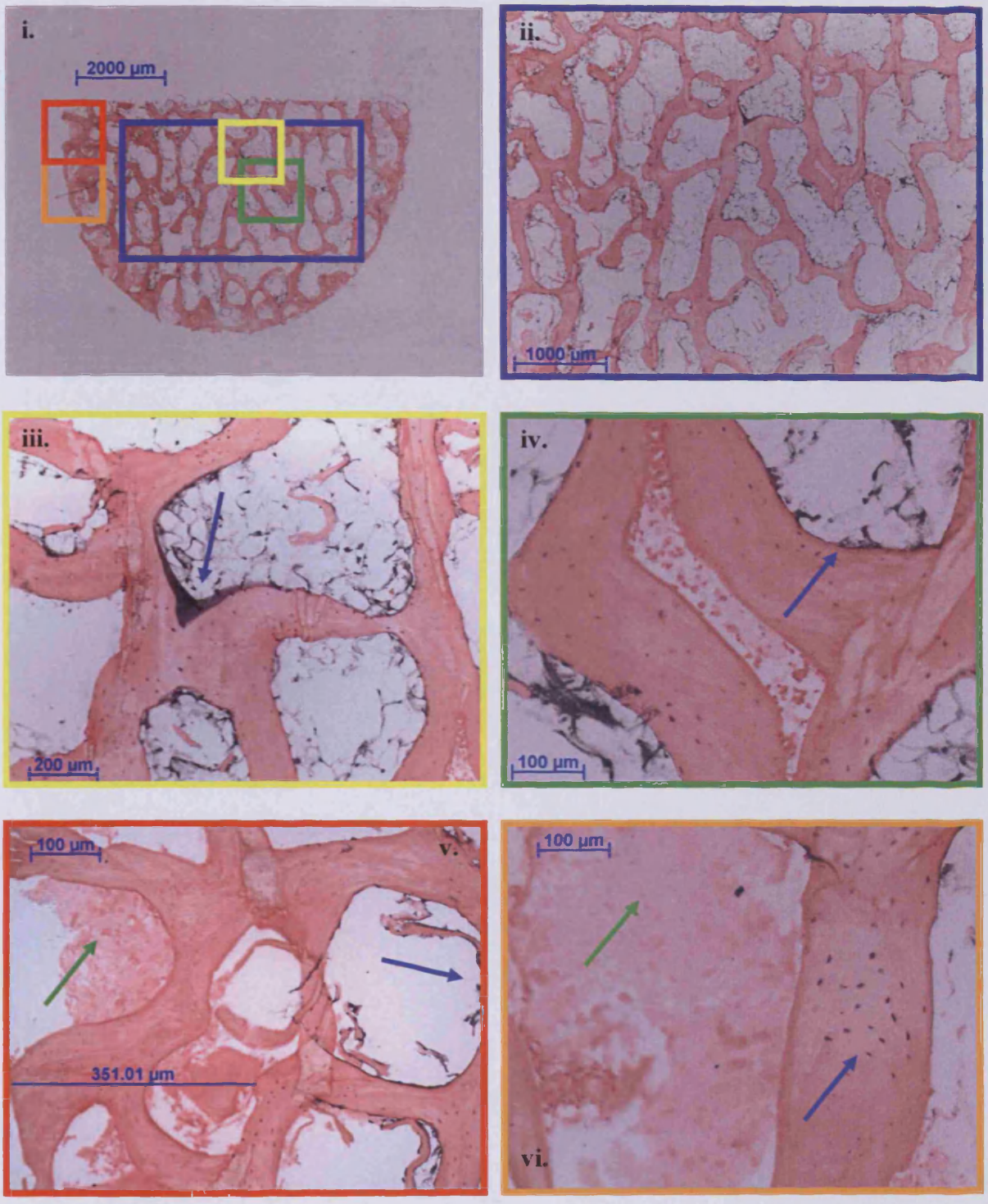

Figure 4c.23. *Transverse-section from bovine tissue (4-months-old) freshly fixed from harvest. Radioactive protein can be seen as black precipitate. Most of the activity can be seen within the soft tissue and osteocytes. Damage to the core was up to 350 µm from the surface that was in contact with the drill. Coloured boxes represent image location within the explant. Blue arrows depict positive labelling, while green arrows depict lack of staining. [Characteristic image from one of ten sections obtained from the surface of the core, providing a representation from a group n=1]*

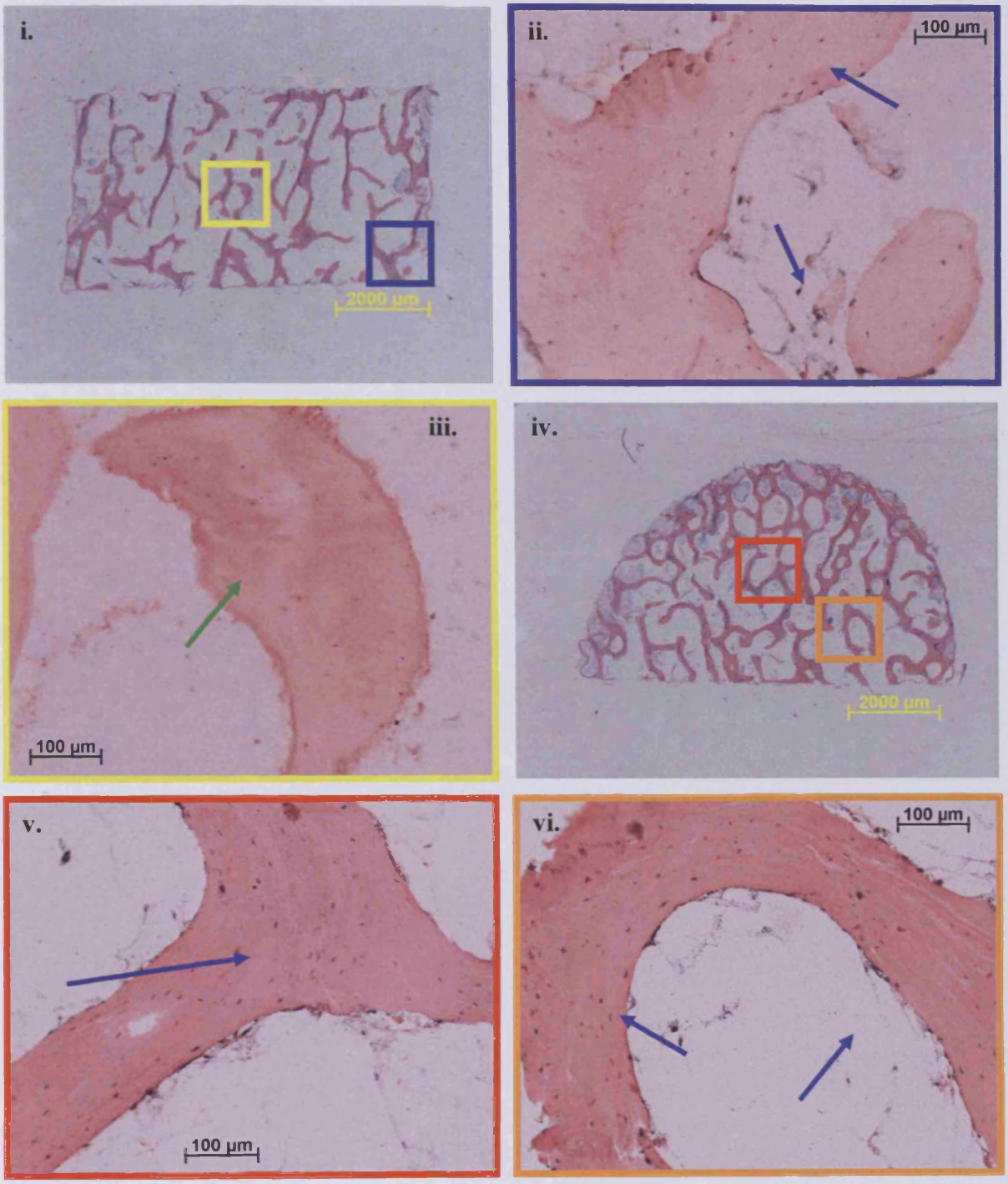

Figure 4c.24. i) *Cross-section from bovine tissue (4-months-old) cultured in a loaded environment of the Zetos culture system for 7 days. Radioactive protein can be seen as black precipitate. Most of the activity can be seen within the fibrous-like tissue surrounding the periphery of the explant. Not much activity seen within the centre. Coloured boxes represent image location within the explant.* **ii)** Transverse *from bovine tissue cultured in a submerged static environment of a centrifuge tube for 7 days. Radioactive protein can be seen within osteocytes and soft tissue. Blue arrows depict positive labelling, while green arrows depict lack of staining. [Characteristic image from one of ten sections obtained from the centre and surface of the core, providing a representation from a group n=1]*

Human Tissue

A number of active cells were observed on the surface of human tissue (71-year-old male) cultured within the loaded Zetos system for 14 days (Fig.4c.25). This was consistent with the results obtained for the ovine and bovine tissue. Localised *de novo* synthesised proteins within osteocyte lacunae, soft tissue, and fibrous-like cells in near proximity to bone debris were observed (Fig.4c.25ii-vi and vi). Single grains of radioactivity could be observed within osteocytes lacunae and osteoblasts (Fig.4c.25v).

Within the cross-section of human tissue (Fig.4c.26), cultured in a loaded manner with the use of the Zetos culture system for 14 days, active cells were observed at the periphery (Fig.4c.26ii) with no active cells visible within the centre of the core (Fig.4c.26iii). High magnification images allowed single grains of radioactivity to be localised within osteocyte lacunae (Fig.4c.26v-vi). However, a number of inactive lacunae were also observed (Fig.4c.26iv).

Zetos cultured, unloaded explants, only contained active cells at the periphery of the core (Fig.4c.27v-vi), whilst the rest of the tissue displayed no metabolically active cells (Fig.4c.27ii-iv). Similarly, submerged static cultured explants maintained *ex vivo* for 14 days in centrifuge tubes also displayed limited cell activity (Fig.4c.28). Active cells were observed at the periphery (Fig.4c.28ii-iii), while the remaining tissue displayed no sign of active protein synthesis (Fig.4c.28iv-vi). As mentioned previously, this lack of radioactive precipitate may be due to either the cells being inactive, or the limitation of label diffusion into the tissue, as previously observed for the fluorochrome labels, as well as viability dyes (Chapter 3).

Loaded tissue appeared to be slightly better maintained than the other culture conditions, though no quantifiable data were obtained. The tissue was more active at day 7 of culture than 14. Active osteoclasts were observed within living Zetos cultured loaded (Fig.4c.29i) and unloaded explants at day 7 (Fig.4c.29ii). Tissue from all culture conditions were comparable to fresh tissue at day 7 with decreased activity observed by day 14. The negative control, dead tissue, did not display any living cells (Fig.4c.30).

Human tissue appeared to survive *ex vivo* culture better than ovine and bovine tissue. This may be due to differences in tissue architecture and composition, allowing a better diffusion of nutrients into and out of the explant.

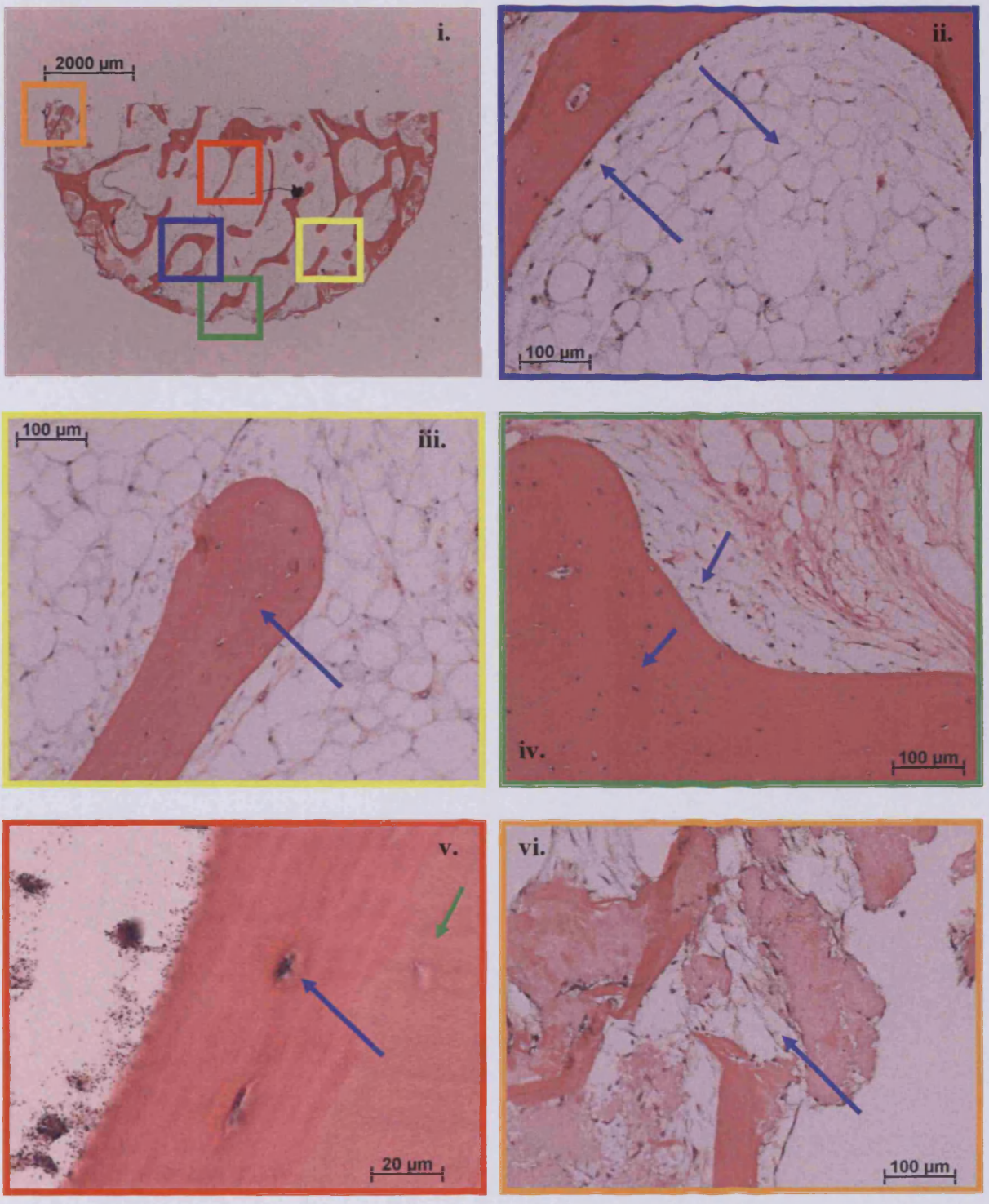

Figure 4c.25. *Transverse-section from human tissue (71-year-old male) cultured in a loaded environment of the Zetos culture system for 14 days. Radioactive protein can be seen as black precipitate. Most of the activity can be seen within the fibrous-like tissue surrounding the periphery of the explant. Individual grains can be seen within the tissue. Coloured boxes represent image location within the explant. Blue arrows depict positive labelling, while green arrows depict lack of staining. [Characteristic image from one of ten sections obtained from the surface of the core, providing a representation from a group n=2]*

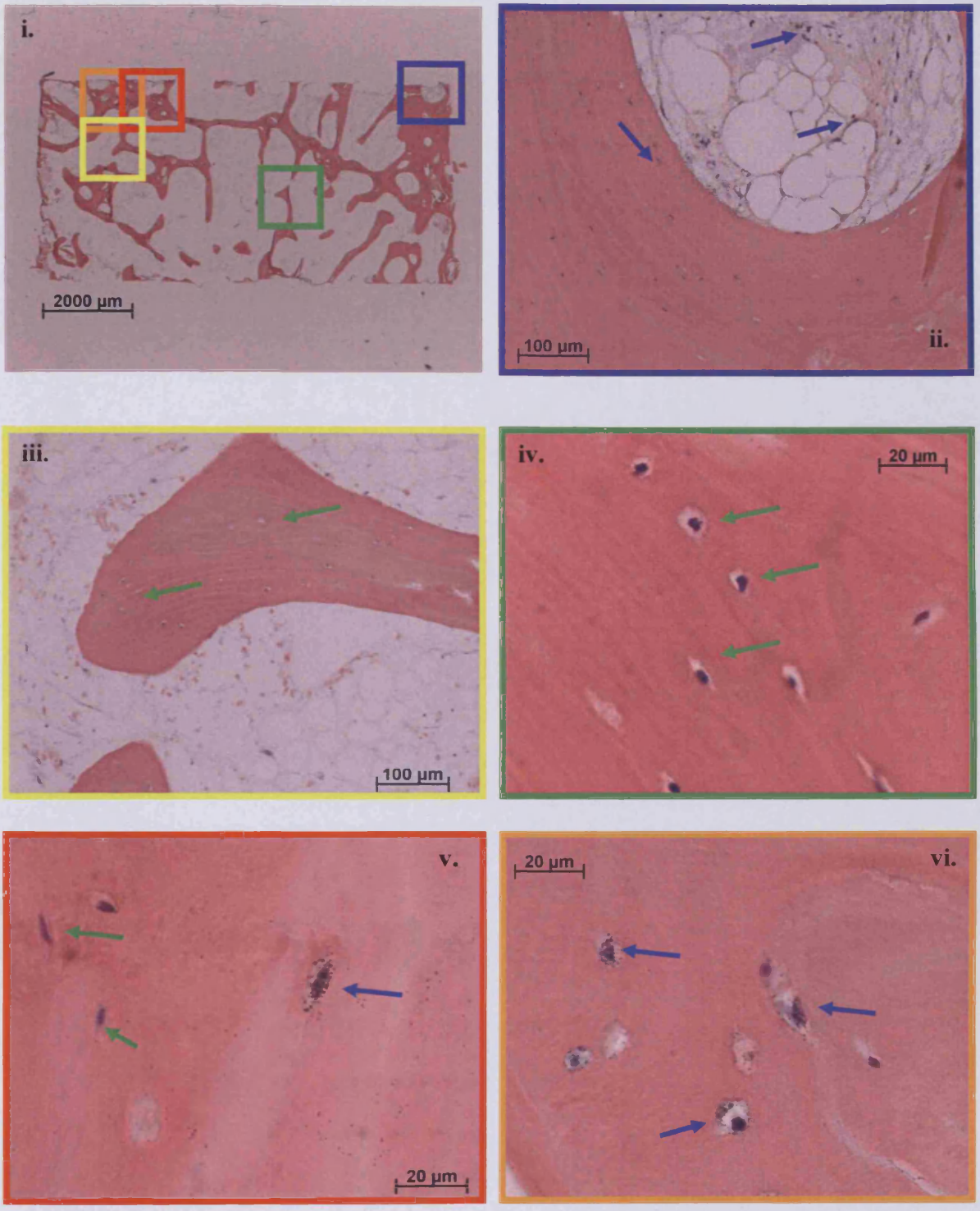

Figure 4c.26. *Cross-section from human tissue (71-year-old male) cultured in a loaded environment of the Zetos culture system for 14 days. Radioactive protein can be seen as black precipitate. Most of the activity can be seen within the fibrous-like tissue surrounding the periphery of the explant. Not much activity seen within the centre. Coloured boxes represent image location within the explant. Blue arrows depict positive labelling, while green arrows depict lack of staining. [Characteristic image from one of ten sections obtained from the centre of the core, providing a representation from a group n=2]*

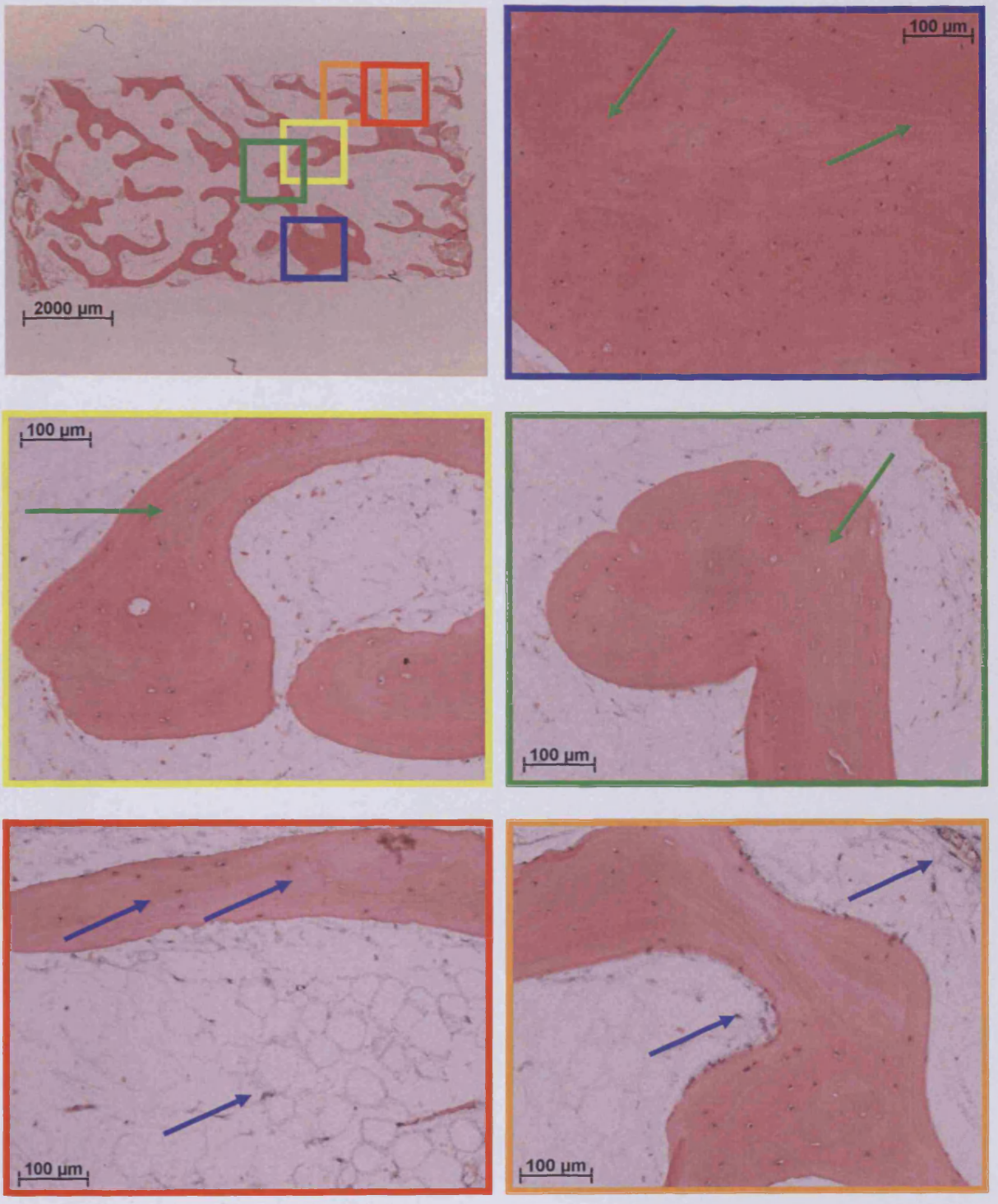

Figure 4c.27. *Cross-section from human tissue (71-year-old male) cultured in an unloaded environment of the Zetos culture system for 14 days. Radioactive protein can be seen as black precipitate. Most of the activity can be seen within the fibrous-like tissue surrounding the periphery of the explant. Not much activity seen within the centre. Coloured boxes represent image location within the explant. Blue arrows depict positive labelling, while green arrows depict lack of staining. [Characteristic image from one of ten sections obtained from the centre of the core, providing a representation from a group n=2]*

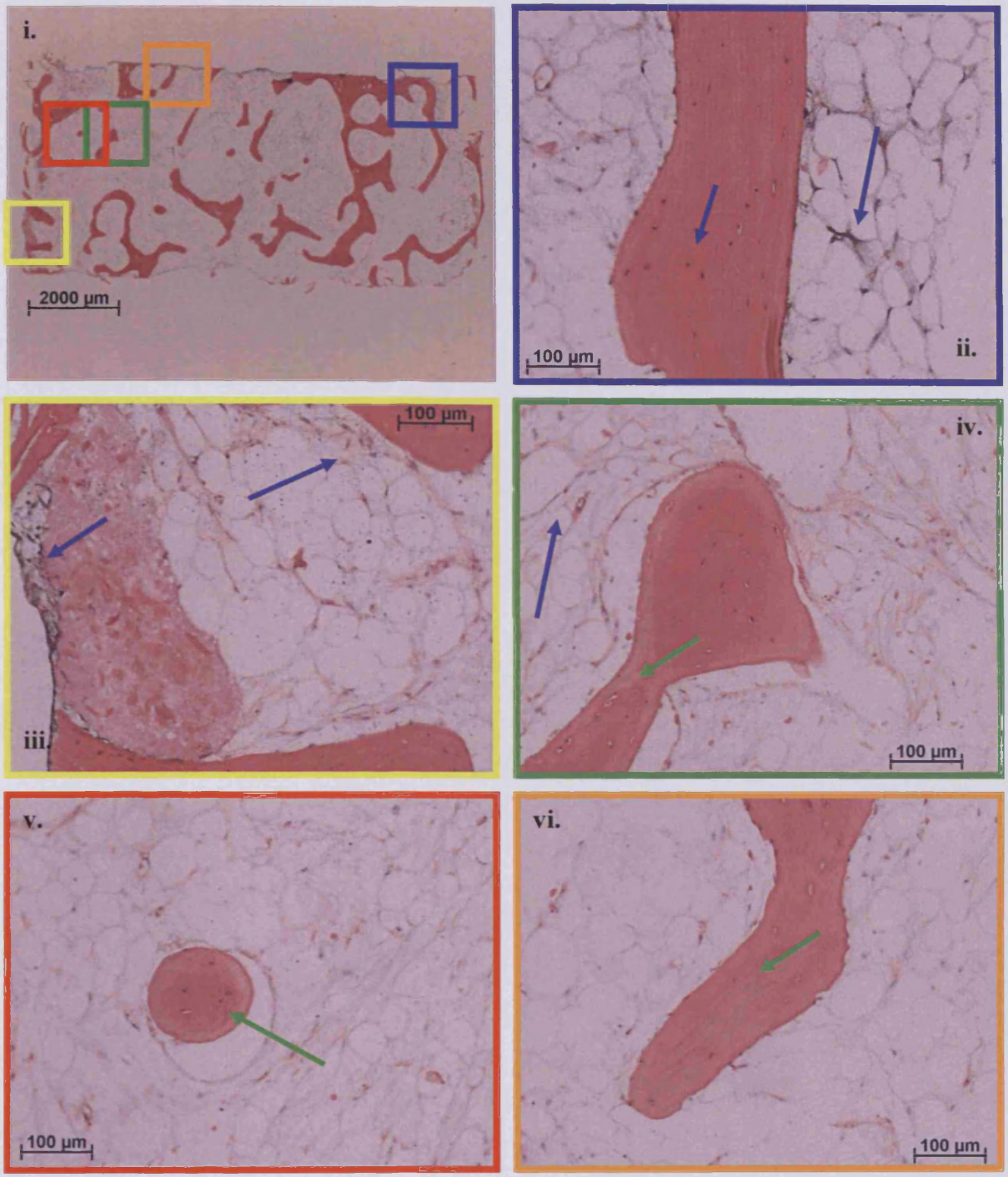

Figure 4c.28. *Cross-section from human tissue (71-year-old male) cultured in a submerged, static environment of a centrifuge tube for 14 days. Radioactive protein can be seen as black precipitate. Most of the activity can be seen within the fibrous-like tissue surrounding the periphery of the explant. Not much activity seen within the centre. Coloured boxes represent image location within the explant. Blue arrows depict positive labelling, while green arrows depict lack of staining. [Characteristic image from one of ten sections obtained from the centre of the core, providing a representation from a group n=2]*

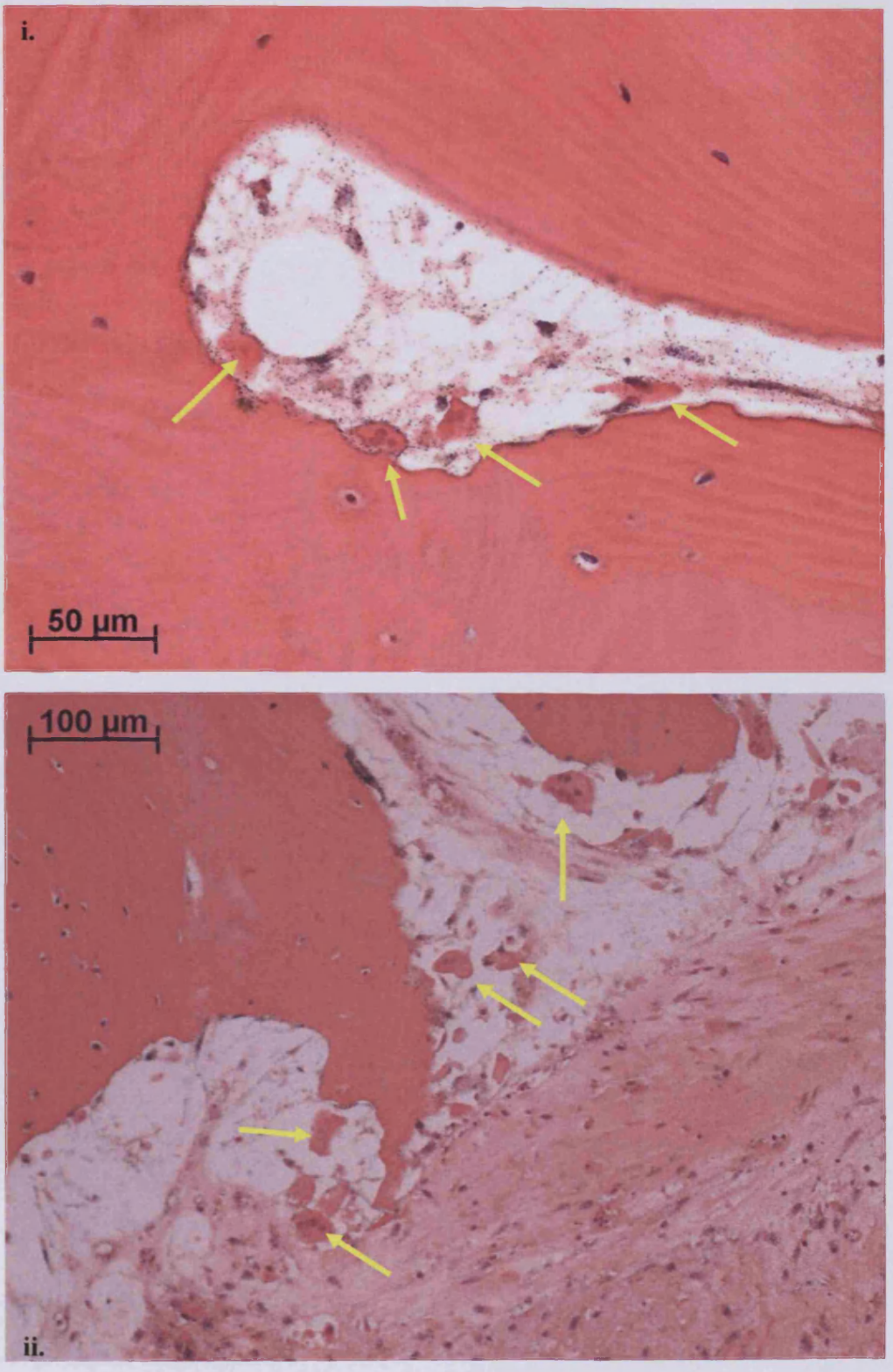

Figure 4c.29. i) *Active osteoclasts observed within a cross-section of human tissue (71-year-old male) cultured in a loaded environment of the Zetos culture system for 7 days.* **ii)** *Numerous osteoclasts observed within a transverse-section of human tissue (71-year-old male) cultured in a loaded environment of the Zetos culture system for 7 days. Osteoclasts are depicted by yellow arrows. [Characteristic image from one of ten sections obtained from the surface of the core, providing a representation from a group n=2]*

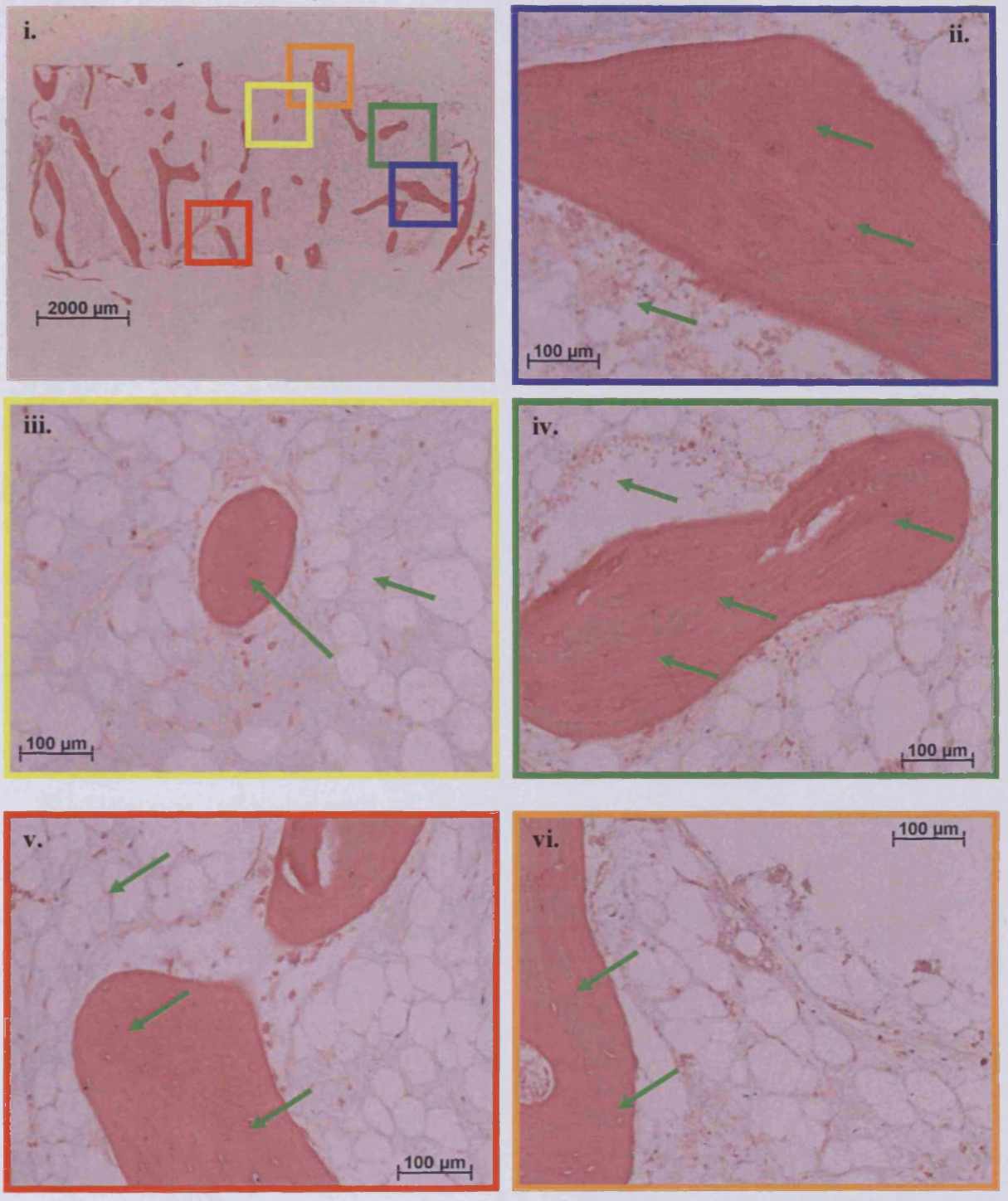

Figure 4c.30. *Cross-section from dead (heat killed) human tissue (71-year-old male) cultured in a loaded environment of the Zetos culture system for 14 days. No radioactive protein can be observed within the explant. Coloured boxes represent image location within the explant. Green arrows depict lack of staining. [Characteristic image from one of ten sections obtained from the centre of the core, providing a representation from a group n=2]*

4.D. Discussion

Due to the inability of fluorescent dyes to determine cell viability directly, and with certainty and accuracy, it was decided to identify metabolically active cells within the *ex vivo* cultured explants, and verify viability in that way. The aim of this chapter was to observe *de novo* matrix synthesis within explants maintained with the Zetos culture system.

The most active and abundant cells within bone tissue are the osteoblasts. They are responsible for synthesising and mineralising the extracellular matrix. Analysis of *de novo* matrix formation was conducted through four various techniques. Immunohistochemistry was used to localise bone matrix proteins; double fluorescent labelling was used to identify areas of bone apposition; tritiated glycine was used to identify protein synthesis at set time points post-harvest; and finally, the media was analysed for the presence of resorption and apposition markers.

The results obtained from the silver enhanced immunogold labelling localised osteonectin, osteopontin, osteocalcin, bone sialoprotein II and collagen type I within the bone cells and surrounding matrix. However, this method did not conclusively demonstrate *de novo* matrix formation, as many of these proteins would have been present in the tissue prior to the explant harvest and maintenance *ex vivo*. Fortunately, the development of this technique with Technovit 9100 New resin will allow the identification of these proteins in future work regarding bone-implant interfaces, the ultimate goal of the Zetos culture system within our group.

Nevertheless, the localisation of these proteins suggested that at least the cells had not dedifferentiated and demonstrated similar localisation patterns as that of fresh tissue, which corresponds to observations in literature (Roach, 1994). Serial sections from ovine, bovine and human explants were assessed. Osteonectin was strongly labelled within the soft tissue of all species (Fig.4c.1vi, 2vi, 3vi). Late osteoblast markers, osteocalcin, osteopontin, bone sialoprotein II and procollagen type I, were not observed within ovine tissue, due to the lack of active osteoblasts synthesising bone matrix (Fig.4c.2). A similar result was observed for human tissue (Fig.4c.3). Osteopontin and bone sialoprotein II was not observed within the mineralised matrix due to lack of specificity of the antibodies for ovine tissue (Yang *et al.*, 2003). All of the late markers (osteocalcin, osteopontin, bone sialoprotein II and procollagen type I) were observed within the cells of bovine tissue

(Fig.4c.1), though, osteocalcin was weakly stained (Fig.4c.1v). Human tissue was strongly stained for osteopontin and bone sialoprotein II at the surfaces of cut tissue (Fig.4c.3vii, viii) and resorption surfaces (Fig.4c.4), but not as strong within the osteoid seams (Fig.4c.4).

In a functionally adaptive response to loading *in vivo*, bone will model or remodel in order to resist applied loads optimally. The core under loading will adjust its mass and architecture to become stronger than it was before loading began. This is the concept behind functional adaptation (Roux, 1885). Bone apposition was evaluated by incorporating Ca^{2+} binding fluorophores at set time points during culture. To limit the amount of time explants were cultured, the first fluorophore (calcein green) was administered on day one post-harvest. The next fluorophore was administered ten days later in order to allow enough bone apposition to take place so that both labels could be distinguished. A number of key observations were made.

The first observation was the lack of staining of the bone cores cultured within the Zetos culture chambers at two different surface areas; one was at the underside of the core (the surface in contact with the base plate), while the other was at the periphery of the core, directly opposite the entry point for the circulating media. Control tissue, which was cultured submerged in static media, was fully stained at each surface, suggesting areas of the chamber were obstructing media from reaching the surface of the tissue and inadequate bathing of the explant was taking place (Fig.4c.5). This observation implies that part of the tissue was not receiving adequate nutrients during the culture period and thus, in consequence, no removal of built up toxic metabolites.

The next key observation made was, that the staining pattern of the tissue depended upon the orientation of the explant during analysis. This was why the location of each image presented within the results section was included. By analysing surface cuts (transverse-sectional images) it became apparent that the entire outer surface area of the trabeculae was in fact stained with alizarin. To the untrained eye, this observation implied that a limited amount of bone apposition was occurring, on every surface, at day 11 of culture, post-harvest. However, it is known that this is highly unlikely and that bone formation occurs far less frequently, and that these fluorophores are not specific to "growing bone" per se, but are bound to areas where free calcium, barium and strontium are to be found. This just so happens to be at the mineralisation front. By examining the explant through its entirety (cross-sectional images) it soon became apparent that there was

a diffusion limitation. After 8 hours of circumfusion/bathing the stain alizarin had only penetrated maximally 600 μm into the tissue at each side (excluding Zetos cultured explants as some surfaces, ie. under surface was not stained) (Fig.4c.7, 10, 14). The other stains (calcein and xylenol orange) had a poorer diffusion depth, and only managed to cover the outer periphery. This may have been due to the size of the molecules, as alizarin was the smallest of the three, followed by calcein green and finally xylenol orange (Fig.4c.6). This diffusion limitation concurs with the results from the previous chapter. It was surprising to note that, Smith *et al.,* (2003) who reported 79% of surfaces labelled with alizarin and 15% of surfaces stained with the double label, could find double labels after such a short incubation period (1 hour) and how they managed to get the stain to penetrate so far into the tissue, unless they were analysing the surface of the tissue only.

Conversely, a contradictory phenomenon occurred with some bovine explants. Explants that contained some of the secondary ossification centre, composed of woven bone apposed to a cartilaginous scaffold, became fully stained throughout the entirety of the trabeculae (Fig.4c.9). It is known that younger bone is more permeable than adult bone (Li *et al.,* 1987), and, therefore, possibly explains why the fluorophores managed to penetrate the collagen-apatite porosity. In more mature bone, this collagen-apatite porosity is believed to be negligible in bone fluid movement, as most of the water in the porosity is bound by interaction with ionic crystal (Neuman and Neuman, 1958). Thus, may explain why entire trabecular uptake of fluorophores was not observed with ovine and human explants utilised in these studies.

In bone, it is known that there are three levels of porosity containing bone fluid. 1) The largest pores are the vascular porosities of cortical bone within the centre of osteons and Volkmann's canals (3-35 μm radius) where the blood vessels are situated. 2) The lacunar-canalicular porosity is smaller (lacunae ~5 μm radius; canaliculi 200 nm radius). This is where the osteocytes and their processes are situated. 3) The smallest porosity is the collagen-apatite porosity (~ 10 nm radius) found between the apatite crystals and collagen.

Several studies have deduced a sieving effect within the lacunar-canalicular porosity, and that there is an upper limit to the molecular cut off size of molecules that can penetrate the tissue (Knothe-Tate *et al.,* 2000; Wang *et al.,* 2004). It was deduced by Wang et al., (2004) that the cutoff size in rat long bone falls between the size of horseradish peroxidase (40,000 Da, approximately 6 nm) and ferritin (440,000 Da, approximately 10 nm). This correlates with the finding of several researchers regarding the structure and

constituents of the osteocyte lacunae. A pericellular matrix (PM) surrounds the osteocytes (Wassermann and Yaeger, 1965; Sauren *et al.*, 1992; Shapiro *et al.*, 1995; and Arden *el al.*, 1996). The size of this space is believed to be between 14-100 nm, but varies depending on species, age of the osteocyte, histological bone type and skeletal location etc. (You *et al.*, 2001). Albumin and proteoglycan are components that are present within the PM. The diameter of albumin is approximately 7 nm, which corresponds to the spacing of the side chains of glycosaminoglycans (GAG) (Buckwalter and Rosenberg, 1982). Thus, these constituents may act as the molecular sieve for solute transport.

Knothe-Tate *et al.*, (2000) determined that load-induced fluid flow enhances the transport of key substances, such as metabolites, nutrients, mineral precursors and osteotropic agents important for cellular activity within cortical tissue. Thus, helping to regulate cellular activity associated with processes of functional adaptation and remodelling. This may also be the key to the success of the viability of bone explants cultured within the loaded Zetos culture system. However, all of these experiments using tracers were conducted *in vivo*, where the tracers had the aid of blood vessels to reach the desired tissue, and therefore did not rely on diffusion alone.

During these studies, false positive results were observed. Double labels were observed on the drill cut surfaces of every single core, irrespective of culture condition or viability status of the tissue. It is known that these fluorophores are not specific for labelling growing bone, and that they bind to free Ca, Ba, and Sr sites within the mineralising matrix (Rahn, 2003). It is highly probable that the damage caused to the tissue during drilling exposes a number of binding sites for these fluorophores to incorporate into the matrix. This was also seen with the high amount of osteopontin and bone sialoprotein within the same regions (Fig.4c.3). Bone debris, blown into the soft tissue during drilling and cutting, was observed to take up the fluorophores throughout its entirety, within all cultured explants.

Though the exposure of binding sites during cutting explains the presence of single labels at the core periphery, it does not explain the presence of double labels, especially with the dead tissue (Fig.4c.14vi). All of the surfaces where double labels were observed at the explant periphery were void of cells. This can only lead to the hypothesis that the supersaturated medium caused calcium phosphate precipitation onto the outer surfaces of the cores.

The standard media (DMEM + 10% FCS) used throughout these studies contained 5 mM β-glycerophosphate (βGP). This organic phosphate acts as a substrate for alkaline phosphates (AlP), resulting in an increased concentration of inorganic phosphate and subsequent mineral deposition. It is thus questioned, whether mineralisation occurring only in the presence of exogenous organic phosphate can be considered physiological. The local increase of inorganic phosphate by the action of AlP upon supplemented organic phosphate is required for mineralisation to proceed once initiated (Bellows *et al.*, 1991; Bellows *et al.*, 1992). It was also noted that the initiation action of AlP on organic phosphate could be replaced by supplementing the medium with inorganic phosphate (Bellow et al., 1992; Marsh *et al.*, 1995). Surprisingly, some evidence has come to light that suggests that high AlP levels in the presence of organic phosphate, or high inorganic phosphate levels may stimulate mineralisation of collagen matrices by fibroblasts (Bellows *et al.*, 1991; Marsh *et al.*, 1995; Khouja *et al.*, 1990). It was also observed that bone matrix alone was sufficient to support mineralisation, even with the absence of viable osteoblasts, if an appropriate level of inorganic phosphate was present (Marsh *et al.*, 1995). This may explain observed double labels upon the surface of trabeculae at the periphery of the cores.

The possibility that hypermineralisation was taking place at the core periphery was acknowledged. However, this was not believed to occur within the explants, as no new mineral deposition was observed within osteocyte lacunae of dead tissue, where loss of cells would have promoted such a case. On the other hand, the lack of empty osteocyte lacunae, and the limitation of diffusion into the explants may have hindered this by preventing the media from reaching deep within the lacunae.

Nevertheless, double labelling of living human tissue was observed, which also correlated with the presence of osteoid seams (Fig.4c.11ii-iv, 12ii, 13iii, 13v, 14ii). Thus, suggesting that active osteoblasts were present within the cancellous tissue cultured *ex vivo* for 15 days. A total of eight different double labels were observed from three Zetos cultured, loaded, explants, while only four double labels were observed within two bathed, static cultured explants maintained within centrifuge tubes. Statistical evaluation of these data is required to determine whether culture in Zetos significantly influenced bone formation. Sadly, these double labels, indicating *de novo* bone formation, were only observed at the outer surfaces of cultured tissue. Due to the diffusion limitations of the fluorochromes, no bone growth was observed within the centre of the tissue, irrespective of culture condition. No double labels were observed within ovine or bovine cultured tissue.

This can only by explained by the fact that active areas within the bovine tissue stained so much that it was impossible to distinguish what was genuine bone apposition and what was artefactual. On the other hand, it was noted that there were very little active surfaces with ovine tissue, possibly due to the age of the animal, or the time of harvest (winter) corresponding to the least active months of bone turnover (Rosen *et al.*, 1999). Success with human tissue can only be attributed to better diffusion within the explants, possibly due to the lower density of extracellular matrix.

Possibly, by increasing the staining time, penetration of the fluorochromes into the tissue would increase. Failing that, increasing the concentration of fluorochromes may help, as a large amount of stain was taken up by bone debris. Care would be needed as many of these stains are toxic to cells and over exposure may cause irreparable damage to the tissue.

The final noted limitation to this technique was the occasional presence of a pseudo double label observed with the same single stain. It was observed, especially in bovine tissue, that two alizarin labels in close proximity to each other, suggested bone apposition had occurred (Fig.4c.8). However, due to the fact that this fluorophore was only administered once, this could not have been possible. This result was artefactual due to the incomplete mineralisation of the tissue, the stain could penetrate deeper within the tissue. This is significant when using the same fluorophore at two different time points, as it would be possible to get false positive results. It is, therefore, suggested that two different fluorophores be used for all future Zetos experiments.

This technique works well *in vivo* as no cell is more than 200 μm from blood vessel. As the blood vessels are no longer functional within cultured explants, this method was slightly limited for conclusively determining the viability of the whole explant during *ex vivo* culture.

In agreement with active bone deposition from osteoblasts within cultured explants was the secretion of AlP within the circulating media, indicating osteoblast activity, and possibly that mineralisation was occurring. The level of secreted AlP was higher in the media of living explants than dead explants and media only controls, up until day 7 (Fig.4c.15). This suggests that mineralisation slows or stops thereafter. It was noted that mechanical stimulation may play a role in stimulating mineralisation as higher levels of AlP were observed within loaded explants compared to unloaded explants. Unloaded explants (which received a single static compression every four days) had higher levels

than submerged, static, cultured explants. This method was only conducted once on human tissue, and thus should be repeated with a greater number of samples to corroborate these findings. This is currently underway at our establishment.

Hydroxyproline, an amino acid only found in collagen, and a marker of bone resorption, was not detected within the media of cultured explants. This suggests that the sensitivity of the technique was not optimal, or unlikely, that no resorption was taking place. Another possibility was that due to the limited number of resorption surfaces and the lack of solute diffusion, only negligible amounts of hydroxyproline was secreted into the media.

The final attempt to ascertain if bone cells present within cancellous bone explants, cultured *ex vivo*, were viable, involved the incorporation of radioactive labelled amino acids into synthesising proteins. The amino acid glycine was chosen due to its high abundance in proteins, including collagen (every third molecule). Tritium was chosen due to its long half-life (12 years). This investigation involved two parts. The cores were incubated after 0, 7, and 14 days cultured with media containing ^{3}H-glycine for 24 hours, to allow adequate protein synthesis. Half of the samples were then fixed and embedded into resin allowing autoradiography to be conducted. This method had the advantage of allowing the active cells to be identified and located within the tissue. The other half of the explants were used to obtain proteins from the tissue (as well as media) allowing radioactive proteins to be located and extracted for gels, with the ultimate aim of identifying which proteins were being synthesised at the given time points.

The results obtained from media and tissue harvested proteins, indicated that cells within loaded, unloaded and static culture were viable, and actively synthesising proteins. This was observed through the presence of radioactive protein bands within the SDS-page gels (4c.17). No radioactive protein was observed from dead tissue. Radioactivity was only observed from proteins harvested from the media, even with fresh controls labelled at day 0. This implied that the technique was not optimum for harvesting all of the protein from the cancellous bone tissue. It also suggested that the majority of active protein synthesis was occurring within the fibrous-like tissue, which was seen to surround the periphery of explants of all culture conditions. This theory was also supported by the lack of radioactive proteins observed from the media of freshly harvested and stained cores (day 0). The extraction of proteins from the tissue was biased towards the harvest of collagen, as this is the most abundant protein in bone. This was confirmed by sequencing the radioactive

bands obtained from the Western blots of the SDS-page gels (Fig.4c.18). Unfortunately, conclusive identification of the proteins was not possible. The limitation to this technique is the ability to successfully determine which cells were responsible for synthesising the radioactive protein.

Analysis of the autoradiographed sections confirmed the above hypothesis that the most active cells within the explants were the surface fibroblast-like cells. This was found to be true of explants from all culture conditions (Fig.4c19, 24v, 24vi, 25,). No radioactivity was detected in control dead tissue (Fig.4c.30). Radioactive protein was observed within ovine, bovine and human tissue; within the cells of the soft tissue and osteocytes; and in human cores, within osteoclasts and osteoblasts. The most activity was observed in fresh tissue, followed by tissue after 7 days of culture, with least activity seen at day 14 post-harvest.

Diffusion limitations were also observed for this method. Highly active cells were observed at the surface of the explants, but active cells within the centre of the core were rarely seen. Maximum penetration was approximately 500 μm into the tissue, after 24 hours diffusion, including fresh tissue (Fig.4c.6, 7, 9ii, 10, 24iii, 26, 27, 28). It was thus, difficult to assess the viability of the whole tissue. Worryingly, if there was insufficient diffusion taking place to allow an amino acid (the smallest one at that) to fully penetrate the tissue, what hope would there be for other molecules? This implies that the centre of the explant was not receiving adequate nutrients and may be dead. However, inadequate concentration of radioactive amino acid cannot be ruled out as the cause for the observed lack of activity at the centre of the tissue. Though active protein synthesis was observed, this method did not allow the proteins to be identified. A number of cells could have been producing bone matrix related proteins, but others could have been producing protein relating to their distress or even their imminent death.

This technique was also seen to substantiate the observed results of the previous chapter, that the drilling of the tissue caused most damage to the explants. Figure 4c.23v demonstrated a lack of active cells seen within the vicinity of the cut surface of freshly harvested bovine tissue. The distance before the first active cells were reached was ~350 μm, similar to that observed when fluorescent live/dead stains were used to analyse cell viability.

To overcome the diffusion limitations observed with this technique, a future technique to be applied could be *in situ* hybridisation for various bone marker proteins.

Though this would not directly confirm active protein synthesis, it could be inferred that the protein would have been made, due to the short half-life of mRNA. The diffusion limitations of the ECM would be eliminated, as this technique would be conducted upon tissue sections.

In conclusion, it was possible to ascertain that not all cells within the tissue were dead. Bone apposition as well as active protein synthesis was observed within tissue cultured *ex vivo*, 15-days post-harvest. To increase the chance of cell survival it may be in the groups best interest to firstly, rethink how to harvest bone cores from the bone tissue, or how to limit the damage caused to the tissue during this procedure. Secondly, create a core with a slightly smaller size, to aid molecular diffusion into the explant centre, but without compromising the ability to load the tissue. The development of other techniques would better enable the viability of the tissue to be established.

Summary

- Qualitative analysis of protein localisation within cells and extracellular matrix within tissue sections from explants maintained *ex vivo* in the Zetos loaded culture system, was not different from fresh tissue and disuse cores maintained in the Zetos culture system or from cores submerged in static media. Thus, suggesting that the explants were all equally viable or that the proteins being localised remained within the cells since harvest. Dead tissue only labelled positively for osteonectin suggesting that heat inactivation of the epitopes had occurred.
- Qualitative analysis of bone apposition within tissue sections was only observed for human tissue. A total of eight different double labels were observed from three Zetos cultured, loaded, explants, while only four double labels were observed within two bathed, static cultured explants maintained within centrifuge tubes. Unfortunately this did not indicate if the new tissue was apposed as an adaptation to the change in loading applied or if it was just a continuation of apposition and mineralisation started *in vivo*.
- Double labelling was also observed on cut surfaces of dead tissue suggesting that the technique was also partially artefactual or that mineral precipitation from the media was adhering to the explant periphery.
- Quantitative analysis of AlP activity within tissue media from explants maintained ex vivo was only conducted once, and thus, not significant. The presence of the enzyme suggested that the tissue was metabolically active and a possible effect of mechanical

influence observed. However, by day 7 a similar quantity to dead tissue and blank media was observed suggesting no more AlP was being produced or that it was not reaching the media.

- Qualitative analysis of protein synthesis from tissue and media suggested that all living explants were synthesising proteins. As most of the radiolabelled protein was found from the media, it suggested that the fibrous tissue was synthesising the detected proteins rather than the bone cells. It was determined that collagen was the protein being synthesised, however, this technique did not let the location of the metabolically active cells be identified. No positive labelling of dead tissue was observed suggesting that technique was reliable and accurate.
- Qualitative analysis of the location of active protein synthesis within cells from all living explants concluded that the fibrous-like cells were synthesising most of the protein. No positive labelling of dead tissue was observed suggesting that technique was reliable and accurate.
- Neither the fluorophores nor the tritiated glycine reached the centre of the cores, which suggests that diffusion of nutrients into the centre of the core is not optimum.

Chapter 5.
General Discussion

The Zetos culture system is an innovative approach to maintaining cancellous bone explants, *ex vivo,* in a dynamically loaded environment, mimicking that of the *in vivo* situation. The role of Zetos is to bridge the gap between cell culture and animal experimentation. Currently, the closest technique that allows bone tissue to be studied in as near a natural milieu as possible is through organ culture. Organ culture consists of maintenance or growth of tissue, or organs (in whole or in part) *in vitro*, which may allow differentiation and preservation of architecture and function. Unfortunately, this culture method is limited in the fact that the tissue rarely receives any mechanical load, a process that is required to maintain skeletal integrity. Also, the explanted tissue quickly dies from necrosis due to too much oxygen at the surface of the tissue and not enough penetrating into the centre. Both cell culture and *in vivo* work suffer from various limitations as discussed in chapter 1a.

The advantages of the Zetos culture system is that compression and force can be applied and measured with high precision (+/- 3%) (Jones *et al.*, 2003) thus allowing reproducible results to be obtained regarding amplitude, direction of load, loading frequency mimicking that of the *in vivo* situation. This is not always the case with *in vivo* and *in vitro* work. The physiochemical environment (pH, temperature, osmotic pressure, and O_2/CO_2 tension) can be strictly controlled. This *ex vivo* bone chamber device allows observation of bone formation and resorption with online readings. On the whole, this culture method is cheap, and avoids the legal, moral, and ethical issues regarding animal experimentation in the *in vivo* situation.

The aim of this work was to validate the Zetos system, to determine if the tissue remained viable during culture and for how long, as well as analysing cell behaviour to establish whether it corresponded to that of the *in vivo* situation. Ultimately, the goal of this study was to provide confirmation that the tissue behaved as it would in its normal environment, allowing this system to be developed as a standard culture technique for cancellous bone research, thus, providing future means to allow bone-biomaterial interactions and bone-biomaterial interfaces to be studied, in the long run, reducing, refining and replacing the need for animal experimentation.

In order to conduct an adequate investigation into the viability of the cancellous tissue maintained within the Zetos culture system, it was first necessary to become familiar with the model systems employed throughout this project. It was possible to utilise cancellous bone tissue from the distal femora of Swiss mountain ewes (aged 3-6 years), the distal metacarpals of Swiss calves (4-months-old), and human femoral heads (aged 70-81 years). No animal was directly sacrificed during the course of this investigation. Ovine and human tissue utilised during this study was regarded as being structurally mature, being composed mainly of lamellar bone while the bovine tissue was regarded as being immature due to the presence of an open growth plate and remaining cartilaginous scaffold and woven bone within the secondary ossification centre. Each of these bones were analysed for cancellous tissue architecture, density and cell types employing techniques such as bone maceration, radiography, microCT, SEM and routine undecalcified bone histology.

The results obtained indicated that the bone cores were highly variable from species to species, location to location in both density and the presence of cell types. Care would be required in order to deduce real experimental results attributed to culture conditions rather than from variations within samples. In this instance, the system suffers from similar limitations to organ culture, in which comparisons between samples are problematic. The analysis of tissue relies mainly on histological observations as biochemical and molecular techniques are difficult to attribute to the correct cell type. In conclusion, cancellous bone is dramatically heterogeneous and great care should be taken to get representative and reproducible results. There is inter-site and inter-individual variability. Caution is required when extrapolating data obtained from one model to other models and to the situation *in vivo*.

Once the cancellous tissues from the model systems were characterised, it was possible to proceed with analysing of the effect of tissue harvest and *ex vivo* maintenance had upon the bone cells. In order to achieve a reliable conclusion regarding the status of tissue's viability, a number of different techniques were employed, some to analyse viability directly and others to observe matrix synthesis.

Explants were maintained within the Zetos culture system for various time points. Loaded explants received daily physiological loading of 4,000 microstrain for 5 min each. Unloaded controls, which simulated "disuse" were loaded every fourth day with a static compressive load for 30 s to measure the samples stiffness (quasi-static loading). Positive control explants for necrotic tissue were placed in a centrifuge tube containing 10 ml media

as in most stationary organ cultures, the tissue degrades when kept at the bottom of a pool of medium. Tissue heated at 55°C for 4-8 hours was used as negative control for all validation techniques. These dead cores were cultured in the Zetos culture system loaded, unloaded and submerged within media at the bottom of a 50 ml centrifuge tube. Heat treating the tissue was chosen as Sharkey *et al.*, (1991) found that cancellous bone cores 8 mm in diameter and 7 mm high incubated at 60°C for 20h displayed an increase of 47% in yield strain and a decrease of 25% in elastic modulus, while bone cores incubated at 56°C for 20 h showed no alterations in mechanical behaviour. Thus, the samples could be used for measuring sample stiffness within the Zetos system. Temperatures above 80°C caused significant reductions in mechanical strength (von Garrel and Knaepler, 1993). It is hypothesised that it is the collagen component that is responsible for the observed changes in mechanical properties. It is known that collagen solubilises at high temperatures. Cleavage of noncovalent bonds may occur at temperatures between 50-70°C and cleavage of covalent cross-links at temperature ranges of 70-100°C (Jackson *et al*, 1974).

The main findings of these experiments were as follows. No differences were observed between the morphology of explants cultured within the Zetos culture system with daily loading, without daily loading, or explants maintained submerged in static media (Fig.3c.4-7) irrespective of species. Each group was comparable to freshly harvested tissue (Fig.2c.37-39). No masses of empty lacunae or a vast number of cells with pyknotic nuclei were observed, which are characteristic of dead cells and tissue. A similar healthy tissue morphology was also seen for dead (heat treated explants) (Fig.3c.7), suggesting the lack of active enzymes present to degrade the tissue, as most enzymes are inactivated at 60°C. Again, no differences were observed with LDH levels measured within circulating media (this may be due to differences in media pH and should thus be repeated) suggesting cells were not continually dying during *ex vivo* maintenance (Fig.3c.23).

Variations in immunolabelling of marker proteins were species specific. No differences were observed due to culture conditions (Fig.4c.1-3). Lack of labelling for late marker proteins (osteocalcin, and type I collagen) in ovine and human tissue was due to the lack of active osteoblasts within the tissue. Lack of labelling of osteopontin and bone sialoprotein in ovine tissue was probably due to the lack of specificity for antibodies raised against human and rabbit antigens to bind to the ovine antigens. Osteonectin was the only protein detected in dead control tissue, suggesting that heat damaged epitope conformation.

Unfortunately, histological morphology of the cultured explants did not relate directly if the tissue was alive, active or functioning as it would *in vivo*. It only provided a visual guide to structure, cell types and location. There was no indication whether the cell's activities were up-regulated, down-regulated or remained the same. The nuclei of osteoclasts and osteoblasts have life-spans within the range of 10-120 days (Parfitt, 1995). Though some osteoclasts may have been created during culture within this system, this is not, on its own, conclusive. Signs of active metabolite synthesis and secretions were required, which lead to the investigation of *de novo* bone formation and protein synthesis.

Double fluorescent labelling of bone apposition showed *de novo* bone formation was occurring on the surface of human tissue cultured in both the Zetos loaded environment and the static cultured control tissue (Fig.4c.11,12, 13, and 14), thus, implying the cancellous tissue was still viable 15 days post-harvest. No actively remodelling areas were observed for the human Zetos cultured unloaded tissue. This lack of remodelling may have been due to the lack of stimulus, or more than likely, due to the nature of those specific explants being mainly in a state of quiescence. Sparse osteoid seams were observed in fresh explants fixed on day of harvest (Fig.2c.39) implying most of the tissue was in a state of quiescence. No double labels were observed with ovine or bovine tissue. The reasons for this result are unclear, but the different hypotheses were discussed in greater detail in chapter 4.

A number of limitations were observed for this technique (see chapter 4). Similar observations were made by other researchers. It was observed that different fluorochromes stained different amounts of tissue (Parfitt *et al.*, 1991). Calcification fronts along osteoid seams can be demonstrated by using morphological stains such as toluidine blue. However, the extent of this staining does not correlate well with the mineralising parameter as measured by tetracycline uptake (Compton *et al.*, 1985). Measurement of osteoid thickness is often influenced by magnification used due to the fact higher magnifications make it difficult to distinguish the osteoid seam from the thin endosteal membrane covering the quiescent bone surface. It is also important to use a staining technique that fully differentiates osteoid from mineralised bone matrix. It has been observed that values obtained from image analysis packages are often lower than those generated manually (Chavassieux *et al.*, 1985).

A technique that allows specific bone growth to be analysed in a non-destructive manner and with time serial examinations would be ideal. Ritman *et al.*, (1998) used the

heavy metal $SrCl_2$ as an X-ray analogue of the fluorophore staining (see chapter 4) for use with the microCT. Strontium can be used as a calcium substitute allowing the heavy metal deposits to be visualised and through the use of predetermined time intervals may be possible to calculate bone formation rate *ex vivo*.

One important question to bear in mind is - though collagen synthesis can be seen to occur *ex vivo* (double label, immunohistochemistry, histology), is it mineralized as it would *in vivo*? Physiological mineralisation is more than just deposition of calcium phosphates. It is a coordinated sequence of events involving the formation of hydroxyapatite and incorporation of specific proteins (collagen, osteocalcin, osteopontin, BSPII, and TGFβ).

The incorporation of the tritiated amino acid glycine into proteins was observed for all living explants, suggesting that some of the tissue was viable 15 days post-harvest. This incorporation was not observed for the dead tissue. Labelled proteins were observed in protein extracts as well as in the tissue sections. It was hypothesised that most of the labelled proteins harvested from the media were produced by the fibrous-like cells at the surfaces of the explants, as no positive labelling was observed for fresh tissue (Fig.4c.17). This hypothesis was confirmed when the radiolabelled sections were analysed. For all culture conditions, irrespective of species, metabolically active cells were observed on the surfaces of the cores (Fig.4c19-29). The most active cells appeared to be the fibroblast-like cells that covered the explant periphery and surrounding bone debris. Cross-sectional images demonstrated limited staining within the centre of the explant, suggesting either inadequate staining time (24h), concentration, or diffusion was taking place. This result correlated with the diffusion limitation observed for the fluorophores used for the double labelling of bone apposition. Autoradiography had the advantage of allowing the localisation of active cells to be pinpointed, but did not disclose which proteins were being synthesised. By sequencing the protein bands from the SDS-page gels it was established that collagen was one of the main types of proteins synthesised.

It was observed that the human tissue appeared to be most active followed by bovine then ovine tissue, which may be related to tissue density and nutrient diffusion. It was also observed that the loaded tissue had qualitatively more activity than static cultured explants, followed by least activity in unloaded Zetos cultured explants. It was difficult to get an accurate representation of events, due to the diffusion limitation observed throughout this validation work. Unfortunately, a system where non-loaded control bones

retain only limited (<35%) osteocyte viability, suggests that the culture method was not suitable even though loading increased the number of viable cells (Skerry, 1998). The absence of loading should not cause so many cells to die. This facet is important to bear in mind when analysing the results.

The results obtained for the levels of AlP present in the circulating media hinted that there may have been a mechanical role in the amount of AlP observed. Loaded explants contained a slightly higher amount of AlP than the unloaded and static cultured cores (Fig.4c.15). A number of factors could account for this, such as loading inducing more mineralisation, specific to individual explants by chance, or the fact that loading the tissue may have aided the movement of solutes into and out of the tissue. The reasoning behind the advantage that loading aids diffusion and mass transport is discussed later.

However, it is has been noted that cellular elements can remain within osteocyte lacunae for up to 16 weeks after bone death (Kenzora *et al.*, 1978). This statement should be borne in mind when considering data from these validation experiments and further highlights the need for an accurate, reliable, and reproducible stain to directly label living and dead cells within the explant.

A number of potential stains were utilised to label live and dead cells simultaneously, but none were found to be satisfactory. Each stain had its own limitation (see Chapter 3). The main drawback of all of the potential labels was the lack of penetration into the tissue (Fig.3c12-15). A maximum penetration depth of around 500 μm was observed. This was also seen for the fluorochrome labels and the tritiated glycine.

An added barrier to the penetration of solutes into the cancellous bone tissue was the development of a fibrous-like skin over the explant periphery. This fibrous-like skin was several cell layers thick (Fig.3c.2). It was the most pronounced in bovine explants, followed by human and then ovine explants, independent of culture method. However, no fibrous like tissue was observed surrounding the periphery of dead (heat killed) control explants, confirming that heat treatment was enough to kill the cells of the core. This fibrous tissue was formed during culture and was observed to be metabolically active and living (Fig.3c.13-14 and Fig.4c19-28). The formation of this fibrous-like tissue was hypothesised to be caused by cells migrating to broken tissue through chemotaxis, mimicking wound healing. However, the amount of fibrous-like cells may have been enhanced by the presence of foetal calf serum (FCS) in the media. It is common to exclude FCS from the media of organ culture to avoid unwanted growth of fibrous-like cells

(Majeska and Gronowicz; 2002). Then again, factors present in serum, may inactivate inhibitors and proteolytic enzymes released during tissue harvest (Bingham and Raisz; 1974) and as a consequence decreases the amount of necrotic cells observed in serum free cultures. It is an experimental dilemma on whether to use FCS or not. One aspect is clear and that is all results observed within this study are only applied to experiments conducted in our laboratory and to one specific batch of serum (Biochrome-S 0113/5 Lot 615B). Future work should include the development of serum-free media.

Another observation was the presence of bone debris within the soft tissue of the cores created during explant harvest (Fig.3c.1). The presence of debris was observed to be worse at the explant periphery, where the drilling of the core took place, with less being formed by the annular saw. The distance that the debris penetrated into the soft tissue was as much as 1mm, causing a potential 36% loss of tissue volume due to damage. This result was correlated to dead tissue observed through viability staining of cores with calcein AM and ethidium homodimer 1 (Fig.3c.10), as well as lack of metabolically active cells observed through autoradiography (Fig.4c.23). The bone debris were also observed to be an attractant to the fibrous-like cells (Fig.3c1vi and 4c.19vi). Ideally, in the future, a new designed drill bit should be implemented. This debris may be blocking the penetration of labels such as alizarin and calcein, as well as hindering the exchange of nutrients and waste from the centre of the bone core, limiting the life-span of the tissue in the culture.

One of the initial observations to be made was the damage the black rubber gaskets caused to the periphery of the explants (Fig.3c.3). This problem was resolved immediately by the removal of all gaskets from the chambers and future studies.

It was observed during all experiments, irrespective of species used, that loaded tissue (live or dead) increased in stiffness during the culture period (Fig.3c.21). It was hypothesised that healthy tissue would have net bone formation and that this could be detected by a rise in sample stiffness due to the fact that compressive strength of bone is approximately proportional to the square of the apparent density, and the compressive modulus is approximately proportional to the cube of the apparent density (Carter and Hayes, 1977). Unloaded samples, which mimic disuse, should decrease in stiffness due to net bone resorption. The static compression that these unloaded cores received every four days should not stimulate the cells as dynamic loading would (Lanyon and Rubin, 1984). Dead tissue was assumed to decrease in stiffness due to the breakdown of tissue. As this was not the case, a different approach to analysing the tissue on line will have to be

adopted. There is an indication that calcium phosphate precipitation may be occurring on the outer surfaces of the tissue, which may be the cause of the observed increase in sample stiffness. It is known from the literature that bone matrix alone is sufficient to support mineralisation, even with the absence of viable osteoblasts, if an appropriate level of inorganic phosphate (β-glycerolphosphate) is present (Marsh *et al.,* 1995). A number of artefactual double labels were observed at the periphery of the explants from dead and living tissue (Fig.4c.6ii, ii and 4c.14vi) supporting this view.

All of these observations require further analysis to prove or disprove formulated hypotheses. A number of changes are required to maximise the potential of the system. There are a number of minor limitations associated with this culture system, such as cost (initial purchase, though maintenance is low), man hours needed to maintain the system and to analyse the results, as well as all limitations associated with organ culture. There is also a limitation of surgery for tissue utilisation (several months). There is also the limitation that not enough healthy cores can be harvested from a single patient to be used for statistical analysis.

The biggest limitation to this culture system is the diffusion constraints associated with the calcified bone matrix. It is known that, *in vivo*, no cell is more than 200 μm away from a blood vessel. Thus, nutrients and waste metabolites are constantly being exchanged. Cartilage, on the other hand, is composed mainly of glycoproteins, thus, it can hold a large amount of water. This composition allows gas, nutrients and waste to be exchanged via diffusion. It is possible that this system may be better directed towards the *ex vivo* culture of cartilage explants.

It is only by being aware of the systems limitations can the results be interpreted correctly, avoiding inappropriate conclusions.

Scientists often require simplified systems in order to better understand biological systems. This system offers just that. It has the advantages over animal experimentations, in that one factor can be altered whilst other variables are constant, thus allowing the effects of one particular agent to be tested. However, the mere fact that systemic factors are absent makes results difficult to extrapolate to the *in vivo* situation.

This system has the advantage that the "3Rs" approach to animal experimentation can be applied. Thus, *reducing* the number of animals used in experiments, *refining* current practices to decrease the suffering of animals, and even *replacing* animals with alternatives—such as the use of human tissue cultures—whenever possible.

A criterion to apply when selecting a loading device is to avoid models used for studies in single publications and not again, or ones confined to single laboratories, especially if that was where it was designed.

Mueller (2003) utilises microcompression in combination with microCT that allows direct 3D visualisation and quantification of fracture progression on the microscopic level (Fig.5a.1). The image over-emphasises how loading the cancellous explant may affect some bone trabeculae more than others. Close examination of the images in figure 5a.1 show that rod shaped trabeculae alter their shape more than plate-like trabeculae. This highlights the reason why not all surfaces of cancellous tissue would be remodelling. Remodelling would only occur on surfaces exposed to unphysiological strain, thus adapting its architecture to better resist the deformation caused during loading. Though this amount of strain would not be applied to cancellous tissue cultured within the Zetos system, or in the *in vivo* situation.

Bone represents a porous tissue containing a fluid phase, solid matrix, and cells. Tissue requires an adequate supply of nutrients for anabolic activity as well as a mechanism for removal of waste products formed during catabolic activities. Interstitual fluid is believed to provide this, as well as the ability to transport mineral ions to the bone tissue allowing storage and retrieval of those mineral ions when they are needed by the body. Interstitial fluid flow is the movement of a fluid phase within the spaces (pores) of the solid matrix. These pores are vascular spaces, lacuno-canalicular systems and matrix micropores (chapter 4). The biochemical composition of the fluid that flows through these pores is unknown due to the practical difficulties to obtain enough to analyse. This interstitial fluid flow is essential to bone vitality. Deformation-driven bone fluid movement in bone tissue, where deformation of the medium influences the flow of fluid and vice versa, is known as poroelasticity. The theory was first proposed in 1935 by Biot regarding soil consolidation (they way structures settled on fluid-saturated porous soils). It has since been applied to problems in rock mechanics as well as bone.

Osteocytes are completely encased in the mineralised matrix of bone, their ability to survive and function is entirely dependent on mass transport through the small interconnecting channels (~200 nm wide) of the lacunar-canalicular system. Transport of solutes (nutrients and bioactive molecules) through the lacunar-canalicular system occurs

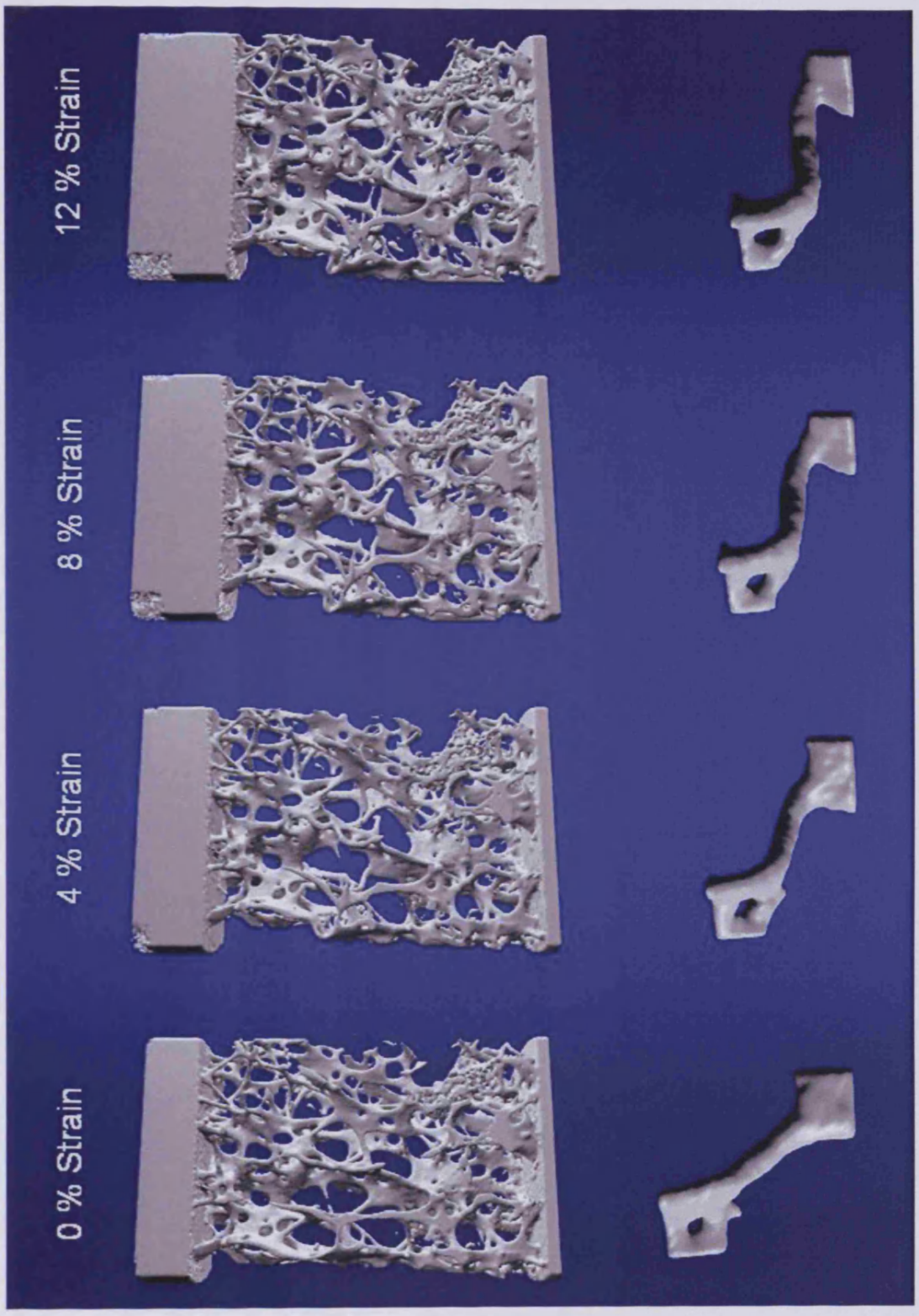

Figure 5a.1. Failure assessment in human spine using time-lapsed microCT imaging. Upper row shows a specimen that is compressed and imaged in steps of 4% strain. The lower row shows how micro-compression can be used to non-invasively monitor the deformation of individual elements. [With permission from Mueller, 2003]

by diffusion and convection. Diffusion alone may not be sufficient to ensure adequate transport to and from osteocytes that are not in close proximity of vascular canals. Bone cells in cancellous bone usually receive nutrients from the diffusion of solutes from the blood vessels within the bone marrow (Dillaman *et al.,* 1991). Intramedullary pressure and pulsatile pressure caused by the heartbeat have been implicated in regulating interstitial fluid flow (Kelly, 1990). Mechanical loading creates pressure gradients which drive fluid flow from areas of bone in compression to those in tension. Knothe-Tate's *in vitro* model (Gatzka *et al.,* 2000; Knothe and Knothe-Tate, 2000; Knothe-Tate and Knothe, 2000) demonstrated a strong positive correlation between transport and number of loading cycles, as well as loading rate. However, mechanical loading did not seem to enhance the diffusion constant of glucose in bone demonstrated by Lang *et al.,* (1974).

It is this drive of fluid through lacunar-canalicular system created by mechanical loading that may aid the maintenance of cancellous bone tissue *ex vivo* for a prolonged time. This would not occur in unloaded and static cultured explants. Currently, the bone debris and fibrous-like tissue layer that surrounds the periphery of the explants may inhibit the full potential of the system. Though this fluid flow effect has only been observed in cortical tissue *in vivo*, it is highly probably the same can be extrapolated to cancellous tissue.

Initial future work with the Zetos culture system would involve developing a better way to harvest bone explants. It may be possible to harvest cubes cut solely with the Exakt band saw or annular saw, or to redesign the drill bit to allow better cooling and dust removal. A new harvest technique, along with the development of serum free media may reduce the problem of diffusion previously observed.

Originally, bone cores (5 mm high and 10 mm in diameter) were chosen for the amount of cells present (~2 million) required for biochemical analysis (Burger, 2001). If the size of the core could be altered to increase its length and reduce its diameter, less diffusion would be required. Minimum size core needed for biomechanical testing would be 7.5 mm in diameter and 6.5 mm in height (Linde, Hvid and Madsen, 1992). Any smaller and the mechanics are effected due to the disintegration of the cut surface in contact with the loading platen (Chapter 1b). Of course, for this to be realistic, a reduction in damage caused to the tissue would have to be implemented. It is possible that using superoxide dismutase, which controls oxygen toxicity by converting the superoxide radical to less toxic forms, would reduce the amount of cell death associated with harvest procedure.

Another limiting factor to the maintenance of cancellous tissue in the Zetos system is the inadequate bathing of the explant with media. The area for diffusion to take place was greatly reduced, and far more inferior to the bathing of explants in centrifuge tubes highlighted in figure 4c.5. By harvesting cores with a smaller diameter, say 9 mm as apposed to 10 mm, better bathing would be observed at the sides of the explant, however, this would not help the barrier the base plate causes to the underside of the core. Presently, at Jones' laboratory, a new chamber is being developed that has a piston-like lower side instead of the base plate. The X-ring causes the lower piston to release from the surface of the core after loading as it does on the upper side, thus, allowing the surface to be bathed in media, aiding diffusion. Another idea would be to create troughs running along the surface of the base plate, allowing media to reach more of the under surface of the tissue. How this will affect samples loading is unknown.

Theoretically, the best structure to increase nutrient diffusion into the centre of the cores would be a doughnut shaped explant. This shape could be achieved by drilling a small 1-2 mm hole in the centre of the explant. Thus, diffusion could occur on both sides. However, the limitation to this would be more cell death caused by the drilling, and the loss of trabecular integrity, which would affect the loading of the tissue.

To overcome the limitations of label diffusion observed while assessing bone cell viability and matrix synthesis, steps are underway to analyse cryo-fixed sections for the presence of LDH with Nobel, Edinburgh. LDH is a stable, cytosolic enzyme, which transfers hydrogen using NAD+ as a hydrogen acceptor, thus, catalysing the oxidation of L-lactate to pyruvate. LDH activity is present in all the cells of the body, predominantly in the cytoplasm. It may also be possible to make *in situ* hybridisation studies on sections for certain bone markers, again avoiding label diffusion.

Further scientific research within our group will analyse the effect of $TGF\beta_3$ and PTH on bone cells, comparing that to *in vivo* and *in vitro* situation. The initial events associated with bone biomaterial integration will also be evaluated, again compared to the *in vivo* and *in vitro* situation.

The Zetos culture system has been validated as having potential to maintain cancellous bone biopsies viable *ex vivo* for at least 14 days. Cell behaviour was observed to correlate to that of the *in vivo* situation (i.e. bone apposition and protein synthesis), though a more thorough analysis would be required to establish this to be genuine. Currently the harvest technique causes a maximal 36% loss of viable tissue due to bone debris, and the

design of the chamber limits the bathing of the tissue in media and in consequence limits the area for the diffusion of nutrients into and out of the explants. Nevertheless, a vast amount of cells were synthesising protein and producing *de novo* bone. If the limitations can be overcome, or at least improved, then there is potential for this system to become routinely used in bone research. Thus, providing future means to allow bone-biomaterial interactions and bone-biomaterial interfaces to be studied, in the long run, reducing, refining and replacing the need for animal experimentation.

Chapter 6.
References

6.a. Journals, Books and Abstracts

- Ahrens M., Schlegel U., and Halm H., (2003). Perfusion culture for cortical bone. *Eur Cell Mater* 2003; **5** (2): 49-50.
- Albinius (1757). Academicarum annotation liber primus (septemus). *Leiden J. and Verbeek H. 1754-1766.* 7: 48-49. *Cited by:* Ricqlès A. de., Meunier F.J., Castanet J., and Francillion-Vieillot H. (1991). Comparative Microstructure of bone. *In:* Hall B.K. (ed.) *Bone Volume 3. Bone matrix and bone specific products.* CRC Press, USA
- Anderson G. and Bancroft J. (2002). Tissue processing and microtomy. *In:* Bancroft J.D. and Gamble M. *Theory and practice of histological techniques. Fifth ed.* Harcourt Publihers. London. pp. 85-107
- ap Gwynn I., Wade S., Ito K., and Richards R.G. (2002). Novel aspects to the structure of rabbit articular cartilage. *Eur Cell Mater.* **4**:18-29.
- Aarden E.M., Wassenaar A.M., Alblas M.J. and Nijweide P.J., (1996). Immunocytochemical demonstration of extracellular matrix proteins in isolated osteocytes. *Histochemistry and Cell Biology* **106**: 495–501.
- Arlot M.E., Delmas P.D., Chappard D., and Meunier P.J. (1990). Trabecular and endocortical bone remodeling in postmenopausal osteoporosis: comparison with normal postmenopausal women. *Osteoporos Int.* **1** (1):41-9.
- Ayalon J., Simkin A., Leichter I., and Raifmann S. (1987). Dynamic bone loading exercises for postmenopausal women: effect on the density of the distal radius. *Arch Phys Med Rehabil.* **68**: 280-3.
- Bartholinus C. (1676). Diaphragmatis structure nova. *Acta Med. Phil. Hafn.* **4**: 14.
- Barlet J.P., Coxam V., and Davicco M.J. (1995). Physical exercise and the skeleton. *Arch Physiol Biochem.* **103** (6):681-98.
- Behrens J.C., Walker P.S., and Shoji H. (1978). Variations in strength and structure of cancellous bone at the knee. *J Biomech.* 7 (3):201-7.
- Belchier J.B. (1736). An account of the bone of animals being changed to a red colour by aliment only. *Phil. Trans. R. Soc. London.* **39**: 299-303.
- Bellows C.G., Aubin J.E., and Heersche J.N. (1991). Initiation and progression of mineralization of bone nodules formed in vitro: the role of alkaline phosphatase and organic phosphate. *Bone Miner.* **14** (1):27-40.
- Bellows C.G, Heersche J.N, and Aubin J.E. (1992). Inorganic phosphate added exogenously or released from beta-glycerophosphate initiates mineralization of osteoid nodules *in vitro*. *Bone Miner.* **17** (1):15-29.

- Bianco P., Fisher L.W., Young M.F., Termine J.D., and Robey P.G. (1990). Expression and localization of the two small proteoglycans biglycan and decorin in developing human skeletal and non-skeletal tissues. *J Histochem Cytochem.* **38** (11):1549-63.
- Bianco P., Fisher L.W., Young M.F., Termine J.D., and Robey P.G. (1991). Expression of bone sialoprotein (BSP) in developing human tissues. *Calcif Tissue Int.* **49** (6):421-6.
- Binderman I., Zor U., Kaye A.M., Shimshoni Z., Harell A., and Somjen D. (1988). The transduction of mechanical force into biochemical events in bone cells may involve activation of phospholipase A2. *Calcif Tissue Int.* **42**(4):261-6.
- Bingham P.J., and Raisz L.G. (1974). Bone growth in organ culture: effects of phosphate and other nutrients on bone and cartilage. *Calcif Tissue Res.* **14** (1):31-48.
- Bolander M.E., Robey P.G., Fisher L.W., Conn K.M., Prabhakar B.S., and Termine J.D. (1989). Monoclonal antibodies against osteonectin show conservation of epitopes across species. *Calcif Tissue Int.* **45** (2):74-80.
- Boppart M.D., Kimmel D.B., Yee J.A., and Cullen D.M. (1998). Time course of osteoblast appearance after in vivo mechanical loading. *Bone.* **23** (5):409-15.
- Boskey A.L. (2001). Bone Mineralization. *In:* Cowin S.C. (ed.) (2001) *Bone Mechanics Handbook.* CRC Press, London.
- Boskey A.L, Gadaleta S., Gundberg C., Doty S.B., Ducy P., and Karsenty G. (1998). Fourier transform infrared microspectroscopic analysis of bones of osteocalcin-deficient mice provides insight into the function of osteocalcin. *Bone.* **23** (3):187-96.
- Boskey A.L. and Paschalis E. (2000). Matrix proteins and biomineralization. *In:* Davies JE. (ed.) *Bone Engineering.* EM Squared Incorporated. Toronto Canada pp.44-63.
- Boyce B.F., Hughes D.E., and Wright K.R. (1998). Methods for studying cell death in bone. *In:* Arnett T.R. and Henderson B. (1998). Methods in Bone Biology. Chapman & Hall, London, UK. Pp127-148.
- Bozzola J.J., & Russell L.D. (1992). Electron microscopy. Jones & Bartlett Publishers, Boston, pp 9 & 199.
- Bronk J.T., Meadows T.H., and Kelly P.J. (1993). The relationship of increased capillary filtration and bone formation. *Clin Orthop Relat Res.* **293**:338-45.
- Buckwalter J.A., and Cooper R.R. (1987). Bone structure and function. *Instr Course Lect.* **36**: 27-48.
- Buckwalter J.A, and Rosenberg L.C. (1982). Electron microscopic studies of cartilage proteoglycans. Direct evidence for the variable length of the chondroitin sulfate-rich region of proteoglycan subunit core protein. *J Biol Chem.* **257**(16):9830-9.
- Burger E.H. (2001). Experiments on cell mechanosensitivity: Bone cells as mechanical engineers. *In:* Cowin S.C. (ed.) (2001). *Bone Mechanics Handbook.* CRC Press, London.
- Butler W.T. (1989). The nature and significance of osteopontin. *Connect Tissue Res.* **23** (2-3):123-36.
- Burr D.B., Schaffler M.B., Yang K.H., Lukoschek M., Sivaneri N., Blaha J.D., and Radin E.L. (1989). Skeletal change in response to altered strain environments: is woven bone a response to elevated strain? *Bone.* **10** (3):223-33.

- Callis G.M. (2002). Bone. *In:* Bancroft J.D. and Gamble M. *Theory and practice of histological techniques. Fifth ed.* Harcourt Publihers. London. pp. 269-301
- Carrel, A. (1912). On the permanent life of tissue outside of the organism. *J. Exp. Med.* **15:** 516-528.
- Carrel, A. (1923). A method for the physiological study of tissues *in vitro. J. Exp. Med.* **38:** 407-418.
- Carter DR. (1982). The relationship between in vivo strains and cortical bone remodeling. *Crit Rev Biomed Eng.* **8** (1):1-28.
- Carter DR., Harris W.H., Vasu R., and Caler W.E (1981). The mechanical and biological response of cortical bone to *in vivo* strain histories. *In:* Cowin S.C. (ed.). *Mechanical Properties of Bone.* ASME, New York, Chapter 6.
- Carter D.R., and Hayes, W.C. (1977). The Compressive Behaviour of Bone as a Two-Phase Porous Structure. *J. Bone Jt Surg.* **59A.** (7) 954-962.
- Chavassieux PM., Arlot M.E., and Meunier PJ. (1985). Intermethod variation in bone histomorphometry: comparison between manual and computerised methods applied to iliac bone biopsies. *Bone.* **12:** 1-6
- Churches A.E., and Howlett C.R. (1982). Functional adaptation of bone in response to sinusoidally varying controlled compressive loading of the ovine metacarpus. *Clin Orthop Relat Res.* **168**:265-80.
- Clarke M.C.H., Savil J., Jones D.B., Nobel B.S., and Brown S.B. (2003). *J. Cell Biol.* **160**:4 577-587.
- Clark R.A.F. (1996). The molecular and cellular biology of wound repair. Plenum Press. New York.
- Colowick S.P. and Kaplan N.O. (1982). Methods in Enzymeology. Volume 82. Structural and Contractile Proteins. Part A. Extracellular Matrix. Edited by Cunningham L.W. & Frederiksen D.W. Chapter 2. Preparation and Characterisation of the different types of collagen. By Miller E.J. and Rhodes R.K. pp 33-44
- Compston J.E. (1994). Connectivity of cancellous bone: assessment and mechanical implications. *Bone.* **15**: 463-466.
- Compston J. (1998). Bone histomorphometry. *In:* Arnett T.R. and Henderson B. (1998). Methods in Bone Biology. Chapman & Hall, London, UK. pp. 177-197
- Compston J.E., Vedi S., and Webb A. (1985). Relationship between toluidine blue-stained calcification fronts and tetracycline labelled surfaces in normal human iliac crest biopsies. *Calcif. Tissue Int.*, **37**: 32-35.
- Coons A.H., Creech H.J., and Jones R.N. (1941). Immunological properties of an antibody containing a fluorescent group. *Proc. Soc. Exp. Biol. Med.* **47**: 200-202.
- Culmann C. (1866). Die Graphische Statik. Zurich.
- Currey J.D. (1984). What should bones be designed to do? *Calcif Tissue Int.* **36** Suppl 1:S7-10.
- Dallas S.L., Zaman G., Pead M.J., and Lanyon L.E. (1993). Early strain-related changes in cultured embryonic chick tibiotarsi parallel those associated with adaptive modeling *in vivo. J Bone Miner Res.* **8** (3):251-9.
- David V., Marino M., Guignandon A., Laroche N., Jones D.B., and Vico L. (2003). Performance of a new cancellous bone explants tissue culture-loading system. *Eur Cell Mater* **5** (2):100.

- Davies J.E., and Hosseini M.M. (2000). Bone formation and healing. *In:* Davies JE. (ed.) *Bone Engineering.* EM Squared Incorporated. Toronto Canada pp.1-14.
- Delany A.M., Amling M., Priemel M., Howe C., Baron R., and Canalis1 E. (1998). Osteopenia and decreased bone formation in osteonectin-deficient mice. *J Clin Invest.* **105** (7): 915–923.
- Denizot F., and Lang R. (1986). Rapid colorimetric assay for cell growth and survival. Modifications to the tetrazolium dye procedure giving improved sensitivity and reliability. *J Immunol Methods.* **89** (2):271-7.
- Doty S.B (1981). Morphological evidence of gap junctions between bone cells. *Calcif. Tissue Int.* **33**: 509-512.
- Ducy P., Desbois C., Boyce B., Pinero G., Story B., Dunstan C., Smith E., Bonadio J., Goldstein S., Gundberg C., Bradley A., and Karsenty G. (1996). Increased bone formation in osteocalcin-deficient mice. *Nature.* **382** (6590):448-52.
- Duhamel H.L. (1739). Su rune racine qui a la faculté de teindre en rouge les os des animaux vivants. *Mem. Acad. R. Sci. Paris.* **52**: 1-13.
- Duhamel H.L. (1740). Observations and experiments with madder root. *Phil. Trans R. Soc. London.* **8**: 420-434.
- Duhamel H.L. (1742). Sur le deéveloppement et la crue des os des animaux. *Mem. Acad. R. Sci. Paris.* **55**: 354-370.
- Duncan RL, and Turner CH. (1995). Mechanotransduction and the functional response of bone to mechanical strain. *Calcif Tissue Int.* **57**(5):344-58.
- Dunstan C.R., Evans R.A., Hills E., Wong S.Y., and Higgs R.J. (1990). Bone death in hip fracture in the elderly. *Calcif Tissue Int.* **47** (5):270-5.
- el Haj A.J., Minter S.L., Rawlinson S.C., Suswillo R., and Lanyon L.E. (1990). Cellular responses to mechanical loading *in vitro. J Bone Miner Res.* **5** (9):923-32.
- Elmardi A.S., Katchburian M.V., and Katchburian E. (1990). Electron microscopy of developing calvaria reveals images that suggest that osteoclasts engulf and destroy osteocytes during bone resorption. *Calcif Tissue Int.* **46** (4):239-45.
- Eriksen E.F., Gundersen H.J., Melsen F., and Mosekilde L. (1984). Reconstruction of the formative site in iliac trabecular bone in 20 normal individuals employing a kinetic model for matrix and mineral apposition. *Metab Bone Dis Relat Res.* **5** (5):243-52.
- Eriksen E.F, Langdahl B., Vesterby A., Rungby J., and Kassem M. (1999). Hormone replacement therapy prevents osteoclastic hyperactivity: A histomorphometric study in early postmenopausal women. *J Bone Miner Res.* **14** (7):1217-21
- Fedarko N.S., Vetter U.K., Weinstein S., and Robey P.G. (1992). Age-related changes in hyaluronan, proteoglycan, collagen, and osteonectin synthesis by human bone cells. *J Cell Physiol.* **151**(2):215-27.
- Feldkamp L.A., Goldstein S.A., Parfitt A.M., Jesion G., and Kleerekoper M. (1989). The direct examination of three-dimensional bone architecture *in vitro* by computed tomography. *J. Bone Miner. Res.* **4**: 3

- Fell, H.B., and Robinson, R. (1929). The growth development and phosphatase activity of embryonic avian femora and limb-buds cultivated *in vitro*. *Biochem. J.* **23**, 767.
- Fisher L.W., McBride O.W., Termine J.D., and Young M.F. (1990). Human bone sialoprotein. Deduced protein sequence and chromosomal localization. *J Biol Chem.* **265** (4):2347-51.
- Fisher L.W., Stubbs J.T. 3rd, and Young M.F. (1995). Antisera and cDNA probes to human and certain animal model bone matrix noncollagenous proteins. Acta *Orthop Scand Suppl.* **266**:61-5.
- Fisher L.W., Termine J.D., and Young M.F. (1989). Deduced protein sequence of bone small proteoglycan I (biglycan) shows homology with proteoglycan II (decorin) and several nonconnective tissue proteins in a variety of species. *J Biol Chem.* **264** (8):4571-6.
- Foellmer H.G., Kawahara K., Madri J.A., Furthmayr H., Timpl R., and Tuderman L. (1983). A monoclonal antibody specific for the amino terminal cleavage site of procollagen type I. *Eur J Biochem.* **134** (1):183-9.
- Freshney R.I. (1986). Animal Cell Culture. IRL Press Oxford & Washington DC pp 183-216.
- Freshney R.I. (2000). Culture of animal cells – a manual of basic techniques, 4th edition. Wiley-Liss. New York, USA. Chapter 1, 2, 8, and 21.
- Freshney R.I. and Morgan D. (1978). Radioisotopic quantitation in microtitration plates by an autofluorographic method. *Cell Biol. Int. Rep.* **2**: 375.
- Freshney R.I., Paul J., and Kane I.M. (1975). Assay of anti-cancer drugs in tissue culture: conditions affecting their ability to incorporate 3H-leucine after drug treatment. *Br. J. Cancer.* **31**: 89.
- Frost H.M.. (1960a). Some aspects of the mechanics and dynamics of blood-bone interchange. *Henery Ford Hosp. Med. Bull.*, **8**: 36.
- Frost H.M.. (1960b). An economical microfluorescence set-up for detection of tetracyclines in bone. *Henry Ford Hosp Med Bull.* **8**:197-8.
- Frost H.M. (1980). Resting seams: "on" and "off" in lamellar bone forming centers. *Metab. Bone Dis Rel. Res.* **2S**: 167-170.
- Frost H.M. (1987). The mechanostat: a proposed pathogenic mechanism of osteoporoses and the bone mass effects of mechanical and nonmechanical agents. *Bone Miner.* **2** (2):73-85.
- Frost H.M. (1999). Muscle, bone, and the Utah paradigm: a 1999 overview. *Med Sci Sports Exerc.* **32** (5):911-7.
- Fuller K., Owens J.M., Jagger C.J., Wilson A., Moss R., and Chambers T.J. (1993). Macrophage colony-stimulating factor stimulates survival and chemotactic behavior in isolated osteoclasts. *J Exp Med.* **178** (5):1733-44.
- Gagliardi D. (1723). Anatome osium. Lugduni Batavorum, apud Henricium Mulhovium. *Cited by:* Ricqlès A. de., Meunier F.J., Castanet J., and Francillion-Vieillot H. (1991). Comparative Microstructure of bone. *In:* Hall B.K. (ed.) *Bone Volume 3. Bone matrix and bone specific products.* CRC Press, USA

- Galileo G.C. (1638). Discorsi e Dimostrazioni matematiche. Leiden. *Cited by:* Ricqlès A. de., Meunier F.J., Castanet J., and Francillion-Vieillot H. (1991). Comparative Microstructure of bone. *In:* Hall B.K. (ed.) *Bone Volume 3. Bone matrix and bone specific products.* CRC Press, USA
- Gegenbaur, C. (1864). Ueber die Bildung Knochenstruktur. *Jena Zeitsch. Med. Naturwiss.* **1**: 343-369. *Cited by:* Ricqlès A. de., Meunier F.J., Castanet J., and Francillion-Vieillot H. (1991). Comparative Microstructure of bone. *In:* Hall B.K. (ed.) *Bone Volume 3. Bone matrix and bone specific products.* CRC Press, USA
- Genant H.K. Wu C.Y., Van Kuijk C., and Nevitt M. (1993). Vertebral fracture assessment using a semiquantitative technique. *J. Bone Miner. Res.* **8**: 1137-1148.
- Giachelli C.M. (1999). Osteopontin. In: Kreis T., and Vale R (e.d.). Guidebook to the Extracellular Matrix, Anchor, and Adhesion Proteins. (Second Ed.) Oxford University Press. Oxford, Uk.
- Gilmour D.T., Lyon G.J., Carlton M.B., Sanes J.R., Cunningham J.M., Anderson J.R., Hogan B.L., Evans M..J, and Colledge W.H. (1998). Mice deficient for the secreted glycoprotein SPARC/osteonectin/BM40 develop normally but show severe age-onset cataract formation and disruption of the lens. *EMBO J.* **17** (7):1860-70.
- Goldstein S.A. (1987). The Mechanical Properties of Trabecular Bone: Dependence on Anatomical Location and Function. *J. Biomechanics.* **20** (11/12) 1055-1061.
- Goldstein J.I., Newbury D.E., Echlin P., Joy D.C., Romig A.D., Lyman C.E., Fiori C., and Lifshun E. (1992). Scanning Electron Microscopy and X-ray Microanalysis Second edition. Plenium Press. New York and London. Chapter 1. pp.2.
- Goldstein S.A., Wilson D.L., Sonstegrad D.A., and Matthews L.S. (1983). The Mechanical Properties of Human Tibial Trabecular Bone as a Function of Metaphyseal Location. *J. Biomechanics.* **16** (12) 965-969.
- Goodship A.E., Lanyon L.E., and McFie H. (1979). Functional adaptation of bone to increased stress. An experimental study. *J Bone Joint Surg Am.* **61**(4):539-46.
- Goodsir J. (1845). The structure and economy of bone. In: Anatomical and Pathalogical Observations. Goodsir J and Goodsir H.D.S. Eds. Myles MacPhail, Edinburgh.
- Gray, H., Pickering Pick, T., and Howden, R. (1974). *Gray's Anatomy.* Running Press. Philadelphia, USA. p183.
- Goshi N., Ogihara A., and Ohno H. (1989). Histological alterations in rat tibia caused by the sciatic neurectomy. J. Electron Microscopy. **38**:219
- Hales S. (1927). Statistical Essays. W&J Innys, London.
- Hales S. (1731). Vegetables Statics. 1731-1733. W Innys, London. *Cited by:* Ricqlès A. de., Meunier F.J., Castanet J., and Francillion-Vieillot H. (1991). Comparative Microstructure of bone. *In:* Hall B.K. (ed.) *Bone Volume 3. Bone matrix and bone specific products.* CRC Press, USA
- Hall B.K. (1992). Historical Overview of Studies on Bone Growth and Repair. *In*: Hall B.K. (ed.) *Bone Volume 6, Bone Growth A.* CRC Press, USA
- Hauschka P.V., Lian J.B., Cole D.E.C. and Gundberg C.M. (1989). Osteocalcin and related Ca2+ - binding proteins in bone. *Physiol. Rev.* **69**:90-1047.

- Hauschka P.V., Lian J.B., and Gallop P.M. (1975). Direct identification of the calcium-binding amino acid, gamma-carboxyglutamate, in mineralized tissue. *Proc Natl Acad Sci USA.* **72** (10):3925-9.
- Havers, C. (1691/1692). Osteologia Nova: or some new observations of the bones, and the parts belonging to them. London (reprinted in Principles of Bone Remodeling, Enlow, D.H.. Ed., Charles C. Thomas, Springfield, IL, 1963).
- Hecker, J.F. (1983). *The Sheep as an Experimantal Animal.* Academic Press. London. p.203.
- Harrison, R. G. (1907). Observations on the living developing nerve fiber. *Proc. Soc. Exp. Biol. Med.* **4:** 140-143.
- Herissant M. (1758). Eclaircissements sur l'ossification. *Mém. Acad. Roy. Sci.* 322-336. *Cited by:* Ricqlès A. de., Meunier F.J., Castanet J., and Francillion-Vieillot H. (1991). Comparative Microstructure of bone. *In:* Hall B.K. (ed.) *Bone Volume 3. Bone matrix and bone specific products.* CRC Press, USA
- Hert J. (1969). Acceleration of the growth after decrease of load on epiphyseal plates by means of spring distractors. *Folia Morphol.* **17** (2):194-203.
- Hert J., Sklenska A., Liskova M. (1971). Reaction of bone to mechanical stimuli. 5. Effect of intermittent stress on the rabbit tibia after resection of the peripheral nerves. *Folia Morphol.* **19** (4):378-87.
- Hillam R.A. and Skerry T.M. (1995). Inhibition of bone resorption and stimulation of formation by mechanical loading of the modeling rat ulna in vivo. *J Bone Miner Res.* **10** (5): 683-9.
- Hobatho M.C., Rho J.Y., and Ashman R.B. (1997) Anatomical variation of human cancellous bone mechanical properties in vitro. *Stud Health Technol Inform.* **40**:157-73.
- Holley R.W. (1975). Control of growth of mammalian cells in cell culture. *Nature.* **258** (5535):487-90.
- Holtrop M.E. (1991). Light and electron microscopic structure of bone forming cells. *In:* Hall. B.K. (ed.) (1991). *The osteoblast and osteocyte.* CRC Press, USA.
- Hopwood D. (2002). Fixation and fixatives. *In:* Bancroft J.D. and Gamble M. *Theory and practice of histological techniques. Fifth ed.* Harcourt Publishers. London. pp. 63-84.
- Howship J. (1817). Experiments and observation in order to ascertain the means employed by the animal economy in the formation of bone. *Med. Chir. Trans.* **6**: 263-295.
- Hulett H.R., Coukell A., and Bodmer W. (1970). Tissue-typing instrumentation using the fluorochromatic cytotoxicity assay. *Transplantation.* **10** (1):135-7.
- Humphrey G.M. (1858). A Treatsie of the Human Skeleton. Cambridge. *Cited by:* Ricqlès A. de., Meunier F.J., Castanet J., and Francillion-Vieillot H. (1991). Comparative Microstructure of bone. *In:* Hall B.K. (ed.) *Bone Volume 3. Bone matrix and bone specific products.* CRC Press, USA
- Hunter J. (1798). Experiments and observations on the growth of long bones. *Hunter's Works.* Palmer D.F. (ed.) 1837. Longman, London, 315. *Cited by:* Ricqlès A. de., Meunier F.J., Castanet J., and Francillion-Vieillot H. (1991). Comparative Microstructure of bone. *In:* Hall B.K. (ed.) *Bone Volume 3. Bone matrix and bone specific products.* CRC Press, USA

- Inaoka T., Lean J.M., Bessho T., Chow J.W., Mackay A., Kokubo T., and Chambers T.J. (1995). Sequential analysis of gene expression after an osteogenic stimulus: c-fos expression is induced in osteocytes. *Biochem Biophys Res Commun.* **217** (1):264-70.
- Ingram R.T., Clarke B.L., Fisher L.W., and Fitzpatrick L.A. (1993). Distribution of noncollagenous proteins in the matrix of adult human bone: evidence of anatomic and functional heterogeneity. *J Bone Miner Res.* **8** (9):1019-29.
- Jackson D.S. Ayad S., and Mechanic G. (1974). Effect of heat on some collagen cross-links. *Biochim. Biophys. Acta.* **336**:100.
- Jaworski Z.F., Liskova-Kiar M., and Uhthoff H.K. (1980). Effect of long-term immobilisation on the pattern of bone loss in older dogs. *J Bone Joint Surg Br.* **62**-B (1):104-10.
- Jayasinghe J.A., Jones S.J., and Boyde A. (1993). Scanning electron microscopy of human lumbar vertebral trabecular bone surfaces. *Virchows Arch A Pathol Anat Histopathol.* **422** (1):25-34.
- Jee W.S.S. (2001). Intergrated bone tissue physiology: anatomy and physiology. *In:* Cowin S.C. (ed.) (2001) *Bone Mechanics Handbook.* CRC Press, London.
- Jiang Y., Zhao J., and Genant H.K. (2002). Macro- and Mircroimaging of Bone Architecture. *In:* Bilezikian J.P., Raisz L.G., and Rodan G.A. (eds.) *Principles of Bone Biology.* Second ed. Academic Press. USA p.1599-1623.
- Jones D.B., and Bingmann D. (1991). How do osteoblasts respond to mechanical stimulation. *Cells and Materials* **1**: 329-340.
- Jones D.B., Boudriot U., Kratz M.., Koller. K., Mertens F. and E.L. Smith (2001). A Trabecular Bone and Marrow Bioreactor. *Eur Cell Mater* **1** (S2) 53.
- Jones D.B., Broeckmann E., Pohl T., and Smith E.L. (2003). Development of a Mechanical Testing and Loading System for Trabecular Bone Studies for Long Term Culture. *Eur Cell Mater* **5**: 48-60
- Jones D.B., Nolte H., Scholubbers J.G., Turner E., and Veltel D. (1991). Biochemical signal transduction of mechanical strain in osteoblast-like cells. *Biomaterials.* **12**(2):101-10.
- Jones H.H., Priest J.D., Hayes W.C., Tichenor C.C., and Nagel D.A. (1977). Humeral hypertrophy in response to exercise. *J Bone Joint Surg Am.* **59** (2):204-8.
- Jones K.H., and Senft J.A. (1985). An improved method to determine cell viability by simultaneous staining with fluorescein diacetate-propidium iodide. *J Histochem Cytochem.* **33** (1):77-9.
- Jowsey, J. (1960). Age changes in human bone. *Clin. Orthop.* **17**: 210–217.
- Kameda T., Mano H., Yuasa T., Mori Y., Miyazawa K., Shiokawa M., Nakamaru Y., Hiroi E., Hiura K., Kameda A., Yang N.N., Hakeda Y., and Kumegawa M. (1997). Estrogen inhibits bone resorption by directly inducing apoptosis of the bone-resorbing osteoclasts. *J Exp Med.* **186** (4):489-95.
- Karaplis A.C. (2002). Embryonic development of bone and the molecular regulation of intramembranous and endochondral bone formation. *In:* Bilezikian J.P., Raisz L.G., and Rodan G.A. (2002). *Principles of bone biology* 2nd Edition. Academic Press. USA. pp. 33-58
- Kaye M., and Henderson J. (1988). Direct functional assessment of human osteoblasts by radioautography: methodology and application in end stage renal disease. *Clin Invest Med.* **11**: 224-33.

- Kenzora JE, Steele RE, Yosipovitch ZH, Glimcher MJ. (1979). Experimental osteonecrosis of the femoral head in adult rabbits. *Clin Orthop Relat Res.* **130**:8-46.
- Kerr J.F.R., Wyllie A.H., and Currie A.R. (1972). Apoptosis: A basic biological phenomenon with wideranging implications in tissue kinetics. *Br. J. Cancer* **26**: 239-257
- Khouja H.I., Bevington A., Kemp G.J., and Russell R.G. (1990). Calcium and orthophosphate deposits in vitro do not imply osteoblast-mediated mineralization: mineralization by betaglycerophosphate in the absence of osteoblasts. *Bone.* **11** (6):385-91.
- Kinney J.H., Lane N.E., and Haupt D.L. (1995). In vivo, three-dimensional microscopy of trabecular bone. *J. Bone Miner. Res.* **13**: 839
- Kinney J.H., and Ladd A.J.C. (1998). The relationship between three-dimensional connectivity and the elastic properties of trabecular bone. *J. Bone Miner. Res.* **10**: 264
- Knothe Tate M. (2001). Interstitial Fluid Flow. *In:* Cowin S.C. (ed.) (2001) *Bone Mechanics Handbook.* CRC Press, London.
- Knothe Tate M.L., Knothe U., and Niederer P. (1998). Experimental elucidation of mechanical load-induced fluid flow and its potential role in bone metabolism and functional adaptation. *Am J Med Sci.* **316** (3):189-95.
- Knothe Tate M.L., Steck R., Forwood M.R., and Niederer P. (2000). *In vivo* demonstration of load-induced fluid flow in the rat tibia and its potential implications for processes associated with functional adaptation. *J Exp Biol.* **203**:2737-45.
- Kobayashi S., Takahashi H.E., Ito A., Saito N., Nawata M., Horiuchi H., Ohta H., Ito A., Iorio R., Yamamoto N, and Takaoka K. (2003). Trabecular minimodeling in human iliac bone. *Bone.* **32** (2):163-9.
- Kölliker A. von (1873). Die normale Resorption des Knochengewebe und ihre Bedeutung für die Entstehung der typischen Knochenformen. Vogel, Leipzig.
- Lang S.M. Moyle D.D., Berg E.W., Detorie N., Gilpin A.T., Pappas N.J., Reynolds J.C., Tkacik M., and Waldron R.L. (1988). Correlation of mechanical properties of vertebral trabecular bone with equivalent mineral density as measured by computed tomography. *J. Bone Joint Surg.* **70A**:1531
- Lang T., Augat P., Majumdar S., Ouyang X., and Genant H.K., Noninvasive assessment of bone density and structure using computed tomography and magnetic resonance. *Bone.* **22**: 149S.
- Lanyon L.E. (1987). Functional strain in bone tissue as an objective, and controlling stimulus for adaptive bone remodelling. *J Biomech.* **20** (11-12):1083-93.
- Lanyon L.E. (1992). Control of bone architecture by functional load bearing. *J Bone Miner Res.* 7 Suppl 2:S 369-75.
- Lanyon L.E, Magee P.T, and Baggott D.G. (1979). The relationship of functional stress and strain to the processes of bone remodelling. An experimental study on the sheep radius. *J Biomech.* **12** (8):593-600.
- Lanyon LE, and Rubin CT. (1984). Static vs dynamic loads as an influence on bone remodelling. *J Biomech.* **17**(12):897-905

- Lean J.M., Jagger C.J., Chambers T.J., and Chow J.W. (1995). Increased insulin-like growth factor I mRNA expression in rat osteocytes in response to mechanical stimulation. *Am J Physiol.* **268** (2 Pt 1):E318-27.
- Leeuwenhoek A. van (1685). Opera omnia seu arcane naturae. *Lugduni Batavorum* **1722**: 135-110. *Cited by:* Ricqlès A. de., Meunier F.J., Castanet J., and Francillion-Vieillot H. (1991). Comparative Microstructure of bone. *In:* Hall B.K. (ed.) *Bone Volume 3. Bone matrix and bone specific products.* CRC Press, USA
- Leeuwenhoek, A. van (1693). An extract of a letter from Mr. Anthoney van Leeuwnhoek, containing several observations on the texture of the bones of animals compared with that of wood: on the bark of trees: on the scales formed on the cuticula, & etc. *Phil. Trans. R. Soc.* **17**: 838.
- Leeuwenhoek A. van (1696). Opera omnia. Lugduni Batavorum. *Epistola.* **107**: 191-192. *Cited by:* Ricqlès A. de., Meunier F.J., Castanet J., and Francillion-Vieillot H. (1991). Comparative Microstructure of bone. *In:* Hall B.K. (ed.) *Bone Volume 3. Bone matrix and bone specific products.* CRC Press, USA.
- Leob, L. (1902). On the growth of epithelium in agar and blood-serum in the living body. *J. med. Res.* **8**, 109.
- Li X.J., Jee W.S., Chow S.Y., and Woodbury D.M. (1990). Adaptation of cancellous bone to aging and immobilization in the rat: a single photon absorptiometry and histomorphometry study. *Anat Rec.* **227** (1):12-24.
- Linde F. and Sorensen H.C.F. (1993). The effect of different storage methods on the mechanical properties of trabecular bone. *J. Biomech.* **26**: 1249
- Linde F., Hvid I., and Madsen F. (1992). The effect of specimen geometry on the mechanical behaviour of trabecular bone specimens. *J Biomech.* **25**(4):359-68.
- Majeska R.J., and Gronowicz G.A. (2002). Current methodologic issues in cell and tissue culture. *In:* Bilezikian J.P., Raisz L.G., and Rodan G.A. (eds.) *Principles of Bone Biology.* Second ed. Academic Press. USA p.1529-1542.
- Malpighi M. (1743). De ossium structura. *Ex. Op. Posth.* Venice. *Cited by:* Ricqlès A. de., Meunier F.J., Castanet J., and Francillion-Vieillot H. (1991). Comparative Microstructure of bone. *In:* Hall B.K. (ed.) *Bone Volume 3. Bone matrix and bone specific products.* CRC Press, USA
- Manolagas S.C., and Jilka R.L. (1995). Bone marrow, cytokines, and bone remodeling. Emerging insights into the pathophysiology of osteoporosis. *N Engl J Med.* **332** (5):305-11.
- Marks SC. and Odgren PR. (2002). Structure and Development of the Skeleton. *In:* Bilezikian J.P., Raisz L.G., and Rodan G.A. (eds.) *Principles of Bone Biology.* Second ed. Academic Press. USA p.3-15.
- Marks SC Jr, and Popoff SN. (1988). Bone cell biology: the regulation of development, structure, and function in the skeleton. *Am J Anat.* **183**(1):1-44.
- Marsh M.E., Munne A.M., Vogel J.J., Cui Y., and Franceschi R.T. (1995). Mineralization of bone-like extracellular matrix in the absence of functional osteoblasts. *J Bone Miner Res.* **10** (11):1635-43.

- Martens F., Smith E., Bröckmann E., and Jones D. (2000). Application of defined compressive strains in a percolation system for very long term culture of trabecular bone. Measurement of trabecular bone mechanical properties. *EORS.* p. 97.
- Martin R.B., and Sharkey N.A. (2001). Mechanical effects of post-mortem changes, preservation, and allograft bone treatments. *In:* Cowin S.C. (ed.) (2001) *Bone Mechanics Handbook.* CRC Press, London.
- May, N.D.S., (1970). *The anatomy of the sheep a dissection manual.* University of Queensland Press, St Lucia, Queensland, Australia. p. 304-5.
- McCabe L.R., Kockx M., Lian J., Stein J., and Stein G. (1995). Selective expression of fos- and jun-related genes during osteoblast proliferation and differentiation. *Exp Cell Res.* **8** (1):255-62.
- Mc Dougal J.S., Martin L.S. Cort S.P., Mozen M., Heldebrant C.M. and Evatt B.L. (1985). Thermal inactivation of the acquired immunodeficiency syndrome virus, human T lymphotropic virus-III lymphadenopathy-associated virus, with specific reference to antihemophilic factor. *J. Clin. Invest.* **76**: 875.
- McKenzie L.S., Horsburgh B.A., Ghosh P., and Taylor T.K. (1977). Organ culture of human articular cartilage: studies on sulphated glycosaminoglycan synthesis. *In Vitro.* **13** (7):423-8.
- Meunier P., Aaron J., Edouard C., and Vignon G. (1971). Osteoporosis and the replacement of cell populations of the marrow by adipose tissue. A quantitative study of 84 iliac bone biopsies. *Clin Orthop Relat Res.* **80**:147-54.
- Milch R.A., Rall D.P., and Tobie J.E. (1957). Bone localization of the tetracyclines. *J Natl Cancer Inst.* **19** (1):87-93.
- Mosmann T. (1983). Rapid colorimetric assay for cellular growth and survival: application to proliferation and cytotoxicity assays. *J Immunol Methods.* **65** (1-2):55-63.
- Mullender M.G., Huskies R., Versleyen H., and Buma P. (1996). Osteocyte density and histomorphometric parameters in cancellous bone of the proximal femur in five mamalian species. *J. Orthop. Res.* **14**: 972.
- Nafei, A., Danielsen, C.C., Linde, F., and Hvid, I. (2000). Properties of growing trabecular ovine bone. *J. Bone Surg Br.* **82** (6): 910-20.
- Neuman, W.F., and Neuman M.W. (195). Skeletal dynamics. *In:* The Chemical Dynamics of Bone Mineral. University of Chicago Press, Chicago, IL. 101.
- Noble B.S., Stevens H.Y. (2003). Techniques for the Study of Apoptosis in Bone. *In:* Helfrich M.H., and Ralston S.H. (e.d.) (2003). Bone Research Protocols. Humana Press. Totowa, New Jersey. pp. 225-236
- Noble B.S., Stevens H., Loveridge N., and Reeve J. (1997). Identification of apoptotic changes in osteocytes in normal and pathological human bone. Bone. **20** (3):273-82.
- Noda M., and Denhardt D.T. (2002). Osteopontin. *In:* Bilezikian J.P., Raisz L.G., and Rodan G.A. (eds.) *Principles of Bone Biology.* Second ed. Academic Press. USA p.239-250.

- Noda M., Yoon K., Rodan G.A., and Koppel D.E. (1987). High lateral mobility of endogenous and transfected alkaline phosphatase: a phosphatidylinositol-anchored membrane protein. *J Cell Biol.* **105** (4):1671-7.
- Nickel R., Schummer A., and Seiferle E. (1992). Lehrbuch der Anatomie der Haustiere Band I 6. Auflage. Knochen der Schultergliedmasse. Verlug Paul, Germany.
- Ninomiya JT, Tracy RP, Calore JD, Gendreau MA, Kelm RJ, Mann KG. (1990). Heterogeneity of human bone. *J Bone Miner Res.* **5** (9):933-8.
- Odgaard A., Hvid I., and Linde F. (1989). Compressive axial strain distributions in cancellous bone specimens. *J Biomech.* **22**: 829-35.
- Owen M. (1967). Uptake of [3H] uridine into precursor pools and RNA in osteogenic cells. *J. Cell Sci.* **2**: 39-56
- Ott S.M. (1993). Bone formation periods studied with triple tetracycline labels in women with postmenopausal osteoporosis. *J Bone Miner Res.* **8** (4):443-50.
- Ott S.M. (2002) Histomophometric analysis of bone remodelling. *In:* Bilezikian J.P., Raisz L.G., and Rodan G.A. (eds.) *Principles of Bone Biology.* Second ed. Academic Press. USA p.303-320.
- Parfitt A.M. (1987). Bone remodeling and bone loss: understanding the pathophysiology of osteoporosis. *Clin Obstet Gynecol.* **30** (4):789-811.
- Parfitt A.M. (1988). Bone histomorphometry: proposed system for standardization of nomenclature, symbols, and units. *Calcif. Tissue Int.*, **42**: 284.
- Parfitt A.M. (1989). Bone-forming cells in clinical conditions. *In:* Hall. B.K. (ed.) (1989). The osteoblast and osteocyte. CRC Press,
- Parfitt A.M. (1994). Osteonal and hemi-osteonal remodeling: the spatial and temporal framework for signal traffic in adult human bone. *J Cell Biochem.* **55** (3):273-86.
- Parfitt A.M. (1995). Problems in the application of in vitro systems to the study of human bone remodeling. *Calcif Tissue Int.* **56** Suppl 1:S5-7.
- Parfitt A.M., Foldes J., Villanueva A.R., and Shih M.S. (1991). Difference in length between demethylchlortetracyline and oxytetracycline: implications for the interpretation of bone histomorphometric data. *Calcif. Tiss. Int.*, **48**: 74-77
- Parfitt A.M., Han Z.H., Palnitkar S., Rao D.S., Shih M.S., and Nelson D. (1997). Effects of ethnicity and age or menopause on osteoblast function, bone mineralization, and osteoid accumulation in iliac bone. *J Bone Miner Res.* **12** (11):1864-73.
- Parfitt A.M., Matthews C.H.E., Villanueva A.R., and Kleerekoper M. (1983). Relationship between surface, volume, and thickness of iliac trabecular bone in aging and in osteoporosis: implications for the microanatomic and cellular mechanism of bone loss. J. Clin. Invest. 72: 1396-1409.
- Parfitt A.M., Mundy G.R., Roodman G.D., Hughes D.E., and Boyce B.F. (1996). A new model for the regulation of bone resorption, with particular reference to the effects of bisphosphonates. *J Bone Miner Res.* **11** (2):150-9.

- Parfitt A.M., Villanueva A.R., Foldes J., and Rao D.S. (1995). Relations between histologic indices of bone formation: implications for the pathogenesis of spinal osteoporosis. *J Bone Miner Res.* **10** (3):466-73.
- Patel S., Pazianas M., Tobias J., Chambers T.J., Fox S., and Chow J. (1999). Early effects of hormone replacement therapy on bone. *Bone.* **24** (3):245-8.
- Paull K.D., Shoemaker R.H., Boyed M.R., Parsons J.L., Risbood P.A., Barbera W.A., Sharma M.N., Baker D.C., Hand E., Scudiero D.A., Monks A., Alley M.C., and Grote M. (1988). The synthesis of XTT: a new tetrazolium reagent that is bioreducible to a water-soluble formazan. *J. Heterocyclic Chem.* **25**: 911
- Pead M.J., Skerry T.M., and Lanyon L.E. (1988). Direct transformation from quiescence to bone formation in the adult periosteum following a single brief period of bone loading. *J Bone Miner Res.* **3** (6):647-56.
- Peck W.A., Birge S.J, Jr, and Fedak S.A. (1964). Bone cells: Biochemical and biological studies after enzymatic isolation. *Science.* **146**: 1476-1477
- Persidsky M.D., and Baillie G.S. (1977). Fluorometric test of cell membrane integrity. *Cryobiology.* **14** (3):322-31.
- Piekarski K., and Munro M. (1977). Transport mechanism operating between blood supply and osteocytes in long bones. *Nature.* **269** (5623):80-2.
- Pitsillides A.A., Rawlinson S.C., Suswillo R.F., Bourrin S., Zaman G., and Lanyon L.E. (1995). Mechanical strain-induced NO production by bone cells: a possible role in adaptive bone (re)modeling? *FASEB J.* **9** (15):1614-22.
- Poole C.A., Brookes N.H., Gilbert R.T., Beaumont B.W., Crowther A., Scott L., and Merrilees M.J. (1996). Detection of viable and non-viable cells in connective tissue explants using the fixable fluoroprobes 5-chloromethylfluorescein diacetate and ethidium homodimer-1. *Connect Tissue Res.* **33**(4):233-41.
- Portal A. (1770). Histoire de l'Anatomie et de la Chirurgie. Didot, Paris.
- Price P.A., Otsuka A.S., Poser J.W., Kristaponis J., and Raman N. (1976). Characterization of a gamma carboxy glutamic acid containing protein from bone. *Proc. Natl. Acad. Sci.* **73**:1447-1451.
- Raab D.M., Crenshaw T.D., Kimmel D.B., and Smith E.L. (1991). A histomorphometric study of cortical bone activity during increased weight-bearing exercise. *J Bone Miner Res.* **6** (7):741-9.
- Raab-Cullen D.M., Thiede M.A., Petersen D.N., Kimmel D.B., and Recker R.R. (1994). Mechanical loading stimulates rapid changes in periosteal gene expression. *Calcif Tissue Int.* **55** (6):473-8.
- Rahn B.A. (2003). Fluorochrome labelling of Bone Dynamics. *Eur Cell Mater* 2003; **5** (2): 41.
- Rahn B.V., Bacellar F.C., Trapp L., and Perren S.M. (1980). A method for morphometry of bone formation using fluorochromes. *Aktuelle Traumatol.* **10** (2):109-15.
- Rahn B.A., and Perren S.M. (1970). Calcein blue as a fluorescent label in bone. *Experientia.* **26**(5):519-20.

- Rahn B.A., and Perren S.M. (1971). Xylenol orange, a fluorochrome useful in polychrome sequential labeling of calcifying tissues. *Stain Technol.* **46** (3):125-9.
- Rahn B.A., and Perren S.M. (1972). Alizarin complexon-fluorochrome for bone and dentine labelling. *Experientia.* **28** (2):180.
- Ranvier L. (1873). Quelques faits relatifs au développement du tissu osseux. *C. R. Acada. Sci. Paris.* 77:1105-1109. *Cited by:* Ricqlès A. de., Meunier F.J., Castanet J., and Francillion-Vieillot H. (1991). Comparative Microstructure of bone. *In:* Hall B.K. (ed.) *Bone Volume 3. Bone matrix and bone specific products.* CRC Press, USA
- Rawlinson S.C., el-Haj A.J., Minter S.L., Tavares I.A., Bennett A., and Lanyon L.E. (1991). Loading-related increases in prostaglandin production in cores of adult canine cancellous bone in vitro: a role for prostacyclin in adaptive bone remodeling? *J Bone Miner Res.* **6** (12):1345-51.
- Rice J.C., Cowin S.C., and Bowman J.A. (1988). On the dependence of the elasticity and strength of cancellous bone on apparent density. *J. Biomech.* **21**: 155.
- Ricqlès A. de., Meunier F.J., Castanet J., and Francillion-Vieillot H. (1991). Comparative Microstructure of bone. In: Hall B.K. (ed.) Bone Volume 3. Bone matrix and bone specific products. CRC Press, USA
- Ritman E.L., Bolander M.E., Fitzpatrick L.A., and Turner R.T. (1998). Micro-CT imaging of structure-to-function relationship of bone microstructure and associated vascular involvement. *Technol. Health Care* **6**: 403.
- Rittling S.R., Matsumoto H.N., McKee M.D., Nanci A., An X.R., Novick K.E., Kowalski A.J., Noda M., and Denhardt D.T. (1998). Mice lacking osteopontin show normal development and bone structure but display altered osteoclast formation *in vitro. J Bone Miner Res.* **13** (7):1101-11.
- Roach H.I. (1994). Why does bone matrix contain non-collagenous proteins? The possible roles of osteocalcin, osteonectin, osteopontin and bone sialoprotein in bone mineralisation and resorption. *Cell Biol Int.* **18** (6):617-28.
- Roach H.I., Erenpreisa J., and Aigner T. (1995). Osteogenic differentiation of hypertrophic chondrocytes involves asymmetric cell divisions and apoptosis. *J Cell Biol.* **131** (2):483-94.
- Robey P.G. (2002). Bone matrix proteoglycans and glycoproteins. *In:* Bilezikian J.P., Raisz L.G., and Rodan G.A. (eds.) *Principles of Bone Biology.* Second ed. Academic Press. USA p.225-238.
- Robins S.P. and Brady J.D. (2002). Collagen Cross-Linking and Metabolism. *In:* Bilezikian J.P., Raisz L.G., and Rodan G.A. (eds.) Principles of Bone Biology. Second ed. Academic Press. USA p.210-223
- Roehm N.W., Rodgers G.H., Hatfield S.M., and Glasebrook A.L. (1991). An improved colorimetric assay for cell proliferation and viability utilizing the tetrazolium salt XTT. *J Immunol Methods.* **142** (2):257-65.
- Rosen CJ., Glowacki J., and Bilezikian J.P. (1999). *The aging skeleton.* Academic press. USA pp 47.
- Rossert J and Crombrugghe B. (2002).Type I Collagen. *In:* Bilezikian J.P., Raisz L.G., and Rodan G.A. (eds.) Principles of Bone Biology. Second ed. Academic Press. USA p.189 -210
- Rotman B., and Papermaster B.W. (1966). Membrane properties of living mammalian cells as studied by enzymatic hydrolysis of fluorogenic esters. *Proc Natl Acad Sci U S A.* **55** (1):134-41.

- Roux W. (1885). Beiträge zur Morphologie der funktionellen anpassung. *Arch. Anat. Physiol. Anat. Abt.* **9**: 120-158.
- Rubin C.T., and Lanyon L.E. (1984). Regulation of bone formation by applied dynamic loads. *J Bone Joint Surg Am.* **66** (3):397-402.
- Rubin C.T. and Lanyon L.E. (1985). Regulation of bone mass by mechanical strain magnitude. *Calcif Tissue Int.* **37**: 411-417.
- Rüegsegger P., Koller B., and Müller R. (1996). A microtomographic system for the nondestructive evaluation of bone architecture. *Calcif. Tiss. Int.,* **58**:24-29.
- Sauren Y.M., Mieremet R.H., Groot C.G., and Scherft J.P. (1992). An electron microscopic study on the presence of proteoglycans in the mineralized matrix of rat and human compact lamellar bone. *Anat Rec.* **232** (1):36-44.
- Schleiden, M.J. (1838). Beiträge zur Phytogenesis. *Arch. Anat., Physiol. u. wiss.* Med. (J. Müller) 1838: 137-176
- Schwann, Th. (1839). *Mikroskopische Untersuchungen über die Übereinstimmung in der Struktur und dem Wachstume der Tiere und Planzen.* Leipzig: W. Engelmann, Nr. 176, Ostwalds Klassiker der exakten Wissenschaften, 1910.
- Shapiro F., Cahill C., Malatantis G. and Nayak R.C. (1995). Transmission electron microscopic demonstration of vimentin in rat osteoblast and osteocyte cell bodies and processes using the immunogold technique. *Anatomical Record.* **241**: 39–48.
- Sharkey N.A., Hollstein S.B., and Martin R.B. (1991). Thermal inactivation of HIV in cadaveric specimens:biochemical effects on bone in Transactions of the Combined Meeting of the Orthopaedic Research Societies of the USA, Japan and Canada, Oct. 21-23, 279.
- Singh I. (1978). The Architecture of Cancellous Bone. *J. Anat.* **127** (2) 305-310
- Singh M., Nagrath A.R., and Maini P.S. (1970). Changes in trabecular-pattern of the upper end of the femur as an index of osteoporosis. *J. Bone Jt. Surg. Am.* **52**: 457-467.
- Skerry T.M. (1998). Models for mechanical loading of bone and bone cells in vivo and in vitro. *In:* Arnett T.R. and Henderson B. (1998). Methods in Bone Biology. Chapman & Hall, London, UK. pp149-176.
- Skerry T.M., Bitensky L., Chayen J., and Lanyon L.E. (1988). Loading-related reorientation of bone proteoglycan in vivo. Strain memory in bone tissue? *J Orthop Res.* **6** (4):547-51.
- Skerry T.M., Bitensky L., Chayen J., and Lanyon L.E. (1989). Early strain-related changes in enzyme activity in osteocytes following bone loading *in vivo. J Bone Miner Res.* **4** (5):783-8.
- Skerry T.M., Suswillo R., el Haj A.J., Ali N.N., Dodds R.A., and Lanyon L.E. (1990). Load-induced proteoglycan orientation in bone tissue *in vivo* and *in vitro. Calcif Tissue Int.* **46**(5):318-26.
- Slater T.F., Sawyer B., and Straeuli U. (1963). Studies on succinate-tetrazolium reductase systems. III. Points of coupling of four different tetrazolium salts. *Biochim Biophys Acta.* 77:383-93.
- Smith E.L., Boudriot U., Daume B., Kratz M.., Recker R.R., Cullen D., Jones D.B. (2003). Long term perfusion loading of trabecular bone cores and formation rate. *Eur Cell Mater* **5** (S2) 48.

- Smith E.L. Jr., Smith P.E., Ensign C.J., and Shea M.M. (1984). Bone involution decrease in exercising middle-aged women. *Calcif Tissue Int.* **36** Suppl 1:S129-38.
- Sodek J., Ganss B., and McKee M.D. (2000). Osteopontin. *Crit Rev Oral Biol Med* **11** (3):279-303.
- Somjen D., Binderman I., Berger E., and Harell A. (1980). Bone remodelling induced by physical stress is prostaglandin E2 mediated. *Biochim Biophys Acta.* **627** (1):91-100.
- Spengler DM, Morey ER, Carter DR, Turner RT, and Baylink DJ. (1983). Effects of spaceflight on structural and material strength of growing bone. *Proc Soc Exp Biol Med.* **174**(2):224-8.
- Spigelius A. (1631). De Formato Foetuliber Singularis opera posthma studio Liberalis cremae tarvisni ed. Ta. Francofurti M. Merianus.
- Spire B., Dormont D., Barre-Sinoussi F., Montagnier L., and Chermann J.C. (1985). Inactivation of lymphadenopathy-associated virus by heat, gamma rays, and ultraviolet light. *Lancet.* **1**(8422): 188
- Stevens A. and Lowe J. (1997). Human histology 2nd Edition. Mosby, Harcourt Publishers Limited. London.
- Stiles C.D., Isberg R.R., Pledger W.J., Antoniades H.N., and Scher C.D. (1979). Control of the Balb/c-3T3 cell cycle by nutrients and serum factors: analysis using platelet-derived growth factor and platelet-poor plasma. *J Cell Physiol.* **99** (3):395-405.
- Strangeways, T.S.P, and Fell, H.B. (1926). Experimental studies on the differentiation of embryonic tissues growing *in vivo* and *in vitro*. (1) The development of the isolated limb-bud (a) when subcutaneously grafted into the post-embryonic chick and (b) The development of the isolated early embryonic eye of the fowl when cultivated *in vitro*. *Proc. Roy. Soc.* **B99**, 340.
- Sumner-Smith, G. (1982). *Bone in Clinical Orthopaedics. A study in comparative osteology.* W.B. Saunders Company. Philadelphia. USA. p. 165
- Suzuki H.K., and Mathews A. (1966). Two-color fluorescent labeling of mineralizing tissues with tetracycline and 2,4-bis[N,N'-di-(carbomethyl)aminomethyl] fluorescein. *Stain Technol.* **41** (1):57-60.
- Termine J.D., Kleinman H.K., Whitson S.W., Conn K.M., McGarvey M.L., and Martin G.R. (1981). Osteonectin, a bone-specific protein linking mineral to collagen. *Cell.* **26**: 99-105.
- Thorsen K., Kristoffersson A., and Lorentzon R. (1996). The effects of brisk walking on markers of bone and calcium metabolism in postmenopausal women. *Calcif Tissue Int.* **58** (4):221-5.
- Tomkinson A., Reeve J., Shaw R.W., and Noble B.S. (1997). The death of osteocytes via apoptosis accompanies estrogen withdrawal in human bone. *J Clin Endocrinol Metab.* **82** (9):3128-35.
- Torrance A.G., Mosley J.R., Suswillo R.F., and Lanyon L.E. (1994). Noninvasive loading of the rat ulna in vivo induces a strain-related modeling response uncomplicated by trauma or periostal pressure. Calcif Tissue Int. **54** (3):241-7.
- Turner C.H., and Burr D.B. (1993). Basic biomechanical measurements of bone: a tutorial. *Bone.* **14** (4):595-608.
- Turner C.H., Woltman T.A., and Belongia D.A. (1992). Structural changes in rat bone subjected to long-term, in vivo mechanical loading. *Bone.* **13** (6):417-22.

- Twentyman P.R., and Luscombe M. (1987). A study of some variables in a tetrazolium dye (MTT) based assay for cell growth and chemosensitivity. *Br J Cancer.* **56** (3):279-85.
- van de Wijngaert F.P., and Burger E.H. (1986). Demonstration of tartrate-resistant acid phosphatase in un-decalcified, glycolmethacrylate-embedded mouse bone: a possible marker for (pre)osteoclast identification. *J Histochem Cytochem.* **34**(10):1317-23.
- Verborgt O., Gibson G.J., and Schaffler M.B. (2000). Loss of osteocyte integrity in association with microdamage and bone remodeling after fatigue *in vivo. J Bone Miner Res.* **15** (1):60-7.
- Versalius A. (1543). *De Humanis Corpori Fabrica.* Basel. *Cited by:* Ricqlès A. de., Meunier F.J., Castanet J., and Francillion-Vieillot H. (1991). Comparative Microstructure of bone. *In:* Hall B.K. (ed.) *Bone Volume 3. Bone matrix and bone specific products.* CRC Press, USA
- Vico L, Chappard D, Alexandre C, Palle S, Minaire P, Riffat G, Morukov B, and Rakhmanov S. (1987). Effects of a 120 day period of bed-rest on bone mass and bone cell activities in man: attempts at countermeasure. *Bone Miner.* **5**:383-94.
- Virchow R. (1851). Die Identität von Knochen-Korpel und Bindergewebskorper schen sowie über Schleingewebe. *Verh. Phys. Med. Ges.* **2**: 150-187.
- von Garrel T., and Knaepler H. (1993). Thermal incubation of allogenic bone transplants. *J. Bone Joint Surg.* 75B Suppl. II. 107.
- von Meyer G.H. (1867). Die Architektur der Spongiosa. *Arch. Anat. Physiol. Wiss. Med. Reichert DuBoisReymonds Arch.* **34**: 615-628.
- Wang L., Ciani C., Doty S.B., and Fritton S.P. (2004). Delineating bone's interstitial fluid pathway *in vivo. Bone.* **34** (3):499-509.
- Warwick R., and Williams P.L. (ed.) (1973). *Gray's Anatomy 35th Edition.* Longman. UK. p. 200-233
- Wassermann F. and Yaeger J.A. (1965). Fine structure of the osteocyte capsule and of the wall of the lacunae in bone. *Zeitschrift fur Zellforschung* **67**: 636–652.
- Weaver J.K. and Chalmers J. (1966). Cancellous bone: its strength and changes with aging and an evaluation of some methods for measuring its mineral content. *J. Bone Joint Surg.* **48A**: 289
- Weinbaum S., Cowin S.C., and Zeng Y. (1994). A model for the excitation of osteocytes by mechanical loading-induced bone fluid shear stresses. *J Biomech.* **27**(3):339-60.
- Weinreb M., Rodan G.A., and Thompson D.D. (1989). Osteopenia in the immobilized rat hind limb is associated with increased bone resorption and decreased bone formation. *Bone.* **10** (3):187-94.
- Woessner J.F. (1961). The determination of hydroxyproline in tissue and protein samples containing small proportions of this imino acid. *Archiv Biochem Biophys.* **93**: 440-447.
- Woo S.L., Kuei S.C., Amiel D., Gomez M.A., Hayes W.C., White F.C., and Akeson W.H. (1991). The effect of prolonged physical training on the properties of long bone: a study of Wolff's Law. *J Bone Joint Surg Am.* **63** (5):780-7.
- Wyllie A.H. (1981). Glucocorticoid-induced thymocyte apoptosis is associated with endogenous withendogenous endonuclease activation. *Nature* **284**: 555-558

- Wyllie A.H., Kerr J.F.R., and Currie A.R. (1980). Cell death: the significance of apoptosis. *Int. Rev. Cytol.* **68:** 251-306
- Whitehouse, W.J., and Dyson, E.D. (1974). Scanning Electron Microscope studies of Trabecular Bone in the Proximal End of the Femur. *J. Anat.* **118** (3) 417-444.
- Whitehouse, W.J., Dyson, E.D., and Jackson, C.K. (1971). The Scanning Electron Microscope in Studies of Trabecular Bone from a Human Vertebral Body. *J. Anat.* **108** (3) 481-496.
- Wolff J. (1870). Ueber die innere Architectur der Konchen und ihre Bedeutung für dir Frage vom Knochenwachstum. *Virchows Arch. Pathol. Anat. Physiol. Klin. Med.* **50**: 389.
- Wolff J. (1892). Das Gesetz der Transformation der Knochen. Hirschwald, Berlin.
- Yan Q., and Sage E.H. (1999). SPARC, a matricellular glycoprotein with important biological functions. *J Histochem Cytochem.* **47** (12):1495-506.
- Yang R., Davies C.M., Archer C.W., and Richards R.G. (2003). Immunohistochemistry of matrix markers in Technovit 9100 New-embedded undecalcified bone sections. *Eur Cell Mater.* **6**: 57-71
- You L.D., Weinbaum S., Cowin S.C., and Schaffler M.B. (2001). Ultrastructure of the osteocyte process and its pericellular matrix. *Anat Rec A Discov Mol Cell Evol Biol.* **278** (2):505-13.
- Zaman G., Dallas .SL., and Lanyon L.E. (1992). Cultured embryonic bone shafts show osteogenic responses to mechanical loading. *Calcif Tissue Int.* **51** (2):132-6.

6.b. Web References

1. http://www.isrvma.org/article/54_4_6.htm [accessed on 18-04-03]
2. http://worldanimalfoundation.homestead.com/WAFDestructiveDairyQA.html [accessed on 18-04-03]
3. http://www.arc.org.uk/about_arth/booklets/6028/6028.htm [accessed on 11-11-04]
4. http://www.ebsciences.com/histology/tartram.htm [accessed on 01-06-01]

6.c. Other References

Thesis

- Koller K (2004) – thesis in submission, Marburg, Germany.
- Roach H.I. (1987). Posibilities and limitations of bone organ culture. PhD thesis, Southhampton University.

Manuals

- Bröckmann E. (2002). Hardware and Software Operating Manual. Zetos version 2. Marburg, Germany.

Chapter 7.
Appendices

7.a. Model Systems

1. MMA I pure MMA. MMA II (always kept in the fridge) 100ml pure MMA 2g catalysts stirred on a magnetic stirrer for 5 to 10 minutes to keep in solution. MMA III 100ml pure MMA 4g catalyst stirred on a magnetic stirrer for 5 to 10 minutes, if the solution was cloudy, it was filtered with a paper filter 595½ before adding the softener 25ml stirred on a magnetic stirrer for a further 5 to 10 minutes. Solution was stored at 2 - 8°C in the refrigerator

2. Preparing Technovit solutions:

Table 7.a.1 Components of the infiltration soloutions for Technovit 9100 New embedding

Solution	xylene	stabilised basic soln	destabilised basic soln	PMMA Powder	hardener 1	hardener 2	Regulator	Storage	Special Instructions / Notes
TMA 1*	60 ml	60 ml						4°C	Mixes immediately
TMA 2*		100 ml			0.5 g			4°C	Dissolves in minutes
TMA 3*			150 ml		0.75 g			4°C	Dissolves in minutes
TMA 4*			150 ml	12 g	0.6 g			4°C	Cloudy. Stir overnight @ 4°C.
Poly A*			360 ml	57.6 g	2.16 g			4°C	Cloudy. Stir overnight @ 4°C.
Poly B*			40 ml			3.2 ml	1.6 ml	4°C	Add regulator 1st then add hardener drop-wise. Mixes immediately

***TMA 1-4 are infiltration solutions. Poly A and Poly B are polymerization solutions which must be mixed up in the ratio of 9A:1B immediately before use.**

3. Masson solution [1 part solution A to 2 parts solution B – Solution A. 1g Acid Fuchsin (Fluka, 84600)100 ml dH_2O boil, let cool,0.3 ml glacial acetic acid (Fluka, 45731) mix, filter. Solution B. 1g Ponceau Xylidine (Fluka, 81465) 100 ml dH_2O boil, let cool, 0.3 ml glacial acetic acid (Fluka, 45731) mix, filter]

4. Phosphomolybdic acid - orange G [4g Phosphomolybdic Acid (Fluka, 79560) 2g Orange G (Fluka, 75380) 100ml dH_2O mix and filter].

5. 0.1% Light green SF yellowish [0.1% light green SF yellowish (Merck, 15941), 100ml dH_2O, 0.2ml glacial acetic acid (Fluka, 45731), mix].

6. 1% Toluidine blue [4g Toluidine Blue (Fluka, 89640), 4g Sodium tetraborate (Fluka, 71998) in 400 ml dH_2O].

7. 1% Alcian Blue (per 100 ml) [1 g Alcian Blue 8GX, 99 ml ddH_2O, 1 ml Glacial Acetic Acid, mix, filter] (stable for 4 weeks)

8. Alkaline Alcohol (per 100ml) [90 ml of 96% Ethanol, 10 ml Ammonia Solution (26%), mix] (make fresh and discard after using).

9. Weigert's Haematoxylin (per 100ml) [50 ml of Weigert's Solution A, 50 ml of Weigert's Solution B] (mixed solution stable for 8 days, solution can be used up to 3 times)

10. Brilliant Crocein / Acid Fuchsin [4 parts of 0.1% Brilliant Crocein, 1 part of 0.1% Acid Fuchsin mix] (mixed solution stable for 3 months). 0.1% Brilliant Crocein (per 100ml) [0.1 g Brilliant Crocein 99.5 ml ddH_2O, 0.5 ml Glacial Acetic Acid stir] (stable for 6 months). 0.1% Acid Fuchsin (per 100ml) [0.1 g Acid Fuchsin, 99.5 ml ddH_2O 0.5 ml Glacial Acetic Acid stir] (stable for 6 months).

11. 0.5 % Acetic Acid (per 100ml) [99.5 ml dH_2O, 0.5 ml Glacial Acetic Acid, stir] (make fresh and discard after using).

12. 5% Phosphotungstic Acid (per 100ml) [5 g Phosphotungstic Acid, 100 ml dH_2O stir] (make fresh and discard after using).

13. Saffron Alcohol (per 100ml) [6 g Safran du Gatinais, 100 ml of 100% Ethanol, stir at length, place into an airtight dark bottle and keep in a 50-58°C incubator for a minimum of 48 hours before using] (solution may be used repeatedly until staining intensity decreases).

7.b. Cell Viability

1. Dulbecco's Modified Eagle Medium, powder (high glucose) 10x1L (Gibco, Cat. No. 12800-017, Lot No. 1143722). Contains L-Glutamine, 4500 mg/L D-Glucose, 110mg/L Sodium Pyruvate, without Sodium Bicarbonate. Stored at 4°C.

Table 7.b.1 Components of Dulbecco's Modified Eagle Medium.

Inorganic Salts	Concentration mg/L	**Vitamins**	Concentration mg/L	**Other Components**	Concentration mg/L
$CaCl_2 \bullet 2H_2O$	-	D-Ca pantothenate	4.00	D-Glucose	4500.00
$CaCl_2$ (anhyd.)	200.00	Choline Chloride	4.00	Phenol Red	15.00
$Fe(NO_3) \bullet 9H_2O$	0.10	Folic Acid	4.00	HEPES	-
KCl	400.00	i-Inositol	7.20	Sodiu Pyruvate	110.00
$MgSO_4$ (anhyd.)	97.67	Niacinamide	4.00		
$MgSO_4 \bullet 7\ H_2O$	-	Pyridoxine HCl	4.00		
NaCl	6400.00	Riboflavin	0.40		
$NaHCO_3$	3700.00	Thiamine HCl	4.00		
$NaH_2PO_4 \bullet 2H_2O$	-				
$NaH_2PO_4 \bullet H_2O$	125.00				

Table 7.b.2 Components of Dulbecco's Modified Eagle Media – continuation.

Amino Acids	mg/L	**Amino Acids**	mg/L	**Amino Acids**	mg/L
L-Alanine	-	L-Alanyl-L-Glutamine	-	L-Phenylalanine	66.00
L-Asparagine	-	Glycyl-L-Glutamine	-	L-Proline	-
L-Arginine • HCl	84.00	Glycine	30.00	L-Serine	42.00
L-Aspartic Acid	-	L-Histidine HCl • H_2O	42.00	L-Threonine	95.00
L-Cystine	-	L-Isoleucine	105.00	L-Tryptophan	13.00
L-Cystine • 2HCl	63.00	L-Leucine	105.00	L-Tyrosine	-
L-Glutamic Acid	-	L-Lysine • HCl	146.00	L-Tyrosine (disodium salt)	104.00
L-Glutamine	584.00	L-Methinonine	30.00	L-Valine	94.00

2. Earle's Balanced Salt Solution (EBSS) (1X), liquid (Gibco, Cat. No. 24010-043, Lot. No. 3067374). Contains Calcium, Magnesium and Phenol Red. Stored at room temperature between 15-30°C. Was previously used as a wash solution in Marburg, but, in atmospheric conditions it resulted in a rapid rise in pH of the culture medium. This caused the phenol red indicator to turn purple, as bone core washing took place in a 37 °C room rather than an incubator with controlled CO_2, therefore, it was decided to change from Earle's salts solution to that of Hanks'.

Table 7.b.3 Components of Earle's Balanced Salt Solution

Inorganic Salts	Concentration (mg/L)	**Other Components**	Concentration (mg/L)
$CaCl_2$ (anhyd.)	0.20	D-Glucose	1.00
KCl	0.40	Phenol Red	0.01
$MgSO_4 \bullet 7H_2O$	0.20		
NaCl	6.80		
$NaHCO_3$	2.20		
$NaH_2PO_4 \bullet 7H_2O$	0.158		

3. Hanks' Balanced Salt Solutions (HBSS) (1X), liquid (Gibco, Cat. No. 24020-133). Contains Calcium, Magnesium and Phenol Red. Stored at room temperature between 15-30°C. Hanks' balanced salt solution is designed for atmospheric equilibrium, based on the physiological relevant pKa of phosphoric acid. The use of Hanks' salts in a CO_2 incubator would result in a drop in pH turning the culture media yellow.

Table 7.b.4 Hanks' Balanced Salt Solutions (HBSS)

Inorganic Salts	Concentration (mg/L)	**Other Components**	Concentration (mg/L)
$CaCl_2$ (anhyd.)	-	D-Glucose	1.00
$CaCl_2 \bullet 2H_2O$	0.185	Phenol Red	0.01
KCl	0.40		
KH_2PO_4	0.06		
$MgCl_2 \bullet 6H2O$	0.10		
$MgSO_4 \bullet 7H_2O$	0.10		
NaCl	8.00		
$NaHCO_3$	0.35		
Na_2PO_4	0.048		
$Na2HPO_4 \bullet 7H_2O$	-		

4. Penicillin/Streptomycin solution (Gibco, Cat.No.15140-122) utilising penicillin G (sodium salt) and streptomycin sulphate prepared in normal saline. Kills gram positive and gram negative bacteria. This solution was aliquated into 10ml Storage at -20°C . Using concentration 50 000 IU (10 000 per ml).

5. Gentamicin, liquid (Gibco, Cat.No.15750-045) containing 50 mg/ml gentamicin sulphate in distilled water. Stored at room temperature between 15-30°C. Using concentration 150 mg gentamicin.

6. Fungizone ® Antimyotic, liquid (Gibco, Cat.No 15290-018) containing 250 µg/ml amphotericin B prepared in distilled water. This solution was aliquated into 10 ml and stored at -20°C . Using concentration 500 µg.
7. Weigert's haematoxylin [1 part Weigert's solution A (Merck, 1.15973./1):1 part Weigert's solution B (Merck, 1.15973./2)]

8. Cell Tracker™ Green [Molecular Probes, C-2925] Cell Tracker Green was placed upon receipt at -20°C until it could be made into a stock solution. A working solution of 25 µM in a 5 ml volume of PBS was required. The stock solution contained 10 mM, thus the working solution needed to be 400x more dilute, (5/400) so 12.5 µl of the stock solution per 5 ml PBS buffer. The molecular weight of CMFDA is 464.84, thus 1 M would contain 464.84g/L and a 10 mM solution would contain 4.6484g/L, though we only have 1 mg. To have a 10 mM stock solution (1/4.6484) 0.215 ml DMSO should be added to 1 mg CMFDA. Before opening the vial the lyophilised powder was allowed to thaw to room temperature (~22°C). All work was conducted under a fume hood as DMSO is toxic (irritating to the eyes, respiratory system and skin). Once the powder had defrosted the vial was flicked in order to drop the powder from the vial wall. Carefully, 215 µl of anhydrous dimethylsulfoxide (DMSO) (prepared by the biochemistry group) was added to the vial containing 1mg of CMFDA. The sample was mixed by pipetting the powder up and down until fully dissolved. This stock solution was aliqoted into 14 vials each containing 15 µl of the solution and stored at -20°C. This working solution had a shelf life of at least 6 months.

9. SYTO24 [Molecular Probes S-7559] SYTO24 was placed upon receipt in a dark box at -20°C until it could be made into a stock solution. A working solution of 5 µM in a 5 ml volume of PBS was required. The stock solution contained 5 mM, thus the working solution needed to be 1000x more dilute, (1/1000) so 5 µl of the stock solution per 5 ml PBS buffer. This dye was already diluted in DMSO and required no other mixing. It was left thaw to room temperature (~22°C), mixed and aliquoted into 10 µl per vial (in order to reduce the number of freeze thaw cycles) and stored at -20°C. This working solution had a shelf life of at least one year. This dye should be protected from light whenever possible and during use a double layer of gloves should be worn as this dye is extremely mutagenic.

7.c. Matrix Synthesis

1. Mayer's haematoxylin [per 100 ml; 0.1 g Haematoxylin, 5 g Potassium Aluminum Sulfate, 0.02 g Sodium Iodate, 100 ml ddH_2O dissolve by mixing and warming solution; 0.1 g Citric Acid, 5 g Chloral Hydrate boil for 5 minutes, let cool, filter]

2. 1% Eosin - Working Solution [1% Eosin - Stock Solution (per 100 ml)1 g Eosin Yellowish 100 ml ddH_2O for 1% Eosin - Working Solution (per 100 ml) 100 ml of 1% Eosin - Stock Solution, 15 drops Glacial Acetic Acid mix while dripping acetic acid]

3. pepsin (SERVA, 31820) [1mg/1ml pepsin in 0.5M acetic acid]

4. The sample buffer was made by diluting 4x buffer [16 ml dH_2O, 4 ml 0.5M Tris-HCL pH 6.8, 3.2 ml glycerol, 6.4 ml 10% SDS stock, 5 mg bromophenol blue and 5.6 (v/v) 2 β-mercaptoethanol].

5. 1x reservoir buffer [50ml x10 reserviour buffer stock, 5ml 10% SDS stock made up to 500 ml with H_2O]